Copyrighted Material

Methods in Cell Biology • Volume 100

# THE ZEBRAFISH: CELLULAR AND DEVELOPMENTAL BIOLOGY, PART A

THIRD EDITION

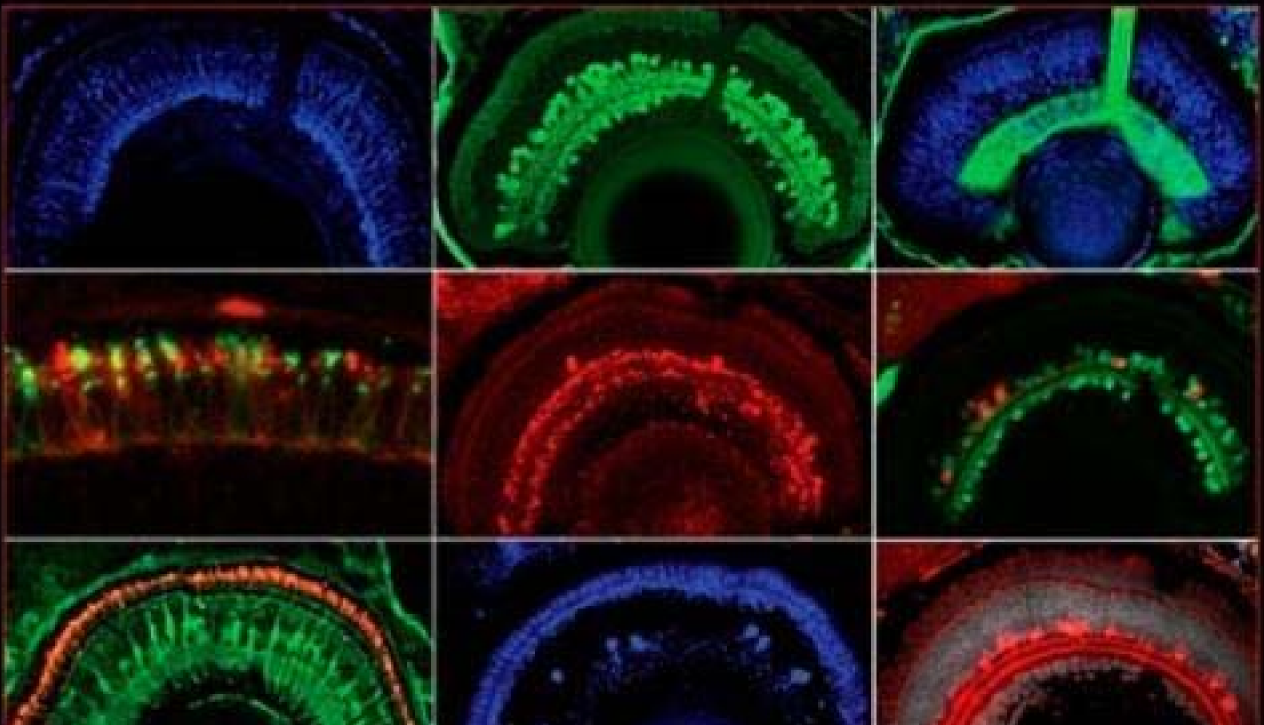

Edited by

H. William Detrich III, Monte Westerfield
and Leonard I. Zon

Copyrighted Material

## Series Editors

**Leslie Wilson**
Department of Molecular, Cellular and Developmental Biology
University of California
Santa Barbara, California

**Paul Matsudaira**
Department of Biological Sciences
National University of Singapore
Singapore

# Methods in Cell Biology

## VOLUME 100

*The Zebrafish: Cellular and Developmental Biology, Part A*
Third Edition

Edited by

**H. William Detrich III**
Department of Biology, Northeastern University, Boston, MA, USA

**Monte Westerfield**
Institute of Neuroscience, University of Oregon, Eugene, OR, USA

**Leonard I. Zon**
Division of Hematology/Oncology, Children's Hospital of Boson,
Department of Pediatrics and Howard Hughes Medical Institute, Harvard Medical School, Boston, MA, USA

ELSEVIER

AMSTERDAM • BOSTON • HEIDELBERG • LONDON
NEW YORK • OXFORD • PARIS • SAN DIEGO
SAN FRANCISCO • SINGAPORE • SYDNEY • TOKYO
Academic Press is an imprint of Elsevier

Academic Press is an imprint of Elsevier
30 Corporate Drive, Suite 400, Burlington, MA 01803, USA
525 B Street, Suite 1900, San Diego, CA 92101-4495, USA
32, Jamestown Road, London NW1 7BY, UK
Linacre House, Jordan Hill, Oxford OX2 8DP, UK

Third edition 2010

Copyright © 2010 Elsevier Inc. All rights reserved

No part of this publication may be reproduced, stored in a retrieval system or transmitted in any form or by any means electronic, mechanical, photocopying, recording or otherwise without the prior written permission of the publisher

Permissions may be sought directly from Elsevier's Science & Technology Rights Department in Oxford, UK: phone (+44) (0) 1865 843830; fax (+44) (0) 1865 853333; email: permissions@elsevier.com. Alternatively you can submit your request online by visiting the Elsevier web site at http://elsevier.com/locate/permissions, and selecting *Obtaining permission to use Elsevier material*

Notice
No responsibility is assumed by the publisher for any injury and/or damage to persons or property as a matter of products liability, negligence or otherwise, or from any use or operation of any methods, products, instructions or ideas contained in the material herein. Because of rapid advances in the medical sciences, in particular, independent verification of diagnoses and drug dosages should be made

ISBN–13: 978-0-12-384892-5
ISSN: 0091-679X

For information on all Academic Press publications
visit our website at elsevierdirect.com

Printed and bound in USA
10 11 12 13 10 9 8 7 6 5 4 3 2 1

Working together to grow
libraries in developing countries

www.elsevier.com | www.bookaid.org | www.sabre.org

ELSEVIER BOOK AID International Sabre Foundation

# DEDICATION

We dedicate the Third Edition of *Methods in Cell Biology: The Zebrafish* to Wolfgang Driever, Mark C. Fishman, Charles Kimmel, and Christiane Nüsslein-Volhard. Through their foresighted embrace of the zebrafish as a model vertebrate and their pursuit of genetic screens to illuminate vertebrate development, they fostered the emergence of the vibrant zebrafish research community.

# CONTRIBUTORS

*Numbers in parentheses indicate the pages on which the authors' contributions begin.*

**Andrei Avanesov**, (153) Division of Craniofacial and Molecular Genetics, Tufts University, Boston, Massachusetts

**Ethan A. Carver**, (295) Department of Biological and Environmental Sciences, The University of Tennessee-Chattanooga, Chattanooga, Tennessee

**Prisca Chapouton**, (73) Institute of Developmental Genetics, Helmholtz Zentrum München, German Research Center for Environmental Health, Neuherberg, Germany

**Chi-Bin Chien**, (3) Department of Neurobiology and Anatomy, University of Utah, Salt Lake City, Utah

**Alan J. Davidson**, (233) Center for Regenerative Medicine, Massachusetts General Hospital, Boston, Massachusetts

**Iain A. Drummond**, (233) Departments of Medicine and Genetics, Harvard Medical School and Nephrology Division, Massachusetts General Hospital, Charlestown, Massachusetts

**James M. Fadool**, (205) Department of Biological Science, Florida State University, Tallahassee, Florida

**John A. Gaynes**, (3) Department of Neurobiology and Anatomy, University of Utah, Salt Lake City, Utah

**Leanne Godinho**, (73) Lehrstuhl für Biomolekulare Sensoren, Institute for Neuroscience, Technische Universität München, Munich, Germany

**Paul D. Henion**, (127) Center for Molecular Neurobiology and Department of Neuroscience, Ohio State University, Columbus, Ohio

**Yunhan Hong**, (55) Department of Biological Sciences, National University of Singapore, Singapore

**Sumio Isogai**, (27) Department of Anatomy, School of Medicine, Iwate Medical University, Morioka, Japan

**Makoto Kamei**, (27) Program in Genomics of Differentiation, National Institute of Child Health and Human Development, Bethesda, Maryland; Cell Biology of Diseases Group, Sansom Institute for Health Research, School of Pharmacy and Medical Science, University of South Australia, Adelaide, South Australia, Australia

**John P. Kanki**, (127) Department of Pediatric Oncology, Dana-Farber Cancer Institute, Harvard Medical School, Boston, Massachusetts

**Robin A. Kimmel**, (261) Institute of Molecular Biology, University of Innsbruck, Innsbruck, Austria

**Martina Lachnit**, (127) Department of Oncological Sciences, Huntsman Cancer Institute, University of Utah, Salt Lake City, Utah

**Mei-Yee Law**, (3) Department of Neurobiology and Anatomy, University of Utah, Salt Lake City, Utah

**Jeong-Soo Lee**, (127) Department of Pediatric Oncology, Dana-Farber Cancer Institute, Harvard Medical School, Boston, Massachusetts

**Charles A. Lessman**, (295) Department of Biological Sciences, The University of Memphis, Memphis, Tennessee

**A. Thomas Look**, (127) Department of Pediatric Oncology, Dana-Farber Cancer Institute, Harvard Medical School, Boston, Massachusetts

**Jarema Malicki**, (153) Division of Craniofacial and Molecular Genetics, Tufts University, Boston, Massachusetts

**Dirk Meyer**, (261) Institute of Molecular Biology, University of Innsbruck, Innsbruck, Austria

**Teresa Nicolson**, (219) Howard Hughes Medical Institute, Oregon Hearing Research Center and Vollum Institute, Oregon Health and Science University, Portland, Oregon

**Wilda Orisme**, (295) Department of Chemical Biology and Therapeutics, St. Jude Children's Research Hospital, Memphis, Tennessee

**Weijun Pan**, (27) Program in Genomics of Differentiation, National Institute of Child Health and Human Development, Bethesda, Maryland

**Brian D. Perkins**, (205) Department of Biology, Texas A&M University, College Station, Texas

**Fabienne E. Poulain**, (3) Department of Neurobiology and Anatomy, University of Utah, Salt Lake City, Utah

**David A. Prober**, (281) Division of Biology, California Institute of Technology, Pasadena, California

**Jason Rihel**, (281) Department of Molecular and Cellular Biology, Harvard University, Cambridge, Massachusetts

**Alexander F. Schier**, (281) Department of Molecular and Cellular Biology, Harvard University, Cambridge, Massachusetts; Division of Sleep Medicine, Harvard University, Cambridge, Massachusetts; Center for Brain Science, Harvard University, Cambridge, Massachusetts; Harvard Stem Cell Institute, Harvard University, Cambridge, Massachusetts

**Cornelia Stacher Hörndli**, (3) Department of Neurobiology and Anatomy, University of Utah, Salt Lake City, Utah

**Rodney A. Stewart**, (127) Department of Oncological Sciences, Huntsman Cancer Institute, University of Utah, Salt Lake City, Utah

**Michael R. Taylor**, (295) Department of Chemical Biology and Therapeutics, St. Jude Children's Research Hospital, Memphis, Tennessee

**Josef G. Trapani**, (219) Howard Hughes Medical Institute, Oregon Hearing Research Center and Vollum Institute, Oregon Health and Science University, Portland, Oregon

**Brant M. Weinstein**, (27) Program in Genomics of Differentiation, National Institute of Child Health and Human Development, Bethesda, Maryland

# PREFACE

The publication of the hundredth volume of *Methods in Cell Biology* is a significant milestone for the Series, indicative both of the success of the volumes in providing state-of-the-art technical protocols and of the commitment of the many contributors, editors, and publisher, Elsevier/Academic Press, to ensuring their widespread dissemination. Two individuals in particular, the Series Editors Leslie Wilson and Paul Matsudaira, deserve our gratitude for fostering the technical and scientific excellence of *Methods in Cell Biology*. Les became the Series Editor beginning with Volume 27 in 1986 and Paul joined to create the "Dynamic Duo" with Volume 37 in 1993. Monte, Len, and I salute Les and Paul for their signal accomplishments in developing the Series into the foremost "go-to" resource for cell and developmental biologists.

Building on the foundation of our first (1999) and second (2004) editions of *Methods in Cell Biology: The Zebrafish*, Monte, Len, and I are pleased to introduce this Third Edition, beginning with *Methods in Cell Biology* Volume 100, *Cellular and Developmental Biology, Part A*. In this volume (and its soon-to-be-released companion, *Part B*), our contributors present the latest technical advances in the Cell, Developmental, and Neural Biology of the zebrafish that have appeared since the second edition. One theme that clearly emerges from these chapters is that the zebrafish is the preeminent vertebrate model for mechanistic *cellular* studies of developmental processes *in vivo*. Subsequent volumes on *Genetics, Genomics, and Informatics* will cover new technologies in Forward and Reverse Genetics, Transgenesis, The Zebrafish Genome and Mapping Technologies, Informatics and Comparative Genomics, and Infrastructure. The Third Edition will also introduce new volumes on *Disease Models and Chemical Screens*, two rapidly emerging and compelling applications of the zebrafish. We trust that these volumes will prove valuable both to seasoned zebrafish investigators and to those who are newly adopting the zebrafish model as part of their research armamentarium.

We thank Les, Paul, and the staff of Elsevier/Academic Press, especially Zoe Kruze, for their enthusiastic support of our Third Edition of *Methods in Cell Biology: The Zebrafish*. Their help, patience, and encouragement are profoundly appreciated.

H. William Detrich, III
Monte Westerfield
Leonard I. Zon

# PART I

# Cellular Biology

## CHAPTER 1

# Analyzing Retinal Axon Guidance in Zebrafish

**Fabienne E. Poulain, John A. Gaynes, Cornelia Stacher Hörndli, Mei-Yee Law, *and* Chi-Bin Chien**
Department of Neurobiology and Anatomy, University of Utah, Salt Lake City, Utah

---

Abstract
I. Introduction
II. Visualizing Retinal Axons
  A. Transgenic Lines
  B. Labeling with Antibodies
  C. Labeling with Lipophilic Dyes
  D. Transiently Expressing DNA Constructs
  E. *In Vivo* Single Cell Electroporation
  F. Time-Lapse Imaging
  G. Protocols for Labeling Methods
III. Perturbing the Retinotectal System
  A. Retinotectal Mutants
  B. Injecting DNA or Morpholinos
  C. Using Heat Shock to Induce Misexpression
  D. Transplanting to Test Cell Autonomy of Gene Function
  E. Protocols for Transplants
IV. Future Directions
References

## Abstract

How neuronal connections are established during development is one of the most fascinating questions in the field of neurobiology. The zebrafish retinotectal system offers distinct advantages for studying axon guidance in an *in vivo* context. Its accessibility and the larva's transparency not only allow its direct visualization, but

Copyright © 2010 Elsevier Inc. All rights reserved.

978-0-12-384892-5
DOI: 10.1016/B978-0-12-384892-5.00001-3

also facilitate experimental manipulations to address the mechanisms of its development. Here we describe methods for labeling and visualizing retinal axons *in vivo*, including transient expression of DNA constructs, injection of lipophilic dyes, and time-lapse imaging. We describe in detail the available transgenic lines for marking retinal ganglion cells (RGCs); a protocol for very precise lipophilic dye labeling; and a protocol for single cell electroporation of RGCs. We then describe several approaches for perturbing the retinotectal system, including morpholino or DNA injection; localized heat shock to induce misexpression of genes; a comprehensive list of known retinotectal mutants; and a detailed protocol for RGC transplants to test cell autonomy. These methods not only provide new ways for examining how retinal axons are guided by their environment, but also can be used to study other axonal tracts in the living embryo.

## I. Introduction

Axon guidance is an essential process for proper formation of neuronal connections during development. This is certainly true in the visual system, where retinal axons must interpret a large variety of signals to navigate to their brain target and establish precise and ordered connections reflecting our perception of the environment. The accessibility of the visual system not only allows its easy visualization, but also facilitates experimental manipulations to test the mechanisms of its development. Many studies have taken advantage of this accessibility to give a precise description of the visual system's anatomy and identify important factors required for its formation. In the past decade, the zebrafish retinotectal system has drawn attention for its distinct advantages. The optical transparency of zebrafish embryos allows direct visualization of retinal axons and is particularly suited for high-resolution imaging, including time-lapse analysis. Chimeric embryos with retinal neurons of different genetic backgrounds can be easily generated by cell transplants. Finally, the short generation time of zebrafish as well as the recent characterization of its genome are especially suited for genetic analysis and have allowed the generation and identification of many mutants with retinotectal defects. These properties establish zebrafish as an excellent model for studying retinal axon guidance and, more generally, for studying cell biology in an *in vivo* context, as many *in vivo* experiments not possible in other systems can be performed.

Retinal ganglion cells (RGCs) are the primary cell type in the innermost cellular layer of the retina, responsible for carrying visual information from the eye to the brain. In zebrafish, the first RGCs are born at 28 h post-fertilization (hpf) (Hu and Easter, 1999; Masai *et al*., 2005) and immediately extend axons that then must pass several landmarks (Fig. 1A). Retinal axons first grow within the retina to the optic disc, where they exit (30–32 hpf). They then join the optic nerve and elongate toward the ventral midline of the diencephalon, where nerves coming from both eyes meet to form the optic chiasm (34–36 hpf). In zebrafish and other species lacking binocular vision, all axons cross the midline. Retinal axons then

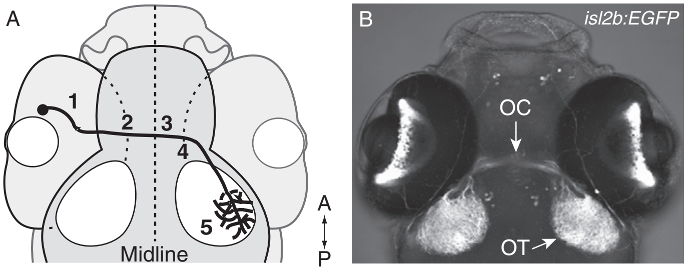

**Fig. 1** The zebrafish retinotectal projection. (A) Diagram of the retinal axon pathway. Retinal axons navigate to the optic nerve head (1), pass through the optic nerve and exit the eye (2), cross the midline at the chiasm (3), and grow dorsally along the optic tract (4) to reach the tectum (5). (B) Dorsal view of a Tg(*isl2b:EGFP)*$^{zc7}$ transgenic embryo, which specifically expresses EGFP in all RGCs, allowing a direct visualization of retinal projections. Courtesy of A. Pittman. A: anterior; P: posterior; OC, optic chiasm; OT, optic tectum. *Maximum intensity projection, confocal microscopy.* (A, B): dorsal views, anterior up.

navigate dorsally through the optic tract to reach their main target, the optic tectum (48 hpf), where they establish a topographic map, making connections according to their position in the retina (Fig. 2C–D). Axons originating from the more rostral retina project to the more posterior tectum, and axons from the dorsal retina project to the ventrolateral tectum. Interestingly, this ordering in the tectum can already be observed along the dorso-ventral axis in the optic tract: dorsal axons grow through the ventral branch of the tract, and ventral axons through its dorsal branch. Once in the tectum, retinal axons mature, arborize, and form synapses with their tectal targets.

Retinal axons encounter many guidance decision points along their pathway and respond to various attractive or repulsive cues to choose the right track. Many factors acting as road signs have been identified, but how retinal axons respond to them *in vivo* still remains poorly understood. Many laboratories, including ours, have developed tools for visualizing retinal axons during their navigation and modifying their nature or their environment to test specific functions. We describe here the different methods used for labeling and visualizing retinal axons, as well as several approaches for perturbing the retinotectal system. Many of these methods are also applicable to nonretinal axons. We finish with an overview of methods likely to be important in the future.

## II. Visualizing Retinal Axons

Understanding how retinal projections develop requires specific labeling and precise visualization of retinal axons *in vivo*. Several methods can be used, depending on which part of the retinotectal pathway is studied, how many axons are observed, and whether the axons are observed live. Thanks to the optical transparency of zebrafish embryos, transgenic lines expressing fluorescent proteins in RGCs can be used to visualize retinal axons as they develop. Lipophilic dyes are particularly useful to label specific groups of axons. Finally, transient expression of DNA constructs and *in vivo* electroporation are specially suited for labeling single axons and imaging them as they elongate. For all these approaches, precise imaging is best achieved using confocal microscopy.

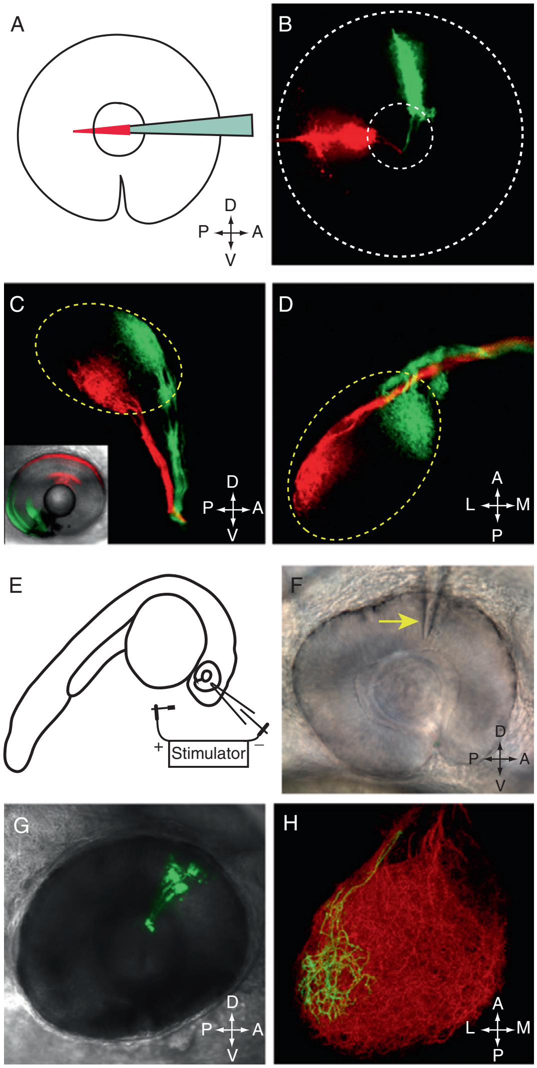

**Fig. 2** *(Continued)*

## A. Transgenic Lines

Several transgenic lines that express fluorescent proteins (FPs) under the control of RGC-specific promoters have been developed (Table I). Their main advantage is to allow clear and direct visualization of retinal projections in live embryos. Labeled embryos are simply obtained by crossing transgenic carriers. Depending on the promoter used, all RGCs or a subset of them are labeled. Promoters from the *isl2b* and *atoh7* (previously named *isl3* and *ath5*) genes drive transgene expression in all RGCs, allowing the visualization of all retinal axons (Fig. 1B, Masai *et al*., 2003; Pittman *et al*., 2008). In contrast, promoters from the *pou4f3* (previously named *brn3c*) gene can be used to label a subset of RGCs (Neumann and Nüsslein-Volhard, 2000; Xiao *et al*., 2005). For instance, the *pou4f3* promoter drives expression in RGCs that project mainly into one of the four retinorecipient layers of the tectum, allowing characterization of laminar targeting of retinal axons (Xiao *et al*., 2005).

Different FPs can be expressed to label RGCs. Enhanced green fluorescent protein (EGFP) is the most frequently used, as it is stable and particularly bright. RGCs can also be labeled in red using TagRFP or mCherry. Adding specific tags to the FP coding sequence allows labeling of specific cellular compartments such as the nucleus or the plasma membrane. For instance, the N-terminal palmitoylation sequence from GAP-43 (Moriyoshi *et al*., 1996) or the CAAX consensus motif from Ras (Choy *et al*., 1999) can target FPs to the plasma membrane, giving better labeling of axonal arbors.

Finally, other transgenic lines express the strong transcriptional activator Gal4-VP16, which drives the expression of DNA constructs containing a UAS (upstream activation sequence) control element (Köster and Fraser, 2001). These lines can be

---

**Fig. 2** Methods for visualizing retinal axons. (A–D) Focal injection of dyes in the retina allows visualization of retinal axons exiting from the retina and making topographic connections in the tectum. (A) After removing lens, a dye-coated glass micropipette is briefly inserted in a peripheral direction into the RGC layer (method described in detail in Section II.G.1). (B) Lateral view of a 48 hpf eye focally injected with DiI (red) and DiO (green). Labeled retinal axons can be observed exiting from the retina. *Maximum intensity projection, confocal microscopy.* (C) Lateral view of a 4 dpf embryo topographically injected with DiI and DiO into the dorsonasal (DN) and ventrotemporal (VT) retina, respectively, using a vibrating-needle injection apparatus (Baier *et al*., 1996). Inset shows the sites of injection in the retina. DN (red) and VT (green) retinal axons navigate through the ventral and dorsal branches of the optic tract, respectively, and terminate topographically in the tectum. Yellow dashed line: tectal border. *Maximum intensity projection, confocal microscopy.* (D) Dorsal view of the projections showed in C. DN axons terminate in the posterolateral tectum, whereas VT axons innervate the antero-medial tectum. Yellow dashed line: tectal border. *Maximum intensity projection, confocal microscopy.* (E–H) *In vivo* single cell electroporation allows visualization of retinal arbors in the tectum. (E) Schematic representation of the electroporation setup: a 22–28 hpf embryo is mounted laterally under a compound microscope. A negatively charged glass microelectrode is filled with DNA solution and placed in the retina, with a positively charged ground electrode placed near the head. (F) DIC picture of the microelectrode (arrow) placed into the DN retina just prior to electroporation. *40× water immersion objective, compound microscope.* (G) Electroporated RGCs expressing GAP43-EGFP (green) in a live 5 dpf embryo mounted laterally with the lens removed. The EGFP image has been merged with a DIC image of the head. *Maximum intensity projection, confocal microscopy.* (H) Dorsal view of the contralateral tectum of the same embryo, with tectal neuropil visualized by *isl2b:mCherry-CAAX* transgene [red; Tg(*isl2b:mCherry-CAAX*)$^{zc23}$] and electroporated RGC axons and arbors visualized with GAP43-EGFP (green). *3D projection from Fluorender software, 40× water immersion objective, confocal microscopy.* A: anterior; P: posterior; D: dorsal; V: ventral; L: lateral; M: medial. (See Plate no. 1 in the Color Plate Section.)

## Table I
## Transgenic Lines that Label RGCs

| Transgenic line | Previous names, ZFIN allele number | Retinal expression | Other expression | References |
|---|---|---|---|---|
| *atoh7:GFP* | *ath5:GFP, rw021* | Newborn RGCs | Forebrain, tectum | Masai *et al.* (2003), Poggi *et al.* (2005) |
| *atoh7:mGFP* | *ath5:mGFP, cu1* | " | " | Vitorino *et al.* (2009), Zolessi *et al.* (2006) |
| *atoh7:mRFP* | *ath5:mRFP, cu2* | " | " | Vitorino *et al.* (2009), Zolessi *et al.* (2006) |
| *atoh7:Gal4-VP16* | *zf138* | " | " | Maddison *et al.* (2009) |
| *pou4f1-hsp70:GFP* | *brn3a-hsp70:GFP, rw0110* | RGCs (likely a subset) | Tectum, habenula, cranial sensory ganglia | Aizawa *et al.* (2005), Sato *et al.* (2007) |
| *pou4f3:mGFP* | *brn3c:mGFP, s273t, s356t* | Subset of RGCs | Inner ear, lateral line neuromasts | Del Bene *et al.* (2008), Xiao *et al.* (2005) |
| *pou4f3:Gal4VP16* | *s311t* | " | " | Xiao and Baier (2007) |
| *isl2b:GFP* | *isl3:GFP, zc7* | All RGCs | Cranial ganglia Rohon-Beard neurons, a few cells in forebrain dorsal midbrain | Pittman *et al.* (2008) |
| *isl2b:mGFP* | *zc20* | " | " | Law and Chien (unpublished) |
| *isl2b:mCherryCAAX* | *zc23, zc25* | " | " | Pittman *et al.* (2008) |
| *isl2b:Gal4VP16* | *zc60* | " | " | Ben Fredj *et al.* (2010) |
| *chrnb3b:GFP* | *jt0021* | RGCs | Trigeminal ganglion, Rohon-Beard neurons, some tectal cells | Matsuda and Mishina (2004), Tokuoka *et al.* (2002), Yoshida and Mishina (2003) |
| *-2.7shh:GFP* | *t10* | RGCs | Amacrine cells, notochord, floor plate, pharyngeal arch endoderm, ventral forebrain | Neumann and Nüsslein-Volhard (2000), Nevin *et al.* (2008), Roeser and Baier (2003) |

mGFP, Membrane-targeted GFP; RGCs, retinal ganglion cells.

particularly useful for expressing DNA constructs at high levels in a few RGCs (described in Section II.D).

## B. Labeling with Antibodies

Alternately, antibodies can be used to label retinal axons. Although they cannot be employed for live visualization, they provide strong staining that can be useful to examine details or specific aspects of retinal axon navigation. Several antibodies have been widely used to label retinal axons using standard whole-mount antibody staining techniques. Anti-acetylated tubulin (Sigma, St. Louis, Missouri) recognizes a form of tubulin found in stable microtubules, and thus labels all axons. This staining has been used to visualize the earliest axons crossing the chiasm (Karlstrom *et al*., 1996) and to label axon bundles within the retina (Li *et al*., 2005). Zn-5 and zn-8 (Zebrafish International Resource Center, Developmental Studies Hybridoma Bank, Iowa City, Iowa) are two monoclonal antibodies, likely derived from the same hybridoma, that recognize the cell surface adhesion molecule Alcam-a (previously named neurolin/DM-GRASP, Laessing *et al*., 1994). Alcam-a is expressed by newly born RGCs that are added in successive peripheral rings around the retina, but turns off in central RGCs by 48 hpf (Laessing and Stuermer, 1996). Consequently, zn-5/8 staining is particularly appropriate to label retinal axons navigating within the retina to the optic nerve head. Finally, anti-GFP (Invitrogen, Carlsbad, California), anti-DsRed (which also recognizes mCherry, Clontech, Mountain View, California) and anti-TagRFP (Evrogen, Moscow, Russia) antibodies can be used to amplify the signal from FPs.

## C. Labeling with Lipophilic Dyes

While transgenic lines and antibodies are appropriate for labeling a large population of axons, they cannot be used to visualize spatially specific sub populations of RGCs. Lipophilic carbocyanine dyes such as DiI, DiO, DiA, or DiD (Invitrogen) offer the great advantage of being easily injected in specific locations within the retina. Structurally, they consist of a fluorophore attached to two long aliphatic alkyl tails responsible for their insertion within membranes. Carbocyanine dyes are highly fluorescent in lipid bilayers, but weakly fluorescent in water. Once applied, they become incorporated into the plasma membrane and diffuse laterally, labeling the entire cell. These properties have made lipophilic dyes the tool of choice for anterograde and retrograde tracing of neurons in both live and fixed tissues (Honig and Hume, 1989).

DiI (red) and DiO (green) are the most commonly used. They can be applied using several methods. The first is to inject DiI or DiO dissolved in chloroform into the eye, which labels the entire projection (“whole eye fills”). This technique is particularly useful for studying guidance at the chiasm, as each eye can be labeled with a different color. It has been described previously (Hutson *et al*., 2004) and is not repeated here.

DiI and DiO can also be delivered into specific regions of the retina, so that only a subset of RGCs is labeled (Fig. 2A–D). In the second method, dyes dissolved in dimethylformamide are focally injected using a vibrating-needle injection apparatus (Baier *et al*., 1996; Trowe, 2000). DiI or DiO is loaded in a reservoir through which passes a tungsten needle. Fixed larvae are mounted in an agarose form. A small loudspeaker vibrates the needle, transporting dye to its tip, where the dye precipitates in the embedded tissue. This method has the advantage of labeling many embryos reproducibly and has been used to analyze projection topography in the tectum and axon ordering in the tract (Karlstrom *et al*., 1996; Lee *et al*., 2004; Trowe *et al*., 1996). However, the custom-built apparatus is not widely available. The third technique uses a dye-coated microneedle to focally deposit dye into the retina. The needle is coated with dye and can be reused several times. It does not require any specialized apparatus and can be used to label very few cells. We describe this method in Section II.G.1. A final method is to focally inject DiI along the retinal pathway to retrogradely label RGCs. Although it is difficult to inject dye precisely enough, this technique can be used to visualize RGC morphology and organization within the retina (Mangrum *et al*., 2002).

## D. Transiently Expressing DNA Constructs

Whereas lipophilic dyes can easily label a subset of RGCs, they are more difficult to use for single axons. These can be better visualized by transiently expressing DNA constructs encoding FPs. Plasmids injected at the one cell stage are expressed mosaically, labeling a few cells randomly. Expression can be targeted to RGCs using the *atoh7* or *isl2b* promoters (Masai *et al*., 2003; Pittman *et al*., 2008). This method has been used to visualize single retinal arbors (Campbell *et al*., 2007) and RGC dendritic outgrowth (Mumm *et al*., 2006). Alternatively, constructs containing a UAS element upstream of an FP coding sequence can be injected into transgenic embryos expressing Gal4-VP16 in RGCs (Table I). The Gal4/UAS system amplifies FP expression and gives better labeling. While DNA methods are very useful for labeling single axons, they cannot yet be used to target specific RGC subtypes or RGCs in particular locations, since the required enhancers have not yet been identified.

## E. *In Vivo* Single Cell Electroporation

Another way to label individual axons is *in vivo* single cell electroporation (Fig. 2E–H). Although technically demanding, this powerful approach offers the possibility of delivering DNA constructs or dextran-coupled indicators to individual RGCs or RGCs in specific locations in the retina. We have used it to visualize projections and arborizations of individual dorsonasal RGCs (Pittman *et al*., 2010). In this approach, an applied voltage generates an electric field across cells in the retina, breaking down the plasma membrane and creating transient pores through which negatively charged DNA molecules move into the cell. Briefly, embryos are mounted laterally on a glass slide in agarose that is windowed to expose the eyes, covered with medium, and viewed under a 40× water immersion objective. A glass microelectrode filled with DNA or tracer solution is poked into the retina with a micromanipulator, and a voltage train applied. Embryos are then unmounted and raised. This approach allows coelectroporation of several indicators or constructs into the same cell, allowing both visualization and perturbation experiments. We describe this technique in detail in Section II.G.2.

## F. Time-Lapse Imaging

Time-lapse imaging of RGC axons is crucial to understand their response to the environment. It has been used by many investigators to monitor axons' behavior (Campbell *et al*., 2007; Hutson and Chien, 2002; Kaethner and Stuermer, 1992; O'Brien *et al*., 2009; Schmidt *et al*., 2000) and can be used with all the labeling techniques described above, except for antibody labeling. Confocal or two-photon microscopy is most appropriate for time-lapse imaging and can be performed with an upright or inverted microscope. Several protocols have been previously described, so we do not discuss them here (Campbell *et al*., 2007; Hutson and Chien, 2002; Hutson *et al*., 2004; Meyer and Smith, 2006).

## G. Protocols for Labeling Methods

Here we describe detailed protocols for focal injections of lipophilic dyes in the retina and for *in vivo* single cell electroporation.

### 1. Method 1: Precise Labeling with Intraretinal Injection of Lipophilic Dyes

This method uses glass microneedles coated with lipophilic carbocyanine dyes to focally deposit dye into the retina (Fig. 2A–B). It can be used to target specific locations in the retina and label very few cells. It was originally developed by Torsten Trowe (2000).

#### a. Solutions Needed

- DiI or DiO crystals (Molecular Probes)
- 4% PFA (4% paraformaldehyde in 0.1 M phosphate buffer, pH 7.4)
- 1% low-melt agarose in PBS (phosphate-buffered saline)
- 50% and 80% glycerol in water

#### b. Protocol

1. Fix zebrafish embryos at required stage in 4% PFA at 4°C for at least 12 h. For growth cone labeling, fix at room temperature for the first 2 h.
2. Use glass capillary with an outer diameter of 1.0 mm and an inner diameter of 0.58 mm to prepare the micropipette for injections. Pull the capillary to a final taper length of 9.0 mm and a tip size of 2 μm. To coat the micropipette with dye, place a few dye crystals on a cover glass and melt them at 100°C on a hot plate. Dip the tip of the micropipette horizontally into the dye paste and roll it to cover the tip equally on all sides. Wipe off as much dye from the tip as possible onto the cover glass.
3. Prepare 30 ml of 1% low-melt agarose and keep on heating block at 45°C to prevent from solidifying. Use a Petri dish lid to embed embryos for dye injection. Coat bottom with a thin layer of 1% low-melt agarose and let solidify. Transfer embryos with as little PFA as possible onto the agarose. Cover embryos with a drop of 1% low-melt agarose and orient them in a lateral position.
4. When the agarose covering is solid, use a sharpened tungsten needle to remove the top-facing lens by carefully cutting the skin covering the eye in a circle along the

border between lens and retina. The lens will become loose and can now be easily removed. The resulting hole should be refilled with 1% low-melt agarose. The embryos are now ready to be injected with the dye.

5. Use a standard pipette holder and three-axis micromanipulator to hold the dye-coated micropipette. Insert it into the RGC layer by placing it in the empty lens cup and advancing in a peripheral direction at a roughly 45° angle (Fig. 2A). Leave the needle in the eye for not more than 2 s to ensure a small injection site and labeling of only a few axons. The coated micropipette can be reused for several injections before it has to be coated again with fresh dye.
6. After finishing the injections, cover embedded embryos with 1× PBS or water to avoid drying. This step also washes off excessive dye. Store the embryos for a few hours at room temperature for fast diffusion of the dye, or keep them at 4°C overnight if slower diffusion is desired. Long incubation times can result in nonspecific diffusion of the dye within the eye, which can prevent clear imaging results later on.
7. Recover embryos from the agarose bed using forceps. Place them in a microfuge tube and wash them in 1× PBS. Transfer embryos to 50% glycerol/$H_2O$ and incubate them for 3 h at 4°C with agitation. Change the medium to 80% glycerol/$H_2O$, and store embryos at 4°C overnight. Now that they are cleared, embryos can be mounted for confocal imaging in 80% glycerol between two coverslips (Fig. 2B).

## 2. Method 2: Single Cell *In Vivo* Electroporation

*In vivo* focal electroporation is used to deliver tracers or transgenes into single RGCs. It can target several or individual cells in precise topographic positions within the retina (Fig. 2E–H). An electric field applied across an RGC progenitor creates transient pores in the plasma membrane through which negatively charged DNA molecules move into the cell. We have used the protocol detailed here to image single RGC arbors in the tectum (Pittman *et al*., 2010); it was slightly modified from a previous method for imaging habenular neurons (Bianco *et al*., 2008).

### a. Solutions Needed

- E2 medium (15 mM NaCl, 0.5 mM KCl, 1 mM $CaCl_2$, 1 mM $MgSO_4$, 0.15 mM $KH_2PO_4$, 1.7 mM $NaHCO_3$)
- 0.1 mM phenylthiourea (PTU) in E3 embryo medium (5 mM NaCl, 0.17 mM KCl, 0.33 mM $CaCl_2$, 0.33 mM $MgSO_4$)
- tricaine stock (0.4% tricaine, 10 mM HEPES, pH 7.4)
- 1% low-melt agarose in E2/GN/tricaine (10 µg/ml gentamicin in E2 medium, 0.02% tricaine)

### b. Protocol

1. Raise embryos at 28.5°C in E3 medium containing 0.1 mM PTU to inhibit pigment formation, and dechorionate them between 22 and 28 hpf. Anesthetize embryos by adding tricaine to a final concentration of 0.02%. Mount laterally in a drop of 1% low-melt agarose in E2/gentamycin/ tricaine, in wells built with quick-hardening

epoxy on a glass microscope slide. Expose the eye by cutting a small window in the agarose with forceps, and cover the embryo with E3-PTU + 0.02% tricaine.

2. After mounting the embryo, place the glass slide under a 40× water immersion objective on an upright compound microscope. Place an Ag/AgCl cathode in the overlying buffer near the head of the embryo. Backfill a glass microelectrode (1–3 μm diameter tip) with 2 μl of solution containing the tracer or DNA (final concentration of 1–3 μg/μl in water or 10 mM Tris-HCl, pH 8.5), and place it in the retina using a micromanipulator. Use a stimulator to deliver 1 s trains of 2 ms negative-going square pulses at 200 Hz, 30–50 V (reverse polarity and use 3–5V for positively charged tracers). An effective train will cause a visible rippling effect (tissue response) in the tissue surrounding the microelectrode tip when the voltage train is applied. A clogged needle will result in a less pronounced tissue response. A "pop" will occasionally appear in the tissue in response to a voltage train, resulting in an ineffective electroporation. While the exact cause of the pop is not known, it occurs less often with a lower DNA concentration and a lower voltage. Each cell is targeted with 3–5 trains, and several cells can be targeted per eye. After electroporation, the embryo is removed from the agarose and raised in E3 + PTU at 28.5°C
3. FP expression can be seen in electroporated RGCs in the eye under a fluorescent dissecting microscope by 12 h after electroporation. Corresponding axons can be visualized in the contralateral optic tract and tectum under a 40× water objective on a compound microscope, or by confocal microscopy. Labeled axons are best observed from a dorsal view in the contralateral tectum, or from a lateral view in the contralateral optic tract after removal of the contralateral eye. Time-lapse imaging can also be performed.

## III. Perturbing the Retinotectal System

Experimental manipulations perturbing axons or their environment are crucial to understand how and by which molecular mechanisms retinotectal projections develop. Many important factors have been discovered through the generation and characterization of mutants with retinotectal defects isolated in large-scale genetic screens. In addition, several approaches including DNA or antisense morpholino oligonucleotide (MO or "morpholino") injections, heat shock experiments, or transplants can be used to assess the function of a particular protein.

### A. Retinotectal Mutants

The first mutants with retinotectal defects were obtained from a large genetic screen performed in Tübingen in the 1990s (Karlstrom *et al*., 1996; Trowe *et al*., 1996). Topographic injections of DiI and DiO in the retina were used as an assay to identify mutants with defects in retinal axon pathfinding, sorting in the tract, and topography in the tectum. Almost all the genes affected in these mutants have now been identified, allowing the discovery of crucial regulators of axon guidance or brain patterning, including the receptors *robo2* and *patched1*, the transcription factor *lhx2*, and the

**Table II**
**Retinotectal Pathfinding Mutants**

| Mutant name (abbreviation) | Region in which pathfinding affected | Gene | Brain defect? | References |
|---|---|---|---|---|
| *acerebellar (ace)* | Chiasm, anterior projection, optic tract, topography | *fgf8* | Yes | Picker *et al*. (1999), Shanmugalingam *et al*. (2000) |
| *astray (ast)* | Chiasm, anterior projection, optic tract, tectum arborization | *robo2* | No | Campbell *et al*. (2007), Fricke *et al*. (2001), Hutson and Chien (2002), Karlstrom *et al*. (1996) |
| *bashful (bal)* | Retinal exit, anterior projection | *laminin* $\alpha 1$ | Yes | Karlstrom *et al*. (1996), Paulus and Halloran (2006) |
| *belladonna (bel)* | Midline crossing | *lhx2* | Yes | Karlstrom *et al*. (1996), Seth *et al*. (2006) |
| *beyond borders (beyo)* | Confinement to tectal neuropil | *?* | Yes | Xiao *et al*. (2005) |
| *blind date (blin)* | Tectum innervation | *?* | No | Muto *et al*. (2005), Xiao *et al*. (2005) |
| *blowout (blw)* | Midline crossing eye shape | *patched 1 (ptc)* | Yes | Karlstrom *et al*. (1996), Lee *et al*. (2008) |
| *blue kite (bluk)* | Tectum innervation | *?* | No | Xiao *et al*. (2005) |
| *blumenkohl (blu)* | Expanded terminations | *slc17a6b (glutamate transporter)* | No | Smear *et al*. (2007), Trowe *et al*. (1996) |
| *bogus journey (boj)* | Midline crossing | *?* | ? | Muto *et al*. (2005) |
| *boxer (box)* | Tract sorting, crossing in posterior commissure | *extl3* | No | Karlstrom *et al*. (1996), Lee *et al*. (2004), Trowe *et al*. (1996) |
| *breaking up (brek)* | Confinement to tectal neuropil | *?* | No | Xiao *et al*. (2005) |
| *chameleon (con)* | Retinal exit, midline crossing | *dispatched homolog 1 (dips1)* | Yes | Karlstrom *et al*. (1996), Nakano *et al*. (2004) |
| *clueless (clew)* | Tectum innervation | *?* | No | Xiao *et al*. (2005) |
| *coming apart (coma)* | Optic tract, tectum innervation | *?* | No | Xiao *et al*. (2005) |
| *cyclops (cyc)* | Midline crossing | *nodal related-2 (ndr2)* | Yes | Karlstrom *et al*. (1996), Rebagliati *et al*. (1998), Sampath *et al*. (1998) |
| *dackel (dak)* | Tract sorting crossing in posterior commissure | *ext2* | No | Karlstrom *et al*. (1996), Lee *et al*. (2004), Trowe *et al*. (1996) |
| *dark half (darl)* | Ventral branch of the optic tract missing, topography | *gdf6a* | No | Gosse and Baier (2009), Muto *et al*. (2005) |
| *detour (dtr)* | Midline crossing | *gli1* | Yes | Karlstrom *et al*. (1996, 2003) |
| *dragnet (drg)* | Laminar specificity in the tectum | *collagen IVa5 (col4a5)* | No | Xiao and Baier (2007), Xiao *et al*. (2005) |
| *esrom (esr)* | Midline crossing, termination | *MYC binding protein 2 (mycbp2) or PAM* | No | D'Souza *et al*. (2005), Karlstrom *et al*. (1996), Trowe *et al*. (1996) |
| *excellent adventure (exa)* | Targeting defect in the tectum | *?* | ? | Muto *et al*. (2005) |

| | | | | |
|---|---|---|---|---|
| *fuzz wuzzy (fuzz)* | Confinement to tectal neuropil | *?* | No | Xiao *et al.* (2005) |
| *gnarled (gna)* | Tectal entry, tectal misrouting | *?* | Yes | Trowe *et al.* (1996), Wagle *et al.* (2004) |
| *grumpy (gup)* | Anterior projection, midline crossing | *laminin* $\beta 1$ | Yes | Karlstrom *et al.* (1996), Parsons *et al.* (2002) |
| *iguana (igu)* | Midline crossing | *DAZ interacting protein 1 (dzip1)* | Yes | Karlstrom *et al.* (1996), Sekimizu *et al.* (2004), Wolff *et al.* (2004) |
| *late bloomer (late)* | Delayed innervation of the tectum | *?* | No | Xiao *et al.* (2005) |
| *no isthmus (noi)* | Chiasm, anterior projection, tectal bypass | *pax2a* | Yes | Brand *et al.* (1996), MacDonald *et al.* (1997), Trowe *et al.* (1996) |
| *macho (mao)* | Expanded terminations | *?* | No | Gnuegge *et al.* (2001), Trowe *et al.* (1996) |
| *michikusa (mich)* | Ectopic arbor after crossing the midline | *?* | ? | Muto *et al.* (2005) |
| *missing link (miss)* | Pretectal targets (AF4, AF9) absent or reduced | *?* | ? | Muto *et al.* (2005) |
| *nevermind (nev)* | Tract sorting, D-V topography | *cyfip2* | No | Pittman *et al.* (2010), Trowe *et al.* (1996) |
| *odysseus (ody)* | Intraretinal guidance defects | *cxcr4b* | No | Knaut *et al.* (2003), Li *et al.* (2005) |
| *parachute (pac)* | Ipsilateral projection\; entering chiasm area | *N-cadherin* | Yes | Lele *et al.* (2002), Masai *et al.* (2003) |
| *pinscher (pic)* | Tract sorting, crossing in posterior commissure | *papst1 (sulfate transporter)* | No | Clément *et al.* (2008), Karlstrom *et al.* (1996), Trowe *et al.* (1996) |
| *shirli-myrli (shir)* | Delayed innervation of the tectum | *?* | No | Muto *et al.* (2005) |
| *sleepy (sly)* | Anterior projection; midline crossing | *laminin* $\gamma 1$ | Yes | Karlstrom *et al.* (1996), Parsons *et al.* (2002) |
| *smooth muscle omitted (smu)* | Midline crossing | *smoothened (smo)* | Yes | Chen *et al.* (2001), Varga *et al.* (2001) |
| *sonic-you (syu)* | Retinal exit, midline crossing | *sonic hedgehog (shh)* | Yes | Brand *et al.* (1996), Schauerte *et al.* (1998) |
| *space cadet (spc)* | Retinal exit, midline crossing | *?* | No | Karlstrom *et al.* (1996), Lorent *et al.* (2001) |
| *tarde demais (tard)* | Delayed innervation of the tectum | *?* | No | Xiao *et al.* (2005) |
| *umleitung (uml)* | Midline crossing | *?* | Yes | Karlstrom *et al.* (1996) |
| *vertigo (vrt)* | Delayed innervation of the tectum | *?* | No | Xiao *et al.* (2005) |
| *walkabout (walk)* | Pretectal target AF4 overinnervated | *?* | ? | Muto *et al.* (2005) |
| *who cares (woe)* | Tract sorting, D-V topography | *?* | No | Trowe *et al.* (1996) |
| *you-too (yot)* | Midline crossing | *gli2* | Yes | Karlstrom *et al.* (1996, 1999) |

?=not known

adhesion molecule *N-cadherin* (see Table II for a complete listing of these mutants). While some genes such as *astray (robo2)* primarily affect axon navigation, others such as *ace (fgf8)* disrupt brain patterning, resulting in mispresented axon guidance cues. More recently, a new screen has been performed using the *pou4f3:mGFP* transgenic line expressing membrane-targeted GFP (mGFP) in a subset of RGCs (Xiao *et al.*, 2005). This approach allowed the identification of novel mutants with various defects in tectum innervation (Table II). Two mutants from this screen have been cloned, revealing new functions for *gdf6a* and *collagenIVa5* in regulating eye dorso-ventral patterning and tectum laminar targeting, respectively (Gosse and Baier, 2009; Xiao and Baier, 2007). Finally, a recent screen using behavioral assays identified mutants with disrupted response to visual motion and/or impaired background adaptation (Muto *et al.*, 2005). Some of these mutants also have abnormal retinotectal projections or a lack of RGCs that are likely responsible for their phenotype. Identifying the mutations generated in these newer screens will give new clues about the factors involved in retinal axon guidance.

## B. Injecting DNA or Morpholinos

A common approach to characterize protein function in zebrafish is to inject stable MOs into one-cell stage embryos. MOs inhibit either protein translation when targeted near the start codon of mRNAs (Nasevicius and Ekker, 2000) or splicing of the pre-mRNAs when they are targeted to exon–intron or intron–exon boundaries (Draper *et al.*, 2001). Under good conditions, MOs can quickly reveal required functions for a targeted gene, though their use is subject to several caveats, including loss of efficacy as they are diluted during development (Eisen and Smith, 2008). We took advantage of this dilution with an MO against the transcription factor *atoh7* to specifically block differentiation of early- but not late-born RGCs, allowing the functional analysis of isotypic interactions between pioneer and follower axons during navigation (Pittman *et al.*, 2008).

Alternatively, DNA constructs encoding dominant negative forms of the protein of interest can be transiently or stably expressed. Temporal or spatial control can be provided by the *hsp70l* heat shock promoter (see following section) or cell-specific promoters, respectively. Similarly, gain-of-function experiments can be performed by misexpressing genes of interest at specific times or locations. For greater precision, DNA constructs or MOs can be delivered to individual RGCs by *in vivo* cell electroporation (described in Section II.E), allowing functional studies at single-cell resolution (Pittman *et al.*, 2010).

## C. Using Heat Shock to Induce Misexpression

A powerful technique to misexpress genes in a temporally or spatially controlled manner is to use heat shock. This approach is particularly useful for studying genes with both early and late roles during development. Heat shocks can be performed after transient injection of DNA constructs or on stable transgenic lines. The *hsp70l* promoter is an inducible element that drives strong gene expression in response to a temperature shift from 28.5°C (normal rearing temperature) to 37–40°C (Halloran *et al*., 2000). Global heat shocks have been widely used to induce ubiquitous gene expression in embryos at specific times. The exact heat shock duration and temperature depend on the age of the embryo, the transgene to be expressed, and the level of expression desired. For instance, raising the temperature to 42°C for 5 min can induce detectable transgene expression in 20 hpf embryos (Thummel *et al*., 2005).

Recently, we developed a technique using a sharpened soldering iron to induce focal heat shocks in restricted regions of the embryo (Hardy *et al*., 2007). For this approach, a copper soldering iron tip with a diameter of 15 μm is heated to 60°C and put directly in contact with the embryo for 3 min. A perfusion chamber keeps fluid flowing over the embryo during heat shock, thereby preventing heating of the medium and restricting the area of activation. This method is rapid and easy, allows the targeting of ~100 μm patches of tissue, and can be used in a variety of tissues and stages. A detailed protocol has been described (Hardy *et al*., 2007). Even more recently, Rolf Karlstrom's group developed another focal heat shock method using an optical fiber to deliver energy to a localized region (Placinta *et al*., 2009).

## D. Transplanting to Test Cell Autonomy of Gene Function

Transplanting cells or tissues is a powerful approach to test cell autonomy of gene function. Different types of transplant can be performed depending on the question (e.g., transplanting all RGCs, or RGCs in specific parts of the retina; labeling donors, hosts, or both labeled). A tricky but elegant approach is to transplant entire eye primordia, yielding mosaic embryos in which the whole eye comes from the donor while the rest of the embryo is derived from the host. A main advantage of this approach is that all retinal axons coming from the transplanted eye share the same genotype and are not influenced by interactions with host retinal axons, as these have been removed. We used eye transplants to demonstrate that *robo2* acts eye-autonomously to regulate retinal axon guidance (Fricke *et al*., 2001). A detailed protocol has been previously described (Hutson *et al*., 2004).

Alternatively, early transplants at blastula stage can be used to test cell autonomy (Ho and Kane, 1990). These are easy to perform and allow quite effective targeting of the retina (Moens and Fritz, 1999). Cells are removed from donor embryos between 4 and 6 hpf and replaced into the animal pole of host embryos. The resulting mosaic embryos display clones of RGCs in the retina, as well as some clones of cells in the brain. An abbreviated protocol is given below. While the presence of donor cells in the brain may make results harder to interpret, this approach is the easiest way to generate mosaic embryos with RGCs from different genetic backgrounds. However, it cannot be employed to target RGCs from or to specific regions within the retina.

Instead, transplants at a later stage are required. We have recently begun to use a technique for transplanting RGCs in a topographic manner (Fig. 3; inspired by Masai *et al*., 2003). Donor and host embryos labeled with different transgenes are grown to 30–33 hpf, when the first RGCs are specified. After mounting embryos laterally in

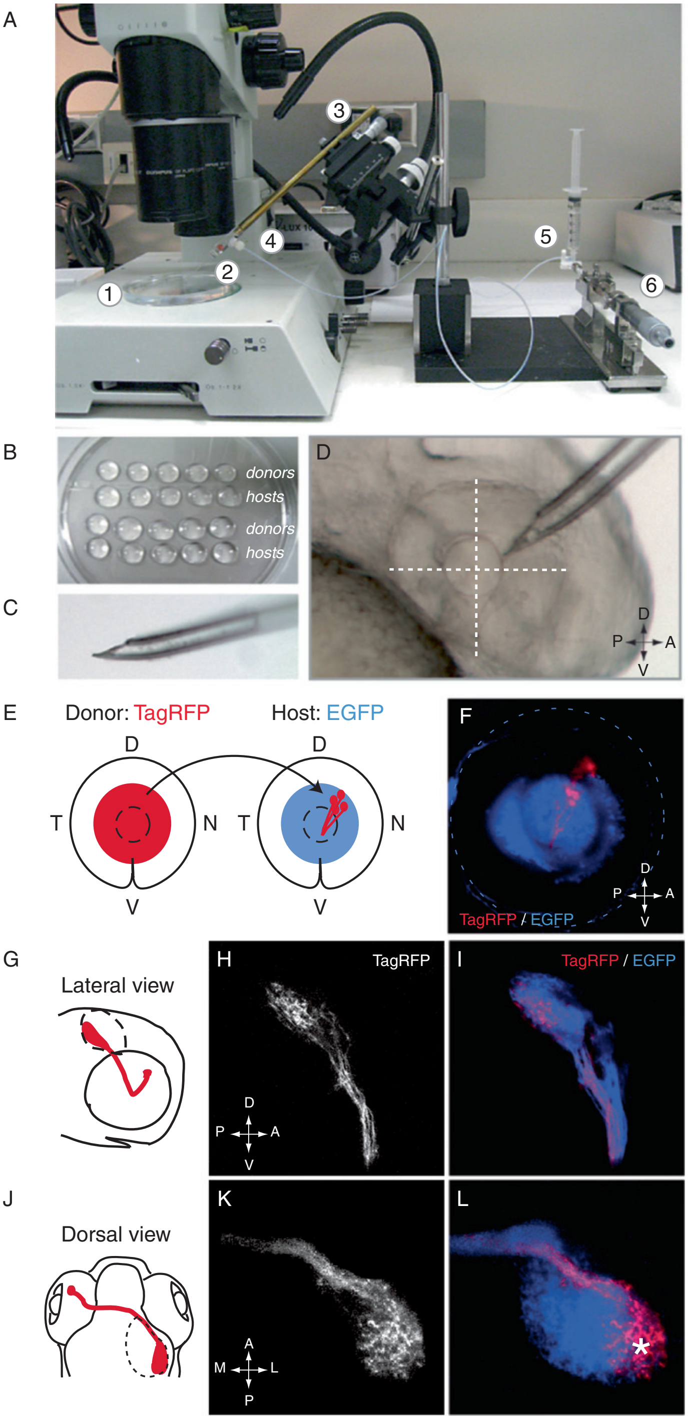
A
1
2
3
4
5
6
B
donors
hosts
donors
hosts
C
D
D
P
A
V
E
Donor: TagRFP
Host: EGFP
D
T
N
V
D
T
N
V
F
D
P
A
V
TagRFP / EGFP
G
Lateral view
H
TagRFP
D
P
A
V
I
TagRFP / EGFP
J
Dorsal view
K
A
M
L
P
L
*

**Fig. 3** *(Continued)*

agarose, donor RGCs are precisely removed from a specific location in the retina with a 40 µm glass micropipette and replaced at the same position in the host retina. The transplant is considered successful if, after raising the host, the transplanted RGCs are observed in the correct area of the retina (from a lateral view), and if in control conditions their arbors terminate in the appropriate part of the tectum (from a dorsal view). We obtain ~25% successful transplants with this approach and provide a detailed protocol below.

## E. Protocols for Transplants

### 1. Method 3: Blastula Transplants

Since blastula stage transplants have been explained in detail elsewhere (Ho and Kane, 1990; Kemp *et al*., 2009), only a succinct description of the method is provided here.

1. Donor embryos are injected at the one-cell stage with 5% Alexa-488 dextran or rhodamine dextran (10,000 MW) as a lineage marker. The light color from the dextran helps to distinguish donors from hosts during later steps. We use agarose-groove dishes for the injections (mold TU-1, Adaptive Science Tools, Worcester, Massachusetts; 1% agarose w/v in E2 or E3 embryo medium). Donor and host embryos are raised at 28.5°C until the sphere (4 hpf) or shield stage (6 hpf).
2. While waiting for the embryos to develop, pull and bevel standard wall, non-filament capillaries for use as transplant needles and prepare an agarose transplant dish (single-well mold; mold PT-1, Adaptive Science Tools; Kane and Kishimoto, 2002).
3. Dechorionate donor and host embryos. Use a clean fire-polished large-bore Pasteur pipette to transfer one donor and four hosts into each row of the transplant dish using an air-filled syringe and fire-polished transplantation pipette. Remove cells

---

**Fig. 3** Perturbing the retinotectal system with late topographic transplants. (A) Embryos are mounted laterally in drops of low-melt agarose deposited on a dish lid that is then placed under a dissecting microscope (1). The transplant needle is mounted in a micropipette holder (2), itself mounted onto a three-axis micromanipulator (3) placed next to the microscope. The micropipette holder is connected via a tube filled with mineral oil (4) to an oil-filled Hamilton syringe with a micrometer drive (6). The syringe is attached by a three-way stopcock to a reservoir filled with mineral oil (5). (B) Donor and host embryos mounted laterally in low-melt agarose drops. Embryos are arranged so that each donor is close to its respective host. (C) The transplant needle has a 40 µm diameter opening with a sharp tip that is slightly bent (around 20°). (D) The transplant needle is inserted into the dorsonasal retina, close to the lens, at a 45° angle. The bend of the needle tip is facing upward, so that ventral RGCs cannot be drawn up. (E) Dorsonasal (DN) RGCs from an *isl2b:TagRFP* donor are isotopically transplanted into the DN retina of an *isl2b:EGFP* host between 30 and 33 hpf. Their axonal projections are then visualized at 4 dpf by live confocal microscopy. (F) Lateral view of a WT *isl2b:EGFP* host eye in which WT TagRFP-positive RGCs have been transplanted. GFP is shown as blue for the best visualization. (G, J) Projections of DN donor axons observed in transplants in lateral (G) and dorsal (J) views. (H, I) Lateral view of TagRFP-positive projections at 4 dpf. DN donor axons navigate along the ventral branch of the tract to reach the tectum. (K, L) Dorsal view of the same projections. DN donor axons project to the posterolateral part of the host tectum (asterisk). *F, H, I, K, L: confocal maximum intensity projections*. (See Plate no. 2 in the Color Plate Section.)

from each donor embryo and transplant 20–50 cells into the animal pole of each corresponding host. While the origin of the transplanted cells is not important, the location where they are placed into the host is crucial. A fate map of the 6 hpf embryo can be used as a reference (Woo *et al.*, 1995).

4. After transplantation, transfer the agarose dish carefully to the 28.5°C incubator. During gastrulation, donor cells will spread out and form a mosaic patch of fluorescently labeled cells; choose those in which this patch includes cells in the eye. Once embryos have developed to bud stage, it is safe to remove them from the transplant dish and put them in 4-well or 24-well dishes. For experiments in which mutant cells are transplanted, donors should be kept together with their respective hosts until genotyped, either by PCR or by mutant phenotype. If necessary, hosts can be genotyped as well.

## 2. Method 4: Late Topographic Transplants

While blastula transplants are useful for testing functional cell autonomy and can be easily performed, they cannot target RGCs within specific regions of the retina. Testing the roles of genes specifically expressed in the dorsal or ventral retina, for instance, requires transplanting at later stages in a topographic manner. Here, we describe a detailed protocol for transplanting dorsonasal RGCs into the host dorsonasal retina. These transplants are performed between 30 and 33 hpf, when the first RGCs are specified and have acquired their positional identity within the retina. Donor and host embryos are labeled with *isl2b:TagRFP* and *isl2b:EGFP* transgenes, respectively, so that axons of transplanted RGCs and their projections can be easily visualized by live confocal miscroscopy at 4 days post-fertilization (dpf).

### a. Solutions Needed

- E2 medium (15 mM NaCl, 0.5 mM KCl, 1 mM $CaCl_2$, 1 mM $MgSO_4$, 0.15 mM $KH_2PO_4$, 1.7 mM $NaHCO_3$)
- 0.1 mM phenylthiourea (PTU) in E3 embryo medium (5 mM NaCl, 0.17 mM KCl, 0.33 mM $CaCl_2$, 0.33 mM $MgSO_4$)
- tricaine stock (0.4% tricaine, 10 mM HEPES, pH 7.4)
- 1% low-melt agarose in E2/GN/tricaine (10 μg/ml gentamicin in E2 medium, 0.02% tricaine)

### b. Protocol

1. The transplant needle is prepared in advance and can be reused several times. The quality of its preparation is the most important parameter for successful transplants. Pull standard wall, non-filament capillaries and polish them using a microforge, so that the tip displays a 20° angle with a 40 μm diameter opening (Fig. 3C).
2. Raise embryos at 28.5°C in E3 medium containing 0.1 mM PTU to inhibit pigment formation, and dechorionate them between 22 and 28 hpf. At 30 hpf, anesthetize embryos by adding tricaine to a final concentration of 0.02%. Mount laterally in a

drop of 1% low-melt agarose in E2/gentamycin/tricaine deposited on the lid of a Petri dish (Fig. 3B). Donors and hosts should be arranged in lines, so that each donor is close to its respective host. Once the drops have solidified, fill the Petri dish with PTU-E3/tricaine and position it under a dissecting scope.

3. Prepare the transplant setup (Fig. 3A): an oil-filled Hamilton syringe with a micrometer drive is connected by a three-way stopcock to a reservoir filled with mineral oil and to a micropipette holder through flexible plastic tubing. It is important to fill the system completely with mineral oil and ensure that air bubbles have been eliminated (air bubbles impair the ability to control suction and pressure). The transplant pipette is mounted in the micropipette holder, itself mounted onto a three-axis micromanipulator positioned next to the dissecting scope.
4. Using the micromanipulator, bring the transplant pipette near the dorsonasal retina, with a 45° angle (Fig. 3C). Make sure that the needle opening is facing upward, so that ventral RGCs cannot be drawn up into the needle. Insert the needle into the dorsonasal retina close to the lens, and slowly and carefully suck up 40–100 cells into the needle. At this stage, the fluorescence of the transgene expressed in RGCs is not yet visible, so the fraction of RGCs among the removed cells can vary. After cells have been taken up, reverse the pressure in the needle to stop the suction, and remove the needle from the donor eye. Insert the needle into the host retina in a similar way, and slowly expel the cells with as little medium as possible. After transplantation, let embryos recover for few minutes, remove them from the agarose, and raise them in E3 + PTU at 28.5°C in 24-well plates. Axons of transplanted RGCs can then be observed after 48 hpf by live imaging.

## IV. Future Directions

The approaches developed over the past decade have greatly improved our ability to label and visualize the retinotectal projection *in vivo,* as well as to perform functional assays for understanding the molecular mechanisms that control its development. Nevertheless, novel techniques will be required for observing retinal axons in greater detail and to ask new biological questions.

Three methods already used in other systems are currently being adapted to study new aspects of zebrafish retinotectal system development. The Brainbow approach, initially developed in mice, allows labeling and mapping of neurons with a wide range of colors by randomly varying the levels of red, green, and blue FPs expressed in individual neurons (Livet *et al*., 2007). It has been used to reconstruct the architecture of neuronal circuits in different systems and will be a powerful tool for analyzing sorting of retinal axons in the tract as well as topographic mapping in the tectum. A second approach is to use enhancer trap (ET) screens to isolate lines expressing transgenes in specific subsets of neurons. For instance, new lines with interesting expression patterns in the tectum have recently been produced with a Gal4 ET screen (Scott and Baier, 2009). Such an approach will potentially allow the identification of new lines driving expression in specific regions of the retina (Picker *et al*., 2009) or RGC subtypes. Finally, calcium imaging has been used *in vitro* to measure growth cone responses to guidance cues (Guan *et al*., 2007; Tojima *et al*., 2010). Adapted to zebrafish, it will give the ability to monitor, *in vivo*, the activity of retinal axons as they elongate. Combined together, these emerging techniques will improve our ability to examine retinal axons as they navigate, shedding new light on axon guidance *in vivo*.

## References

Aizawa, H., Bianco, I. H., Hamaoka, T., Miyashita, T., Uemura, O., Concha, M. L., Russell, C., Wilson, S. W., and Okamoto, H. (2005). Laterotopic representation of left-right information onto the dorso-ventral axis of a zebrafish midbrain target nucleus. Curr. Biol. **15**, 238–243.

Baier, H., Klostermann, S., Trowe, T., Karlstrom, R. O., Nusslein-Volhard, C., and Bonhoeffer, F. (1996). Genetic dissection of the retinotectal projection. Development **123**, 415–425.

Ben Fredj, N., Hammond, S., Otsuna, H., Chien, C. B., Burrone, J., and Meyer, M. P. (2010). Synaptic activity and activity-dependent competition regulates axon arbor maturation, growth arrest, and territory in the retinotectal projection. J. Neurosci. **30**, 10939–10951.

Bianco, I. H., Carl, M., Russell, C., Clarke, J. D., and Wilson, S. W. (2008). Brain asymmetry is encoded at the level of axon terminal morphology. Neural Dev. **3**, 9.

Brand, M., Heisenberg, C. P., Jiang, Y. J., Beuchle, D., Lun, K., Furutani-Seiki, M., Granato, M., Haffter, P., Hammerschmidt, M., Kane, D. A., Kelsh, R. N., Mullins, M. C., *et al*., (1996). Mutations in zebrafish genes affecting the formation of the boundary between midbrain and hindbrain. Development **123**, 179–190.

Campbell, D. S., Stringham, S. A., Timm, A., Xiao, T., Law, M. Y., Baier, H., Nonet, M. L., and Chien, C. B. (2007). Slit1a inhibits retinal ganglion cell arborization and synaptogenesis via Robo2-dependent and -independent pathways. Neuron **55**, 231–245.

Chen, W., Burgess, S., and Hopkins, N. (2001). Analysis of the zebrafish smoothened mutant reveals conserved and divergent functions of hedgehog activity. Development **128**, 2385–2396.

Choy, E., Chiu, V. K., Silletti, J., Feoktistov, M., Morimoto, T., Michaelson, D., Ivanov, I. E., and Philips, M. R. (1999). Endomembrane trafficking of ras: The CAAX motif targets proteins to the ER and Golgi. Cell **98**, 69–80.

Clement, A., Wiweger, M., von der Hardt, S., Rusch, M. A., Selleck, S. B., Chien, C. B., and Roehl, H. H. (2008). Regulation of zebrafish skeletogenesis by ext2/dackel and papst1/pinscher. PLoS Genet. **4**, e1000136.

Del Bene, F., Wehman, A. M., Link, B. A., and Baier, H. (2008). Regulation of neurogenesis by interkinetic nuclear migration through an apical-basal notch gradient. Cell **134**, 1055–1065.

Draper, B. W., Morcos, P. A., and Kimmel, C. B. (2001). Inhibition of zebrafish fgf8 pre-mRNA splicing with morpholino oligos: A quantifiable method for gene knockdown. Genesis **30**, 154–156.

D'Souza, J., Hendricks, M., Le Guyader, S., Subburaju, S., Grunewald, B., Scholich, K., and Jesuthasan, S. (2005). Formation of the retinotectal projection requires Esrom, an ortholog of PAM (protein associated with Myc). Development **132**, 247–256.

Eisen, J. S., and Smith, J. C. (2008). Controlling morpholino experiments: Don't stop making antisense. Development **135**, 1735–1743.

Fricke, C., Lee, J. S., Geiger-Rudolph, S., Bonhoeffer, F., and Chien, C. B. (2001). Astray, a zebrafish roundabout homolog required for retinal axon guidance. Science **292**, 507–510.

Gnuegge, L., Schmid, S., and Neuhauss, S. C. (2001). Analysis of the activity-deprived zebrafish mutant macho reveals an essential requirement of neuronal activity for the development of a fine-grained visuotopic map. J. Neurosci. **21**, 3542–3548.

Gosse, N. J., and Baier, H. (2009). An essential role for Radar (Gdf6a) in inducing dorsal fate in the zebrafish retina. Proc. Natl. Acad. Sci. U.S.A. **106**, 2236–2241.

Guan, C. B., Xu, H. T., Jin, M., Yuan, X. B., and Poo, M. M. (2007). Long-range Ca2+ signaling from growth cone to soma mediates reversal of neuronal migration induced by slit-2. Cell **129**, 385–395.

Halloran, M. C., Sato-Maeda, M., Warren, J. T., Su, F., Lele, Z., Krone, P. H., Kuwada, J. Y., and Shoji, W. (2000). Laser-induced gene expression in specific cells of transgenic zebrafish. Development **127**, 1953–1960.

Hardy, M. E., Ross, L. V., and Chien, C. B. (2007). Focal gene misexpression in zebrafish embryos induced by local heat shock using a modified soldering iron. Dev. Dyn. **236**, 3071–3076.

Ho, R. K., and Kane, D. A. (1990). Cell-autonomous action of zebrafish spt-1 mutation in specific mesodermal precursors. Nature **348**, 728–730.

Honig, M. G., and Hume, R. I. (1989). Dil and diO: Versatile fluorescent dyes for neuronal labelling and pathway tracing. Trends Neurosci. **12**, 333–335, 340–341.

Hu, M., and Easter, S. S. (1999). Retinal neurogenesis: The formation of the initial central patch of postmitotic cells. Dev. Biol. **207**, 309–321.

Hutson, L. D., Campbell, D. S., and Chien, C. B. (2004). Analyzing axon guidance in the zebrafish retinotectal system. Methods Cell Biol. **76**, 13–35.

Hutson, L. D., and Chien, C. B. (2002). Pathfinding and error correction by retinal axons: The role of astray/robo2. Neuron **33**, 205–217.

Kaethner, R. J., and Stuermer, C. A. (1992). Dynamics of terminal arbor formation and target approach of retinotectal axons in living zebrafish embryos: A time-lapse study of single axons. J. Neurosci. **12**, 3257–3271.

Kane, D. A., and Kishimoto, Y. (2002). Cell labelling and transplantation techniques. In "Zebrafish, Practical Approach" (C. Nϋsslein-Volhard, R. Dahm, eds.) No. 261, pp. 95–120, Oxford University Press, Tubingen, Germany.

Karlstrom, R. O., Talbot, W. S., and Schier, A. F. (1999). Comparative synteny cloning of zebrafish you-too: Mutations in the Hedgehog target gli2 affect ventral forebrain patterning. Genes Dev. **13**, 388–393.

Karlstrom, R. O., Trowe, T., Klostermann, S., Baier, H., Brand, M., Crawford, A. D., Grunewald, B., Haffter, P., Hoffmann, H., Meyer, S. U., Muller, B. K., Richter, S., *et al.* (1996). Zebrafish mutations affecting retinotectal axon pathfinding. Development **123**, 427–438.

Karlstrom, R. O., Tyurina, O. V., Kawakami, A., Nishioka, N., Talbot, W. S., Sasaki, H., and Schier, A. F. (2003). Genetic analysis of zebrafish gli1 and gli2 reveals divergent requirements for gli genes in vertebrate development. Development **130**, 1549–1564.

Kemp, H. A., Carmany-Rampey, A., and Moens, C. (2009). Generating chimeric zebrafish embryos by transplantation. J. Vis. Exp. Jul 17;(29). pii: 1394. doi: 10.3791/1394.

Knaut, H., Werz, C., Geisler, R., and Nusslein-Volhard, C. (2003). A zebrafish homologue of the chemokine receptor Cxcr4 is a germ-cell guidance receptor. Nature **421**, 279–282.

Koster, R. W., and Fraser, S. E. (2001). Tracing transgene expression in living zebrafish embryos. Dev. Biol. **233**, 329–346.

Laessing, U., Giordano, S., Stecher, B., Lottspeich, F., and Stuermer, C. A. (1994). Molecular characterization of fish neurolin: A growth-associated cell surface protein and member of the immunoglobulin superfamily in the fish retinotectal system with similarities to chick protein DM-GRASP/SC-1/BEN. Differentiation **56**, 21–29.

Laessing, U., and Stuermer, C. A. (1996). Spatiotemporal pattern of retinal ganglion cell differentiation revealed by the expression of neurolin in embryonic zebrafish. J. Neurobiol. **29**, 65–74.

Lee, J. S., von der Hardt, S., Rusch, M. A., Stringer, S. E., Stickney, H. L., Talbot, W. S., Geisler, R., Nusslein-Volhard, C., Selleck, S. B., Chien, C. B., and Roehl, H. (2004). Axon sorting in the optic tract requires HSPG synthesis by ext2 (dackel) and extl3 (boxer). Neuron **44**, 947–960.

Lee, J. S., Willer, J. R., Willer, G. B., Smith, K., Gregg, R. G., and Gross, J. M. (2008). Zebrafish blowout provides genetic evidence for Patched1-mediated negative regulation of Hedgehog signaling within the proximal optic vesicle of the vertebrate eye. Dev. Biol. **319**, 10–22.

Lele, Z., Folchert, A., Concha, M., Rauch, G. J., Geisler, R., Rosa, F., Wilson, S. W., Hammerschmidt, M., and Bally-Cuif, L. (2002). Parachute/n-cadherin is required for morphogenesis and maintained integrity of the zebrafish neural tube. Development **129**, 3281–3294.

Li, Q., Shirabe, K., Thisse, C., Thisse, B., Okamoto, H., Masai, I., and Kuwada, J. Y. (2005). Chemokine signaling guides axons within the retina in zebrafish. J. Neurosci. **25**, 1711–1717.

Livet, J., Weissman, T. A., Kang, H., Draft, R. W., Lu, J., Bennis, R. A., Sanes, J. R., and Lichtman, J. W. (2007). Transgenic strategies for combinatorial expression of fluorescent proteins in the nervous system. Nature **450**, 56–62.

Lorent, K., Liu, K. S., Fetcho, J. R., and Granato, M. (2001). The zebrafish space cadet gene controls axonal pathfinding of neurons that modulate fast turning movements. Development **128**, 2131–2142.

Macdonald, R., Scholes, J., Strahle, U., Brennan, C., Holder, N., Brand, M., and Wilson, S. W. (1997). The Pax protein Noi is required for commissural axon pathway formation in the rostral forebrain. Development **124**, 2397–2408.

Maddison, L. A., Lu, J., Victoroff, T., Scott, E., Baier, H., and Chen, W. (2009). A gain-of-function screen in zebrafish identifies a guanylate cyclase with a role in neuronal degeneration. Mol. Genet. Genomics **281**, 551–563.

Mangrum, W. I., Dowling, J. E., and Cohen, E. D. (2002). A morphological classification of ganglion cells in the zebrafish retina. Vis. Neurosci. **19**, 767–779.

Masai, I., Lele, Z., Yamaguchi, M., Komori, A., Nakata, A., Nishiwaki, Y., Wada, H., Tanaka, H., Nojima, Y., Hammerschmidt, M., Wilson, S. W., and Okamoto, H. (2003). N-cadherin mediates retinal lamination, maintenance of forebrain compartments and patterning of retinal neurites. Development **130**, 2479–2494.

Masai, I., Yamaguchi, M., Tonou-Fujimori, N., Komori, A., and Okamoto, H. (2005). The hedgehog-PKA pathway regulates two distinct steps of the differentiation of retinal ganglion cells: The cell-cycle exit of retinoblasts and their neuronal maturation. Development **132**, 1539–1553.

Matsuda, N., and Mishina, M. (2004). Identification of chaperonin CCT gamma subunit as a determinant of retinotectal development by whole-genome subtraction cloning from zebrafish no tectal neuron mutant. Development **131**, 1913–1925.

Meyer, M. P., and Smith, S. J. (2006). Evidence from in vivo imaging that synaptogenesis guides the growth and branching of axonal arbors by two distinct mechanisms. J. Neurosci. **26**, 3604–3614.

Moens, C. B., and Fritz, A. (1999). Techniques in neural development. Methods Cell Biol. **59**, 253–272.

Moriyoshi, K., Richards, L. J., Akazawa, C., O'Leary, D. D., and Nakanishi, S. (1996). Labeling neural cells using adenoviral gene transfer of membrane-targeted GFP. Neuron **16**, 255–260.

Mumm, J. S., Williams, P. R., Godinho, L., Koerber, A., Pittman, A. J., Roeser, T., Chien, C. B., Baier, H., and Wong, R. O. (2006). In vivo imaging reveals dendritic targeting of laminated afferents by zebrafish retinal ganglion cells. Neuron **52**, 609–621.

Muto, A., Orger, M. B., Wehman, A. M., Smear, M. C., Kay, J. N., Page-McCaw, P. S., Gahtan, E., Xiao, T., Nevin, L. M., Gosse, N. J., Staub, W., Finger-Baier, K., *et al.*, (2005). Forward genetic analysis of visual behavior in zebrafish. PLoS Genet. **1**, e66.

Nakano, Y., Kim, H. R., Kawakami, A., Roy, S., Schier, A. F., and Ingham, P. W. (2004). Inactivation of dispatched 1 by the chameleon mutation disrupts Hedgehog signalling in the zebrafish embryo. Dev. Biol. **269**, 381–392.

Nasevicius, A., and Ekker, S. C. (2000). Effective targeted gene "knockdown" in zebrafish. Nat. Genet. **26**, 216–220.

Neumann, C. J., and Nuesslein-Volhard, C. (2000). Patterning of the zebrafish retina by a wave of sonic hedgehog activity. Science **289**, 2137–2139.

Nevin, L. M., Taylor, M. R., and Baier, H. (2008). Hardwiring of fine synaptic layers in the zebrafish visual pathway. Neural Dev. **3**, 36.

O'Brien, G. S., Rieger, S., Martin, S. M., Cavanaugh, A. M., Portera-Cailliau, C., and Sagasti, A. (2009). Two-photon axotomy and time-lapse confocal imaging in live zebrafish embryos. J. Vis. Exp. Feb 16;(24). pii: 1129. doi: 10.3791/1129.

Parsons, M. J., Pollard, S. M., Saude, L., Feldman, B., Coutinho, P., Hirst, E. M., and Stemple, D. L. (2002). Zebrafish mutants identify an essential role for laminins in notochord formation. Development **129**, 3137–3146.

Paulus, J. D., and Halloran, M. C. (2006). Zebrafish bashful/laminin-alpha 1 mutants exhibit multiple axon guidance defects. Dev. Dyn. **235**, 213–224.

Picker, A., Brennan, C., Reifers, F., Clarke, J. D., Holder, N., and Brand, M. (1999). Requirement for the zebrafish mid-hindbrain boundary in midbrain polarisation, mapping and confinement of the retinotectal projection. Development **126**, 2967–2978.

Picker, A., Cavodeassi, F., Machate, A., Bernauer, S., Hans, S., Abe, G., Kawakami, K., Wilson, S. W., and Brand, M. (2009). Dynamic coupling of pattern formation and morphogenesis in the developing vertebrate retina. PLoS Biol. **7**, e1000214.

Pittman, A. J., Gaynes, J. A., and Chien, C. B. (2010). nev (cyfip2) is required for retinal lamination and axon guidance in the zebrafish retinotectal system. Dev. Biol. **344**, 784–794.

Pittman, A. J., Law, M. Y., and Chien, C. B. (2008). Pathfinding in a large vertebrate axon tract: Isotypic interactions guide retinotectal axons at multiple choice points. Development **135**, 2865–2871.

Placinta, M., Shen, M. C., Achermann, M., and Karlstrom, R. O. (2009). A laser pointer driven microheater for precise local heating and conditional gene regulation in vivo. Microheater driven gene regulation in zebrafish. BMC Dev. Biol. **9**, 73.

Poggi, L., Vitorino, M., Masai, I., and Harris, W. A. (2005). Influences on neural lineage and mode of division in the zebrafish retina in vivo. J. Cell Biol. **171**, 991–999.

Rebagliati, M. R., Toyama, R., Haffter, P., and Dawid, I. B. (1998). cyclops encodes a nodal-related factor involved in midline signaling. Proc. Natl. Acad. Sci. U.S.A. **95**, 9932–9937.

Roeser, T., and Baier, H. (2003). Visuomotor behaviors in larval zebrafish after GFP-guided laser ablation of the optic tectum. J. Neurosci. **23**, 3726–3734.

Sampath, K., Rubinstein, A. L., Cheng, A. M., Liang, J. O., Fekany, K., Solnica-Krezel, L., Korzh, V., Halpern, M. E., and Wright, C. V. (1998). Induction of the zebrafish ventral brain and floorplate requires cyclops/nodal signalling. Nature **395**, 185–189.

Sato, T., Hamaoka, T., Aizawa, H., Hosoya, T., and Okamoto, H. (2007). Genetic single-cell mosaic analysis implicates ephrinB2 reverse signaling in projections from the posterior tectum to the hindbrain in zebrafish. J. Neurosci. **27**, 5271–5279.

Schauerte, H. E., van Eeden, F. J., Fricke, C., Odenthal, J., Strahle, U., and Haffter, P. (1998). Sonic hedgehog is not required for the induction of medial floor plate cells in the zebrafish. Development **125**, 2983–2993.

Schmidt, J. T., Buzzard, M., Borress, R., and Dhillon, S. (2000). MK801 increases retinotectal arbor size in developing zebrafish without affecting kinetics of branch elimination and addition. J. Neurobiol. **42**, 303–314.

Scott, E. K., and Baier, H. (2009). The cellular architecture of the larval zebrafish tectum, as revealed by gal4 enhancer trap lines. Front Neural Circuits **3**, 13.

Sekimizu, K., Nishioka, N., Sasaki, H., Takeda, H., Karlstrom, R. O., and Kawakami, A. (2004). The zebrafish iguana locus encodes Dzip1, a novel zinc-finger protein required for proper regulation of Hedgehog signaling. Development **131**, 2521–2532.

Seth, A., Culverwell, J., Walkowicz, M., Toro, S., Rick, J. M., Neuhauss, S. C., Varga, Z. M., and Karlstrom, R. O. (2006). belladonna/(Ihx2) is required for neural patterning and midline axon guidance in the zebrafish forebrain. Development **133**, 725–735.

Shanmugalingam, S., Houart, C., Picker, A., Reifers, F., Macdonald, R., Barth, A., Griffin, K., Brand, M., and Wilson, S. W. (2000). Ace/Fgf8 is required for forebrain commissure formation and patterning of the telencephalon. Development **127**, 2549–2561.

Smear, M. C., Tao, H. W., Staub, W., Orger, M. B., Gosse, N. J., Liu, Y., Takahashi, K., Poo, M. M., and Baier, H. (2007). Vesicular glutamate transport at a central synapse limits the acuity of visual perception in zebrafish. Neuron **53**, 65–77.

Thummel, R., Burket, C. T., Brewer, J. L., Sarras, M. P., Jr., Li, L., Perry, M., McDermott, J. P., Sauer, B., Hyde, D. R., and Godwin, A. R. (2005). Cre-mediated site-specific recombination in zebrafish embryos. Dev. Dyn. **233**, 1366–1377.

Tojima, T., Itofusa, R., and Kamiguchi, H. (2010) Asymmetric clathrin-mediated endocytosis drives repulsive growth cone guidance. Neuron **66**, 370–377.

Tokuoka, H., Yoshida, T., Matsuda, N., and Mishina, M. (2002). Regulation by glycogen synthase kinase-3beta of the arborization field and maturation of retinotectal projection in zebrafish. J. Neurosci. **22**, 10324–10332.

"Analyse von Mutationen mit Einfluss aud die topographische Ordnung von Axonen im retinotektalen System des Zebrabärblings, Danio rerio. PhD Thesis, Eberhard-Karls-Universität Tübingen, Tübingen, Germany.

Trowe, T., Klostermann, S., Baier, H., Granato, M., Crawford, A. D., Grunewald, B., Hoffmann, H., Karlstrom, R. O., Meyer, S. U., Muller, B., Richter, S., Nusslein-Volhard, C., *et al.*, (1996). Mutations disrupting the ordering and topographic mapping of axons in the retinotectal projection of the zebrafish, Danio rerio. Development **123**, 439–450.

Varga, Z. M., Amores, A., Lewis, K. E., Yan, Y. L., Postlethwait, J. H., Eisen, J. S., and Westerfield, M. (2001). Zebrafish smoothened functions in ventral neural tube specification and axon tract formation. Development **128**, 3497–3509.

Vitorino, M., Jusuf, P. R., Maurus, D., Kimura, Y., Higashijima, S., and Harris, W. A. (2009). Vsx2 in the zebrafish retina: Restricted lineages through derepression. Neural Dev. **4**, 14.

Wagle, M., Grunewald, B., Subburaju, S., Barzaghi, C., Le Guyader, S., Chan, J., and Jesuthasan, S. (2004). EphrinB2a in the zebrafish retinotectal system. J. Neurobiol. **59**, 57–65.

Wolff, C., Roy, S., Lewis, K. E., Schauerte, H., Joerg-Rauch, G., Kirn, A., Weiler, C., Geisler, R., Haffter, P., and Ingham, P. W. (2004). iguana encodes a novel zinc-finger protein with coiled-coil domains essential for Hedgehog signal transduction in the zebrafish embryo. Genes Dev. **18**, 1565–1576.

Woo, K., Shih, J., and Fraser, S. E. (1995). Fate maps of the zebrafish embryo. Curr. Opin. Genet. Dev. **5**, 439–443.

Xiao, T., and Baier, H. (2007). Lamina-specific axonal projections in the zebrafish tectum require the type IV collagen Dragnet. Nat. Neurosci. **10**, 1529–1537.

Xiao, T., Roeser, T., Staub, W., and Baier, H. (2005). A GFP-based genetic screen reveals mutations that disrupt the architecture of the zebrafish retinotectal projection. Development **132**, 2955–2967.

Yoshida, T., and Mishina, M. (2003). Neuron-specific gene manipulations to transparent zebrafish embryos. Methods Cell Sci. **25**, 15–23.

Zolessi, F. R., Poggi, L., Wilkinson, C. J., Chien, C. B., and Harris, W. A. (2006). Polarization and orientation of retinal ganglion cells in vivo. Neural Dev. **1**, 2.

## CHAPTER 2

# Imaging Blood Vessels in the Zebrafish

**Makoto Kamei**[*,‡], **Sumio Isogai**[†], **Weijun Pan**[*],
*and* **Brant M. Weinstein**[*]

[*]Program in Genomics of Differentiation, National Institute of Child Health and Human Development, Bethesda, Maryland

[†]Department of Anatomy, School of Medicine, Iwate Medical University, Morioka, Japan

[‡]Cell Biology of Diseases Group, Sansom Institute for Health Research, School of Pharmacy and Medical Science, University of South Australia, Adelaide, South Australia, Australia

Abstract
I. Introduction
II. Imaging Vascular Gene Expression
III. Non-vital Blood Vessel Imaging
  A. Micro-Dye and Micro-Resin Injection
  B. Alkaline Phosphatase Staining for 3 dpf Embryos
IV. Vital Imaging of Blood Vessels
  A. Microangiography
  B. Imaging Blood Vessels in Transgenic Zebrafish
V. Conclusion
References

## Abstract

Understanding on the mechanisms of vascular branching morphogenesis has become a subject of enormous scientific and clinical interest. Zebrafish, which have small, accessible, transparent embryos and larvae, provides a unique living animal model to facilitating high-resolution imaging on ubiquitous and deep localization of vessels within embryo development and also in adult tissues. In this chapter, we have summarized various methods for vessel imaging in zebrafish, including in situ hybridization for vascular-specific genes, resin injection- or dye injection-based vessel visualization, and alkaline phosphatase staining. We also described detail protocols for live imaging of vessels by microangiography or using various transgenic zebrafish lines.

METHODS IN CELL BIOLOGY, VOL. 100
Copyright © 2010 Elsevier Inc. All rights reserved.

978-0-12-384892-5
DOI: 10.1016/B978-0-12-384892-5.00002-5

# I. Introduction

The circulatory system is one of the first organ systems to begin functioning during vertebrate development, and its proper assembly is critical for embryonic survival. Blood vessels innervate all other tissues, supplying them with oxygen, nutrients, hormones, and cellular and humoral immune factors. The heart pumps blood through a complex network of blood vessels comprised of an inner single-cell thick endothelial epithelium surrounded by outer supporting pericyte or smooth muscle cells embedded in a fibrillar matrix. The mechanisms of blood vessel growth and morphogenesis are a subject of intensive investigation, and a large number of genes important for blood vessel formation have been identified in recent years. This has been achieved through developmental studies in mice and other animal models. However, our understanding of how these genes work together to orchestrate the proper assembly of the intricate system of blood vessels in the living animal remains limited, in part because of the challenging nature of these studies. The architecture and context of blood vessels are difficult to reproduce *in vitro*, and most developing blood vessels *in vivo* are relatively inaccessible to observation and experimental manipulation. Furthermore, since a properly functioning vasculature is required for embryonic survival and major defects lead to early death and embryonic resorption in amniotes, genetic analysis of blood vessel formation has been largely limited to reverse-genetic approaches.

The zebrafish provides a number of advantages for *in vivo* analysis of vascular development. As noted elsewhere in this book, zebrafish embryos are readily accessible to observation and experimental manipulation. Genetic and experimental tools and methods are available for functional manipulation of the entire organism, vascular tissues, or even single vascular- or non-vascular cells. Two features in particular make zebrafish especially useful for studying vascular development. First, developing zebrafish are very small—a 2 dpf embryo is just 2 mm long. Their embryos are so small, in fact, that the cells and tissues of the zebrafish receive enough oxygen by passive diffusion to survive and develop in a reasonably normal fashion for the first 3–4 days of development, even in the complete absence of blood circulation. This makes it fairly straightforward to assess the cardiovascular specificity of genetic or experimental defects that affect the circulation. Second, zebrafish embryos and early larvae are virtually transparent. The embryos of zebrafish (and many other teleosts) are telolecithic—yolk is sequestered in a single large cell separate from the embryo proper. The absence of obscuring yolk proteins gives embryos and larvae a high degree of optically clarity. Genetic variants deficient in pigment cells or pigment formation are even more transparent. This remarkable transparency is probably the most valuable feature of the fish for studying blood vessels, facilitating high-resolution imaging *in vivo.*

In this chapter we review some of the methods used to image and assess the pattern and function of the zebrafish vasculature, both in developing animals and in adults. First, we briefly touch on visualizing vascular gene expression (*in situ* hybridization, immunohistochemistry). In the next section we detail methods for imaging blood vessels in fixed developing and adult zebrafish specimens (resin and dye injection, alkaline phosphatase (AP) staining). In the final section we describe several methods for imaging blood vessels in living animals (microangiography, time-lapse imaging of transgenic zebrafish with fluorescently tagged blood vessels). Collectively, these methods provide an unprecedented capability to image blood vessels in developing and adult animals.

## II. Imaging Vascular Gene Expression

Experimental analysis of blood vessel formation during development requires the use of methods for visualizing the expression of particular genes within blood vessels and their progenitors. There are two general methods available to visualize endogenous gene expression within zebrafish embryos and larvae, *in situ* hybridization and immunohistochemistry. Neither of the methods is specific to the vasculature, and detailed protocols for these methods are available elsewhere (Hauptmann and Gerster, 1994; Westerfield, 2000). *In situ* hybridization is used routinely to assay the spatial and temporal patterns of vascular genes. A variety of different probes are available, some of which are listed in Table I. The *fli1a* and *scl* genes are early markers of vascular and hematopoietic lateral mesoderm. The expression of the *fli1a* becomes restricted to endothelial cells, a subset of circulating myeloid cells, and cranial neural crest derivatives (Brown *et al*., 2000; Thompson *et al*., 1998), while *scl* expression becomes restricted to the hematopoietic lineage at later stages (Gering *et al*., 1998). The *tie2* and *cdh5* genes are zebrafish orthologs of angiopoietin-1 receptor and VE-Cadherin, respectively, and are expressed in a vascular-specific manner (Lyons *et al*., 1998; Sumanas *et al*., 2005). The *kdrl* and *flt4* genes (Fouquet *et al*., 1997; Sumoy *et al*., 1997; Thompson *et al*., 1998) are zebrafish orthologs of mammalian endothelial-specific tyrosine kinase receptors for the important vascular signaling molecule

**Table I**
**Common Marker Genes Used in Zebrafish Vasculature Research**

| Marker genes | Expression pattern | Reference |
|---|---|---|
| *Fli1a* | Pan-endothelial | Brown *et al*. (2000); Thompson *et al*. (1998) |
| *tie2* | Pan-endothelial | Lyons *et al*. (1998) |
| *Kdrl (flk1)* | Initially pan-endothelial, enriched in arteries at later stages | (Bussmann *et al*., 2008); Sumoy *et al*. (1997) |
| *cdh5* | Pan-endothelial | Sumanas *et al*. (2005) |
| *efnb2* | Artery only | Lawson *et al*. (2001); Zhong *et al*. (2000) |
| *Grl* | Artery only | Zhong *et al*. (2000) |
| *notch5* | Artery only | Lawson *et al*. (2001) |
| *dll4* | Artery only | Herpers *et al*. (2008) |
| *tbx20* | Artery only | Szeto *et al*. (2002) |
| *dab2* | Vein only | Herpers *et al*. (2008) |
| *ephb4* | Vein only | Lawson *et al*. (2001) |
| *flt4* | Initially pan-endothelial. Later restricted to vein only. | Thompson *et al*. (1998) |
| *prox1* | Lymphatic vessel | Yaniv *et al*. (2006) |
| *lyve1* | Lymphatic vessel | Hogan *et al*. (2009) |
| *Scl* | Hematopoietic | Gering *et al*. (1998) |

*vascular endothelial growth factor (vegf).* They are initially expressed in hemangiogenic lateral mesoderm then become restricted to angioblasts and endothelium. In the axial vessels of the trunk (dorsal aorta and posterior cardinal vein) *kdrl* becomes preferentially expressed in the aorta while *flt4* becomes preferentially expressed in the posterior cardinal vein (similar expression patterns of the corresponding orthologs are observed in mouse) (Kaipainen *et al*., 1995; Thompson *et al*., 1998). Other genes such as *efnb2, grl, Dll4, Tbx20*, and *notch5* are useful as markers of specification of arterial rather than venous endothelium, although all of these markers also exhibit substantial expression in non-vascular tissues, particularly the nervous system (Herpers *et al*., 2008; Lawson *et al*., 2001; Szeto *et al*., 2002; Zhong *et al*., 2000). The most commonly used venous marker is *ephb4*, although *flt4* has also been used to identify venous endothelium as noted above. *Disabled-2 (Dab2)*, a cytosolic adaptor regulating endocytosis, also localizes very specifically to venous but not arterial endothelium in both *Xenopus* and *Zebrafish* embryos (Cheong *et al*., 2006; Herpers *et al*., 2008). The lymphatic endothelial markers Prox-1 and Lyve-1 are both conserved between mammals and fish, and both are useful zebrafish markers of lymphatic specification (Hogan *et al*., 2009; Yaniv *et al*., 2006). *Prox-1* functions as a key transcriptional factor for the differentiation of lymphatic endothelial cells. *Lyve-1* has been identified as a major receptor for HA (extracellular matrix glycosaminoglycan hyaluronan) on the lymph vessel wall, although its function in lymphangiogenesis is unclear.

## III. Non-vital Blood Vessel Imaging

A number of methods are available for visualizing the pattern of blood vessels in fixed specimens. Micro-dye injection and micro-resin injection can be used to delineate the patent vasculature (lumenized or open blood vessels connected to the systemic circulation). Both of these methods rely on injection to fill blood vessels with dye or plastic resin that can be visualized in detail following the procedure. Dye injection methods are most useful in embryos and larvae up to a few weeks old. At later juvenile stages, and in adults, tissue opacity and thickness interfere with dye visualization in deeper vessels and resin injections can be more useful. Resin injections are difficult to perform on small specimens (such as embryos) but could be used to visualize vessels at almost any stage of development. While technically challenging, resin injection provides excellent visualization of the adult vasculature, since tissues surrounding the plastic resin are digested away and do not interfere with vessel observation. In addition to these two injection methods for lumenized vessels, staining for the endogenous AP activity of vascular endothelium can also be used to visualize vessels in fixed specimens. This method is useful for easy, rapid observation of vessel patterns, and does not require the vessel be patent, but it cannot be used effectively prior to approximately 3 days post-fertilization due to low signal and high background staining. Even at 3 dpf the method gives a relatively high background and is not particularly useful for visualizing cranial vessels. This method is also less useful at later stages due to increasing background. We describe the procedures for all of these methods in detail below.

## A. Micro-Dye and Micro-Resin Injection

Since the 19th century, the dye injection method has been the most widely used tool for visualizing the developing circulatory system. Pioneering vascular embryologists such as Florence Sabin carried out their groundbreaking descriptive studies by injecting India ink into blood vessels of vertebrate embryos to reveal their patterns (for example, Evans, 1910; Sabin, 1917). In the 1970s the corrosive resin casting method, previously employed to visualize larger adult blood vessels, was combined with scanning electron microscopy to permit its use for visualizing vessels on a microscopic scale, such as in the developing renal vasculature (Murakami, 1972). Although microangiography and vascular-specific transgenic fish have now become the tools of choice in most cases for visualizing vessels in living zebrafish embryos (see below), these newer methods have limited usefulness in later stage larvae, juveniles, and adult fish. At these later stages the "classical" dye or resin injection methods still provide the best visualization of the majority of blood vessels (via direct injection into the dorsal aorta or caudal artery) or lymphatic vessels (via direct injection into the thoracic duct) (Yaniv *et al*., 2006). The resin casting method involves injection of a plastic resin that is allowed to harden *in situ*, followed by etching away of tissues to leave behind only the plastic cast. The cast is rotary shadowed and visualized by scanning electron microscopy. The dye injection method described below involves injection of Berlin Blue dye followed by fixation and clearing of the embryos or larvae and whole-mount microscopic visualization.

### 1. Resin Injection Method

#### a. Materials

- Paraffin bed (see Fig. 2)
- Injection apparatus for circulating saline buffer (x2; see Fig. 4)
- Injection apparatus for fixative
- Injection apparatus for resin injection (one apparatus per sample to be injected)
- Physiological saline buffer suitable for bony fish
- 2% glutaraldehyde solution in saline buffer (Sigma cat# G6403, 50% solution in water)
- Methacrylate resin components

Methyl methacrylate monomer (Aldrich cat# M55909 or Fluka cat# 03989)
Ethyl methacrylate monomer (Aldrich cat# 234893 or Fluka cat# 65852)
2-Hydroxypropyl methacrylate monomer (Aldrich cat# 268542 or Fluka cat# 17351)

#### b. Protocol

*Preparation of the apparatus*

1. The *paraffin bed* is made in a 9 cm glass petri dish by pouring molten paraffin wax (Fig. 1). While the wax is solidifying, tilt the dish approximately 15° to create a gentle slope. A depression is made in the middle of the bed for settling a fish.

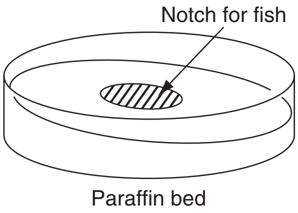

**Fig. 1** Paraffin bed used for holding adult zebrafish.

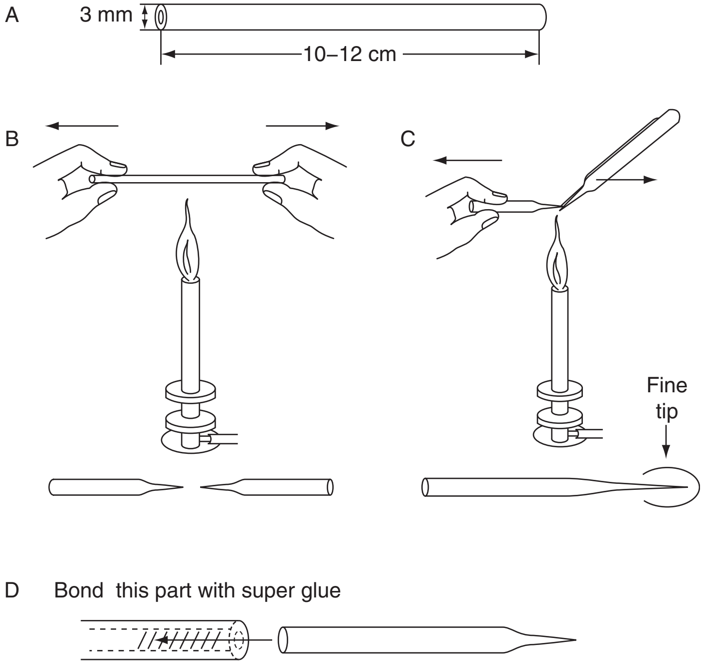

**Fig. 2** Preparation of glass needles for injection of adult zebrafish. Glass stock (A) is pulled on a Bunsen burner (B), the tips are re-pulled (C), and then the needles are bonded to vinyl tubing with super glue (D).

2. The *glass needles* are made from stock glass tubing (3 mm outside diameter). The tubes are cut into 10–12 cm lengths (Fig. 2). The needles are pulled from the tube by heating the middle of the tube with a Bunsen burner. When the color of the glass tube is changed to red and the tubes feel soft, remove the tube from the heat, and pull on both ends. This should produce two injection needles with length of 5–6 cm. Let the needles cool down. Then holding the thick end of the needle by hand, and the sharp end of the needle by a pair of forceps, re-heat the sharp end on a Bunsen burner, and pull as before. By pulling the needles twice, it is possible to create

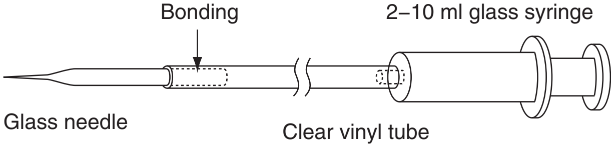

**Fig. 3** Apparatus for injecting adult zebrafish with saline and fixative. For injecting resin, the glass syringe is replaced with a disposable plastic syringe.

needles with very fine points. The tip of the needles made in this manner is closed, and the tip needs to be broken open just before use.

3. The *apparatus for injecting physiological saline buffer* is made by attaching a glass needle (see step 2 above) to a clear vinyl tubing (3 mm inside diameter, 20 cm in length). When plugging the needle in, a small amount of superglue is applied to reinforce the attachment. For injection of the buffer a 2–10 ml glass syringe is attached as shown (Fig. 3).
4. The *apparatus for injecting fixative* is prepared as described in step 3 above.
5. The *apparatus for injecting resin* is prepared as described in step 3, except that a 10 ml disposable syringe is attached instead of a glass syringe and heat-resistant silicone tubing is used.

**** IMPORTANT CAUTION ON RESIN USE ****

As resin polymerizes, heat is generated and the viscosity of the resin increases. The heated vinyl tube can detach from the syringe suddenly, causing pressurized, viscous hot resin to splatter. The resin is harmful to skin and mucous membranes, and personal safety measures should always be taken when performing this procedure (e.g., use of goggles, face masks, gloves, and other protective clothing). In addition, make sure that the end of the vinyl tubing is securely attached to the syringe and use heat-resistant silicone tubing for the resin injection apparatus.

6. *Preparing resin (methyl methacrylate and ethyl methacrylate monomers)*. Commercially available methacrylate monomers contain monomethyl ether hydroxyquinone to prevent polymerization, and it is necessary to remove this before use. Prepare 500 ml of 5% NaOH. Pour 100 ml methacrylate monomer and 50 ml 5% NaOH in a separating funnel and shake (Fig. 4A). Wait until the two solutions separate, and then remove the lower 5% NaOH layer (should be brown in color). Repeat until the NaOH solution remains clear, then remove the NaOH by extracting the methacrylate monomer (upper layer) with distilled water. Pour 100 ml of distilled water in the separating funnel containing the methacrylate monomer, shake, and wait until the two layers separate. Remove the lower distilled water layer. Repeat three to four times. Filter methacrylate monomer using double filter paper (Whatman) and incubate the monomer in a 150 ml air-tight container with sodium sulfite overnight (Fig. 4B). Place this container within a desiccator containing silica-gel, and store in a refrigerator at 4°C.

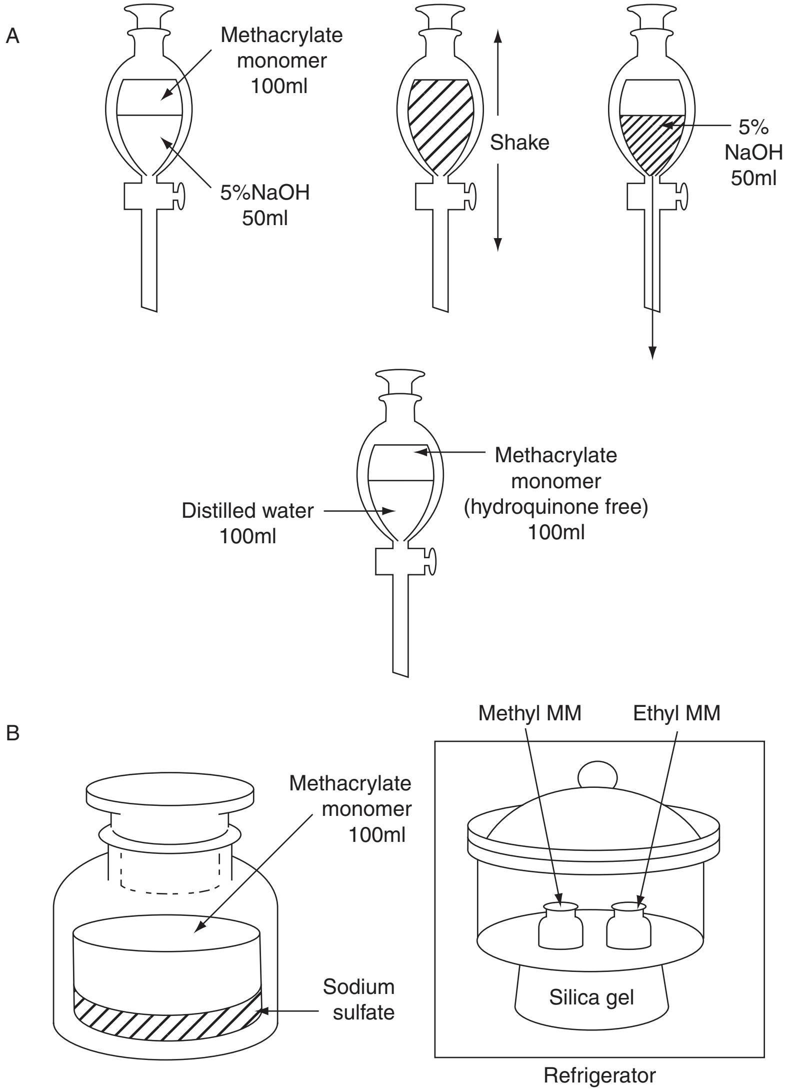
A
Methacrylate monomer 100ml
5%NaOH 50ml
Shake
5% NaOH 50ml
Distilled water 100ml
Methacrylate monomer (hydroquinone free) 100ml
B
Methacrylate monomer 100ml
Sodium sulfate
Methyl MM
Ethyl MM
Silica gel
Refrigerator

**Fig. 4** Preparation of resin for injection. Commercial resin is supplied with monomethyl ether hydroxyquinone to prevent polymerization. This must be extracted before use (A) as described in the text. After extraction resin is stored refrigerated over sodium sulfate in a desiccator (B).

*Experimental procedure*

Steps 1, 2, and 4 are to be carried out under a dissecting microscope.

1. *Washing the circulatory system with saline buffer*. Place anesthetized adult zebrafish on the depressed part of the paraffin bed ventral side up. Use a pair of watchmaker's forceps and a pair of fine surgical or iridectomy scissors to remove the outer skin

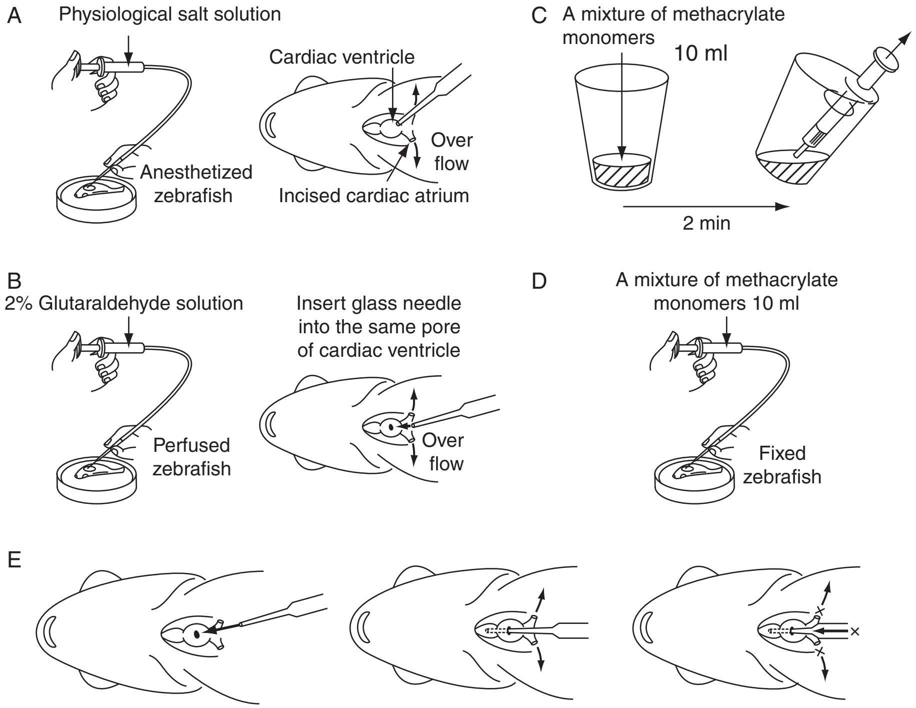
A
Physiological salt solution
Cardiac ventricle
Over
flow
Anesthetized
zebrafish
Incised cardiac atrium
C
A mixture of methacrylate
monomers
10 ml
2 min
B
2% Glutaraldehyde solution
Insert glass needle
into the same pore
of cardiac ventricle
Perfused
zebrafish
Over
flow
D
A mixture of methacrylate
monomers 10 ml
Fixed
zebrafish
E

**Fig. 5** Resin injection of adult zebrafish. Anesthetized animal is thoroughly flushed with physiological salt solution (A), then with glutaraldehyde fixative (B). Mixed resin is taken up into plastic syringe (C) which is attached to the rest of the resin injection apparatus and injection is performed (D). Injection should be stopped when resin hardens and flow ceases (E). See text for details.

and pericardial sac surrounding the heart. Use the forceps to sever the sinus venosus to allow blood to drain. Break the tip of the needle to the size of the ventricle and attached to a glass syringe containing saline buffer. Stab the glass needle into the ventricle in the direction of the head, and apply pressure on the syringe to flush the circulatory system with buffer (Fig. 5A). Do not stop until the system is very well flushed out; flushing should be continued well after the flow from the sinus venosus has become clear saline.

2. *Fixation with 2% glutaraldehyde*. Break a glass needle as above, attach to a syringe containing the 2% glutaraldehyde solution, and start circulating the fixative in the same manner as for the saline buffer (Fig. 5B). Fix well (overnight preferable).
3. *Mixing the resin.* Mix together 3 ml methyl methacrylate monomer, 1.75 ml ethyl methacrylate monomer, and 5.25 ml 2-hydroxypropyl methacrylate monomer (to make 10 ml final volume) in a disposable plastic 100 ml cup (Fig. 5C). To this mixture, add 0.15 g benzoyl peroxide (catalyst), 0.15 ml *N,N*-dimethylaniline (polymerization agent), and Sudan III (dye), then mix well and sonicate for 2 min.

4. *Resin injection*. Immediately after sonication, aspirate the resin mixture into a 10 ml disposable plastic syringe, and attach a glass needle. This time break the needle so that it will have a slightly larger bore. Make sure the vinyl tubing is attached to the end of the syringe firmly. Push the needle in the direction of the head of the fish through the same hole used for washing and fixing (Fig. 5D). If possible, push the tip of the needle all the way into the arterial cone (back of the ventricle) before beginning the injection. At first the injection will be easy since the viscosity is low, but after 3–5 min, the viscosity will increase, and the resin will start to heat up. Keep pushing down on the syringe. After 10–12 min, the resin hardens sufficiently for resin flow to stop, at which point the injection should be stopped (Fig. 5E). Wait about 10 min more for resin to fully harden.
5. *Digestion of tissue*. The injected adult zebrafish is digested with 10–20% KOH for a few days, and gently washed with distilled water to remove tissue. The resin cast is dissected out using watchmaker's forceps and small scissors. Sometimes sonication is used to remove bones and hard-to-remove tissues, but care is required not to destroy the cast itself. For SEM (scanning electron microscopy) observation, each local vascular system is divided and trimmed. These procedures must be performed under water using dissecting microscope. Each block is frozen in distilled water then freeze-dried.
6. *Scanning electron microscopy*. The dried block is mounted on a metal stub and coated with osmium or platinum. Observations are performed with a scanning electron microscope using an acceleration voltage of 5–10 kV.

## 2. Dye Injection Method

### a. Materials

- Berlin blue dye solution
- Injection apparatus for embryos and early larvae (as described for microangiography, below) *OR*
- Injection apparatus for juvenile and adult fish as described for resin injection, above)
- Paraffin bed (for juvenile and adult injections—see resin injection above)

### b. Protocol

*Dye injection of embryos and early larvae*

1. Prepare Berlin blue dye solution by adding 0.5–0.75 g Berlin blue powder (Aldrich cat# 234125, Prussian blue) to 100 ml distilled water and dissolving thoroughly. Filter solution through double layers of Whatman 3MM filter paper and store in an air-tight bottle.
2. Glass microneedles are prepared as for microangiography (see below).
3. Agarose embed embryos/larvae as follows (Fig. 6A): Immobilize embryo in 1X tricaine methanesulfonate (MS-222) in embryo media (Westerfield, 2000). Place embryo on slide in a drop of tricaine embryo media and them remove as much of liquid as possible with a pipette. Place a single drop of 1% molten low-melting

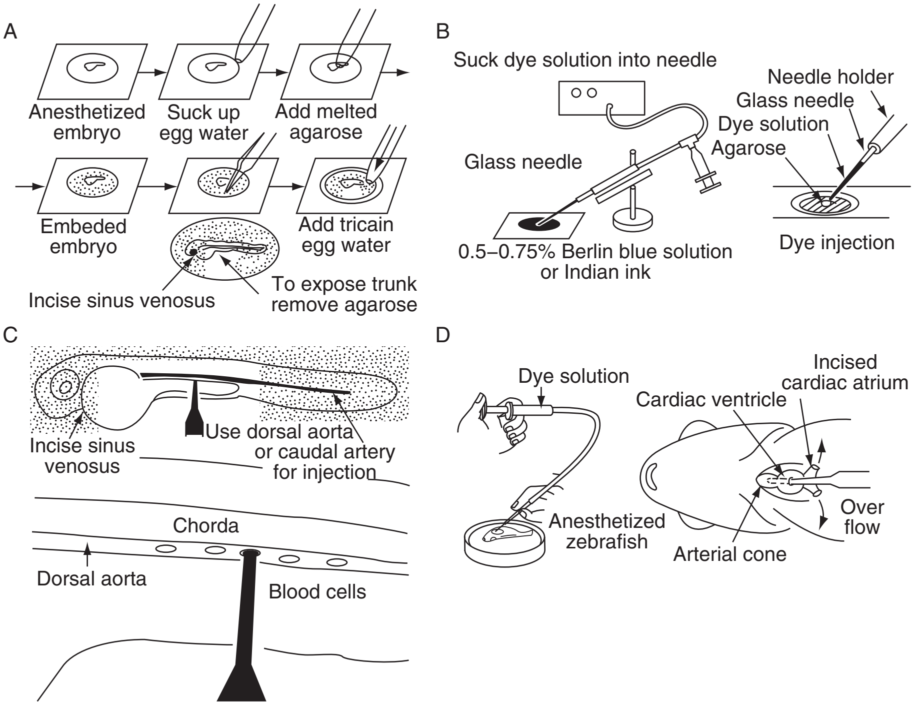
A
Anesthetized embryo
Suck up egg water
Add melted agarose
Embeded embryo
Add tricain egg water
Incise sinus venosus
To expose trunk remove agarose
B
Suck dye solution into needle
Glass needle
0.5–0.75% Berlin blue solution or Indian ink
Needle holder
Glass needle
Dye solution
Agarose
Dye injection
C
Incise sinus venosus
Use dorsal aorta or caudal artery for injection
Chorda
Dorsal aorta
Blood cells
D
Dye solution
Anesthetized zebrafish
Cardiac ventricle
Incised cardiac atrium
Over flow
Arterial cone

**Fig. 6** Mounting and dye injection of developing and adult zebrafish. Embryos and larvae are embedded in agarose on a glass slide for dye injection (A). Injection is performed into the dorsal aorta or caudal artery, with the sinus venosus incised to permit dye to flow through the vasculature (B). The apparatus used for dye injection is shown in (C). For dye injection of adult zebrafish, an apparatus similar to that used for saline and fixative injection prior to resin injection is employed (D). See text for further details.

temperature agarose on the embryo, allowing it to harden and embed the embryo. Attempt to orient the embryo before the agarose hardens such that either its left or its right side is facing up.

4. In order to allow blood drain, sever the sinus venosus using the watchmaker's forceps.
5. Remove the agarose covering the caudal half of the trunk or cranial half of the tail with the forceps, and then add a drop of 1X tricaine.
6. Break the fine tip of needle to the size of the dorsal aorta or the caudal artery, and, from the needle tip, aspirate enough Berlin blue solution to cannulate all the vessels thoroughly (Fig. 6B).
7. To pierce precisely the dorsal aorta or the caudal artery with the fine tip, the point just beneath the notochord must be targeted. To make sure the tip is in the correct position with respect to these vessels, inject the dye for 0.1 s using a picopump. The blood cells move according to the pumping if the tip is in the right position. Inject the dye for 1–2 s, and continue the procedure until all the vessels are cannulated

thoroughly (Fig. 6C). For lymphangiography, attempt to pierce the thoracic duct, which lies ventral to the dorsal aorta above the posterior cardinal vein, instead of the dorsal aorta. This vessel is more difficult to visualize and more challenging to inject than the dorsal aorta, so repeated attempts and patience will likely be needed. One can distinguish when the lymphatic rather than the blood vascular system has been injected because the dye will fill the thoracic duct but will not be visible or highly diluted in blood vessels such as the cardinal vein and dorsal aorta.

8. Fix the dye injected embryos.

*Dye injection of juvenile and adult zebrafish*

Note: This method is similar to the resin injection method described above.

1. The injection of dye is carried out under a dissecting microscope. Place an anesthetized adult zebrafish on the depressed part of the paraffin bed ventral side up.
2. Use a pair of watchmaker's forceps and a pair of fine surgical or iridectomy scissors to remove the outer skin and pericardial sac surrounding the heart. Use the forceps to sever the sinus venosus to allow blood to drain during injection (Fig. 6D).
3. Break the tip of the needle to the size of the ventricle and attach to a glass syringe containing 0.5~0.7% Berlin blue solution buffer (apparatus is very similar to that used for saline injection in the resin injection method described above). Stab the glass needle into the ventricle in the direction of the head, and apply pressure on the syringe to flush the circulatory system with buffer. Continue injection well after dye begins to flow from sinus venosus; make sure that the dye is thoroughly injected.
4. Fix the dye injected sample immediately in either 4% paraformaldehyde or 10% neutral formaldehyde; store in fixative.
5. For observation lightly wash the samples and then clear them by passing through 50%, 70%, 80%, 90%, and then 100% glycerol solution (1 solution change per day for a total of 5 days). Image samples under a dissecting microscope, dissecting away tissues as needed for observation of deeper vessels.

## B. Alkaline Phosphatase Staining for 3 dpf Embryos

Zebrafish blood vessels possess endogenous AP activity. Endogenous AP activity is not detectable in 24 hpf embryos, but is weakly detectable by 48 hpf and strongly at 72 hpf. Staining vessels by endogenous AP activity is useful for easy and rapid visualization of the vasculature in many specimens, but provides less resolution than many of the other methods. We use a protocol modified from Childs *et al*. (2002)

### a. Materials

- Fixation Buffer: 10 ml 4% paraformaldehyde + 1 ml 10% Triton-X100; makes 11 ml, scale up or down as needed.
- Rinse Buffer: 10 ml 10X PBS + 5 ml 10% Triton-X100 + 1 ml normal horse serum + 84 ml distilled water; makes 100 ml, scale up or down as needed.

- Staining Buffer: 1 ml 5M NaCl + 2.5 ml 1M MgCl2 + 5 ml 1M Tris pH 9.0 – 9.5 + 500 µl 10% Tween-20 + 41 ml distilled water; makes 50 ml, scale up or down as needed.
- Staining Solution: 10 ml staining buffer + 45 µl NBT + 35 µl BCIP; scale up or down as needed.
- NBT 4-Nitro Blue Tetrazolium (Boehringer-Mannheim Cat# 1-383-213), 100 mg/ml in 70% dimethylformamide.
- BCIP X-Phosphate or 5-Bromo-4-Chloro-3-indolyl-phosphate (Boehringer-Mannheim Cat# 1-383-221), 50 mg/ml in dimethylformamide.

**b. Protocol**

1. Fix embryos at room temperature for 1 h in fixation buffer.
2. Rinse 1× in rinse buffer.
3. Wash 5× 10 min at room temperature in rinse buffer **or** leave washing in rinse buffer at 4°C for up to several days. If doing the latter, wash again at RT for 10 min before going on to the next step.
4. Wash 2× 5 min in staining buffer.
5. Stain in 1 ml of staining solution. Color development takes about 5–30 min.
6. To stop reaction, wash 3X in rinse buffer without horse serum, then fix in 4% paraformaldehyde for 30 min, and store in fixative at 4°C.

**c. Important Notes**

1. Avoid putting the embryos in methanol (this destroys endogenous AP activity). If embryos have been placed in methanol, some AP activity can be reconstituted by washing embryos in PBT overnight or even over a weekend before starting the staining procedure, although staining will be weaker than in non-methanol-exposed embryos.
2. If combined AP staining and antibody staining (e.g., anti-EGFP) staining is desired, antibody staining should be done first. After the DAB (3,3′-diaminobenzidine) staining, do a quick post-fix and go straight into the washes for the AP protocol. AP staining works very well after an antibody stain. Alternatively, stain for exogenous AP phosphatase at a time point when the endogenous vascular form is not active (24 hpf).

## IV. Vital Imaging of Blood Vessels

While the methods described above are useful for visualizing vascular patterns in fixed zebrafish specimens, particularly at later developmental stages and in adults, the zebrafish is perhaps best known for its accessibility to vital imaging methods. A number of vascular imaging methods are available that take advantage of the optical clarity and experimental accessibility of zebrafish embryos and larvae. Confocal microangiography can be used for imaging blood vessels with active circulation and to detect defects in their patterning and/or function. Confocal microangiography is

**Table II**
**Zebrafish Transgenic Lines for Time-Lapse Vascular Imaging**

| Transgenic zebrafish line | Reference |
|---|---|
| *Tg(fli1a:EGFP)*$^{y1}$ | Lawson and Weinstein (2002) |
| *Tg(flii1a:nEGFP)*$^{y7}$ | Yaniv *et al.* (2006) |
| *Tg(flii1a:EGFP–cdc42wt)*$^{y48}$ | Kamei *et al.* (2006) |
| *Tg(mTie2:GFP)* | Motoike *et al.* (2000) |
| *Tg(kdrl:G-RCFP)* | Cross *et al.* (2003) |
| *Tg(kdrl:memCherry)*$^{s896}$ | Chi *et al.* (2008) |
| *Tg(kdrl:EGFP)*$^{s843}$ | Jin *et al.* (2005) |
| *Tg(fli1a: DsRed)* | Geudens *et al.* (2010) |
| *Tg(fli1a:EGFP; kdrl:ras-cherry)* | Hogan *et al.* (2009) |
| Tg*(flt1:YFP, kdrl:mCherryRed)* | Hogan *et al.* (2009) |
| *Tg(stabilin:YFP)*$^{hu4453}$ | Hogan *et al.* (2009) |
| *Tg(gata1:DsRed)*$^{sd2}$ | Traver *et al.* (2003) |

performed by injecting fluorescent microspheres into the circulation of living embryos, and then collecting 3-dimensional image "stacks" of the fluorescently labeled vasculature in the living animal using a confocal or (preferably) multiphoton microscope. This method can be used from the initiation of circulation at approximately 1 dpf out to 10 dpf or even older larvae, although injections become progressively more technically challenging to perform after about 2 dpf. Increasing tissue depth makes high-resolution imaging of deep vessels increasingly difficult at later stages. Repeated microangiographic imaging of the same animal and microangiography on animals with impaired circulation may be difficult or impossible to perform.

Numerous transgenic zebrafish lines have been generated with endogenous fluorescent labeling of blood or blood and lymphatic vessels (Table II). These animals facilitate high-resolution imaging of the vasculature *in vivo* and make possible long-term time-lapse imaging of the dynamics of vessel growth and remodeling. Unlike dye or resin injection methods, transgenic animals can be repeatedly re-imaged over an extended period of time with continued normal development of the imaged vessels, particularly when multiphoton imaging is employed.

Zebrafish *fli1a*:*EGFP* (Lawson and Weinstein, 2002), *kdrl*:*EGFP* (Cross *et al.*, 2003) and other transgenic zebrafish lines have already been widely used in studies of vasculogenesis and angiogenesis in the zebrafish. Since these lines permit imaging of the endothelial cells themselves, rather than vessel lumens, they can be used to image vessels that are not carrying circulation, cords of endothelial cells lacking a vascular lumens, or even isolated migrating angioblasts. The *fli1a*:*EGFP* line permits visualization of both blood and lymphatic vessels, while only blood endothelial cells are marked in the *kdrl*:*EGFP* line. The *fli1a*:*EGFP* line has already been used in a very large variety of studies, including examination of the mechanisms of cranial (Lawson and Weinstein, 2002) and trunk (Isogai *et al.*, 2003) blood vessel formation, lymphatic vessel formation (Yaniv *et al.*, 2006), and tumorigenesis (Stoletov *et al.*, 2007). The *fli1a* and *kdrl* promoters have also both been used to generate additional lines expressing other fluorescent proteins. Transgenic lines expressing nuclear-targeted EGFP (nEGFP) or membrane-targeted EGFP (EGFP-cdc42wt) have been derived. Multiphoton time-lapse imaging using *Tg*(*fli1a*:*nEGFP*)$^{y7}$ transgenic embryos has been used to trace the migration and lineage of individual endothelial cells and to quantify their proliferation (Yaniv *et al*., 2006). The *Tg*(*fli1a*:*EGFP–cdc42wt*)$^{y48}$ line has been used to visualize the dynamics of endothelial vacuoles and their contribution to vascular lumens formation (Kamei *et al*., 2006). By combining microangiographic imaging of functional vascular lumens using red quantum dots, and imaging of forming lumenal compartments using the *Tg*(*fli1a*:*EGFP–cdc42wt*)$^{y48}$, the details of progressive formation of vascular lumens (via formation and intracellular/intercellular fusion of endothelial vacuoles) and their connection to the rest of the vascular circulation could be followed dynamically *in vivo* for the first time (Kamei *et al*., 2006).

More recently, transgenic lines have been established with a variety of fluorescent proteins expressed under the control of a number of different endothelial promoters (Table II). Taking advantage of differences in the preferential labeling of different vascular promoters, double transgenic animals were generated for the specific observation on blood/lymph vessels, like *Tg*(*fli1a*:*EGFP; kdrl*:*ras-cherry*), or artery/venous sprouts *Tg*(*flt1*:*YFP; kdrl*:*mCherryRed*) (Hogan *et al*., 2009).

In addition to endothelial promoter-driven transgenic lines, hematopoietic-specific transgenic lines such as *Tg*(*gata1*:*DsRed*)$^{sd2}$ have proven useful for applications in vascular analysis. Motion-based imaging of blood flow has been used to characterize lumens formation, distinguish lymphatic vessels from blood vessels, and examine which vessels are patent and carrying blood flow in (*Tg*(*fli1a*:*EGFP; gata1*:*DsRed*) double transgenic animals (Tong *et al*., 2009; Yaniv *et al*., 2006).

Methods for confocal microangiography and time-lapse multiphoton imaging of transgenic animals are described in more detail below. Finally, we describe some of the novel insights into *in vivo* vessel formation processes that have already been obtained through use of time-lapse imaging methods.

## A. Microangiography

Confocal microangiography is useful for visualizing and assessing the patent circulatory system; blood vessels that are actually carrying blood flow or that at least have open lumens connected to the functioning vasculature. The method facilitates detailed study of the pattern, function, and integrity (leakiness) of vessels. The method is relatively easy to perform, particularly on younger animals, and does not require that the animal be of any particular genotype (although animals with impaired circulation may be difficult or impossible to infuse with fluorescent microspheres).

### a. Materials

- 0.02–0.04 μm fluoresceinated carboxylated latex beads, available from Invitrogen. The yellow-green (cat # F8787), red-orange (cat # F8794), or dark red (cat # F8783) beads are suitable for confocal imaging using the laser lines on standard Krypton–Argon laser confocal microscopes. Other colors may be used for when multiphoton imaging is employed. Quantum dots (QD) are fluorescent semiconductors that are especially suited for multiphoton imaging with their high quantum yield, as well as the fact that the same excitation wavelength could be used for obtaining multiple different colors depending on the QD used. For microangiography, PEG-coated non-targeted QDs are available from Invitrogen. Qtracker 565, 655, 705, and 800 (cat# Q21031MP, Q21021MP, Q21061MP, and Q21071MP, respectively) are suitable for multiphoton confocal imaging. The fluorescent bead suspension as supplied is diluted 1:1 with 2% BSA (Sigma) in deionized distilled water, sonicated approximately 25 cycles of 1" each at maximum power on a Branson sonifier equipped with a microprobe, and subjected to centrifugation for 2 min at top speed in an Eppendorf microcentrifuge. The quantum dots in supernatant are used as supplied.

- 1 mm OD glass capillaries (World Precision Instruments, Cat # TW100-4 without filament or TW100F-4 with an internal filament) for preparing holding and microinjection pipettes.
- 2 Coarse micromanipulators with magnetic holders and base plates.
- 30% Danieu's solution (1X Danieu's: 58 mM NaCl, 0.7 mM KCl, 0.4 mM MgSO4, 0.6 mM Ca(NO3)2, 5 mM Hepes, pH 7.6).
- Holding and microinjection pipettes.
- 6 cm culture dish (Falcon).
- Micromanipulator and microinjection apparatus.
- Dissecting microscope equipped with epifluorescence optics.

### b. Protocol

*Preparation of the apparatus*

1. The *glass microinjection needles* are prepared from 1 mm capillaries with internal filaments using a Kopf vertical pipette puller (approximate settings: heat = 12, solenoid = 4.5; see Fig. 7A for desired shape of microneedle). Needles are broken open with a razor blade just behind their tip to give an opening of approximately 5–10μm in width.
2. The *holding pipettes* are prepared from 1 mm capillaries WITHOUT filaments by partially melting one end of the capillary with a Bunsen burner, such that the opening is narrowed to approximately 0.2 mm (slightly smaller for younger embryos, slightly larger for older larvae). A photographic image of the end of the tip of a holding pipette is shown in Fig. 7B.
3. The *apparatus for microinjection* is made by attaching a glass microinjection needle (step 1) to a pipette holder (World Precision Inst Cat # MPH6912; adapter for holder and tubing to attach to picopump, WPI Cat # 5430). The pipette holder is attached to a controlled air pressure station such as World Precision Instruments Pneumatic Picopump (catalog # PV820).
4. The *apparatus for holding embryos* is made by attaching a glass holding pipette (step 2) to a pipette holder (World Precision Inst Cat # MPH6912). The holding pipettes and their holders are attached via mineral-oil filled tubing (Stoelting

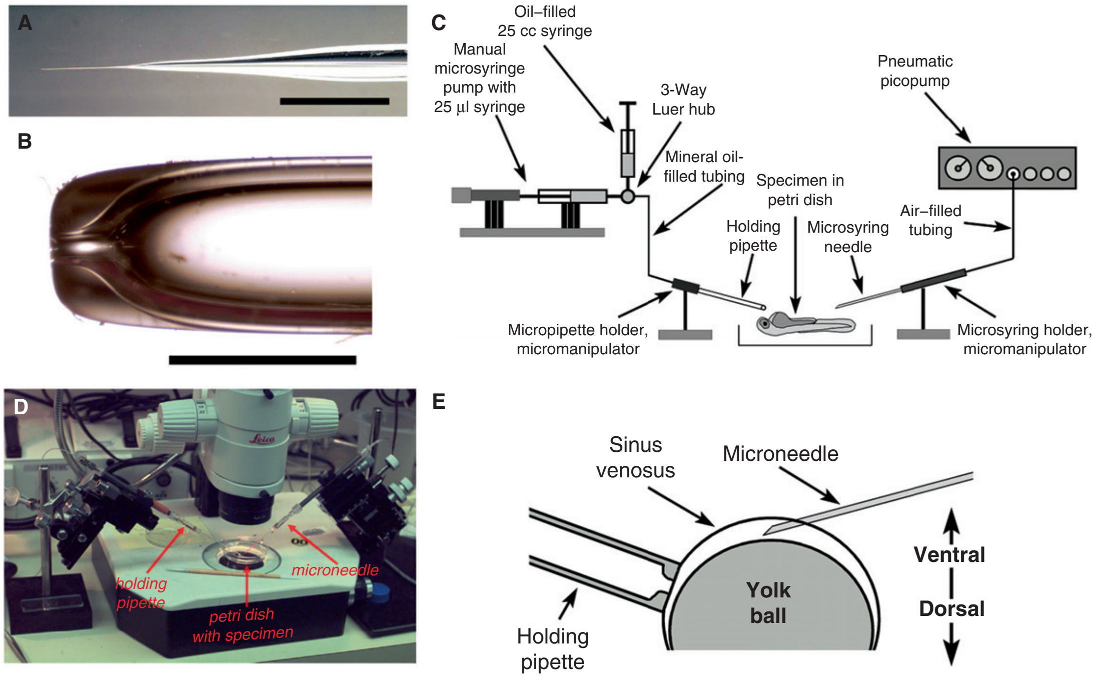
A
B
C
Oil–filled 25 cc syringe
Manual microsyringe pump with 25 µl syringe
3-Way Luer hub
Pneumatic picopump
Mineral oil-filled tubing
Specimen in petri dish
Holding pipette
Microsyring needle
Air–filled tubing
Micropipette holder, micromanipulator
Microsyring holder, micromanipulator
D
holding pipette
microneedle
petri dish with specimen
E
Sinus venosus
Microneedle
Ventral
Yolk ball
Dorsal
Holding pipette

**Fig. 7** Microangiography of developing zebrafish embryos and larvae. The desired configurations for injection needles (A) and holding pipettes (B) are shown. A schematic diagram of the apparatus used is shown in (C) and a photographic image of an actual setup is shown in (D). For injection, an embryo is held ventral side up with suction applied through the holding pipette and injected obliquely through the sinus venosus (E). Older larvae are injected by direct intracardiac injection. See text for details. Scale bars are 3 mm (A) and 1 mm (B).

Instruments, Clay-Adams cat # 427415) to a manual microsyringe pump (Stoelting Instruments cat # 51222, with 25 µl syringe).

5. Holding pipettes and microneedles and their associated holders and other equipment are arranged on either side of a stereo dissecting microscope as diagrammed in Fig. 7C. A photographic image of a typical arrangement is shown in Fig. 7D.

*Experimental procedure*

1. Embryos are collected and incubated to the desired stage of development. Use of albino mutant lines or PTU (1-phenyl-2-thiourea) treatment improves visualization of many vascular beds at later stages (see Westerfield 2000 for PTU treatment protocol).
2. A few microliters of fluorescent microsphere suspension are used to backfill a glass microneedle for injection. The tip should be broken off to the desired diameter just before use.
3. Embryos are dechorionated and anesthetized with tricaine in embryo media.

4. 1- to 3-day-old embryos and larvae are held ventral side up for injection using a holding pipette applied to the side of the yolk ball (Fig. 7E), with suction applied via a microsyringe driver. Care should be taken to not allow the holding pipette to rupture the yolk ball. 4- to 7–day-old larvae are held ventral side up for injection by embedding in 0.5% low-melting temperature agarose.
5. For 1- to 3-day-old embryos a broken glass microneedle is inserted obliquely into the sinus venosus (as diagrammed in Fig. 7E). For 4- to 7-day-old larvae a broken glass microneedle is inserted through the pericardium directly into the ventricle.

   For lymphangiographic labeling of the lymphatic vasculature injections are performed directly into the thoracic duct, located between the dorsal aorta and the cardinal vein. Lymphangiographic injections are generally significantly more difficult than angiographic injections of comparable stage embryos.

   Labeling of the lymphatic vasculature in living animals can also be accomplished by subcutaneous or intramuscular injections after insertion of the broken glass microneedle through the tough outer periderm of the developing animal. The dyes or microspheres are preferentially taken up by and drained through the lymphatic vessels. Injections should be performed at a site relatively distant to (preferably caudal to) the area to be imaged and the animal monitored after injection to choose the optimal time for imaging. This is when the dye has filled the lymphatic vessels, but has not yet diffused far from the site of injection through other tissues (which creates a high background labeling outside the lymphatics). Subcutaneous dye injection labeling of the lymphatics is most effective in older larvae (2 weeks +) in which the lymphatic vasculature is well developed.
6. Following microneedle insertion, many (20+) small boluses of bead suspension are delivered over the course of up to a minute. Smaller numbers of overly large boluses can cause temporary or permanent cardiac arrest. The epifluorescence attachment on the dissecting microscope can be used to monitor the success of the injection.
7. Embryos or larvae are allowed to recover from injection briefly (approximately 1 min) in tricaine-free embryo media, then rapidly mounted in 5% methylcellulose (Sigma) or low-melt agarose (both made up in embryo media with tricaine). For short-term imaging (generally one stack of images) methylcellulose is applied to the bottom of a thick depression well slide. The rest of the well is carefully filled with 30% Danieu's solution containing 1× Tricaine, trying not to disturb the methylcellulose layer below. The injected zebrafish embryo is placed in the well, moved on top of the methylcellulose, and then gently pushed into the methylcellulose in the desired orientation to fully immobilize. Methylcellulose is only useful for short-term mounting because the embryo gradually sinks in the methylcellulose (which also loses viscosity by absorbing additional water over time). For longer term or repeated imaging animals can be mounted in agarose, using methods such as that described below.
8. Injected, mounted animals are imaged on a confocal or multiphoton microscope using the appropriate laser lines/wavelengths. Although the fluorescent beads are initially distributed uniformly throughout the vasculature of the embryo, within minutes they

begin to be phagocytosed by and concentrated in selected cells lining the vessels (cf. "tail reticular cells" in Westerfield 2000). Because of this, specimens must be imaged as rapidly as possible, generally within 15 min after injection. Generally between 20 and 50 frame-averaged (5 frames) optical sections are collected with a spacing of 2–5 µm between sections, depending on the magnification (smaller spacing at higher magnifications). Three-dimensional reconstructions can be generated using a variety of commercial packages (see below).

## B. Imaging Blood Vessels in Transgenic Zebrafish

Confocal microangiography is a valuable tool for imaging developing blood vessels, but it has limitations. The method is well suited for delineating the luminal spaces of functional blood vessels, but those that lack circulation, vessels that have not yet formed open lumens, and isolated endothelial progenitor cells are essentially invisible. Much of the "action" of early blood vessel formation occurs prior to the initiation of circulation through the relevant vessels. The first, major axial vessels of the zebrafish trunk, the dorsal aorta and cardinal vein, coalesce as defined cords of cells at the trunk midline with distinct molecular arterial-venous identities many hours before they actually begin to carry circulation. Later-developing vessels generally form by sprouting and migration of strings of endothelial cells or even individual cells that are likewise undetectable by angiography until well after their initial growth has been completed. Furthermore, because of leakage of low molecular weight dyes, or pinocytotic clearance of microspheres, injected animals can only be imaged for a short time (up to 1/2 h) after injection and repeated imaging requires re-injection of microspheres with different excitation and emission spectra. Thus, for most practical purposes dynamic imaging of blood vessel growth using this method is not possible. What is needed is a specific and durable fluorescent "tag" for endothelial cells and their angioblast progenitors.

As already described, autofluorescent proteins such as GFP have been used to mark a variety of tissues in transgenic zebrafish embryos and larvae. Methods for generating germline transgenic zebrafish are now widely used and their application and resulting lines have been thoroughly reviewed elsewhere (Lin, 2000; Udvadia and Linney, 2003). Tissue-specific expression of fluorescent (or other) proteins in germline transgenic animals is achieved through the use of tissue-specific promoters, and a number of different promoters have been used to drive fluorescent protein expression in zebrafish vascular endothelium. Murine *Tie2* (a tyrosine kinase receptor expressed in endothelium activated by angiopoietin ligands) promoter constructs drive GFP expression in endothelial cells in mice and zebrafish, and stable germline transgenic lines have been prepared in both species (Motoike *et al*., 2000). The usefulness of mTie2-GFP has been limited in fish by the fact that germline transgenic zebrafish show substantial non-vascular expression of GFP in the hindbrain and more posterior neural tube. The overall level of expression from the murine promoter is also relatively low in fish compared to mice. Germline transgenic zebrafish have also been generated expressing EGFP (enhanced green fluorescent protein) in the vasculature under the control of the zebrafish *fli1a* promoter (Lawson and Weinstein, 2002). The *fli1a* is a transcription factor expressed in the presumptive hemangioblast lineage, and later restricted to vascular endothelium, cranial neural crest derivatives, and a small subset of myeloid derivatives (Brown *et al*., 2000). These lines express abundant EGFP in the vasculature, faithfully recapitulating the expression pattern of the endogenous *fli1a* gene, and permitting resolution of very fine cellular features of vascular endothelial cells *in vivo*. The *fli1*a:*EGFP* transgenic lines have become the most widely used resource for transgenic visualization of blood vessels and have already been used in a variety of different published studies to examining developing trunk and cranial vessels (Isogai *et al*., 2003; Lawson and Weinstein, 2002; Roman *et al*., 2002) and regenerating vessels in the adult fin (Huang *et al*., 2003). Most recently, transgenic zebrafish with fluorescently labeled blood vessels have also been generated by using the promoter for the *kdrl* receptor tyrosine kinase to drive EGFP expression in endothelium (Cross *et al*., 2003).

Here, we review methods for exploiting what is perhaps the most important feature of these transgenics, that they permit repeated and continuous imaging of the fluorescently labeled blood vessels. This has made it possible, for the first time, to image the dynamics of blood vessel growth and development of vascular networks in living animals. We describe methods for mounting embryos and larvae for long-term observation and for time-lapse multiphoton microscopy of blood vessels within these animals. The mounting of animals for time-lapse imaging is much more difficult and in some ways more critical to the success of the experiment than the actual imaging, which is relatively straightforward to set up on most imaging systems.

## 1. Long-Term Mounting for Time-Lapse Imaging

For time-lapse imaging of blood vessels in transgenic fish over the course of hours or even days, the animals must be carefully mounted in a way that maintains the region of the animal being imaged in a relatively fixed position, yet keeps the animal alive and developing normally throughout the course of the experiment. This task is complicated further by the fact that developing zebrafish are continuously growing and undergoing morphogenetic movements and this must be accommodated in whatever scheme is used to hold them in place. We describe below a relatively simple mounting method that is adaptable to imaging different areas of embryos or larvae and holds them in place over the course of hours. For time-lapse experiments that run up to a day or more imaging chambers with buffer circulation are employed.

### a. Materials

- Imaging chambers (see below)
- 2% low-melting temperature agarose made up in 30% Danieu's solution containing 1X PTU (if non-albino animals are used) and 1.25X Tricaine (if non-paralyzed animals are used)

- 30% Danieu's solution with or without 1× PTU and 1.25× Tricaine (see above)
- Fine forceps (Dumont #55)

### b. Method

*Preparation of imaging chambers*

1. Imaging vessels are prepared from 6 cm polystyrene culture dishes (Falcon 3002) and 14 ml polypropylene tubes (Falcon 2059). Model cement is also required for assembly.
2. The polypropylene tube is sliced into 5 mm segments (rings) using a heated razor blade. One ring is glued to the bottom plate of the culture dish using model cement. Care should be taken to glue the slice of the polypropylene tube to the center of the dish and to avoid smearing the glue inside the polypropylene ring (to avoid obscuring the optical clarity). See Fig. 8A.
3. The glue should be allowed to dry overnight before use.
4. Just before use the polypropylene ring in the imaging chamber should be slightly overfilled with the low-melting temperature agarose to make a slightly convex dome (Fig. 8A).
5. Time-lapse imaging for longer duration (more than 1 day) requires a modified version of this chamber. Instead of using a 6 cm polystyrene culture dish, a T-25 tissue culture flask (Nalge Nunc cat# 163371) is used. A 1–1/2" square is cut from the upper side of the flask with a coping saw. The opening should stretch from one side of the flask to the other, and be large enough to accommodate the objective lens to be used in the observation. Portions of the adjoining walls of the flask should also be cut down as shown in (Fig. 8B) in order to allow the objective lens to enter the imaging chamber. A second opening is made in the bottom of the flask opposite the cap by drilling a 3/32" hole using an electric drill. This second opening is to be used for the inflow port, and it should be large enough to accommodate the female Luer bulkhead (Small Parts, Inc., 3/32" barb, cat# LCN-FB-093-25). A silicone O-ring (Small Parts, Inc., 1/4" ID × 3/8" OD × 1/16" wide, cat# ORS-010-25) is inserted over the bulkhead before its attachment to the flask, and then secured onto the flask with a locking nut (Small Parts, Inc., cat# LCN-LN0-25). A 5 mm-wide slice of a 14 ml Falcon tube is glued to the center of the chamber opposite the large opening using Z-Poxy resin (Small Parts, Inc., cat# EPX-PT38). Baffles are made from a lid of a 14 ml Falcon tube, and also glued on inside of the chamber, one over the inlet port and another one before the outlet. Another small hole on the top of the chamber was made by drilling to allow the insertion of a temperature probe into the chamber. The cap of the flask needs to be modified so that the Luer bulkhead can be attached. The center portion of the lid is excised and discarded. The Luer female bulkhead is then screwed tightly onto the lid with an O-ring. To prevent flooding of the stage should accidental overflow of the chamber occur a safety drain is installed into the side of the chamber ("Gutter" in Fig. 8B). The safety drain is constructed from a plastic drinking straw connected to a cutoff disposable

pipette. The bulb and first 1” of the pipette are removed. A quarter of the wall of the main pipette body was also removed to form a catchment opening for chamber overflow. This piece is attached to the side of the chamber at an angle of 25–30° using Z-Poxy resin. After drying, a plastic drinking straw is connected to the drain to lead the overflow to a container. The completed chamber is air-dried for overnight to allow all resin to cure, and then tested for any leakage by filling it with distilled water before use.

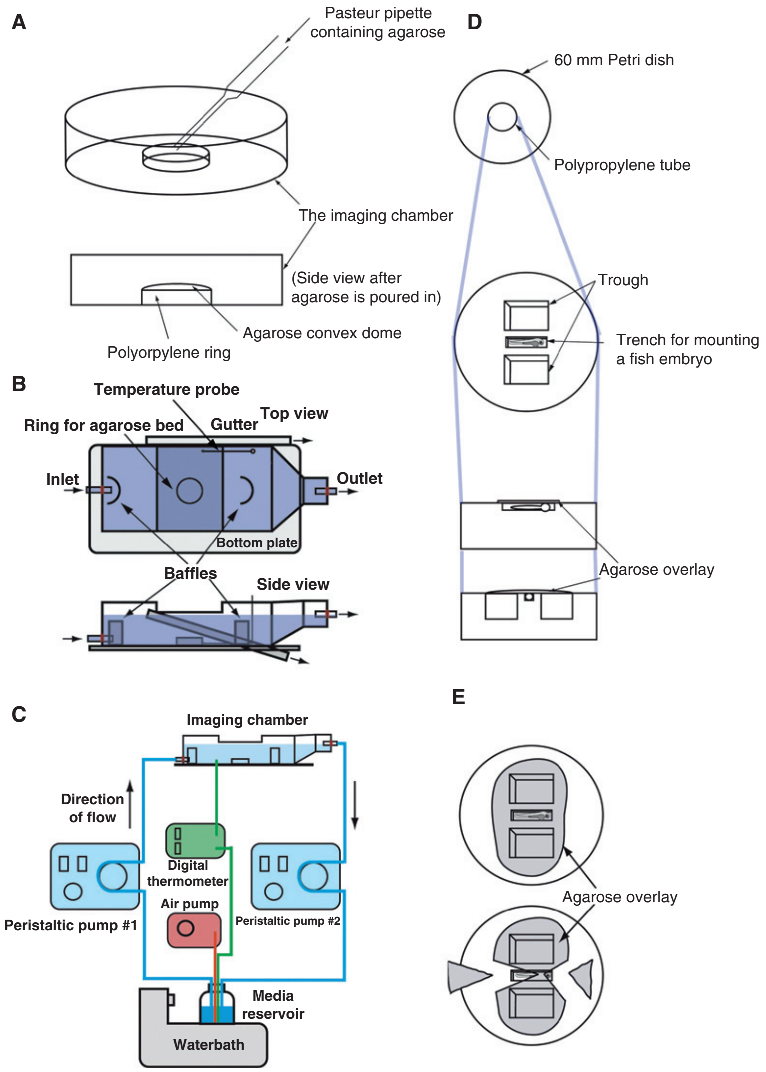
A
Pasteur pipette containing agarose
The imaging chamber
(Side view after agarose is poured in)
Agarose convex dome
Polyorpylene ring
B
Temperature probe
Ring for agarose bed
Gutter
Top view
Inlet
Outlet
Bottom plate
Baffles
Side view
C
Imaging chamber
Direction of flow
Digital thermometer
Air pump
Peristaltic pump #1
Peristaltic pump #2
Media reservoir
Waterbath
D
60 mm Petri dish
Polypropylene tube
Trough
Trench for mounting a fish embryo
Agarose overlay
E
Agarose overlay

**Fig. 8** *(Continued)*

6. The imaging chamber forms part of a loop of fluid circulation connected together with silicone tubing (Fig. 8B and C). Embryo media warmed in a bottle in a waterbath is carried through silicone tubing to the chamber by a peristaltic pump. Excess media is continuously removed from the chamber and returned to the media reservoir by a second peristaltic pump. The embryo media in the reservoir is aerated by an aquarium air pump. The temperature of the waterbath is calibrated to warm the media sufficiently to maintain a constant temperature (28.5°C) in the imaging chamber (an electronic temperature probe measures the temperature in the imaging chamber). The required waterbath temperature should be determined empirically and depends on a number of factors including the ambient temperature of the room, the length and diameter of the tubing between the reservoir and imaging chamber, and the flow rate. In a cool room with long tubing the temperature of the waterbath may need to be 37°C or even higher.

*Mounting animals in imaging chambers*

These procedures are done on a dissecting microscope.

1. Dechorionate and select embryos for mounting. Only a single embryo is generally mounted per imaging chamber.
2. Fill the imaging vessel with the 30% Danieu's solution to just below the rim of the petri dish. If pigment-free albino mutant embryos are used, the PTU can be left out, and if paralyzed mutant embryos are used the tricaine can be left out of the Danieu's solution.
3. Pick an embryo for mounting, and drop it in the middle of the agarose bed (it may begin to roll of because of the convex surface).
4. Using the fine forceps blades, make a shallow, narrow trench in the center of the agarose dome. This trench should be slightly wider than the dimensions of the embryo in its desired orientation for imaging, with the animal below the surface of the agarose but not too deep (Fig. 8D). It is critical that the trench be carved out carefully to make a space that holds the animal relatively motionless at rest. For imaging most portions of later stage embryos and larvae the animal should lie on its side in the trench, for lateral view. A larger cavity should be carved out posterior to

---

**Fig. 8** Mounting zebrafish embryos and larvae for time-lapse imaging. For shorter-term imaging, imaging chambers are prepared from a ring of polypropylene tube glued to a 60 mm petri dish (A). For long-term (greater than 1 day) time-lapse imaging, an imaging chamber is constructed from a modified tissue culture flask (B). The approximate areas filled with water in an operating chamber are noted in blue. For details on construction, see text and Kamei & Weinstein (2005). The imaging chamber is a key part of the apparatus used for long-term time-lapse imaging of developing zebrafish, diagrammed schematically here (C). Tubing carrying water is noted in blue, wires for temperature probe are shown in green, and the air line is shown in red. The inlet and outlet ports of the imaging chamber are each connected via silicone tubing through two separate peristaltic pumps to a heated, aerated reservoir of embryo buffer, forming a continuous circuit of fluid. Temperature of the imaging chamber and fluid reservoir are both monitored using separate temperature probes, and the reservoir is continuously aerated with an aquarium air pump. See text and Kamei & Weinstein (2005) for additional details. In either short- or long-term imaging chambers the polypropylene ring in the center is filled with low-melt agarose and cavities carved out to accommodate the animal and to act as anchor points for top agarose (D). After covering the animal with top agarose much of the agarose over the animal is carved away in wedges (E). See text for further details. (See Plate no. 3 in the Color Plate Section.)

the tail to accommodate additional increases in trunk/tail length. Additional space should also be left around the head to accommodate shifting and growth, particularly in younger animals.

5. Two additional large cavities should also be carved out perpendicular to the trench on either side (Fig. 8D). These cavities will act as anchor points for the agarose layer that is overlaid on top of the embryo.
6. Place the embryo in the trench, and slowly overlay with molten agarose. It should be warm enough to freely flow in the buffer, but not too hot to kill the embryo. We typically use glass Pasteur pipette for this since it offers more precise control. Start from one well next to the trench. Apply the agarose at steady rate, and once it filled the well, move over to the other well by moving the pipette over the embryo. Once positioned over the other well, fill up this well also (Fig. 8E). This should create an agarose bridge over the embryo and should hold the embryo down.
7. Cut excess agarose away by using the blades of a pair of fine forceps. For imaging the trunk, we slice away a triangle of agarose over the trunk and tail and over the rostral region, leaving a "bridge" of agarose over the yolk sac, posterior head, and anterior-most trunk sufficient to hold the embryo firmly in place (Fig. 8E). This ensures the optical clarity of the trunk vessels. These cuts are necessary, since the embryo is growing in anterior-posterior axis, and straightening. Without removing these wedges of agarose, continued growth and straightening of the embryo/larva could not be accommodated.

## 2. Multiphoton Time-Lapse Imaging

Once animals are properly mounted they can be imaged by relatively straightforward time-lapse imaging methods. It is strongly recommended that a multiphoton microscopy system be used for this rather than a standard confocal microscope. The advantages of multiphoton microscopy and its use in developmental studies have been reviewed elsewhere (Denk and Svoboda, 1997; Weinstein, 2002). Multiphoton imaging reduces photodamage over the course of long imaging experiments, improves resolution of fluorescent structures deep in tissues, and improves the "three dimensionality" of resulting image reconstructions. Most imaging systems designed for or adaptable to multiphoton imaging (Leica, Zeiss, Olympus, etc.) have software interfaces that allow simple implementation of "4-D imaging" (*x, y, z*, time) experiments. Below we provide a cursory experimental description with some of the important parameters and experimental considerations. The melanophores in developing embryos interfere with multiphoton imaging when 976 nm excitation (EGFP two-photon excitation wavelength) is used. This interference can be avoided either by imaging techniques (moving the field of view), by treating embryos with PTU, or by using genetic mutants lacking or with reduced melanophores (such as *albino, nacre,* or *casper*) (Lister *et al*., 1999; White *et al*., 2008). PTU should be used carefully in later stage embryos because it may cause developmental defects. Use of tricaine (MS-222) for extended periods of time can also be problematic as the proper dosage for the drug becomes difficult to control, and excess tricaine can easily kill the animal. For imaging experiment lasting longer than 1 day, the use of paralyzed *nic1* mutant animals (Westerfield *et al*., 1990) is strongly encouraged.

1. Transfer the imaging chamber with mounted animal very carefully to the stage of a multiphoton microscope, taking care not to dislodge the animal. If the animal is very easily dislodged in transfer then it was likely not well enough mounted and should be more securely held when re-mounted.
2. After locating the field to be imaged, the time-lapse parameters should be set. Below are listed some guidelines for a few of the important parameters for multiphoton transgenic blood vessel imaging:

| | |
|---|---|
| Maximal imaging depth: | approximately 250 μm for best image quality |
| Objectives: | 10–100X, must pass long wavelength light |
| Spacing between planes: | 1–5 μm, depending on magnification |
| Number of planes imaged: | 10–60, depending on region and magnification |
| Interval between time points: | 1–15 min (5 min is most typical) |
| Length of timelapse: | Up to 24 h, longer if a chamber is used with circulation of warmed buffer. With such a chamber, we have successfully imaged an animal for 5 days (Kamei and Weinstein, 2005). The chamber without flow described above is mainly used for shorter time-lapse experiments, and some developmental delay may be noted in longer runs. |
| Laser power setting: | Minimum necessary to obtain good images; if possible increase power with greater depth and use sensitive detectors to permit further decreases in required power. |
| Frames averaged: | 5 frames averaged/plane |

3. Once an imaging run has been initiated the images being collected should be checked frequently for shifting of the field being imaged. Often some shifting occurs due to growth or morphogenetic movements of the developing animal. Some shifting is also sometimes seen at the beginning of a time-lapse run as the animal “settles in.” The field being imaged will sometimes need to be adjusted several times during the course of an experiment to maintain the vessels being imaged within the field. The stage can be adjusted to reset the X and Y positions. The Z positions (bottom and top of the images stack) may also need to be reset, usually by stopping and restarting the time-lapse program. If excessive shifting occurs due to the embryo being improperly mounted a new animal should be re-mounted.

## V. Conclusion

Recent evidence suggests that genetic factors are critical in the formation of major vessels form during early development. Understanding the mechanisms behind the emergence of these early vascular networks will require the use of genetically and experimentally accessible model vertebrates. The accessibility and optical clarity of the zebrafish embryo and larva make it particularly useful for studies of vascular development. Studies of developing vessels are likely to have far-reaching implications for human health, since understanding mechanisms underlying the growth and morphogenesis of blood vessels has become critical for a number of important emerging clinical applications. Pro- and anti-angiogenic therapies show great promise for treating cancer and ischemia, respectively, and a great deal of effort is currently going into uncovering and characterizing factors that can be used to promote or inhibit vessel growth *in vivo*. Since many of the molecules that play key roles in developing vessels carry out analogous functions during postnatal angiogenesis, it seems likely that the zebrafish will yield many important clinically applicable insights in the future.

## References

Brown, L.A., Rodaway, A.R., Schilling, T.F., Jowett, T., Ingham, P.W., Patient, R.K., and Sharrocks, A.D. (2000). Insights into early vasculogenesis revealed by expression of the ETS-domain transcription factor Fli-1 in wild-type and mutant zebrafish embryos. *Mech. Dev.* **90**, 237–252.

Bussmann, J., Lawson, N., Zon, L., and Schulte-Merker, S. ( 2008). Zebrafish VEGF receptors: A guideline to nomenclature. *PLoS Genet*. **4**, e1000064.

Cheong, S.M., Choi, S.C., and Han, J.K. ( 2006). Xenopus Dab2 is required for embryonic angiogenesis. *BMC Dev. Biol*. **6**, 63.

Chi, N.C., Shaw, R.M., De Val, S., Kang, G., Jan, L.Y., Black, B.L., and Stainier, D.Y. (2008). Foxn4 directly regulates tbx2b expression and atrioventricular canal formation. *Genes Dev.* **22**, 734–739.

Childs, S., Chen, J.N., Garrity, D.M., and Fishman, M.C. ( 2002). Patterning of angiogenesis in the zebrafish embryo. *Development* **129**, 973–982.

Cross, L.M., Cook, M.A., Lin, S., Chen, J.N., and Rubinstein, A.L. (2003). Rapid analysis of angiogenesis drugs in a live fluorescent zebrafish assay. *Arterioscler. Thromb. Vasc. Biol.* **23**, 911–912.

Denk, W., and Svoboda, K. ( 1997). Photon upmanship: Why multiphoton imaging is more than a gimmick. *Neuron* **18**, 351–357.

Evans, H. (1910). "Manual of Human Embryology." J. B. Lippincott & Company, Philadelphia, PA and London.

Fouquet, B., Weinstein, B.M., Serluca, F.C., and Fishman, M.C. (1997). Vessel patterning in the embryo of the zebrafish: Guidance by notochord. *Dev. Biol.* **183**, 37–48.

Gering, M., Rodaway, A.R., Gottgens, B., Patient, R.K., and Green, A.R. (1998). The SCL gene specifies haemangioblast development from early mesoderm. *EMBO J.* **17**, 4029–4045.

Geudens, I., Herpers, R., Hermans, K., Segura, I., Ruiz de Almodovar, C., Bussmann, J., De Smet, F., Vandevelde, W., Hogan, B.M., Siekmann, A., *et al*. (2010). Role of Dll4/Notch in the Formation and Wiring of the Lymphatic Network in Zebra Fish. *Arterioscler. Thromb. Vasc. Biol.* **30**, 1695–1702.

Hauptmann, G., and Gerster, T. (1994). Two-color whole-mount in situ hybridization to vertebrate and Drosophila embryos. *Trends Genet*. **10**, 266.

Herpers, R., van de Kamp, E., Duckers, H.J., and Schulte-Merker, S. (2008). Redundant roles for sox7 and sox18 in arteriovenous specification in zebrafish. *Circ. Res*. **102**, 12–15.

Hogan, B.M., Bos, F.L., Bussmann, J., Witte, M., Chi, N.C., Duckers, H.J., and Schulte-Merker, S. (2009). Ccbe1 is required for embryonic lymphangiogenesis and venous sprouting. *Nat. Genet*. **41**, 396–398.

Huang, C.C., Lawson, N.D., Weinstein, B.M., and Johnson, S.L. (2003). reg6 is required for branching morphogenesis during blood vessel regeneration in zebrafish caudal fins. *Dev. Biol*. **264**, 263–274.

Isogai, S., Lawson, N.D., Torrealday, S., Horiguchi, M., and Weinstein, B.M. (2003). Angiogenic network formation in the developing vertebrate trunk. *Development* **130**, 5281–5290.

Jin, S.W., Beis, D., Mitchell, T., Chen, J.N., and Stainier, D.Y. (2005). Cellular and molecular analyses of vascular tube and lumen formation in zebrafish. *Development* **132**, 5199–5209.

Kaipainen, A., Korhonen, J., Mustonen, T., van Hinsbergh, V.W., Fang, G.H., Dumont, D., Breitman, M., and Alitalo, K. (1995). Expression of the fms-like tyrosine kinase 4 gene becomes restricted to lymphatic endothelium during development. *Proc. Natl. Acad. Sci. U.S.A*. **92**, 3566–3570.

Kamei, M., Saunders, W.B., Bayless, K.J., Dye, L., Davis, G.E., and Weinstein, B.M. (2006). Endothelial tubes assemble from intracellular vacuoles *in vivo*. *Nature* **442**, 453–456.

Kamei, M., and Weinstein, B.M. (2005). Long-term time-lapse fluorescence imaging of developing zebrafish. *Zebrafish* **2**, 113–123.

Lawson, N.D., Scheer, N., Pham, V.N., Kim, C.H., Chitnis, A.B., Campos-Ortega, J.A., and Weinstein, B.M. (2001). Notch signaling is required for arterial-venous differentiation during embryonic vascular development. *Development* **128**, 3675–3683.

Lawson, N.D., and Weinstein, B.M. (2002). *In vivo* imaging of embryonic vascular development using transgenic zebrafish. *Dev. Biol.* **248**, 307–318.

Lin, S. (2000). Transgenic zebrafish. *Methods Mol. Biol*. **136**, 375–383.

Lister, J.A., Robertson, C.P., Lepage, T., Johnson, S.L., and Raible, D.W. (1999). Nacre encodes a zebrafish microphthalmia-related protein that regulates neural-crest-derived pigment cell fate. *Development* **126**, 3757–3767.

Lyons, M.S., Bell, B., Stainier, D., and Peters, K.G. (1998). Isolation of the zebrafish homologues for the tie-1 and tie-2 endothelium-specific receptor tyrosine kinases. *Dev. Dyn*. **212**, 133–140.

Motoike, T., Loughna, S., Perens, E., Roman, B.L., Liao, W., Chau, T.C., Richardson, C.D., Kawate, T., Kuno, J., Weinstein, B.M., *et al*. (2000). Universal GFP reporter for the study of vascular development. *Genesis* **28**, 75–81.

Murakami, T. (1972). Vascular arrangement of the rat renal glomerulus: A scanning electron microscope study of corrosion casts. *Arch. Histol. Jap*. **34**, 87–107.

Roman, B.L., Pham, V.N., Lawson, N.D., Kulik, M., Childs, S., Lekven, A.C., Garrity, D.M., Moon, R.T., Fishman, M.C., Lechleider, R.J., *et al*. (2002). Disruption of acvrl1 increases endothelial cell number in zebrafish cranial vessels. *Development* **129**, 3009–3019.

Sabin, F.R. (1917). Origin and development of the primitive vessels of the chick and of the pig. *Carnegie Contrib. Embryol*. **6**, 61–124.

Stoletov, K., Montel, V., Lester, R.D., Gonias, S.L., and Klemke, R. (2007). High-resolution imaging of the dynamic tumor cell vascular interface in transparent zebrafish. *Proc. Natl. Acad. Sci. U.S.A*. **104**, 17406–17411.

Sumanas, S., Jorniak, T., and Lin, S. (2005). Identification of novel vascular endothelial-specific genes by the microarray analysis of the zebrafish cloche mutants. *Blood* **106**, 534–541.

Sumoy, L., Keasey, J.B., Dittman, T.D., and Kimelman, D. (1997). A role for notochord in axial vascular development revealed by analysis of phenotype and the expression of VEGR-2 in zebrafish flh and ntl mutant embryos. *Mech. Dev*. **63**, 15–27.

Szeto, D.P., Griffin, K.J., and Kimelman, D. (2002). HrT is required for cardiovascular development in zebrafish. *Development* **129**, 5093–5101.

Thompson, M.A., Ransom, D.G., Pratt, S.J., MacLennan, H., Kieran, M.W., Detrich, H. W.3rd, Vail, B., Huber, T.L., Paw, B., Brownlie, A.J., *et al*. (1998). The cloche and spadetail genes differentially affect hematopoiesis and vasculogenesis. *Dev. Biol.* **197**, 248–269.

Tong, E.Y., Collins, G.C., Greene-Colozzi, A.E., Chen, J.L., Manos, P.D., Judkins, K.M., Lee, J.A., Ophir, M.J., Laliberte, F.M., and Levesque, T.J. (2009). Motion-based angiogenesis analysis: A simple method to quantify blood vessel growth. *Zebrafish* **6**, 239–243.

Traver, D., Paw, B.H., Poss, K.D., Penberthy, W.T., Lin, S., and Zon, L.I. (2003). Transplantation and *in vivo* imaging of multilineage engraftment in zebrafish bloodless mutants. *Nat. Immunol.* **4**, 1238–1246.

Udvadia, A.J., and Linney, E. (2003). Windows into development: Historic, current, and future perspectives on transgenic zebrafish. *Dev. Biol.* **256**, 1–17.

Weinstein, B. (2002). Vascular cell biology *in vivo*. A new piscine paradigm?*Trends Cell Biol*. **12**, 439–445.

Westerfield, M.(2000). “The Zebrafish Book. A Guide for the Laboratory Use of Zebrafish (Danio Rerio),” 4th ed. University of Oregon Press, Eugene.

Westerfield, M., Liu, D.W., Kimmel, C.B., and Walker, C. (1990). Pathfinding and synapse formation in a zebrafish mutant lacking functional acetylcholine receptors. *Neuron* **4**, 867–874.

White, R.M., Sessa, A., Burke, C., Bowman, T., LeBlanc, J., Ceol, C., Bourque, C., Dovey, M., Goessling, W., Burns, C.E., *et al*. (2008). Transparent adult zebrafish as a tool for *in vivo* transplantation analysis. *Cell Stem Cell*. **2**, 183–189.

Yaniv, K., Isogai, S., Castranova, D., Dye, L., Hitomi, J., and Weinstein, B.M. (2006). Live imaging of lymphatic development in the zebrafish. *Nat. Med.* **12**, 711–716.

Zhong, T.P., Rosenberg, M., Mohideen, M.A., Weinstein, B., and Fishman, M.C. (2000). gridlock, an HLH gene required for assembly of the aorta in zebrafish. *Science* **287**, 1820–1824.

## CHAPTER 3

# Medaka Haploid Embryonic Stem Cells

**Yunhan Hong**
Department of Biological Sciences, National University of Singapore, Singapore 117543

---

Abstract
I. Introduction
  A. Haploidy in Evolution
  B. History Toward Haploid ES Cell Culture
  C. Rationale
II. Methods
  A. Production of Haploid Embryos
  B. Cell Culture Derivation
  C. Culture Condition
  D. Generation of Stable Haploid ES Cell Lines
  E. Characterization of Haploid ES Cells
  F. Stable Growth and Genetic Stability
III. Applications of Haploid ES Cells
  A. Semicloning
  B. Analysis of Gene Function
  C. Haploid Genetic Screens
IV. Summary
Acknowledgments
References

## Abstract

The appearance of diploidy, the presence of two genomes or chromosome sets, is a fundamental hallmark of eukaryotic evolution and bisexual reproduction, because diploidy offers the basis for the bisexual life cycle, allowing for oscillation between diploid and haploid phases. Meiosis produces haploid gametes. At fertilization, male and female gametes fuse to restore diploidy in a zygote, which develops into a new life. At sex maturation, diploid cells enter into meiosis, culminating in the production of haploid gametes. Therefore, diploidy ensures pluripotency, cell proliferation, and

Copyright © 2010 Elsevier Inc. All rights reserved.

978-0-12-384892-5
DOI: 10.1016/B978-0-12-384892-5.00003-7

functions, whereas haploidy is restricted only to the post-meiotic gamete phase of germline development and represents the end point of cell growth. Diploidy is advantageous for evolution. Haploidy is ideal for genetic analyses, because any recessive mutations of essential genes will show a clear phenotype in the absence of a second gene copy. Recently, my laboratory succeeded in the generation of medaka haploid embryonic stem (ES) cells capable of whole animal production. Therefore, haploidy in a vertebrate is able to support stable cell culture and pluripotency. This finding anticipates the possibility to generate haploid ES cells in other vertebrate species such as zebrafish. These medaka haploid ES cells elegantly combine haploidy and pluripotency, offering a unique yeast-like system for *in vitro* genetic analyses of molecular, cellular, and developmental events in various cell lineages. This chapter is aimed to describe the strategy of haploid ES cell derivation and their characteristics, and illustrate the perspectives of haploid ES cells for infertility treatment, genetic screens, and analyses.

## I. Introduction

Our interest in creating haploid embryonic stem (ES) cells comes from the curiosity and need. It has been well known for centuries that haploidy, the presence of a single genome or a complete set of chromosomes or genes within a cell, is an excellent system for genetic analyses of molecular events, because any recessive mutations of genes essential, for example, tumor suppressors and pluripotency will show a clear phenotype in the absence of a second gene copy. However, haploidy in eukaryotes is usually restricted to single-celled organisms, among them is the yeast (*Saccharomyces cerevisiae*), which has been best employed in genetic analyses (Botstein and Fink, 1988). Multicellular organisms, in particular vertebrates, are usually diploid and contain two genomes, one from the father and the other from the mother. The absence of haploid vertebrates has raised a fundamental question as to whether haploidy can support normal development in these organisms. Curiously, it is completely unknown about the absence of haploid vertebrates.

ES cells are an excellent system for experimental analyses of cellular and developmental events *in vitro*. ES cells are derived from early fertilization embryos (Evans and Kaufman, 1981), and induced pluripotent stem (iPS) cells can even be derived by reprogramming from various differentiated types of cells (Takahashi and Yamanaka, 2006). These are diploid fertilization ES or iPS cells, because they originate directly from fertilization embryos or indirectly from their differentiated derivatives and contain two chromosome sets. Although these diploid ES cells have been widely used for studying vertebrate development *in vitro*, a direct analysis of recessive phenotypes has been hampered by their diploidy. Therefore, it is highly desirable to create haploid ES cells to combine haploidy and pluripotency for developmental genetic analyses in biomedicine, because any recessive and disease phenotypes of essential genes can easily be dissected *in vitro* either in an undifferentiated state or under various differentiation schemes to follow molecular, cellular, and developmental events during the restriction of various cell lineages and differentiation of various cell types. Similarly, genes essential for normal and diseased cellular metabolism can also be investigated on a well-defined genetic background.

In this chapter, we will discuss the practice for our recent success in the generation of first haploid ES cells from the fish medaka (*Oryzias latipes*) (Yi *et al.*, 2009). We will focus on the rationale and strategies we have used to help readers develop an intuitive understanding of the possibility and approach to derive haploid ES cells from other organisms. Detailed experimental protocols will be published elsewhere (Yi *et al.*, 2010). We will also discuss problems and future directions.

## A. Haploidy in Evolution

In most bisexual animals, haploidy oscillates with diploidy. Diploidy ensures mitotic divisions and pluripotency throughout life, whereas haploidy exists only in the post-meiotic germline and lacks the mitotic ability, and thus represents the dead end of the life unless fertilization to restore diploidy in a zygote. Haploidy is the ancestral status of evolution. In a broad sense, all viruses and prokaryotic organisms are haploid. They often possess a single RNA or DNA molecule as their genome. In single-celled eukaryotic organisms such as yeast, the genome usually comprises several DNA molecules that are compacted with proteins into individual chromosomes. In these single-celled organisms, haploidy prevails, and cell divisions by fission or budding lead to individual propagation. This is asexual reproduction. Under defined conditions such as starvation, these haploid organisms fuse together to form transient diploid cells, which immediately undergo meiosis and become haploid cells. In plants, haploid callus and pollens in culture can form plantlets. It is well known in certain invertebrates such as the honeybee (Heimpel and de Boer, 2008) that parthenogenetic haploid embryos can develop into adult animals. Therefore, haploidy in these unicellular organisms, in plants, and in invertebrates is associated with the intrinsic ability for continuous cell divisions, pluripotency *in vivo*, fertility, and heredity. However, haploid organisms have so far been absent in vertebrates.

## B. History Toward Haploid ES Cell Culture

Driven by the enormous potential for genetic analyses in biomedicine, haploid cell cultures have attracted considerable interest. Pioneer work was done in frog, where androgenetic embryos at the late tail-bud stage produced two cell lines, which consisted of diploid and near-haploid populations but could not give rise to pure near-haploid cultures (Freed and Mezger-Freed, 1970). Later on in *Drosophila*, several cultures were derived from haploid embryos, which initially had a high percentage of 80–90% of haploid cells but were quickly overgrown by diploidy and aneuploidy in serial culture (Debec, 1978, 1984). In human, a heterogeneous culture called KBM7 was obtained from near-haploid chronic myeloid leukemia, which was unstable and quickly overgrown by diploid cells (Andersson *et al.*, 1987). By making use of their expertise in the derivation of first mouse ES cells, Kaufman *et al*. (1983) repeatedly attempted to derive mouse haploid ES cells. In their experiments, they used 7% ethanol to activate eggs to develop into parthenogenetic embryos, which predominantly (>80%) contained only haploid mitoses when examined at the morula stage. When reaching the blastocyst stage, these embryos were used for cell initiation, resulting in several stable ES cell lines. “However, chromosome analysis at early passage cell lines revealed that all were diploid with a modal number of 40 chromosomes” (Kaufman *et al*., 1983). Therefore, this work demonstrated the ability to derive homozygous diploid cell lines of parthenogenetic origin but the inability to generate haploid ES cells in mouse. These studies provided valuable data on haploid cell cultures but also led to a generally accepted hypothesis that haploidy is associated with inferior growth and genetic instability due to diploidization and aneuploidy.

### C. Rationale

As outlined above, there are two pros for the feasibility to derive haploid ES cells in a vertebrate: (1) haploidy has the start point of evolution into multicellular organism and must be able to support cell division and (2) haploidy *per se* can even sufficiently support embryonic and adult development in plants and invertebrate animals. There are also two cons, which are (1) the lack of report on any haploid organism in vertebrates and (2) the unsuccessful attempts in *Drosophila*, frog, and mouse. The curiosity to understanding these controversial aspects, the great potential of haploid ES cells and our expertise in generating stable cell lines of diploid ES cells and adult germ stem cells have been the driving force for us to create haploid ES cells.

Technically, we envisioned that the successful generation of haploid ES cells might depend on three critical factors (Yi *et al*., 2009): (1) a pure or highly inbred strain in which many—if not all—deleterious (recessive) alleles have been deleted; (2) conditions most conducive to stem cell proliferation rather than differentiation; and (3) ability to maintain the genetic stability/integrity. These considerations have led us to choose the medaka as a test organism. This laboratory fish is an excellent model for analyzing vertebrate development (Wittbrodt *et al*., 2002) and has given rise to several diploid lines of ES cells (Hong and Schartl, 2006; Hong *et al*., 1996, 1998b) and male germ stem cell spermatogonia (Hong *et al*., 2004b). This fish also has many inbred strains known to be permissive to ES cell derivation (Hong *et al*., 1998a). Experience of nearly 20 years working with medaka stem cells has been an encouraging force for haploid ES cell derivation.

## II. Methods

Detailed procedures are the topics of several papers. The focus here is on those that are particularly important for haploid ES cells.

## A. Production of Haploid Embryos

One exception is the need to obtain haploid embryos as the start point. There are two approaches. One is haploid androgenesis, in which the oocyte is genetically inactivated before fertilization with a normal sperm. The other is haploid gynogenesis, in which sperm are inactivated before they are used for insemination with normal eggs. We adopt gynogenesis to obtain haploid embryos (Fig. 1). Sperm are small, and their nuclei can easily be inactivated by UV-light irradiation without affecting their ability to trigger egg development. To ensure haploid gynogenesis, we made use of two inbred albino medaka strains, $i^1$ and $i^3$, which produce genetically pigmented hybrids. In the absence of one nucleus, namely the sperm nucleus, the embryo will be haploid and albino. The haploidy can also be judged by the so-called haploid syndrome. Direct evidence comes from chromosome analysis demonstrating the presence of 24 chromosomes for the haploid set in medaka. Once 100% efficiency of haploid gynogenesis is achieved, embryos thus obtained can be used for cell culture initiation.

## B. Cell Culture Derivation

The strategy to obtain haploid ES cells is similar to that for diploid ES cells. Blastomere cells were dissociated from gynogenetic embryos at the midblastula stage and seeded in gelatin-coated 48-well plates for culture under feeder-free conditions (Hong and Schartl, 2006). Blastomeres moved around by forming pseudopodia and underwent rapid divisions during the first hours of culture, and reached the final

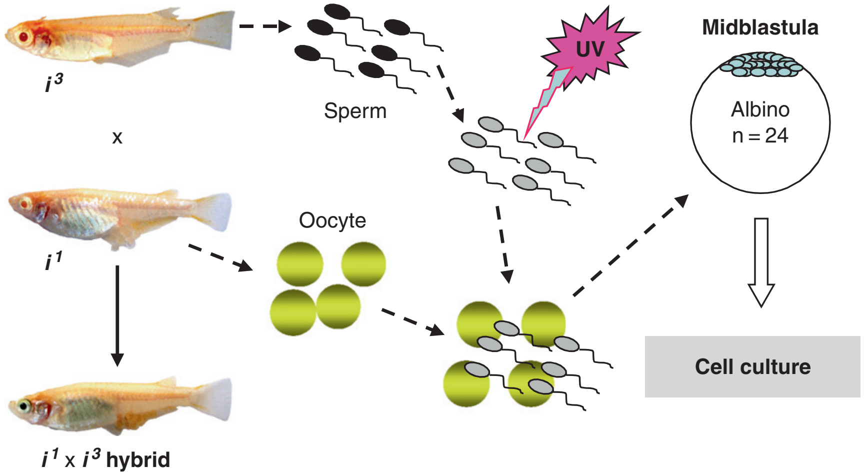

**Fig. 1** Flow chart illustrating how to produce haploid embryos. Two different albino strains are used to phenotype successful induction of haploid gynogenesis. Solid lines depict normal fertilization, resulting in hybrids with black pigmentation as clearly seen in the eye. Broken lines depict steps in producing gynogenetic haploid embryos for cell initiation. The haploid embryos are genetically albino and possess a haploid set of 24 chromosomes.

small size and attached by day 1 of culture. Serial passages led to stable cultures. We initiated five primary cultures and obtained three ES cell lines designated as HX1, HX2, and HX3, because they predominantly comprise haploid X-chromosome-carrying cells of gynogenetic origin. Albinism, haploid syndrome, and haploid metaphases demonstrated uniparental haploidy for the embryos from which the cell lines were derived. Direct evidence for the parental origin came from genotyping. In all the three cell lines we failed to detect sperm-derived autosomal tyrosinase allele (Hong *et al*., 1998b), convincingly demonstrating a gynogenetic origin. In addition, the Y-chromosomal dmrt1y (Matsuda *et al*., 2007) is absent, confirming a female genotype in accordance with the maternal origin.

All the three cell lines had similar stable growth and phenotype following more than 120 passages during more than 400 days of culture. Chromosome examination revealed that 77% cells were haploid. These haploid ES cells have a round or polygonal shape, little cytoplasm, and large nuclei with prominent nucleoli. Importantly, the number of nucleoli serves as a marker to monitor haploidy in living cell cultures. The medaka karyotype has a single nucleolar organizer region (Uwa and Ojima, 1981), indicating that the haploid genome can form only one nucleolus. The nucleolus is easily visible in living cells and its number delineates ploidy levels in culture. During the nucleolar cycle, a haploid medaka cell may have one (interphase), no (metaphase and anaphase), or two nucleoli (telophase with two daughter nuclei). A diploid medaka cell displays a similar picture except for up to a doubled number of nucleoli. In culture, the small cells indeed have one nucleolus per nucleus, whereas the large cells have one (fused from two) to two nucleoli per nucleus. Nucleolar silver staining of fixed cells confirmed these observations. We found that haploid blastula-derived cultures invariantly have ~20% diploid cells (Fig. 2).

## C. Culture Condition

Cell dissociation and feeder-free culture conditions for the derivation of gynogenetically haploid ES cells are similar to those established for fertilization diploid ES cells (Hong and Schartl, 1996). One big difference is a more demanding culture medium for haploid ES cell initiation. We found that a mixture of MES1-conditioned medium and MO1-conditioned medium enhanced the efficiency of haploid ES cell initiation and early passage culture up to 100 days. Afterward, the parental haploid ES cell lines and their pure haploid clones can easily be maintained in normal medaka ES cell media. MO1 is an uncharacterized cell culture derived from the adult medaka ovary. MES1 is one of the three medaka diploid ES cell lines derived from fertilization midblastula embryos of strain HB32C (Hong *et al*., 1996). HX cells originated from medaka strain $i^1$. It remains to be determined whether the requirement for conditioned medium for initial culture is due to differences in ploidy and/or medaka strain, as we have found that under conditions for MES1 cell derivation, only certain strains are permissive for ES cell derivation, whereas others are not (Hong *et al*., 1998a).

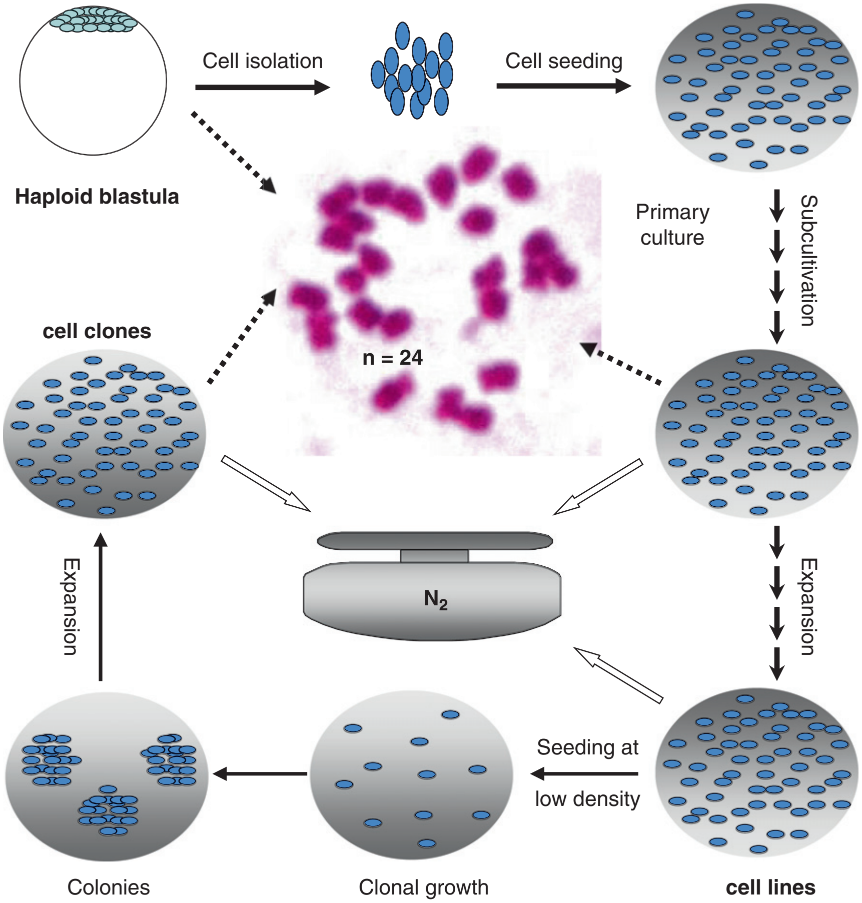
Cell isolation
Cell seeding
Haploid blastula
Primary
culture
Subcultivation
n = 24
cell clones
$N_2$
Expansion
Expansion
Seeding at
low density
Colonies
Clonal growth
cell lines

**Fig. 2** Flow chart illustrating how to create pure haploid ES cells. Solid arrows depict major steps to derive haploid ES cells and pure ES cell clones. Broken arrows depict major steps for characterization by, e.g., chromosome analysis. Open arrows depict when cells are frozen for cryostorage. Cell initiation and subculture are in multiwell plates. Clonal growth and expansion are often in 10-cm dishes.

## D. Generation of Stable Haploid ES Cell Lines

Fortunately, medaka haploid ES cells can easily be dissociated into single cells. When seeded at a low cell density, they can form distinct colonies during clonal growth. Importantly, colonies comprising undifferentiated cells were capable of expansion to stable clones of homogeneous cells exhibiting high alkaline phosphatase activity, a general marker for undifferentiated stem cells (Hong and Schartl, 2006; Hong *et al*., 1996, 1998b, 2004b). Medaka gynogenetic ES cells have the intrinsic ability for stable growth. In our experiment, 100 colonies were randomly picked up and seeded in 96-well plates. We obtained 60 clones and expanded them for cytogenetic analyses. Chromosome examination revealed that 45 clones were haploid with the remainder being diploid. This ratio is again in accordance with the haploid/diploid ratio observed in parental cell cultures. Flow cytometry analyses revealed that the parental cell lines indeed had haploid and diploid peaks, whereas haploid clones essentially had only the haploid peak (Yi *et al*., 2009). Taken together, both haploid and diploid clones of HX1 comprise essentially pure haploid and diploid cells capable of stable growth.

## E. Characterization of Haploid ES Cells

Besides stable growth and phenotype, there are several other experiments to characterize the pluripotency of diploid ES cells. These procedures apply also to haploid ES cells. These include pluripotency gene expression profile, induced differentiation in suspension culture to form embryoid bodies followed by phenotypic monitoring and immunostaining, and chimera formation by cell transplantation into early developing embryos. Interestingly, upon transplantation into fertilization embryo hosts, haploid ES cells are not different from diploid counterparts in the ability to take part in chimeric embryogenesis, generating functional cells that contribute to several organ systems, including the heart, blood cells, skeletal muscles, and fin epithelia (Yi *et al*., 2009).

## F. Stable Growth and Genetic Stability

It is widely accepted that three factors are against haploid cell culture (Andersson *et al*., 1987; Debec, 1978, 1984; Freed and Mezger-Freed, 1970). Diploidization has been thought to be a major cause to prevent haploid cell derivation. Conceivably, somatic cells in culture may undergo spontaneous fusion and/or endomitosis. The reverse situation, somatic haploidization to convert diploidy to haploidy, has not been reported, because haploidization has so far been found only in the meiotic division of germ cells. Consequently, diploid and even polyploid cells will gradually accumulate during serial culture, ultimately overgrowing haploid cells. Haploid cells in culture may intrinsically have genetic instability and become aneuploid cells, abolishing in part haploid cell cultures. Inferior growth has also been ascribed to haploid cells in culture and accepted as an important factor for outgrowth by diploid cells. Stable growth and the retention of a constant ratio between haploidy and diploidy in all the three HX cell lines indicate that these factors are essentially absent in medaka haploid ES cells. The availability of pure haploid ES cell clones, diploid gynogenetic ES cell clones, and fertilization diploid ES cell lines enabled us to address the stability issue. We found that haploid and diploid ES cells are not different in doubling time and proliferation during attachment and suspension cocultures. Interestingly, we found that di- and polyploidization events rarely occur in self-renewing haploid ES cells, but do occur during differentiation. These di- and polyploidized differentiation products usually disappear by cell death, without overgrowing haploid ES cells (Yi *et al*., 2009). Conceivably, the three parental cell lines maintained a dynamically stable proportion of haploid cells during serial culture because under standard culture conditions, spontaneous differentiation is a rare event (≤1%), and occasional diploidization does not accumulate. These results demonstrate that the haploidy retains pluripotency-dependent genetic stability *in vitro*.

The ploidy levels in the parental HX cell lines and their haploid clones remain fairly constant during continuous culture. However, we noticed that diploid cells will increase when cell cultures are re-initiated from frozen vials. But we do not know when diploidization occurs (unpublished data). Therefore, it is a routine to regularly monitor the ploidy level by the nucleolus number and cytogenetic analyses. In the case that pure haploid cells are required, clonal growth and expansion can lead to new haploid ES cell clones.

## III. Applications of Haploid ES Cells

### A. Semicloning

In normal reproduction, fertilization combines two haploid meiotic nuclei of the sperm and egg, and ensures a high efficiency of normal development and genetic diversity in progeny. By mimicking fertilization, intracytoplasmic sperm injection has been developed and increasingly used for treating infertile men who have germ cells but defects in post-meiotic progression. Embryos by diploid somatic cell nuclear transfer to enucleated oocytes produced viable offspring in frogs, fish, and mammals (Campbell *et al*., 1996; Gurdon and Melton, 2008; Lee *et al*., 2002; Wakamatsu *et al*., 2001), providing a powerful tool for animal cloning, human ES cell derivation, and analyzing nuclear reprogramming. However, the application of this cloning strategy to human-assisted reproduction has widely been debated because of low efficacy and ethical concern about identical progeny to the nuclear donor. Recently, a new assisted reproductive technology on the basis of creating mosaic oocytes has been proposed to treat infertile patients lacking any germ cells. This approach, called semicloning, uses nuclear transfer to combine a haploid somatic nucleus and a haploid gamete nucleus in the oocyte. Semicloning has remained hypothetical because viable offspring has not yet been obtained (Tsai *et al*., 2000).

Haploid ES cells and sperm are similar to each other in terms of a complete single genome. However, they are different in terms of mitotic or meiotic products. In addition, haploid ES cells lack the ability of sperm to penetrate eggs. It is curious to know whether haploid ES cells can replace sperm for reproduction. The availability of haploid ES cells enabled us to directly test semicloning by producing mosaic oocytes. To this end, $i^1$-derived HX1 cells were labeled with nuclear GFP and their nuclei were transplanted into non-enucleated matured oocytes of $i^3$ albino. The nuclear transplants exhibited black pigmentation (Fig. 3), similar to the fertilization hybrid between $i^1$ and $i^3$ albinos (Fig. 1), demonstrating the functional contribution from both the oocyte and the HX1 nuclei. Furthermore, nuclear transplant embryos also displayed nuclear GFP in all tissues (Fig. 3B and C). One of the nuclear transplant fry grew into a pigmented fertile female (Fig. 3D), namely NT1, which also exhibited continuous GFP expression from the hES genome. Most importantly, NT1 showed normal fertility and germline

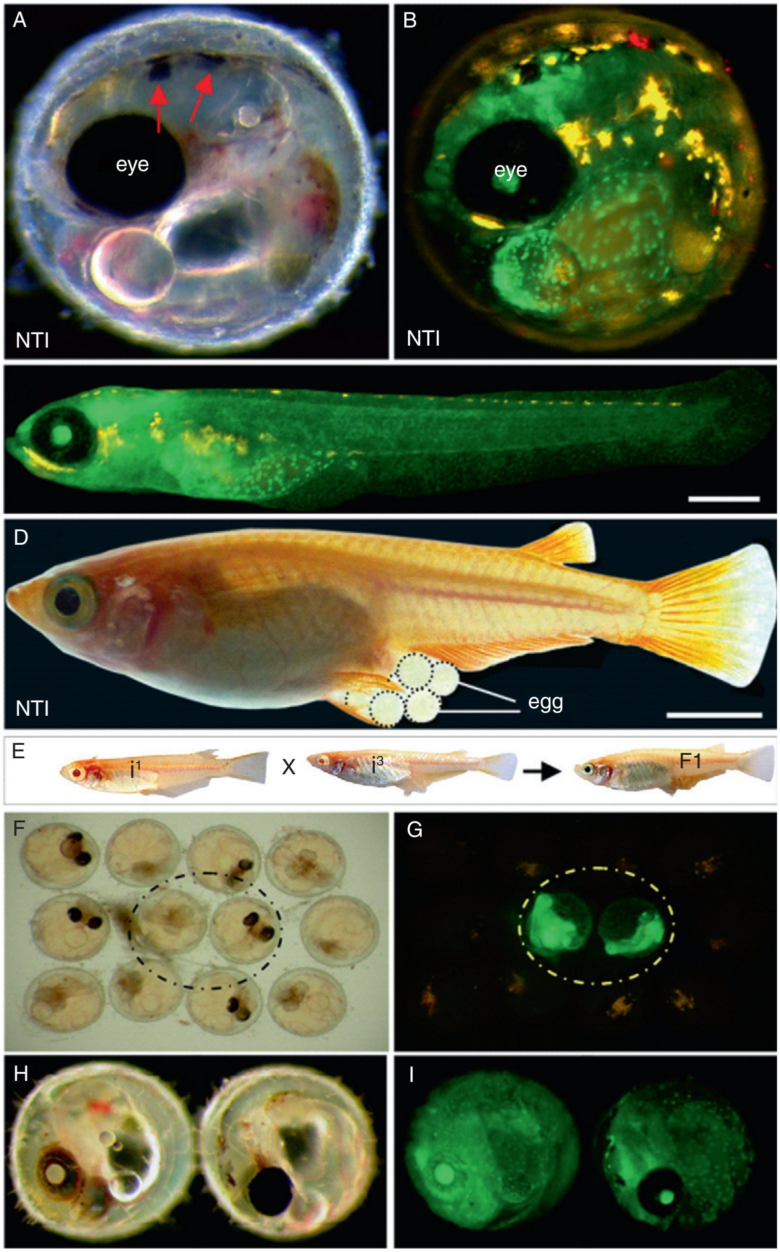
A
eye
NTI
B
eye
NTI
D
NTI
egg
E
i1
X
i3
F1
F
G
H
I

**Fig. 3** *(Continued)*

transmission upon test-crosses to both $i^1$ and $i^3$ males (Fig. 3E), producing four types of F1 progeny, namely albino or pigmented and GFP-positive or GFP-negative (Fig. 3F–I). Pigmented and albino progeny were segregated at the Mendelian 1:1 ratio (Fig. 3F–I), demonstrating that the HX1-derived and oocyte genomes were not different in germline transmission. We termed this first semicloned medaka Holly. Holly lived for 18 months, and her albino and transgene expression has been passed over four generations. Since embryos with genomic abnormalities cannot reach advanced stages of development in mouse and human (Yanagimachi, 2005), germline transmission demonstrates the retention of genetic stability and integrity in hES cultures. Most importantly, mosaic oocytes comprising a haploid mitotic nucleus from haploid ES cells and a haploid meiotic nucleus from the oocyte can generate viable and fertile offspring, demonstrating the feasibility of semicloning for reproductive medicine.

Compared to cloning through diploid somatic nuclear transfer, semicloning would not only ensure the biparental contribution to the progeny but also create a new and unpredictable combination of genetic traits from both parents similar to normal fertilization (Fig. 4). However, semicloning at its present form can treat only male infertility and produce female individuals. Future work is needed to determine whether male haploid ES cells can also be obtained.

## B. Analysis of Gene Function

Gene targeting by homologous recombination in ES cells is a powerful routine in mouse developmental genetics. This complicated approach starts with targeted gene disruption in ES cells, production of whole animals by germline chimera formation from gene-targeted ES cell clones, and breeding the founder to produce F1 heterozygous animals, which in turn are intercrossed to obtain heterozygous and, more importantly, homozygous null embryos/animals for phenotypic analyses. This series of steps are aimed at generating a null locus at the homozygous state. Although this approach is tedious and experimentally demanding, it remains the standard in creating homozygous null vertebrates, because precise genetic alterations mediated by homologous recombination in mouse ES cells occur at an exceedingly low efficiency of $\sim 10^{-6}$. The frequency for independent and simultaneous disruption within a particular cell of both copies of a gene in question would be $\sim 10^{-12}$, which is well beyond the

---

**Fig. 3** Semicloning and germline transmission. (A, B) Nuclear transplant founder NT1 embryo at day 7. The $i^1$-derived HX1a was stably labeled with nuclear GFP, and its nuclei were transplanted into non-enucleated oocytes of strain $i^3$. Wild-type pigmentation is seen in the eye and body surface (arrows; A), and nuclear GFP is throughout the embryo (B). (C) Fry NT1 showing GFP expression and eye pigmentation. (D) NT1 fertile female laying eggs. (E) Crossing between albino strains $i^1$ and $i^3$. F1 hybrids have wild-type black pigmentation in the eye. (F–I) Germline transmission. (F, G) Cluster of embryos between NT1 and $i^1$ male showing germline transmission into four classes of progeny: GFP-positive albino or pigmented and GFP-negative albino or pigmented. (H, I) Higher magnification of GFP-positive albino or pigmented progeny as circled in (F, G). Embryos are 1 mm in diameter. Bars, 0.2 mm (C) and 0.5 mm (D). (reproduced with permission from the Science Publisher).

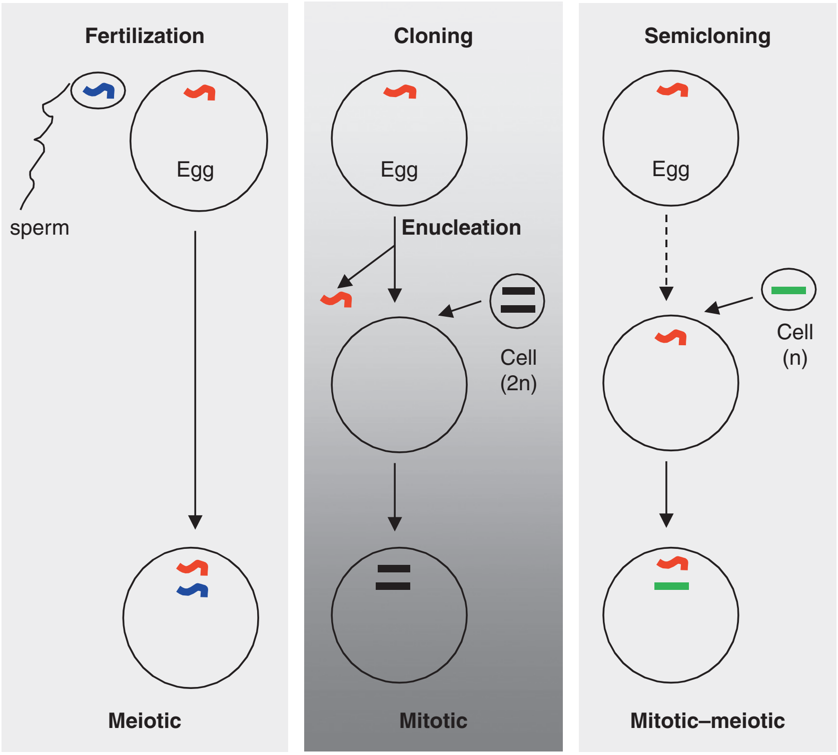

| | | | |
|---|---|---|---|
| Parent: | 2 | 1 | 2 |
| Sexuality: | Sexual | Asexual | Semisexual |
| parent–offspring: | 50% | 100% | 50% |
| siblings: | 50% | 100% | 75% |

**Fig. 4** Genetic consequences of semicloning. (Top) Comparisons between fertilization, cloning by diploid somatic nuclear transfer, and semicloning by haploid nuclear transfer. (Bottom) Genetic consequences of the three reproduction modes. Semicloning omits the enucleation step and mimics fertilization in the production of diversity in an unpredictable way. Curved line, meiotic genome; straight line, mitotic genome.

practical limit of screening for putative homozygous null mutants. In the case of haploid ES cells, the approach becomes straightforward, because the disruption of a single gene copy will directly show the loss-of-function phenotype at molecular and cellular levels. If the gene concerned is involved in pluripotency maintenance or lineage restriction and differentiation, the role of the gene can also be easily investigated by induced ES differentiation under defined culture conditions.

In theory, genes encoding cell cycle repressors and tumor suppressors such as p53 are perfect candidates for gene targeting in haploid ES cells. Conceivably, disruption of such genes alone or in combination will not compromise but promote haploid ES cell growth. In fact, the work with fish gene targeting began ~20 years ago, when I and

Manfred Schartl (Würzburg, Germany) initiated ES cell derivation and attempted gene targeting by using p53 as a model. Although the medaka ES cell work has been a success, germline chimera production from ES cell cultures has remained open. Recent work by Schartl and colleagues led to the notion that the medaka germline is cell-autonomously specified, pointing to the possible inaccessibility of this organism to germline contribution by ES cell cultures. Recently, we showed that p53 is expressed in both diploid and haploid medaka ES cells. By using a homologous recombination vector we previously designed for gene targeting in diploid medaka ES cells (Chen *et al.*, 2002) and drug selection conditions established for diploid medaka ES cells (Hong *et al.*, 2004a), we showed that p53 disruption in haploid ES cells can easily be detected by genomic PCR for the targeted locus and RT-PCR for the loss of the endogenous p53 expression, thus its absence. Importantly, the p53-disrupted haploid ES cells indeed exhibit a clear phenotype, including the loss of sensitivity for induced cell cycle arrest and senescence (unpublished data), a well-conserved role of this gene in diverse organisms examined so far. In medaka haploid ES cells, a typical gene-targeting experiment starting with available vectors can often be achieved within 3 months to offer targeted cell clones in large quantity for phenotypic analyses.

### C. Haploid Genetic Screens

Mutagenesis screening is a powerful tool for generating, identifying, and analyzing genes involved in a particular process or pathway. Such screens have so far been performed in several model organisms including *Drosophila*, zebrafish, and medaka. These are diploid genetic screens because they are also based on the production of homozygous animals containing a particular mutation. In this regard, haploid ES cells offer a paradigm for high-throughput haploid genetic screens for random mutations (e.g., chemical mutagenesis), designed genetic modifications (gene targeting), and endogenous genes involved in particular pathways and processes. Recently, it has been reported that haploid genetic screens in human cells identify host factors used by pathogens (Carette *et al.*, 2009). Similar approaches toward identifying host genes responsible for sensitivity to infection by viruses will shed light on new strategies to disrupt the virus susceptibility/sensitivity in aquaculture species by gene transfer technology.

## IV. Summary

We have developed a strategy for generating haploid ES cell lines from gynogenetic blastula embryos of a highly inbred medaka strain. We can reproducibly obtain and stably cultivate haploid ES cells capable of forming pure haploid clones. We have demonstrated that haploidy in medaka has the intrinsic ability to support stable growth and pluripotency in culture. Most importantly, we have shown that haploidy after long-term culture and even genetic engineering is capable of producing fertile animals, demonstrating that haploidy retains the genetic integrity, and providing a powerful tool for germline transmission in this organism. Most strikingly, we have generated oocyte creatures comprising a haploid mitotic nucleus and a haploid meiotic nucleus and demonstrated their ability to develop into fertile offspring. Most recently, we have also shown that the medaka haploid ES cells are excellent for gene-targeting experiments. Future work will determine whether these haploid cells are also a paradigm for genetic screens.

## Acknowledgments

The author thanks Professors Manfred Schartl and Jochen Wittbrodt (Germany) for encouragement, and the members of his Developmental Genetics Lab for discussions and unpublished data. This work was supported by the Biomedical Research Council of Singapore (R-08-1-21-19-585 and SBIC-SSCC C-002-2007) and the National University of Singapore (R-154-000-153-720).

## References

Andersson, B. S., Beran, M., Pathak, S., Goodacre, A., Barlogie, B., and McCredie, K. B. (1987). Ph-positive chronic myeloid leukemia with near-haploid conversion *in vivo* and establishment of a continuously growing cell line with similar cytogenetic pattern. *Cancer Genet. Cytogenet.* **24**, 335–343.

Botstein, D., and Fink, G. R. (1988). Yeast: An experimental organism for modern biology. *Science* **240**, 1439–1443.

Campbell, K. H., McWhir, J., Ritchie, W. A., and Wilmut, I. (1996). Sheep cloned by nuclear transfer from a cultured cell line. *Nature* **380**, 64–66.

Carette, J. E., Guimaraes, C. P., Varadarajan, M., Park, A. S., Wuethrich, I., Godarova, A., Kotecki, M., Cochran, B. H., Spooner, E., Ploegh, H. L., and Brummelkamp, T. R. (2009). Haploid genetic screens in human cells identify host factors used by pathogens. *Science* **326**, 1231–1235.

Chen, S., Hong, Y., and Schartl, M. (2002). Development of a positive–negative selection procedure for gene targeting in fish cells. *Aquaculture* **214**, 67–79.

Debec, A. (1978). Haploid cell cultures of *Drosophila melanogaster*. *Nature* **274**, 255–256.

Debec, A. (1984). Evolution of karyotype in haploid cell lines of *Drosophila melanogaster*. *Exp. Cell Res.* **151**, 236–246.

Evans, M. J., and Kaufman, M. H. (1981). Establishment in culture of pluripotential cells from mouse embryos. *Nature* **292**, 154–156.

Freed, J. J., and Mezger-Freed, L. (1970). Stable haploid cultured cell lines from frog embryos. *Proc. Natl. Acad. Sci. U. S. A.* **65**, 337–344.

Gurdon, J. B., and Melton, D. A. (2008). Nuclear reprogramming in cells. *Science* **322**, 1811–1815.

Heimpel, G. E., and de Boer, J. G. (2008). Sex determination in the Hymenoptera. *Annu. Rev. Entomol.* **53**, 209–230.

Hong, Y., and Schartl, M. (1996). Establishment and growth responses of early medakafish *(Oryzias latipes)* embryonic cells in feeder layer-free cultures. *Mol. Mar. Biol. Biotechnol*. **5**, 93–104.

Hong, Y., Chen, S., Gui, J., and Schartl, M. (2004a). Retention of the developmental pluripotency in medaka embryonic stem cells after gene transfer and long-term drug selection for gene targeting in fish. *Transgenic Res.* **13**, 41–50.

Hong, Y., Liu, T., Zhao, H., Xu, H., Wang, W., Liu, R., Chen, T., Deng, J., and Gui, J. (2004b). Establishment of a normal medakafish spermatogonial cell line capable of sperm production *in vitro*. *Proc. Natl. Acad. Sci. U. S. A.* **101**, 8011–8016.

Hong, Y., and Schartl, M. (2006). Isolation and differentiation of medaka embryonic stem cells. *Methods Mol. Biol.* **329**, 3–16.

Hong, Y., Winkler, C., and Schartl, M. (1996). Pluripotency and differentiation of embryonic stem cell lines from the medakafish (*Oryzias latipes*). *Mech. Dev.* **60**, 33–44.

Hong, Y., Winkler, C., and Schartl, M. (1998a). Efficiency of cell culture derivation from blastula embryos and of chimera formation in the medaka (*Oryzias latipes*) depends on donor genotype and passage number. *Dev. Genes Evol.* **208**, 595–602.

Hong, Y., Winkler, C., and Schartl, M. (1998b). Production of medakafish chimeras from a stable embryonic stem cell line. *Proc. Natl. Acad. Sci. U. S. A.* **95**, 3679–3684.

Kaufman, M. H., Robertson, E. J., Handyside, A. H., and Evans, M. J. (1983). Establishment of pluripotential cell lines from haploid mouse embryos. *J. Embryol. Exp. Morphol.* **73**, 249–261.

Lee, K. Y., Huang, H., Ju, B., Yang, Z., and Lin, S. (2002). Cloned zebrafish by nuclear transfer from long-term-cultured cells. *Nat. Biotechnol.* **20**, 795–799.

Matsuda, M., Shinomiya, A., Kinoshita, M., Suzuki, A., Kobayashi, T., Paul-Prasanth, B., Lau, E. L., Hamaguchi, S., Sakaizumi, M., and Nagahama, Y. (2007). DMY gene induces male development in genetically female (XX) medaka fish. *Proc. Natl. Acad. Sci. U. S. A.* **104**, 3865–3870.

Takahashi, K., and Yamanaka, S. (2006). Induction of pluripotent stem cells from mouse embryonic and adult fibroblast cultures by defined factors. *Cell* **126**, 663–676.

Tsai, M. C., Takeuchi, T., Bedford, J. M., Reis, M. M., Rosenwaks, Z., and Palermo, G. D. (2000). Alternative sources of gametes: Reality or science fiction? *Hum. Reprod.* **15**, 988–998.

Uwa, H., and Ojima, Y. (1981). Detailed and banding karyotype analyses of the medaka, *Oryzias latipes* in cultured cells. *Proc. Jpn. Acad.* **57**, 39–43.

Wakamatsu, Y., Ju, B., Pristyaznhyuk, I., Niwa, K., Ladygina, T., Kinoshita, M., Araki, K., and Ozato, K. (2001). Fertile and diploid nuclear transplants derived from embryonic cells of a small laboratory fish, medaka (*Oryzias latipes*). *Proc. Natl. Acad. Sci. U. S. A.* **98**, 1071–1076.

Wittbrodt, J., Shima, A., and Schartl, M. (2002). Medaka—a model organism from the far East. *Nat. Rev. Genet.* **3**, 53–64.

Yanagimachi, R. (2005). Intracytoplasmic injection of spermatozoa and spermatogenic cells: Its biology and applications in humans and animals. *Reprod. Biomed. Online* **10**, 247–288.

Yi, M., Hong, N., and Hong, Y. (2009). Generation of medaka fish haploid embryonic stem cells. *Science* **326**, 430–433.

Yi, M., Hong, N., and Hong, Y. (2010). Derivation and characterization of haploid embryonic stem cell cultures in medaka fish. *Nat. Protoc.* **5**, 1418–1430.

# PART II

# Developmental and Neural Biology

# CHAPTER 4

# Neurogenesis

**Prisca Chapouton*** *and* **Leanne Godinho**[‡]

*Institute of Developmental Genetics, Helmholtz Zentrum München, German Research Center for Environmental Health, Neuherberg, Germany

[‡]Lehrstuhl für Biomolekulare Sensoren, Institute for Neuroscience, Technische Universität München, Munich, Germany

---

Abstract
I. Introduction
II. Neurogenesis During Development and in the Adult Brain
  A. Morphogenesis: Formation of the Neural Plate and Neural Tube
  B. Molecular Determinants and Patterning of the Neural Plate
  C. Proneural Domains, Lateral Inhibition, and Neurogenic Cascade
  D. Zones of Delayed Differentiation
  E. Signaling Centers and Downstream Neuronal Specification
  F. Generation of Glial Cells
  G. Neurogenesis at Juvenile and Adult Stages
III. Methods for Studying Neurogenesis in the Developing and Adult Brain
  A. Molecular Markers
  B. Methods to Label Live Cells
  C. *In Vivo* Imaging
  D. Methods to Follow Cell Cycle Events
  E. Manipulating the Expression of Genes Involved in Neurogenesis
  F. Methods for Targeted Cell Ablations
IV. Specific Protocols to Study Adult Neurogenesis
  A. Fixation of the Adult Brain for Immunohistochemistry and *In Situ* Hybridization
  B. Immunohistochemistry on Vibratome Sections
  C. *In Situ* Hybridization on Whole Mount Adult Brains
  D. *In Situ* Hybridization on Gelatine–Albumin Sections
  E. Intraperitoneal Injections of BrdU
  F. Lipofections/Electroporations of the Adult Brain *In Vivo*
  G. Slice Culture
V. Conclusion
Acknowledgements
References

Copyright © 2010 Elsevier Inc. All rights reserved.

978-0-12-384892-5
DOI: 10.1016/B978-0-12-384892-5.00004-9

## Abstract

For more than a decade, the zebrafish has proven to be an excellent model organism to investigate the mechanisms of neurogenesis during development. The often cited advantages, namely external development, genetic, and optical accessibility, have permitted direct examination and experimental manipulations of neurogenesis during development. Recent studies have begun to investigate adult neurogenesis, taking advantage of its widespread occurrence in the mature zebrafish brain to investigate the mechanisms underlying neural stem cell maintenance and recruitment. Here we provide a comprehensive overview of the tools and techniques available to study neurogenesis in zebrafish both during development and in adulthood. As useful resources, we provide tables of available molecular markers, transgenic, and mutant lines. We further provide optimized protocols for studying neurogenesis in the adult zebrafish brain, including *in situ* hybridization, immunohistochemistry, *in vivo* lipofection and electroporation methods to deliver expression constructs, administration of bromodeoxyuridine (BrdU), and finally slice cultures. These currently available tools have put zebrafish on par with other model organisms used to investigate neurogenesis.

## I. Introduction

The mechanisms by which undifferentiated neural progenitor cells generate mature, functioning neurons are referred to as neurogenesis. Because neural progenitors also generate glial cells (oligodendrocytes and astrocytes), we also include gliogenesis in this chapter. The earliest step in neurogenesis (and gliogenesis) begins with the specification of neural progenitors, followed by proliferative cell divisions that amplify the progenitor pool, cell fate specification and determination, exit from the cell cycle, and finally terminal differentiation. Each of these steps is precisely orchestrated to generate multiple cell-types that ultimately will populate the mature central nervous system (CNS).

For more than a decade, the vertebrate organism zebrafish has been highly productive for studies of neurogenesis, because it harbors the most advantageous features of several different model organisms. Like mice and *Drosophila*, zebrafish are amenable to genetic analysis and like *Xenopus*, fertilization and subsequent development occurs externally, making them particularly accessible for examination and experimental manipulation.

Although neurogenesis during development has been the subject of the vast majority of studies conducted thus far, neurogenesis in the adult zebrafish brain has also recently received attention. Our goal in this chapter is to provide an overview of the tools and techniques currently available to study neurogenesis in zebrafish both during development and in adulthood. We begin, however, with a brief description of how neurogenesis is initiated during development and how it occurs in the adult brain of zebrafish.

## II. Neurogenesis During Development and in the Adult Brain

### A. Morphogenesis: Formation of the Neural Plate and Neural Tube

As early as the 16-cell stage of development, it is possible to identify the cells (4 central blastomeres) that will give rise to the future CNS (Helde *et al*., 1994). The descendents of these four cells are located in the dorsal blastoderm and become assembled into a two-dimensional neural plate by the end of gastrulation. A detailed fate mapping study (Woo and Fraser, 1995) that traced dorsal blastula cells at the shield stage to their corresponding locations in the neural plate revealed that cells located at the animal pole are fated to anterior locations, whereas more laterally located cells are fated to more posterior brain regions. Territories along the anterior–posterior (A–P) axis of the neural plate are fated to give rise to distinct brain regions (retina and telencephalon, diencephalon, mesencephalon, hindbrain, and spinal cord) and can be labeled by specific patterning markers (see II-B and Fig. 1A). At the 6–10 somite stages, the neural plate becomes a three-dimensional keel and subsequently a rod (Kimmel *et al*., 1995). During this morphogenetic process, medial cells of the neural plate reach ventral locations, while lateral cells become located in dorsal midline domains (Papan and Campos-Ortega, 1997; see Fig. 1B–E). Cells in the rod gradually become polarized, with the apical localization of ZO1 and N cadherin, followed by Lin7c and Nok (Yang *et al*., 2009). This gradual polarization, as well as mirror symmetric type divisions that occur medially in the neural rod, with the localization of Par3 at the cleavage furrow, induces the formation of a lumen (Tawk *et al*., 2007; Yang *et al*., 2009), thereby forming a neural tube. Thus, the establishment of apico-basal polarity by neuroepithelial cells is critical to neural tube formation. This polarity, which involves the apical localization of structural proteins [ZO-1, Par3 (von Trotha *et al*., 2006), Nok (Yamaguchi *et al*., 2010), lin7 (Wei *et al*., 2006)] and of enzymatic proteins [aPKC (Alexandre *et al*., 2010; Rohr *et al*., 2006; Tawk *et al*., 2007)], and the basolateral localization of Numb (Reugels *et al*., 2006) and lgl2 (Reischauer *et al*., 2009) is also essential at later stages of development for progenitor maintenance and neuronal fate specification throughout the CNS (Roberts and Appel, 2009). Mutants exhibiting defects in apico-basal polarity are listed in Tables V and VI. As another aspect of tissue polarization, the nuclei of dividing progenitors in the neural tube move between the ventricular (apical) and basal (pial) surfaces in a process called interkinetic nuclear migration (INM), with nuclear position correlating with specific phases of the cell cycle. INM continues to occur at later stages of neurogenesis throughout the CNS and has been well characterized in the developing zebrafish retina where the extent of nuclear movement during INM was shown to correlate with the fate of daughter cells: the more basal a progenitor cell nucleus migrates, the more likely it is to generate a postmitotic daughter cell (Baye and Link, 2007b).

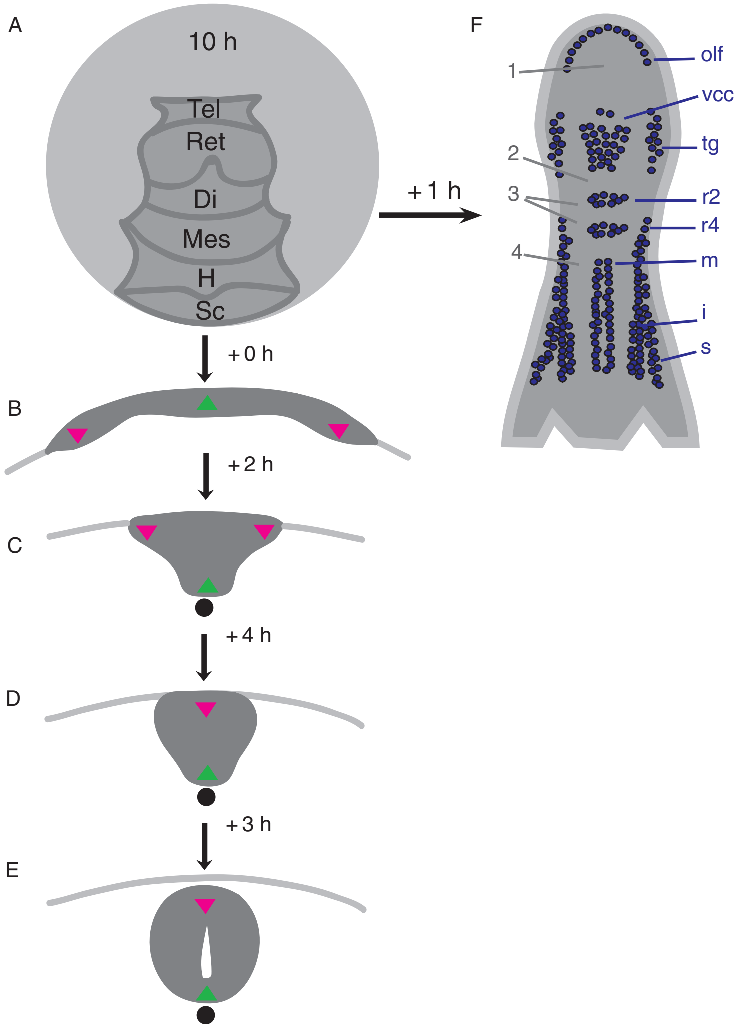

**Fig. 1** Fate map, neurogenesis, and early proneural clusters. (A) Fate map of the neural plate at tail-bud stage (10 h post-fertilization, dorsal view). Schematization adapted from Woo and Fraser (1995). The different neural territories are organized in partially overlapping domains that align along the A–P axis during gastrulation. (Tel, telencephalon; Ret, retina; Di, diencephalon; Mes, mesencephalon; H, hindbrain; Sc, spinal cord). (B–E) Morphogenesis of the neural tube at tail-bud (B), 5 somites (C), 14 somites (D), and 20 somites (E) after (Papan and Campos-ortega, 1994; Schmitz *et al*., 1993). Lateral neural plate bulges converge toward the midline, which folds inward leading to the formation of a neural keel (C) and rod (D). A process of cavitation then shapes a lumen, and thus a tube (E). Prospective dorsal neural tube cells originate from lateral neural plate domains (indicated by red triangles) while ventral neural tube cells originate from medial neural plate domains (indicated by a green triangle). At the keel/ rod stage, progenitors undergo mirror symmetric divisions and contribute to cells on both sides of the future neural tube. (F) Early proneural clusters at the 3-somite stage, visualized on a schematically represented flat mounted embryo (anterior to the top) after *neurog1* whole mount in situ hybridization. The following proneural clusters are visible: olf, olfactory neuron progenitors; tg, trigeminal ganglia; vcc, ventro-caudal cluster; r2, motoneuron progenitors of rhombomere 2; r4 motoneuron progenitors of rhombomere 4; m, spinal motoneuron progenitors; i, spinal interneuron progenitors; s, spinal sensory neuron progenitors. These clusters are separated by prepatterned zones of delayed differentiation (1, ANP, anterior neural plate; 2, intervening zone at the mid-hindbrain boundary, 3, longitudinal stripes in r2 and r4; 4, longitudinal stripes in the spinal cord). (See Plate no. 4 in the Color Plate Section.)

## B. Molecular Determinants and Patterning of the Neural Plate

The neural territory is marked and specified by members of the SoxB1 family, *sox1a/b, sox2, sox3*, and *sox 19a/b* (Dee *et al*., 2008; Okuda *et al*., 2006; Vriz *et al*., 1996), which are already expressed at blastula stages and in the neural plate. The SoxB transcription factors regulate, both positively and negatively, several transcriptional programs (Okuda *et al*., 2010) implicated in the patterning of the neural plate (*bmp2b/7*) and in neural differentiation (*her3* and *neurog1*, positively regulated and *ascl1*, negatively regulated). As in other vertebrates, SoxB1 family members are involved generally in imparting neural fate and preventing further differentiation (Bylund *et al*., 2003). Upstream and in combination with Sox2, the Pou transcription factor pou5f1/Oct4/pou2/Spg (Belting *et al*., 2001; Reim and Brand, 2006) also activates repressors of differentiation that specify neural progenitors, such as *hesx1* and *her3* (Onichtchouk *et al*., 2010).

The anterior neural plate (ANP) border is delimited by the placodal field territory and expresses *dlx3b, dlx5a*, and *foxi1* (Akimenko *et al*., 1994; Nissen *et al*., 2003; Quint *et al*., 2000; Solomon and Fritz, 2002; Solomon *et al*., 2003; Whitlock and Westerfield, 2000), whereas posteriorly the neural plate is delimited by the future neural crest and Rohon-Beard neurons and is marked by *snail1b, foxd3, sox9b*, and *sox10* (Dutton *et al*., 2001; Li *et al*., 2002; Odenthal and Nusslein-Volhard, 1998; Thisse *et al*., 1995). Along the A–P axis of the neural plate, patterning genes subdivide presumptive brain regions and are involved in their growth and specification. An early ANP marker is *otx2*, whereas *hoxb1b* marks the hindbrain territory, from rhombomere 4 to more caudal regions (Koshida *et al*., 1998; Li *et al*., 1994; Prince *et al*., 1998). The anterior neural border, expressing the Wnt inhibitor Sfrp (Houart *et al*., 2002), is a crucial organizing center that inhibits posterior fates and induces the formation of the telencephalon in the ANP. Within the ANP, *rx3* expression specifies the eye field territory (Stigloher *et al*., 2006). Along the dorso-ventral (D-V) axis, BMP signaling is an important regulator defining the territories of distinct neurons (Barth *et al*., 1999). Markers subdividing domains of the developing anterior brain from 17 somites to 1 day have been described in (Hauptmann and Gerster, 2000a, c; Hauptmann *et al*., 2002).

## C. Proneural Domains, Lateral Inhibition, and Neurogenic Cascade

At the 3 somite stage, the first proneural clusters can be identified in the neural plate by their expression of several markers (see below and Fig. 1F). Within these clusters, a few progenitors are specified toward the neurogenic cascade to exit the cell cycle and differentiate as neurons. This complete neurogenic program takes place for a few cells very early in development so that the first nuclei and axonal tracts can be traced as early as 18 h post-fertilization (hpf) using HRP, diI, or acetylated tubulin antibody staining (Wilson *et al*., 1990). This early wave of neuron production results in the establishment of a basic functional neuronal network that allows newly hatched fish to exhibit escape responses as early as 2 days post-fertilization (dpf) (O'Malley *et al*., 1996).

Within the proneural clusters, specified progenitors express proneural genes, such as *neurog1, ascl1a*, and *coe2* (Allende and Weinberg, 1994; Bally-Cuif *et al*., 1998; Blader *et al*., 1997) (other proneural genes are listed in Tables I and II), neurogenic genes (*deltaA, deltaB, deltaD*, and *deltaC, jagged 1a, 1b, and 2*) (Haddon *et al*., 1998; Julich *et al*., 2005; Yeo and Chitnis, 2007), and, as they eventually exit the cell cycle, the early postmitotic neuronal marker *elavl3* (Park *et al*., 2000b). A dynamic process of lateral inhibition allows some cells within the proneural clusters to follow the neurogenic cascade while keeping their neighbors in a progenitor state. The expression of the genes named above in these clusters is therefore visible as a "salt and pepper" pattern.

Lateral inhibition involves the interaction between cells expressing Notch ligands (Delta A, B, C, D, Jagged1a, 1b, 2) and their neighbors expressing Notch receptors (Notch1a, Notch1b, Notch2, Notch3) (see Tables I and II). Upon ligand binding, Notch is cleaved intracellularly and transported to the nucleus, where it acts together with the transcription factor Su(H) and its coactivator Mastermind to induce the transcription of the family of Hairy/Enhancer of Split genes, such as *her4* (Bray and Furriols, 2001; Takke *et al*., 1999). Her proteins, in turn, inhibit the expression of proneural genes. Notch activation requires not only binding of the ligand to the receptor but also an internalization of the ligand (Matsuda and Chitnis, 2009), which is intracellularly bound by the Mindbomb ring ubiquitin ligase (Itoh *et al*., 2003). The dAsb11 ubiquitin ligase is also required in the ligand-expressing cells for correct Notch activity (Diks *et al*., 2008). Thus, lateral inhibition ensures the maintenance of progenitors within the proneural clusters while permitting the generation of different neuronal phenotypes, owing, in most cases, to a temporal difference of cell cycle exit (Aizawa *et al*., 2007; Appel *et al*., 2001; Cau *et al*., 2008; Yeo and Chitnis, 2007). Pathways and markers involved in the coordination of cell cycle exit and differentiation have been shown to involve Cdkn1c (Park *et al*., 2005) and histone deacetylase (Yamaguchi *et al*., 2005) but are in general not well characterized in the zebrafish.

## D. Zones of Delayed Differentiation

Zones of delayed neurogenesis, or non-neurogenic zones, are found around the proneural clusters (areas marked 1–4 in Fig. 1F). In several of these non-neurogenic zones, members of the hairy/enhancer of split family genes have been shown to prevent neural progenitors from entering the neurogenic cascade (Stigloher *et al*., 2008). The intervening zone around the mid-hindbrain boundary which expresses *her5* and *her11* (Geling *et al*., 2003, 2004; Ninkovic *et al*., 2005, 2008); the longitudinal domains in the spinal cord, which express *her9* and *her3* (Bae *et al*., 2005; Hans *et al*., 2004) and separate the columns of motoneurons, interneurons, and Rohon-Beard sensory neurons; and the ANP (containing the prospective telencephalon, diencephalon, and eyes), by the action of Foxg1 (Bourguignon *et al*., 1998), constitute zones in which neurogenesis is inhibited. Notably, not only in the neural plate but also later in brain development and at adult stages, several regions of the zebrafish brain maintain pools of undifferentiated neural progenitors that express *her* genes (Chapouton et al., in revision).

## E. Signaling Centers and Downstream Neuronal Specification

Positive signals that induce the first proneural clusters and ongoing neurogenesis involve sources of signaling activity within or adjacent to the neural plate, and at later stages within the developing brain. These signals not only induce the neurogenic cascade (i.e., Shh induces *neurog1* expression Blader *et al*., 1997) but also specify neuronal identity and the size of the neuronal clusters, for example, the role of Wnt in the diencephalic dopaminergic population (Lee *et al*., 2006; Russek-Blum *et al*., 2008). Such signaling centers include the floor plate which secretes Shh and Twhh (Ribes *et al*., 2010; Strahle *et al*., 2004), the roof plate with Wnt signaling activity (Amoyel *et al*., 2005), the interrhombomeric boundary cells in the hindbrain conveying Wnt1 signaling activity and inducing *deltaA* expression in rhombomeres (Amoyel *et al*., 2005), rhombomere 4 conveying FGF3 and FGF8 signaling activity (Maves *et al*., 2002), the zona limitans intrathalamica (ZLI), with Shh and Twhh (Scholpp *et al*., 2006, 2009), and the isthmic organizer at the mid-hindbrain boundary (Raible and Brand, 2004; Wurst and Bally-Cuif, 2001) with FGF and Wnt signaling activity orchestrating the growth of the midbrain and rhombomere 1. Downstream of these signaling pathways, transcription factor combinations are activated in a temporal and region-specific manner and define specific differentiation programs, thereby producing a variety of neuronal phenotypes. One example illustrating this diversity of programs is the specification of three types of interneurons in the ventral spinal cord, V3 neurons, and the two classes of Kolmer–Agduhr cells (Ka″ and Ka′) (Yang *et al*., 2010). V3 and KA″ interneurons are generated by lateral floor plate progenitors and are intercalated on the same ventral level in the spinal cord. The slightly more dorsally located KA′ interneurons are generated by the *olig2*-expressing motoneuron progenitor pool. Initially all three neuron types depend on Shh. Subsequently, the activation cascade generating the V3 identity goes through the transcription factors Gli, Nkx2.2a, Nkx 2.2b, Nkx 9, Olig2, and Sim1 (a leucine zipper transcription factor) whereas the generation of the KA″ identity goes through the transcription factors Gli, Nkx2.2a, Nkx 2.2b, Nkx 9, Olig2, Gata2, Tal2, and Gata3. The generation of KA′ neurons involves Olig2, Gata3, and Tal2. Interestingly, although both KA″ and KA′ inhibitory interneurons express the enzyme Gad67 at the end of their differentiation program, the expression of *gad67* is acquired via two distinct transcriptional cascades. Tables I and II list some of the markers specific to diverse neuronal populations generated in the neural tube and developing brain, Tables III and IV list transgenic lines, and Tables V and VI mutants affecting neurogenesis and signaling pathways.

## F. Generation of Glial Cells

Neural progenitors give rise not only to neurons but also to oligodendrocytes and to radial glial cells. The generation of oligodendrocytes has mostly been studied in the spinal cord (Park *et al*., 2002) and in the hindbrain (Zannino and Appel, 2009) and takes place after motoneurons have been generated, sharing the same progenitors and some of the molecular determinants of motoneuron progenitors, such as Shh and Olig 2 (Park *et al*., 2002, 2004). Molecular markers of radial glial cells such as GFAP and *nestin* are expressed in neural plate progenitors (Kim *et al*., 2008; Mahler and Driever, 2007; Tawk *et al*., 2007). The radial glial morphology, however, characterized by the long processes spanning from the ventricle to the pial surface, becomes visible from juvenile stages onward (Kim *et al*., 2008; Tawk *et al*., 2007). Radial glial cells function as neural progenitors (Bernardos *et al*., 2007; Chapouton *et al*., 2010; Kim *et al*., 2008; Lam *et al*., 2009; März *et al*., 2010; Pellegrini *et al*., 2007b) and may also subserve an astrocytic function in the mature brain. A parenchymal astrocytic population, in addition to radial glia, may also exist in the zebrafish brainstem. Evidence for their existence comes from a study in which immunostaining using a monoclonal antibody revealed cells with a stellar morphology reminiscent of parenchymal astrocytes in other vertebrates (Kawai *et al*., 2001). Interestingly, these cells also express GFAP.

## G. Neurogenesis at Juvenile and Adult Stages

Zebrafish grow throughout life with growth occurring in all organs, including the brain. In accordance with this, neurons continue to be generated within the adult fish brain. This continued neurogenesis is made possible by the maintenance of undifferentiated progenitors in specific niches throughout the brain that can be recruited into the neurogenic cascade even at adult stages. Indeed, many more zones of proliferation and neurogenesis have been identified in the zebrafish brain than in mammals (Adolf *et al*., 2006; Chapouton *et al*., 2006, 2010; Grandel *et al*., 2006; Ito *et al*., 2010; Kaslin *et al*., 2009; März *et al*., 2010) (reviewed in Chapouton *et al*., 2007; Kaslin *et al*., 2008; Fig. 2). The generation of neurons of distinct neurotransmitter phenotypes (GABAergic, glutamatergic, Tyrosine hydroxylase (TH)-expressing, serotonergic) as well as the generation of oligodendrocytes has been reported. Except for the cerebellum (Chaplin *et al*., 2010; Kaslin *et al*., 2009), dividing progenitors in the adult CNS are located in ventricular regions. These dividing progenitors express radial glial markers and/or early differentiation markers (Adolf *et al*., 2006; Berberoglu *et al*., 2009; Chapouton *et al*., 2010; Ganz *et al*., 2010; März *et al*., 2010; Menuet *et al*., 2005; Pellegrini *et al*., 2007b; Raymond *et al*., 2006). Efforts to characterize progenitors (radial glial cells) in the adult telencephalon have revealed that they can exist in a quiescent or proliferating state and can switch back and forth between these two states (Chapouton *et al*., 2010; März *et al*., 2010). Additionally, BrdU tracing and marker analysis have revealed that radial glial cells generally proceed along the following lineage to generate new neurons: quiescent radial glial cells (state I progenitors) enter the cell cycle, thus becoming dividing radial glial cells (state II progenitors), which in turn generate progenitors expressing early proneural genes such as *ascl1a*, and the neural cell adhesion molecule PSA-NCAM and are thus committed to differentiation (state III progenitors) (Chapouton *et al*., 2010; März *et al*., 2010).

The pronounced neurogenic activity in the mature zebrafish CNS translates to a capacity for a strong regenerative response following injury. Thus injury models have also begun to be used to uncover the molecular and cellular features of the regenerative response in the adult CNS particularly in the spinal cord (Reimer *et al*., 2008, 2009) and in the retina (Bernardos *et al*., 2007; Fausett and Goldman, 2006; Fausett *et al*., 2008; Fimbel *et al*., 2007; Hieber *et al*., 1998a; Kassen *et al*., 2007; Thummel *et al*., 2008a,c, 2010).

# III. Methods for Studying Neurogenesis in the Developing and Adult Brain

The tools and techniques currently available to study neurogenesis allow for the identification of progenitors and their progeny, permit dynamic visualization of mitotic divisions and the behavior of proliferating and postmitotic cells, as well as manipulations of cell fate. We discuss each technique briefly and provide tables of available resources (cell-specific markers, transgenic lines, mutants etc.) and references to detailed protocols where appropriate. Finally, although the tools and methods to study neurogenesis during development can, in principle, be used to examine neurogenesis in the adult zebrafish brain, optimization is necessary. We therefore provide detailed protocols for performing a handful of methods including immunostaining, *in situ* hybridization, slice cultures, BrdU injections, lipofections, and electroporations that have been optimized for application in the adult zebrafish brain (see Section IV).

## A. Molecular Markers

Comprehensive analysis of how neurogenesis proceeds during development and adulthood requires the ability to identify progenitor cells at different stages of the cell cycle, maturation and commitment, as well as the various types of progeny they generate. Antibodies and antisense RNA probes (listed in Tables I and II) have been indispensable in providing tools for such analyses. For example, antibodies directed against proliferating cell nuclear antigen (PCNA) are used to mark all proliferating cells, while expression of phosphohistone H3 marks only those proliferating cells in the late G2- and M-phase of the cell cycle. Furthermore, the expression of specific genes can be used to identify progenitors committed to the neuronal fate (e.g., neurod) or mark newly generated postmitotic neurons (e.g., HuC and HuD; Kim *et al*., 1996; Mueller and Wullimann, 2002; Park *et al*., 2000b), and specific neuronal subtypes (e.g., glyt2 for glycinergic neurons, Higashijima *et al*., 2004). Whether performed on whole mount embryos or on sections, immunostaining and *in situ* hybridization also provide spatial information about where specific progenitors and cell-types reside in the nervous system. Detailed protocols for performing *in situ* hybridization and immunostaining on embryonic tissue can be found in Hauptmann and Gerster (2000b) and Jowett (1999). A protocol that has been optimized for examining RNA and protein expression in the adult zebrafish brain is provided in Section IV.

## B. Methods to Label Live Cells

Although the expression of specific transcripts and proteins can be used to uniquely label and identify cells, they permit analysis only in fixed specimens. Other labeling methods are required to visualize cells dynamically *in vivo*, either to trace lineages or to study the behavior of cells. One of the classical methods to label cells involves iontophoresis or pressure injection of fluorescent dyes. Lineage analysis can be performed when single cells are labeled as the dye is passed on to the ensuing progeny

**Table I**
**Markers of Distinct States and Fates: Antibodies and Antisense Probes—Distinct Cellular States**

| Name | Ab/RNA | Type of cells labeled | Reference |
|---|---|---|---|
| **Cell cycle markers** | | | |
| Phosphohistone 3 | Polyclonal Ab | Cells in late G2- and M-phase | Wei and Allis (1998) |
| Ccnb1 | RNA | Cells in late G2- and M-phase | Kassen *et al*. (2008) |
| Cdkn1c | RNA | | Park *et al*. (2005) |
| PCNA | Ab, monoclonal and polyclonal | All proliferating cells (the antigen remains present for about 24 h) | Wullimann and Knipp (2000); Thummel *et al*. (2008b) |
| MCM5 | RNA, Ab | All proliferating cells | Ryu *et al*. (2005) |
| Histone H1 | Ab | Cells in G1-phase | Huang and Sato (1998); Tarnowka *et al*. (1978) |
| BrdU | mAb | Cells in S-phase permanently labeled after BrdU treatment | Adolf *et al*. (2006); Park *et al*. (2004) |
| Histone H2A | | Visualization of mitotic figures | Pauls *et al*. (2001) |
| **Undifferentiated progenitor markers** | | | |
| *gfap* | RNA, Ab | Radial glial cells | Bernardos and Raymond (2006) |
| S100ß | Ab | Radial glial cells | Grandel *et al*. (2006); März *et al*. (2010) |
| Glutamine synthetase | Ab | Mueller glia cells | Thummel *et al*. (2008a) |
| BLBP/*FABP* | RNA, Ab | Radial glial cells | Adolf *et al*. (2006) |
| *nestin* | RNA | Radial glial cells | Mahler and Driever (2007) |
| *Cyp19b* (AroB) | RNA, Ab | Radial glial cells | Pellegrini *et al*. (2007a) |
| *pou3 (tai-ji)* | RNA | Progenitor cells | Huang and Sato (1998) |
| *pou5f1 (pou2)* | RNA | Progenitors | Hauptmann and Gerster (1996) |
| *sox2* | RNA, Ab | Progenitors | März *et al*. (2010) |
| *sox19* | RNA | Progenitors | Vriz *et al*. (1996) |
| *sox31* | RNA | Progenitors | Girard *et al*. (2001) |
| *sox11a* | RNA | Progenitors | de Martino *et al*. (2000) |
| *sox11b* | RNA | Progenitors | de Martino *et al*. (2000) |
| *sox21* | RNA | Progenitors | Rimini *et al*. (1999) |
| *her3* | RNA | Progenitors | Bae *et al*. (2005) |
| *her4* | RNA | Progenitors, radial glial cells | Yeo *et al*. (2007) |
| *her5, her11* | RNA | Midbrain progenitors | Chapouton *et al*. (2006); Ninkovic *et al*. (2005); Tallafuss and Bally-Cuif (2003) |
| *her6* | RNA | Progenitors | Scholpp *et al*. (2009) |
| *her9* | RNA | Progenitors | Latimer *et al*. (2005) |
| *id2* | RNA | Progenitors | Chong *et al*. (2005) |
| *id3* | RNA | Progenitors | Dickmeis *et al*. (2002) |
| *notch1a* | RNA | Progenitors | Mueller and Wullimann (2002); Westin and Lardelli (1997) |
| *notch1b* | RNA | Progenitors | Thisse et al. (2001), http://zfin.org |
| *notch2* | RNA | Progenitors | Thisse et al. (2001), http://zfin.org |
| *notch3* | RNA | Progenitors | Thisse et al. (2001), http://zfin.org |
| **Committed progenitor markers** | | | |
| *dlA* | RNA, Ab | Progenitors | Chapouton *et al*. (2010); Haddon (1998); Mueller and Wullimann (2002); Tallafuss *et al*. (2009) |
| *dlD* | RNA | Progenitors | Dornseifer *et al*. (1997); Haddon (1998) |
| *dlB* | RNA | Subpopulation of *deltaA* and *deltaD* expressing cells: singled-out primary neurons | Haddon (1998) |

**Table I**
**(*Continued*)**

| Name | Ab/RNA | Type of cells labeled | Reference |
|---|---|---|---|
| *dlC* | RNA, Ab | Progenitors, early expression mainly in presomitic mesoderm | Julich *et al.* (2005); Matsuda and Chitnis (2009) |
| *jagged1a, jagged1b, jagged2* | | Progenitors | Gwak *et al.* (2010); Yeo and Chitnis (2007); Zecchin *et al.* (2005) |
| *onecut1* | RNA | Progenitors, early differentiating neurons, except in the telencephalon | Hong *et al.* (2002) |
| *coe2* | | Progenitors, early postmitotic neurons | Bally-Cuif *et al.* (1998) |
| *neurog1* (*ngn1*) | RNA<br>Ab | Progenitors, early postmitotic neurons | Blader *et al.* (1997); Mueller and Wullimann (2003); Thummel *et al.* (2008a) |
| *neurod* | RNA, Ab | | Kani *et al.* (2010); Korzh *et al.* (1998); Mueller and Wullimann (2002) |
| *neurod2* | RNA | Progenitors | Liao *et al.* (1999) |
| *neurod4 (zath3)* | RNA | Progenitors, early postmitotic neurons | Park *et al.* (2003); Wang *et al.* (2003) |
| *ascl1a* | RNA | Progenitors | Allende and Weinberg (1994) |
| *ascl1b* | RNA | Progenitors | Allende and Weinberg (1994) |
| *atoh1a, atoh1b, atoh1c* | RNA | Progenitors of the rhombic lip | Adolf *et al.* (2004); Chaplin *et al.* (2010) |
| *olig1* | RNA | Oligodendrocytes progenitors | Schebesta and Serluca (2009) |
| *olig2* | RNA | Oligodendrocytes and motoneurons progenitors; cerebellar eurydendroid cells | Bae *et al.* (2009); Park *et al.* (2002) |
| *Pax6.1, pax6.2* | RNA, Ab | Retinal and brain progenitors | Adolf *et al.* (2006); Blader *et al.* (2004); Thummel *et al.* (2010) |
| **Early differentiating markers** | | | |
| *dcc* | RNA | First neuronal clusters | Hjorth *et al.* (2001) |
| *ß-thymosin* | RNA | Early differentiating neurons | Roth *et al.* (1999) |
| Polysialic acid (PSA) | Ab | Differentiating neurons, expression on cell bodies | Marx *et al.* (2001); März *et al.* (2010) |
| *cntn2 (tag1)* | RNA | Outgrowing and migrating neurons | Warren *et al.* (1999) |
| L2/HNK1 | mAb Zn12 | Outgrowing neurons | Metcalfe *et al.* (1990) |
| *elavl3 (HuC)* | RNA | Early differentiating and mature neurons. Start at 1 somite | Kim *et al.* (1996) |
| | | | Park *et al.* (2000a) |
| Elavl3 + 4 (HuC+D) | Ab | | Mueller and Wullimann (2002) |
| *elavl4 (HuD)* | RNA | Subset of postmitotic neurons. Start at 10 somites | Park *et al.* (2000a) |
| *tuba1 (α1-Tubulin)* | RNA | Early differentiating and regenerating neurons | Hieber *et al.* (1998b) |
| *β1-Tubulin* | RNA | Early differentiating, start at 24 hpf | Oehlmann *et al.* (2004) |
| *gap43* | RNA | Postmitotic neurons in the phase of axonal growth and regenerating neurons start at 17 hpf | Reinhard *et al.* (1994) |
| Eno2 | RNA | Neurons | Bai *et al.* (2007) |
| *α2-Tubulin* | RNA | Mature neurons | Hieber *et al.* (1998b) |
| Acetylated Tubulin | Ab | Membrane staining of all differentiated neurons | |
| Neurofilament | Ab | Mature neurons, reticulospinal neurons (bodies+axons) | Gray *et al.* (2001); Lee *et al.* (1987) |

(*Continued*)

**Table I**
**(*Continued*)**

| Name | Ab/RNA | Type of cells labeled | Reference |
|---|---|---|---|
| | RMO-44 | | |
| Gefiltin (intermediate filament) | Ab | Retinal ganglion cells | Leake *et al.* (1999) |
| *Plasticin* (intermediate filament) | Ab | Subset of neurons extending axons | Canger *et al.* (1998) |
| | RNA | | |
| *nadl1.1 (L1.1)* | RNA | Reticulospinal neurons during axonogenesis | Becker *et al.* (1998) |
| E587 (L1 related) | mAb E17 | Axons of primary tracts and commissures. start at 17 hpf | Weiland *et al.* (1997) |
| | CON1 | Subset of axons | Bernhardt *et al.* (1990) |
| | zn-1 | All neurons | Trewarrow *et al.* (1990) |

**Table II**
**Markers of Distinct States and Fates: Antibodies and Antisense Probes—Neuronal Identity Markers**

| Neuronal identity | Marker | Ab/RNA | Reference |
|---|---|---|---|
| **GABAergic neurons** | | | |
| | | Antibodies | Extensive list in Marc and Cameron (2001); Yazulla and Studholme (2001) |
| | Gad1 | | MacDonald *et al.* (2010) |
| | *gad2 (gad65)* | RNA | Martin *et al.* (1998) |
| | *gad1 (gad67)* | RNA | Martin *et al.* (1998) |
| **Monoaminergic neurons** | | | |
| | *Vmat2* | RNA | Wen *et al.* (2008) |
| **Catecholaminergic neurons (dopamine, noradrenalin, adrenalin)** | | | |
| Dopaminergic | *TH* (tyrosine hydroxylase) | RNA<br>Ab(Chemicon) | Guo *et al.* (1999b) |
| | *Uch-L1* | RNA | Son *et al.* (2003) |
| | *nr4a2a (Nurr1)* | RNA | Blin *et al.* (2008); Filippi *et al.* (2007); Luo *et al.* (2008) |
| | *Nr4a2b* | | |
| | *slc6a3 (dat)* | RNA | Bai and Burton (2009); Holzschuh *et al.* (2001) |
| | *Otpa,otpb* | RNA, Ab | Blechman *et al.* (2007); Ryu *et al.* (2007) |
| Noradrenergic and adrenergic neurons | *dbh* (*dopamine β hydroxylase*) | RNA | Guo *et al.* (1999b) |
| | *TH* (tyrosine hydroxylase) | RNA<br>Ab(Chemicon) | Guo *et al.* (1999b) |
| **Serotonergic neurons** | | | |
| | 5HT (serotonin) | Ab (Chemicon) | |
| | *tph (tphD1)* | RNA | Bellipanni *et al.* (2002) |

**Table II**
**(*Continued*)**

| Neuronal identity | Marker | Ab/RNA | Reference |
|---|---|---|---|
| | *tph2 (tphD2)* | RNA | Bellipanni *et al.* (2002) |
| | *tphR* | RNA | Teraoka *et al.* (2004) |
| | *Pet1* | RNA | Lillesaar *et al.* (2007, 2009) |
| | *slc6a4a; slc6a4b* | RNA | Norton *et al.* (2008) |
| **Glutamatergic neurons** | | | |
| | | Antibodies | Extensive list in Marc and Cameron (2001); Yazulla and Studholme (2001); |
| | *vglut1* and *vglut2* | RNA | Higashijima *et al.* (2004) |
| **Cholinergic neurons** | | | |
| | | Antibodies | Extensive list in Marc and Cameron (2001); Yazulla and Studholme (2001) |
| **Glycinergic neurons** | | | |
| | *glyt2* | RNA | Higashijima *et al.* (2004) |
| | *glra1, glra4a, glrb (glyR* subunits) | RNA | Imboden *et al.* (2001) |
| **Histaminergic neurons** | | | |
| | *L-histidine decarboxylase*, HA | RNA, Ab | Eriksson *et al.* (1998); Kaslin and Panula (2001b) |
| **Orexin/Hypocretin neurons** | | | |
| | *preproORX* | RNA, antibodies | Kaslin *et al.* (2004) |
| **Isotocynergic neurons** | | | |
| | Otp | Antibody | Blechman *et al.* (2007) |
| **Motoneurons** | | | |
| Primary and secondary motoneurons | HB9 | | Flanagan-Steet *et al.* (2005) |
| Primary motoneurons, early processes | znp-1 | mAb | Melancon *et al.* (1997); Trewarrow *et al.* (1990) |
| Secondary motoneurons during axonal growth | Alcam (DM-GRASP/ neurolin) | Ab zn-5 | Fashena and Westerfield (1999); Ott *et al.* (2001) |
| Primary (RoP, MiP, VaP, CaP) and secondary motoneurons | *lhx3 (lim3)* | RNA | Appel *et al.* (1995) |
| | | pAb | Glasgow *et al.* (1997) |
| MiP+RoP, secondary motoneurons and cranial motoneurons | *islet1* | RNA | Inoue *et al.* (1994) |
| | | Ab(DSHB, 40.2D6 and 39.5D5) | Korzh *et al.* (1993); Segawa *et al.* (2001) |
| CaP and VaP | *islet2* | RNA | Appel *et al.* (1995) |
| Primary motoneurons | *pnx* | RNA | Bae *et al.* (2003) |
| Primary motoneurons | *olig2* | RNA | Park *et al.* (2002) |
| Cranial motoneurons | *tbx20* | RNA | Ahn *et al.* (2000) |
| Occulomotor and trochlear motoneurons | *phox2a* | RNA | Guo *et al.* (1999a) |

(*Continued*)

**Table II**
**(*Continued*)**

| Neuronal identity | Marker | Ab/RNA | Reference |
|---|---|---|---|
| Spinal motoneurons (transiently)+ vagal motor nucleus(nX) | *sst1 (ppss1)* (somatostatin) | RNA | Devos *et al.* (2002) |
| **Reticulospinal interneurons** | | | |
| | *tlx3a (tlxA)* | RNA | Andermann and Weinberg (2001) |
| Mauthner neuron | 3A10 | Ab | Hatta (1992) |
| Mauthner neuron | *RMO-44* | mAb | Gray *et al.* (2001); Lee *et al.* (1987) |
| Mauthner neuron | *glra1, glra4a, glrb (glyR* subunits) | RNA | Imboden *et al.* (2001) |
| **Spinal cord commissural interneurons** | | | |
| | *pax2a (pax2.1)* | RNA<br>Ab | Mikkola *et al.* (1992) |
| **Interneurons of the spinal cord** | | | |
| | *pnx* | RNA | Bae *et al.* (2003) |
| | *dbx1a (hlx1)* | RNA | Fjose *et al.* (1994) |
| | *cxcr4a* | RNA | Chong *et al.* (2001) |
| Small number of interneurons | *islet1* | RNA, Ab | Korzh *et al.* (1993) |
| **Rohon-Beard primary sensory neurons** | | | |
| | *pnx* | RNA | Bae *et al.* (2003) |
| | *cxcr4b* | RNA | Chong *et al.* (2001) |
| | *islet1* | RNA<br>Ab | Korzh *et al.* (1993) |
| | *islet2* | RNA | Segawa *et al.* (2001) |
| | *tlx3a (tlxA)* | RNA | Andermann and Weinberg (2001); Langenau *et al.* (2002) |
| | *tlx3b* | RNA | Langenau *et al.* (2002) |
| | *cbfb* | RNA | Blake *et al.* (2000) |
| | *runx3* | RNA | Kalev-Zylinska *et al.* (2003) |
| Subpopulation of RB | *ntrk3a (trkC)* | RNA | Williams *et al.* (2000) |
| **Cerebellar populations** | | | |
| Upper rhombic lip, granule cells precursors | *atoh1a, atoh 1b* | RNA | Adolf *et al.* (2004); Koster and Fraser (2001) |
| Rhombic lip and granule cells | *zic1*<br>*Ptf1a* | RNA | Chaplin *et al.* (2010) |
| Eurydendroid cells | *olig2* | RNA | McFarland *et al.* (2008) |
| Purkinje cells | zebrin2 | mAb | Jaszai *et al.* (2003) |
| | M1 | mAb | Miyamura and Nakayasu (2001) |
| **Retinal cells** | | | |
| | See extensive reviews | Antibodies | Marc and Cameron (2001); Yazulla and Studholme (2001) |
| | *Brn3a* | | Sato *et al.* (2007a) |
| Amacrine cells | *pax6a (pax6.1)* | RNA | Kay *et al.* (2001); Raymond *et al.* (2006); Thummel *et al.* (2008b) |
| Ganglion cells (RGC) | *atoh7 (ath5)* | RNA | Kay *et al.* (2001); Masai *et al.* (2000) |
| RGC and INL | *islet 1* | RNA, Ab | Korzh *et al.* (1993); Masai *et al.* (2000) |
| | *islet3* | | Kikuchi *et al.* (1997) |
| RGC and INL | *lhx3 (lim3)* | RNA, Ab | Glasgow *et al.* (1997); Masai *et al.* (2000) |

**Table II**
**(*Continued*)**

| Neuronal identity | Marker | Ab/RNA | Reference |
|---|---|---|---|
| RGC | *cxcr4b* | RNA | Chong *et al.* (2001) |
| RGC | *dacha* | RNA | Hammond *et al.* (2002) |
| RGC | zn-5 | mAb | Kawahara *et al.* (2002) |
| **Pineal/habenula neurons** | | | |
| | *brn3a* | | Aizawa *et al.* (2007) |
| | *Serotonin-N-acetyltransferase-2* (*aanat2*) | RNA | Gothilf *et al.* (2002a) |
| | *islet1* | RNA, Ab | Korzh *et al.* (1993) |
| | *lhx3 (lim3)* | RNA, pAb | Glasgow *et al.* (1997) |
| | *tph (tphD1)* | RNA | Bellipanni *et al.* (2002) |
| | *cxcrb* | RNA | Chong *et al.* (2001) |
| **Pituitary gland neurons** | | | |
| | *tbx20* | RNA | Ahn *et al.* (2000) |
| | *lhx3 (lim3)* | RNA, pAb | Glasgow *et al.* (1997) |
| **Hypothalamic clusters** | | | |
| | histamine | Ab | Kaslin and Panula (2001a) |
| | *neurog3 (ngn2, ngn3)*, expression start at 24 hpf | RNA | Wang *et al.* (2003) |
| | *cxcrb* | RNA | Chong *et al.* (2001) |
| | *sst1 (ppss1)*, start at 5dpf | RNA | Devos *et al.* (2002) |
| | *tph (tphD1)* | RNA | Bellipanni *et al.* (2002) |
| | *dacha* | RNA | Hammond *et al.* (2002) |

(Li *et al*., 2000; Woo and Fraser, 1995). Caged fluorescent dyes can also be injected at the one-cell stage and subsequently uncaged in brain regions of interest at specific developmental times to allow fate-mapping studies. Photolysis of the caging group to reveal fluorescein in small numbers of cells can be achieved by UV irradiation using an epifluorescence microscope fitted with a 4′,6-diamidino-2-phenylindole (DAPI) filter set and a pinhole in the light-path to restrict the illumination to a small area (Kozlowski and Weinberg, 2000; Tallafuss and Bally-Cuif, 2003). Uncaging in individual cells can be accomplished by two-photon excitation (Russek-Blum *et al*., 2009). Although fluorescent dyes have been successfully used in several fate mapping studies, photobleaching and loss of label can pose problems; successive divisions dilute the dye making it difficult to verify whether all of a cell's descendants have been labeled.

The advent of genetically encoded fluorescent proteins has provided the most effective method thus far to indelibly label cells. Genetically encoded fluorescent proteins are generally non-toxic, do not dilute with cell divisions, and are less prone to photobleaching because new fluorescent proteins are constantly generated by the cell. Fluorescent proteins can be delivered to cells via DNA or RNA expression constructs. The purpose of the experiment and the degree of labeling specificity desired will determine which method should be employed. Ubiquitous labeling may be useful

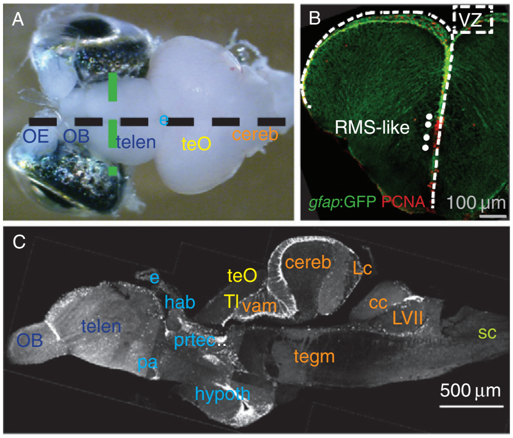

**Fig. 2** Neural progenitors in the adult brain. (A) Whole mount preparation of an adult brain of a 3-month-old zebrafish, anterior to the left, depicting the different brain regions and the levels of sections shown in B (green dashed line) and in C (gray dashed line). (B) Cross section of 100 µm thickness through the telencephalon of a *gfap*:GFP transgenic zebrafish depicting in green the cell bodies of GFP-positive radial glial cells located along a single layer at the medial and dorsal ventricular surface (VZ, white dashed line), their processes extending toward the pial surface, and in red the nuclei of dividing cells stained by an anti-PCNA antibody. Dividing cells are scattered along all levels of the VZ and are concentrated in a rostral migratory stream-like stripe (depicted by a white dotted line) situated along the A–P length of the telencephalic midline (see März *et al*., 2010). (C) Sagittal medial section depicting in white the nuclei of dividing cells stained by a PCNA antibody. Dividing progenitors are located along all ventricular regions of the brain, as well as in the cerebellum (see Kaslin *et al*., 2009). OE, olfactory epithelium; OB, olfactory bulb; telen, telencephalon; pa, preoptic area; e, epiphysis; hab, habenula; prtec, pretectal nucleus; hypo, hypothalamus; teO, optic tecum; Tl, torus longitudinalis; vam, medial valvula cerebelli; cereb, cerebellum; Lc, lobus caudalis; tegm, tegmentum; cc, crista cerebellaris; LVII facial lobe, sc spinal cord. For more details see the adult brain atlas (Wullimann *et al*., 1996). (See Plate no. 5 in the Color Plate Section.)

to obtain information about general morphogenesis either during normal development or when things go awry in mutants. However, mosaic labeling provides a powerful way to highlight individual or small numbers of cells allowing their fates and behavior to be studied with greater precision.

## 1. Transient Expression of RNA and DNA

Ubiquitous labeling of the entire embryo will result when capped RNA is injected at the one-cell stage. To achieve mosaic expression using RNA constructs, injections should be performed at later stages (16–128 cell stages) and into individual blastomeres (e.g., Alexandre *et al*., 2010). It should be noted that as RNA degrades over time, persistence of the fluorescent label is usually limited to the first 2 days of development. Injecting DNA constructs will result in mosaic expression even when injections are performed at the one-cell stage and when ubiquitous promoters are used. The resulting expression pattern, however, will be stochastic rather than cell specific. When specific cell populations need to be targeted, cell-type-specific promoters and regulatory

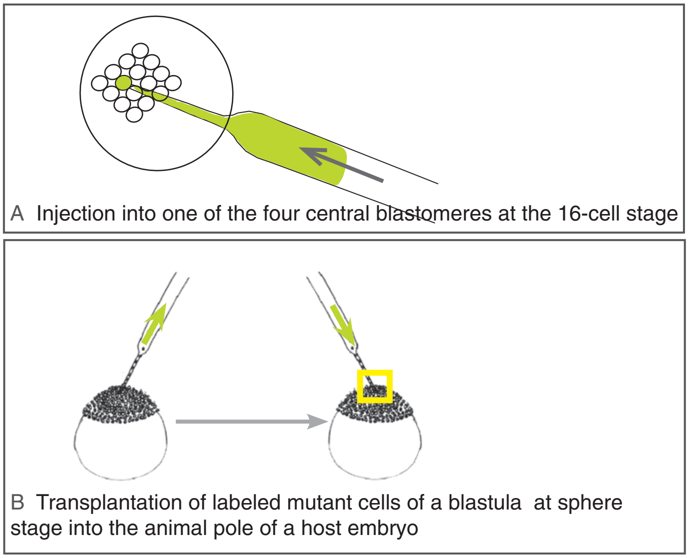
A Injection into one of the four central blastomeres at the 16-cell stage
B Transplantation of labeled mutant cells of a blastula at sphere stage into the animal pole of a host embryo

**Fig. 3** Targeting the neural plate by injection into one central blastomere at the 16-cell stage or by blastula transplantation. (A) Injection of DNA or RNA in one of the 4 central blastomeres at the 16-cell stage; (B) Transplantation of blastomeres at sphere stage. Both the injection in one of the 4 central blastomeres and the transplantation into the dorsal side of the blastula lead to a mosaic organization of injected/transplanted cells and their descendants in the neural tube. Prior to transplantation, donor embryos should be injected at the one-cell stage with a fluorescent or biotinylated dextran. Alternatively, donor embryos are transgenically labeled. The dorsal part of the host embryo, depicted by a square, is the targeted area of transplantation.

elements should be used. Although such DNA constructs are used to generate stable transgenic lines, they can also simply be injected at the one-cell stage to generate transient transgenic zebrafish. The resulting mosaic but nonetheless largely cell-specific labeling provides the ability to visualize cells in isolation. It should be noted that transient injections of DNA constructs with cell-specific promoters can sometimes also result in non-specific expression patterns. If it is necessary to restrict expression specifically to the CNS, plasmids can be introduced into one of the 4 central cells at the 16-cell stage, as these cells give rise to the CNS (Helde *et al.*, 1994) (Fig. 3A).

## 2. Stable Transgenic Lines

To obtain reproducible cell-specific expression patterns for every experiment, stable transgenic lines should be used. A vast array of stable transgenic lines has been generated, where cell-type-specific regulatory elements drive the expression of fluorescent proteins [most commonly green fluorescent protein (GFP)] in progenitors and postmitotic cells of diverse fates (see Table III). Additionally, stable transgenic lines as well as libraries of enhancer trap lines driving the expression of the transcriptional activator Gal4 have been generated (Asakawa and Kawakami, 2009;

Asakawa *et al*., 2008; Choo *et al*., 2006; Distel *et al*., 2009; Ogura *et al*., 2009; Scott and Baier, 2009; Scott *et al*., 2007). These Gal4 "driver" lines can be crossed to "effector" transgenic lines expressing fluorescent proteins under the control of the Gal4-specific Upstream Activating Sequence (UAS) promoter (UAS:GFP; UAS: RFP, UAS:Kaede; see Table IV). Alternatively, UAS reporter constructs can be injected into eggs from specific Gal4 driver lines, or vice versa, enhancer-specific Gal4 constructs can be injected into eggs from UAS effector lines to achieve mosaic expression patterns. Expression of the reporter is maintained as long as the cell-specific enhancer and promoter elements drive Gal4 expression. A new UAS effector transgenic line, however, allows continuous expression of a reporter gene once activated. To generate this line, a bicistronic construct was used to express both a reporter gene (GFP) and the Gal4 transcriptional activator, KalTA4, under UAS promoter elements (Distel *et al*., 2009). Activation of UAS thus results in the expression of both GFP and KalTA4. The expression of KalTA4 allows reiterative activation of UAS and therefore maintenance of expression.

**Table III**
**Transgenic Lines to Visualize Distinct States and Fates**

| Cell type/brain region | Transgenic line | Reference |
|---|---|---|
| **Ubiquitous** | H2A.F/Z:GFP | Pauls *et al*. (2001) |
| | H2Afx:H2A-mCherry | McMahon et al. (2009) |
| | αactin:GFP | Higashijima et al. (1997) |
| | αactin:M.GFP | Cooper et al. (2005) |
| | Pax6-DF4:gap43-CFPQ$^{01}$ | Godinho *et al*. (2005) |
| **Cell cycle phases** | Cecyil double transgenic line | Sugiyama *et al*. (2009) |
| **Progenitors, radial glial cells** | | |
| Neural progenitors; radial glial cells | her4:rfp<br>her4:gfp | Yeo *et al*. (2007) |
| Radial glial cells | Fezf2:GFP | Berberoglu *et al*. (2009) |
| Radial glial cells | Cyp19a1b:gfp | Tong *et al*. (2009) |
| Radial glial cells | gfap:gfp | Bernardos and Raymond (2006); Lam *et al*. (2009) |
| Radial glial cells | nestin:gfp | Kaslin *et al*. (2009); Lam *et al*. (2009) |
| Mid-hindbrain boundary progenitors | her5:gfp | Chapouton *et al*. (2006); Tallafuss and Bally-Cuif (2003) |
| **Committed progenitors** | | |
| Rhombic lip progenitors | Atoh1a:egfp<br>Atoh1a:dTomato | Kani *et al*. (2010) |
| Neuronal progenitors<br>DRG-sensory neurons | neurog1:gfp | Blader *et al*. (2004); McGraw *et al*. (2008) |
| Neuronal progenitors | deltaA:gfp | Chapouton *et al*. (2010) |
| Neuronal progenitors and early differentiating neurons | α1-tubulin:gfp | Fausett *et al*. (2008); Goldman *et al*. (2001) |
| **Differentiating and early postmitotic neurons** | | |
| Early differentiating neurons | HuC:gfp<br>HuC:Kaede | Park *et al*. (2000c); Sato *et al*. (2006) |

**Table III**
**(*Continued*)**

| Cell type/brain region | Transgenic line | Reference |
|---|---|---|
| Neurons | Eno2:gfp | Bai *et al.* (2009) |
| | Eno2:rfp | |
| Differentiating and regenerating neurons | gap43:gfp | Kusik *et al.* (2010) |
| Oligodendrocyte progenitors | olig1:mgfp | Schebesta and Serluca (2009) |
| Oligodendrocyte progenitors | sox10:mrfp | Kucenas *et al.* (2008) |
| Motoneurons and oligodendrocyte progenitors | olig2:GFP | Shin *et al.* (2003) |
| | olig2:dsred2 | Kucenas *et al.* (2008) |
| | olig2:Kaede | Zannino and Appel (2009) |
| Motoneurons and oligodendrocyte progenitors<br>Differentiated neurons and glia | nkx2.2a: EGFP | Kirby *et al.* (2006) |
| Oligodendrocytes | plp:gfp | Yoshida and Macklin (2005) |
| **Neuronal subtypes** | | |
| Motoneurons | hb9:GFP | Flanagan-Steet *et al.* (2005) |
| | hb9:mGFP | |
| Cranial motoneurons | isl1:GFP | Higashijima *et al.* (2000) |
| Sensory neurons | sensory:GFP | Sagasti *et al.* (2005) |
| Excitatory interneurons | alx:GFP | Kimura *et al.* (2006) |
| V2 interneurons | vsx1:GFP | Kimura *et al.* (2008) |
| Caudal primary neurons | nrp1a:GFP | Sato-Maeda *et al.* (2008) |
| Spinal cord commissural interneurons | pax2.1:GFP | Picker *et al.* (2002) |
| Olfactory sensory neurons | pOMP$^{2k}$:gap-CFP | Sato *et al.* (2005) |
| | pOMP$^{2k}$:lyn-RFP | |
| | pTRPC2$^{9k}$:gap-Venus | |
| | pTRPC2$^{4.5k}$:gap-Venus | Sato *et al.* (2007b) |
| | OR111-7:YFP | |
| | OR1031:CFP | Feng *et al.* (2005) |
| | rag1:gfp | |
| Glycinergic neurons | glyt2:gfp | McLean *et al.* (2007) |
| Monoaminergic neurons | vmat2:gfp | Wen *et al.* (2008) |
| TH-positive neurons | TH:Mmgfp | Meng *et al.* (2008a) |
| Serotonergic neurons | pet1:gfp | Lillesaar *et al.* (2009) |
| Glutamatergic neurons | vglut2a:egfp | Bae *et al.* (2009) |
| | vglut2a:dsred2 | Kani *et al.* (2010) |
| | Xeom:gfp | Mione *et al.* (2008) |
| GABAergic neurons | ptf1a:gfp | Kani *et al.* (2010); Pisharath *et al.* (2007) |
| | ptf1a:gal4VP16 | Zerucha *et al.* (2000) |
| | 1.4dlx5a-6a:GFP | MacDonald *et al.* (2010) |
| | Dlx1a/2aIG:GFP | |
| Gonadotropin releasing hormone neurons | gnrh:gfp | Palevitch *et al.* (2007) |
| Pineal neurons | aanat2:gfp | Gothilf *et al.* (2002b) |
| Dorsal hindbrain neurons | gad2:gal4VP16 | Sassa *et al.* (2007) |
| Dorsal hindbrain neurons | zic1:gal4VP16 | Sassa *et al.* (2007) |
| Retinal and habenular neurons | Brn3ahsp70:gfp | Aizawa *et al.* (2007) |
| Telencephalic neurons | Tbr1:yfp | Mione *et al.* (2008) |

(*Continued*)

### Table III
### (*Continued*)

| Cell type/brain region | Transgenic line | Reference |
|---|---|---|
| **Reporter transgenes for specific signaling activity** | | |
| Cells containing Notch activity | TP1bglob:gfp<br>TP1bglob:rfp | Parsons *et al.* (2009) |
| Cells containing wnt activity | Top:dgfp | Dorsky *et al.* (2002) |
| Cells containing fgf activity | Dusp6:gfp | Molina *et al.* (2007) |
| Hedgehog-expressing cells | shh:gfp | Ertzer *et al.* (2007) |
| | twhh:gfp | Du and Dienhart (2001) |
| **Retinal cells** | | |
| Rod photoreceptors (pan) | Rhodopsin:GFP | Hamaoka *et al.* (2002) |
| | Xenopus rhodopsin:GFP | Fadool (2003) |
| Cone photoreceptors (pan) | TransducinαC:GFP | Kennedy *et al.* (2007) |
| UV cone photoreceptors (pan) | SWS1:GFP | Takechi *et al.* (2003) |
| Blue cone photoreceptors (pan) | SWS2:GFP | Takechi *et al.* (2003) |
| Green cone photoreceptors | RH2-1:GFP, RH2-2:GFP, RH2-3:GFP, RH2-4:GFP | Tsujimura *et al.* (2007) |
| Horizontal cells (pan) | ptf1a:GFP | Godinho *et al.* (2005) |
| Bipolar cells | vsx1:GFP | Vitorino *et al.* (2009) |
| Bipolar cells (subset) | vsx2:GFP | Vitorino *et al.* (2009) |
| Bipolar cells (subset) | nyctalopin:Gal4VP16 UAS:memYFP | Schroeter *et al.* (2006) |
| Amacrine cells (pan) | ptf1a:GFP | Godinho *et al.* (2005) |
| Amacrine cells (subset) | Pax6DF4:memYFP | Kay *et al.* (2004) |
| | Pax6DF4:memCFP | Godinho *et al.* (2005) |
| Amacrine cells (subset) | 12th:MmGFP | Meng et al. (2008) |
| Ganglion cells (subset) | brn3c: memGFP | Xiao *et al.* (2005) |
| Ganglion cells (all or vast majority) | isl2b:mCherry | Pittman *et al.* (2008) |
| Müller glial cells (pan) | gfap:GFP | Bernardos and Raymond (2006); Kassen *et al.* (2007); Lam *et al.* (2009) |
| **Miscellaneous** | | |
| Enhancer trap-viral insertion | yfp | Ellingsen *et al.* (2005) |
| Enhancer trap | gfp | Parinov *et al.* (2004) |
| Enhancer trap screen | gal4 | Asakawa and Kawakami (2009); Asakawa *et al.* (2008); Choo *et al.* (2006); Distel *et al.* (2009); Ogura *et al.* (2009); Scott and Baier (2009); Scott *et al.* (2007) |

### Table IV
### Uas Effector Lines

| Purpose/manipulation | Transgenic line | Reference |
|---|---|---|
| Visualization | uas:gfp | Asakawa *et al.* (2008) |
| Visualization | uas:rfp | Asakawa *et al.* (2008) |
| Photoconvertible fluorescent protein | uas: kaede | Asakawa *et al.* (2008) |
| Blocking synaptic transmission | uas:tetxLC | Davison *et al.* (2007) |
| Overexpression of Notch intracellular domain | uas:nicd | Scheer and Campos-Ortega (1999) |

### 3. Electroporation and Lipofections

When promoter elements that target specific cell populations are unknown, but restricted spatial and/or temporal labeling is still required, DNA or RNA can be transfected into cells either by electroporation or by lipofection. Electroporation methods have been developed for embryonic, juvenile, and adult zebrafish. Following the focal injection of DNA or RNA into the desired brain region to target groups of cells (Bianco *et al.*, 2008; Kera *et al.*, 2010) or using microelectrodes to target individual cells (Cerda *et al.*, 2006; Tawk *et al.*, 2009), a small current is applied. In the adult zebrafish brain, radial glial cells, by virtue of their location near the ventricular surface, can be specifically targeted for lipofection or electroporation by injecting DNA expression constructs into the ventricles (Chapouton *et al.*, 2010) (Fig. 5, see Section IV).

### 4. Blastomere Transplantation

Mosaic labeling can also be achieved by taking advantage of classical embryological techniques of transplantation (Fig. 3B). Briefly, cells from a transgenically labeled embryo, or from an embryo injected at one-cell stage with rhodamine dextran, are transplanted at sphere stage into unlabeled embryos at the same developmental age, into the region that will develop into the future brain. This region is, however, determined at shield stage (dorsal part of the blastula at shield stage Woo and Fraser, 1995), so that not all transplantations will contribute cells to the brain. Correctly transplanted embryos need to be sorted at later stages. This technique is described in detail in Kemp *et al.* (2009).

## C. *In Vivo* Imaging

By permitting direct observations of processes as they occur *in vivo*, time-lapse imaging is proving to be a powerful tool to study neurogenesis. Several characteristics of embryonic and larval zebrafish make them particularly accessible to *in vivo* time-lapse imaging. First, their relative transparency and external development permit imaging without manipulative surgery. Second, genetic tools can be used to label progenitors and their progeny fluorescently (See Section III.B). Third, the speed with which development occurs makes it feasible to follow the fate of individual progenitors over multiple rounds of divisions (Lyons *et al.*, 2003) and until the terminal differentiation of their progeny. Indeed, it has been possible to visualize directly the behavior of neural progenitor cells (including INM), mitotic divisions, where these mitoses occur, and the outcomes of the divisions, whether these are symmetric and proliferative, symmetric and terminal, or asymmetric, with a progenitor and a postmitotic cell being generated (Baye and Link, 2007b; Das *et al.*, 2003; Godinho *et al.*, 2007; Poggi *et al.*, 2005; Norden *et al.*, 2009).

Although largely transparent, zebrafish harbor pigment cells (melanophores and iridophores) which can be problematic for imaging beyond 24 hpf. Melanophores (black pigment cells) are first detectable around 24 hpf, whereas iridophores (silver pigment cells) can be detected beginning at 42 hpf. Chemical inhibition of melanin formation, by rearing the embryos in *N*-phenylthiourea (PTU) and mutants that lack melanophores (*nacre*; Lister *et al*., 1999) or iridophores (*roy orbison*; Ren *et al*., 2002) can be used to circumvent pigment-associated problems. By treating *roy orbison* embryos with PTU, transparency can be maintained until larval stages, whereas breeding *nacre* with *roy orbison* permits transparency to be maintained into adulthood (*mitfa;roy*; White *et al*., 2008).

In stark contrast to the abundant reports of *in vivo* time-lapse imaging studies of neurogenesis during development, no such reports exist thus far for adult fish. Lack of transparency in adults and the difficulty of immobilizing adult fish are likely contributors. The pigmentation mutants *nacre, roy orbison*, and *mitfa;roy* should, in principle, permit imaging of the intact adult zebrafish CNS. However, using pigmentation mutants to conduct imaging studies, whether during development or at maturity, requires careful verification that physiological processes occur in a normal and timely manner. Although keeping embryonic and larval zebrafish immobilized and alive for imaging is relatively easy, the situation is more challenging for adult fish. Embryonic and larval fish can be embedded in low-melt agarose and continually anesthetized in tricaine for periods of up to 24 h continuously while largely maintaining normal development. For adult fish, it will be necessary to construct special devices to restrain the animal while superfusing the gills with anesthetic-containing water, methods used in electrophysiological recordings of goldfish (Szabo *et al*., 2008).

The most effective way to indelibly label cells for imaging has been to use genetically encoded fluorescent proteins. Several methods now exist to restrict fluorescent labeling to individual or a few cells, easing fate tracking during time-lapse imaging (see Section III.B). Despite the vast array of available fluorescent proteins (Rizzo *et al*., 2009; Shaner *et al*., 2005, 2008), green fluorescent protein (GFP) remains the most commonly used in reporter constructs and in stable transgenic lines (see Table III). When multicolor imaging is required, either to label different compartments of a cell (e.g., nucleus and cytoplasm) or to label different cell populations concurrently, it is worth noting the fluorescent proteins with non-overlapping spectra (Shaner *et al*., 2005). Although combinations of GFP and RFP have been the most commonly used (Alexandre *et al*., 2010), CFP and YFP have also been demonstrated to work well in combination (Mumm *et al*., 2006). A notable addition to the palette of fluorescent proteins is the growing number of photoconvertable and photoswitchable fluorescent proteins which can serve to highlight one or a few cells among a larger labeled population, thus allowing cells to be tracked more confidently (Lippincott-Schwartz and Patterson, 2009). Kaede and Dronpa are the only examples reported to be used in zebrafish thus far (Aramaki and Hatta, 2006; Hatta *et al*., 2006; Sato *et al*., 2006). Kaede converts from green to red fluorescence in response to irradiation with UV light (Ando *et al*., 2002), while Dronpa can be switched on or off by excitation with 405 and 488 nm respectively (Habuchi *et al*., 2005). Additionally, two-photon excitation can be used to turn on Dronpa, thus making it possible to target individual cells in a volume (Aramaki and Hatta, 2006).

With its ability to capture images at depths 30–50 μm from the surface and optical sectioning capability, confocal microscopy has been the workhorse of most of the imaging studies conducted in zebrafish so far. Confocal microscopes equipped with the appropriate laser lines to excite the most commonly used fluorescent proteins (440 nm for CFP, 488 nm for GFP, 514 nm for YFP, and 559 or 568 nm for RFP) and several detectors (photomultiplier tubes) allow multichannel imaging. A 405 nm laser line or other source of UV illumination is necessary when working with many photoactivatable fluorescent proteins (e.g., Kaede). Imaging deeper structures, several hundred microns below the surface, can be accomplished only by multiphoton microscopy, which requires a tunable pulsed infrared laser. Additionally, because multiphoton excitation is confined only to the focal plane, repetitive imaging over long time frames produces less phototoxic effects than confocal microscopy (Helmchen and Denk, 2005). When fast acquisition and detection of cellular or intracellular events and optical sectioning are required, spinning disk confocals are more suitable than slow scanning confocal and multiphoton microscopes.

Finally, recent developments in light microscopy that allow imaging at high speeds and at greater depths, while keeping phototoxicity at low levels, have provided unprecendented three dimensional (3D) reconstructions of early zebrafish embryogenesis in its entirety. These new microscopy approaches promise to contribute to studies of neurogenesis by providing not only qualitative data but also quantitative data. As the name implies, digital scanned laser light sheet fluorescence microscopy (DSLM) uses a sheet of laser light to illuminate a transparent, fluorescently labeled specimen in a single plane and a camera to detect images placed at a 90° angle from the axis of illumination. DSLM was used to record the first 24 h of zebrafish embryogenesis with high temporal and spatial resolution allowing the mitotic divisions and movements of every cell to be tracked (Keller *et al*., 2008). Modifications of DSLM, using structured illumination to overcome the difficulties of imaging older zebrafish embryos which scatter light, allowed imaging up to the third day of development (Keller *et al*., 2010). Another approach to acquire complete views of zebrafish embryonic development exploited the intrinsic non-linear optical properties of cells to image mitotic spindles and membranes without the need for fluorescent labeling (Olivier *et al*., 2010). Furthermore, optimizing the scanning mode to capture images of the deepest structures at higher frame rates allowed entire 3D reconstructions of embryogenesis for the first 10 cell division cycles. The vast amounts of data acquired through such imaging approaches have also necessitated the development of software to allow for automated image reconstruction and cell tracking (Keller *et al*., 2008, 2010; Olivier *et al*., 2010).

## D. Methods to Follow Cell Cycle Events

One of the simplest and yet powerful tools to examine the dynamics of the cell cycle takes advantage of the incorporation of thymidine analogues into newly synthesized DNA. The most commonly used among these analogues is bromodeoxyuridine

(BrdU), followed by chlorodeoxyuridine (CldU), iododeoxyuridine (IdU), and ethynyldeoxyuridine (EdU).

Because DNA is newly synthesized during S-phase, BrdU incorporation, which can be detected by antibody labeling, can be used to mark cells undergoing the S-phase of the cell cycle. BrdU incorporation can also be used to measure other cell cycle parameters. The relative cell cycle speed of a progenitor population can be inferred by calculating the proportion of cells residing in S-phase (BrdU-positive) within the total number of cycling cells (i.e., PCNA-positive), given that the S-phase remains relatively constant, while the G1-phase is more variable. The fates of cells "born" (i.e., that permanently leave the cell cycle) at specific times can be determined by administering BrdU over a short time window and sacrificing the animal after several days or weeks. Because the incorporated BrdU will not be diluted by cells that have left the cell cycle, double labeling with antibodies against BrdU and specific cell-type markers will reveal the fate of the cells. After long chase periods, some BrdU label-retaining cells remain in the stem cell niche without having divided many times, therefore without having diluted BrdU. The cycling status of these label-retaining cells can be determined by a co-staining for PCNA (Adolf *et al*., 2006; Alunni *et al*., 2010; Chapouton *et al*., 2006; Kaslin *et al*., 2009) or by the incorporation of a second thymidine analogue, such as IdU (Aluni et al., 2010). BrdU and the other base analogues can be administered to the living animal in different ways: embryos can be soaked in a BrdU solution (although the skin can be difficult to permeabilize) (Kim *et al*., 2008; Park *et al*., 2004) or BrdU can be directly injected into the brain region of interest (Baye and Link, 2007b). To examine cell proliferation in the adult CNS, BrdU can be injected intraperitoneally (detailed protocol provided in Section IV, Fig. 4) (Adolf *et al*., 2006) or added to the swimming water (Grandel *et al*., 2006).

An alternative to using BrdU incorporation to determine the birthdates of cells takes advantage of the photoconversion properties of Kaede. By using transgenic lines in which neurons express Kaede shortly following their birth (Huc:Kaede), selective photoconversion can highlight neurons generated at specific developmental times. The fates that these Kaede-marked new-born cells adopt can be examined by their subsequent expression of cell-type-specific transgenic markers. This method termed BAPTISM (birthdating analysis by photoconverted fluorescent protein tracing *in vivo* combined with subpopulation markers), permits continuous observation of the birthdated cells throughout their development (Caron *et al*., 2008).

Taking advantage of the upregulation of specific proteins at distinct phases of the cell cycle, a new technique, Fucci (fluorescent ubiquitination-based cell cycle indicator), allows an *in vivo* glimpse into cell cycle progression (Sugiyama *et al*., 2009). By crossing two transgenic lines in which the ubiquitination domain of Cdt1 is fused to Kusabira Orange 2 and the ubiquitination domain of geminin is fused to Azami Green, respectively, it is possible to distinctly mark the G1-phase (orange) and the S/G2/M-phase (green) of the cell cycle. This new tool permits cycling progenitors to be imaged *in vivo*, while displaying the phase of the cell cycle they are in. It will thus be possible to investigate whether progenitors in specific brain regions or at different developmental times display heterogeneous cell cycle behaviors.

## E. Manipulating the Expression of Genes Involved in Neurogenesis

To investigate the genetic mechanisms underlying neurogenesis, loss-of-function and gain-of-function approaches can be used. Gain-of-function approaches typically involve the overexpression or misexpression of genes by RNA injection or transient or stable transgene expression. Restricting gene expression temporally and/or to specific cell-types can be achieved by using cell-type-specific promoters or inducible systems (discussed below). Loss-of-function studies examine the effects of disruptions in gene function. Antisense morpholino oligonucleotides to knock-down gene expression (Knowlton *et al*., 2008), the use of dominant negative constructs, and analysis of mutant fish can provide insights into the genetic underpinnings of neurogenesis. Mutants have been isolated in several mutagenesis screens (Tables V and VI) generated using TILLING (Targeting induced local lesions in genomes) libraries (Wienholds et al., 2002) or by the more recent technology of zinc finger nucleases (Doyon *et al*., 2008; Meng *et al*., 2008b). The use of small interfering RNAs (siRNAs) to knock-down-specific genes in zebrafish has not proved successful so far due to strong developmental side effects. These side effects have been attributed to an interference with the microRNA processing machinery (Fjose and Zhao, 2010), leading to an impairment of microRNA function.

Many loss- and gain-of-function approaches disrupt gene expression early in development and potentially throughout the embryo. Thus it may be difficult to decipher a specific role for a gene in neurogenesis if it also plays a role in early embryonic development. To circumvent this, genetic perturbations that can be spatially and/or temporally restricted are required.

**Table V**
**Mutants and Transgenics Allowing for Manipulation of the Whole Embryo**

| | Transgenic, mutant, or chemical inhibitor | Affected protein | Reference |
|---|---|---|---|
| **Mutants affecting cell cycle** | | | |
| | mcm5 | MCM5 | Ryu *et al*. (2005) |
| | disarrayed | – | Baye and Link (2007a) |
| | perplexed | carbamoyl-phosphate synthetase2-aspartate transcarbamylase-dihydroorotase (cad) | Link *et al*. (2001b); Willer *et al*. (2005) |
| | pescadillo | Pescadillo | Allende *et al*. (1996) |
| | APC | APC | Wehman *et al*. (2007) |
| | curly fry(cfy) | - | Song *et al*. (2004) |
| | flotte lotte (flo) | Elys/Ahctf1 | Cerveny et al. (2010) |
| | Transgenic: hsp70: cdkn1c-myc | | Park *et al*. (2005) |
| **Mutant of the neurogenic cascade** | | | |
| | Notch pathway mutants (see below) | | |
| | *neurog1* | Neurog1 | Golling *et al*. (2002) |
| | *ascl1a* | Ascl1a | http://zfin.org |

(*Continued*)

**Table V**
**(*Continued*)**

| | Transgenic, mutant, or chemical inhibitor | Affected protein | Reference |
|---|---|---|---|
| **Cell polarity mutants** | | | |
| | ncad | N-Cadherin | Lele *et al*. (2002); Malicki *et al*. (2003); Yamaguchi *et al*. (2010) |
| | nagy oko (nok) | Pals1/Stardust | Bit-Avragim *et al*. (2008); Wei and Malicki (2002) |
| | mosaic eyes (moe) | FERM domain protein | Jensen and Westerfield (2004) |
| | heart and sould (has) | aPKCλ | Horne-Badovinac *et al*. (2001) |
| | oko meduzy (ome) | Crumbs2 | Malicki and Driever (1999); Omori and Malicki (2006) |
| | pen/lgl2 | Lgl2 | Reischauer *et al*. (2009); Sonawane *et al*. (2005) |
| | ale oko | P50 component of dynactin complex | Jing and Malicki (2009) |
| **Signalling pathway mutants or inhibitors** | | | |
| FGF-pathway | Hsp:dn-fgfR1 | | Gonzalez-Quevedo *et al*. (2010); Lee *et al*. (2005) |
| | Hsp: ca-fgfR | | Marques *et al*. (2008) |
| | Hagoromo FGF upregulation mutant | | Amsterdam *et al*. (2009) |
| | fgf20 mutant | | Gonzalez-Quevedo *et al*. (2010) |
| | fgf8 mutant | | Reifers *et al*. (1998) |
| | Inhibitor | SU5402 | Furthauer *et al*. (2001) |
| Shh-pathway | smoothened (smo) | Smoothened receptor | Chen *et al*. (2001) |
| | Sonic you (Syu) | Shh | Schauerte *et al*. (1998) |
| | detour | Gli1 | Odenthal *et al*. (2000); Vanderlaan *et al*. (2005) |
| | you too (yot) | Gli2 | Vanderlaan *et al*. (2005) |
| | broad minded (bromi) | | Ko *et al*. (2010) |
| | Inhibitor: cyclopamine | | Chen *et al*. (2001) |
| Notch-pathway | deadly seven (des) | Notch1a | Gray *et al*. (2001); Liu *et al*. (2003) |
| | dla$^{dx2}$ | DeltaA | Appel *et al*. (1999) |
| | after eight (aei) | DeltaD | Holley *et al*. (2000) |
| | Beamter (bea) | DeltaC | Julich *et al*. (2005) |
| | mind bomb (mib) | E3 ubiquitin ligase that is required for Delta endocytosis | Itoh *et al*. (2003) |
| | Transgenic: hsp70:dnSu(H) | Dominant negative effect on Su(H) and block of Notch activity | Latimer *et al*. (2005) |
| | Transgenic: hsp:gal4 x uas:nicd-myc | Activation of Notch signalling | Scheer *et al*. (2001) |
| | Inhibitor: DAPT | | Chapouton *et al*. (2010); Geling *et al*. (2002) |
| BMP pathway | swirl (swr) | Bmp2 | Kishimoto *et al*. (1997); Nguyen *et al*. (1998) |
| | Snailhouse (snh) | Bmp7 | Nguyen *et al*. (1998) |
| | chordino (chd) | Chordin | Schulte-Merker *et al*. (1997) |
| | Somitabun (sbn) | Smad5 | Hild *et al*. (1999) |
| Nodal pathway | one eyed pinhead (oep) | EGF-CFC class protein | Gritsman *et al*. (1999) |
| | cyclops | TGFß of nodal class | Feldman *et al*. (2000) |
| | squint | TGFß of nodal class | Feldman *et al*. (2000) |

**Table V**
**(*Continued*)**

| | Transgenic, mutant, or chemical inhibitor | Affected protein | Reference |
|---|---|---|---|
| | Inhibitor: SB431542 | | Ribes *et al.* (2010) |
| Wnt pathway | masterblind | Axin1 | Heisenberg *et al.* (1996); Masai *et al.* (1997) |
| | headless | TCF3 | Kim *et al.* (2000) |
| | GSK3ß Inhibitor: OTDZT | | Ninkovic *et al.* (2008) |
| | Activator: LiCl | | Ninkovic *et al.* (2008) |
| **Mutant collections** | Viral mutagenesis screen | | Wang *et al.* (2007) |
| | Insertional mutagenesis screen | | Amsterdam *et al.* (1999); Golling *et al.* (2002) |
| | Gene trap screen | | Asakawa *et al.* (2008) |
| | TILLING mutants | | Moens *et al.* (2008) |

**Table VI**
**Mutants Affecting Neuronal Specification**

| Mutant name | Abbreviation | Mutated gene | Phenotype | Reference |
|---|---|---|---|---|
| *narrowminded* | *nrd* | *prdm1* (SET/ zinc finger transcription factor) | Loss of Rohon-Beard and decrease in neural crests neurons | Artinger *et al.* (1999); Hernandez-Lagunas *et al.* (2005) |
| *motionless* | *mot* | *Med* (component of the Mediator complex) | Less dopaminergic hypothalamic neurons, lacking brain ventricles, cell death in telencephalon and lens by 50 hpf. | Guo *et al.* (1999b); Wang *et al.* (2006) |
| *foggy* | *fog* | *supt5h* (*spt5*) | Lack of dopaminergic neurons in hypothalamus, telencephalon and retina, and lack of noradrenergic neurons in the locus Coeruleus (+cardiovascular defects) | Guo *et al.* (1999b); Guo *et al.* (2000) |
| *too few* | *tof* | *fezl* | Reduction of hypothalamic dopaminergic neurons | Guo *et al.* (1999b); Levkowitz *et al.* (2003) |
| *opta* | *m866* | *orthopedia* | Fewer dopaminergic neurons in the hypothalamus and caudal posterior tuberculum | Ryu *et al.* (2007) |
| *soulless* | *sll* | *phox2a* | Loss of locus coeruleus and arch associated catecholaminergic neurons | Guo *et al.* (1999a) |
| *lakritz* | *lak* | *atoh7 (ath5)* | Loss of retinal ganglion cells | Kay *et al.* (2001) |
| *young* | *yng* | *smarca4* | Blocked final differentiation of retinal cells | Gregg *et al.* (2003); Link *et al.* (2000) |
| *perplexed* | *plx* | carbamoyl-phosphate synthetase2-aspartate transcarbamylase-dihydroorotase (cad) | Cell death of retinal cells before exiting the cell cycle | Link *et al.* (2001b); Willer *et al.* (2005) |
| *confused* | *cfs* | | Cell death in a subset of retinal postmitotic cells | Link *et al.* (2001a) |
| *ascending and descending* | *add* | Hdac1 | Retinal cells do not exit the cell cycle | Yamaguchi *et al.* (2005) |

## 1. Spatial Control of Genetic Manipulations

Blastomere transplantation is one approach to spatially restrict genetic perturbations. Mosaic mutants can be generated by transplanting a few cells at the sphere stage from tracer-labeled (rhodamine dextran or other fluorophore) mutant embryos into the dorsal blastula of unlabeled wild-type embryos. Because the dorsal blastula is the site of the future presumptive brain (Woo and Fraser, 1995), integration of the transplanted mutant cells will be restricted to this region. Genetic mosaic animals have the added benefit of allowing studies of the effect of a mutation in isolated cells and whether a phenotype resulting from a mutated gene is cell autonomous or non-autonomous (Ho and Kane, 1990).

Genetic perturbations can also be targeted to specific brain regions or even single cells at selected times (from early embryos until adulthood) by the electroporation (Bianco *et al*., 2008; Cerda *et al*., 2006; Chapouton *et al*., 2010; Kera *et al*., 2010; Tawk *et al*., 2009) or lipofection (Chapouton *et al*., 2010) of constructs (e.g., overexpression, dominant-negative). Additionally, electroporation can be used to deliver antisense morpholinos directly into CNS regions of interest even at adult stages (Fausett *et al*., 2008; Thummel *et al*., 2008c). The ability to knock-down genes at later ages using this approach circumvents the declining efficacy of morpholinos injected at the one-cell stage. (Morpholinos are usually not effective at knocking down genes beyond the first 2 days of development, presumably due to their dilution with cell divisions and/or due to the synthesis of new mRNA.) Recombinant sindbis and rabies viruses can also be used to deliver transgenic constructs by infecting neurons in larval or adult zebrafish brains (Zhu *et al*., 2009). CMV-based retro- and lentiviruses can be used to target the adult brain ventricular zones (Rothenaigner and Bally-Cuif, personal communication).

Cell-type-specific promoters can be used to target genetic manipulations to specific cell populations using either transient transgenic approaches or stable transgenic lines. Additionally, one can take advantage of the vast array of available Gal4 driver lines generated through enhancer trap screens, some of whose expression patterns have been characterized. Specific Gal4 driver lines can be crossed with UAS effector transgenic lines that allow for genetic manipulation (e.g., *UAS:NICD* that produces overexpression of the Notch intracellular domain; Table IV). Alternatively, in the absence of UAS effector transgenic lines, UAS constructs can be injected into eggs obtained from Gal4 driver lines.

In a similar manner to the Gal4-UAS bipartite system, but leading to permanent genetic recombination, the Cre-loxP system can be used to achieve spatial control of gene expression. Cre recombinase expressed under a specific enhancer in one transgenic line can be used to excise loxP sites in a second transgenic line carrying a ubiquitously expressed reporter. Recombination will occur in cells expressing Cre and in the progeny they generate, providing a way to mark clones of cells genetically. Conversely, the reporter can be expressed under a specific enhancer and Cre expressed ubiquitously (Seok *et al*., 2009) (see Table VII).

**Table VII**
**Cell-Type-Specific Manipulations: Simple and Combined Driver + Effector Transgenic Lines**

| Description | Transgenic line | Reference |
|---|---|---|
| Tracing of cells progeny | Tissue-specific:KalTA4 (several enhancer trap lines)uas: gfpT2ATalTA4 | Distel *et al.* (2009) |
| | http://plover.imcb.a-star.edu.sg/~zetrap/ZETRAP.htm | Asakawa *et al.* (2008); Choo *et al.* (2006); Davison *et al.* (2007); Scott *et al.* (2007) |
| Permanent ubiquitous deletion of gfp and expression of dsred. | EF1α-lox-gfp-lox-dsred2 | Yoshikawa *et al.* (2008); Sinha *et al.* (2010) |
| Permanent ubiquitous deletion of dsred and expression of gfp. | EF1α-lox-dsred2-lox-egfp | Hans *et al.* (2009) |
| Permanent expression of KRAS in progenitors after Cre- induced recombination. | Nestin-lox-Cherry-lox-EGFP-KRAS | Seok *et al.* (2009) |
| Permanent ubiquitous expression of KRAS after Cre- induced recombination. | ß-actin-lox-egfp-lox- KRasG12D | Le *et al.* (2007) |

## 2. Temporally Controlled Genetic Manipulations

Approaches that allow inducible gene expression permit temporal control of genetic manipulation. One of the most widely used inducible systems in zebrafish involves the use of the heat shock promoter *hsp70* (Collins *et al.*, 2010; Le *et al.*, 2007; Thummel *et al.*, 2005). Expression of genes cloned downstream of the *hsp70* promoter involves exposure of the embryos to 37°C which can be spatially restricted to single cells by using a laser beam (Halloran *et al.*, 2000). Other methods developed to achieve temporal control of gene expression (Table VIII) use substrate-dependant transcriptional activation. Although some of these methods have not been used specifically in studies of the nervous system, they should in principle work. For example, the expression of a glucocorticoid receptor fused to Gal4 (de Graaf *et al.*, 1998) or of a modified Ecdysone receptor from insect fused to Gal4 (Esengil *et al.*, 2007) induces expression of a UAS-driven target gene only upon administration of a chemical compound (i.e., dexamethasone or tebufenozide, respectively). Similarly, the lexPR operator line is activated by the administration of the steroid Mifepristone, thereby inducing expression of the LexOP-driven effector line (Emelyanov and Parinov, 2008). Furthermore, a recent report suggests that the Tet system, used in mammals (Schonig and Bujard, 2003), has been successfully transferred to zebrafish (Zhu *et al.*, 2009). Here the Tet-Off system was used to conditionally repress transgenes upon doxycycline application (Zhu *et al.*, 2009). Temporal control of recombination using the Cre-LoxP system can also be achieved by using the ligand-inducible form of the Cre recombinase, CreER$^{T2}$, whose expression occurs only upon administration of the drug tamoxifen or its active metabolite 4-hydroxy-tamoxifen (Hans *et al.*, 2009). CreER$^{T2}$ can also be activated in single cells when two-photon excitation is used to uncage a caged ER ligand, 4-hydroxy-cyclofen (Sinha *et al.*, 2010).

**Table VIII**
**Time Controlled Cell-Type-Specific Manipulation: Driver + Effector Transgenic Lines + Substrate Administration**

| Description | Transient induction by | Transgenic line or constructs | Reference |
|---|---|---|---|
| | Targeted heat shock on single cells via laser beam | hsp70:egfp | Halloran *et al.* (2000) |
| | Heat shock | hsp:cre<br>hsp:egfp-cre | Le *et al.* (2007)Thummel *et al.* (2005) |
| | Heat shock | hsp:gal4 | Scheer and Campos-Ortega (1999) |
| HOTcre | Heat shock | hsp:lox-mcherry-lox-H2Bgfp | Hesselson *et al.* (2009) |
| | 4OH-Tamoxifen | Pax2.1:cre$^{ERT2}$ | Hans *et al.* (2009) |
| | Light-induced uncaging of 4OH-cyclofen | cre$^{ERT2}$ transient ubiquitous expression | Sinha *et al.* (2010) |
| Self-excising Cre;Mosaic Clonal analysis | Heat shock | EF1α-L-hsp:cre-L-gal4VP16-uas-nlsRFP | Collins *et al.* (2010) |
| Glucocorticoid receptor | Dexamethasone | No stable line-but construct: CMV: GalGR | de Graaf *et al.* (1998) |
| Insect-derived Ectysone receptor | Tebufenozide | No stable line, but construct: CMV:EcR-gal4-VP16 | Esengil *et al.* (2007) |
| Fusion between bacterial repressor/ activator domain/ human progesterone receptor | Mifepristone (Ru486) | Driver+operator line:<br>Krt8:LexPR-LexOP:egfp<br>Krt8:LexPR-LexOP:Kras<br>Operator line:<br>Cry:cfp-LexOP:mCherry | Emelyanov and Parinov (2008) |
| | Transient inactivation by administration of doxycyclin | Activator lines:<br>HuC:itTA<br>*dlx4/6:itTA*<br>Effector lines:<br>Ptet:venus<br>Ptet:ChR2YFP | Zhu *et al.* (2009) |
| Cell ablation | NTR substrate: Metronidazole | *uas:nfsBmCherry*<br>*uas:nfs-cfp* | Davison *et al.* (2007)Curado *et al.* (2008)Review Pisharath and Parsons (2009) |

## F. Methods for Targeted Cell Ablations

Cell ablation studies can be used to reveal the importance of specific cell-types during development, examine lineage relationships, or probe the mechanisms that trigger proliferation and neurogenesis in the regenerative response to injury. Laser-mediated cell ablation (Gahtan and Baier, 2004; Yang *et al.*, 2004) and the use of diphtheria toxin under the control of specific promoters to mediate cell death have both been reported in zebrafish (Kurita *et al.*, 2003; Li *et al.*, 2009; Wan *et al.*, 2006). It should be noted, however, that reports of diphtheria toxin-mediated cell ablation in the zebrafish nervous system are currently lacking.

A relatively recent addition to the array of cell ablation techniques takes advantage of the ability of the bacterial nitroreductase enzyme to convert the prodrug, metronidazole into a cytotoxic agent (Bridgewater *et al*., 1995). Using cell-specific promoters to express nitroreductase in specific cell populations and exposure to metronidazole allows targeted cell ablation that can be spatially and temporally controlled (Curado *et al*., 2008; Davison *et al*., 2007; Montgomery *et al*., 2009; Pisharath *et al*., 2007; Zhao *et al*., 2009). Fusing fluorescent proteins to the nitroreductase coding sequence allows cells to be monitored before being ablated.

Another enzyme prodrug combination, thymidine kinase–ganciclovir, which is used as a therapy for cancer, can also be employed to ablate cells (Springer and Niculescu-Duvaz, 2000). The herpes simplex virus thymidine kinase phosphorylates the drug, ganciclovir, which then acts by inhibiting DNA polymerase and thus arresting the cell cycle and causing subsequent cell death. No report of its use exists in zebrafish to date. Additionally, it should also be noted that, as a result of its mechanism of action, cell ablation would be restricted to proliferating cells. Finally, expression of the fluorescent protein KillerRed has the potential to mediate cell death. When illuminated with green light, KillerRed generates reactive oxygen species thereby killing the cells that express it (Bulina *et al*., 2006). No reports of cell ablation using KillerRed in zebrafish currently exist.

## IV. Specific Protocols to Study Adult Neurogenesis

### A. Fixation of the Adult Brain for Immunohistochemistry and *In Situ* Hybridization

Anesthetize adult fish on an ice/water mix for 3–5 min and decapitate with a scalpel. Either dissect the brain immediately in phosphate-buffered saline (PBS) and fix for 4–6 h at 4°C in 4% paraformaldehyde (PFA) or fix the whole head at 4°C in 4% PFA overnight on a shaker and dissect the brain the next day. After washing out the PFA in PBS, proceed to a methanol series (sequentially: 25% MeOH (in PBS+0.1%Tween), 50%, 75%, and 100% MeOH). Freeze the brain in 100% Methanol at –20°C for at least 1 h. The brains can be preserved for several months in MeOH at –20°C.

### B. Immunohistochemistry on Vibratome Sections

Brains stored in MeOH at –20°C must be processed through a descending methanol series, back to PBS (sequentially 75% MeOH (in PBS+0.1% Tween=PBT); 50% MeOH, 25% MeOH, PBS). It should be noted that some antigens (e.g., lipid soluble) do not tolerate methanol treatment (recommended above for preparing brains). Some antigens do not require any methanol treatment. Some antibodies require a special pretreatment, such as a second methanol series, treatment with hydrochloric acid (HCl), or a citrate buffer treatment (see antigen retrieval, below).

Embed the brain in 3% agarose in PBS. Cool the agarose and cut a block around the brain.

Cut 70–100 μm-thick sections on a vibratome.

Incubate the sections in a blocking solution (PBS containing 0.5% Triton X-100 and 5–10% normal immune goat serum).

Primary antibody (diluted in blocking solution) incubation should proceed for 2 h at room temperature or overnight at 4°C on a shaking incubator.

Wash 2–3× for 5 min in PBS.

Incubate the sections in secondary antibody (1:1000 dilution, e.g., Alexa Fluor-coupled antibodies from Molecular Probes-Invitrogen) in PBS containing 0.5% Triton and 10% normal goat serum for 30–45 min at room temperature in the dark.

Wash 2–3× in PBS

The sections are mounted on slides in Aqua polymount (Polyscience) or any other water-based mounting medium.

### Pretreatments, Antigen Retrieval

**Hydrochloric Acid Pretreatment** Detection of BrdU by immunostaining requires HCl pretreatment which denatures DNA and thus exposes the BrdU epitope. HCl pretreatment might destroy other antigens and should therefore be performed after the completion of immunohistochemistry for the other markers. Incubate the sections with freshly made 2M HCl (1:4.4 of 32% HCl solution) for 30 min at room temperature. Wash once quickly, and twice for 5 min each, with PBS. The BrdU antibody should then be diluted in PBS containing 0.5% Triton X-100 but no serum.

**Citrate Retrieval** Some antigens require a retrieval step in citrate buffer. Slices are incubated at 85°C for 30 min in 10 mM sodium citrate in PBS, pH 6, and washed three times in PBS.

## C. *In Situ* Hybridization on Whole Mount Adult Brains

Fix brains as described above. Incubate the brains in a descending methanol series until PBS, as described above in (B).

Place fixed, methanol-treated brains into a 48-well-plate. Treat with proteinase K (10 μg/ml) for 30 min at room temperature. Proceed through to *in situ* hybridization using the standard protocol for zebrafish embryos (Hauptmann and Gerster, 2000b), until all post-hybridization washes have been performed. Embed the brain in 3% agarose and cut 70–100 μm sections at the vibratome. Block the sections in blocking buffer (PBS; 0.1% Tween; 2% normal goat serum (NGS); 2 mg/ml bovine serum albumin) and incubate them in anti-DIG antibodies and continue following the standard embryo *in situ* protocol.

## D. *In Situ* Hybridization on Gelatine–Albumin Sections

For weak RNA probes which do not reveal a strong signal following whole mount *in situ* hybridization, gelatine–albumin sections are better suited. However, it is not possible to perform fluorescence immunohistochemistry following *in situ* hybridization, due to the high level of autofluorescence resulting from the embedding mixture.

Prepare the gelatine–albumin mixture: To 4.5 g gelatine in a beaker add PBS up to the 250 ml mark and dissolve by heating at 50°C. In a separate beaker, to 270 g albumin and 80 g sucrose, add PBS up to the 750 ml mark and dissolve overnight at room temperature. Filter the solution.

Mix both solutions after the gelatine solution has cooled down. The mixture can be aliquoted and stored at –20°C.

Immediately before embedding the brain, add 200–500 µl glutaraldehyde to 5 ml of the gelatine–albumin mixture. Embed the brain very quickly, as the gelatine–albumin polymerizes within 30 s to 1 min.

Trim a block around the brain and cut 70–100 µm sections on a vibratome. Process the sections through an ascending methanol series and freeze in 100% methanol at –20°C for a minimum of 1 h. Reverse the methanol series to 100% PBS and process for *in situ* hybridization, following the standard zebrafish embryo (Hauptmann and Gerster, 2000b) protocol, without proteinase K pretreatment.

## E. Intraperitoneal Injections of BrdU

As described in (Adolf *et al*., 2006), dissolve BrdU in a saline solution (110 mM NaCl pH 7.2) at a concentration of 2.5 mg/ml. Add a few drops of methylene blue to color the solution. Vortex the solution for about 5 min to ensure that the BrdU is completely dissolved. The BrdU solution can be stored for up to one week at 4°C.

Inject the fish intraperitoneally with BrdU solution (5 µl per 0.1 g body weight). As illustrated in Fig. 4, the required injection volume is pipetted as a drop onto a piece of Parafilm (Fig. 4A), aspirated into a small syringe (insulin syringe). The fish is held on its side in a net on a wet Petri dish (Fig. 4B) and injected right below the skin at the level of the belly (Fig. 4C). The procedure is rapid and does not require anesthetizing the fish.

## F. Lipofections/Electroporations of the Adult Brain *In Vivo*

Prepare a piece of plastic foam to fit into in a 6 cm Petri dish, with a slit to hold a fish, as illustrated in Fig. 5A (Chapouton *et al*., 2010). Fill the Petri dish and foam

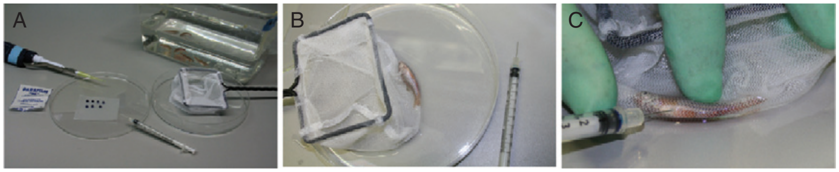

**Fig. 4** Intraperitoneal injection of BrdU into the adult fish. (A) The desired volume of BrdU solution (5 µl/0.1 g body mass) is dropped onto a piece of Parafilm. (B) The fish is immobilized for a short time in a net in a wet Petri dish. (C) Stabilize the fish on its side and inject the BrdU solution using a small syringe, inserted at an oblique angle, into the peritoneum.

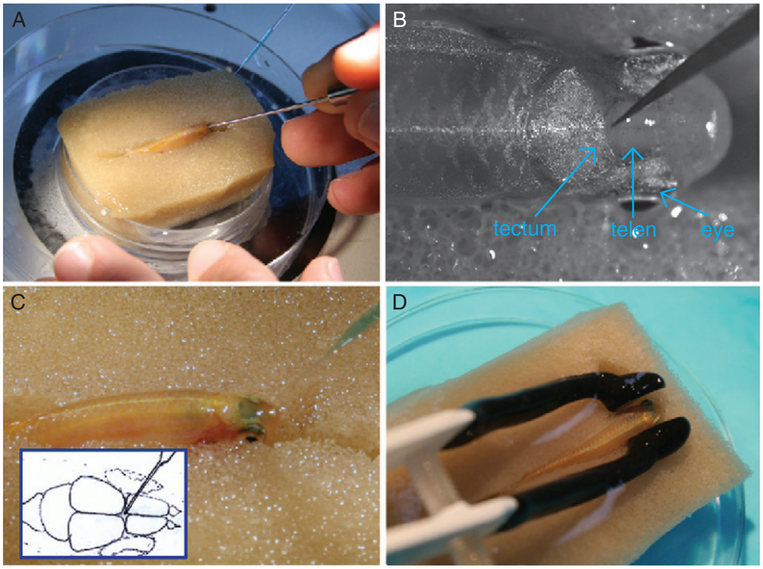

**Fig. 5** Lipofection and electroporation *in vivo* in the adult zebrafish brain. (A) The anesthetized fish is placed into a slit in a block of wet foam and a hole is made in its skull at the level of the epiphysis, as shown in (B). (C) The capillary containing DNA (with lipofectamine if lipofecting) is inserted through the hole and the solution is pressure injected into the brain ventricles. The propagation of the solution through the ventricles can be visualized easily due to the presence of a dye (Fast Green). (D) For electroporation, tweezertrodes are placed on both sides of the head and electroshocks are given.

plastic with fish water containing 0.02% tricaine (MS-222). Anesthetize an adult fish in 0.02% tricaine and place it into the slit of the plastic foam so that its dorsal-side faces up (Fig. 5A). With the help of a microsurgery tool (i.e., Fine Science Tools 10055-12) under a stereomicroscope, make a small hole in the skull at the level of the epiphysis (as in Fig. 5A and B). Introduce an injection capillary (as used for injections of embryos at the one-cell stage), containing DNA solution (see below) through the hole at the posterior end of the telencephalon into the diencephalic ventricle and pressure inject the solution (Fig. 5C). The presence of Fast Green should make it relatively easy to visualize the propagation of the DNA solution into all the ventricles. Propagation of the solution is easier to visualize when working with brass fish, and slightly more difficult to detect in the AB, Tü, or EK lines, due to their stronger pigmentation. It should be possible to distinguish between a successful injection that fills the ventricles from an injection which results in the DNA solution only being distributed on the surface of the brain, outside the meninges.

To deliver DNA into the living brain using lipofection, prepare a mixture of DNA and lipofectant (Lipofectamine 2000, Invitrogen). Dissolve Lipofectamine in a ratio of 1:2 in water or Hank's buffered salt solution (HBSS) (solution A). Prepare 2–5 μg of DNA (a single plasmid or two plasmids) in a 5 μl volume (solution B). Mix 5 μl each of solution A and solution B at room temperature and incubate 20 min before use. This mixture should be used within a few hours of preparation. Prior to injection, add 2 μl of a 2 mg/ml Fast Green solution to the lipofection mix.

For electroporations, inject DNA (2–5 μg/μl) in a solution containing 0.2 mg/ml fast green. Remove the fish from the plastic foam and place it into fish water containing tricaine. Connect electrodes (e.g., Tweezertrodes 520, Harvard Apparatus) to an electroporator (Ovodyne) and current amplifier (TSS20 and EP21; Intracell), and position the electrodes laterally on both sides of the head, slightly anterior to the eyes. Deliver 5 pulses (40 V, with 50 ms pulse width and 1000 ms time interval) (Fig. 5D).

Both lipofection and electroporation work equally well and allow isolated cells located on the ventricular surface to be transduced (about 20–50 cells per telencephalon). Lipofection presents the advantage of avoiding electroshocks to the fish.

## G. Slice Culture

Culture medium (modified artificial cerebrospinal fluid, ACSF) to be prepared fresh: for 1 l:

| | | |
|---|---|---|
| 100 mM | NaCl | 5.84 g |
| 2.46 mM | KCl | 0.183 g |
| 1 mM | $MgCl_2$.6H2O | 0.203 g |
| 0.44 mM | $NaH_2$PO4.H2O | 0.060 g |
| 1.13 mM | $CaCl_2$ | 0.166 g |
| 5 mM | $NaHCO_3$ | 0.420 g |
| 10 mM | Glucose | 1.802 g |
| pH 7.2 | | |

Sterile filter the solution

**Brain Embedding, Cutting, and Culture** Dissect brains in cold culture medium and embed in 2% low gelling agarose cooled down to 28°C. Cut 270 μm slices on a vibratome. Collect the slices gently using a spatula or a plastic Pasteur pipette with a large bore. Lay the slices on a Millicell-CM (Millipore) culture plate insert placed in a 6-well plate filled with 1.5 ml culture medium (containing penicillin/streptomycin) per well. The slices should not float, they should only be covered by a thin layer of medium. Culture the slices at -28°C, in a normal egg incubator. Change the medium every second day. Slices can be cultured for about 4–5 days.

**Fixation** Remove the medium and fill the wells with about 3 ml of 4% PFA, drop some more PFA gently onto the slices. Fix for 1 h at 4°C. Wash the slices in PBS and proceed to a methanol series, freeze in 100% methanol at –20°C for at least 1 h, before proceeding for immunohistochemistry.

## V. Conclusion

Both as an embryo and as an adult, the zebrafish continues to contribute to our understanding of neurogenesis. Many methods of manipulation, mutants, and transgenic lines are available, as well as genetic methods to manipulate the zebrafish in a conditional (spatially and temporally) manner. Optical methods to image processes *in vivo* and to manipulate neuronal activity have been implemented. In the future, more genetic and optical tools will be developed, making neurogenesis in the zebrafish a rich field to explore.

## Acknowledgments

We are very grateful to Laure Bally-Cuif, Philip Williams, and Thomas Misgeld for their helpful comments and suggestions while writing this chapter.

## References

Adolf, B., Bellipanni, G., Huber, V., and Bally-Cuif, L. (2004). atoh1.2 and beta3.1 are two new bHLH-encoding genes expressed in selective precursor cells of the zebrafish anterior hindbrain. *Gene Expr. Patterns* **5**, 35–41.

Adolf, B., Chapouton, P., Lam, C. S., Topp, S., Tannhauser, B., Strahle, U., Gotz, M., and Bally-Cuif, L. (2006). Conserved and acquired features of adult neurogenesis in the zebrafish telencephalon. *Dev. Biol.* **295**, 278–293.

Ahn, D., Ruvinsky, I., Oates, A., Silver, L., and Ho, R. (2000). tbx20, a new vertebrate T-box gene expressed in the cranial motor neurons and developing cardiovascular structures in zebrafish. *Mech. Dev.* **95**, 253–258.

Aizawa, H., Goto, M., Sato, T., and Okamoto, H. (2007). Temporally regulated asymmetric neurogenesis causes left-right difference in the zebrafish habenular structures. *Dev. Cell* **12**, 87–98.

Akimenko, M. A., Ekker, M., Wegner, J., Lin, W., and Westerfield, M. (1994). Combinatorial expression of three zebrafish genes related to distal-less: Part of a homeobox gene code for the head. *J. Neurosci.* **14**, 3475–3486.

Alexandre, P., Reugels, A. M., Barker, D., Blanc, E., and Clarke, J. D. (2010). Neurons derive from the more apical daughter in asymmetric divisions in the zebrafish neural tube. *Nat. Neurosci.* **13**, 673–679.

Allende, M. L., Amsterdam, A., Becker, T., Kawakami, K., Gaiano, N., and Hopkins, N. (1996). Insertional mutagenesis in zebrafish identifies two novel genes, pescadillo and dead eye, essential for embryonic development. *Genes Dev.* **10**, 3141–3155.

Allende, M. L., and Weinberg, E. S. (1994). The expression pattern of two zebrafish achaete-scute homolog (ash) genes is altered in the embryonic brain of the cyclops mutant. *Dev. Biol.* **166**, 509–530.

Alunni, A., Hermel, J. M., Heuze, A., Bourrat, F., Jamen, F., and Joly, J. S. (2010). Evidence for neural stem cells in the medaka optic tectum proliferation zones. *Dev. Neurobiol.* **70**, 693–713.

Amoyel, M., Cheng, Y. C., Jiang, Y. J., and Wilkinson, D. G. (2005). Wnt1 regulates neurogenesis and mediates lateral inhibition of boundary cell specification in the zebrafish hindbrain. *Development* **132**, 775–785.

Amsterdam, A., Burgess, S., Golling, G., Chen, W., Sun, Z., Townsend, K., Farrington, S., Haldi, M., and Hopkins, N. (1999). A large-scale insertional mutagenesis screen in zebrafish. *Genes Dev.* **13**, 2713–2724.

Amsterdam, A., Lai, K., Komisarczuk, A. Z., Becker, T. S., Bronson, R. T., Hopkins, N., and Lees, J. A. (2009). Zebrafish Hagoromo mutants up-regulate fgf8 postembryonically and develop neuroblastoma. *Mol. Cancer Res.* **7**, 841–850.

Andermann, P., and Weinberg, E. (2001). Expression of zTlxA, a Hox11-like gene, in early differentiating embryonic neurons and cranial sensory ganglia of the zebrafish embryo. *Dev. Dyn.* **222**, 595–610.

Ando, R., Hama, H., Yamamoto-Hino, M., Mizuno, H., and Miyawaki, A. (2002). An optical marker based on the UV-induced green-to-red photoconversion of a fluorescent protein. *Proc. Natl. Acad. Sci. U.S.A.* **99**, 12651–12656.

Appel, B., Fritz, A., Westerfield, M., Grunwald, D. J., Eisen, J. S., and Riley, B. B. (1999). Delta-mediated specification of midline cell fates in zebrafish embryos. *Curr. Biol.* **9**, 247–256.

Appel, B., Givan, L. A., and Eisen, J. S. (2001). Delta-Notch signaling and lateral inhibition in zebrafish spinal cord development. *BMC Dev. Biol.* **1**, 13.

Appel, B., Korzh, V., Glasgow, E., Thor, S., Edlund, T., Dawid, I. B., and Eisen, J. S. (1995). Motoneuron fate specification revealed by patterned LIM homeobox gene expression in embryonic zebrafish. *Development* **121**, 4117–4125.

Aramaki, S., and Hatta, K. (2006). Visualizing neurons one-by-one *in vivo*: Optical dissection and reconstruction of neural networks with reversible fluorescent proteins. *Dev. Dyn.* **235**, 2192–2199.

Artinger, K. B., Chitnis, A. B., Mercola, M., and Driever, W. (1999). Zebrafish narrowminded suggests a genetic link between formation of neural crest and primary sensory neurons. *Development* **126**, 3969–3979.

Asakawa, K., and Kawakami, K. (2009). The Tol2-mediated Gal4-UAS method for gene and enhancer trapping in zebrafish. *Methods* **49**, 275–281.

Asakawa, K., Suster, M. L., Mizusawa, K., Nagayoshi, S., Kotani, T., Urasaki, A., Kishimoto, Y., Hibi, M., and Kawakami, K. (2008). Genetic dissection of neural circuits by Tol2 transposon-mediated Gal4 gene and enhancer trapping in zebrafish. *Proc. Natl. Acad. Sci. U.S.A.* **105**, 1255–1260.

Bae, Y. K., Kani, S., Shimizu, T., Tanabe, K., Nojima, H., Kimura, Y., Higashijima, S., and Hibi, M. (2009). Anatomy of zebrafish cerebellum and screen for mutations affecting its development. *Dev. Biol.* **330**, 406–426.

Bae, Y. K., Shimizu, T., and Hibi, M. (2005). Patterning of proneuronal and inter-proneuronal domains by hairy- and enhancer of split-related genes in zebrafish neuroectoderm. *Development* **132**, 1375–1385.

Bae, Y. K., Shimizu, T., Yabe, T., Kim, C. H., Hirata, T., Nojima, H., Muraoka, O., Hirano, T., and Hibi, M. (2003). A homeobox gene, pnx, is involved in the formation of posterior neurons in zebrafish. *Development* **130**, 1853–1865.

Bai, Q., and Burton, E. A. (2009). Cis-acting elements responsible for dopaminergic neuron-specific expression of zebrafish slc6a3 (dopamine transporter) *in vivo* are located remote from the transcriptional start site. *Neuroscience* **164**, 1138–1151.

Bai, Q., Garver, J. A., Hukriede, N. A., and Burton, E. A. (2007). Generation of a transgenic zebrafish model of Tauopathy using a novel promoter element derived from the zebrafish eno2 gene. *Nucleic Acids Res.* **35**, 6501–6516.

Bai, Q., Wei, X., and Burton, E. A. (2009). Expression of a 12-kb promoter element derived from the zebrafish enolase-2 gene in the zebrafish visual system. *Neurosci. Lett.* **449**, 252–257.

Bally-Cuif, L., Dubois, L., and Vincent, A. (1998). Molecular cloning of Zcoe2, the zebrafish homolog of Xenopus Xcoe2 and mouse EBF-2, and its expression during primary neurogenesis. *Mech. Dev.* **77**, 85–90.

Barth, K. A., Kishimoto, Y., Rohr, K. B., Seydler, C., Schulte-Merker, S., and Wilson, S. W. (1999). Bmp activity establishes a gradient of positional information throughout the entire neural plate. *Development* **126**, 4977–4987.

Baye, L. M., and Link, B. A. (2007a). The disarrayed mutation results in cell cycle and neurogenesis defects during retinal development in zebrafish. *BMC Dev. Biol.* **7**, 28.

Baye, L. M., and Link, B. A. (2007b). Interkinetic nuclear migration and the selection of neurogenic cell divisions during vertebrate retinogenesis. *J. Neurosci.* **27**, 10143–10152.

Becker, T., Bernhardt, R. R., Reinhard, E., Wullimann, M. F., Tongiorgi, E., and Schachner, M. (1998). Readiness of zebrafish brain neurons to regenerate a spinal axon correlates with differential expression of specific cell recognition molecules. *J. Neurosci.* **18**, 5789–5803.

Bellipanni, G., Rink, E., and Bally-Cuif, L. (2002). Cloning of two tryptophane hydroxylase genes expressed in the diencephalon of the developing zebrafish brain. *Mech. Dev.* **119S**, S215–S220.

Belting, H. G., Hauptmann, G., Meyer, D., Abdelilah-Seyfried, S., Chitnis, A., Eschbach, C., Soll, I., Thisse, C., Thisse, B., Artinger, K. B., *et al.* (2001). spiel ohne grenzen/pou2 is required during establishment of the zebrafish midbrain-hindbrain boundary organizer. *Development* **128**, 4165–4176.

Berberoglu, M. A., Dong, Z., Mueller, T., and Guo, S. (2009). fezf2 expression delineates cells with proliferative potential and expressing markers of neural stem cells in the adult zebrafish brain. *Gene Expr. Patterns* **9**, 411–422.

Bernardos, R. L., Barthel, L. K., Meyers, J. R., and Raymond, P. A. (2007). Late-stage neuronal progenitors in the retina are radial Muller glia that function as retinal stem cells. *J. Neurosci.* **27**, 7028–7040.

Bernardos, R. L., and Raymond, P. A. (2006). GFAP transgenic zebrafish. *Gene Expr. Patterns* **6**, 1007–1013.

Bernhardt, R. R., Chitnis, A. B., Lindamer, L., and Kuwada, J. Y. (1990). Identification of spinal neurons in the embryonic and larval zebrafish. *J. Comp. Neurol.* **302**, 603–616.

Bianco, I. H., Carl, M., Russell, C., Clarke, J. D., and Wilson, S. W. (2008). Brain asymmetry is encoded at the level of axon terminal morphology. *Neural Dev.* **3**, 9.

Bit-Avragim, N., Hellwig, N., Rudolph, F., Munson, C., Stainier, D. Y., and Abdelilah-Seyfried, S. (2008). Divergent polarization mechanisms during vertebrate epithelial development mediated by the Crumbs complex protein Nagie oko. *J. Cell. Sci.* **121**, 2503–2510.

Blader, P., Fischer, N., Gradwohl, G., Guillemot, F., and Strahle, U. (1997). The activity of neurogenin1 is controlled by local cues in the zebrafish embryo. *Development* **124**, 4557–4569.

Blader, P., Lam, C. S., Rastegar, S., Scardigli, R., Nicod, J. C., Simplicio, N., Plessy, C., Fischer, N., Schuurmans, C., Guillemot, F., *et al*. (2004). Conserved and acquired features of neurogenin1 regulation. *Development* **131**, 5627–5637.

Blake, T., Adya, N., Kim, C. H., Oates, A. C., Zon, L., Chitnis, A., Weinstein, B. M., and Liu, P. P. (2000). Zebrafish homolog of the leukemia gene CBFB: Its expression during embryogenesis and its relationship to scl and gata-1 in hematopoiesis. *Blood* **96**, 4178–4184.

Blechman, J., Borodovsky, N., Eisenberg, M., Nabel-Rosen, H., Grimm, J., and Levkowitz, G. (2007). Specification of hypothalamic neurons by dual regulation of the homeodomain protein Orthopedia. *Development* **134**, 4417–4426.

Blin, M., Norton, W., Bally-Cuif, L., and Vernier, P. (2008). NR4A2 controls the differentiation of selective dopaminergic nuclei in the zebrafish brain. *Mol. Cell. Neurosci.* **39**, 592–604.

Bourguignon, C., Li, J., and Papalopulu, N. (1998). XBF-1, a winged helix transcription factor with dual activity, has a role in positioning neurogenesis in Xenopus competent ectoderm. *Development* **125**, 4889–4900.

Bray, S., and Furriols, M. (2001). Notch pathway: Making sense of suppressor of hairless. *Curr. Biol.* **11**, R217–R221.

Bridgewater, J. A., Springer, C. J., Knox, R. J., Minton, N. P., Michael, N. P., and Collins, M. K. (1995). Expression of the bacterial nitroreductase enzyme in mammalian cells renders them selectively sensitive to killing by the prodrug CB1954. *Eur. J. Cancer* **31A**, 2362–2370.

Bulina, M. E., Lukyanov, K. A., Britanova, O. V., Onichtchouk, D., Lukyanov, S., and Chudakov, D. M. (2006). Chromophore-assisted light inactivation (CALI) using the phototoxic fluorescent protein KillerRed. *Nat. Protoc.* **1**, 947–953.

Bylund, M., Andersson, E., Novitch, B. G., and Muhr, J. (2003). Vertebrate neurogenesis is counteracted by Sox1-3 activity. *Nat. Neurosci.* **6**, 1162–1168.

Canger, A., Passini, M., Asch, W., Leake, D., Zafonte, B., Glasgow, E., and Schechter, N. (1998). Restricted expression of the neuronal intermediate filament protein plasticin during zebrafish development. *J. Comp. Neurol.* **399**, 561–572.

Caron, S. J., Prober, D., Choy, M., and Schier, A. F. (2008). *In vivo* birthdating by BAPTISM reveals that trigeminal sensory neuron diversity depends on early neurogenesis. *Development* **135**, 3259–3269.

Cau, E., Quillien, A., and Blader, P. (2008). Notch resolves mixed neural identities in the zebrafish epiphysis. *Development* **135**, 2391–2401.

Cerda, G. A., Thomas, J. E., Allende, M. L., Karlstrom, R. O., and Palma, V. (2006). Electroporation of DNA, RNA, and morpholinos into zebrafish embryos. *Methods* **39**, 207–211.

Cerveny, K. L., Cavodeassi, F., Turner, K. J., de Jong-Curtain, T. A., Heath, J. K., and Wilson, S. W. (2010). The zebrafish flotte lotte mutant reveals that the local retinal environment promotes the differentiation of proliferating precursors emerging from their stem cell niche. *Development* 137, 2107–2115.

Chaplin, N., Tendeng, C., and Wingate, R. J. (2010). Absence of an external germinal layer in zebrafish and shark reveals a distinct, anamniote ground plan of cerebellum development. *J. Neurosci.* **30**, 3048–3057.

Chapouton, P., Adolf, B., Leucht, C., Tannhauser, B., Ryu, S., Driever, W., and Bally-Cuif, L. (2006). her5 expression reveals a pool of neural stem cells in the adult zebrafish midbrain. *Development* **133**, 4293–4303.

Chapouton, P., Jagasia, R., and Bally-Cuif, L. (2007). Adult neurogenesis in non-mammalian vertebrates. *Bioessays* **29**, 745–757.

Chapouton, P., Skupien, P., Hesl, B., Coolen, M., Moore, J. C., Madelaine, R., Kremmer, E., Faus-Kessler, T., Blader, P., Lawson, N. D., *et al*. (2010). Notch activity levels control the balance between quiescence and recruitment of adult neural stem cells. *J. Neurosci.* **30**, 7961–7974.

Chen, W., Burgess, S., and Hopkins, N. (2001). Analysis of the zebrafish smoothened mutant reveals conserved and divergent functions of hedgehog activity. *Development* **128**, 2385–2396.

Chong, S., Emelyanov, A., Gong, Z., and Korzh, V. (2001). Expression pattern of two zebrafish genes, cxcr4a and cxcr4b. *Mech. Dev.* **109**, 347–354.

Chong, S. W., Nguyen, T. T., Chu, L. T., Jiang, Y. J., and Korzh, V. (2005). Zebrafish id2 developmental expression pattern contains evolutionary conserved and species-specific characteristics. *Dev. Dyn.* **234**, 1055–1063.

Choo, B. G., Kondrichin, I., Parinov, S., Emelyanov, A., Go, W., Toh, W. C., and Korzh, V. (2006). Zebrafish transgenic Enhancer TRAP line database (ZETRAP). *BMC Dev. Biol.* **6**, 5.

Collins, R. T., Linker, C., and Lewis, J. (2010). MAZe: A tool for mosaic analysis of gene function in zebrafish. *Nat. Methods* **7**, 219–223.

Cooper, M. S., Szeto, D. P., Sommers-Herivel, G., Topczewski, J., Solnica-Krezel, L., Kang, H. C., Johnson, I., Kimelman, D. (2005). Visualizing morphogenesis in transgenic zebrafish embryos using BODIPY TR methyl ester dye as a vital counterstain for GFP. *Dev. Dyn.* **232**, 359–368.

Curado, S., Stainier, D. Y., and Anderson, R. M. (2008). Nitroreductase-mediated cell/tissue ablation in zebrafish: A spatially and temporally controlled ablation method with applications in developmental and regeneration studies. *Nat. Protoc.* **3**, 948–954.

Das, T., Payer, B., Cayouette, M., and Harris, W. A. (2003). *In vivo* time-lapse imaging of cell divisions during neurogenesis in the developing zebrafish retina. *Neuron* **37**, 597–609.

Davison, J. M., Akitake, C. M., Goll, M. G., Rhee, J. M., Gosse, N., Baier, H., Halpern, M. E., Leach, S. D., and Parsons, M. J. (2007). Transactivation from Gal4-VP16 transgenic insertions for tissue-specific cell labeling and ablation in zebrafish. *Dev. Biol.* **304**, 811–824.

de Graaf, M., Zivkovic, D., and Joore, J. (1998). Hormone-inducible expression of secreted factors in zebrafish embryos. *Dev. Growth Differ.* **40**, 577–582.

de Martino, S., Yan, Y. L., Jowett, T., Postlethwait, J. H., Varga, Z. M., Ashworth, A., and Austin, C. A. (2000). Expression of sox11 gene duplicates in zebrafish suggests the reciprocal loss of ancestral gene expression patterns in development. *Dev. Dyn.* **217**, 279–292.

Dee, C. T., Hirst, C. S., Shih, Y. H., Tripathi, V. B., Patient, R. K., and Scotting, P. J. (2008). Sox3 regulates both neural fate and differentiation in the zebrafish ectoderm. *Dev. Biol.* **320**, 289–301.

Devos, N., Deflorian, G., Biemar, F., Bortolussi, M., Martial, J., Peers, B., and Argenton, F. (2002). Differential expression of two somatostatin genes during zebrafish embryonic development. *Mech. Dev.* **115**, 133–137.

Dickmeis, T., Rastegar, S., Lam, C. S., Aanstad, P., Clark, M., Fischer, N., Rosa, F., Korzh, V., and Strahle, U. (2002). Expression of the helix-loop-helix gene id3 in the zebrafish embryo. *Mech. Dev.* **113**, 99–102.

Diks, S. H., Sartori da Silva, M. A., Hillebrands, J. L., Bink, R. J., Versteeg, H. H., Van Rooijen, C., Brouwers, A., Chitnis, A. B., Peppelenbosch, M. P., and Zivkovic, D. (2008). d-Asb11 is an essential mediator of canonical Delta-Notch signalling. *Nat. Cell Biol.* **10**, 1190–1198.

Distel, M., Wullimann, M. F., and Koster, R. W. (2009). Optimized Gal4 genetics for permanent gene expression mapping in zebrafish. *Proc. Natl. Acad. Sci. U.S.A.* **106**, 13365–13370.

Dornseifer, P., Takke, C., and Campos-Ortega, J. A. (1997). Overexpression of a zebrafish homologue of the Drosophila neurogenic gene Delta perturbs differentiation of primary neurons and somite development. *Mech. Dev.* **63**, 159–171.

Dorsky, R. I., Sheldahl, L. C., and Moon, R. T. (2002). A transgenic Lef1/beta-catenin-dependent reporter is expressed in spatially restricted domains throughout zebrafish development. *Dev. Biol.* **241**, 229–237.

Doyon, Y., McCammon, J. M., Miller, J. C., Faraji, F., Ngo, C., Katibah, G. E., Amora, R., Hocking, T. D., Zhang, L., Rebar, E. J., *et al*. (2008). Heritable targeted gene disruption in zebrafish using designed zinc-finger nucleases. *Nat. Biotechnol.* **26**, 702–708.

Du, S. J., and Dienhart, M. (2001). Zebrafish tiggy-winkle hedgehog promoter directs notochord and floor plate green fluorescence protein expression in transgenic zebrafish embryos. *Dev. Dyn.* **222**, 655–666.

Dutton, K. A., Pauliny, A., Lopes, S. S., Elworthy, S., Carney, T. J., Rauch, J., Geisler, R., Haffter, P., and Kelsh, R. N. (2001). Zebrafish colourless encodes sox10 and specifies non-ectomesenchymal neural crest fates. *Development* **128**, 4113–4125.

Ellingsen, S., Laplante, M. A., Konig, M., Kikuta, H., Furmanek, T., Hoivik, E. A., and Becker, T. S. (2005). Large-scale enhancer detection in the zebrafish genome. *Development* **132**, 3799–3811.

Emelyanov, A., and Parinov, S. (2008). Mifepristone-inducible LexPR system to drive and control gene expression in transgenic zebrafish. *Dev. Biol.* **320**, 113–121.

Eriksson, K. S., Peitsaro, N., Karlstedt, K., Kaslin, J., and Panula, P. (1998). Development of the histaminergic neurons and expression of histidine decarboxylase mRNA in the zebrafish brain in the absence of all peripheral histaminergic systems. *Eur. J. Neurosci.* **10**, 3799–3812.

Ertzer, R., Muller, F., Hadzhiev, Y., Rathnam, S., Fischer, N., Rastegar, S., and Strahle, U. (2007). Cooperation of sonic hedgehog enhancers in midline expression. *Dev. Biol.* **301**, 578–589.

Esengil, H., Chang, V., Mich, J. K., and Chen, J. K. (2007). Small-molecule regulation of zebrafish gene expression. *Nat. Chem. Biol.* **3**, 154–155.

Fadool, J. M. (2003). Development of a rod photoreceptor mosaic revealed in transgenic zebrafish. *Dev. Biol.* **258**, 277–290.

Fashena, D., and Westerfield, M. (1999). Secondary motoneuron axons localize DM-GRASP on their fasciculated segments. *J. Comp. Neurol.* **406**, 415–424.

Fausett, B. V., and Goldman, D. (2006). A role for alpha1 tubulin-expressing Muller glia in regeneration of the injured zebrafish retina. *J. Neurosci.* **26**, 6303–6313.

Fausett, B. V., Gumerson, J. D., and Goldman, D. (2008). The proneural basic helix-loop-helix gene ascl1a is required for retina regeneration. *J. Neurosci.* **28**, 1109–1117.

Feldman, B., Dougan, S. T., Schier, A. F., and Talbot, W. S. (2000). Nodal-related signals establish mesendodermal fate and trunk neural identity in zebrafish. *Curr. Biol.* **10**, 531–534.

Feng, B., Bulchand, S., Yaksi, E., Friedrich, R. W., and Jesuthasan, S. (2005). The recombination activation gene 1 (Rag1) is expressed in a subset of zebrafish olfactory neurons but is not essential for axon targeting or amino acid detection. *BMC Neurosci.* **6**, 46.

Filippi, A., Durr, K., Ryu, S., Willaredt, M., Holzschuh, J., and Driever, W. (2007). Expression and function of nr4a2, lmx1b, and pitx3 in zebrafish dopaminergic and noradrenergic neuronal development. *BMC Dev. Biol.* **7**, 135.

Fimbel, S. M., Montgomery, J. E., Burket, C. T., and Hyde, D. R. (2007). Regeneration of inner retinal neurons after intravitreal injection of ouabain in zebrafish. *J. Neurosci.* **27**, 1712–1724.

Fjose, A., Izpisua-Belmonte, J. C., Fromental-Ramain, C., and Duboule, D. (1994). Expression of the zebrafish gene hlx-1 in the prechordal plate and during CNS development. *Development* **120**, 71–81.

Fjose, A., and Zhao, X. F. (2010). Inhibition of the microRNA pathway in zebrafish by siRNA. *Methods Mol. Biol.* **629**, 239–255.

Flanagan-Steet, H., Fox, M. A., Meyer, D., and Sanes, J. R. (2005). Neuromuscular synapses can form *in vivo* by incorporation of initially aneural postsynaptic specializations. *Development* **132**, 4471–4481.

Furthauer, M., Reifers, F., Brand, M., Thisse, B., and Thisse, C. (2001). sprouty4 acts *in vivo* as a feedback-induced antagonist of FGF signaling in zebrafish. *Development* **128**, 2175–2186.

Gahtan, E., and Baier, H. (2004). Of lasers, mutants, and see-through brains: Functional neuroanatomy in zebrafish. *J. Neurobiol.* **59**, 147–161.

Ganz, J., Kaslin, J., Hochmann, S., Freudenreich, D., and Brand, M. (2010). Heterogeneity and Fgf dependence of adult neural progenitors in the zebrafish telencephalon. *Glia* **58**, 1345–1363.

Geling, A., Itoh, M., Tallafuss, A., Chapouton, P., Tannhauser, B., Kuwada, J. Y., Chitnis, A. B., and Bally-Cuif, L. (2003). bHLH transcription factor Her5 links patterning to regional inhibition of neurogenesis at the midbrain-hindbrain boundary. *Development* **130**, 1591–1604.

Geling, A., Plessy, C., Rastegar, S., Strahle, U., and Bally-Cuif, L. (2004). Her5 acts as a prepattern factor that blocks neurogenin1 and coe2 expression upstream of Notch to inhibit neurogenesis at the midbrain-hindbrain boundary. *Development* **131**, 1993–2006.

Geling, A., Steiner, H., Willem, M., Bally-Cuif, L., and Haass, C. (2002). A gamma-secretase inhibitor blocks Notch signaling *in vivo* and causes a severe neurogenic phenotype in zebrafish. *EMBO Rep.* **3**, 688–694.

Girard, F., Cremazy, F., Berta, P., and Renucci, A. (2001). Expression pattern of the Sox31 gene during Zebrafish embryonic development. *Mech. Dev.* **100**, 71–73.

Glasgow, E., Karavanov, A., and Dawid, I. (1997). Neuronal and neuroendocrine expression of lim3, a lim class homeobox gene, is altered in mutant zebrafish with axial signaling defects. *Dev. Biol.* **192**, 405–419.

Godinho, L., Mumm, J. S., Williams, P. R., Schroeter, E. H., Koerber, A., Park, S. W., Leach, S. D., and Wong, R. O. (2005). Targeting of amacrine cell neurites to appropriate synaptic laminae in the developing zebrafish retina. *Development* **132**, 5069–5079.

Godinho, L., Williams, P. R., Claassen, Y., Provost, E., Leach, S. D., Kamermans, M., and Wong, R. O. (2007). Nonapical symmetric divisions underlie horizontal cell layer formation in the developing retina *in vivo*. *Neuron* **56**, 597–603.

Goldman, D., Hankin, M., Li, Z., Dai, X., and Ding, J. (2001). Transgenic zebrafish for studying nervous system development and regeneration. *Transgenic Res.* **10**, 21–33.

Golling, G., Amsterdam, A., Sun, Z., Antonelli, M., Maldonado, E., Chen, W., Burgess, S., Haldi, M., Artzt, K., Farrington, S., *et al*. (2002). Insertional mutagenesis in zebrafish rapidly identifies genes essential for early vertebrate development. *Nat. Genet.* **31**, 135–140.

Gonzalez-Quevedo, R., Lee, Y., Poss, K. D., and Wilkinson, D. G. (2010). Neuronal regulation of the spatial patterning of neurogenesis. *Dev. Cell* **18**, 136–147.

Gothilf, Y., Toyama, R., Coon, S., Du, S., Dawid, I., and Klein, D. (2002). Pineal-specific expression of green fluorescent protein under the control of the serotonin-N-acetyltransferase gene regulatory regions in transgenic zebrafish. *Dev. Dyn.* **225**, 241–249.

Grandel, H., Kaslin, J., Ganz, J., Wenzel, I., and Brand, M. (2006). Neural stem cells and neurogenesis in the adult zebrafish brain: Origin, proliferation dynamics, migration and cell fate. *Dev. Biol.* **295**, 263–277.

Gray, M., Moens, C. B., Amacher, S. L., Eisen, J. S., and Beattie, C. E. (2001). Zebrafish deadly seven functions in neurogenesis. *Dev. Biol.* **237**, 306–323.

Gregg, R. G., Willer, G. B., Fadool, J. M., Dowling, J. E., and Link, B. A. (2003). Positional cloning of the young mutation identifies an essential role for the Brahma chromatin remodeling complex in mediating retinal cell differentiation. *Proc. Natl. Acad. Sci. U.S.A.* **100**, 6535–6540.

Gritsman, K., Zhang, J., Cheng, S., Heckscher, E., Talbot, W. S., and Schier, A. F. (1999). The EGF-CFC protein one-eyed pinhead is essential for nodal signaling. *Cell* **97**, 121–132.

Guo, S., Brush, J., Teraoka, H., Goddard, A., Wilson, S. W., Mullins, M. C., and Rosenthal, A. (1999a). Development of noradrenergic neurons in the zebrafish hindbrain requires BMP, FGF8, and the homeodomain protein soulless/Phox2a. *Neuron* **24**, 555–566.

Guo, S., Wilson, S. W., Cooke, S., Chitnis, A. B., Driever, W., and Rosenthal, A. (1999b). Mutations in the zebrafish unmask shared regulatory pathways controlling the development of catecholaminergic neurons. *Dev. Biol.* **208**, 473–487.

Guo, S., Yamaguchi, Y., Schilbach, S., Wada, T., Lee, J., Goddard, A., French, D., Handa, H., and Rosenthal, A. (2000). A regulator of transcriptional elongation controls vertebrate neuronal development. *Nature* **408**, 366–369.

Gwak, J. W., Kong, H. J., Bae, Y. K., Kim, M. J., Lee, J., Park, J. H., and Yeo, S. Y. (2010). Proliferating neural progenitors in the developing CNS of zebrafish require Jagged2 and Jagged1b. *Mol. Cells* **30**, 155–159.

Habuchi, S., Ando, R., Dedecker, P., Verheijen, W., Mizuno, H., Miyawaki, A., and Hofkens, J. (2005). Reversible single-molecule photoswitching in the GFP-like fluorescent protein Dronpa. *Proc. Natl. Acad. Sci. U.S.A.* **102**, 9511–9516.

Haddon, C., Smithers, L., Schneider-Maunoury, S., Coche, T., Henrique, D., and Lewis, J. (1998). Multiple delta genes and lateral inhibition in zebrafish primary neurogenesis. *Development* **125**, 359–370.

Halloran, M. C., Sato-Maeda, M., Warren, J. T., Su, F., Lele, Z., Krone, P. H., Kuwada, J. Y., and Shoji, W. (2000). Laser-induced gene expression in specific cells of transgenic zebrafish. *Development* **127**, 1953–1960.

Hamaoka, T., Takechi, M., Chinen, A., Nishiwaki, Y., and Kawamura, S. (2002). Visualization of rod photoreceptor development using GFP-transgenic zebrafish. *Genesis* **34**, 215–220.

Hammond, K. L., Hill, R. E., Whitfield, T. T., and Currie, P. D. (2002). Isolation of three zebrafish dachshund homologues and their expression in sensory organs, the central nervous system and pectoral fin buds. *Mech. Dev.* **112**, 183–189.

Hans, S., Kaslin, J., Freudenreich, D., and Brand, M. (2009). Temporally-controlled site-specific recombination in zebrafish. *PLoS One* **4**, e4640.

Hans, S., Scheer, N., Riedl, I., v Weizsacker, E., Blader, P., and Campos-Ortega, J. A. (2004). her3, a zebrafish member of the hairy-E(spl) family, is repressed by Notch signalling. *Development* **131**, 2957–2969.

Hatta, K. (1992). Role of the floor plate in axonal patterning in the zebrafish CNS. *Neuron* **9**, 629–642.

Hatta, K., Tsujii, H., and Omura, T. (2006). Cell tracking using a photoconvertible fluorescent protein. *Nat. Protoc.* **1**, 960–967.

Hauptmann, G., and Gerster, T. (1996). Complex expression of the zp-50 pou gene in the embryonic zebrafish brain is altered by overexpression of sonic hedgehog. *Development* **122**, 1769–1780.

Hauptmann, G., and Gerster, T. (2000a). Combinatorial expression of zebrafish Brn-1- and Brn-2-related POU genes in the embryonic brain, pronephric primordium, and pharyngeal arches. *Dev. Dyn.* **218**, 345–358.

Hauptmann, G., and Gerster, T. (2000b). Multicolor whole-mount in situ hybridization. *Methods Mol. Biol.* **137**, 139–148.

Hauptmann, G., and Gerster, T. (2000c). Regulatory gene expression patterns reveal transverse and longitudinal subdivisions of the embryonic zebrafish forebrain. *Mech. Dev.* **91**, 105–118.

Hauptmann, G., Soll, I., and Gerster, T. (2002). The early embryonic zebrafish forebrain is subdivided into molecularly distinct transverse and longitudinal domains. *Brain Res. Bull.* **57**, 371–375.

Heisenberg, C. P., Brand, M., Jiang, Y. J., Warga, R. M., Beuchle, D., van Eeden, F. J., Furutani-Seiki, M., Granato, M., Haffter, P., Hammerschmidt, M., *et al.* (1996). Genes involved in forebrain development in the zebrafish, Danio rerio. *Development* **123**, 191–203.

Helde, K. A., Wilson, E. T., Cretekos, C. J., and Grunwald, D. J. (1994). Contribution of early cells to the fate map of the zebrafish gastrula. *Science* **265**, 517–520.

Helmchen, F., and Denk, W. (2005). Deep tissue two-photon microscopy. *Nat. Methods* **2**, 932–940.

Hernandez-Lagunas, L., Choi, I. F., Kaji, T., Simpson, P., Hershey, C., Zhou, Y., Zon, L., Mercola, M., and Artinger, K. B. (2005). Zebrafish narrowminded disrupts the transcription factor prdm1 and is required for neural crest and sensory neuron specification. *Dev. Biol.* **278**, 347–357.

Hesselson, D., Anderson, R. M., Beinat, M., and Stainier, D. Y. (2009). Distinct populations of quiescent and proliferative pancreatic beta-cells identified by HOTcre mediated labeling. *Proc. Natl. Acad. Sci. U.S.A.* **106**, 14896–14901.

Hieber, V., Dai, X., Foreman, M., and Goldman, D. (1998). Induction of alpha1-tubulin gene expression during development and regeneration of the fish central nervous system. *J. Neurobiol.* **37**, 429–440.

Higashijima, S., Okamoto, H., Ueno, N., Hotta, Y., Eguchi, G. (1997). High-frequency generation of transgenic zebrafish which reliably express GFP in whole muscles or the whole body by using promoters of zebrafish origin. *Dev. Biol.* **192**, 289–299.

Higashijima, S., Hotta, Y., and Okamoto, H. (2000). Visualization of cranial motor neurons in live transgenic zebrafish expressing green fluorescent protein under the control of the islet-1 promoter/enhancer. *J. Neurosci.* **20**, 206–218.

Higashijima, S., Mandel, G., and Fetcho, J. R. (2004). Distribution of prospective glutamatergic, glycinergic, and GABAergic neurons in embryonic and larval zebrafish. *J. Comp. Neurol.* **480**, 1–18.

Hild, M., Dick, A., Rauch, G. J., Meier, A., Bouwmeester, T., Haffter, P., and Hammerschmidt, M. (1999). The smad5 mutation somitabun blocks Bmp2b signaling during early dorsoventral patterning of the zebrafish embryo. *Development* **126**, 2149–2159.

Hjorth, J. T., Gad, J., Cooper, H., and Key, B. (2001). A zebrafish homologue of deleted in colorectal cancer (zdcc) is expressed in the first neuronal clusters of the developing brain. *Mech. Dev.* **109**, 105–109.

Ho, R. K., and Kane, D. A. (1990). Cell-autonomous action of zebrafish spt-1 mutation in specific mesodermal precursors. *Nature* **348**, 728–730.

Holley, S. A., Geisler, R., and Nusslein-Volhard, C. (2000). Control of her1 expression during zebrafish somitogenesis by a delta-dependent oscillator and an independent wave-front activity. *Genes Dev.* **14**, 1678–1690.

Holzschuh, J., Ryu, S., Aberger, F., and Driever, W. (2001). Dopamine transporter expression distinguishes dopaminergic neurons from other catecholaminergic neurons in the developing zebrafish embryo. *Mech. Dev.* **101**, 237–243.

Hong, S., Kim, C., Yoo, K., Kim, H., Kudoh, T., Dawid, I., and Huh, T. (2002). Isolation and expression of a novel neuron-specific onecut homeobox gene in zebrafish. *Mech. Dev.* **112**, 199–202.

Horne-Badovinac, S., Lin, D., Waldron, S., Schwarz, M., Mbamalu, G., Pawson, T., Jan, Y., Stainier, D. Y., and Abdelilah-Seyfried, S. (2001). Positional cloning of heart and soul reveals multiple roles for PKC lambda in zebrafish organogenesis. *Curr. Biol.* **11**, 1492–1502.

Houart, C., Caneparo, L., Heisenberg, C., Barth, K., Take-Uchi, M., and Wilson, S. (2002). Establishment of the telencephalon during gastrulation by local antagonism of Wnt signaling. *Neuron* **35**, 255–265.

Huang, S., and Sato, S. (1998). Progenitor cells in the adult zebrafish nervous system express a Brn-1-related Pou gene, Tai-ji. *Mech. Dev.* **71**, 23–35.

Imboden, M., Devignot, V., Korn, H., and Goblet, C. (2001). Regional distribution of glycine receptor messenger RNA in the central nervous system of zebrafish. *Neuroscience* **103**, 811–830.

Inoue, A., Takahashi, M., Hatta, K., Hotta, Y., and Okamoto, H. (1994). Developmental regulation of islet-1 mRNA expression during neuronal differentiation in embryonic zebrafish. *Dev. Dyn.* **199**, 1–11.

Ito, Y., Tanaka, H., Okamoto, H., and Ohshima, T. (2010). Characterization of neural stem cells and their progeny in the adult zebrafish optic tectum. *Dev. Biol.* **342**, 26–38.

Itoh, M., Kim, C. H., Palardy, G., Oda, T., Jiang, Y. J., Maust, D., Yeo, S. Y., Lorick, K., Wright, G. J., Ariza-McNaughton, L., *et al.* (2003). Mind bomb is a ubiquitin ligase that is essential for efficient activation of Notch signaling by Delta. *Dev. Cell* **4**, 67–82.

Jaszai, J., Reifers, F., Picker, A., Langenberg, T., and Brand, M. (2003). Isthmus-to-midbrain transformation in the absence of midbrain-hindbrain organizer activity. *Development* **130**, 6611–6623.

Jensen, A. M., and Westerfield, M. (2004). Zebrafish mosaic eyes is a novel FERM protein required for retinal lamination and retinal pigmented epithelial tight junction formation. *Curr. Biol.* **14**, 711–717.

Jing, X., and Malicki, J. (2009). Zebrafish ale oko, an essential determinant of sensory neuron survival and the polarity of retinal radial glia, encodes the p50 subunit of dynactin. *Development* **136**, 2955–2964.

Jowett, T. (1999). Analysis of protein and gene expression. *Methods Cell Biol.* **59**, 63–85.

Julich, D., Hwee Lim, C., Round, J., Nicolaije, C., Schroeder, J., Davies, A., Geisler, R., Lewis, J., Jiang, Y. J., and Holley, S. A. (2005). beamter/deltaC and the role of Notch ligands in the zebrafish somite segmentation, hindbrain neurogenesis and hypochord differentiation. *Dev. Biol.* **286**, 391–404.

Kalev-Zylinska, M. L., Horsfield, J. A., Flores, M. V., Postlethwait, J. H., Chau, J. Y., Cattin, P. M., Vitas, M. R., Crosier, P. S., and Crosier, K. E. (2003). Runx3 is required for hematopoietic development in zebrafish. *Dev. Dyn.* **228**, 323–336.

Kani, S., Bae, Y. K., Shimizu, T., Tanabe, K., Satou, C., Parsons, M. J., Scott, E., Higashijima, S., and Hibi, M. (2010). Proneural gene-linked neurogenesis in zebrafish cerebellum. *Dev. Biol.* **343**, 1–17.

Kaslin, J., Ganz, J., and Brand, M. (2008). Proliferation, neurogenesis and regeneration in the non-mammalian vertebrate brain. *Philos. Trans. R. Soc. Lond., B, Biol. Sci.* **363**, 101–122.

Kaslin, J., Ganz, J., Geffarth, M., Grandel, H., Hans, S., and Brand, M. (2009). Stem cells in the adult zebrafish cerebellum: Initiation and maintenance of a novel stem cell niche. *J. Neurosci.* **29**, 6142–6153.

Kaslin, J., Nystedt, J. M., Ostergard, M., Peitsaro, N., and Panula, P. (2004). The orexin/hypocretin system in zebrafish is connected to the aminergic and cholinergic systems. *J. Neurosci.* **24**, 2678–2689.

Kaslin, J., and Panula, P. (2001). Comparative anatomy of the histaminergic and other aminergic systems in zebrafish (Danio rerio). *J. Comp. Neurol.* **440**, 342–377.

Kassen, S. C., Ramanan, V., Montgomery, J.E., C., T.B., Liu, C. G., Vihtelic, T. S., and Hyde, D. R. (2007). Time course analysis of gene expression during light-induced photoreceptor cell death and regeneration in albino zebrafish. *Dev. Neurobiol.* **67**, 1009–1031.

Kassen, S. C., Thummel, R., Burket, C. T., Campochiaro, L. A., Harding, M. J., and Hyde, D. R. (2008). The Tg(ccnb1:EGFP) transgenic zebrafish line labels proliferating cells during retinal development and regeneration. *Mol. Vis.* **14**, 951–963.

Kawahara, A., Chien, C. B., and Dawid, I. B. (2002). The homeobox gene mbx is involved in eye and tectum development. *Dev. Biol.* **248**, 107–117.

Kawai, H., Arata, N., and Nakayasu, H. (2001). Three-dimensional distribution of astrocytes in zebrafish spinal cord. *Glia* **36**, 406–413.

Kay, J., Finger-Baier, K., Roeser, T., Staub, W., and Baier, H. (2001). Retinal ganglion cell genesis requires lakritz, a zebrafish atonal homolog. *Neuron* **30**, 725–736.

Kay, J. N., Roeser, T., Mumm, J. S., Godinho, L., Mrejeru, A., Wong, R. O., and Baier, H. (2004). Transient requirement for ganglion cells during assembly of retinal synaptic layers. *Development* **131**, 1331–1342.

Keller, P. J., Schmidt, A. D., Santella, A., Khairy, K., Bao, Z., Wittbrodt, J., and Stelzer, E. H. (2010). Fast, high-contrast imaging of animal development with scanned light sheet-based structured-illumination microscopy. *Nat. Methods* **7**, 637–642.

Keller, P. J., Schmidt, A. D., Wittbrodt, J., and Stelzer, E. H. (2008). Reconstruction of zebrafish early embryonic development by scanned light sheet microscopy. *Science* **322**, 1065–1069.

Kemp, H. A., Carmany-Rampey, A., and Moens, C. (2009). Generating chimeric zebrafish embryos by transplantation. *J. Vis. Exp.*17; (29). pii: 1394. doi: 10.379/-1394.

Kennedy, B. N., Alvarez, Y., Brockerhoff, S. E., Stearns, G. W., Sapetto-Rebow, B., Taylor, M. R., and Hurley, J. B. (2007). Identification of a zebrafish cone photoreceptor-specific promoter and genetic rescue of achromatopsia in the nof mutant. *Invest. Ophthalmol. Vis. Sci.* **48**, 522–529.

Kera, S. A., Agerwala, S. M., and Horne, J. H. (2010). The temporal resolution of *in vivo* electroporation in zebrafish: A method for time-resolved loss of function. *Zebrafish* **7**, 97–108.

Kikuchi, Y., Segawa, H., Tokumoto, M., Tsubokawa, T., Hotta, Y., Uyemura, K., and Okamoto, H. (1997). Ocular and cerebellar defects in zebrafish induced by overexpression of the LIM domains of the islet-3 LIM/homeodomain protein. *Neuron* **18**, 369–382.

Kim, C. H., Oda, T., Itoh, M., Jiang, D., Artinger, K. B., Chandrasekharappa, S. C., Driever, W., and Chitnis, A. B. (2000). Repressor activity of Headless/Tcf3 is essential for vertebrate head formation. *Nature* **407**, 913–916.

Kim, C. H., Ueshima, E., Muraoka, O., Tanaka, H., Yeo, S. Y., Huh, T. L., and Miki, N. (1996). Zebrafish elav/HuC homologue as a very early neuronal marker. *Neurosci. Lett.* **216**, 109–112.

Kim, H., Shin, J., Kim, S., Poling, J., Park, H. C., and Appel, B. (2008). Notch-regulated oligodendrocyte specification from radial glia in the spinal cord of zebrafish embryos. *Dev. Dyn.* **237**, 2081–2089.

Kimmel, C. B., Ballard, W. W., Kimmel, S. R., Ullmann, B., and Schilling, T. F. (1995). Stages of embryonic development of the zebrafish. *Dev. Dyn.* **203**, 253–310.

Kimura, Y., Okamura, Y., and Higashijima, S. (2006). alx, a zebrafish homolog of Chx10, marks ipsilateral descending excitatory interneurons that participate in the regulation of spinal locomotor circuits. *J. Neurosci.* **26**, 5684–5697.

Kimura, Y., Satou, C., and Higashijima, S. (2008). V2a and V2b neurons are generated by the final divisions of pair-producing progenitors in the zebrafish spinal cord. *Development* **135**, 3001–3005.

Kirby, B. B., Takada, N., Latimer, A. J., Shin, J., Carney, T. J., Kelsh, R. N., and Appel, B. (2006). *In vivo* time-lapse imaging shows dynamic oligodendrocyte progenitor behavior during zebrafish development. *Nat. Neurosci.* **9**, 1506–1511.

Kishimoto, Y., Lee, K. H., Zon, L., Hammerschmidt, M., and Schulte-Merker, S. (1997). The molecular nature of zebrafish swirl: BMP2 function is essential during early dorsoventral patterning. *Development* **124**, 4457–4466.

Knowlton, M. N., Li, T., Ren, Y., Bill, B. R., Ellis, L. B., and Ekker, S. C. (2008). A PATO-compliant zebrafish screening database (MODB): Management of morpholino knockdown screen information. *BMC Bioinformatics* **9**, 7.

Ko, H. W., Norman, R. X., Tran, J., Fuller, K. P., Fukuda, M., and Eggenschwiler, J. T. (2010). Broad-minded links cell cycle-related kinase to cilia assembly and hedgehog signal transduction. *Dev. Cell* **18**, 237–247.

Korzh, V., Edlund, T., and Thor, S. (1993). Zebrafish primary neurons initiate expression of the LIM homeodomain protein Isl-1 at the end of gastrulation. *Development* **118**, 417–425.

Korzh, V., Sleptsova, I., Liao, J., He, J., and Gong, Z. (1998). Expression of zebrafish bHLH genes ngn1 and nrd defines distinct stages of neural differentiation. *Dev. Dyn.* **213**, 92–104.

Koshida, S., Shinya, M., Mizuno, T., Kuroiwa, A., and Takeda, H. (1998). Initial anteroposterior pattern of the zebrafish central nervous system is determined by differential competence of the epiblast. *Development* **125**, 1957–1966.

Koster, R. W., and Fraser, S. E. (2001). Direct imaging of *in vivo* neuronal migration in the developing cerebellum. *Curr. Biol.* **11**, 1858–1863.

Kozlowski, D. J., and Weinberg, E. S. (2000). Photoactivatable (caged) fluorescein as a cell tracer for fate mapping in the zebrafish embryo. *Methods Mol. Biol.* **135**, 349–355.

Kucenas, S., Takada, N., Park, H. C., Woodruff, E., Broadie, K., and Appel, B. (2008). CNS-derived glia ensheath peripheral nerves and mediate motor root development. *Nat. Neurosci.* **11**, 143–151.

Kurita, R., Sagara, H., Aoki, Y., Link, B. A., Arai, K., and Watanabe, S. (2003). Suppression of lens growth by alphaA-crystallin promoter-driven expression of diphtheria toxin results in disruption of retinal cell organization in zebrafish. *Dev. Biol.* **255**, 113–127.

Kusik, B. W., Hammond, D. R., and Udvadia, A. J. (2010). Transcriptional regulatory regions of gap43 needed in developing and regenerating retinal ganglion cells. *Dev. Dyn.* **239**, 482–495.

Lam, C. S., Marz, M., and Strahle, U. (2009). gfap and nestin reporter lines reveal characteristics of neural progenitors in the adult zebrafish brain. *Dev. Dyn.* **238**, 475–486.

Langenau, D., Palomero, T., Kanki, J., Ferrando, A., Zhou, Y., Zon, L., and Look, A. (2002). Molecular cloning and developmental expression of Tlx (Hox11) genes in zebrafish (Danio rerio). *Mech. Dev.* **117**, 243–248.

Latimer, A. J., Shin, J., and Appel, B. (2005). her9 promotes floor plate development in zebrafish. *Dev. Dyn.* **232**, 1098–1104.

Le, X., Langenau, D. M., Keefe, M. D., Kutok, J. L., Neuberg, D. S., and Zon, L. I. (2007). Heat shock-inducible Cre/Lox approaches to induce diverse types of tumors and hyperplasia in transgenic zebrafish. *Proc. Natl. Acad. Sci. U.S.A.* **104**, 9410–9415.

Leake, D., Asch, W., Canger, A., and Schechter, N. (1999). Gefiltin in zebrafish embryos: Sequential gene expression of two neurofilament proteins in retinal ganglion cells. *Differentiation* **65**, 181–189.

Lee, J. E., Wu, S. F., Goering, L. M., and Dorsky, R. I. (2006). Canonical Wnt signaling through Lef1 is required for hypothalamic neurogenesis. *Development* **133**, 4451–4461.

Lee, V. M., Carden, M. J., Schlaepfer, W. W., and Trojanowski, J. Q. (1987). Monoclonal antibodies distinguish several differently phosphorylated states of the two largest rat neurofilament subunits (NF-H and NF-M) and demonstrate their existence in the normal nervous system of adult rats. *J. Neurosci.* **7**, 3474–3488.

Lee, Y., Grill, S., Sanchez, A., Murphy-Ryan, M., and Poss, K. D. (2005). Fgf signaling instructs position-dependent growth rate during zebrafish fin regeneration. *Development* **132**, 5173–5183.

Lele, Z., Folchert, A., Concha, M., Rauch, G. J., Geisler, R., Rosa, F., Wilson, S. W., Hammerschmidt, M., and Bally-Cuif, L. (2002). parachute/n-cadherin is required for morphogenesis and maintained integrity of the zebrafish neural tube. *Development* **129**, 3281–3294.

Levkowitz, G., Zeller, J., Sirotkin, H. I., French, D., Schilbach, S., Hashimoto, H., Hibi, M., Talbot, W. S., and Rosenthal, A. (2003). Zinc finger protein too few controls the development of monoaminergic neurons. *Nat. Neurosci.* **6**, 28–33.

Li, M., Zhao, C., Wang, Y., Zhao, Z., and Meng, A. (2002). Zebrafish sox9b is an early neural crest marker. *Dev. Genes Evol.* **212**, 203–206.

Li, Y., Allende, M. L., Finkelstein, R., and Weinberg, E. S. (1994). Expression of two zebrafish orthodenticle-related genes in the embryonic brain. *Mech. Dev.* **48**, 229–244.

Li, Z., Joseph, N. M., and Easter, S. S. Jr. (2000). The morphogenesis of the zebrafish eye, including a fate map of the optic vesicle. *Dev. Dyn.* **218**, 175–188.

Li, Z., Korzh, V., and Gong, Z. (2009). DTA-mediated targeted ablation revealed differential interdependence of endocrine cell lineages in early development of zebrafish pancreas. *Differentiation* **78**, 241–252.

Liao, J., He, J., Yan, T., Korzh, V., and Gong, Z. (1999). A class of neuroD-related basic helix-loop-helix transcription factors expressed in developing central nervous system in zebrafish. *DNA Cell Biol.* **18**, 333–344.

Lillesaar, C., Stigloher, C., Tannhauser, B., Wullimann, M. F., and Bally-Cuif, L. (2009). Axonal projections originating from raphe serotonergic neurons in the developing and adult zebrafish, Danio rerio, using transgenics to visualize raphe-specific pet1 expression. *J. Comp. Neurol.* **512**, 158–182.

Lillesaar, C., Tannhauser, B., Stigloher, C., Kremmer, E., and Bally-Cuif, L. (2007). The serotonergic phenotype is acquired by converging genetic mechanisms within the zebrafish central nervous system. *Dev. Dyn.* **236**, 1072–1084.

Link, B., Fadool, J., Malicki, J., and Dowling, J. (2000). The zebrafish young mutation acts non-cell-autonomously to uncouple differentiation from specification for all retinal cells. *Development* **127**, 2177–2188.

Link, B. A., Kainz, P. M., Ryou, T., and Dowling, J. E. (2001). The perplexed and confused mutations affect distinct stages during the transition from proliferating to post-mitotic cells within the zebrafish retina. *Dev. Biol.* **236**, 436–453.

Lippincott-Schwartz, J., and Patterson, G. H. (2009). Photoactivatable fluorescent proteins for diffraction-limited and super-resolution imaging. *Trends Cell Biol.* **19**, 555–565.

Lister, J. A., Robertson, C. P., Lepage, T., Johnson, S. L., and Raible, D. W. (1999). nacre encodes a zebrafish microphthalmia-related protein that regulates neural-crest-derived pigment cell fate. *Development* **126**, 3757–3767.

Liu, K. S., Gray, M., Otto, S. J., Fetcho, J. R., and Beattie, C. E. (2003). Mutations in deadly seven/notch1a reveal developmental plasticity in the escape response circuit. *J. Neurosci.* **23**, 8159–8166.

Luo, G. R., Chen, Y., Li, X. P., Liu, T. X., and Le, W. D. (2008). Nr4a2 is essential for the differentiation of dopaminergic neurons during zebrafish embryogenesis. *Mol. Cell. Neurosci.* **39**, 202–210.

Lyons, D. A., Guy, A. T., and Clarke, J. D. (2003). Monitoring neural progenitor fate through multiple rounds of division in an intact vertebrate brain. *Development* **130**, 3427–3436.

MacDonald, R. B., Debiais-Thibaud, M., Talbot, J. C., and Ekker, M. (2010). The relationship between dlx and gad1 expression indicates highly conserved genetic pathways in the zebrafish forebrain. *Dev. Dyn.* **239**, 2298–2306.

Mahler, J., and Driever, W. (2007). Expression of the zebrafish intermediate neurofilament Nestin in the developing nervous system and in neural proliferation zones at postembryonic stages. *BMC Dev. Biol.* **7**, 89.

Malicki, J., and Driever, W. (1999). oko meduzy mutations affect neuronal patterning in the zebrafish retina and reveal cell-cell interactions of the retinal neuroepithelial sheet. *Development* **126**, 1235–1246.

Malicki, J., Jo, H., and Pujic, Z. (2003). Zebrafish N-cadherin, encoded by the glass onion locus, plays an essential role in retinal patterning. *Dev. Biol.* **259**, 95–108.

Marc, R., and Cameron, D. (2001). A molecular phenotype atlas of the zebrafish retina. *J. Neurocytol.* **30**, 593–654.

Marques, S. R., Lee, Y., Poss, K. D., and Yelon, D. (2008). Reiterative roles for FGF signaling in the establishment of size and proportion of the zebrafish heart. *Dev. Biol.* **321**, 397–406.

Martin, S., Heinrich, G., and Sandell, J. H. (1998). Sequence and expression of glutamic acid decarboxylase isoforms in the developing zebrafish. *J. Comp. Neurol.* **396**, 253–266.

Marx, M., Rutishauser, U., and Bastmeyer, M. (2001). Dual function of polysialic acid during zebrafish central nervous system development. *Development* **128**, 4949–4958.

März, M., Chapouton, P., Diotel, N., Vaillant, C., Hesl, B., Takamiya, M., Lam, C. S., Kah, O., Bally-Cuif, L., and Strahle, U. (2010). Heterogeneity in progenitor cell subtypes in the ventricular zone of the zebrafish adult telencephalon. *Glia* **58**, 870–888.

Masai, I., Heisenberg, C. P., Barth, K. A., Macdonald, R., Adamek, S., and Wilson, S. W. (1997). floating head and masterblind regulate neuronal patterning in the roof of the forebrain. *Neuron* **18**, 43–57.

Masai, I., Stemple, D., Okamoto, H., and Wilson, S. (2000). Midline signals regulate retinal neurogenesis in zebrafish. *Neuron* **27**, 251–263.

Matsuda, M., and Chitnis, A. B. (2009). Interaction with Notch determines endocytosis of specific Delta ligands in zebrafish neural tissue. *Development* **136**, 197–206.

Maves, L., Jackman, W., and Kimmel, C. B. (2002). FGF3 and FGF8 mediate a rhombomere 4 signaling activity in the zebrafish hindbrain. *Development* **129**, 3825–3837.

McFarland, K. A., Topczewska, J. M., Weidinger, G., Dorsky, R. I., and Appel, B. (2008). Hh and Wnt signaling regulate formation of olig2+ neurons in the zebrafish cerebellum. *Dev. Biol.* **318**, 162–171.

McGraw, H. F., Nechiporuk, A., and Raible, D. W. (2008). Zebrafish dorsal root ganglia neural precursor cells adopt a glial fate in the absence of neurogenin1. *J. Neurosci.* **28**, 12558–12569.

McLean, D. L., Fan, J., Higashijima, S., Hale, M. E., and Fetcho, J. R. (2007). A topographic map of recruitment in spinal cord. *Nature* **446**, 71–75.

McMahon, C., Gestri, G., Wilson, S. W., Link, B. A. (2009). Lmx1b is essential for survival of periocular mesenchymal cells and influences Fgf-mediated retinal patterning in zebrafish. *Dev. Biol.* **332**, 287–298.

Melancon, E., Liu, D. W., Westerfield, M., and Eisen, J. S. (1997). Pathfinding by identified zebrafish motoneurons in the absence of muscle pioneers. *J. Neurosci.* **17**, 7796–7804.

Meng, S., Ryu, S., Zhao, B., Zhang, D. Q., Driever, W., and McMahon, D. G. (2008a). Targeting retinal dopaminergic neurons in tyrosine hydroxylase-driven green fluorescent protein transgenic zebrafish. *Mol. Vis.* **14**, 2475–2483.

Meng, X., Noyes, M. B., Zhu, L. J., Lawson, N. D., and Wolfe, S. A. (2008b). Targeted gene inactivation in zebrafish using engineered zinc-finger nucleases. *Nat. Biotechnol.* **26**, 695–701.

Menuet, A., Pellegrini, E., Brion, F., Gueguen, M. M., Anglade, I., Pakdel, F., and Kah, O. (2005). Expression and estrogen-dependent regulation of the zebrafish brain aromatase gene. *J. Comp. Neurol.* **485**, 304–320.

Metcalfe, W., Myers, P., Trevarrow, B., Bass, M., and Kimmel, C. (1990). Primary neurons that express the L2/HNK-1 carbohydrate during early development in the zebrafish. *Development* **110**, 491–504.

Mikkola, I., Fjose, A., Kuwada, J. Y., Wilson, S., Guddal, P. H., and Krauss, S. (1992). The paired domain-containing nuclear factor pax[b] is expressed in specific commissural interneurons in zebrafish embryos. *J. Neurobiol.* **23**, 933–946.

Mione, M., Baldessari, D., Deflorian, G., Nappo, G., and Santoriello, C. (2008). How neuronal migration contributes to the morphogenesis of the CNS: Insights from the zebrafish. *Dev. Neurosci.* **30**, 65–81.

Miyamura, Y., and Nakayasu, H. (2001). Zonal distribution of Purkinje cells in the zebrafish cerebellum: Analysis by means of a specific monoclonal antibody. *Cell Tissue Res.* **305**, 299–305.

Moens, C. B., Donn, T. M., Wolf-Saxon, E. R., and Ma, T. P. (2008). Reverse genetics in zebrafish by TILLING. *Brief Funct. Genomic Proteomic* **7**, 454–459.

Molina, G. A., Watkins, S. C., and Tsang, M. (2007). Generation of FGF reporter transgenic zebrafish and their utility in chemical screens. *BMC Dev. Biol.* **7**, 62.

Montgomery, J. E., Parsons, M. J., and Hyde, D. R. (2009). A novel model of retinal ablation demonstrates that the extent of rod cell death regulates the origin of the regenerated zebrafish rod photoreceptors. *J. Comp. Neurol.* **518**, 800–814.

Mueller, T., and Wullimann, M. F. (2002). BrdU-, neuroD (nrd)- and Hu-studies reveal unusual non-ventricular neurogenesis in the postembryonic zebrafish forebrain. *Mech. Dev.* **117**, 123–135.

Mueller, T., and Wullimann, M. F. (2003). Anatomy of neurogenesis in the early zebrafish brain. *Brain Res. Dev. Brain Res.* **140**, 137–155.

Mumm, J. S., Williams, P. R., Godinho, L., Koerber, A., Pittman, A. J., Roeser, T., Chien, C. B., Baier, H., and Wong, R. O. (2006). *In vivo* imaging reveals dendritic targeting of laminated afferents by zebrafish retinal ganglion cells. *Neuron* **52**, 609–621.

Nguyen, V. H., Schmid, B., Trout, J., Connors, S. A., Ekker, M., and Mullins, M. C. (1998). Ventral and lateral regions of the zebrafish gastrula, including the neural crest progenitors, are established by a bmp2b/swirl pathway of genes. *Dev. Biol.* **199**, 93–110.

Ninkovic, J., Stigloher, C., Lillesaar, C., and Bally-Cuif, L. (2008). Gsk3beta/PKA and Gli1 regulate the maintenance of neural progenitors at the midbrain-hindbrain boundary in concert with E(Spl) factor activity. *Development* **135**, 3137–3148.

Ninkovic, J., Tallafuss, A., Leucht, C., Topczewski, J., Tannhauser, B., Solnica-Krezel, L., and Bally-Cuif, L. (2005). Inhibition of neurogenesis at the zebrafish midbrain-hindbrain boundary by the combined and dose-dependent activity of a new hairy/E(spl) gene pair. *Development* **132**, 75–88.

Nissen, R. M., Yan, J., Amsterdam, A., Hopkins, N., and Burgess, S. M. (2003). Zebrafish foxi one modulates cellular responses to Fgf signaling required for the integrity of ear and jaw patterning. *Development* **130**, 2543–2554.

Norden, C., Young, S., Link, B. A., Harris, W. A. (2009). Actomyosin is the main driver of interkinetic nuclear migration in the retina. *Cell* **138**, 1195–1208.

Norton, W. H., Folchert, A., and Bally-Cuif, L. (2008). Comparative analysis of serotonin receptor (HTR1A/HTR1B families) and transporter (slc6a4a/b) gene expression in the zebrafish brain. *J. Comp. Neurol.* **511**, 521–542.

O'Malley, D. M., Kao, Y. H., and Fetcho, J. R. (1996). Imaging the functional organization of zebrafish hindbrain segments during escape behaviors. *Neuron* **17**, 1145–1155.

Odenthal, J., and Nusslein-Volhard, C. (1998). Fork head domain genes in zebrafish. *Dev. Genes Evol.* **208**, 245–258.

Odenthal, J., van Eeden, F. J., Haffter, P., Ingham, P. W., and Nusslein-Volhard, C. (2000). Two distinct cell populations in the floor plate of the zebrafish are induced by different pathways. *Dev. Biol.* **219**, 350–363.

Oehlmann, V., Berger, S., Sterner, C., and Korsching, S. (2004). Zebrafish beta tubulin expression is limited to the nervous system throughout development, and in the adult brain is restricted to a subset of proliferative regions. *Gene Expr. Patterns* **4**, 191–198.

Ogura, E., Okuda, Y., Kondoh, H., and Kamachi, Y. (2009). Adaptation of GAL4 activators for GAL4 enhancer trapping in zebrafish. *Dev. Dyn.* **238**, 641–655.

Okuda, Y., Ogura, E., Kondoh, H., and Kamachi, Y. (2010). B1 SOX coordinate cell specification with patterning and morphogenesis in the early zebrafish embryo. *PLoS Genet.* **6**, e1000936.

Okuda, Y., Yoda, H., Uchikawa, M., Furutani-Seiki, M., Takeda, H., Kondoh, H., and Kamachi, Y. (2006). Comparative genomic and expression analysis of group B1 sox genes in zebrafish indicates their diversification during vertebrate evolution. *Dev. Dyn.* **235**, 811–825.

Olivier, N., Luengo-Oroz, M. A., Duloquin, L., Faure, E., Savy, T., Veilleux, I., Solinas, X., Debarre, D., Bourgine, P., Santos, A., *et al*. (2010). Cell lineage reconstruction of early zebrafish embryos using label-free nonlinear microscopy. *Science* **329**, 967–971.

Omori, Y., and Malicki, J. (2006). oko meduzy and related crumbs genes are determinants of apical cell features in the vertebrate embryo. *Curr. Biol.* **16**, 945–957.

Onichtchouk, D., Geier, F., Polok, B., Messerschmidt, D. M., Mossner, R., Wendik, B., Song, S., Taylor, V., Timmer, J., and Driever, W. (2010). Zebrafish Pou5f1-dependent transcriptional networks in temporal control of early development. *Mol. Syst. Biol.* **6**, 354.

Ott, H., Diekmann, H., Stuermer, C., and Bastmeyer, M. (2001). Function of neurolin (DM-GRASP/SC-1) in guidance of motor axons during zebrafish development. *Dev. Biol.* **235**, 86–97.

Palevitch, O., Kight, K., Abraham, E., Wray, S., Zohar, Y., and Gothilf, Y. (2007). Ontogeny of the GnRH systems in zebrafish brain: In situ hybridization and promoter-reporter expression analyses in intact animals. *Cell Tissue Res.* **327**, 313–322.

Papan, C., and Campos-Ortega, J. (1997). A clonal analysis of spinal cord development in the zebrafish. *Dev. Genes Evol.* **207**, 71–81.

Papan, C., and Campos-ortega, J. A. (1994). On the formation of the neural keel and neural tube in the zebrafish Danio (Brachydanio) rerio. *Rouxs Arch. Dev. Biol.* **203**, 178–186.

Parinov, S., Kondrichin, I., Korzh, V., and Emelyanov, A. (2004). Tol2 transposon-mediated enhancer trap to identify developmentally regulated zebrafish genes *in vivo*. *Dev. Dyn.* **231**, 449–459.

Park, H. C., Hong, S. K., Kim, H. S., Kim, S. H., Yoon, E. J., Kim, C. H., Miki, N., and Huh, T. L. (2000a). Structural comparison of zebrafish Elav/Hu and their differential expressions during neurogenesis. *Neurosci. Lett.* **279**, 81–84.

Park, H. C., Boyce, J., Shin, J., and Appel, B. (2005). Oligodendrocyte specification in zebrafish requires notch-regulated cyclin-dependent kinase inhibitor function. *J. Neurosci.* **25**, 6836–6844.

Park, H. C., Kim, C. H., Bae, Y. K., Yeo, S. Y., Kim, S. H., Hong, S. K., Shin, J., Yoo, K. W., Hibi, M., Hirano, T., *et al*. (2000b). Analysis of upstream elements in the HuC promoter leads to the establishment of transgenic zebrafish with fluorescent neurons. *Dev. Biol.* **227**, 279–293.

Park, H. C., Mehta, A., Richardson, J. S., and Appel, B. (2002). olig2 is required for zebrafish primary motor neuron and oligodendrocyte development. *Dev. Biol.* **248**, 356–368.

Park, H. C., Shin, J., and Appel, B. (2004). Spatial and temporal regulation of ventral spinal cord precursor specification by Hedgehog signaling. *Development* **131**, 5959–5969.

Park, S. H., Yeo, S. Y., Yoo, K. W., Hong, S. K., Lee, S., Rhee, M., Chitnis, A. B., and Kim, C. H. (2003). Zath3, a neural basic helix-loop-helix gene, regulates early neurogenesis in the zebrafish. *Biochem. Biophys. Res. Commun.* **308**, 184–190.

Parsons, M. J., Pisharath, H., Yusuff, S., Moore, J. C., Siekmann, A. F., Lawson, N., and Leach, S. D. (2009). Notch-responsive cells initiate the secondary transition in larval zebrafish pancreas. *Mech. Dev.* **126**, 898–912.

Pauls, S., Geldmacher-Voss, B., and Campos-Ortega, J. A. (2001). A zebrafish histone variant H2A.F/Z and a transgenic H2A.F/Z:GFP fusion protein for *in vivo* studies of embryonic development. *Dev. Genes Evol.* **211**, 603–610.

Pellegrini, E., Mouriec, K., Anglade, I., Menuet, A., Le Page, Y., Gueguen, M. M., Marmignon, M. H., Brion, F., Pakdel, F., and Kah, O. (2007). Identification of aromatase-positive radial glial cells as progenitor cells in the ventricular layer of the forebrain in zebrafish. *J. Comp. Neurol.* **501**, 150–167.

Picker, A., Scholpp, S., Bohli, H., Takeda, H., and Brand, M. (2002). A novel positive transcriptional feedback loop in midbrain-hindbrain boundary development is revealed through analysis of the zebrafish pax2.1 promoter in transgenic lines. *Development* **129**, 3227–3239.

Pisharath, H., and Parsons, M. J. (2009). Nitroreductase-mediated cell ablation in transgenic zebrafish embryos. *Methods Mol. Biol.* **546**, 133–143.

Pisharath, H., Rhee, J. M., Swanson, M. A., Leach, S. D., and Parsons, M. J. (2007). Targeted ablation of beta cells in the embryonic zebrafish pancreas using E. coli nitroreductase. *Mech. Dev.* **124**, 218–229.

Pittman, A. J., Law, M. Y., and Chien, C. B. (2008). Pathfinding in a large vertebrate axon tract: Isotypic interactions guide retinotectal axons at multiple choice points. *Development* **135**, 2865–2871.

Poggi, L., Vitorino, M., Masai, I., and Harris, W. A. (2005). Influences on neural lineage and mode of division in the zebrafish retina *in vivo*. *J. Cell Biol.* **171**, 991–999.

Prince, V. E., Moens, C. B., Kimmel, C. B., and Ho, R. K. (1998). Zebrafish hox genes: Expression in the hindbrain region of wild-type and mutants of the segmentation gene, valentino. *Development* **125**, 393–406.

Quint, E., Zerucha, T., and Ekker, M. (2000). Differential expression of orthologous Dlx genes in zebrafish and mice: Implications for the evolution of the Dlx homeobox gene family. *J. Exp. Zool.* **288**, 235–241.

Raible, F., and Brand, M. (2004). Divide et Impera–the midbrain-hindbrain boundary and its organizer. *Trends Neurosci.* **27**, 727–734.

Raymond, P. A., Barthel, L. K., Bernardos, R. L., and Perkowski, J. J. (2006). Molecular characterization of retinal stem cells and their niches in adult zebrafish. *BMC Dev. Biol.* **6**, 36.

Reifers, F., Bohli, H., Walsh, E. C., Crossley, P. H., Stainier, D. Y., and Brand, M. (1998). Fgf8 is mutated in zebrafish acerebellar (ace) mutants and is required for maintenance of midbrain-hindbrain boundary development and somitogenesis. *Development* **125**, 2381–2395.

Reim, G., and Brand, M. (2006). Maternal control of vertebrate dorsoventral axis formation and epiboly by the POU domain protein Spg/Pou2/Oct4. *Development* **133**, 2757–2770.

Reimer, M. M., Kuscha, V., Wyatt, C., Sorensen, I., Frank, R. E., Knuwer, M., Becker, T., and Becker, C. G. (2009). Sonic hedgehog is a polarized signal for motor neuron regeneration in adult zebrafish. *J. Neurosci.* **29**, 15073–15082.

Reimer, M. M., Sorensen, I., Kuscha, V., Frank, R. E., Liu, C., Becker, C. G., and Becker, T. (2008). Motor neuron regeneration in adult zebrafish. *J. Neurosci.* **28**, 8510–8516.

Reinhard, E., Nedivi, E., Wegner, J., Skene, J. H., and Westerfield, M. (1994). Neural selective activation and temporal regulation of a mammalian GAP-43 promoter in zebrafish. *Development* **120**, 1767–1775.

Reischauer, S., Levesque, M. P., Nusslein-Volhard, C., and Sonawane, M. (2009). Lgl2 executes its function as a tumor suppressor by regulating ErbB signaling in the zebrafish epidermis. *PLoS Genet.* **5**, e1000720.

Ren, J. Q., McCarthy, W. R., Zhang, H., Adolph, A. R., and Li, L. (2002). Behavioral visual responses of wild-type and hypopigmented zebrafish. *Vision Res.* **42**, 293–299.

Reugels, A. M., Boggetti, B., Scheer, N., and Campos-Ortega, J. A. (2006). Asymmetric localization of Numb:EGFP in dividing neuroepithelial cells during neurulation in Danio rerio. *Dev. Dyn.* **235**, 934–948.

Ribes, V., Balaskas, N., Sasai, N., Cruz, C., Dessaud, E., Cayuso, J., Tozer, S., Yang, L. L., Novitch, B., Marti, E., *et al*. (2010). Distinct Sonic Hedgehog signaling dynamics specify floor plate and ventral neuronal progenitors in the vertebrate neural tube. *Genes Dev.* **24**, 1186–1200.

Rimini, R., Beltrame, M., Argenton, F., Szymczak, D., Cotelli, F., and Bianchi, M. E. (1999). Expression patterns of zebrafish sox11A, sox11B and sox21. *Mech. Dev.* **89**, 167–171.

Rizzo, M. A., Davidson, M. W., and Piston, D. W. (2009). Fluorescent protein tracking and detection: Applications using fluorescent proteins in living cells. *Cold Spring Harb. Protoc. 2009, pdb top64.*

Roberts, R. K., and Appel, B. (2009). Apical polarity protein PrkCi is necessary for maintenance of spinal cord precursors in zebrafish. *Dev. Dyn.* **238**, 1638–1648.

Rohr, S., Bit-Avragim, N., and Abdelilah-Seyfried, S. (2006). Heart and soul/PRKCi and nagie oko/Mpp5 regulate myocardial coherence and remodeling during cardiac morphogenesis. *Development* **133**, 107–115.

Roth, L., Bormann, P., Bonnet, A., and Reinhard, E. (1999). beta-thymosin is required for axonal tract formation in developing zebrafish brain. *Development* **126**, 1365–1374.

Russek-Blum, N., Gutnick, A., Nabel-Rosen, H., Blechman, J., Staudt, N., Dorsky, R. I., Houart, C., and Levkowitz, G. (2008). Dopaminergic neuronal cluster size is determined during early forebrain patterning. *Development* **135**, 3401–3413.

Russek-Blum, N., Nabel-Rosen, H., and Levkowitz, G. (2009). High resolution fate map of the zebrafish diencephalon. *Dev. Dyn.* **238**, 1827–1835.

Ryu, S., Holzschuh, J., Erhardt, S., Ettl, A. K., and Driever, W. (2005). Depletion of minichromosome maintenance protein 5 in the zebrafish retina causes cell cycle defect and apoptosis. *Proc. Natl. Acad. Sci. U.S.A.* **102**, 18467–18472.

Ryu, S., Mahler, J., Acampora, D., Holzschuh, J., Erhardt, S., Omodei, D., Simeone, A., and Driever, W. (2007). Orthopedia homeodomain protein is essential for diencephalic dopaminergic neuron development. *Curr. Biol.* **17**, 873–880.

Sagasti, A., Guido, M. R., Raible, D. W., and Schier, A. F. (2005). Repulsive interactions shape the morphologies and functional arrangement of zebrafish peripheral sensory arbors. *Curr. Biol.* **15**, 804–814.

Sassa, T., Aizawa, H., and Okamoto, H. (2007). Visualization of two distinct classes of neurons by gad2 and zic1 promoter/enhancer elements in the dorsal hindbrain of developing zebrafish reveals neuronal connectivity related to the auditory and lateral line systems. *Dev. Dyn.* **236**, 706–718.

Sato, T., Hamaoka, T., Aizawa, H., Hosoya, T., and Okamoto, H. (2007a). Genetic single-cell mosaic analysis implicates ephrinB2 reverse signaling in projections from the posterior tectum to the hindbrain in zebrafish. *J. Neurosci.* **27**, 5271–5279.

Sato, T., Takahoko, M., and Okamoto, H. (2006). HuC:Kaede, a useful tool to label neural morphologies in networks *in vivo*. *Genesis* **44**, 136–142.

Sato, Y., Miyasaka, N., and Yoshihara, Y. (2005). Mutually exclusive glomerular innervation by two distinct types of olfactory sensory neurons revealed in transgenic zebrafish. *J. Neurosci.* **25**, 4889–4897.

Sato, Y., Miyasaka, N., and Yoshihara, Y. (2007b). Hierarchical regulation of odorant receptor gene choice and subsequent axonal projection of olfactory sensory neurons in zebrafish. *J. Neurosci.* **27**, 1606–1615.

Sato-Maeda, M., Obinata, M., and Shoji, W. (2008). Position fine-tuning of caudal primary motoneurons in the zebrafish spinal cord. *Development* **135**, 323–332.

Schauerte, H. E., van Eeden, F. J., Fricke, C., Odenthal, J., Strahle, U., and Haffter, P. (1998). Sonic hedgehog is not required for the induction of medial floor plate cells in the zebrafish. *Development* **125**, 2983–2993.

Schebesta, M., and Serluca, F. C. (2009). olig1 Expression identifies developing oligodendrocytes in zebrafish and requires hedgehog and notch signaling. *Dev. Dyn.* **238**, 887–898.

Scheer, N., and Campos-Ortega, J. A. (1999). Use of the Gal4-UAS technique for targeted gene expression in the zebrafish. *Mech. Dev.* **80**, 153–158.

Scheer, N., Groth, A., Hans, S., and Campos-Ortega, J. A. (2001). An instructive function for Notch in promoting gliogenesis in the zebrafish retina. *Development* **128**, 1099–1107.

Schmitz, B., Papan, C., and Campos-Ortega, J. A. (1993). Neurulation in the anterior trunk region of the zebrafish Brachydanio rerio. *Rouxs Arch. Dev. Biol.* **202**, 250–259.

Scholpp, S., Delogu, A., Gilthorpe, J., Peukert, D., Schindler, S., and Lumsden, A. (2009). Her6 regulates the neurogenetic gradient and neuronal identity in the thalamus. *Proc. Natl. Acad. Sci. U.S.A.* **106**, 19895–19900.

Scholpp, S., Wolf, O., Brand, M., and Lumsden, A. (2006). Hedgehog signalling from the zona limitans intrathalamica orchestrates patterning of the zebrafish diencephalon. *Development* **133**, 855–864.

Schonig, K., and Bujard, H. (2003). Generating conditional mouse mutants via tetracycline-controlled gene expression. *Methods Mol. Biol.* **209**, 69–104.

Schroeter, E. H., Wong, R. O., and Gregg, R. G. (2006). *In vivo* development of retinal ON-bipolar cell axonal terminals visualized in nyx::MYFP transgenic zebrafish. *Vis. Neurosci.* **23**, 833–843.

Schulte-Merker, S., Lee, K. J., McMahon, A. P., and Hammerschmidt, M. (1997). The zebrafish organizer requires chordino. *Nature* **387**, 862–3.

Scott, E. K., and Baier, H. (2009). The cellular architecture of the larval zebrafish tectum, as revealed by gal4 enhancer trap lines. *Front Neural Circuits* **3**, 13.

Scott, E. K., Mason, L., Arrenberg, A. B., Ziv, L., Gosse, N. J., Xiao, T., Chi, N. C., Asakawa, K., Kawakami, K., and Baier, H. (2007). Targeting neural circuitry in zebrafish using GAL4 enhancer trapping. *Nat. Methods* **4**, 323–326.

Segawa, H., Miyashita, T., Hirate, Y., Higashijima, S., Chino, N., Uyemura, K., Kikuchi, Y., and Okamoto, H. (2001). Functional repression of Islet-2 by disruption of complex with Ldb impairs peripheral axonal outgrowth in embryonic zebrafish. *Neuron* **30**, 423–436.

Seok, S. H., Na, Y. R., Han, J. H., Kim, T. H., Jung, H., Lee, B. H., Emelyanov, A., Parinov, S., and Park, J. H. (2009). Cre/loxP-regulated transgenic zebrafish model for neural progenitor-specific oncogenic Kras expression. *Cancer Sci.* **101**, 149–154.

Shaner, N. C., Lin, M. Z., McKeown, M. R., Steinbach, P. A., Hazelwood, K. L., Davidson, M. W., and Tsien, R. Y. (2008). Improving the photostability of bright monomeric orange and red fluorescent proteins. *Nat. Methods* **5**, 545–551.

Shaner, N. C., Steinbach, P. A., and Tsien, R. Y. (2005). A guide to choosing fluorescent proteins. *Nat. Methods* **2**, 905–909.

Shin, J., Park, H. C., Topczewska, J. M., Mawdsley, D. J., and Appel, B. (2003). Neural cell fate analysis in zebrafish using olig2 BAC transgenics. *Methods Cell Sci.* **25**, 7–14.

Sinha, D. K., Neveu, P., Gagey, N., Aujard, I., Le Saux, T., Rampon, C., Gauron, C., Kawakami, K., Leucht, C., Bally-Cuif, L., *et al.* (2010). Photoactivation of the CreER T2 recombinase for conditional site-specific recombination with high spatiotemporal resolution. *Zebrafish* **7**, 199–204.

Solomon, K. S., and Fritz, A. (2002). Concerted action of two dlx paralogs in sensory placode formation. *Development* **129**, 3127–3136.

Solomon, K. S., Kudoh, T., Dawid, I. B., and Fritz, A. (2003). Zebrafish foxi1 mediates otic placode formation and jaw development. *Development* **130**, 929–940.

Son, O., Kim, H., Ji, M., Yoo, K., Rhee, M., and Kim, C. (2003). Cloning and expression analysis of a Parkinson's disease gene, uch-L1, and its promoter in zebrafish. *Biochem. Biophys. Res. Commun.* **312**, 601–607.

Sonawane, M., Carpio, Y., Geisler, R., Schwarz, H., Maischein, H. M., and Nuesslein-Volhard, C. (2005). Zebrafish penner/lethal giant larvae 2 functions in hemidesmosome formation, maintenance of cellular morphology and growth regulation in the developing basal epidermis. *Development* **132**, 3255–3265.

Song, M. H., Brown, N. L., and Kuwada, J. Y. (2004). The cfy mutation disrupts cell divisions in a stage-dependent manner in zebrafish embryos. *Dev. Biol.* **276**, 194–206.

Springer, C. J., and Niculescu-Duvaz, I. (2000). Prodrug-activating systems in suicide gene therapy. *J. Clin. Invest.* **105**, 1161–1167.

Stigloher, C., Chapouton, P., Adolf, B., and Bally-Cuif, L. (2008). Identification of neural progenitor pools by E(Spl) factors in the embryonic and adult brain. *Brain Res. Bull.* **75**, 266–273.

Stigloher, C., Ninkovic, J., Laplante, M., Geling, A., Tannhauser, B., Topp, S., Kikuta, H., Becker, T. S., Houart, C., and Bally-Cuif, L. (2006). Segregation of telencephalic and eye-field identities inside the zebrafish forebrain territory is controlled by Rx3. *Development* **133**, 2925–2935.

Strahle, U., Lam, C. S., Ertzer, R., and Rastegar, S. (2004). Vertebrate floor-plate specification: Variations on common themes. *Trends Genet.* **20**, 155–162.

Sugiyama, M., Sakaue-Sawano, A., Iimura, T., Fukami, K., Kitaguchi, T., Kawakami, K., Okamoto, H., Higashijima, S. I., and Miyawaki, A. (2009). Illuminating cell cycle progression in the developing zebrafish embryo. *Proc. Natl. Acad. Sci. U.S.A.* **106**, 20812–20817.

Szabo, T. M., Brookings, T., Preuss, T., and Faber, D. S. (2008). Effects of temperature acclimation on a central neural circuit and its behavioral output. *J. Neurophysiol.* **100**, 2997–3008.

Takechi, M., Hamaoka, T., and Kawamura, S. (2003). Fluorescence visualization of ultraviolet-sensitive cone photoreceptor development in living zebrafish. *FEBS Lett.* **553**, 90–94.

Takke, C., Dornseifer, P., v Weizsacker, E., and Campos-Ortega, J. A. (1999). her4, a zebrafish homologue of the Drosophila neurogenic gene E(spl), is a target of NOTCH signalling. *Development* **126**, 1811–1821.

Tallafuss, A., and Bally-Cuif, L. (2003). Tracing of her5 progeny in zebrafish transgenics reveals the dynamics of midbrain-hindbrain neurogenesis and maintenance. *Development* **130**, 4307–4323.

Tallafuss, A., Trepman, A., and Eisen, J. S. (2009). DeltaA mRNA and protein distribution in the zebrafish nervous system. *Dev. Dyn.* **238**, 3226–3236.

Tarnowka, M. A., Baglioni, C., and Basilico, C. (1978). Synthesis of H1 histones by BHK cells in G1. *Cell* **15**, 163–171.

Tawk, M., Araya, C., Lyons, D. A., Reugels, A. M., Girdler, G. C., Bayley, P. R., Hyde, D. R., Tada, M., and Clarke, J. D. (2007). A mirror-symmetric cell division that orchestrates neuroepithelial morphogenesis. *Nature* **446**, 797–800.

Tawk, M., Bianco, I. H., and Clarke, J. D. (2009). Focal electroporation in zebrafish embryos and larvae. *Methods Mol. Biol.* **546**, 145–151.

Teraoka, H., Russell, C., Regan, J., Chandrasekhar, A., Concha, M., Yokoyama, R., Higashi, K., Take-Uchi, M., Dong, W., Hiraga, T., *et al.* (2004). Hedgehog and Fgf signaling pathways regulate the development of tphR-expressing serotonergic raphe neurons in zebrafish embryos. *J. Neurobiol.* **60**, 275–288.

Thisse, B., Pflumio, S., Fürthauer, M., Loppin, B., Heyer, V., Degrave, A., Woehl, R., Lux, A., Steffan, T., Charbonnier, X. Q., and Thisse, C.. (2001) Expression of the zebrafish genome during embryogenesis. ZFIN Direct Data Submission (http://zfin.org).

Thisse, C., Thisse, B., and Postlethwait, J. H. (1995). Expression of snail2, a second member of the zebrafish snail family, in cephalic mesendoderm and presumptive neural crest of wild-type and spadetail mutant embryos. *Dev. Biol.* **172**, 86–99.

Thummel, R., Burket, C. T., Brewer, J. L., Sarras, M. P. Jr., Li, L., Perry, M., McDermott, J. P., Sauer, B., Hyde, D. R., and Godwin, A. R. (2005). Cre-mediated site-specific recombination in zebrafish embryos. *Dev. Dyn.* **233**, 1366–1377.

Thummel, R., Enright, J. M., Kassen, S. C., Montgomery, J. E., Bailey, T. J., and Hyde, D. R. (2010). Pax6a and Pax6b are required at different points in neuronal progenitor cell proliferation during zebrafish photoreceptor regeneration. *Exp. Eye Res.* **90**, 572–582.

Thummel, R., Kassen, S. C., Enright, J. M., Nelson, C. M., Montgomery, J. E., and Hyde, D. R. (2008a). Characterization of Muller glia and neuronal progenitors during adult zebrafish retinal regeneration. *Exp. Eye Res.* **87**, 433–444.

Thummel, R., Kassen, S. C., Enright, J. M., Nelson, C. M., Montgomery, J. E., and Hyde, D. R. (2008b). Characterization of Muller glia and neuronal progenitors during adult zebrafish retinal regeneration. *Exp. Eye Res.* **87**, 433–444. Epub 2008 Aug 5.

Thummel, R., Kassen, S. C., Montgomery, J. E., Enright, J. M., and Hyde, D. R. (2008c). Inhibition of Muller glial cell division blocks regeneration of the light-damaged zebrafish retina. *Dev. Neurobiol.* **68**, 392–408.

Tong, S. K., Mouriec, K., Kuo, M. W., Pellegrini, E., Gueguen, M. M., Brion, F., Kah, O., and Chung, B. C. (2009). A cyp19a1b-gfp (aromatase B) transgenic zebrafish line that expresses GFP in radial glial cells. *Genesis* **47**, 67–73.

Trewarrow, B., Marks, D., and Kimmel, C. B. (1990). Organization of hindbrain segments in the zebrafish embryos. *Neuron* **4**, 669–679.

Tsujimura, T., Chinen, A., and Kawamura, S. (2007). Identification of a locus control region for quadruplicated green-sensitive opsin genes in zebrafish. *Proc. Natl. Acad. Sci. U.S.A.* **104**, 12813–12818.

Vanderlaan, G., Tyurina, O. V., Karlstrom, R. O., and Chandrasekhar, A. (2005). Gli function is essential for motor neuron induction in zebrafish. *Dev. Biol.* **282**, 550–570.

Vitorino, M., Jusuf, P. R., Maurus, D., Kimura, Y., Higashijima, S., and Harris, W. A. (2009). Vsx2 in the zebrafish retina: Restricted lineages through derepression. *Neural Dev.* **4**, 14.

von Trotha, J. W., Campos-Ortega, J. A., and Reugels, A. M. (2006). Apical localization of ASIP/PAR-3: EGFP in zebrafish neuroepithelial cells involves the oligomerization domain CR1, the PDZ domains, and the C-terminal portion of the protein. *Dev. Dyn.* **235**, 967–977.

Vriz, S., Joly, C., Boulekbache, H., and Condamine, H. (1996). Zygotic expression of the zebrafish Sox-19, an HMG box-containing gene, suggests an involvement in central nervous system development. *Brain Res. Mol. Brain Res.* **40**, 221–228.

Wan, H., Korzh, S., Li, Z., Mudumana, S. P., Korzh, V., Jiang, Y. J., Lin, S., and Gong, Z. (2006). Analyses of pancreas development by generation of gfp transgenic zebrafish using an exocrine pancreas-specific elastaseA gene promoter. *Exp. Cell Res.* **312**, 1526–1539.

Wang, D., Jao, L. E., Zheng, N., Dolan, K., Ivey, J., Zonies, S., Wu, X., Wu, K., Yang, H., Meng, Q., *et al.* (2007). Efficient genome-wide mutagenesis of zebrafish genes by retroviral insertions. *Proc. Natl. Acad. Sci. U.S.A.* **104**, 12428–12433.

Wang, X., Emelyanov, A., Korzh, V., and Gong, Z. (2003). Zebrafish atonal homologue zath3 is expressed during neurogenesis in embryonic development. *Dev. Dyn.* **227**, 587–592.

Wang, X., Yang, N., Uno, E., Roeder, R. G., and Guo, S. (2006). A subunit of the mediator complex regulates vertebrate neuronal development. *Proc. Natl. Acad. Sci. U.S.A.* **103**, 17284–17289.

Warren, J. T. Jr., Chandrasekhar, A., Kanki, J. P., Rangarajan, R., Furley, A. J., and Kuwada, J. Y. (1999). Molecular cloning and developmental expression of a zebrafish axonal glycoprotein similar to TAG-1. *Mech. Dev.* **80**, 197–201.

Wehman, A. M., Staub, W., and Baier, H. (2007). The anaphase-promoting complex is required in both dividing and quiescent cells during zebrafish development. *Dev. Biol.* **303**, 144–156.

Wei, X., Luo, Y., and Hyde, D. R. (2006). Molecular cloning of three zebrafish lin7 genes and their expression patterns in the retina. *Exp. Eye Res.* **82**, 122–131.

Wei, X., and Malicki, J. (2002). nagie oko, encoding a MAGUK-family protein, is essential for cellular patterning of the retina. *Nat. Genet.* **31**, 150–157.

Wei, Y., and Allis, C. (1998). Pictures in cell biology. *Trends Cell Biol.* **8**, 266.

Weiland, U., Ott, H., Bastmeyer, M., Schaden, H., Giordano, S., and Stuermer, C. A. (1997). Expression of an l1-related cell adhesion molecule on developing cns fiber tracts in zebrafish and its functional contribution to axon fasciculation. *Mol. Cell. Neurosci.* **9**, 77–89.

Wen, L., Wei, W., Gu, W., Huang, P., Ren, X., Zhang, Z., Zhu, Z., Lin, S., and Zhang, B. (2008). Visualization of monoaminergic neurons and neurotoxicity of MPTP in live transgenic zebrafish. *Dev. Biol.* **314**, 84–92.

Westin, J., and Lardelli, M. (1997). Three novel Notch genes in zebrafish: Implications for vertebrate Notch gene evolution and function. *Dev. Genes Evol.* **207**, 51–63.

White, R. M., Sessa, A., Burke, C., Bowman, T., LeBlanc, J., Ceol, C., Bourque, C., Dovey, M., Goessling, W., Burns, C. E., *et al.* (2008). Transparent adult zebrafish as a tool for *in vivo* transplantation analysis. *Cell Stem Cell* **2**, 183–189.

Whitlock, K. E., and Westerfield, M. (2000). The olfactory placodes of the zebrafish form by convergence of cellular fields at the edge of the neural plate. *Development* **127**, 3645–3653.

Wienholds, E., Schulte-Merker, S., Walderich, B., Plasterk, R. H. (2002). Target-selected inactivation of the zebrafish rag1 gene. *Science* **297**, 99–102.

Willer, G. B., Lee, V. M., Gregg, R. G., and Link, B. A. (2005). Analysis of the Zebrafish perplexed mutation reveals tissue-specific roles for de novo pyrimidine synthesis during development. *Genetics* **170**, 1827–1837.

Williams, J. A., Barrios, A., Gatchalian, C., Rubin, L., Wilson, S. W., and Holder, N. (2000). Programmed cell death in zebrafish rohon beard neurons is influenced by TrkC1/NT-3 signaling. *Dev. Biol.* **226**, 220–230.

Wilson, S. W., Ross, L. S., Parrett, T., and Easter, S. S. Jr. (1990). The development of a simple scaffold of axon tracts in the brain of the embryonic zebrafish, Brachydanio rerio. *Development* **108**, 121–145.

Woo, K., and Fraser, S. E. (1995). Order and coherence in the fate map of the zebrafish nervous system. *Development* **121**, 2595–2609.

Wullimann, M., and Knipp, S. (2000). Proliferation pattern changes in the zebrafish brain from embryonic through early postembryonic stages. *Anat. Embryol.* **202**, 385–400.

Wullimann, M. F., Rupp, B., and Reichert, H. (1996). Neuroanatomy of the zebrafish brain. *Birkhäuser verlag.*

Wurst, W., and Bally-Cuif, L. (2001). Neural plate patterning: Upstream and downstream of the isthmic organizer. *Nat. Rev. Neurosci.* **2**, 99–108.

Xiao, T., Roeser, T., Staub, W., and Baier, H. (2005). A GFP-based genetic screen reveals mutations that disrupt the architecture of the zebrafish retinotectal projection. *Development* **132**, 2955–2967.

Yamaguchi, M., Imai, F., Tonou-Fujimori, N., and Masai, I. (2010). Mutations in N-cadherin and a Stardust homolog, Nagie oko, affect cell cycle exit in zebrafish retina. *Mech. Dev.* **127**, 247–264.

Yamaguchi, M., Tonou-Fujimori, N., Komori, A., Maeda, R., Nojima, Y., Li, H., Okamoto, H., and Masai, I. (2005). Histone deacetylase 1 regulates retinal neurogenesis in zebrafish by suppressing Wnt and Notch signaling pathways. *Development* **132**, 3027–3043.

Yang, C. T., Sengelmann, R. D., and Johnson, S. L. (2004). Larval melanocyte regeneration following laser ablation in zebrafish. *J. Invest. Dermatol.* **123**, 924–929.

Yang, L., Rastegar, S., and Strahle, U. (2010). Regulatory interactions specifying Kolmer-Agduhr interneurons. *Development* **137**, 2713–2722.

Yang, X., Zou, J., Hyde, D. R., Davidson, L. A., and Wei, X. (2009). Stepwise maturation of apicobasal polarity of the neuroepithelium is essential for vertebrate neurulation. *J. Neurosci.* **29**, 11426–11440.

Yazulla, S., and Studholme, K. (2001). Neurochemical anatomy of the zebrafish retina as determined by immunocytochemistry. *J. Neurocytol.* **30**, 551–592.

Yeo, S. Y., and Chitnis, A. B. (2007). Jagged-mediated Notch signaling maintains proliferating neural progenitors and regulates cell diversity in the ventral spinal cord. *Proc. Natl. Acad. Sci. U.S.A.* **104**, 5913–5918.

Yeo, S. Y., Kim, M., Kim, H. S., Huh, T. L., and Chitnis, A. B. (2007). Fluorescent protein expression driven by her4 regulatory elements reveals the spatiotemporal pattern of Notch signaling in the nervous system of zebrafish embryos. *Dev. Biol.* **301**, 555–567.

Yoshida, M., and Macklin, W. B. (2005). Oligodendrocyte development and myelination in GFP-transgenic zebrafish. *J. Neurosci. Res.* **81**, 1–8.

Yoshikawa, S., Kawakami, K., and Zhao, X. C. (2008). G2R Cre reporter transgenic zebrafish. *Dev. Dyn.* **237**, 2460–2465.

Zannino, D. A., and Appel, B. (2009). Olig2+ precursors produce abducens motor neurons and oligodendrocytes in the zebrafish hindbrain. *J. Neurosci.* **29**, 2322–2333.

Zecchin, E., Conigliaro, A., Tiso, N., Argenton, F., and Bortolussi, M. (2005). Expression analysis of jagged genes in zebrafish embryos. *Dev. Dyn.* **233**, 638–645.

Zerucha, T., Stuhmer, T., Hatch, G., Park, B. K., Long, Q., Yu, G., Gambarotta, A., Schultz, J. R., Rubenstein, J. L., and Ekker, M. (2000). A highly conserved enhancer in the Dlx5/Dlx6 intergenic region is the site of cross-regulatory interactions between Dlx genes in the embryonic forebrain. *J. Neurosci.* **20**, 709–721.

Zhao, X. F., Ellingsen, S., and Fjose, A. (2009). Labeling and targeted ablation of specific bipolar cell types in the zebrafish retina. *BMC Neurosci.* **10**, 107.

Zhu, P., Narita, Y., Bundschuh, S. T., Fajardo, O., Scharer, Y. P., Chattopadhyaya, B., Bouldoires, E. A., Stepien, A. E., Deisseroth, K., Arber, S., *et al.* (2009). Optogenetic Dissection of Neuronal Circuits in Zebrafish using Viral Gene Transfer and the Tet System. *Front Neural Circuits* **3**, 21.

## CHAPTER 5

# Studying Peripheral Sympathetic Nervous System Development and Neuroblastoma in Zebrafish

**Rodney A. Stewart**[*], **Jeong-Soo Lee**[†], **Martina Lachnit**[*], **A. Thomas Look**[†], **John P. Kanki**[†], ***and*** **Paul D. Henion**[‡]

[*]Department of Oncological Sciences, Huntsman Cancer Institute, University of Utah,
Salt Lake City, Utah

[†]Department of Pediatric Oncology, Dana-Farber Cancer Institute, Harvard Medical School,
Boston, Massachusetts

[‡]Center for Molecular Neurobiology and Department of Neuroscience, Ohio State University,
Columbus, Ohio

---

Abstract
I. Introduction
II. The Peripheral Autonomic Nervous System
  A. Overview
  B. Molecular Pathways Underlying PSNS Development
III. The Zebrafish as a Model System for Studying PSNS Development
  A. Overview
  B. Development of the PSNS in Zebrafish
  C. Mutations Affecting PSNS Development
IV. Zebrafish as a Novel Model for Studying Neuroblastoma
  A. Overview of Neuroblastoma
  B. Using Zebrafish to Study Neuroblastoma
V. Conclusion and Future Directions
VI. Acknowledgments
References

## Abstract

The combined experimental attributes of the zebrafish model system, which accommodates cellular, molecular, and genetic approaches, make it particularly

Copyright © 2010 Elsevier Inc. All rights reserved.

978-0-12-384892-5
DOI: 10.1016/B978-0-12-384892-5.00005-0

well-suited for determining the mechanisms underlying normal vertebrate development as well as disease states, such as cancer. In this chapter, we describe the advantages of the zebrafish system for identifying genes and their functions that participate in the regulation of the development of the peripheral sympathetic nervous system (PSNS). The zebrafish model is a powerful system for identifying new genes and pathways that regulate PSNS development, which can then be used to genetically dissect PSNS developmental processes, such as tissue size and cell numbers, which in the past haves proved difficult to study by mutational analysis in vivo. We provide a brief review of our current understanding of genetic pathways important in PSNS development, the rationale for developing a zebrafish model, and the current knowledge of zebrafish PSNS development. Finally, we postulate that knowledge of the genes responsible for normal PSNS development in the zebrafish will help in the identification of molecular pathways that are dysfunctional in neuroblastoma, a highly malignant cancer of the PSNS.

## I. Introduction

The cellular, molecular, and genetic attributes of the zebrafish system make it particularly well suited for studying mechanisms underlying normal vertebrate developmental processes and disease states, such as cancer. The ability to analyze developing tissues in the optically clear embryo, combined with the unbiased nature of forward genetic screens, allows the identification of genes that function during vertebrate organogenesis. These genes may also contribute to diseases of a specific tissue/organ, providing new drug targets for development of therapies to treat the analogous human disease.

In this chapter, we focus on the advantages of the zebrafish system for analyzing the developing peripheral sympathetic nervous system (PSNS). We provide a brief overview of the genetic pathways involved in the PSNS development, our current understanding of zebrafish PSNS development and discuss the rationale for developing a zebrafish model. We also include examples that illustrate the potential of mutant analysis in zebrafish PSNS research. Finally, we explore the potential of the zebrafish system for discovering genes that are disrupted in neuroblastoma (NB), a highly malignant cancer of the PSNS.

## II. The Peripheral Autonomic Nervous System

### A. Overview

The internal organs, smooth muscles, skin, and exocrine glands of the vertebrate body are innervated by the peripheral autonomic nervous system (ANS), which comprises the PSNS and the parasympathetic (PAS) and enteric nervous systems (ENS). The three components of the ANS differ structurally and functionally in their characteristic location of the cell bodies, the targets they innervate, the neurotransmitters they utilize, and the molecular pathways controlling their development (Ernsberger and Rohrer, 2009; Young *et al.*, 2010). These structural and functional differences allow the sympathetic and parasympathetic systems to function largely in complementary opposition to each other in order to maintain organ homeostasis by adjusting vascular tone, heart rate, and endocrine secretion to specific environmental challenges, which can in turn generate the fight-or-flight response.

The ANS in general consists of central preganglionic and peripheral postganglionic neurons that regulate the function of a target organ. In the sympathetic nervous system, the preganglionic neurons are short, mainly cholinergic and their cell bodies are generally found in the thoracic and lumbar areas of the spinal cord. Their axons exit ventrally and innervate long adrenergic postganglia lying near the spinal cord that will innervate the target organs. A preganglionic PSNS neuron can innervate up to 20 postganglionic neurons, resulting in a massive signal amplification and eventual ubiquitous activation of all organ systems. Sympathetic neurons are predominantly adrenergic, producing the neurotransmitter noradrenalin along with one or more other neuropeptides, including adenosine triphosphate. For example, sympathetic neurons that stimulate smooth muscle cells (e.g., cardiac muscle cells) depend on a postsynaptic receptor in the target cell, activation of which can be mimicked by administering appropriate receptor ligand analogous (β-blockers), causing the heart to beat faster and blood vessels to constrict. In contrast, the preganglionic neurons of the PAS are long and their cell bodies lie in the cranial (brain stem) and sacral regions of the spinal cord. They synapse with maximally five, but normally only one short postganglionic neuron, which happens to be located within a specific target organ or its immediate vicinity. Signal transmission therefore results in localized low-dose organ innervations. Both pre- and postganglionic PAS neurons are cholinergic, releasing the neurotransmitter acetylcholine along with other neuromodulators (Thexton, 2001).

Chromaffin cells located in the adrenal medulla represent a unique subset of the PSNS that develop into endocrine cells (instead of postganglion neurons) that release hormones directly into the blood stream, instead of sending out processes. The adrenal medulla may therefore be considered as a modified sympathetic ganglion. Chromaffin cells are the bodies' main source of circulating catecholamines (adrenaline, noradrenaline) and endorphins, which are stored in intracellular granules and released in response to stress. As such they play an important role in the generation of the fight-or-flight response. Chromaffin cells can also be found in fewer numbers in structures such as the carotid aorta, vagus nerve, bladder, and prostate. While it is generally accepted that chromaffin cells and sympathetic neurons are derived from a common precursor population (the sympathoadrenal (SA) cell), there is evidence that these cell populations can also develop independently from the neural crest (NC) in the absence of a common progenitor (Huber, 2006). Importantly, chromaffin cells can develop into malignant tumors, called pheochromocytomas, which produce excessive amounts of catecholamines, usually adrenaline and noradrenaline, which cause severely high blood pressure. Pheochromocytomas are tumors of the multiple endocrine neoplasia syndromes type IIA and type IIB (also known as MEN IIA/B), with up to 25% being hereditary. Mutations in *VHL, RET, NF1, SDHB*, and *SDHD* are associated with familial pheochromocytomas, and recent studies suggest that loss of developmentally regulated apoptosis (resistance to neurotrophic withdrawal) is the mechanism driving tumor formation in these cases (Nakamura and Kaelin, 2006; Schlisio *et al*., 2008).

The function of the ENS is relatively independent of the CNS and other components of the ANS. In most vertebrates, the enteric neurons form two layers of ganglionic plexuses located along the entire length of the gastrointestinal tract consisting of a microscopic meshwork of ganglia connected to each other by short nerve trunks. The inner myenteric plexus (termed Auerbach plexus), situated between the longitudinal and the circular muscle layers, is mainly responsible for muscle contraction. Neurons in the Auerbach plexus regulate peristaltic waves, which move digestive products. The submucosal plexus (termed Meissners plexus) controls motility, secretion, and microcirculation processes as well as blood flow in the gut. The functions of the ENS are complex, and 17 different neuronal types have been identified, which can be classified into sensory neurons, interneurons, and motor neurons. Each type produces a variety of different neurotransmitters including nitric oxide, ATP, and 5-hydroxytryptamine. Enteric ganglia integrate sensory and reflex signals from the parasympathetic and sympathetic neurons, which innervate the gastrointestinal tract to coordinate peristalsis (Hansen, 2003).

## B. Molecular Pathways Underlying PSNS Development

The early development of the PSNS can be divided into four overlapping stages, based on both morphologic and molecular criteria: (i) formation and fate specification of NC cells that will develop into SA progenitors, (ii) bilateral migration of SA cells and their coalescence in regions adjacent to the dorsal aorta, (iii) neuronal and noradrenergic differentiation of SA progenitors, and (iv) maintenance of PSNS neurons in fully developed ganglia and the establishment of their efferent synaptic connections.

Considerable progress has been made elucidating the cellular and molecular mechanisms underlying PSNS development, which represents one of the best described genetic pathways establishing vertebrate neuronal and neurotransmitter identity (Anderson, 1993; Apostolova and Dechant, 2009; Ernsberger and Rohrer, 2009; Francis and Landis, 1999; Goridis and Rohrer, 2002; Young *et al*., 2010). Briefly, NC progenitors form at the border between the neural and non-neural ectoderm through a process regulated by bone morphogenetic proteins (BMPs), fibroblast growth factors (FGFs), Retinoic acid (RA), and Wnt signaling (Knecht and Bronner-Fraser, 2002). These NC progenitor cells express genes such as *Snai1l/2, Tfap2$\alpha$*, and *Foxd3* that appear to play roles in their induction and/or early specification (Sauka-Spengler and Bronner-Fraser, 2008). Subsequent to the morphogenetic movements that result in neural tube closure, NC progenitors are localized to the most dorsal aspect of the neural tube. The premigratory NC then undergoes an epithelial–mesenchymal transition and migrates away from the neural tube (Acloque *et al*., 2009). NC cells first migrate ventromedially and later others follow a dorsolateral pathway (Fig. 1A; Goridis and Rohrer, 2002; LeDouarin and Kalcheim, 1999). Ventral-migrating NC cells aggregate in the vicinity of the dorsal aorta, where they form primary sympathetic ganglia, and then migrate to the secondary sympathetic ganglia and adrenal gland, where they undergo neuronal and catecholaminergic differentiation (Anderson and Axel, 1986; Anderson *et al*., 1991; Huber, 2006).

During the premigratory stage, NC cells may become fate-restricted to specific lineages. Indeed, lineage-tracing studies in mice show that the expression of

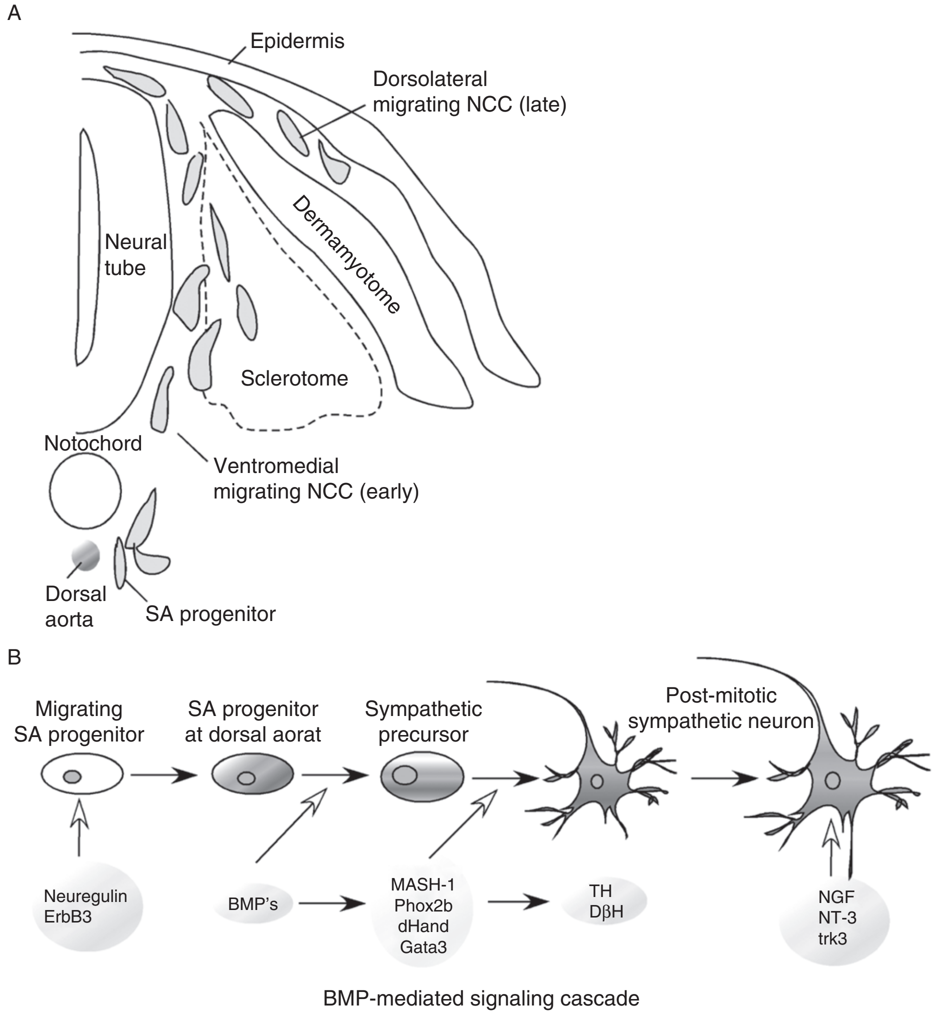
A
Epidermis
Dorsolateral
migrating NCC (late)
Dermamyotome
Neural
tube
Sclerotome
Notochord
Ventromedial
migrating NCC (early)
Dorsal
aorta
SA progenitor
B
Migrating
SA progenitor
SA progenitor
at dorsal aorat
Sympathetic
precursor
Post-mitotic
sympathetic neuron
Neuregulin
ErbB3
BMP's
MASH-1
Phox2b
dHand
Gata3
TH
DβH
NGF
NT-3
trk3
BMP-mediated signaling cascade

**Fig. 1** Neural crest-derived SA progenitors migrate along a ventromedial pathway to bilateral regions adjacent to the dorsal aorta. (A) Schematic diagram of a transverse section through the trunk of a vertebrate embryo (embryonic day 10.5 in the mouse, 2.5 in the chick, and approximately 28 hpf in the zebrafish embryo). In avian and rodent embryos, presumptive SA progenitor cells derived from the neural crest migrate ventromedially within the sclerotome region of the somites and ultimately cease migration in the region of the dorsal aorta. In zebrafish, neural crest-derived SA precursors migrate ventromedially between the neural tube and the somites to the dorsal aorta region. (B) Molecular pathways governing sympathetic neuron development. During migration, signaling via the neuregulin-1 growth factor is required for the development of at least some SA progenitors. Once the SA progenitor cells arrive at the dorsal aorta, BMP signaling activates the transcriptional regulators MASH-1 and Phox2b that ultimately lead to the expression of the transcription factors Phox2a, GATA-3, and dHand. Together, these factors are responsible for differentiation of SA progenitors into noradrenergic neurons. Fully differentiated neurons express biosynthetic enzymes responsible for the synthesis of noradrenalin, such as tyrosine hydroxylase and dopamine-β-hydroxylase. Survival of the differentiated sympathetic neurons is governed by a number of neurotrophic factors, such as NGF and NT-3.

Neurogenin-2 in pre- and early migrating NC cells promotes the differentiation of sensory neurons at the expense of sympathetic neurons (Zirlinger *et al.*, 2002). These results are consistent with single cell labeled studies in zebrafish, which show that the SA lineage is specified at early migratory stages (Raible and Eisen, 1994). Unfortunately, the molecular mechanisms governing these decisions (including what determines *Ngn2* expression in a sub-population of NC) are not known. Instead, most of our knowledge of PSNS development comes from studies during or after NC migration.

During ventrolateral migration, precursors of the SA lineage are exposed to signaling factors from the somites, ventral neural tube, and notochord, such as sonic hedgehog (Shh) and Neuregulin-1, an EGF-like growth factor (Crone and Lee, 2002; Krauss *et al.*, 1993; Patten and Placzek, 2000; Williams *et al.*, 2000b). Neuregulin-1 expression is associated with the origin, migration, and target site of SA progenitors. Mice and zebrafish lacking components of the Neuregulin-1 pathway, such as the ErbB3 receptor, exhibit severe hypoplasia of the primary sympathetic ganglion chain while the migration of cranial NC-derived enteric neurons appears normal (Britsch *et al.*, 1998). Migrating trunk NC cells of *ErbB3* mutants cannot recognize their target location and instead accumulate dorsal to the sites of normal sympathetic ganglion formation (Britsch *et al.*, 1998; Crone and Lee, 2002; Murphy *et al.*, 2002). A number of other signaling molecules also function to restrict the migration path of SA precursors toward the dorsal aorta. For example, trunk NC cell migration is restricted to the anterior somite by EphrinB ligands, which repel early migrating NC cells from the dorsolateral pathway and redirects them toward the ventrolateral migration path (Santiago and Erickson, 2002; Schwarz *et al.*, 2009). Semaphorin-3A and 3F, Neuropilin-1 and -2, and F-Spondin are also involved in restricting migration to the anterior somite (Debby-Brafman *et al.*, 1999; Gammill *et al.*, 2006; Kawasaki *et al.*, 2002). Once the migrating NC cells reach the dorsal aorta, N-Cadherin, Eph/ephrin, CXCL12, and Artemin signaling are required for the subsequent formation and segmental organization of sympathetic ganglia (Honma *et al.*, 2002; Kasemeier-Kulesa *et al.*, 2005, 2006).

As the SA precursors aggregate in the vicinity of the dorsal aorta, a molecular signaling cascade is initiated in response to BMPs secreted by these cells (Fig. 1B). Dose-dependent BMP signaling appears to be essential and sufficient to initiate the development of both noradrenergic sympathetic neurons (*Phox2b/Th*; high BMP concentration) and cholinergic parasympathetic neurons (*Phox2b /Chat*; low BMP concentration) of the autonomic lineage (Huber and Ernsberger, 2006; Morikawa *et al.*, 2009; Muller and Rohrer, 2002). Response to the BMP gradient occurs through the ALK3 receptor (BMP receptor IA) in mice, as conditional deletion of *Alk3* in NC cells caused death of these cells immediately after reaching the dorsal aorta (Morikawa *et al.*, 2009). BMP signaling induces the expression of the proneural gene *Mash-1*, a mammalian *achaete-scute* homolog, and the homeodomain transcription factor PHOX2B in sympathetic neuroblasts (Ernsberger *et al.*, 1995; Groves *et al.*, 1995; Guillemot *et al.*, 1993; Hirsch *et al.*, 1998). PHOX2B is essential for the maintained expression of *Mash-1* and proliferation of sympathoadrenergic precursor cells, as SA precursors fail to proliferate and degenerate before differentiation is induced in *Phox2b* mouse mutants (Huber, 2006; Pattyn *et al.*, 1999, 2000). MASH-1 appears to support sympathoblast differentiation, and *Mash-1* deficient mice show delay of sympathoadrenergic differentiation that eventually leads to their loss (Pattyn *et al.*, 2006). It is still not clear how BMP signaling results in *Mash-1* or *Phox2b* expression, although it is likely that multiple BMP pathways, including *Smad4*-dependent and-independent pathways are required for proliferation, survival, and differentiation of PSNS precursors (Morikawa *et al.*, 2009).

Several other critical transcription factors are activated downstream or in parallel to MASH-1 and PHOX2B, including the homeobox proteins PHOX2A, bHLH transcription factor HAND2, and the zinc-finger proteins GATA-2/3 (Howard *et al.*, 2000; Huber, 2006; Tsarovina *et al.*, 2004). PHOX2A and PHOX2B are not functionally equivalent, though both appear to bind and activate the noradrenergic marker genes, tyrosine hydroxylase (*Th*) and dopamine-β-hydroxylase (*Dβh*), that are essential enzymes in the production of noradrenaline (Coppola *et al.*, 2005). HAND2 (also known as dHAND) is essential for the differentiation of noradrenergic neurons and is expressed in the early noradrenergic sympathetic chain but not in the cholinergic parasympathetic system (Lucas *et al.*, 2006; Muller and Rohrer, 2002; Schmidt *et al.*, 2009). Expression of HAND2 in terminally differentiated sympathetic neurons maintains their neurotransmitter properties by promoting the expression of noradrenergic genes, while suppressing cholinergic genes (Apostolova and Dechant, 2009; Schmidt *et al.*, 2009). In contrast, HAND1 (also known as eHAND) appears to have no significant impact on *Dbh* expression (Doxakis *et al.*, 2008). GATA 2/3 expression is initiated after MASH-1, PHOX2A, PHOX2B, and HAND2 expression, but before the onset of the noradrenergic marker genes, and is maintained throughout development (Huber, 2006; Tsarovina *et al.*, 2004). However, GATA2/3 overexpression results in the formation of ectopically non-autonomic TH-negative neurons, which may reflect a dependence on additional cofactors for induction of sympathetic neurons (Tsarovina *et al.*, 2004). The transcriptional activity of GATA 2/3 appears to be directly regulated via protein–protein interactions with the transcription factor CREB, which also seems to interact with Phox2a and to influence noradrenergic differentiation (Benjanirut *et al.*, 2006; Hong *et al.*, 2006; Rudiger *et al.*, 2009). Together, these genes drive SA differentiation, which is further modulated by cAMP and MAPK signaling to activate *Dbh* and *Th* expressions (Ernsberger *et al.*, 2000; Kim *et al.*, 2001; Seo *et al.*, 2002).

As mentioned above, a later stage of PSNS development consists of modeling of the sympathetic ganglia. The neurotrophic factors, NGF and NT-3, have been shown to control sympathetic neuron survival and the maintenance of their synaptic connections (Birren *et al.*, 1993; DiCicco-Bloom *et al.*, 1993; Francis and Landis, 1999). In the embryo, NGF is secreted from sympathetic target tissues upon arrival of sympathetic neurons (Chun and Patterson, 1977; Heumann *et al.*, 1984; Korsching and Thoenen, 1983; Shelton and Reichardt, 1984). Analysis of NGF and its high affinity receptor, TrkA, in mouse mutants confirmed their requirement for the *in vivo* survival of sympathetic neurons (Fagan *et al.*, 1996; Smeyne *et al.*, 1994). In their absence, sympathetic neuron development proceeds normally, but is then followed by neuronal cell death. A similar phenotype is observed in NT-3 mutants, although neuronal death occurs at later embryonic stages (Ernfors *et al.*, 1994; Farinas *et al.*, 1994; Francis and Landis, 1999; Wyatt *et al.*, 1997). HAND1 and HAND2 support NGF-dependent neurotrophic survival by enhancing the expression of *TrkA* in sympathetic neurons (Doxakis *et al*., 2008; Ma *et al*., 2000; Schmidt *et al*., 2009). Interestingly, adrenalin transporter and TrkA co-localize in noradrenergic cells, which suggests that TrkA ligands (NGF or NT3) might indirectly support a positive selection of noradrenergic cells (Brodski *et al*., 2002). In summary, neurotrophic factors (such as NT-3 and NGF) appear to be largely responsible for establishing and maintaining mature ganglion cell numbers during embryonic or early postnatal development in chick and rodents.

Although many of the inductive signaling pathways affecting different stages of NC development have been identified, the regulatory mechanisms controlling these pathways remain poorly understood. While substantial evidence links BMP signaling with the induction of SA progenitor cell development, the genetic control of SA cell responsiveness to BMP signals and their specification remain unclear. While sympathetic precursors are competent to express MASH1 and PHOX2B in response to BMP signaling near the dorsal aorta, they do not respond to BMPs present in the overlying ectoderm during earlier premigratory stages. Furthermore, the molecular mechanisms regulating the interactions of transcription factors and downstream pathways, specifying neuronal and noradrenergic differentiation, are incompletely understood. Other signaling pathways, such as cAMP (Lo *et al*., 1999), may also contribute to this process. Finally, proliferation of sympathoblasts and differentiated sympathetic neurons occurs throughout embryogenesis (Birren *et al*., 1993; Marusich *et al*., 1994; Rohrer and Thoenen, 1987; Rothman *et al*., 1978). An inability to control cell proliferation in sympathetic ganglia is of particular medical interest, since it can lead to NB, the most common human cancer in infants less than 1 year of age. While the study of PSNS development in tetrapods will continue to contribute to our knowledge of PSNS development, a goal of this chapter is to demonstrate the power of the zebrafish, *Danio rerio*, exploiting its forward genetic potential and advantages as an embryologic system, for making significant contributions to PSNS research. We also propose that the study of zebrafish PSNS development will contribute to our understanding of both normal and abnormal PSNS development and may ultimately provide a genetic model for human NB.

## III. The Zebrafish as a Model System for Studying PSNS Development

### A. Overview

One of the most powerful attributes of the zebrafish system is its capacity for large-scale genetic screens due to its rapid embryonic development and high expansion rate. The unbiased nature of phenotype-based genetic screens enables new genes to be identified without prior knowledge of their function or expression in the tissue of interest. This approach is particularly attractive for study of the PSNS, as many signaling components involved in determining sympathetic fate are incompletely understood. Also, most of our current understanding of PSNS development has relied on functional assays on isolated sympathetic cells in culture or gene misexpression analyses (Francis and Landis, 1999; Goridis and Rohrer, 2002). While these studies can determine whether certain genes are sufficient to direct sympathetic development, they do not address whether those genes are normally required for PSNS development. Murine gene knock-out models have been used in loss-of-function studies to confirm the *in vivo* requirement for particular genes in PSNS development (Guillemot *et al*., 1993; Lim *et al*., 2000; Morin *et al*., 1997; Pattyn *et al*., 1999). For example, although both *Phox2a* and *Phox2b* can induce a sympathetic phenotype when misexpressed in chick, only the selective knock-out of *Phox2b* eliminates PSNS development *in vivo*, as the PSNS in *Phox2a*$^{-/-}$ mutant mice appears relatively normal (Morin *et al*., 1997; Pattyn *et al*., 1999).

These studies provide valuable insights into the regulatory pathways directing sympathetic neuron development and emphasize the advantages of using mutants to dissect genetic pathways *in vivo*. The capacity for experimental mutagenesis and manipulation of gene expression in the developing embryo is a major strength of the zebrafish system. Forward genetic zebrafish screens can be especially valuable for identifying genes affecting complex signaling pathways that rely upon interactions between the developing PSNS and the surrounding tissues, which may be impossible to address using *in vitro* assays. Critical roles for extrinsic factors are particularly evident in PSNS development and SA progenitors migrate past a number of tissues expressing different signaling molecules, such as the neural tube, notochord, and floor-plate. In addition, zebrafish mutant embryos often survive for longer periods of time during embryogenesis than knock-out mice lacking orthologous genes due to their *ex-utero* development. This allows the analysis of the PSNS to extend through later stages of sympathetic neuron differentiation and maintenance. Finally, the zebrafish system offers the most amenable vertebrate model for performing large-scale mutagenesis screens to identify novel genes affecting all aspects of PSNS development, as the time, space, and expense associated with mutagenesis techniques in mice can be prohibitive.

Establishing the zebrafish as a useful vertebrate model for identifying new genes important for PSNS development will require (i) an analysis of zebrafish sympathetic neuron development and its comparison with other vertebrates, (ii) an analysis of the genetic programs regulating zebrafish PSNS development and their conservation in other vertebrates, (iii) the generation of efficient mutagenesis protocols and screening assays for the isolation of PSNS mutants. These areas are addressed below.

## B. Development of the PSNS in Zebrafish

### 1. Neural Crest Development and Migration

A number of studies have now analyzed the anatomical and molecular mechanisms underlying the different stages of PSNS development in the zebrafish (An *et al*., 2002; Raible and Eisen, 1994). The findings show that the morphogenesis and differentiation of sympathetic neurons in zebrafish are qualitatively very similar to other vertebrates. Migration and cell fate specification of trunk sympathetic precursors in zebrafish were initially analyzed by labeling single NC cells with vital dyes and following their subsequent development (Raible and Eisen, 1994). In the trunk, NC migration begins around 16 h postfertilization hpf, at the level of somite 7 and sympathetic neurons are only derived from NC cells migrating along the ventromedial pathway. Hence, the ventromedial migration of SA precursor cells is conserved in zebrafish. These studies also demonstrated the existence of both multipotent and fate-restricted NC precursors that generate a limited number of derivatives, such as sympathetic neurons, before or during the initial stages of migration (Raible and Eisen, 1994). Although little is known about the molecular mechanisms underlying such fate decisions, the ability to analyze the fate-restriction of sympathetic neurons in zebrafish, using different NC mutants, affords a powerful method to dissect the genetic pathways underlying this process.

## 2. Gene Expression in Migrating SA Progenitors

Many of the genes capable of inducing the development of SA progenitors in birds and rodents have been identified in zebrafish (Table I). Furthermore, the expression of some of these genes in dorsal aorta cells and in NC-derived cells in its vicinity, where noradrenergic neurons form, is consistent with their role in fish PSNS development (Cheung *et al*., 2005; Elworthy *et al*., 2005; Lucas *et al*., 2006; Sakai *et al*., 2006; Tsarovina *et al*., 2004). A number of BMP homologues have been identified in zebrafish and some have been shown to be expressed by the dorsal aorta (Dick *et al*., 2000; Nguyen *et al*., 1998). Several zebrafish mutants exhibit midline defects affecting structures that may be responsible for BMP signaling. In *flh* mutant embryos, the notochord and dorsal aorta fail to develop and *bmp4* expression is absent (Talbot *et al*., 1995). The loss of the local source of BMP signaling corresponds with a failure of sympathetic neurons (Hu$^+$/TH$^+$) to form (P. Henion, unpublished data). Interestingly, NC-derived cells (*crestin*$^+$) continue to populate this region where sympathetic neurons would normally develop. These observations suggest that, like other vertebrates, dorsal aorta-derived BMPs are required for SA development in zebrafish. In

**Table I**
**Expression of Conserved PSNS Genes in Zebrafish**

| Genes | Expression during PSNSdevelopment | References |
|---|---|---|
| ErbB3 | N/A | Lo *et al*. (2003) |
| BMP4 | Dorsal aorta | Fig. 2A, Dick *et al*. (2000), Nguyen *et al*. (1998) |
| Crestin | Migrating SA, nascent SCG | Luo *et al*. (2001) |
| Zash1a (Ascl1) | SCG | Lucas *et al*. (2006), Stewart *et al*. (2006) |
| Phox2a | SCG | Guo *et al*. (1999a), Holzschuh *et al*. (2003) |
| Phox2b | Migrating SA, SCG | Elworthy *et al*. (2005), Lucas *et al*. (2006), Stewart *et al*. (2006) |
| HuC (Elavl3) | SCG, Trunk sympathetic ganglia | An *et al*. (2002) |
| Gata2 | SCG | Neave *et al*. (1995) |
| dHand | SCG | Fig. 2C and D, Yelon *et al*. (2000) |
| Th | SCG, Trunk sympathetic ganglia | An *et al*. (2002), Guo *et al*. (1999b), Holzschuh *et al*. (2001) |
| Dβh | SCG, Trunk sympathetic ganglia | An *et al*. (2002), Holzschuh *et al*. (2003) |
| Pnmt | SCG | R. Stewart (unpublished) |

contrast, floor-plate cells, which are lacking in the *cyclops* mutant, do not appear to be required for dorsal aorta development, BMP expression or SA development, and all of these functions appear to be normal in these mutant embryos (P. Henion, unpublished data). Interestingly, SA development appears normal in *no tail* mutants (Fig. 2A and B) even though dorsal aorta development is impaired (Fouquet *et al*., 1997) and BMP expression is reduced. It is possible that weak BMP persists in *ntl* due to the continued presence of notochord precursor cells that fail to differentiate properly in this mutant (Melby *et al*., 1997). However, whether the notochord is directly responsible for BMP expression and dorsal aorta development is unclear.

Most of the described transcription factors known to direct the development of the sympathetic precursors in other species are present in the zebrafish and exhibit appropriate gene expression patterns. The zebrafish *zash1a* gene, a homolog of *Mash-1*, is transiently expressed in cells near the dorsal aorta by 48 hpf (Allende and Weinberg, 1994). Preliminary gene knockdown experiments using antisense morpholinos to specifically target the *zash1a* gene resulted in the loss of *th*-expressing noradrenergic neurons in the developing PSNS (R. Stewart, unpublished data). The *phox2a, phox2b, gata-2/3*, and *hand2* genes have also been cloned in zebrafish, and they are all expressed in cells adjacent to the dorsal aorta by 2 days postfertilization (dpf) (Guo *et al*., 1999a; Holzschuh *et al*., 2003; Neave *et al*., 1995; Yelon *et al*., 2000). Initial reports of embryos deficient for *phox2b* suggest that, unlike other vertebrates, it is not required for normal PSNS development, but instead is required for development of the ENS (Elworthy *et al*., 2005). This may be due to the fact that Phox2b is only transiently expressed in nascent

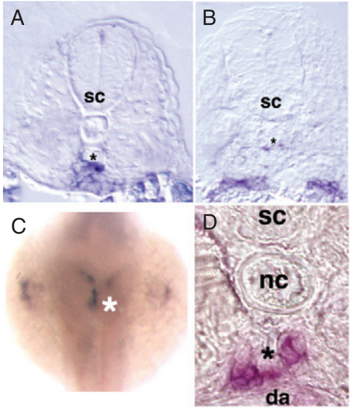

**Fig. 2** Expression of *bmp* by the dorsal aorta and dHand by sympathetic neurons. (A) Expression of *bmp4* in transverse sections at the mid-trunk level in wild-type (top) and *ntl* mutant embryos at 48 hpf. *bmp4* expression is evident in cells of the dorsal aorta (asterisk) of wild-type embryos. (B) In *ntl* mutants, the dorsal aorta does not form completely (asterisk) although expression of *bmp4* is present albeit to a reduced extent. (C) Expression of zebrafish dHand at 58 hpf in cervical sympathetic neurons (asterisk). (D) Co-expression of dHand (blue) and TH (red) in sympathetic neurons (asterisk) in a transverse section in the anterior trunk

sympathetic ganglia (Lucas *et al*., 2006) or it could be due to incomplete knockdown of *phox2b* that is commonly observed using antisense morpholinos technologies. Analysis of PSNS development in *phox2b* mutants will be needed to resolve this issue. Noradrenergic differentiation requires *hand2* in zebrafish, as the zebrafish *hand2* deletion mutant, *hands off*, fails to express the noradrenergic genes *th* and *dbh*, even though the pan-neuronal marker *HuC* (*elav13*) and other PSNS precursor markers are normally expressed (Lucas *et al*., 2006). Further analysis of *Zash1a, Phox2b, Phox2a, Gata-2/3*, and *Hand2* expression, together with the examination of Th and Dβh expression in SA precursors, will provide insight into the functions of these genes with respect to sympathetic neuron differentiation (see below). Importantly, analysis of compound mutants utilizing existing zebrafish mutants such as *soulless* (*phox2a*; Guo *et al*., 1999a and *hands off*; Lucas *et al*., 2006) together with other mutants described in this chapter will contribute to our understanding of the functional roles of these genes in sympathetic neuron development. The combination of transient gene knockdown techniques using morpholinos, and the identification of new zebrafish mutants affecting other regulators of sympathetic neuron development, should also contribute to novel insights relevant to PSNS development across vertebrate species.

## 3. Neuronal Differentiation and Coalescence into Sympathetic Ganglia

The timing of overt neuronal differentiation of sympathetic precursors and their transition to fully differentiated NA-producing neurons has been described in detail in zebrafish (An *et al*., 2002). The pan-neuronal antibody 16A11 recognizes members of the Hu family of RNA-binding proteins and labels sympathetic precursors located ventrolateral to the notochord and adjacent to the dorsal aorta (An *et al*., 2002). Sympathetic neurons were found to differentiate at different times in the zebrafish embryo, and two populations of sympathetic ganglion neurons were defined. The most rostral population develops at 2 dpf and comprises the superior cervical ganglion (SCG) complex that consists of two separate ganglia arranged in an hourglass shape. Several days later, more caudal trunk sympathetic neurons develop as irregular, bilateral rows of single neurons adjacent to the dorsal aorta, presumably analogous to the primary sympathetic chain in other vertebrates. These neurons differentiate in an anterior to posterior temporal progression, extending caudally as far as the level of the anus, and eventually form regular arrays of segmentally distributed sympathetic ganglia (An *et al*., 2002). The reason for the delay in the differentiation of the caudal sympathetic neurons is not known, since the formation of the dorsal aorta (Fouquet *et al*., 1997) and its expression of BMPs (Martinez-Barbera *et al*., 1997) occur well before the differentiation of sympathetic neurons is observed. Importantly, ventrally migrating NC-derived cells populate the region adjacent to the dorsal aorta between 24 and 36 hpf. Thus, the delay in caudal PSNS development may be due to a delay in their becoming competent to respond to BMP signaling. Since the expression of some zebrafish BMPs has not been examined in the dorsal aorta, it remains possible that different types of BMPs may be selectively expressed by dorsal aorta cells and/or that SA progenitors exhibit differential responsiveness to different BMPs.

## 4. Differentiation of Noradrenergic Neurons

One of the key events in PSNS differentiation is the acquisition of the NA-neurotransmitter phenotype indicated by the expression of noradrenalin and genes such as *tyrosine hydroxylase* (*th*) and *dopamine-β-hydroxylase* (*dbh*) that are required for the enzymatic conversion of the amino acid L-tyrosine to noradrenalin (Goridis and Rohrer, 2002; Huber, 2006). In zebrafish, *th* expression has been used as the principal marker for the presence and formation of fully differentiated sympathetic neurons although it is also expressed by other catecholaminergic neurons in the central nervous system (CNS) (Figs. 3A–D; An *et al*., 2002; Guo *et al*., 1999b; Holzschuh *et al*., 2001). Expression of Dβh protein and mRNA is also used as markers of PSNS differentiation because of its requirement for the conversion of dopamine to noradrenaline in sympathetic neurons of the PSNS and a subset of dopaminergic neurons in the CNS (An *et al*., 2002; Holzschuh *et al*., 2003). By 10 dpf, all of the sympathetic ganglia contain neurons expressing *th*, although some neurons within the nascent sympathetic ganglia do not express Th protein. However, by 28 dpf, all of the neurons uniformly express Th, suggesting the complete maturation of sympathetic ganglia by this time. Both Th protein and mRNA are detectable in the SCG complex beginning at 48 hpf. Consistent with the expression of Hu proteins, most sympathetic neurons located posterior to the SCG complex do not begin to express *th* mRNA until approximately 5 dpf, in a few of the more rostral trunk segments (Fig. 3D). It should be noted that a second tyrosine hydroxylase gene has been identified in zebrafish, called *th2* (Filippi *et al*., 2009; Schweitzer and Driever, 2009; Yamamoto *et al*., 2010). The expression of *th2* overlaps that of *th1* in the CNS; however, it is not known if *th2* also labels PSNS. The expression of *dbh* is generally observed slightly later than *th* in differentiating sympathetic neurons (An *et al*., 2002). However, *dbh* is expressed along with *th* as early as 2 dpf in the SCG complex (Holzschuh *et al*., 2003). Once noradrenergic identity has been established, the continued expression of *hand2* appears to be essential for the maintenance and proliferation of sympathetic neurons (Hendershot *et al*., 2008; Lucas *et al*., 2006; Morikawa *et al*., 2007).

Another element of PSNS function is the regulated release of adrenalin and noradrenalin by chromaffin cells of the adrenal gland, which form in and/or around the developing kidney (Liu, 2007; Unsicker *et al*., 2005). Chromaffin cells represent a specialized component of the PSNS, and most of these cells express an additional enzyme in the catecholaminergic pathway, called phenylethanolamine *N*-methyltransferase (PNMT), which converts noradrenaline into adrenaline (Kalcheim *et al*., 2002; Schober *et al*., 2000). As in other species, both noradrenergic and adrenergic chromaffin cells have been described in zebrafish (Hsu *et al*., 2003; Liu *et al*., 2003). However, in contrast to mammals, where chromaffin cells are located in the adrenal medulla separated from steroidogenic cells in the adrenal cortex, the chromaffin cells in zebrafish and other teleost fish are interspersed with adrenocortical cells in a specialized region of the kidney called the interrenal gland (Liu, 2007). Initial observations indicated that non-neuronal (16A11-negative), Th and Dβh-positive cells are present in the SCG complex at 2 dpf, which continue to migrate ventrally to the

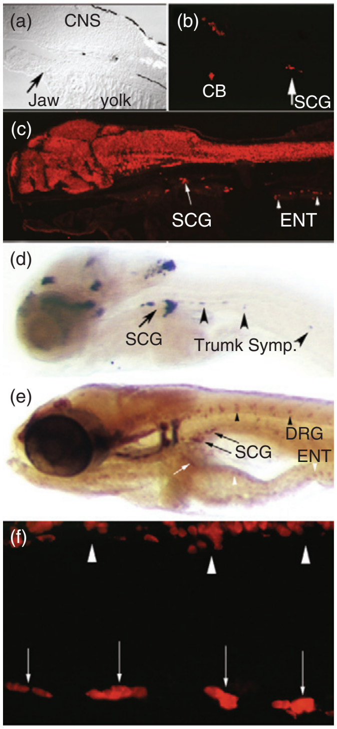

**Fig. 3** Development of the peripheral sympathetic nervous system in zebrafish embryos. (A–C) Parasagittal section of 3.5 dpf embryo. High-magnification DIC (A) and fluorescence (B) of the same field showing TH-IR (red) in the SCG (arrow), carotid body (CB), and a group of anterior cells in the midbrain (CNS). (C) Low-magnification view of 3.5 dpf embryo labeled with anti-Hu to reveal all neurons. A subset of cervical sympathetic neurons are indicated by the arrow and enteric neurons (ENT) by arrowheads. (D) Lateral view of whole-mount *TH* RNA *in situ* preparation at 5 dpf. *TH* RNA is strongly expressed in the SCG (arrow) at this stage and is beginning to be expressed in the trunk sympathetic chain (arrowheads). A description of *TH* RNA expression in the head is described in Guo *et al*., 1999b. (E) Whole-mount antibody preparation of a 7 dpf larvae labeled with anti-Hu to reveal neurons. Black arrows indicate SCG, black arrowheads indicate dorsal root ganglion (DRG) sensory neurons, and white arrow and white arrowheads indicate enteric neurons (ENT). (F) Parasagittal section in the mid-trunk region of a 17 dpf embryo labeled with anti-Hu. Ventral spinal cord neurons are evident at the top (arrowheads). Four segmental sympathetic ganglia (arrows) are located ventral to the notochord adjacent to the dorsal aorta.

interrenal gland (Fig. 4; An *et al*., 2002). Consistent with these studies, mRNA *in situ* hybridization assays using *pnmt* expression show that double positive $pnmt^{+}/th^{+}$ cells are present in the SCG at 3 dpf, suggesting that chromaffin cells can be specified before migration to the kidney (R. Stewart, unpublished). Once chromaffin cells reach the kidney, signaling from the pituitary gland and endothelial cells appears to be required for continued maintenance and development of a functional interrenal gland (Liu, 2007; To *et al*., 2007).

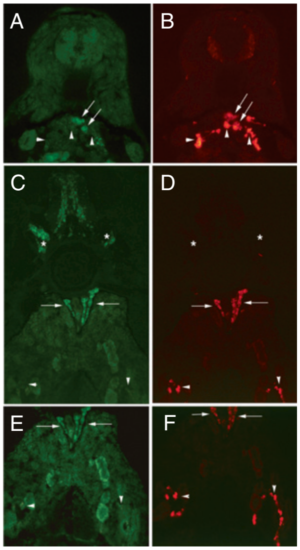

**Fig. 4** Sympathoadrenal derivatives in embryonic and juvenile zebrafish. (A, B) Transverse section of a 3.5 dpf embryo double labeled with anti-Hu (green) and DβH (red). Arrows indicate $Hu^+/D\beta H^+$ sympathetic neurons of the cervical ganglion. Arrowheads indicate $Hu^-/D\beta H^+$ presumptive chromaffin cells. (C, D) Transverse section through the mid-trunk region at 28 dpf double labeled with anti-Hu (green) and anti-TH (red). (E, F) Higher magnification of C and D, including a slightly more ventral region. Arrows indicate sympathetic neurons, arrowheads indicate chromaffin cells, and asterisks denote dorsal root ganglia. (See Plate no. 7 in the Color Plate Section.)

## 5. Modeling of Sympathetic Ganglia

In rodents and birds, neurotrophic factors, such as NGF and NT-3, control sympathetic neuron cell numbers through the regulation of their survival and continued maintenance of their synaptic connections (Francis and Landis, 1999; Schober and Unsicker, 2001). In zebrafish, the ability of these factors to control the survival of sympathetic neurons is unknown. However, NT-3 has been shown to act as a neurotrophic factor regulating cell death in Rohon-Beard sensory neurons (Williams *et al.*, 2000a). In teleost sympathetic ganglia, the proliferation of cells occurs during early development and may possibly continue throughout adult life (An *et al.*, 2002; Weis, 1968). Recent data suggest that Hand2 in combination with Hand1 appears to enhance the NGF response by upregulating *TrkA* expression (Doxakis *et al.*, 2008; Lucas *et al.*, 2006; Ma *et al.*, 2000; Schmidt *et al.*, 2009). Analysis of BrdU incorporation and phospho-histone H3 immunoreactivity indicate that cells proliferate and undergo cell division within the developing sympathetic ganglia (An *et al.*, 2002). Interestingly, some of these cells also expressed the pan-neuronal marker, 16A11, suggesting that pre-existing neuronal cells proliferated within the ganglia, a process that has also been observed in both chick and mouse PSNS (Birren *et al.*, 1993; Cohen, 1974; DiCicco-Bloom *et al.*, 1993; Marusich *et al.*, 1994; Rohrer and Thoenen, 1987; Rothman *et al.*, 1978). However, in chick and rodents sympathetic neurons become post-mitotic during embryonic development, while they may remain competent to divide throughout life in the zebrafish (Weis, 1968).

## C. Mutations Affecting PSNS Development

### 1. Introduction

PSNS development, from the induction of NC through the overt differentiation of sympathetic ganglia, can be readily observed within the first 5 days of zebrafish development (An *et al*., 2002). During this time, dynamic changes in both the numbers and the distribution of sympathetic cells within the SCG can be easily visualized by *th* mRNA whole-mount *in situ* hybridization. At 2 dpf, bilateral rows containing approximately 5–10 *th*-positive cells are ventrally located near the dorsal aorta. By 5 dpf, the number of *th*-positive cells have increased fivefold and coalesced into a V-shaped ganglia, including some appearing to migrate ventrally toward the kidney, which may represent putative adrenal chromaffin cells (An *et al*., 2002). Thus, the evaluation of SCG formation at 3- and 5 dpf represents an excellent assay for early PSNS development that can be used in combination with forward genetic screens to detect novel mutations affecting different stages of PSNS development. Assaying the SCG would also be able to confirm mutations found to affect very early NC development. Such mutagenesis screens have been performed and examples of the different mutant classes that have been isolated thus far are discussed below.

### 2. Mutations Affecting PSNS Development

Mutations affecting PSNS development can be divided into a number of classes. Mutants can be identified that either fail to (1) form NC precursors, (2) migrate to the dorsal aorta, (3) differentiate into SA progenitors, or (4) proliferate and survive once they differentiate. So far, most of the zebrafish PSNS mutants described disrupt the early phases of PSNS development, notably failure of NC precursors to be specified before cell migration commences. One example is *sympathetic mutant 1* (*sym1*), which was discovered in a diploid gynogenetic screen designed to identify mutations disrupting *th* expression in the SCG complex at 5 dpf (Fig. 5; Stewart *et al*., 2006). The *sym1* mutation causes a severe reduction or absence of *th*- and *pnmt*-expressing cells in the SCG complex of the PSNS, but *th* expression is not affected in other regions of the CNS. Subsequent cloning of the *sym1* mutation revealed that it was a deletion within the *foxd3* gene (and renamed *foxd3*$^{zdf10}$), which was previously shown to be essential for early NC development in other vertebrates (Fig. 5A and C; Stewart *et al*., 2006). Analysis of the *sym1* phenotype showed that early NC survival, migration, and specification is impaired in these embryos, and they exhibit a reduction in the expression of a number of early NC markers, including *snai1b, crestin*, and *sox10* (Luo *et al*., 2001). Thus, Foxd3 is required at multiple stages in early NC progenitors for the specification and migration of PSNS progenitors.

Another NC mutant that displays defects in PSNS development is the zebrafish *colorless* (*cls*) mutant, which disrupts the *sox10* gene required for development of most

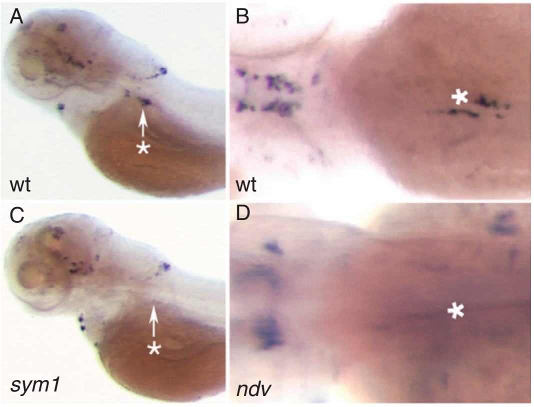

**Fig. 5** Isolation of PSNS mutants in zebrafish. Whole-mount *TH in situ* preparation showing expression of *TH* mRNA in wild-type (A, B), *sym1* (C), and *nosedive* (D) mutant embryos. (A, C) Lateral view of *TH* expression at 5 dpf. The *sym1* mutant phenotype (C) was identified in an *in situ* screen at 5 dpf for mutations that specifically lack *TH* expression in the SCG (C, asterisk), but leave others areas of TH expression in the CNS and carotid body unaffected. (B, D) Dorsal view of *TH* expression in the SCG region at 3 dpf in wild-type embryos (B, asterisk). Expression of *TH* is absent in the SCG in *nosedive* mutants (D, asterisk). Analysis of Hu immunoreactivity revealed that the lack of *TH* expression in the cervical region in *nosedive* mutant embryos is due to the absence of sympathetic neurons (data not shown).

non-ectomesenchymal NC lineages, including the PSNS (Dutton *et al.*, 2001; Kelsh and Eisen, 2000). The mutation was originally isolated in a screen for NC mutants affecting pigment cell development (Kelsh and Eisen, 2000). Analysis of the *cls* phenotype shows that Sox10 appears to be required for the early survival and migration of NC-derived cells, as well as for their specification into certain sub-lineages and glial formation at a later developmental stage (Arduini *et al.*, 2009; Dutton *et al.*, 2001; Kelsh and Eisen, 2000; McKeown *et al.*, 2005). *cls* homozygotes have a complete absence of the ENS, glia and pigment cells, and a strong reduction of sensory neurons, although craniofacial derivatives are unaffected (Dutton *et al.*, 2001). Interestingly, the *sym1* and *cls* mutations affect complementary sets of NC derivatives. For example, unlike *cls, sym1* mutants have severe defects in craniofacial cartilage development, while unlike *sym1*, the *cls* mutant lacks pigment cells (Kelsh and Eisen, 2000). These phenotypes suggest that multiple genetic pathways control NC fate specification, including the specification of PSNS progenitors. Indeed, analysis of *foxd3* and *tfap2a* double mutants revealed that these genes act in parallel to regulate cell specification within the premigratory NC, at least in part by controlling the expression of *soxE* group genes, such as *sox10* (Arduini *et al.*, 2009).

Similar to the *foxd3* and *sox10* mutant phenotypes, the *lockjaw* or *mount blanc* mutant (*tfap2a*) also shows a lack of *th*- and *dbh*-positive neurons in the region of the SCG complex (Holzschuh *et al.*, 2003; Knight *et al.*, 2003). The *tfap2a* gene is normally expressed both in the premigratory NC and again in the region of the developing SCG. Recent studies have demonstrated that *tfap2a*, along with *foxd3*, clearly plays an important role in the early specification of all NC lineages (Arduini *et al.*, 2009). Therefore it is likely that *tfap2a* is involved in both specification of premigratory crest toward the PSNS lineage and differentiation of PSNS progenitors once they reach the dorsal aorta. Indeed, in the absence of *tfap2a* function, a subset of NC cells can still migrate and undergo neural differentiation to SA progenitors at the SCG, as determined by 16A11 immunoreactivity (Holzschuh *et al*., 2003; O'Brien *et al*., 2004). Furthermore, the expression of *phox2a* in cells in the region of the SCG in *tfap2a* mutants indicates that the signaling cascade required to induce the initial stages of noradrenergic differentiation at the dorsal aorta is intact in these mutants (Holzschuh *et al*., 2003). The failure of *tfap2a* mutants to express the noradrenergic differentiation markers *th* and *dbh* is therefore likely due to the requirement for Tfap2a to activate these genes, as Tfap2a has conserved DNA binding regions in both *th* and *dbh* promoters (Holzschuh *et al*., 2003; Seo *et al*., 2002). Retinoic acid (RA) signaling pathways function upstream of *tfap2a* in the differentiation of noradrenergic neurons because incubation of wild-type zebrafish embryos in RA induces ectopic *th*-positive cells in the region of the SCG, and this affect is blocked in *tfap2a* mutants (Holzschuh *et al*., 2003). In addition, mutations in *neckless/rald2*, which disrupt the biosynthesis of RA from vitamin A, have fewer *th*-expressing cells in the SCG (Holzschuh *et al*., 2003).

The expression of *tfap2a* in PSNS precursors is also controlled by Hand2, as the zebrafish *hands off* mutant (deletion of *hand2)* fails to express normal levels of *tfap2a* and *gata2* in PSNS precursors that have arrived at the dorsal aorta, which in turn causes a strong reduction in the number of *dbh*- and *th*-expressing cells in the SCG (Lucas *et al*., 2006). The loss of noradrenergic identity in *hands off* mutants may also be due to the direct loss of *dbh* expression in these precursors, as Hand2 has been shown to function with Phox2b to directly activate the *dbh* expression in other vertebrates (Rychlik *et al*., 2003; Xu *et al*., 2003).

In a screen for mutations affecting NC derivatives (Henion *et al*., 1996), three mutants were identified based on the absence of dorsal root ganglion (DRG) sensory neurons, based on the loss of 16A11 immunoreactivity. Subsequently, it has been found that these mutants, one of which is called *nosedive*, also completely lack sympathetic and enteric neurons based on the expression of *th* mRNA and 16A11, respectively (Fig. 5B and D). In contrast, the development of trunk NC-derived chromatophores and glia appears normal in all three mutants. These observations suggest that the genes disrupted by these mutations do not affect all NC derivatives, but selectively function during the development of crest-derived neurons. It is tempting to speculate that the phenotypes of these mutants further indicate an early lineage segregation of neurogenic precursors and/or suggest the function of these genes in the development of multiple NC-derived neuronal subtypes.

## IV. Zebrafish as a Novel Model for Studying Neuroblastoma

### A. Overview of Neuroblastoma

Neuroblastoma (NB) is an embryonic tumor of the PSNS that affects 650 children in the United States each year, making it the most common extracranial solid tumor and the leading cause of cancer death in children 1–4 years of age (Goodman, 1999). Clinically, NB most often arises in the adrenal medulla (40% of cases); however, it manifests diverse behavior and can spontaneously regress or differentiate without treatment in infants less than 1-year-old (Maris, 2010; Maris and Matthay, 1999). Unfortunately, older children with advanced disease account for 70% of all NB patients, and their long-term survival rate remains a dismal 20–30% (Maris, 2010; Maris and Matthay, 1999). Cytogenetic analyses of NB have identified a number of aberrant chromosomal regions in NB cells. These regions include allelic losses of 1p36.1, 2q, 3p, 4p, 5q, 9p, 11q23, 14q23-qter, 16p12–13 and 18q –, which have been identified in 15–44% of primary NB (Brodeur, 2003; Brodeur *et al*., 1997; Maris and Matthay, 1999). Although the majority of critical target genes within these chromosomal regions remain to be identified, the findings suggest that multiple tumor suppressor genes may function during different stages of NB pathogenesis. Extensive interrogation of the 1p36 deletion has identified potential tumor suppressor genes that include *KIF1B* and *miR34a* (Schlisio *et al*., 2008; Welch *et al*., 2007; Westermann and Schwab, 2002). Furthermore, increased single nucleotide polymorphisms detected in *BRAD1* (*BRCA1*-associated domain 1 located at 2q35) and the putative gene *FLJ22536* at 6p22, along with copy number variations in a novel NB breakpoint family gene 23 (*NBPF23*), have been recently been implicated in NB (Capasso *et al*., 2009; Diskin *et al*., 2009; Maris *et al*., 2008). However, the functional roles of these genes in the pathogenesis of NB remain unclear.

Amplification of the potent proto-oncogene *MYCN* is found in over 20% of NB patients and is the most reliable marker of poor prognosis. Aberrant *MYCN* expression is believed to mediate NB formation by promoting cell proliferation and survival of NC-derived PSNS cells while blocking cell death (Brodeur, 2003). Other genetic factors in NB include the *PHOX2B* gene, which encodes a homeobox transcription factor that is essential to the development of the sympathoadrenal lineage cells (see above). Heterozygous mutations in *PHOX2B* have been identified in both familial and sporadic NB, albeit at low frequencies (Bourdeaut *et al*., 2005; van Limpt *et al*., 2004). Recently, the mutation and amplification of the anaplastic lymphoma kinase (*ALK*) gene were identified in up to 15% of both familial and sporadic NB cases (Chen *et al*., 2008; George *et al*., 2008; Janoueix-Lerosey *et al*., 2008; Mosse *et al*., 2008). The *ALK* gene encodes a receptor tyrosine kinase that regulates cell proliferation, differentiation, and apoptosis through a number of different signaling pathways including the PI3K/Akt pathway, MAPK pathway, and the STAT3 pathway (Palmer *et al*., 2009). These recent significant findings are sure to be among many other disrupted genetic pathways yet to be identified, and lack of understanding of their functional roles in this disease poses a major obstacle to understanding the molecular pathology of NB and to the development of effective therapies to treat this devastating disease.

## B. Using Zebrafish to Study Neuroblastoma

Previous studies of NB pathogenesis have relied on cell lines derived from NB patient samples that are cultured *in vitro*. Also, an *in vivo* animal model of NB has been established in mice by specifically driving the overexpression of *MYCN* under the control of the tyrosine hydroxylase (Th) promoter, which resembles human NB (Weiss *et al*., 1997). Another murine transgenic mice expressing H-Ras chimerically under the dopamine-beta-hydroxylase (DβH) promoter was reported to develop tumors similar to human ganglioneuroma and NB (Sweetser *et al.*, 1997). The development of a new zebrafish model of NB can contribute substantially to the analysis of NB *in vivo* based upon the strengths of the zebrafish as a genetic and tumor model system. These strengths include (1) direct visualization of tumor formation and progression in adult pigment mutants by observing the expression of fluorescently tagged oncogenes in the tumor tissues and (2) the relative ease of maintaining large numbers of animals for tumor sample collection and genetic and chemical modifier screens. In addition, the ability to simultaneously misexpress mRNAs and knockdown genes of interest in zebrafish embryos using morpholinos (Eisen and Smith, 2008) and shRNA techniques (Dong *et al.*, 2009) allow genetic epistasis analyses to be performed that provide insights into the molecular pathways that are dysfunctional in this disease. Furthermore, the zebrafish is especially amenable to the generation of transgenic lines that express human oncogenes, such as *MYCN*, to the analysis of the cellular properties of transformation and to mutagenic techniques, such as TILLING (Moens *et al.*, 2008) and Zinc-Finger Nuclease strategies (Doyon *et al.*, 2008; Foley *et al.*, 2009; Meng *et al.*, 2008), which allow the contribution and cooperation of potential tumor suppressors to be assessed *in vivo*. Importantly, the zebrafish NB model represents a platform that can be used in large high-throughput drug screens to foster the development of therapies to successfully target this deadly cancer.

## V. Conclusion and Future Directions

Impressive advances have been made in understanding the genetic mechanisms that regulate PSNS development through studies in birds and rodents. Zebrafish studies that further define the anatomical and morphological aspects of the developing PSNS have accelerated the pace of discovery in this field. Exploiting the forward genetic and imaging capacity of the zebrafish system can contribute significantly to the identification of new genes and pathways that regulate PSNS development, and these mutants also provide the means to genetically dissect PSNS developmental processes *in vivo*. Finally, we postulate that knowledge of the genes responsible for normal PSNS development, such as Phox2b and Alk, will help define the molecular pathways that are affected in NB. Ultimately, second-generation suppressor screens based on established PSNS mutants exhibiting proliferative abnormalities, or on new transgenic NB models themselves, can be used to identify potential genes and pathways that may be relevant to the development of effective therapies for this disease.

## VI. Acknowledgments

We would like to thank Hermann Rohrer for comments on the first edition of this manuscript. This work was supported by grant R01 CA104605 (A.T.L.). J.S.L. was supported by the Hope Street Kids foundation. R.A.S is supported by NIH/NINDS award R00 NS058608.

## References

Acloque, H., Adams, M. S., *et al*. (2009). Epithelial-mesenchymal transitions: The importance of changing cell state in development and disease. *J. Clin. Invest.* **119**(6), 1438–1449.

Allende, M. L., and Weinberg, E. S. (1994). The expression pattern of two zebrafish achaete-scute homolog (ash) genes is altered in the embryonic brain of the cyclops mutant. *Dev. Biol.* **166**(2), 509–530.

An, M., Luo, R., *et al*. (2002). Differentiation and maturation of zebrafish dorsal root and sympathetic ganglion neurons. *J. Comp. Neurol.* **446**(3), 267–275.

Anderson, D. J. (1993). Cell fate determination in the peripheral nervous system: The sympathoadrenal progenitor. *J. Neurobiol.* **24**(2), 185–198.

Anderson, D. J., and Axel, R. (1986). A bipotential neuroendocrine precursor whose choice of cell fate is determined by NGF and glucocorticoids. *Cell* **47**(6), 1079–1090.

Anderson, D. J., Carnahan, J. F., *et al*. (1991). Antibody markers identify a common progenitor to sympathetic neurons and chromaffin cells in vivo and reveal the timing of commitment to neuronal differentiation in the sympathoadrenal lineage. *J. Neurosci.* **11**(11), 3507–3519.

Apostolova, G., and Dechant, G. (2009). Development of neurotransmitter phenotypes in sympathetic neurons. *Auton. Neurosci.* **151**(1), 30–38.

Arduini, B. L., Bosse, K. M., *et al*. (2009). Genetic ablation of neural crest cell diversification. *Development* **136**(12), 1987–1994.

Benjanirut, C., Paris, M., *et al*. (2006). The cAMP pathway in combination with BMP2 regulates Phox2a transcription via cAMP response element binding sites. *J. Biol. Chem.* **281**(5), 2969–2981.

Birren, S. J., Lo, L., *et al*. (1993). Sympathetic neuroblasts undergo a developmental switch in trophic dependence. *Development* **119**(3), 597–610.

Bourdeaut, F., Trochet, D., *et al*. (2005). Germline mutations of the paired-like homeobox 2B (PHOX2B) gene in neuroblastoma. *Cancer Lett.* **228**(1–2), 51–58.

Britsch, S., Li, L., *et al*. (1998). The ErbB2 and ErbB3 receptors and their ligand, neuregulin-1, are essential for development of the sympathetic nervous system. *Genes Dev.* **12**(12), 1825–1836.

Brodeur, G. M. (2003). Neuroblastoma: Biological insights into a clinical enigma. *Nat. Rev. Cancer* **3**(3), 203–216.

Brodeur, G. M., Maris, J. M., *et al*. (1997). Biology and genetics of human neuroblastomas. *J. Pediatr. Hematol. Oncol.* **19**(2), 93–101.

Brodski, C., Schaubmar, A., *et al*. (2002). Opposing functions of GDNF and NGF in the development of cholinergic and noradrenergic sympathetic neurons. *Mol. Cell. Neurosci.* **19**(4), 528–538.

Capasso, M., Devoto, M., *et al*. (2009). Common variations in BARD1 influence susceptibility to high-risk neuroblastoma. *Nat. Genet.* **41**(6), 718–723.

Chen, Y., Takita, J., *et al*. (2008). Oncogenic mutations of ALK kinase in neuroblastoma. *Nature* **455**(7215), 971–974.

Cheung, M., Chaboissier, M. C., *et al*. (2005). The transcriptional control of trunk neural crest induction, survival, and delamination. *Dev. Cell* **8**(2), 179–192.

Chun, L. L., and Patterson, P. H. (1977). Role of nerve growth factor in the development of rat sympathetic neurons in vitro. I. Survival, growth, and differentiation of catecholamine production. *J. Cell Biol.* **75**(3), 694–704.

Cohen, A. M. (1974).DNA synthesis and cell division in differentiating avian adrenergic neuroblasts. In "Wenner-Gren Center International Symposium Series: Dynamics of Degeneration and Growth in Neurons" (K. Fuxe, L. Olson, and Y. Zotterman, eds) 359–370. Pergamon, Oxford.

Coppola, E., Pattyn, A., *et al*. (2005). Reciprocal gene replacements reveal unique functions for Phox2 genes during neural differentiation. *EMBO J.* **24**(24), 4392–4403.

Crone, S. A., and Lee, K. F. (2002). Gene targeting reveals multiple essential functions of the neuregulin signaling system during development of the neuroendocrine and nervous systems. *Ann. N. Y. Acad. Sci.* **971**, 547–553.

Debby-Brafman, A., Burstyn-Cohen, T., *et al*. (1999). F-Spondin, expressed in somite regions avoided by neural crest cells, mediates inhibition of distinct somite domains to neural crest migration. *Neuron* **22**(3), 475–488.

DiCicco-Bloom, E., Friedman, W. J., *et al*. (1993). NT-3 stimulates sympathetic neuroblast proliferation by promoting precursor survival. *Neuron* **11**(6), 1101–1111.

Dick, A., Hild, M., *et al*. (2000). Essential role of Bmp7 (snailhouse) and its prodomain in dorsoventral patterning of the zebrafish embryo. *Development* **127**(2), 343–354.

Diskin, S. J., Hou, C., *et al*. (2009). Copy number variation at 1q21.1 associated with neuroblastoma. *Nature* **459**(7249), 987–991.

Dong, M., Fu, Y. F., *et al*. (2009). Heritable and lineage-specific gene knockdown in zebrafish embryo. *PLoS One* **4**(7), e6125.

Doxakis, E., Howard, L., *et al*. (2008). HAND transcription factors are required for neonatal sympathetic neuron survival. *EMBO Rep.* **9**(10), 1041–1047.

Doyon, Y., McCammon, J. M., *et al*. (2008). Heritable targeted gene disruption in zebrafish using designed zinc-finger nucleases. *Nat. Biotechnol.* **26**(6), 702–708.

Dutton, K. A., Pauliny, A., *et al*. (2001). Zebrafish colourless encodes sox10 and specifies non-ectomesenchymal neural crest fates. *Development* **128**(21), 4113–4125.

Eisen, J. S., and Smith, J. C. (2008). Controlling morpholino experiments: Don't stop making antisense. *Development* **135**(10), 1735–1743.

Elworthy, S., Pinto, J. P., *et al*. (2005). Phox2b function in the enteric nervous system is conserved in zebrafish and is sox10-dependent. *Mech. Dev.* **122**(5), 659–669.

Ernfors, P., Lee, K. F., *et al*. (1994). Lack of neurotrophin-3 leads to deficiencies in the peripheral nervous system and loss of limb proprioceptive afferents. *Cell* **77**(4), 503–512.

Ernsberger, U., Patzke, H., *et al*. (1995). The expression of tyrosine hydroxylase and the transcription factors cPhox-2 and Cash-1: Evidence for distinct inductive steps in the differentiation of chick sympathetic precursor cells. *Mech. Dev.* **52**(1), 125–136.

Ernsberger, U., Reissmann, E., *et al*. (2000). The expression of dopamine beta-hydroxylase, tyrosine hydroxylase, and Phox2 transcription factors in sympathetic neurons: Evidence for common regulation during noradrenergic induction and diverging regulation later in development. *Mech. Dev.* **92**(2), 169–177.

Ernsberger, U., and Rohrer, H. (2009). Development of the autonomic nervous system: New perspectives and open questions. *Auton. Neurosci.* **151**(1), 1–2.

Fagan, A. M., Zhang, H., *et al*. (1996). TrkA, but not TrkC, receptors are essential for survival of sympathetic neurons in vivo. *J. Neurosci.* **16**(19), 6208–6218.

Farinas, I., Jones, K. R., *et al*. (1994). Severe sensory and sympathetic deficits in mice lacking neurotrophin-3. *Nature* **369**(6482), 658–661.

Filippi, A., Mahler, J., *et al*. (2009). Expression of the paralogous tyrosine hydroxylase encoding genes th1 and th2 reveals the full complement of dopaminergic and noradrenergic neurons in zebrafish larval and juvenile brain. *J. Comp. Neurol.* **518**(4), 423–438.

Foley, J. E., Yeh, J. R., *et al*. (2009). Rapid mutation of endogenous zebrafish genes using zinc finger nucleases made by Oligomerized Pool ENgineering (OPEN). *PLoS One* **4**(2), e4348.

Fouquet, B., Weinstein, B. M., *et al*. (1997). Vessel patterning in the embryo of the zebrafish: Guidance by notochord. *Dev. Biol.* **183**(1), 37–48.

Francis, N. J., and Landis, S. C. (1999). Cellular and molecular determinants of sympathetic neuron development. *Annu. Rev. Neurosci.* **22**, 541–566.

Gammill, L. S., Gonzalez, C., *et al*. (2006). Guidance of trunk neural crest migration requires neuropilin 2/semaphorin 3F signaling. *Development* **133**(1), 99–106.

George, R. E., Sanda, T., *et al*. (2008). Activating mutations in ALK provide a therapeutic target in neuroblastoma. *Nature* **455**(7215), 975–978.

Goodman, N. W. (1999). An open letter to the Director General of the Cancer Research Campaign. *J. R Coll. Physicians Lond.* **33**(1), 93.

Goridis, C., and Rohrer, H. (2002). Specification of catecholaminergic and serotonergic neurons. *Nat. Rev. Neurosci.* **3**(7), 531–541.

Groves, A. K., George, K. M., *et al*. (1995). Differential regulation of transcription factor gene expression and phenotypic markers in developing sympathetic neurons. *Development* **121**(3), 887–901.

Guillemot, F., Lo, L. C., *et al*. (1993). Mammalian achaete-scute homolog 1 is required for the early development of olfactory and autonomic neurons. *Cell* **75**(3), 463–476.

Guo, S., Brush, J., *et al*. (1999a). Development of noradrenergic neurons in the zebrafish hindbrain requires BMP, FGF8, and the homeodomain protein soulless/Phox2a. *Neuron* **24**(3), 555–566.

Guo, S., Wilson, S. W., *et al*. (1999b). Mutations in the zebrafish unmask shared regulatory pathways controlling the development of catecholaminergic neurons. *Dev. Biol.* **208**(2), 473–487.

Hansen, M. B. (2003). The enteric nervous system I: Organisation and classification. *Pharmacol. Toxicol.* **92**(3), 105–113.

Hendershot, T. J., Liu, H., *et al*. (2008). Conditional deletion of Hand2 reveals critical functions in neurogenesis and cell type-specific gene expression for development of neural crest-derived noradrenergic sympathetic ganglion neurons. *Dev. Biol.* **319**(2), 179–191.

Henion, P. D., Raible, D. W., *et al*. (1996). Screen for mutations affecting development of Zebrafish neural crest. *Dev. Genet.* **18**(1), 11–17.

Heumann, R., Korsching, S., *et al*. (1984). Relationship between levels of nerve growth factor (NGF) and its messenger RNA in sympathetic ganglia and peripheral target tissues. *EMBO J.* **3**(13), 3183–3189.

Hirsch, M. R., Tiveron, M. C., *et al*. (1998). Control of noradrenergic differentiation and Phox2a expression by MASH1 in the central and peripheral nervous system. *Development* **125**(4), 599–608.

Holzschuh, J., Barrallo-Gimeno, A., *et al*. (2003). Noradrenergic neurons in the zebrafish hindbrain are induced by retinoic acid and require tfap2a for expression of the neurotransmitter phenotype. *Development* **130**(23), 5741–5754.

Holzschuh, J., Ryu, S., *et al*. (2001). Dopamine transporter expression distinguishes dopaminergic neurons from other catecholaminergic neurons in the developing zebrafish embryo. *Mech. Dev.* **101**(1–2), 237–243.

Hong, S. J., Huh, Y., *et al*. (2006). GATA-3 regulates the transcriptional activity of tyrosine hydroxylase by interacting with CREB. *J. Neurochem.* **98**(3), 773–781.

Honma, Y., Araki, T., *et al*. (2002). Artemin is a vascular-derived neurotropic factor for developing sympathetic neurons. *Neuron* **35**(2), 267–282.

Howard, M. J., Stanke, M., *et al*. (2000). The transcription factor dHAND is a downstream effector of BMPs in sympathetic neuron specification. *Development* **127**(18), 4073–4081.

Hsu, H. J., Lin, G., *et al*. (2003). Parallel early development of zebrafish interrenal glands and pronephros: Differential control by wt1 and ff1b. *Development* **130**(10), 2107–2116.

Huber, K. (2006). The sympathoadrenal cell lineage: Specification, diversification, and new perspectives. *Dev. Biol.* **298**(2), 335–343.

Huber, K., and Ernsberger, U. (2006). Cholinergic differentiation occurs early in mouse sympathetic neurons and requires Phox2b. *Gene Expr.* **13**(2), 133–139.

Janoueix-Lerosey, I., Lequin, D., *et al*. (2008). Somatic and germline activating mutations of the ALK kinase receptor in neuroblastoma. *Nature* **455**(7215), 967–970.

Kalcheim, C., Langley, K., *et al*. (2002). From the neural crest to chromaffin cells: Introduction to a session on chromaffin cell development. *Ann. N. Y. Acad. Sci.* **971**, 544–546.

Kasemeier-Kulesa, J. C., Bradley, R., *et al*. (2006). Eph/ephrins and N-cadherin coordinate to control the pattern of sympathetic ganglia. *Development* **133**(24), 4839–4847.

Kasemeier-Kulesa, J. C., Kulesa, P. M., *et al*. (2005). Imaging neural crest cell dynamics during formation of dorsal root ganglia and sympathetic ganglia. *Development* **132**(2), 235–245.

Kawasaki, T., Bekku, Y., *et al*. (2002). Requirement of neuropilin 1-mediated Sema3A signals in patterning of the sympathetic nervous system. *Development* **129**(3), 671–680.

Kelsh, R. N., and Eisen, J. S. (2000). The zebrafish colourless gene regulates development of non-ectomesenchymal neural crest derivatives. *Development* **127**(3), 515–525.

Kim, H. S., Hong, S. J., *et al*. (2001). Regulation of the tyrosine hydroxylase and dopamine beta-hydroxylase genes by the transcription factor AP-2. *J. Neurochem.* **76**(1), 280–294.

Knecht, A. K., and Bronner-Fraser, M. (2002). Induction of the neural crest: A multigene process. *Nat. Rev. Genet.* **3**(6), 453–461.

Knight, R. D., Nair, S., *et al*. (2003). lockjaw encodes a zebrafish tfap2a required for early neural crest development. *Development* **130**(23), 5755–5768.

Korsching, S., and Thoenen, H. (1983). Nerve growth factor in sympathetic ganglia and corresponding target organs of the rat: Correlation with density of sympathetic innervation. *Proc. Natl. Acad. Sci. U.S.A* **80**(11), 3513–3516.

Krauss, S., Concordet, J. P., *et al*. (1993). A functionally conserved homolog of the Drosophila segment polarity gene hh is expressed in tissues with polarizing activity in zebrafish embryos. *Cell* **75**(7), 1431–1444.

LeDouarin, N., and Kalcheim, C. (1999). "The Neural Crest". Cambridge University Press, Cambridge; New York.

Lim, K. C., Lakshmanan, G., *et al*. (2000). Gata3 loss leads to embryonic lethality due to noradrenaline deficiency of the sympathetic nervous system. *Nat. Genet.* **25**(2), 209–212.

Liu, Y. W. (2007). Interrenal organogenesis in the zebrafish model. *Organogenesis* **3**(1), 44–48.

Liu, Y. W., Gao, W., *et al*. (2003). Prox1 is a novel coregulator of Ff1b and is involved in the embryonic development of the zebra fish interrenal primordium. *Mol. Cell. Biol.* **23**(20), 7243–7255.

Lo, J., Lee, S., *et al*. (2003). 15000 unique zebrafish EST clusters and their future use in microarray for profiling gene expression patterns during embryogenesis. *Genome Res.* **13**(3), 455–466.

Lo, L., Morin, X., *et al*. (1999). Specification of neurotransmitter identity by Phox2 proteins in neural crest stem cells. *Neuron* **22**(4), 693–705.

Lucas, M. E., Muller, F., *et al*. (2006). The bHLH transcription factor hand2 is essential for noradrenergic differentiation of sympathetic neurons. *Development* **133**(20), 4015–4024.

Luo, R., An, M., *et al*. (2001). Specific pan-neural crest expression of zebrafish Crestin throughout embryonic development. *Dev. Dyn.* **220**(2), 169–174.

Ma, L., Merenmies, J., *et al*. (2000). Molecular characterization of the TrkA/NGF receptor minimal enhancer reveals regulation by multiple cis elements to drive embryonic neuron expression. *Development* **127**(17), 3777–3788.

Maris, J. M. (2010). Recent advances in neuroblastoma. *N. Engl. J. Med.* **362**(23), 2202–2211.

Maris, J. M., and Matthay, K. K. (1999). Molecular biology of neuroblastoma. *J. Clin. Oncol.* **17**(7), 2264–2279.

Maris, J. M., Mosse, Y. P., *et al*. (2008). Chromosome 6p22 locus associated with clinically aggressive neuroblastoma. *N. Engl. J. Med.* **358**(24), 2585–2593.

Martin, S. C., Marazzi, G., *et al*. (1995). Five Trk receptors in the zebrafish. *Dev. Biol.* **169**(2), 745–758.

Martinez-Barbera, J. P., Toresson, H., *et al*. (1997). Cloning and expression of three members of the zebrafish Bmp family: Bmp2a, Bmp2b and Bmp4. *Gene* **198**(1–2), 53–59.

Marusich, M. F., Furneaux, H. M., *et al*. (1994). Hu neuronal proteins are expressed in proliferating neurogenic cells. *J. Neurobiol.* **25**(2), 143–155.

McKeown, S. J., Lee, V. M., *et al*. (2005). Sox10 overexpression induces neural crest-like cells from all dorsoventral levels of the neural tube but inhibits differentiation. *Dev. Dyn.* **233**(2), 430–444.

Melby, A. E., Kimelman, D., *et al*. (1997). Spatial regulation of floating head expression in the developing notochord. *Dev. Dyn.* **209**(2), 156–165.

Meng, X., Noyes, M. B., *et al*. (2008). Targeted gene inactivation in zebrafish using engineered zinc-finger nucleases. *Nat. Biotechnol.* **26**(6), 695–701.

Moens, C. B., Donn, T. M., *et al*. (2008). Reverse genetics in zebrafish by TILLING. *Brief. Funct. Genomic. Proteomic.* **7**(6), 454–459.

Morikawa, Y., D'Autreaux, F., *et al*. (2007). Hand2 determines the noradrenergic phenotype in the mouse sympathetic nervous system. *Dev. Biol.* **307**(1), 114–126.

Morikawa, Y., Zehir, A., *et al*. (2009). BMP signaling regulates sympathetic nervous system development through Smad4-dependent and -independent pathways. *Development* **136**(21), 3575–3584.

Morin, X., Cremer, H., *et al*. (1997). Defects in sensory and autonomic ganglia and absence of locus coeruleus in mice deficient for the homeobox gene Phox2a. *Neuron* **18**(3), 411–423.

Mosse, Y. P., Laudenslager, M., *et al*. (2008). Identification of ALK as a major familial neuroblastoma predisposition gene. *Nature* **455**(7215), 930–935.

Muller, F., and Rohrer, H. (2002). Molecular control of ciliary neuron development: BMPs and downstream transcriptional control in the parasympathetic lineage. *Development* **129**(24), 5707–5717.

Murphy, S., Krainock, R., *et al*. (2002). Neuregulin signaling via erbB receptor assemblies in the nervous system. *Mol. Neurobiol.* **25**(1), 67–77.

Nakamura, E., and Kaelin, W. G. Jr. (2006). Recent insights into the molecular pathogenesis of pheochromocytoma and paraganglioma. *Endocr. Pathol.* **17**(2), 97–106.

Neave, B., Rodaway, A., *et al*. (1995). Expression of zebrafish GATA 3 (gta3) during gastrulation and neurulation suggests a role in the specification of cell fate. *Mech. Dev.* **51**(2–3), 169–182.

Nguyen, V. H., Schmid, B., *et al*. (1998). Ventral and lateral regions of the zebrafish gastrula, including the neural crest progenitors, are established by a bmp2b/swirl pathway of genes. *Dev. Biol.* **199**(1), 93–110.

O'Brien, E. K., d'Alencon, C., *et al*. (2004). Transcription factor Ap-2alpha is necessary for development of embryonic melanophores, autonomic neurons and pharyngeal skeleton in zebrafish. *Dev. Biol.* **265**(1), 246–261.

Palmer, R. H., Vernersson, E., *et al*. (2009). Anaplastic lymphoma kinase: Signalling in development and disease. *Biochem. J.* **420**(3), 345–361.

Patten, I., and Placzek, M. (2000). The role of Sonic hedgehog in neural tube patterning. *Cell Mol. Life Sci.* **57**(12), 1695–1708.

Pattyn, A., Goridis, C., *et al*. (2000). Specification of the central noradrenergic phenotype by the homeobox gene Phox2b. *Mol. Cell. Neurosci.* **15**(3), 235–243.

Pattyn, A., Guillemot, F., *et al*. (2006). Delays in neuronal differentiation in Mash1/Ascl1 mutants. *Dev. Biol.* **295**(1), 67–75.

Pattyn, A., Morin, X., *et al*. (1999). The homeobox gene Phox2b is essential for the development of autonomic neural crest derivatives. *Nature* **399**(6734), 366–370.

Raible, D. W., and Eisen, J. S. (1994). Restriction of neural crest cell fate in the trunk of the embryonic zebrafish. *Development* **120**(3), 495–503.

Rohrer, H., and Thoenen, H. (1987). Relationship between differentiation and terminal mitosis: Chick sensory and ciliary neurons differentiate after terminal mitosis of precursor cells, whereas sympathetic neurons continue to divide after differentiation. *J. Neurosci.* **7**(11), 3739–3748.

Rothman, T. P., Gershon, M. D., *et al*. (1978). The relationship of cell division to the acquisition of adrenergic characteristics by developing sympathetic ganglion cell precursors. *Dev. Biol.* **65**(2), 322–341.

Rudiger, R., Binder, E., *et al*. (2009). In vivo role for CREB signaling in the noradrenergic differentiation of sympathetic neurons. *Mol. Cell. Neurosci.* **42**(2), 142–151.

Rychlik, J. L., Gerbasi, V., *et al*. (2003). The interaction between dHAND and Arix at the dopamine beta-hydroxylase promoter region is independent of direct dHAND binding to DNA. *J. Biol. Chem.* **278**(49), 49652–49660.

Sakai, D., Suzuki, T., *et al*. (2006). Cooperative action of Sox9, Snail2 and PKA signaling in early neural crest development. *Development* **133**(7), 1323–1333.

Santiago, A., and Erickson, C. A. (2002). Ephrin-B ligands play a dual role in the control of neural crest cell migration. *Development* **129**(15), 3621–3632.

Sauka-Spengler, T., and Bronner-Fraser, M. (2008). A gene regulatory network orchestrates neural crest formation. *Nat. Rev. Mol. Cell Biol.* **9**(7), 557–568.

Schlisio, S., Kenchappa, R. S., *et al*. (2008). The kinesin KIF1Bbeta acts downstream from EglN3 to induce apoptosis and is a potential 1p36 tumor suppressor. *Genes Dev.* **22**(7), 884–893.

Schmidt, M., Lin, S., *et al*. (2009). The bHLH transcription factor Hand2 is essential for the maintenance of noradrenergic properties in differentiated sympathetic neurons. *Dev. Biol.* **329**(2), 191–200.

Schober, A., Krieglstein, K., *et al*. (2000). Molecular cues for the development of adrenal chromaffin cells and their preganglionic innervation. *Eur. J. Clin. Invest.* **30**(Suppl 3), 87–90.

Schober, A., and Unsicker, K. (2001). Growth and neurotrophic factors regulating development and maintenance of sympathetic preganglionic neurons. *Int. Rev. Cytol.* **205**, 37–76.

Schwarz, Q., Maden, C. H., *et al*. (2009). Neuropilin 1 signaling guides neural crest cells to coordinate pathway choice with cell specification. *Proc. Natl. Acad. Sci. U.S.A* **106**(15), 6164–6169.

Schweitzer, J., and Driever, W. (2009). Development of the dopamine systems in zebrafish. *Adv. Exp. Med. Biol.* **651**, 1–14.

Seo, H., Hong, S. J., *et al*. (2002). A direct role of the homeodomain proteins Phox2a/2b in noradrenaline neurotransmitter identity determination. *J. Neurochem.* **80**(5), 905–916.

Shelton, D. L., and Reichardt, L. F. (1984). Expression of the beta-nerve growth factor gene correlates with the density of sympathetic innervation in effector organs. *Proc. Natl. Acad. Sci. U.S.A* **81**(24), 7951–7955.

Smeyne, R. J., Klein, R., *et al*. (1994). Severe sensory and sympathetic neuropathies in mice carrying a disrupted Trk/NGF receptor gene. *Nature* **368**(6468), 246–249.

Stewart, R. A., Arduini, B. L., *et al*. (2006). Zebrafish foxd3 is selectively required for neural crest specification, migration and survival. *Dev. Biol.* **292**(1), 174–188.

Sweetser, D. A., Kapur, R. P., *et al*. (1997). Oncogenesis and altered differentiation induced by activated Ras in neuroblasts of transgenic mice. *Oncogene* **15**(23), 2783–2794.

Talbot, W. S., Trevarrow, B., *et al*. (1995). A homeobox gene essential for zebrafish notochord development. *Nature* **378**(6553), 150–157.

Thexton, A. (2001). Vertebrate peripheral nervous system. Encyclopedia of Life Sciences. Retrieved 2001.

To, T. T., Hahner, S., *et al*. (2007). Pituitary-interrenal interaction in zebrafish interrenal organ development. *Mol. Endocrinol.* **21**(2), 472–485.

Tsarovina, K., Pattyn, A., *et al*. (2004). Essential role of Gata transcription factors in sympathetic neuron development. *Development* **131**(19), 4775–4786.

Unsicker, K., Huber, K., *et al*. (2005). The chromaffin cell and its development. *Neurochem. Res.* **30**(6–7), 921–925.

van Limpt, V., Schramm, A., *et al*. (2004). The Phox2B homeobox gene is mutated in sporadic neuroblastomas. *Oncogene* **23**(57), 9280–9288.

Weis, J. S. (1968). Analysis of the development of nervous system of the zebrafish, Brachydanio rerio. I. The normal morphology and development of the spinal cord and ganglia of the zebrafish. *J. Embryol. Exp. Morphol.* **19**(2), 109–119.

Weiss, W. A., Aldape, K., *et al*. (1997). Targeted expression of MYCN causes neuroblastoma in transgenic mice. *EMBO J.* **16**(11), 2985–2995.

Welch, C., Chen, Y., *et al*. (2007). MicroRNA-34a functions as a potential tumor suppressor by inducing apoptosis in neuroblastoma cells. *Oncogene* **26**(34), 5017–5022.

Westermann, F., and Schwab, M. (2002). Genetic parameters of neuroblastomas. *Cancer Lett.* **184**(2), 127–147.

Williams, J. A., Barrios, A., *et al*. (2000a). Programmed cell death in zebrafish rohon beard neurons is influenced by TrkC1/NT-3 signaling. *Dev. Biol.* **226**(2), 220–230.

Williams, Z., Tse, V., *et al*. (2000b). Sonic hedgehog promotes proliferation and tyrosine hydroxylase induction of postnatal sympathetic cells in vitro. *NeuroReport* **11**(15), 3315–3319.

Wyatt, S., Pinon, L. G., *et al*. (1997). Sympathetic neuron survival and TrkA expression in NT3-deficient mouse embryos. *EMBO J.* **16**(11), 3115–3123.

Xu, H., Firulli, A. B., *et al*. (2003). HAND2 synergistically enhances transcription of dopamine-beta-hydroxylase in the presence of Phox2a. *Dev. Biol.* **262**(1), 183–193.

Yamamoto, K., Ruuskanen, J. O., *et al*. (2010). Two tyrosine hydroxylase genes in vertebrates New dopaminergic territories revealed in the zebrafish brain. *Mol. Cell. Neurosci.* **43**(4), 394–402.

Yelon, D., Ticho, B., *et al*. (2000). The bHLH transcription factor hand2 plays parallel roles in zebrafish heart and pectoral fin development. *Development* **127**(12), 2573–2582.

Young, H. M., Cane, K. N., *et al*. (2010). Development of the autonomic nervous system: A comparative view. *Auton. Neurosci.* Mar 24. [Epub ahead of print]. PMID: 20346736

Zirlinger, M., Lo, L., *et al*. (2002). Transient expression of the bHLH factor neurogenin-2 marks a subpopulation of neural crest cells biased for a sensory but not a neuronal fate. *Proc. Natl. Acad. Sci. U.S.A* **99**(12), 8084–8089.

## CHAPTER 6

# Analysis of the Retina in the Zebrafish Model

**Andrei Avanesov** *and* **Jarema Malicki**
Division of Craniofacial and Molecular Genetics, Tufts University, Boston, Massachusetts

I. Introduction
II. Development of the Zebrafish Retina
    A. Early Morphogenetic Events
    B. Neurogenesis
    C. Development of Retinotectal Projections
    D. Non-Neuronal Tissues
III. Analysis of Wild-Type and Mutant Visual System
    A. Histological Analysis
    B. The Use of Molecular Markers
    C. Analysis of Cell Movements and Lineage Relationships
    D. Analysis of Cell and Tissue Interactions
    E. Analysis of Cell Proliferation
    F. Behavioral Studies
    G. Electrophysiological Analysis of Retinal Function
    H. Biochemical Approaches
    I. Chemical Screens
IV. Analysis of Gene Function in the Zebrafish Retina
    A. Reverse Genetic Approaches
    B. Forward Genetics
V. Summary
Acknowledgments
References

## Abstract

The zebrafish is one of the leading models for the analysis of the vertebrate visual system. A wide assortment of molecular, genetic, and cell biological approaches is available to study zebrafish visual system development and function. As new techniques

Copyright © 2010 Elsevier Inc. All rights reserved.

978-0-12-384892-5
DOI: 10.1016/B978-0-12-384892-5.00006-2

become available, genetic analysis and imaging continue to be the strengths of the zebrafish model. In particular, recent developments in the use of transposons and zinc finger nucleases to produce new generations of mutant strains enhance both forward and reverse genetic analysis. Similarly, the imaging of developmental and physiological processes benefits from a wide assortment of fluorescent proteins and the ways to express them in the embryo. The zebrafish is also highly attractive for high-throughput screening of small molecules, a promising strategy to search for compounds with therapeutic potential. Here we discuss experimental approaches used in the zebrafish model to study morphogenetic transformations, cell fate decisions, and the differentiation of fine morphological features that ultimately lead to the formation of the functional vertebrate visual system.

## I. Introduction

The vertebrate central nervous system (CNS) is enormously complex. The human cerebral cortex alone is estimated to contain in excess of $10^9$ neurons (Jacobson, 1991), each characterized by the morphology of its soma and processes, synaptic connections with other cells, receptors expressed on its surface, the neurotransmitters it releases, and numerous other molecular and cellular features. Together these characteristics define cell identity. To understand the development of the CNS, multiple steps involved in the formation of numerous cell identities must be determined. One way to approach this enormously complicated task is to study a relatively simple and accessible region of the CNS. The retina is such a region.

Several characteristics make the retina more approachable than most other areas of the CNS. Most importantly, the retina contains a relatively small number of neuronal cell classes, and these are characterized by stereotypical positions and distinctive morphologies. Even in very crude histological preparations, the identity of individual cells can be frequently and correctly determined based on their location. Cajal noted that the separation of different cells into distinct layers, the small size of dendritic fields, and the presence of layers consisting almost exclusively of neuronal projections are fortuitous characteristics of the retina (Cajal, 1893). In addition, the eye becomes isolated from other parts of the CNS early in embryogenesis, and consequently cell migrations into the retina are limited to the optic nerve and the optic chiasm only (Burrill and Easter, 1994; Watanabe and Raff, 1988). Such anatomical isolation simplifies the interpretation of developmental events within the retina. Taken together, all these qualities make the retina an excellent model system for the studies of vertebrate neuronal development and function.

Teleost retinae have been studied for over a century (Cajal, 1893; Dowling, 1987; Malicki, 2000; Muller, 1857; Rodieck, 1973). The eyes of teleosts in general and zebrafish in particular are large and their neuroanatomy is well characterized. An important advantage of the zebrafish retina for genetic and developmental research is that it is formed and becomes functional very early in development. Neurogenesis in the central retina of the zebrafish eye is essentially complete by 60 hours post fertilization (hpf) (Nawrocki, 1985) and, as judged by behavioral responses to visual stimuli, the zebrafish eye detects light surprisingly early, starting between 2.5 and 3.5 days post fertilization (dpf) (Clark, 1981; Easter and Nicola, 1996). Studies of the zebrafish retina benefit from many general qualities of the system: high fecundity, transparency, embryogenesis that occurs outside the maternal organism, the ease of maintenance in large numbers, the short length of the life cycle, the ability to study haploid development, and most recently the progress in zebrafish genomics, including the genome sequencing project.

The neuronal architecture of the vertebrate retina has been remarkably conserved in evolution. Early investigators noted that even retinae of divergent vertebrate phyla, including teleosts and mammals, display similar organization (Cajal, 1893; Muller, 1857). Gross morphological and histological features of mammalian and teleost retinae display few differences. Accordingly, human and zebrafish retinae contain the same major cell classes organized in the same layered pattern, where light-sensing photoreceptors occupy the outermost layer, while the retinal projection neurons, the ganglion cells, reside in the innermost neuronal layer, proximal to the lens. The retinal interneurons, the amacrine, bipolar, and horizontal cells, localize in between the photoreceptor and ganglion cell layers (Fig. 2). Similarities extend beyond histology and morphology. Pax-2/noi and Chx10/Vsx-2 expression patterns, for example, are very similar in mouse and zebrafish eyes (Liu *et al*., 1994; Macdonald and Wilson, 1997; Nornes *et al*., 1990; Passini *et al*., 1997), and a number of genetic loci display closely related phenotypes in humans and zebrafish alike. These observations stimulated efforts to use the zebrafish as a model of human eye disorders (reviewed in Gross and Perkins, 2008). Consequently, zebrafish eye mutants have been proposed as models of pyruvate dehydrogenase deficiency, choroidemia, achromatopsia, as well as June, Joubert, and Hermansky–Pudlak syndromes (Bahadori *et al*., 2006; Brockerhoff *et al*., 2003; Duldulao *et al*., 2009; Hudak *et al*., 2010; Krock *et al*., 2007; Taylor *et al*., 2004). This is a fortuitous circumstance, considering that throughout the world diseases of the retina affect millions (Cedrone *et al*., 1997; Dryja and Li, 1995; Hartong *et al*., 2006; Seddon, 1994). Thus, in addition to being an excellent model for the studies of vertebrate neurogenesis, the zebrafish retina is likely to provide medically relevant insights. In this chapter, following an introduction to zebrafish eye development, we focus on tools currently used to study various aspects of the zebrafish visual system. Since many techniques described in this chapter are also applied to the analysis of other organs, the reader is encouraged to search for more information in other sections of this volume.

## II. Development of the Zebrafish Retina

### A. Early Morphogenetic Events

Fate-mapping studies indicate that during early gastrulation the retina originates from a single field of cells positioned roughly between the telencephalic and the diencephalic precursor fields (Woo and Fraser, 1995). During late gastrulation, the anterior and lateral migrations of diencephalic precursors are thought to subdivide the retinal field into two separate primordia (Rembold *et al*., 2006; Varga *et al*., 1999). Neurulation in teleosts proceeds somewhat differently than in higher vertebrates. First, the primordium of the CNS does not take the form of a tube (the neural tube), and instead is shaped in the form of a solid rod called the neural keel (Fig. 1B and C) (Kimmel *et al*., 1995; Lowery and Sive, 2004; Schmitz *et al*., 1993). Consistent with that, optic vesicles are not present, and the equivalent structures are called optic lobes. These first become evident as bilateral thickenings of the anterior neural keel at about 11.5 hpf, and gradually become more and

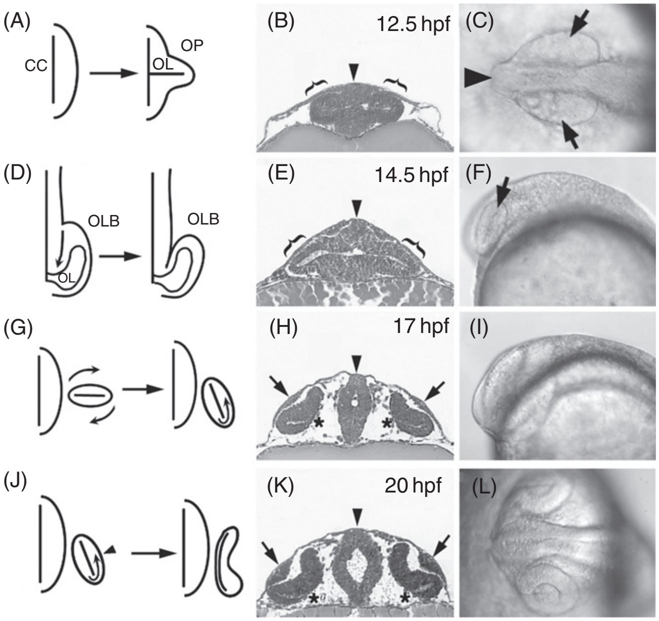

**Fig. 1** Early morphogenetic events leading to the formation of the optic cup. (A) A diagram of a transverse section through anterior neural keel illustrating morphogenetic transformation that leads to the formation of optic lobes. Solid horizontal line represents the ventricular lumen (OL) of the optic lobe. (B) A transverse plastic section through the anterior portion of the neural keel and optic lobes (brackets). (C) Dorsal view of anterior neural keel and optic lobes (arrows) at 12.5 hpf. (D) A schematic representation of anterior neural keel (dorsal view, anterior down). Wing-shaped optic primordia gradually detach from the neural keel starting posteriorly (arrow). (E) A transverse plastic section through anterior neural keel and optic lobes (brackets) at 14.5 hpf. (F) Lateral view of anterior neural keel and optic lobe (arrow) at the same stage. (G) A diagram of dorsoventral reorientation of the optic lobe. (H) A transverse plastic section through neural keel and optic lobes during the reorientation at ca. 17 hpf. At about the same time, lens rudiments start to form (arrows) and the medial layer of the optic lobe becomes thinner as it begins to differentiate into the pigmented epithelium (asterisks). The lateral surface of the optic lobe starts to invaginate. (I) A lateral view of anterior neural keel during optic cup formation. (J) A schematic representation of morphogenetic movements that accompany optic cup formation. Cells migrate (arrow) from the medial to the lateral cell layer around the ventral edge of the lobe. Simultaneously, the initially flat lobe invaginates (arrowhead) to become the concave eye cup. (K) A transverse plastic section through the anterior neural tube during optic cup formation at 20 hpf. Lens rudiments are quite prominent by this stage (arrows). Most of the medial cell layer already displays a flattened morphology, except for the ventralmost regions, which still retain columnar appearance (asterisks). (L) A dorsal view of anterior neural tube and optic lobes at 20 hpf. Vertical arrowheads in B, E, H, and K indicate the midline. CC, central canal; OL, optic lumen; OP, optic primordium; OLB, optic lobe; hpf, hours post fertilization. Except D, C and L, in all panels dorsal is up. Panels A, D, G, and J are based on Easter and Malicki (2002). The remaining panels reprinted from Pujic and Malicki (2001) with permission from Elsevier.

more prominent (Fig. 1A–C) (Schmitt and Dowling, 1994). They are initially flattened and protrude laterally on both sides of the brain (brackets and arrows, respectively in Fig. 1B and C). At approximately 13 hpf, the posterior portion of the optic lobe starts to separate from the brain, while its anterior part remains attached (Fig. 1D). This attachment will persist throughout eye development, at later stages forming the optic stalk. As its morphogenesis advances, the optic lobe turns around its anteroposterior axis so that its

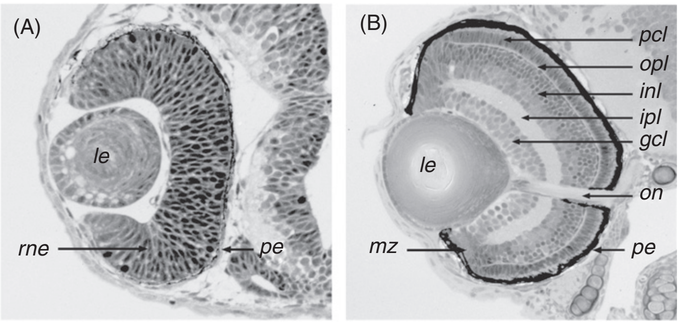

**Fig. 2** Histology of the zebrafish retina. (A) A section through the zebrafish eye during early stages of neurogenesis at approximately 36 hpf. At this stage, the retina mostly consists of two epithelial layers: the pigmented epithelium and the retinal neuroepithelium. Although some retinal cells are already postmitotic at this stage, they are not numerous enough to form a distinct layer. (B) A section through the zebrafish eye at 72 hpf. With the exception of the marginal zone, where cell proliferation will continue throughout the lifetime of the animal, retinal neurogenesis is mostly completed. The major nuclear and plexiform layers, as well as the optic nerve and the pigmented epithelium, are well differentiated. gcl: ganglion cell layer; inl: inner nuclear layer; ipl: inner plexiform layer; le: lens; mz: marginal zone; on: optic nerve; opl: outer plexiform layer; pcl: photoreceptor cell layer; pe: pigmented epithelium; rne: retinal neuroepithelium.

ventral surface becomes directed toward the brain while the dorsal surface starts to face the outside environment (Fig. 1G). Cells forming the outside surface will differentiate into the neural retina. Fate-mapping studies suggest that starting at ca. 15 hpf, cells migrate from the medial to lateral epithelial layer of the optic lobe (Li *et al.*, 2000b). The medial layer becomes thinner and subsequently differentiates as the retinal pigmented epithelium (RPE) (asterisks in Fig. 1H and K). At about the same time, an invagination forms on the lateral (upper, before turning) surface of the optic lobe (Schmitt and Dowling, 1994). This is accompanied by the appearance of a thickening in the epithelium overlying the optic lobe: the lens rudiment (arrows in Fig. 1H). Subsequently, over a period of several hours, both the invagination and the lens placode become increasingly more prominent, transforming the optic lobe into the optic cup (Fig. 1J–L). The choroid fissure forms in the rim of the optic cup next to the optic stalk. The lens placode continues to grow and by 24 hpf it is detached from the epidermis. At the beginning of day 2, the optic cup consists of two closely connected sheets of cells: the pseudostratified columnar neuroepithelium (rne) and the cuboidal pigmented epithelium (pe) (Fig. 2A). Starting at about 24 hpf, melanin granules appear in the cells of the pigmented epithelium. In the first half of day 2, concomitant to the expansion of the ventral diencephalon, the eye rotates so that the choroid fissure, which at 24 hpf was pointing above the yolk sac, is now directed toward the heart (Kimmel *et al.*, 1995; Schmitt and Dowling, 1994). Throughout this period, the optic stalk gradually becomes less prominent. In the first half of day 2 as ganglion cells begin to differentiate, the optic stalk provides support for their axons. Later in development, it is no longer present as a distinct structure and its cells may contribute the optic nerve (Macdonald *et al.*, 1997). Lastly, the optic cup rotates around its mediolateral axis (Schmitt and Dowling, 1994). This is the final major morphological transformation in zebrafish eye development.

## B. Neurogenesis

At the beginning of the second day of development, the zebrafish neural retina still consists of a single sheet of pseudostratified neuroepithelium. Similar to other epithelia, the retinal neuroepithelium is a highly polarized tissue, characterized by apicobasal nuclear movements, which correlate with cell cycle phase (Baye and Link, 2007; Das *et al*., 2003; Hinds and Hinds, 1974). Nuclei of cells that are about to divide migrate to the apical surface of the neuroepithelium, where both nuclear division and cytokinesis take place. After the division, the newly formed nuclei move back to more basal locations. Although it has been assumed for a long time that dividing cells lose their contact with the basal surface of the neuroepithelium (Hinds and Hinds, 1974), more recent two-photon imaging studies in zebrafish show that this view is most likely incorrect, as a tenuous cytoplasmic process extends toward the basal surface during nuclear division of the neuroepithelial cell (Das *et al*., 2003). Interestingly, in the brain neuroepithelium, and possibly in the retina, this process splits into two or more prior to the cytokinesis, and the daughter processes are inherited either symmetrically or asymmetrically by the daughter cells (Kosodo *et al*., 2008).

In between mitotic divisions, the movement of cell nuclei is stochastic most of the time, so that persistent nuclear movements, directed either basally or apically, occur during less than 10% of the cell cycle (Norden *et al*., 2009). The maximum depth of basally directed translocation is very heterogeneous, ranging from 10% to 90% of neuroepithelial thickness. Interestingly, deeper nuclear migration correlates with divisions that generate postmitotic cells (Baye and Link, 2007). Mitotic divisions are observed nearly exclusively at the apical surface of the neuroepithelium until about 1.5 dpf. Following that, between 40 and 50 hpf, ca. 50% of mitoses occur in the inner nuclear layer (INL) (Godinho *et al*., 2005). Very few mitotic divisions are observed in the central retina at later stages.

Despite its uniform morphology, the retinal neuroepithelium is the site of many transformations, apparent in the changes of cell cycle length and in the dynamic characteristics of gene expression patterns. After a period of very slow cell cycle progression during early stages of optic cup morphogenesis, the cell cycle shortens to ca. 10 h by 24 hpf, and later its duration appears even shorter (Baye and Link, 2007; Hu and Easter, 1999; Li *et al*., 2000a; Nawrocki, 1985). Imaging of individual neuroepithelial cells between 24 and 40 hpf revealed that their cell cycle varies greatly in length from about 4 to 11 h, averaging ca. 6.5 h (Baye and Link, 2007). The significance of changes in the length of the cell cycle, or the genetic mechanisms that regulate them, are not understood.

In parallel to fluctuations of cell cycle length, the expression patterns of numerous genes display dramatic changes in the retinal neuroepithelium during this time. While the transcription of some early expressed genes, such as *rx3* or *six3*, is downregulated, other genes become active. The zebrafish *atonal 5* homolog, *lakritz*, is one interesting example of an important genetic regulator characterized by a dynamic expression pattern. The *lakritz* gene becomes transcriptionally active in a small group of cells in the ventral retina by 25 hpf, and from there its expression spreads into the nasal, dorsal, and finally temporal eye (Masai *et al*., 2000). This gradual advance of expression around the retinal surface is noteworthy because it characterizes many other developmental regulators and neuronal differentiation markers (reviewed in Pujic and Malicki, 2004).

Another noteworthy feature of neuroepithelial cells is the orientation of their mitotic spindles. The mitotic spindle position and its role in cell fate determination has been interesting, albeit contentious issue. It has been proposed that in some species the vertical (apico-basal) reorientation of the mitotic spindle characterizes asymmetric cell divisions, which produce cells of different identities: a progenitor cell and a postmitotic neuron for example (Cayouette and Raff, 2003; Cayouette *et al*., 2001). As such divisions first appear in the neuroepithelium at the onset of neurogenesis, so should vertically oriented mitotic spindles. The analysis of zebrafish neuroepithelial cells found, however, little support for the presence of vertically oriented mitotic spindles: the majority, if not all, of zebrafish neuroepithelial cells divide horizontally (Das *et al*., 2003).

As the morphogenetic movements that shape and orient the optic cup come to completion, the first retinal cells become postmitotic and differentiate. Gross morphological characteristics of the major retinal cell classes are very well conserved in all vertebrates. Six major classes of neurons arise during neurogenesis: ganglion, amacrine, bipolar, horizontal, interplexiform, and photoreceptor cells. The Müller glia are also generated in the same period. Ganglion cell precursors are the first to become postmitotic in a small patch of ventrally located cells between 27 and 28 hpf (Hu and Easter, 1999; Nawrocki, 1985). The early onset of ganglion cell differentiation is again conserved in many vertebrate phyla (Altshuler *et al*., 1991). Similar to expression patterns that characterize the genetic regulators of retinal neurogenesis, differentiated ganglion cells first appear in the ventral retina, nasal to the optic nerve (Burrill and Easter, 1995; Schmitt and Dowling, 1996). The rudiments of the ganglion cell layer are recognizable in histological sections by 36 hpf. Approximately 10 h after the first ganglion neuron progenitors exit the cell cycle, cells that contribute to the INL also become postmitotic. Again, this first happens in a small ventral group of cells (Hu and Easter, 1999). By 34–36 hpf, and possibly even earlier, terminal divisions of retinal progenitor cells give rise to pairs of ganglion and photoreceptor cells, indicating that these two cell classes are generated in overlapping windows of time (Poggi *et al*., 2005).

By 60 hpf, over 90% of neurons in the central retina are postmitotic, and the major neuronal layers are distinguishable by morphological criteria. Cells of different layers become postmitotic in largely non-overlapping windows of time. This is particularly obvious for ganglion cell precursors, most of which, if not all, are postmitotic before the first INL cells exit the cell cycle (Hu and Easter, 1999). This is different from *Xenopus*, where the times of cell cycle exit for different cell classes overlap extensively (Holt *et al*., 1988). In contrast to mammals, neurogenesis in teleosts and larval amphibians continues at the retinal margin throughout the lifetime of the organism (Marcus *et al*., 1999). In adult zebrafish, as well as in other teleosts, neurons are also added in the outer nuclear layer. In contrast to the marginal zone, where many cell types are generated, only rods are added in the outer nuclear layer of the adult (Mack and Fernald, 1995; Marcus *et al*., 1999).

Photoreceptor morphogenesis starts shortly after the exit of photoreceptor precursor cells from the cell cycle (reviewed in Tsujikawa and Malicki, 2004a). The photoreceptor cell layer can be distinguished in histological sections by 48 hpf. The expression of visual pigments, opsins, is necessary for photoreceptor outer segment differentiation. Rods are the first to express opsin around 50 hpf, shortly followed by blue and red cones, and somewhat later by short single cones (Raymond *et al*., 1995; Robinson *et al*., 1995; Takechi *et al*., 2003). Photoreceptor outer segments first appear in the ventral patch by 60 hpf, and ribbon synapses of photoreceptor synaptic termini are detectable by 62 hpf (Branchek and Bremiller, 1984; Schmitt and Dowling, 1999). The photoreceptor cell layer of the zebrafish retina contains five types of photoreceptor cells: rods, short single cones, long single cones, and short and long members of double cone pairs. The differentiation of morphologically distinct photoreceptor types becomes apparent by 4 dpf, and by 12 dpf all zebrafish photoreceptor classes can be distinguished on the basis of their morphology (Branchek and Bremiller, 1984).

The photoreceptor cells of the zebrafish retina are organized in a regular pattern, referred to as the "photoreceptor mosaic." In the adult, cones form regular rows. The spaces between these rows are occupied by rods, which do not display any obvious pattern. Within a single row of cones, double cones are separated from each other by alternating long and short single cones. Adjacent rows of cones are staggered relative to each other so that short single cones of one row are flanked on either side by long single cones of the two neighboring rows (Fadool, 2003; Larison and Bremiller, 1990). In addition to morphology, individual types of photoreceptors are uniquely characterized by spectral sensitivities and visual pigment expressions. Long single cones express blue light-sensitive opsin; short single cones, ultraviolet (UV)-sensitive opsin; double cones, red-sensitive and green-sensitive opsins; whereas rods express rod opsin (Hisatomi *et al*., 1996; Raymond *et al*., 1993). The number of opsin genes exceeds the number of photoreceptor types, as two and four independent loci encode red and green opsins, respectively (Chinen *et al*., 2003). Each green and red opsin gene is expressed in a different subpopulation of double cones. Of the two red opsin genes, LWS-2 is expressed in the central retina, while LWS-1 in the retinal periphery (Takechi and Kawamura, 2005). Similarly, the expression domains of green opsin genes RH2-1 and RH2-2 occupy largely overlapping areas in the central retina, while RH2-3 and RH3-4 are expressed at the retinal circumference in what appears to be non-overlapping regions (Takechi and Kawamura, 2005).

## C. Development of Retinotectal Projections

As this aspect of retinal development is discussed at length in an accompanying chapter (Chapter 1), here we comment on some of the most basic observations only. The neuronal network of the retina is largely self-contained. The only retinal neurons that send their projections outside are the ganglion cells. Their axons navigate through the midline of the ventral diencephalon into the dorsal part of the midbrain, the optic tectum. The ganglion cells extend axons shortly after their final mitosis, already while they are migrating toward the vitreal surface (Bodick and Levinthal, 1980). The projections proceed toward the inner surface of the retina and subsequently along the inner limiting membrane toward the optic nerve head. In zebrafish, the first ganglion cell axons exit the eye between 34 and 36 hpf and navigate along the optic stalk and through the ventral region of the brain toward the midline (Burrill and Easter, 1995; Macdonald and Wilson, 1997). At about 2 dpf, the zebrafish optic nerve contains ca. 1800 axons at the exit point from the retina (Bodick and Levinthal, 1980). Cross sections near the nerve head reveal a crescent-shaped optic nerve. Axons of centrally located ganglion cells occupy the outside (dorsal) surface of the crescent whereas the axons of more peripheral (younger) cells localize to the inside (ventral) surface of the optic nerve. With the exception of the axonal trajectories of cells separated by the choroid fissure, axons of neighboring ganglion cells travel together in the optic nerve (Bodick and Levinthal, 1980). In addition to ganglion cell axons, the optic nerve contains retinopetal projections, which appear considerably later, after 5 dpf, and originate in the nucleus olfactoretinalis of the rostral telencephalon (Burrill and Easter, 1994). After crossing the midline, the axonal projections of the ganglion cells split into the dorsal and ventral branches of the optic tract. The ventral branch contains mostly axons of the dorsal retinal ganglion cells, and the dorsal branch mostly of the ventral cells (Baier *et al*., 1996). The growth cones of the retinal ganglion cells first enter the optic tectum between 46 and 48 hpf. In addition to the optic tectum, the retinal axons innervate nine other, much smaller targets in the zebrafish brain (Burrill and Easter, 1994).

Spatial relationships between individual ganglion cells in the retina are precisely reproduced by their projections in the tectum. The exactitude of this pattern has long fascinated biologists and has been a subject of intensive research in many vertebrate species (Drescher *et al*., 1997; Fraser, 1992; Sanes, 1993). The spatial coordinates of the retina and the tectum are reversed. The ventral-nasal ganglion cells of the zebrafish retina project to the dorsal-posterior optic tectum whereas the dorsal-temporal cells innervate the ventral-anterior tectum (Karlstrom *et al*., 1996; Stuermer, 1988; Trowe *et al*., 1996). By 72 hpf, axons from all quadrants of the retina are in contact with their target territories in the optic tectum.

In summary, development of the zebrafish retina proceeds at a rapid pace. By the end of day 3, all major retinal cell classes have been generated and are organized in distinct layers (Fig. 2B), the photoreceptor cells have developed outer segments, and the ganglion cell axons have innervated their target, the optic tectum. It is also about this time that the zebrafish visual system becomes functional (Clark, 1981; Easter and Nicola, 1996). The brevity of eye morphogenesis and retinal neurogenesis is a major advantage of the zebrafish eye as a model system.

## D. Non-Neuronal Tissues

In many vertebrates, the retina is intimately associated with some form of the vascular system (Wise *et al*., 1971). The mature zebrafish retina features two vessel systems: the choroidal and retinal vasculatures. The first of these tightly surrounds the retinal pigment epithelium, while the second differentiates on the inner surface of the retina (Alvarez *et al*., 2007; Kitambi *et al*., 2009). The development of the eye vasculature can be efficiently visualized using transgenic lines. Carriers of the fli-GFP and flk-GFP transgenes are suitable for this purpose (Choi *et al*., 2007; Lawson and Weinstein, 2002). In these strains, GFP-positive cells first appear in the retinal choroid fissure and the retina toward the end of the first 24 h of embryogenesis (Kitambi *et al*., 2009). By 48 hpf, a vascular bed forms on the medial surface of the lens (Alvarez *et al*., 2007; Kitambi *et al*., 2009). Initially, retinal blood vessels appear to adhere tightly to the lens. As the organism matures, however, vasculature appears to progressively lose contact with the lens and starts to adhere to the vitreal surface of the eye (Alvarez *et al*., 2007). In contrast to many mammals, including primates, blood vessels do not penetrate the neural retina in zebrafish (Alvarez *et al*., 2007). In addition to the vasculature, several other non-neuronal ocular tissues, such as the cornea, the iris, the ciliary body, and the lens, have been characterized in the zebrafish in detail (Dahm *et al*., 2007; Gray *et al*., 2009; Soules and Link, 2005; Zhang *et al*., 2009; Zhao *et al*., 2006).

## III. Analysis of Wild-Type and Mutant Visual System

A major goal of eye research in zebrafish is to characterize phenotypes obtained in the course of new generations of forward and reverse genetic studies as well as small-molecule screens. Diverse research approaches are available to study the zebrafish retina. This chapter provides an overview of the available methods. While some techniques are described in detail, the majority are discussed only briefly because of space constraints, and references to sources of more comprehensive protocols are provided. Where applicable, other chapters of this volume are referenced as the source of more complete information. Table I lists some of the most important techniques currently available for the analysis of the zebrafish retina.

After 30 hpf, the observations of retinal development in the zebrafish embryo are hampered by the differentiation of pigment granules in the RPE. In immunohistochemical experiments, for example, the staining pattern is not accessible to visual inspection in whole embryos unless they are sectioned or their pigmentation is inhibited. To inhibit pigmentation, embryos are raised in media containing 1-phenyl-2-thiourea (PTU). Concentrations ranging from 75 to 200 μM are recommended (Karlsson *et al*., 2001; Westerfield, 2000). Starting between 2 and 3 dpf, embryogenesis is somewhat delayed in PTU-treated embryos, hatching is inhibited, and pectoral fins are abnormal (Karlsson *et al*., 2001). Appropriate controls have to be included to account for these deviations from normal embryogenesis. An additional disadvantage of using PTU is that it does not inhibit the differentiation of iridophores, which are present on the surface of the eye by 42 hpf, and by 4 dpf are dense enough to impair visualization of retinal cells with fluorescent probes. An alternative to using PTU is to conduct experiments on pigmentation-deficient animals. *albino; roy* double mutant line is the most useful for this purpose as it lacks both RPE pigmentation and iridophores (Ren *et al*., 2002). As crossing a mutation of interest into a pigmentation-deficient background takes two generations (or about 6 months), this approach is, however, time consuming.

### A. Histological Analysis

Following morphological description, the first and the simplest step in the analysis of a phenotype is histological examination. It allows one to evaluate the major cell classes in the retina at the resolution that whole-mount preparations do not offer. Given the exquisitely precise organization of retinal neurons, histological analysis on tissue sections is frequently very informative. Plastic sections in particular offer very good tissue preservation and thus reveal fine detail. Prior to sectioning, tissue samples are usually embedded in either epoxy (epon, araldite) or in methacrylate (JB4) resins (Polysciences Inc.). Epoxy resins can be used for both light and electron microscopy. Several fixation methods suitable for plastic sections are routinely used (Li *et al*., 2000b; Malicki *et al*., 1996). For light microscopy, plastic sections are frequently prepared at 1–8 μm thickness

**Table I**
**Techniques Available to Study the Zebrafish Retina and Their Sources/Examples of Use**

| Protocol | Goal | Sources/Examples of Use |
|---|---|---|
| **Histological analysis** | | |
| Electron microscopy | Evaluation of phenotype on a subcellular level | Allwardt *et al*. (2001), Doerre and Malicki (2002), Kimmel *et al*. (1981) |
| Light microscopy | Evaluation of phenotype on a cellular level | Malicki *et al*. (1996), Schmitt and Dowling (1994) |
| **Molecular marker analysis** | | |
| Antibody staining (whole mount) | Determination of expression pattern on protein level | Schmitt and Dowling (1996) |
| Antibody staining (sections) | Determination of expression pattern on protein level | Pujic and Malicki (2001), Wei and Malicki (2002) |
| *In situ* hybridization—double labeling | Parallel determination of two expression patterns on transcript level | Hauptmann and Gerster (1994), Jowett (2001), Jowett and Lettice (1994), Strahle *et al*. (1994) |
| *In situ* hybridization—frozen sections | Determination of expression pattern on transcript level | Barthel and Raymond (1993), Hisatomi *et al*. (1996) |
| *In situ* hybridization—whole mount | Determination of expression pattern on transcript level | Oxtoby and Jowett (1993), Thisse *et al*. (2004) |
| **Gene function analysis** | | |
| Implantation | Test of function for a factor (most often diffusible) via the implantation of a bead saturated with this substance | Hyatt *et al*. (1996), Martinez-Morales *et al*. (2005) |
| Morpholino knockdown | Test of gene function based on antisense inhibition of its activity | Eisen and Smith (2008), Nasevicius and Ekker (2000), Tsujikawa and Malicki (2004a) |
| Overexpression (DNA injections) | Test of gene function based on enhancement of its activity through DNA injections | Koster and Fraser (2001), Mumm *et al*. (2006) |
| Overexpression (light-mediated RNA/DNA uncaging) | Identification of gene function through enhancement of its activity in selected tissues at specific developmental stages | Ando *et al*. (2001), Ando and Okamoto (2003) |
| Overexpression (RNA injections) | Test of gene function based on enhancement of its activity through RNA injections | Macdonald *et al*. (1995), reviewed in Malicki *et al*. (2002) |
| Overexpression (UAS–GAL4 system) | Test of gene function in selected tissues using stable transgenic lines | Del Bene *et al*. (2008), Scheer and Campos-Ortega (1999) |
| TILLING (targeting induced local lesions in genomes) | Identification of chemically induced mutant alleles in a specific genetic locus | Colbert *et al*. (2001), Wienholds *et al*. (2002) |
| Zinc finger nucleases | Identification of mutant alleles in a specific locus | Doyon *et al*. (2008), Meng *et al*. (2008) |

(*Continued*)

**Table I**
**(*Continued*)**

| Protocol | Goal | Sources/Examples of Use |
|---|---|---|
| **Embryological techniques** | | |
| Cell labeling (caged fluorophore) | Fate determination for a specific group of cells | Take-uchi *et al.* (2003) |
| Cell labeling (iontophoretic) | Determination of morphogenetic movements or cell lineage relationships | Li *et al.* (2000b), Varga *et al.* (1999), Woo and Fraser (1995) |
| Cell labeling (lipophilic tracers) | Analysis of ganglion cell development (for example, retino tectal projection) | Baier *et al.* (1996), Malicki and Driever (1999) Mangrum *et al.* (2002) |
| Cell labeling (fluorescent protein transgenes) | Determination of cell fate and fine differentiation features in living animals | Hatta *et al.* (2006), Mumm *et al.* (2006), Neumann and Nuesslein-Volhard (2000) |
| Mitotic activity detection (BrdU) | Identification of mitotically active cell populations; birth dating | Hu and Easter (1999), Larison and Bremiller (1990), Del Bene *et al.* (2008) |
| Mitotic activity detection (tritiated thymidine) | Identification of mitotically active cell populations; birth dating | Nawrocki (1985) |
| Tissue ablation | Functional test for a field of cells via their removal by surgical means | Masai *et al.* (2000) |
| Transplantation (whole eye) | Test whether a defect (in axonal navigation, for example) originates within or outside the eye | Fricke *et al.* (2001) |
| Transplantation (fragment of tissue) | Functional test for a field of cells via their transplantation to an ectopic position by surgical means | Masai *et al.* (2000) |
| Transplantation (blastomere) | Test of cell autonomy of a mutant phenotype by generating a genetically mosaic embryo | Ho and Kane (1990), Jensen *et al.* (2001), Malicki and Driever (1999), Jing and Malicki (2009) |
| **Behavioral tests** | | |
| Optokinetic response | Test of vision based on eye movements; allows for evaluation of visual acuity | Brockerhoff *et al.* (1995), Clark (1981), Neuhauss *et al.* (1999) |
| Optomotor response | Test of vision based on swimming behavior | Clark (1981), Neuhauss *et al.* (1999) |
| Startle response | Simple test of vision based on swimming behavior | Easter and Nicola (1996) |
| **Electrophysiological tests** | | |
| ERG | Test of retinal function based on the detection of electrical activity of retinal neurons and glia | Avanesov *et al.* (2005), Brockerhoff *et al.* (1995) |

**Table I**
**(*Continued*)**

| Protocol | Goal | Sources/Examples of Use |
|---|---|---|
| **Biochemical approaches** | | |
| Co-immunoprecipitation from embryo extracts | Identification of direct and indirect protein binding partners | Insinna *et al*. (2008), Krock and Perkins (2008) |
| Tandem affinity purification from embryo extracts | Identification of direct and indirect protein binding partners | Omori *et al*. (2008) |
| **Chemical screens** | | |
| Screens of small-molecule libraries | Identification of chemicals that affect a developmental process | Kitambi *et al*. (2008) |
| **Genetic screens** | | |
| Behavioral | Detection of mutant phenotypes by behavioral tests | Muto *et al*. (2005), Neuhauss *et al*. (1999) |
| Histological | Detection of mutant phenotypes via histological analysis of sections | Mohideen *et al*. (2003) |
| Marker/tracer labeling | Detection of mutant phenotypes via staining with antibodies, RNA probes, or lipophilic tracers | Baier *et al*. (1996), Guo *et al*. (1999) |
| Morphological | Detection of mutant phenotypes by morphological criteria | Malicki *et al*. (1996) |
| Transgene guided | Detection of mutant phenotypes in transgenic lines expressing fluorescent proteins in specific cell populations | Xiao *et al*. (2005) |

In this table, we primarily cite experiments performed on the retina. Only where references to work on the eye are not available, we refer to studies of other organs. Most forward genetic approaches such as mutagenesis, mapping, and positional cloning methods do not contain visual system-specific features and thus are not listed in this table. These approaches are discussed in depth in other sections of this volume. Entries are listed alphabetically within each section of the table.

and stained with an aqueous solution of 1% methylene blue and 1% azure II (Humphrey and Pittman, 1974; Malicki *et al*., 1996; Schmitt and Dowling, 1999).

Following transmitted light microscopy, histological analysis of mutant phenotypes can be performed at a higher resolution using electron microscopy. This allows one to inspect morphological details of subcellular structures, such as the photoreceptor outer segments, cell junctions, cilia, synaptic ribbons, mitochondria, and many other organelles (Allwardt *et al*., 2001; Doerre and Malicki, 2002; Schmitt and Dowling, 1999; Tsujikawa and Malicki, 2004b). These subcellular features frequently offer insight into the nature of the process being studied (Avanesov *et al*., 2005; Emran *et al*., 2010). Electron microscopy can be used in combination with diaminobenzidine (DAB) labeling of specific cell populations. Oxidation of DAB results in the formation of polymers which are chelated with osmium tetroxide and subsequently observed in the electron microscope (Hanker, 1979). Prior to microscopic analysis, cells can be selectively DAB-labeled using several approaches: photoconversion (Burrill and Easter, 1995), antibody staining combined with peroxidase detection (Metcalfe *et al*., 1990), or retrograde labeling with horseradish peroxidase (HRP) (Metcalfe, 1985).

## B. The Use of Molecular Markers

A variety of molecular markers are used to study the zebrafish retina before, during, and after neurogenesis. Endogenous transcripts and proteins are among the most frequently used markers, although smaller molecules, such as neurotransmitters, and neuropeptides can also be used (Avanesov *et al*., 2005; Cameron and Carney, 2000). During early embryogenesis, the analysis of marker distribution allows one to determine whether the eye field is specified correctly. Several RNA probes are available to visualize the optic lobe during embryogenesis (Table II). Some of them label all cells of the optic lobe uniformly, while others can be used to monitor the optic stalk area (Table II). After the completion of neurogenesis, cell class-specific markers are used to determine whether particular cell populations are specified and occupy correct positions. Some of these markers are listed in Table II. Many transcript and protein detection methods have been described. Detailed protocols for most of these are available and we reference many of them in Table II. Below we discuss in detail the main types of molecular probes used to study the zebrafish visual system.

### 1. Antibodies

Antibody staining experiments can be performed in several ways. Staining of whole embryos is the least laborious. One has to keep in mind, however, that many antibodies produce high background in whole-mount experiments, and the eye pigmentation needs to be eliminated after 30 hpf as described above. At later stages of development, tissue penetration may become an additional problem. This can be circumvented by permeabilizing larvae via increasing detergent concentration above the standard level of 0.5% (2.5% Triton in both blocking and staining solution works well for anti Pax-2 antibody; see Riley *et al*., 1999) or by enzymatic digestion of embryos (for example

**Table II**
**Selected Molecular Markers Available to Study the Zebrafish Retina**

| Name | Type | Expression pattern | References[a]/Sources |
|---|---|---|---|
| **Optic lobe, optic stalk markers** | | | |
| pax2a (pax 2) | RNA probe & Ab (poly) | Nasal retina, optic stalk (≤24 hpf); ON (2 dpf) | Kikuchi *et al.* (1997), Macdonald *et al.* (1997), *Covance PRB-276P* |
| rx1 (zrx1) | RNA probe | Anterior neural keel, optic primordia (≤11 hpf) | Chuang *et al.* (1999), Pujic and Malicki (2001) |
| rx2 (zrx2) | RNA probe | Anterior neural keel, optic primordia (≤11 hpf) | Chuang *et al.* (1999), Pujic and Malicki (2001) |
| rx3 (zrx3) | RNA probe | Anterior neural plate (≤9 hpf); optic primordia (≤12 hpf) | Chuang *et al.* (1999), Pujic and Malicki (2001) |
| six3a (six3) | RNA probe | Neural keel, optic primordia (≤11 hpf) | Pujic and Malicki (2001), Seo *et al.* (1998) |
| six3b (six6) | RNA probe | Anterior neural keel, optic primordia (≤11 hpf) | Pujic and Malicki (2001), Seo *et al.* (1998) |
| vax2 | RNA probe | Optic stalk (≤15 hpf); optic stalk, ventral retina (≤18 hpf) | Take-uchi *et al.* (2003) |
| **Ganglion cell markers** | | | |
| alcam[b] (neurolin) | RNA probe, Ab (mono & poly) | Ganglion cells (28 hpf, RNA; ≤32 hpf protein) | Fashena and Westerfield (1999), Laessing *et al.* (1994), Laessing and Stuermer (1996), *Zn-5/Zn-8 DSHB* and *ZIRC* |
| cxcr4b | RNA probe | Ganglion cells (30 hpf) | Pujic *et al.* (2006) |
| gc34 | RNA probe | Ganglion cells (≤36 hpf) | Pujic *et al.* (2006) |
| L3 | RNA probe | Ganglion cells (30 hpf) | Brennan *et al.* (1997) |
| Tg (ath5:GFP) | Transgene | Ganglion cells (25 hpf) | Masai *et al.* (2003, 2005) |
| Tg (brn3c: gap43-GFP) | Transgene | Ganglion cells (42 hpf) | Xiao *et al.* (2005) |
| **Amacrine cell markers** | | | |
| Ap2α | RNA probe | Amacrine cells (1.5–2 dpf) | Pujic *et al.* (2006) |
| Ap2β | RNA prove | Amacrine cells (≤36 hpf) | Pujic *et al.* (2006) |
| Choline acetyltransferase | Ab (poly) | Subset in INL and GCL, IPL (≤5 dpf) | Avanesov *et al.* (2005), *Millipore, cat# AB144P* |
| GABA | Ab (poly) | Subset in INL and GCL, IPL (2.5 dpf); ON (2 dpf) | Sandell *et al.* (1994), *Millipore, cat# AB131; Sigma, cat# A2052* |
| GAD67 | Ab (poly) | Subset in INL and few in GCL, IPL (≤7 dpf) | Connaughton *et al.* (1999), Kay *et al.* (2001), *Millipore, cat# AB9706* |
| Hu C/D | Ab (mono) | INL and GCL (≤3 dpf) | Kay *et al.* (2001), Link *et al.* (2000), *Invitrogen, cat# A21271* |
| Neuropeptide Y | Ab (poly) | Subset in INL, IPL (≤4 dpf) | Avanesov *et al.* (2005), *ImmunoStar, cat# 22940* |
| Parvalbumin | Ab (mono) | Subset in INL and GCL, IPL (≤3 dpf) | Malicki *et al.* (2003), *Millipore, cat# MAB1572* |
| pax6a (pax6.1) | RNA probe Ab (poly) | Neuroepithelium (12–34 hpf); INL and GCL (2 dpf); INL (5 dpf) | Hitchcock *et al.* (1996), Macdonald and Wilson (1997) |

(*Continued*)

**Table II**
**(*Continued*)**

| Name | Type | Expression pattern | References[a]/Sources |
|---|---|---|---|
| Serotonin | Ab (poly) | Subset in INL (≤5 dpf) | Avanesov *et al.* (2005), *Sigma, cat# S5545* |
| Somatostatin | Ab (poly) | Subset in INL (≤5 dpf) | Malicki Lab, unpublished data; *ImmunoStar, cat# 20067* |
| Substance P | Ab (mono) | Subset in INL (≤5 dpf) | Malicki Lab, unpublished data; *AbCam, cat# AB6338* |
| Tyrosine hydroxylase | Ab (mono) | Subset in INL (3–3.5 dpf) | Biehlmaier *et al.* (2003), Pujic and Malicki (2001), *ImmunoStar, cat# 22941; Millipore, cat# MAB318* |
| **Bipolar cell markers** | | | |
| vsx1 | RNA probe | Neuroepithelium (31 hpf); outer INL (50 hpf) | Passini *et al.* (1997) |
| vsx2 | RNA probe | Neuroepithelium (24 hpf); primarily or exclusively in the bipolar cells (50 hpf) | Passini *et al.* (1997) |
| Protein kinase C-β1 | Ab (poly) | IPL, OPL (2.5 dpf); bipolar cell somata (4 dpf) | Biehlmaier *et al.* (2003), Kay *et al.* (2001), *Santa Cruz, cat# sc-209* |
| Tg(nyx::Gal4VP16; UAS::MYFP) | Transgene | ON bipolar cells (2.5 dpf) | Schroeter *et al.* (2006) |
| **Horizontal cell markers** | | | |
| Cx 52.6 | Ab (poly) | Horizontal cells (≤7 dpf?) | Shields *et al.* (2007) |
| Cx 55.5 | Ab (poly) | Horizontal cells (≤7 dpf?) | Shields *et al.* (2007) |
| Horizin | RNA probe | Horizontal cells, weak staining in GCL and inner INL (≤60 hpf) | Pujic *et al.* (2006) |
| **Photoreceptor markers** | | | |
| Blue opsin | Ab (poly) | Blue cones (≤3 dpf) | Doerre and Malicki (2001), Vihtelic *et al.* (1999) |
| Blue opsin[c] | RNA probe | Blue cones (52 hpf) | Chinen *et al.* (2003), Raymond *et al.* (1995), Vihtelic *et al.* (1999) |
| Green opsin | Ab (poly) | Green cones (≤3 dpf) | Doerre and Malicki (2001), Vihtelic *et al.* (1999) |
| Green opsins (four genes) | RNA probes | Green cones (40–45 hpf) | Chinen *et al.* (2003), Takechi and Kawamura (2005), Vihtelic *et al.* (1999) |
| NDRG1 | RNA probe | Photoreceptors (36–48 hpf) | Pujic *et al.* (2006) |
| Red opsin | Ab (poly) | Red cones (≤3 dpf) | Doerre and Malicki (2001), Vihtelic *et al.* (1999) |
| Red opsins (two genes) | RNA probes | Red cones (40–45 hpf) | Chinen *et al.* (2003), Raymond *et al.* (1995), Takechi and Kawamura (2005) |
| Rod opsin | Ab (poly) | Rods (≤3 dpf) | Doerre and Malicki (2001), Vihtelic *et al.* (1999) |
| Rod opsin[c] | RNA probe | Rods (50 hpf) | Chinen *et al.* (2003), Raymond *et al.* (1995) |
| Tg (opn1sw1: EGFP) | Transgene | UV cones (≤56 hpf) | Takechi *et al.* (2003) |
| Tg (xops: GFP) | Transgene | Rods | Fadool (2003) |

**Table II**
**(*Continued*)**

| Name | Type | Expression pattern | References[a]/Sources |
|---|---|---|---|
| UV opsin | RNA probe | UV cones (56 hpf) | Hisatomi *et al*. (1996), Takechi *et al*. (2003) |
| UV opsin | Ab (poly) | UV cones (≤3 dpf) | Doerre and Malicki (2001), Vihtelic *et al*. (1999) |
| Zpr1 (FRet 43) | Ab (mono) | Double cones in larvae (48 hpf); double cones &bipolar cell subpopulation in the adult | Larison and Bremiller (1990), *ZIRC* |
| Zpr3 (FRet 11) | Ab (mono) | Rods (50 hpf) | Schmitt and Dowling (1996), *ZIRC* |
| Zs-4 | Ab (mono) | Rod inner segments (adult), onset unknown | Vihtelic and Hyde (2000), *ZIRC* |
| **Müller glia markers** | | | |
| cahz (carbonic anhydrase) | RNA probe Ab (poly) | Müller glia (≤4 dpf) | Peterson *et al*. (1997, 2001) |
| GFAP | Ab (poly) | Müller glia (5 dpf) | Malicki Lab, unpublished data; *DAKO, cat# Z0334* |
| Glutamine synthetase | Ab (poly) | Müller glia (60 hpf) | Peterson *et al*. (2001) |
| Tg (gfap: GFP) | Transgene | Müller glia (48 hpf) | Bernardos and Raymond (2006) |
| **Plexiform layer markers** | | | |
| Phalloidin | Fungal toxin | IPL, OPL, ON (≤60 hpf) | Malicki *et al*. (2003), *Invitrogen, cat# A-12379* |
| Snap-25 | Ab (poly) | OPL, IPL (≤2.5 dpf) | Biehlmaier *et al*. (2003), *StressGen, cat# VAP-SV002* |
| SV2 | Ab (mono) | IPL, OPL (≤2.5 dpf) | Biehlmaier *et al*. (2003), *DSHB* |
| Syntaxin-3 | Ab (poly) | OPL (2.5 dpf); faint IPL (5 dpf) | Biehlmaier *et al*. (2003), *Alamone Labs, cat# ANR-005* |

Approximate time of the expression onset is indicated in parenthesis. Sources of commercially available reagents are listed, including catalog numbers where appropriate. Names of markers are listed alphabetically within each section.

DSHB = Developmental Studies Hybridoma Bank (http://dshb.biology.uiowa.edu); ZIRC = Zebrafish International Resource Center (http://zfin.org/zirc/home/guide.php). dpf = days post fertilization; hpf = hours post fertilization; GCL = ganglion cell layer; INL = inner nuclear layer; IPL = inner plexiform layer; OPL = outer plexiform layer; ON = optic nerve.

[a] When references to work performed on zebrafish are not available, experiments on related fish species are cited.

[b] Zn-5 and Zn-8 antibodies both recognize neurolin (Kawahara *et al*., 2002).

[c] Transcript expression onset was estimated by using goldfish probes (Raymond *et al*., 1995).

collagenase treatment; see Doerre and Malicki, 2002). When background or tissue penetration is a problem, useful alternatives to using whole embryos is staining of either frozen or paraffin sections. Confocal microscopy of retinal sections reduces the background even further, while also enhancing the details of cell architecture.

For cryosectioning, embryos should be fixed as appropriate for a particular antigen and infiltrated in 30% sucrose/phosphate buffered saline (PBS) solution for cryoprotection. While for many antigens simple overnight fixation in 4% paraformaldehyde (PFA) at 4°C is sufficient, some others require special treatments. For example, anti-gamma aminobutyric acid (GABA) staining of amacrine cells requires fixation in both glutaraldehyde and paraformaldehyde (2% each; see Avanesov *et al*., 2005; Sandell *et al*., 1994) (Fig. 3F). Glyoxal-based fixatives (such as Prefer fix supplied by Anatech)

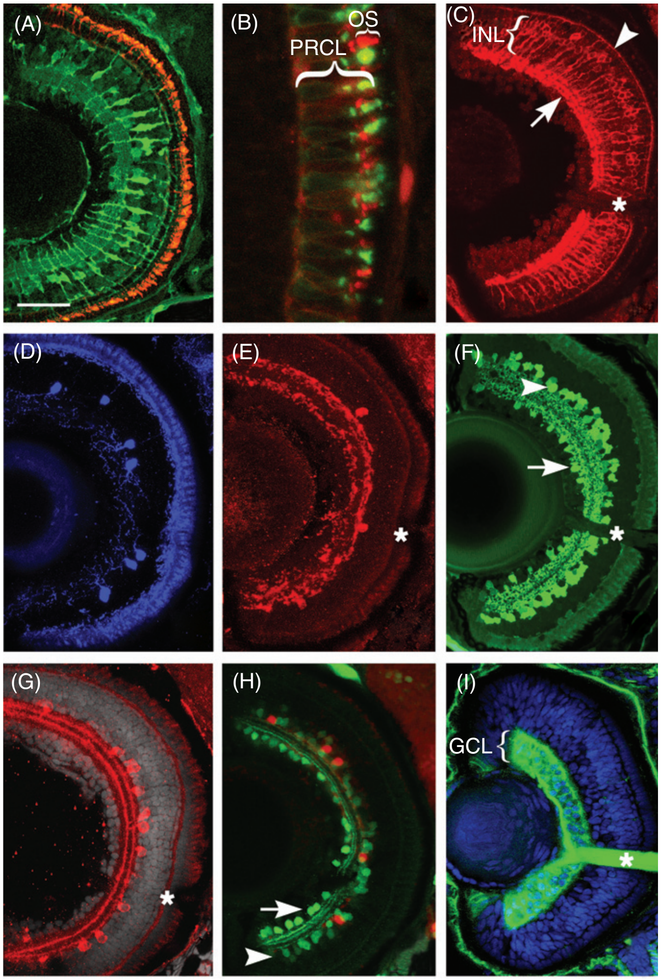

**Fig. 3** *(Continued)*

may also be useful when testing new antibodies (Dapson, 2007; Pathak *et al*., 2007). Fixed specimen can be oriented as desired using molds prepared from Eppendorf tubes that are cut transversely into ca. 3–4 mm wide rings. These are then placed flat on a glass slide and filled with embedding medium (Richard-Allan Scientific Inc.). Embryos are placed in the medium, oriented with a needle, and transferred into a cryostat chamber that is cooled to −20°C. Once the medium solidifies, plastic rings are removed with a razor blade.

Antibody staining can be efficiently performed on 15–30 μm frozen sections, and analyzed by confocal microscopy. For conventional epifluorescence microscopy, thinner sections may be desired. Upon the application of modified infiltration and embedding protocols, 3 μm sections of the zebrafish embryos can be prepared and analyzed using a conventional microscope equipped with UV illumination (Barthel and Raymond, 1990). Some antigens require the application of additional steps during staining protocols, such as antigen retrieval. Sections are immersed in near-boiling solution of 10 mM sodium citrate for 10 min prior to the application of blocking solution. This method significantly improves the labeling of amacrine cell populations by anti-serotonin or anti-choline acetyltransferase antibodies (Fig. 3G and H) (Avanesov *et al*., 2005). Immersion in cold acetone is another treatment that improves staining with some immunoreagents, such as certain anti-gamma-tubulin antibodies (Pujic and Malicki, 2001).

Alternatively, antibody staining can be performed on plastic sections. Anti-GABA antibodies, for example, work very well with this method. Both epoxy (Epon-812,

**Fig. 3** Transverse sections through the center of the zebrafish eye reveal several major retinal cell classes and their subpopulations. (A) Anti-rod opsin antibody detects rod photoreceptor outer segments (red), which are fairly uniformly distributed throughout the outer perimeter of the retina by 5dpf. On the same section, an antibody to carbonic anhydrase labels cell bodies of Müller glia in the INL as well as their radially oriented processes. (B) A higher magnification of the photoreceptor cell layer shows the distribution of rod opsin (red signal) and UV opsin (green signal) in the outer segments (OSs) of rods and short single cones, respectively. (C) A subpopulation of bipolar cells is detected using antibody directed to protein kinase C-β (PKC). While cell bodies of PKC-positive bipolar neurons are situated in the central region of the INL, their processes travel radially into the inner (arrow) and outer (arrowhead) plexiform layers, where they make synaptic connections. (D) Tyrosine hydroxylase-positive interplexiform cells are relatively sparse in the larval retina. (E) Similarly, the distribution of neuropeptide Y is limited to only a few cells per section. (F) The distribution of GABA, a major inhibitory neurotransmitter. GABA is largely found in amacrine neurons in the INL (arrowhead), although some GABA-positive cells are also found in the GCL (arrow). (G) Choline acetyltransferase, an enzyme of acetylcholine biosynthetic pathway, is restricted to a relatively small amacrine cell subpopulation. (H) Antibodies directed to a calcium-binding protein, parvalbumin, recognize another fairly large subpopulation of amacrine cells in the INL (green, arrowhead). Some parvalbumin-positive cells localize also to the GCL and most likely represent displaced amacrine neurons (arrow). By contrast, serotonin-positive neurons (red) are exclusively found in the INL. (I) Ganglion cells stain with the Zn-8 antibody directed to neurolin, a cell surface antigen (Fashena and Westerfield, 1999). In addition to neuronal somata, strong Zn-8 staining exists in the optic nerve (asterisk). In all panels lens is left, dorsal is up. A–H show the retina at 5dpf, while I shows a 3dpf retina. Asterisks indicate the optic nerve. Scale bar equals 50 μm in A and C–I and 10 μm in B. dpf, days post fertilization; GCL, ganglion cell layer; INL, inner nuclear layer; OS, outer segments; PRCL, photoreceptor cell layer. Panels D, G, and H are reprinted from Pujic and Malicki (2004) with permission from Elsevier. (See Plate no. 8 in the Color Plate Section.)

Electron Microscopy Sciences Inc.) and methacrylate (JB-4, Polysciences Inc.) resins can be used as the embedding medium. This improves the quality of staining, as plastic sections preserve tissue morphology better, compared to frozen ones. In the GABA staining protocol, primary antibody can be detected using avidin–HRP conjugate (Vector Laboratories Inc.) or a fluorophore-conjugated secondary antibody (Fig. 2F and Malicki and Driever, 1999; Sandell *et al*., 1994). An extensive collection of antibodies that can be used to visualize features of the retina in the adult zebrafish has been also characterized (Yazulla and Studholme, 2001).

## 2. mRNA Probes

*In situ* hybridization with most RNA probes works very well on whole embryos (Oxtoby and Jowett, 1993). Following hybridization, embryos are gradually dehydrated in a series of ethanol solutions of increasing concentration, and embedded in plastic as described above (Pujic and Malicki, 2001). An additional fixation step prior to dehydration reduces the leaching of *in situ* signal (Westerfield, 2000). Expression patterns are then analyzed on 1–5 μm thick sections. Several *in situ* protocols are available to monitor the expression of two genes simultaneously (Jowett, 2001, and references in Table II; Jowett and Lettice, 1994). In the experiment shown in Fig. 4B, expression patterns of two opsins are detected simultaneously using two different chromogenic substrates of alkaline phosphatase (AP) (Hauptmann and Gerster, 1994). *In situ* hybridization can also be combined with antibody staining (Novak and Ribera, 2003; Prince *et al*., 1998). In embryos older than 5 dpf, *in situ* reagents sometimes do not penetrate to the center of the retina. In such cases, hybridization procedures can be performed more successfully on sections (Hisatomi *et al*., 1996). Given the small size of zebrafish embryos, *in situ* hybridization experiments can be performed in a high-throughput fashion using hundreds or even thousands of probes to screen for genes expressed in specific organs, tissues, or even specific cell types (Thisse *et al*., 2004). In recent years, *in situ* hybridization could also be performed using robotic devices that carry out most of the tedious steps, including hybridizations and washes (Intavis Bioanalytical Instruments AG). This approach was also applied to the retina and led to the identification of numerous transcripts expressed in subpopulations of retinal cells (Pujic *et al*., 2006). Some of these transcripts can be used as markers of specific retinal cell classes (Table II).

## 3. Lipophilic Tracers

Details of cell morphology can also be studied using lipophilic carbocyanine dyes, DiI, DiO, and others, which label cell membranes (Honig and Hume, 1986; 1989). In the retina, these are especially useful in the analysis of ganglion cells. Carbocyanine dyes can be used as anterograde as well as retrograde tracers. When applied to the retina, DiI and DiO allow one to trace the retinotectal projections (Baier *et al*., 1996). When applied to the optic tectum or the optic tract, they can be used to determine the position of ganglion cell perikarya, and even to study the stratification and branching

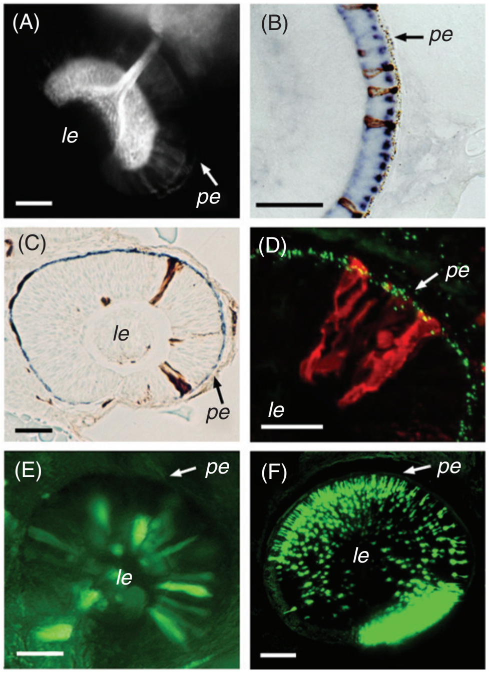

**Fig. 4** Selected techniques available to study neurogenesis in the zebrafish retina. (A) DiI incorporation into the optic tectum retrogradely labels the optic nerve and ganglion cell somata. (B) A transverse plastic section through the zebrafish retina at 3 dpf. *In situ* mRNA hybridization using two probes, each targeted to a different opsin transcript and detected using a different enzymatic reaction, visualizes two types of photoreceptor cells. (C) A plastic section through a genetically mosaic retina at ca. 30 hpf. Biotinylated dextran-labeled donor-derived cells incorporate into retinal neuroepithelial sheet of a host embryo and can be detected using HRP staining (brown precipitate). (D) A transverse cryosection through a genetically mosaic zebrafish eye at 36 hpf. In this case, donor-derived clones of neuroepithelial cells are detected with fluorophore-conjugated avidin (red). The apical surface of the neuroepithelial sheet is visualized with anti-γ-tubulin antibody, which stains centrosomes (green). (E) GPF expression in the eye of a zebrafish embryo following injection of a DNA construct containing the GFP gene under the control of a heat-shock promoter. The transgene is expressed in only a small subpopulation of cells. (F) A confocal z-series through the eye of a living transgenic zebrafish, carrying a GFP transgene under the control of a rod opsin promoter (Fadool, 2003). Bright expression is present in rod photoreceptor cells (ca. 3 dpf). Scale bar, 50 μm. pe, pigmented epithelium; le, lens. Panel E reprinted from Malicki *et al*. (2002) with permission from Elsevier.

of ganglion cell dendrites (Burrill and Easter, 1995; Malicki and Driever, 1999; Mangrum *et al*., 2002). Since DiI and DiO have different emission spectra, they can be used simultaneously to label different cell populations (Baier *et al*., 1996).

## 4. Fluorescent Proteins

Fluorescent proteins (hereafter FPs), frequently fused to other polypeptides, offer a very rich source of markers to visualize tissues, cells, and even subcellular structures.

These can be expressed in embryos either transiently or from stably integrated transgenes. Numerous derivatives of two FPs—green fluorescent protein (GFP, from jellyfish, *Aequorea victoria*) and red fluorescent protein (RFP, from coral species)—are currently available (reviewed in Shaner *et al*., 2007) and differ in brightness as well as emission spectra. Many of them have been applied in zebrafish. The uses of FPs can be grouped in at least three categories:

1. **Visualization of gene activity**. The purpose of these experiments is to determine where and when a gene of interest is transcribed. Although the same goal can be accomplished using *in situ* hybridization, the use of FP fusions may result in higher sensitivity of detection (see for example a sonic hedgehog study by Neumann and Nuesslein-Volhard, 2000), and, importantly, allow one to create time-lapse images tracking spatial-temporal changes in gene expression. The biggest challenge in this type of study is the need to include all regulatory elements in the transgene to faithfully recapitulate the expression of the endogenous transcript. The best way to accomplish that is to insert an FP coding sequence into the open reading frame of a gene derived from a phage or bacterial artificial chromosome (PAC or BAC). For example, to study the expression of zebrafish green opsin genes, a modified PAC clone of ca. 85 kb was used to generate transgenic lines. To visualize expression, the first exon after the initiation codon was replaced with a GFP sequence in each of these genes (Tsujimura *et al*., 2007). The use of artificial chromosomes is frequently necessary as distant regulatory elements are likely to affect the expression of a given gene. One has to note, however, that even using an artificial chromosome does not assure that all relevant regulatory elements will be included in the transgene.

   In some experiments, when temporal characteristics of expression need to be faithfully reproduced, excessive stability of FP may pose a problem. FPs tend to be stable in the cell's cytoplasm and may persist for much longer than the transcript of the gene being studied, making it difficult to determine when the gene of interest is turned off. To circumvent this difficulty, FPs characterized by reduced stability, such as dRFP (destabilized RFP) or short half-life GFP, are available (Yeo *et al*., 2007; Yu *et al*., 2007). dRFP was used, for example, to study Notch pathway activity in the zebrafish retinal neuroepithelium (Del Bene *et al*., 2008).
2. **Visualization of the subcellular localization of proteins**. In this type of experiment, it is not necessary to recapitulate the tissue distribution of the protein being studied and thus expression can be driven ubiquitously. Consequently, transient expression methods based on mRNA or DNA injection are preferred. Although they usually do not allow for the targeting of expression to particular tissues, they are much less time consuming, compared to using stable transgenic lines. The expression of FP fusions is especially valuable when antibodies are difficult to generate, as has been the case for the Elipsa protein, for example (Omori *et al*., 2008). This procedure is not without drawbacks, however. First, adding GFP polypeptide to a protein may change its binding properties, and thus cause aberrant localization in the cell. Second, as FP fusions are frequently expressed at a higher level compared to their wild-type

counterparts, they may display nonspecific binding. Finally, fusion proteins may be toxic to cells. These problems can be largely, although not entirely, eliminated by placing FP tags in multiple locations and testing whether the resulting fusion proteins can rescue mutant/morphant phenotypes.

3. **Monitoring of fate, differentiation, and cell physiology**. In these studies, FP fusions are used solely to mark cells and/or subcellular structures. In the simplest case, this approach can be used to monitor the gross morphology of the cell and its survival. In more sophisticated variants of this technique, one monitors cell division patterns, migration trajectories, or specific aspects of cell morphology, such as the shape of dendritic processes, subcellular distribution of organelles, or intracellular transport. Zebrafish FP transgenic lines have been generated to monitor the differentiation of fine morphological features of various retinal cell classes, including bipolar interneurons (Schroeter *et al.*, 2006), horizontal interneurons (Shields *et al.*, 2007), amacrine interneurons (Godinho *et al.*, 2005; Kay *et al.*, 2004), ganglion cells (Xiao *et al.*, 2005), and Müller glia (Bernardos and Raymond, 2006) (Table II). These transgenic lines allow one to continuously observe fine features of cells, and even follow the entire trajectory of the retinotectal projection, or the phylopodia of differentiating bipolar cell axon terminals. In most studies conducted so far, FP fusions were expressed from stably integrated transgenes, although in some cases the GAL4–VP16-based system (Koster and Fraser, 2001, see below) is used to drive transient expression in retinal interneurons (Mumm *et al.*, 2006; Shields *et al.*, 2007). While generating stable transgenic lines, it is necessary to compare expression patterns from at least two different transgenic lines since the integration of same construct can produce very different expression patterns in different lines, due to position-specific effects. For example, depending on the integration site, a hexamer of the DF4 regulatory element of the Pax6 gene can drive expression either throughout the retina or in subsets of amacrine cells (Godinho *et al.*, 2005; Kay *et al.*, 2004).

In some experimental contexts, FPs can also be used to monitor the behavior of cellular organelles. This is accomplished by generating FPs fused to subcellular localization signals or to entire proteins that display a desirable subcellular localization. The H2A-GFP transgene, for example, allows one not only to visualize cell nuclei but also to distinguish when cells undergo mitosis, and even to determine the orientation of mitotic spindles in the retinal neuroepithelium (Cui *et al.*, 2007; Pauls *et al.*, 2001). Similarly, GFP-centrin can be used to monitor the position of the centrosome in differentiating ganglion cells (Zolessi *et al.*, 2006), and GFP fused to a mitochondrial localization sequence can be applied to observe the distribution of mitochondria (Kim *et al.*, 2008). GFP fused to the 44 C-terminal amino acids of rod opsin is targeted to the photoreceptor outer segment and can be used as a specific marker of this structure (Perkins *et al.*, 2002). FPs can also be applied to mark specific cell membrane domains: PAR-3/EGFP fusion, for example, labels the apical surface of retinal neuroepithelial cells (Zolessi *et al.*, 2006).

Photoconvertible FPs are yet another class of markers that can be used to visualize cell morphology. Kaede and Dronpa have been used most frequently in the zebrafish so far (Aramaki and Hatta, 2006; Hatta *et al*., 2006; Sato *et al*., 2006). Kaede is irreversibly converted from green to red fluorescence using UV irradiation, whereas Dronpa green fluorescence can be reversibly activated and deactivated multiple times by irradiating it with blue and UV light, respectively. The advantage of these FPs is that they can be used to reveal morphology of single neurons by selective photoconversion in the cell soma (anterograde labeling) or in cell processes (retrograde labeling). This is particularly useful when appropriate regulatory elements are not available to drive FP expression in specific cell populations. Moreover, one can potentially use photoactivatable FPs to trace the journey of tagged proteins within cells. Although as yet this approach has not been applied in the zebrafish retina, it is potentially useful to analyze protein trafficking in photoreceptor cells.

The number of different FPs and the variety of their applications in zebrafish have been growing at a breathtaking pace. Given the multitude of available promoter sequences, the diversity of spectral variants, and the variety of methods for protein expression in the zebrafish embryo, one is frequently confronted with the task of generating multiple combinations of regulatory elements and FP tags. This is made easier by recombination cloning approaches (Kwan *et al*., 2007; Villefranc *et al*., 2007; see the description of the Gateway cloning system on page 241). The use of FPs to monitor the divisions, movements, and differentiation of cells and their organelles has been one of the fastest growing approaches in the studies of zebrafish embryogenesis.

## C. Analysis of Cell Movements and Lineage Relationships

The best-established and the most versatile approach to cell labeling in living zebrafish embryos is iontophoresis. This technique was applied in numerous zebrafish cell fate studies (Collazo *et al*., 1994; Devoto *et al*., 1996; Raible *et al*., 1992). In the context of visual system development, iontophoretic cell labeling was used to determine the developmental origins of the optic primordium (Woo and Fraser, 1995) and later to study cell rearrangements that accompany optic cup morphogenesis (Li *et al*., 2000b). A potentially very informative variant of cell fate analysis is to perform it in the retinae of mutant animals (Poggi *et al*., 2005; Varga *et al*., 1999). Iontophoretic cell labeling has been applied to study cell lineage relationships in the developing retina of *Xenopus laevis* (Holt *et al*., 1988; Wetts and Fraser, 1988). Lineage analysis has been performed in the zebrafish retina to a very limited extent, perhaps because of the perception that it would be unlikely to add much to the results previously obtained in higher vertebrates (Holt *et al*., 1988; Turner and Cepko, 1987; Turner *et al*., 1990). An alternative to iontophoresis is the activation of caged fluorophores using a laser beam. Caged flourescein (Molecular Probes, Inc.) is particularly popular in this type of experiment, and was applied to study cell fate changes caused by a double knockdown of *vax1* and *vax2* gene function (Take-uchi *et al*., 2003). One study of lineage relationships in the zebrafish eye also took advantage of a transgenic line that expresses GFP in retinal progenitor cells (Poggi *et al*., 2005).

## D. Analysis of Cell and Tissue Interactions

Transplantation techniques are used to reveal cell or tissue interactions. The size of a transplant varies from a small group of cells, or even a single cell, to the entire organ. In the case of mutations that affect retinotectal projections, it is important to determine whether defects originate in the eye or in brain tissues. This can be accomplished by transplanting the entire optic lobe at 12 hpf, and allowing the animals to develop until desired stages (Fricke *et al*., 2001). Smaller size fragments of tissue can be transplanted to document cell–cell signaling events within the optic cup. This approach was used to demonstrate inductive properties of the optic stalk tissue, and to test the presence of cell–cell interactions within the optic cup (Kay *et al*., 2005; Masai *et al*., 2000). Transplantation can also be used to study interactions between the lens and the retina. Lens transplantation is performed following a procedure similar to that developed for *Astyanax mexicanus* (Yamamoto and Jeffery, 2002) and recently applied to zebrafish (Zhang *et al*., 2009)

Mosaic analysis is a widely used approach that combines genetic and embryological manipulations (Ho and Kane, 1990). The goal of such experiments is to determine the site of the genetic defect responsible for a mutant phenotype. In simple terms, cell-autonomous phenotypes are caused by gene function defects within the affected cells, while cell-nonautonomous phenotypes are caused by defects in other (frequently neighboring) cells. In contrast to approaches used in *Drosophila*, genetic mosaics in zebrafish are generated via blastomere transplantation, essentially a surgical procedure performed on the early embryo (Ho and Kane, 1990; Westerfield, 2000). As this technique has been widely used in zebrafish, also in the context of eye development, we provide a more extensive description of how it is applied.

In the first step, the donor embryos are labeled at the one- to eight-cell stage with a cell tracer. Dextrans conjugated with biotin or a fluorophore are the most commonly used tracers, and frequently a mix of both is used. The choice of the tracer depends on how it is going to be detected during later stages of the experiment, when the fate of donor-derived cells is analyzed. Within a few minutes after injection into the yolk, tracers diffuse throughout the embryo, labeling all blastomeres. Subsequently, starting at about 3 hpf, blastomeres are transplanted from tracer-labeled donor embryos to unlabeled host embryos using a glass needle. The number of transplanted blastomeres usually varies from a few to hundreds, depending on the experimental context. One donor embryo is frequently sufficient to supply blastomeres for several hosts. The transplanted blastomeres become incorporated into the host embryo and randomly contribute to various tissues, including those of experimental interest. To increase the frequency of donor-derived cells in the retina, blastomeres should be transplanted into the animal pole of a host embryo (Moens and Fritz, 1999). Cells in that region will later contribute to eye and brain structures (Woo and Fraser, 1995). Embryos that contain descendants of donor blastomeres in the eye are identified using UV illumination between 24 and 30 hpf, when the retina is only weakly pigmented and contains large radially oriented neuroepithelial cells (Fig. 4C and D). An elegant way to control cell autonomy tests is to transplant cells from two donor embryos—one wild type, one mutant—into a single host (Ho and Kane, 1990). In such a case, each of the donors has to be labeled with a different tracer.

Tracer purity and the quality of the transplantation needle are two important technical aspects of mosaic analysis. To increase the survival rate of donor embryos and transplanted cells, it is important to purify dextran by filtering it through a spin column several times (Microcon YM-3, Millipore Inc.). This procedure removes small molecular weight contaminants that are toxic for cells. The preparation of transplantation needle requires considerable manual dexterity, and is fairly time consuming. A good transplantation needle has several features: (1) a smooth opening with a diameter that is slightly larger than blastomeres at the "high" stage (Kimmel *et al*., 1995); (2) a fairly constant width near the tip; (3) lumen free of glass debris, which frequently accumulate when the needle is beveled; and (4) a sharp glass spike at the very tip, to help in penetrating the embryo. Needle preparation requires two instruments: a beveler and a microforge, available from WPI and Narishige, respectively. Useful technical details of needle preparation and other aspects of blastomere transplantation protocol are provided in *The Zebrafish Book* (Westerfield, 2000).

Following successful transplantations, the analysis of donor-derived cells in mosaic embryos can proceed in several ways. In the simplest case, the donor-derived cells are labeled with a fluorescent tracer or a transgene and directly analyzed in whole embryos using conventional or confocal miscroscopy (Zolessi *et al*., 2006). Such analysis is sufficient to provide information about the position and sometimes the morphology of donor-derived cells. When more detailed analysis is necessary, the donor-derived cells can be further analyzed on frozen or plastic sections (Avanesov *et al*., 2005). In such cases, the donor blastomeres are usually labeled with both fluorophore- and biotin-conjugated dextrans. The fluorophore-conjugated tracer is used to distinguish which embryos contain donor-derived cells in the desired tissue as described above. The biotin-conjugated dextran, on the other hand, is used in detailed analysis at later developmental stages. The HRP-conjugated streptavidin version of the ABC kit (Vector Laboratories Inc.) or fluorophore-conjugated avidin (Jackson ImmunoResearch Inc., Molecular Probes, Inc.) can be used to detect biotinylated dextran (Fig. 4C and D, respectively). HRP detection can be performed on whole mounts and analyzed on plastic sections, as described above for histological analysis. In contrast to that, fluorophore-conjugated avidin is preferably used after sectioning of the frozen tissue, owing to degradation of some flurophores during embedding of specimen in plastic. In these experiments, cryosections are prepared as described for antibody staining above. In some experiments, it is desirable to analyze the donor-derived cells for the expression of molecular markers (see Fig. 4D for an example). On frozen sections, avidin detection of donor-derived cells can be combined with antibody staining. Another way to visualize donor-derived cells and analyze expression at the same time is to combine HRP detection of donor-derived cells with *in situ* hybridization or antibody staining (Halpern *et al*., 1993; Schier *et al*., 1997). When HRP is used for the detection of donor-derived cells, the resulting reaction product inhibits the detection of the *in situ* probe with AP (Schier *et al*., 1997). Because of this, the opposite sequence of enzymatic detection reactions is preferred: *in situ* probe detection first and HRP staining second.

When mosaic analysis is performed in the zebrafish retina at 3 dpf or later, the dilution of a donor-cell tracer can make the interpretation of the results difficult. This is because the descendants of a single transplanted blastomere divide a variable number of times. Thus in the donor-derived cells which undergo the highest number of divisions the label may be diluted so much that it is no longer detectable. In mosaic animals, such a situation can lead to the appearance of a mutant phenotype or to the rescue of a mutant phenotype in places seemingly not associated with the presence of donor cells and complicate the interpretation of experimental results. Increasing the concentration of the tracer or, in the case of whole-mount experiments, improving the penetration of staining reagents can sometimes alleviate this problem. Alternatively, collagenase treatment of fixed embryos improves reagent penetration during the detection of donor-derived cells (Doerre and Malicki, 2001). The amount of injected dextran should be increased carefully as excessively high concentrations are lethal for labeled cells.

If the dilution of tracer cannot be circumvented, an excellent alternative is the use of transgenes. An ideal transgene to mark donor cells in mosaic analysis would drive the expression of FP at a high level in all cells throughout development. In the context of the retina, the mCFP Q01 line largely meets these requirements, although its expression becomes somewhat dimmer as development advances (Godinho *et al*., 2005). This line has been used, for example, to study photoreceptor and glia defects in *ale oko* mutant retinae (Jing and Malicki, 2009). An additional advantage of using transgenic FP tracers is that they eliminate the need for tracer injections into the donors, which decreases mechanical damage to embryos. Lastly, FP are relatively nontoxic, which increases the survival of donor-derived cells further. A disadvantage of transgene use in this context is that it takes one generation to in-cross an FP transgene into a mutant line. In summary, mosaic analysis is an important approach that has been widely used to study zebrafish retinal mutants (Avanesov *et al*., 2005; Cerveny *et al*., 2010; Doerre and Malicki, 2001; 2002; Goldsmith *et al*., 2003; Jensen *et al*., 2001; Jing and Malicki, 2009; Krock *et al*., 2007; Link *et al*., 2000; Malicki and Driever, 1999; Malicki *et al*., 2003; Pujic and Malicki, 2001; Wei and Malicki, 2002; Yamaguchi *et al*., 2010).

## E. Analysis of Cell Proliferation

Several techniques are available to study cell proliferation in the retina. The amount of cell proliferation, the timing of cell cycle exit (birth date), and cell cycle length can be evaluated by $H^3$-thymidine labeling (Nawrocki, 1985) or via bromodeoxyuridine (BrdU) injections into the embryo (Hu and Easter, 1999). Such studies can be very informative in mutant animals (Kay *et al*., 2001; Link *et al*., 2000; Yamaguchi *et al*., 2008). To identify the population of cells that exit the cell cycle in a particular window of time, BrdU labeling can be combined with iododeoxyuridine (IdU) (Del Bene *et al*., 2008). Finally, another useful technique that can be used to test for cell cycle defects in mutant strains is fluorescence activated cell sorting (FACS) of dissociated retinal cells (Plaster *et al*., 2006; Yamaguchi *et al*., 2008).

## F. Behavioral Studies

Several vision-dependent behavioral responses have been described in zebrafish larvae and adults: the optomotor response (Clark, 1981), the optokinetic response (Clark, 1981; Easter and Nicola, 1996), the startle response (Easter and Nicola, 1996), the phototaxis (Brockerhoff *et al*., 1995), the escape response (Li and Dowling, 1997), and the dorsal light reflex (Nicolson *et al*., 1998). Not surprisingly, larval feeding efficiency also depends on vision (Clark, 1981). While some of these behaviors are already present by 72 hpf, others have been described in adult fish only (for a review see Neuhauss, 2003). The vision-dependent behaviors of zebrafish proved to be very useful in genetic screening (see *Phenotype Detection Methods* on page 244). The optokinetic response appears to be the most robust and versatile. It is useful both in quick tests of vision and in quantitative estimates of visual acuity. In addition to genetic screens, behavioral tests have been used to study the function of the zebrafish optic tectum (Roeser and Baier, 2003).

## G. Electrophysiological Analysis of Retinal Function

In addition to behavioral tests, measurements of electrical activity in the eye are another, more precise way to evaluate retinal function. Electrical responses of the zebrafish retina can be evaluated by electroretinography (ERG) already by 4 dpf (for example, Avanesov *et al*., 2005). Similar to other vertebrates, the zebrafish ERG response contains two main waves: a small negative a-wave, originating from the photoreceptor cells, and a large positive b-wave, which reflects the function of the INL (Dowling, 1987; Makhankov *et al*., 2004). The goal of an ERG study in zebrafish is no different from that of a similar procedure performed on the human eye. ERG can be used to evaluate the site of retinal defects in mutant animals. Ganglion cell defects do not affect the ERG response (Gnuegge *et al*., 2001), whereas the absence of the a-wave or the b-wave suggests a defect in photoreceptors or in the INL, respectively. The a-wave appears small in ERG measurements because of an overlap with the b-wave. To measure the a-wave amplitude, the b-wave has to be blocked pharmacologically (Kainz *et al*., 2003). An additional ERG wave, the d-wave, is produced when longer (ca. 1 s) flashes of light are used. Referred to as the OFF response, the d-wave is thought to reflect the activity of OFF-bipolar cells and photoreceptors (Kainz *et al*., 2003; Makhankov *et al*., 2004).

Retinal responses are usually elicited using a series of light stimuli that vary by several orders of magnitude in intensity (Allwardt *et al*., 2001; Kainz *et al*., 2003). This allows the evaluation of the visual response threshold, a parameter that is sometimes abnormal in mutant animals (Li and Dowling, 1997). Another important variable in ERG measurements is the level of background illumination. ERG measurements can be performed on light-adapted retinae using background illumination of a constant intensity, or on dark-adapted retinae, which are maintained in total darkness for at least 20 min prior to measurements (Kainz *et al*., 2003). Most frequently recordings are performed on intact anesthetized animals (Makhankov *et al*., 2004). Alternatively, eyes may be gently removed from larvae and bathed in an oxygenated buffer solution. The latter ensures the oxygen supply to the retina in the absence of blood circulation (Kainz *et al*., 2003). ERG recordings have become a standard assay when evaluating zebrafish eye mutants (Allwardt *et al*., 2001; Avanesov *et al*., 2005; Biehlmaier *et al*., 2007; Brockerhoff *et al*., 1998; Kainz *et al*., 2003; Makhankov *et al*., 2004; Morris *et al*., 2005).

In addition to ERG, other more technically sophisticated electrophysiological measurements can be used to evaluate zebrafish (mutant) retinae. The ganglion cell function, for example, can be evaluated by recording action potentials from the optic nerve (Emran *et al*., 2007). Such measurements revealed ganglion cell defects in the retinae of *nbb* and *mao* mutants (Gnuegge *et al*., 2001; Li and Dowling, 2000). Similarly, photoreceptor function has been evaluated by measuring outer segment currents in isolated cells (Brockerhoff *et al*., 2003).

## H. Biochemical Approaches

Genetic experiments in animal models are frequently supplemented with studies of protein–protein interactions. Although this type of analysis has not been traditionally a strength of the zebrafish model, zebrafish embryos can be used to analyze binding interactions. In the context of the visual system, biochemical analysis has been largely applied to study the intraflagellar transport (IFT) in photoreceptor outer segment formation. As IFT occurs in many tissues, it can be studied via co-immunoprecipitation from embryonic or larval extracts (Krock and Perkins, 2008). Alternatively, extracts from the retinae of adult animals can be used in this type of experiment (Insinna *et al*., 2008). A clear advantage of using larvae is that one can apply biochemical methods to analyze mutant phenotypes. As most zebrafish mutants are lethal at embryonic or larval stages, adult retinae are not suitable for this purpose. In addition to immunoprecipitation experiments, a more sophisticated but also more laborious and technically demanding approach is to identify binding partners by tandem affinity purification (TAP) (reviewed in Collins and Choudhary, 2008). The TAP tag procedure involves attaching a peptide tag to the protein of interest, and expressing it in zebrafish embryos. Following the preparation of embryonic extract, the peptide tag is used to purify the bait protein along with its binding partners using appropriate affinity columns. The identities of the binding partners are established using mass spectrometry. The TAP tag approach was applied in the zebrafish to identify the binding partners of Elipsa, a determinant of outer segment differentiation (Omori *et al*., 2008). It is a relatively demanding technique, as it requires the expression of the bait protein in thousands of embryos. As more efficient affinity purification tags are engineered (Burckstummer *et al*., 2006), TAP is likely to become easier to apply in the zebrafish.

## I. Chemical Screens

Another approach that is gaining popularity in the zebrafish model is the screening of chemical libraries for compounds that affect developmental processes. The characteristics that render the zebrafish embryo suitable for genetic experiments—small size, rapid development, and transparency—also make it exceptionally useful for small-molecule screening (Kokel *et al*., 2010; Peterson *et al*., 2000; Tran *et al*., 2007; Zon and Peterson, 2005). In this type of experiment, hundreds or even thousands of small batches of embryos are each exposed to a different chemical compound, and analyzed for developmental or behavioral changes. Such an approach has been applied either to wild-type embryos or to carriers of genetic defects (Cao *et al*., 2009; North *et al*., 2007, 2009; Peterson *et al*., 2004). In the latter case, compounds that rescue a mutant phenotype can be screened for. When mutations that resemble human abnormalities are used, this approach can be a powerful way to identify chemicals of potential therapeutic importance (Cao *et al*., 2009; Hong *et al*., 2006; Peterson *et al*., 2004).

Chemical compound libraries ranging in size from hundreds to tens of thousands of molecules are commercially available. Phenotype detection approaches in a small-molecule screen are potentially as varied as in a genetic screen (Kaufman *et al*., 2009; *Phenotype Detection Methods* on page 244). Gross evaluation of morphological features is the simplest option. Transgenic lines that express FPs in target tissues make it possible to detect subtle phenotypes. In a recent experiment, for example, an flk-GFP transgenic line was used to screen ca. 2000 small molecules for their effects on retinal vasculature (Kitambi *et al*., 2009). Although little precedent exists at this time for small-molecule screens focusing on retinal development, this approach has been successful in the analysis of several zebrafish organs and behaviors (Hong *et al*., 2006; Kokel *et al*., 2010; North *et al*., 2007; Sachidanandan *et al*., 2008), and thus is also likely to find its way into the studies of the visual system.

## IV. Analysis of Gene Function in the Zebrafish Retina

### A. Reverse Genetic Approaches

A series of mutant alleles of varying severity is arguably the most informative tool of gene function analysis. Although a great variety of mutant lines have been identified in forward genetic sceens, for many loci chemically induced mutant alleles are not yet available. In these cases, other approaches must be applied to study gene function. In this section, we briefly discuss advantages and disadvantages of different loss-of-function and gain-of-function approaches in the context of the zebrafish visual system, and provide references to more comprehensive discussions of each.

#### 1. Loss-of-Function Analysis

In the absence of loss-of-function mutations, antisense-based interference is by far the most common way to obtain information about gene function in the zebrafish embryo (Nasevicius and Ekker, 2000). The reasons for this popularity are low cost and low labor expense involved in their use. Although antisense morpholino-modified oligonucleotides have been shown to reproduce mutant phenotypes quite well, their use suffers from two main disadvantages. First, they become progressively less effective as development proceeds, presumably because of degradation. Second, some morpholinos produce nonspecific toxicity, which must be distinguished from specific features of a morpholino-induced phenotype. Morpholino oligos can be used to interfere either with translation initiation or with splicing. Importantly, the efficiency of splice-site morpholinos can be monitored by reverse transcription polymerase chain reaction (RT-PCR) (Draper *et al*., 2001; Tsujikawa and Malicki, 2004b). In general, splice-site morpholinos reduce wild-type transcript expression below the level of RT-PCR detection throughout the first 36 h of development, although some have been reported to remain active until 3 or even 5 dpf (Tsujikawa and Malicki, 2004b). Most morpholinos are thus sufficient to interfere with genetic pathways involved in retinal neurogenesis but not to study later differentiation events or retinal function. Some help in designing morpholinos can be obtained from their manufacturer (Gene Tools LLC). Detailed protocols for the use of morpholinos, including their target site homology requirements, injection protocols, and methods to control for specificity, are available in literature (reviewed by Eisen and Smith, 2008; Malicki *et al*., 2002).

A powerful alternative to the use of morpholinos in loss-of-function studies is TILLING (targeted induced local lesions in genomes) (Colbert *et al*., 2001; McCallum *et al*., 2000; Wienholds *et al*., 2002). This approach combines chemical mutagenesis with a PCR-based protocol for detecting mutations in a locus of choice, and yields a series of mutant alleles that vary in strength. Its main disadvantage is the vast amount of preparation that needs to be done to initiate these experiments. One particularly labor-intensive step is the collection of thousands of sperm and DNA samples from F1 males. Because of this limitation, TILLING experiments are frequently performed by core facilities, which serve a group of laboratories, or the entire research community.

A recent addition to mutagenesis approaches in zebrafish is the use of zinc finger nucleases (ZFNs) to induce lesions in desired genes. ZFNs consist of a DNA recognition module, essentially a tandem array of two to four zinc finger-type DNA binding domains, and a catalytic module, which is usually derived from the Fok I restriction endonuclease (reviewed in Porteus and Carroll, 2005). ZFN binding to its target sequence induces double-stranded DNA breaks, which results in heritable defects because of improper repair. Needless to say, DNA binding specificity is critical for the application of ZFNs in animal models. The ability to manipulate binding is based on several findings: individual zinc fingers primarily interact with a single triplet of the DNA sequence; this interaction involves a significant degree of sequence specificity; and multiple zinc fingers can be assembled together to recognize longer target sequences (Porteus and Carroll, 2005). In zebrafish, pilot studies confirmed that ZFNs can be used to induce mutations in desired genes with good efficiency and specificity (Doyon *et al*., 2008; Meng *et al*., 2008). Nonetheless, the engineering of zinc finger binding domains of predetermined specificities remains laborious as it requires lengthy *in vitro* and/or *in vivo* selection procedures (Doyon *et al*., 2008; Meng *et al*., 2008). Detailed protocols for the selection of zinc finger combinations that will efficiently target predetermined DNA sequences and for the subsequent generation of mutant zebrafish have been described (Foley *et al*., 2009; Wright *et al*., 2006).

## 2. Approaches to Gene Overexpression

To obtain a comprehensive understanding of gene function, one often needs to supplement loss-of-function analysis with overexpression data. In the simplest scenario, this can be accomplished in zebrafish by RNA or DNA injections into the embryo. Several variants of this procedure exist, each with unique advantages and drawbacks (reviewed in Malicki *et al*., 2002). The main disadvantage of injecting RNA into embryos is its limited stability. The injection of DNA constructs, on the other hand, produces expression for a much longer period of time but only in a small number of cells. The fraction of cells that express a gene of interest following the injection of a DNA construct into the embryo can be increased by placing the gene to be studied under the control of UAS (Upstream Activating Sequence, multiple copies are used in tandem) and driving its expression using GAL4–VP16 fusion protein expressed from either a ubiquitous or a tissue-specific promoter (Koster and Fraser, 2001). Alternatively, transgene integration efficiency (estimated as the fraction of cells that express DNA construct) can be greatly improved by using Tol2 transposon-based vectors (Kawakami, 2004). These are injected into one- to two-cell embryos (the earlier the better) along with transposase mRNA (Kawakami, 2004; Kwan *et al*., 2007). The integration of these constructs into the genome relies on terminal transposon sequences, including the terminal inverted repeats (TIRs). The Tol2-derived sequences can be as short as 150–200 bp, but tend to be longer in older vectors, such as T2KXIG (Kawakami, 2004; Urasaki *et al*., 2006). In addition to transposon terminal sequences, these vectors contain an FP marker that helps to follow the pattern of transgene inheritance in embryonic tissues. Genes of interest can also be placed in these vectors under the control of appropriate regulatory elements. The heat-shock promoter has been used, for example, to drive the expression of a *crumbs* gene from a Tol2-based vector in the zebrafish retinal neuroepithelium. This approach produced expression in nearly half of neuroepithelial cells (Omori *et al*., 2008).

Overexpression phenotypes can also be studied in stable transgenic lines, provided that the resulting dominant phenotype is viable or can be conditionally induced. Several efficient methods for generating transgenic zebrafish are available. To develop a good understanding of its function, a gene under investigation may have to be expressed under the control of several regulatory elements and/or as a fusion with more than one tag (FP tags with different spectral characteristics and/or a myc tag, for example). As generating appropriate expression constructs using traditional cloning approaches is laborious, recombination cloning-based strategies have been specifically tailored for use in zebrafish (Kwan *et al*., 2007; Villefranc *et al*., 2007). These methods utilize a set of bacteriophage λ recombination enzymes to transfer DNA fragments from so-called entry vectors into so-called destination vectors, and are referred to as Gateway cloning (Hartley *et al*., 2000). One of the most obvious advantages of the Gateway system is that it allows one to combine several different DNA elements relatively efficiently in a single enzymatic reaction. In one example of how this method can be applied, three entry clones were assembled in the correct configuration into a Tol2-based zebrafish destination vector in a single step (Kwan *et al*., 2007). The use of the Gateway system requires some preparatory work. Recombination sites need to be added to generate entry vectors, and, similarly, the destination vectors have to be prepared by inserting recombination sites and selection markers. These procedures are nonetheless straightforward, and most standard laboratory vectors can be fairly easily converted into destination vectors. To make this approach even more attractive, several destination vectors are already available for use in the zebrafish (Kwan *et al*., 2007; Villefranc *et al*., 2007).

A frequent limitation of overexpression studies is the pleiotropy of mutant phenotypes: for many loci, early embryonic phenotypes are so severe that they preclude the analysis of late developmental processes, such as retinal neurogenesis. Several experimental tools are available to overcome this problem, including the use of heat-shock promoters, the GAL4–UAS overexpression system, and caged nucleic acids. Similar to invertebrate model systems, the use of heat-shock-induced expression in zebrafish relies on the hsp70 promoter (Halloran *et al*., 2000). An interesting variant of this protocol involves the activation of a heat-shock promoter-driven transgene in a small group of cells in a living embryo by heating them gently with a laser beam, which provides both temporal and spatial control of overexpression pattern (Halloran *et al*., 2000).

GAL4–UAS system is another method to achieve spatial control of gene expression. Modeled after *Drosophila* (Brand and Perrimon, 1993), the GAL4–UAS overexpression approach takes advantage of two transgenic strains. The activator strain expresses the GAL4 transcriptional activator in a desired subset of tissues, while the effector strain carries the gene of interest under the control of a GAL4 responsive promoter (UAS, upstream activating sequence). The effector transgene is activated by crossing its carrier strain to a line that carries the activator transgene (Scheer *et al*., 2002). One variant of this system involves a fusion of the Gal4 DNA binding domain to the viral VP16 activation domain and uses a multimer of 14 UAS sites in the reporter construct (Koster and Fraser, 2001; see also comments above). The GAL4–UAS system was initially used in the zebrafish eye to study *notch* function (Scheer *et al*., 2001), and since then has gained popularity (Del Bene *et al*., 2008; Godinho *et al*., 2005; Mumm *et al*., 2006; Yeo *et al*., 2007). Importantly, enhancer trap screens have generated hundreds of transgenic strains that express the Gal4 activator in a variety of patterns and can be used to drive the expression of UAS effector transgenes in many organs, including the eye (Asakawa and Kawakami, 2008; Scott *et al*., 2007). Finally, an interesting method to control gene overexpression patterns is the use of Bhc-caged nucleic acids (Ando *et al*., 2001). In this approach, embryos are injected with an inactive form of an overexpression construct, which is then later activated in a selected tissue using UV illumination. Both RNA and DNA templates can be used to produce overexpression in this approach (Ando and Okamoto, 2003).

## B. Forward Genetics

The use of zebrafish in genetic studies offers several obvious advantages. The most important of these is the possibility of performing efficient forward genetic screens. Genetic screening is feasible because adult zebrafish are highly fecund and are easily maintained in large numbers in a fairly small laboratory space. Screens performed in on the zebrafish so far identified hundreds of visual system mutants (Baier *et al*., 1996; Fadool *et al*., 1997; Malicki *et al*., 1996; Muto *et al*., 2005; Neuhauss *et al*., 1999). While designing a genetic screen, one has to consider three important variables: the type of mutagen to be used, the design of the breeding scheme, and mutant defect recognition criteria. Each of these is discussed below.

### 1. Mutagenesis Approaches

The majority of screens performed in zebrafish so far involved the use of *N*-ethyl-*N*-nitrosourea (ENU) (Mullins *et al*., 1994; Solnica-Krezel *et al*., 1994). This mutagenesis approach is very effective as evidenced by the fact that the vast majority of mutations isolated so far are ENU induced. A powerful alternative to chemical mutagenesis is insertional retroviral mutagenesis. Although the efficiency of this mutagenesis approach is still lower than that of chemical methods, an obvious advantage of a retroviral mutagen is that it provides means for very rapid identification of mutant genes (Amsterdam *et al*., 1999; Golling *et al*., 2002). Retroviral mutagenesis has also been applied on a large scale to identify hundreds of mutant strains (Golling *et al*., 2002). The photoreceptor mutant *nrf* is an example of a retinal defect induced using this approach (Becker *et al*., 1998). More recently, a rescreen of 250 retrovirus-induced mutants led to the identification of defects in several aspects of eye development (Gross *et al*., 2005).

In addition to chemical mutagens and retroviral vectors, transposons provide another option for effective mutagenesis. Transposable elements of the *Tc-1/mariner* (*Sleeping beauty*) and *hAT* (*Tol2*) families integrate into the zebrafish genome in a transposase-dependent manner (Fadool *et al*., 1998; Kawakami *et al*., 2000; Raz *et al*., 1998). Although initial efforts to induce mutations using transposon-based vectors were unsuccessful (Balciunas *et al*., 2004; Kawakami *et al*., 2004), recent experiments that rely on improved vector design generate mutants with high efficiency (Nagayoshi *et al*., 2008; Sivasubbu *et al*., 2006). Both *Tol2*- and *Sleeping beauty*-based constructs were used in these efforts. Transposon-based mutagenesis is an attractive alternative to retrovirus-mediated one because transposon-based vectors efficiently integrate into the zebrafish genome, and their mutagenicity (measured as the fraction of genome insertion events that lead to mutant phenotypes in homozygous animals) already exceeds that of retroviral mutagenesis (Nagayoshi *et al*., 2008; Sivasubbu *et al*., 2006). The use of transposons does not require technically difficult packaging of DNA into viral particles, and also appears to pose few safety concerns. An added bonus of using transposons is that they can be remobilized from preexisting lines to generate additional insertions (Kondrychyn *et al*., 2009). One has to bear in mind, however, that just like in the case of viral insertions, transposon integration is not entirely random (Kondrychyn *et al*., 2009). As the efficiency of transposable element-mediated mutagenesis is gradually improving, future genetic screens are likely to be performed with the help of transposons.

Transposon-mediated mutagenesis is usually performed using enhancer or gene trap vectors, which carry FP reporter genes (reviewed in Balciunas *et al*., 2004; Nagayoshi *et al*., 2008). Such a design is important for several reasons. First, it allows one to visually detect integration events that occur in the vicinity of genes because the nearby regulatory elements frequently drive FP reporter expression. Such integrations are much more likely to produce phenotypic defects, compared to insertions into non-transcribed regions of the genome. Second, as different integration events tend to produce different expression patterns, at least in some cases one can distinguish them from each other via simple inspection of living embryos. Consequently, potentially mutagenic insertions can be driven to homozygocity already in the F2 generation of a screen (Nagayoshi *et al*., 2008). Moreover, as gene/enhancer trap expression patterns suggest the function for genes in which insertions have occurred, they may allow one to focus a genetic screen on a specific developmental or physiological process. Finally, trap-induced mutant alleles are easier to maintain as their presence can be selected for in heterozygotes based on expression pattern. Although retroviral mutagenesis vectors can also be engineered to function as traps (Ellingsen *et al*., 2005), mutants generated using retroviral trap vectors have not been reported in zebrafish so far.

## 2. Breeding Schemes

The second important consideration is the type of breeding scheme that will carry genetic defects from mutagenized animals (G0) to the generation in which the screening for mutant phenotypes is performed. The most straightforward option, but also the most space- and time-consuming one, is screening for recessive defects in F3 generation embryos. This procedure was used in early large-scale genetic screens (Amsterdam *et al*., 1999; Driever *et al*., 1996; Haffter *et al*., 1996). Its main disadvantage is that it requires a very large number of tanks to raise the F2 generation to adulthood. As the majority of laboratories do not have access to several thousands of fish tanks, more space-efficient procedures are frequently required. In this regard, the zebrafish offers some possibilities not available in other genetically studied vertebrates—haploid and early pressure screens (for a review see Malicki, 2000). The major asset of these screening strategies is that one generation of animals is omitted and consequently time and the amount of laboratory space required is dramatically reduced. Although there are obvious advantages, these two screening strategies also suffer from some limitations. The most significant disadvantage of haploids is that their development does not proceed in the same way as wild-type embryogenesis. Haploid embryos do not survive beyond 5 dpf, and even at earlier stages of development they display obvious defects. Although the eyes of haploid zebrafish appear fairly normal at least until 3 dpf, the architecture of their retinae tends to be disorganized. By 5 dpf, haploid embryos are markedly smaller than the wild type and display numerous abnormalities. In the context of the visual system, haploid screens appear useful to search for early patterning defects prior to the onset of neurogenesis.

Screening of embryos generated via the application of early pressure (Streisinger *et al*., 1981) is another strategy that can be used to save both time and space. Similar to haploidization, this technique also allows one to screen for recessive defects in F2 generation embryos. The early pressure technique also involves some shortcomings. Embryos produced via this method display a high background of developmental abnormalities, which complicate the detection of mutant phenotypes, especially at early developmental stages. Another limitation of early pressure screens is that the fraction of homozygous mutant animals in a clutch of early pressure-generated embryos depends on the distance of a mutant locus from the centromere. For centromeric loci, the fraction of mutant embryos approaches 50%, whereas for telomeric genes it decreases below 10% (Streisinger *et al*., 1986). In other types of screens, mutant phenotypes can be distinguished from non-genetic developmental abnormalities based on their frequencies (25% in the case of screens on F3 embryos). Clearly, this criterion cannot be used in early pressure screens. Despite these limitations, early pressure screens are useful, especially in small-scale endeavors. The experimental techniques involved in haploid and early pressure screens have been previously reviewed in depth (Beattie *et al*., 1999; Walker, 1999).

While the approaches discussed above are used to identify recessive mutant phenotypes, an entirely different breeding scheme is used in searches for dominant defects. These can already be detected in embryos, larvae, or adults of the F1 generation. Although this category of screens requires just a single generation and consequently a very small amount of laboratory space, few experiments focusing on dominant defects have been performed in zebrafish so far (van Eeden *et al*., 1999). An example of a search for dominant defects of the visual system is provided by a small behavioral screen of adult animals for defects of visual perception, which identified a late-onset photoreceptor degeneration phenotype (Li and Dowling, 1997).

## 3. Phenotype Detection Methods

The third important consideration while designing a genetic screen is the mutant phenotype detection method. This aspect of screening allows for substantial creativity. Phenotype detection criteria range from very simple to very sophisticated. Ideally, the mutant phenotype recognition strategy should fulfill the following requirements: (1) involve minimal effort, (2) detect gross abnormalities as well as subtle changes, and (3) exclude phenotypes irrelevant to the targeted process. One class of irrelevant phenotypes are nonspecific defects. In large-scale mutagenesis screens performed so far, more than two-thirds of all phenotypes were classified as nonspecific (Driever *et al*., 1996; Golling *et al*., 2002; Haffter *et al*., 1996). The most frequent nonspecific phenotypes in zebrafish are early degeneration spreading across the entire embryo, and developmental retardation affecting brain, eyes, fins, and jaw. The latter class of mutants affects tissues that display robust proliferation between 3 and 5 dpf. Nonspecific phenotypes are not necessarily without value, but are usually considered uninteresting because they are likely to be produced by defects in a broad range of housekeeping mechanisms (such as metabolic pathways or DNA replication machinery; see for example Allende *et al*., 1996; Plaster *et al*., 2006). Another category of irrelevant phenotypes includes specific defects that are of no interest to investigators performing the screen. Such phenotypes are isolated when a screening procedure detects mutations affecting multiple organs, only one of which is of interest. A good example of such a situation is provided by behavioral screens involving the optomotor response. Lack of the optomotor response may be due to defects of photoreceptor neurons or skeletal muscles. These two cell types are seldom interesting to the same group of investigators. It is one of the virtues of a well-designed screen that irrelevant phenotypes are efficiently selected against.

The simplest way to screen for mutant phenotypes is by visual inspection. The most significant disadvantage of this method is that it detects changes only in structures easily recognizable using a microscope (preferably a dissecting scope). Thus visual inspection screens are suitable to search for defects in trunk blood vessels (which are easy to see in larvae), but would not detect a loss of a small population of neurons hidden in the depths of the retina or the brain. Visual inspection criteria work well when the aim of a screen is to detect gross morphological changes. Within the eye, such changes may reflect specific defects in a single neuronal lamina. In many mutants, the changes of eye size are caused by a degeneration of photoreceptor cells (Doerre and Malicki, 2002; Jing and Malicki, 2009; Malicki *et al*., 1996). In this case, the affected cell population is numerous enough to cause a major change of morphology. Most likely, a morphological screen would not detect abnormalities in a less numerous cell class.

Changes confined to small populations of cells cannot usually be identified in a visual inspection screen. To detect these changes, the target cell population must somehow be made accessible to inspection. Several options exist in this regard: analysis of histological sections, whole-mount antibody staining, *in situ* hybridization, retrograde or anterograde labeling of neurons, and cell class-specific FP transgenes. One technically simple but rather laborious approach is to embed zebrafish larvae in paraffin and prepare histological sections. This approach was used to screen more than 2000 individuals from ca. 50 clutches of F2 early pressure-generated mutagenized larvae and led to the identification of two photoreceptor mutants (Mohideen *et al*., 2003). In addition to histological analysis, individual cell populations can be visualized in mutgenized animals using antibody staining or *in situ* hybridization. In one screening endeavor, staining of 700 early pressure-generated egg clutches with anti-tyrosine hydroxylase antibody led to the isolation of two retinal mutants (Guo *et al*., 1999).

An excellent example of a genetic screen that involves labeling of a specific neuronal population has been performed to uncover defects of the retinotectal projection (Baier *et al*., 1996; Karlstrom *et al*., 1996; Trowe *et al*., 1996). In this screen, two subpopulations of retinal ganglion cells were labeled with the carbocyanine tracers, DiI and DiO. Labeling procedures usually make screening much more laborious. To reduce the workload in this screen, DiI and DiO labeling were highly automated. For tracer injection, fish larvae were mounted in a standardized fashion in a temperature-controlled mounting apparatus. After filling the apparatus with liquid agarose and mounting the larvae, the temperature was lowered allowing the agarose to solidify. Subsequently, the blocks of agarose containing mounted larvae were transferred into the injection setup. Upon injection, the larvae were stored overnight at room temperature to allow for the diffusion of the injected tracer, and then transferred to a microscope stage for phenotypic analysis. The authors of this experiment estimate that using this highly automated screening procedure allowed them to inspect over 2000 larvae per day and to reduce the time spent on the analysis of a single individual to less than 1 min (Baier *et al*., 1996). Other labeling procedures can also be scaled up to process many clutches of embryos in a single experiment. Antibody or *in situ* protocols, for example, involve multiple changes of staining and washing solutions. To perform these protocols on many embryos in parallel, one can use multiwell staining dishes with stainless steel mesh at the bottom. Such staining dishes can be quickly transferred from one solution to another. Since many labeling procedures are time consuming, it is essential that during a screen they are performed in parallel on many embryos.

Recent advances provide an additional way to label specific cell populations in a much less labor-intensive way by using FP transgenes, such as the ones described earlier in this chapter. Transgenic FP lines can be either directly mutagenized or crossed to mutagenized males. Then the resulting progeny is used to search for defects in fine features of retinal cell populations. In contrast to other cell labeling procedures, the use of FP transgenes requires very little additional effort, compared to simple morphological observations of the external phenotype.

Behavioral tests are yet another screening alternative. Several screens based on behavioral criteria have been performed in recent years, leading to the isolation of interesting developmental defects (Brockerhoff *et al*., 1997; 2003; Li and Dowling, 1997; Muto *et al*., 2005; Neuhauss *et al*., 1999). Behavioral screens allow one to detect subtle functional defects of the retina that might evade other search criteria. They can be used to search for both recessive and dominant defects in larvae as well as in adult fish (Li and Dowling, 1997). Similar to many labeling procedures, however, behavioral screens tend to be laborious. In one instance of a screen involving the optokinetic response, the authors estimate that screening of a single zebrafish larva took, on average, 1 min. (Brockerhoff *et al*., 1995). Since optomotor tests can be performed on populations of animals, they tend to be less time consuming, compared to optokinetic response tests. They do, however, produce more false-positive hits (Muto *et al*., 2005). In addition, since behavioral responses usually involve the cooperation of many cell classes, screens of this type tend to detect a wide range of defects. The optokinetic response screens, for example, may lead to the isolation of defects in the differentiation of lens cells, the specification of the retinal neurons or glia, the formation of synaptic connections, the mechanisms of neurotransmitter release, or the development of ocular muscles. Additional tests are necessary to assure that the isolated mutants belong to the desired category. To be useful for screening, the behavioral response should be robust and reproducible, and should involve the simplest possible neuronal circuitry. In light of these criteria, the optokinetic response appears to be superior to other behaviors; both optomotor and startle responses require functional optic tecta while the optokinetic response does not (Clark, 1981; Easter and Nicola, 1996). The optokinetic response also appears to be more robust than the optomotor response and phototaxis (Brockerhoff *et al*., 1995; Clark, 1981). The most extensive visual behavior-based screen conducted so far relied on two tests conducted in parallel: optokinetic and optomotor responses (Muto *et al*., 2005). Although the results of this experiment are quite informative, they also illustrate inconsistencies associated with the use of behavioral tests as a screening tool. First, the initial round of screening was characterized by a very high false-positive rate (> 90% for the optomotor test). Second, surprisingly, the two behavioral tests used in this study uncovered largely non-overlapping sets of mutants. Following retests it turned out, however, that all mutants display both optomotor and optokinetic defects to varying degrees. Finally, as pointed out above, a broad range of phenotypic abnormalities in different cell classes were found in this experiment.

### 4. Positional and Candidate Cloning

Molecular characterization of defective loci is usually a crucial step that follows the isolation of mutant lines. The development of positional and candidate gene cloning strategies is one of the most significant advances in the field of zebrafish genetics within the last decade. These approaches are currently well established and have played a key role in many important contributions to the understanding of eye development and function. The positional cloning strategy involves a standard set of steps, such as mapping, chromosomal walking, transcript identification, and the delivery of a proof that the correct gene has been cloned. These steps are largely the same, regardless of the nature of a mutant phenotype. An example of a positional cloning strategy, laborious but eventually successful, is the cloning of the *nagie oko* locus (Wei and Malicki, 2002).

### 5. Mutant Strains Available

Large and small mutagenesis screens identified numerous genetic defects of retinal development in zebrafish. Mutant phenotypes affect a broad range of developmental stages, starting with the specification of the eye primordia, through optic lobe morphogenesis, the specification of neuronal identities, and include the final steps of differentiation, such as outer segment development in photoreceptor cells. Lists of mutant lines, excluding those that produce nonspecific degeneration of the entire retina, have been provided previously (Avanesov and Malicki, 2004; Malicki, 1999). Although these are still useful, many new mutants have been generated in recent years. The descriptions of these are available in the Zebrafish Model Organism Database (ZFIN, http://zfin.org).

## V. Summary

Relative simplicity, rapid development, and accessibility to genetic analysis make the zebrafish retina an excellent model system for the studies of neurogenesis in the vertebrate CNS. Numerous genetic screens have led to isolation of many mutants affecting the retina and the retinotectal projection in zebrafish. Mutant phenotypes are being studied using a rich variety of markers: antibodies, RNA probes, retrograde and anterograde tracers, as well as transgenic lines. A particularly impressive progress has been made in the characterization of the zebrafish genome. Consequently, positional and candidate cloning of mutant loci are now fairly easy in zebrafish. Many mutant genes have been cloned, and their analysis has provided insights into genetic circuitries that regulate retinal pattern formation, and the differentiation of retinal neurons and glia. Genetic screens for visual system defects will continue in the future, and progressively more sophisticated screening approaches will make it possible to detect an increasingly broad and varied assortment of mutant phenotypes. The remarkable evolutionary conservation of the vertebrate eye provides the basis for the use of the zebrafish retina as a model of human-inherited eye defects. As new techniques are being introduced and rapidly improved, the zebrafish will continue to be an important organism for the studies of the vertebrate visual system.

## Acknowledgments

The authors are grateful to Brian Perkins, Ichiro Masai, and Brian Link for critical reading of earlier versions of this manuscript and helpful comments. The authors' research on the retina is supported by grants from the National Eye Institute to JM (R01 EY018176 and R01EY016859).

## References

Allende, M. L., Amsterdam, A., Becker, T., Kawakami, K., Gaiano, N., and Hopkins, N. (1996). Insertional mutagenesis in zebrafish identifies two novel genes, pescadillo and dead eye, essential for embryonic development. *Genes Dev.* **10**, 3141–3155.

Allwardt, B. A., Lall, A. B., Brockerhoff, S. E., and Dowling, J. E. (2001). Synapse formation is arrested in retinal photoreceptors of the zebrafish nrc mutant. *J. Neurosci.* **21**, 2330–2342.

Altshuler, D., Turner, D., and Cepko, C. (1991). Specification of cell type in the vertebrate retina. *In* "Development of the Visual System" (D. Lam, and C. Shatz, eds.) pp. 37–58. The MIT Press, Cambridge, MA.

Alvarez, Y., Cederlund, M. L., Cottell, D. C., Bill, B. R., Ekker, S. C., Torres-Vazquez, J., Weinstein, B. M., Hyde, D. R., Vihtelic, T. S., and Kennedy, B. N. (2007). Genetic determinants of hyaloid and retinal vasculature in zebrafish. *BMC Dev. Biol.* **7**, 114.

Amsterdam, A., Burgess, S., Golling, G., Chen, W., Sun, Z., Townsend, K., Farrington, S., Haldi, M., and Hopkins, N. (1999). A large-scale insertional mutagenesis screen in zebrafish. *Genes Dev.* **13**, 2713–2724.

Ando, H., Furuta, T., Tsien, R. Y., and Okamoto, H. (2001). Photo-mediated gene activation using caged RNA/DNA in zebrafish embryos. *Nat. Genet.* **28**, 317–325.

Ando, H., and Okamoto, H. (2003). Practical procedures for ectopic induction of gene expression in zebrafish embryos using Bhc-diazo-caged mRNA. *Methods Cell Sci.* **25**, 25–31.

Aramaki, S., and Hatta, K. (2006). Visualizing neurons one-by-one *in vivo*: optical dissection and reconstruction of neural networks with reversible fluorescent proteins. *Dev. Dyn.* **235**, 2192–2199.

Asakawa, K., and Kawakami, K. (2008). Targeted gene expression by the Gal4–UAS system in zebrafish. *Dev. Growth. Differ.* **50**, 391–399.

Avanesov, A., Dahm, R., Sewell, W. F., and Malicki, J. J. (2005). Mutations that affect the survival of selected amacrine cell subpopulations define a new class of genetic defects in the vertebrate retina. *Dev. Biol.* **285**, 138–155.

Avanesov, A., and Malicki, J. (2004). Approaches to study neurogenesis in the zebrafish retina. *Methods Cell Biol.* **76**, 333–384.

Bahadori, R., Rinner, O., Schonthaler, H. B., Biehlmaier, O., Makhankov, Y. V., Rao, P., Jagadeeswaran, P., and Neuhauss, S. C. (2006). The zebrafish fade out mutant: a novel genetic model for Hermansky–Pudlak syndrome. *Invest. Ophthalmol. Vis. Sci.* **47**, 4523–4531.

Baier, H., Klostermann, S., Trowe, T., Karlstrom, R. O., Nusslein-Volhard, C., and Bonhoeffer, F. (1996). Genetic dissection of the retinotectal projection. *Development* **123**, 415–425.

Balciunas, D., Davidson, A. E., Sivasubbu, S., Hermanson, S. B., Welle, Z., and Ekker, S. C. (2004). Enhancer trapping in zebrafish using the sleeping beauty transposon. *BMC Genomics* **5**, 62.

Barthel, L. K., and Raymond, P. A. (1990). Improved method for obtaining 3-microns cryosections for immunocytochemistry. *J. Histochem. Cytochem.* **38**, 1383–1388.

Barthel, L. K., and Raymond, P. A. (1993). Subcellular localization of alpha-tubulin and opsin mRNA in the goldfish retina using digoxigenin-labeled cRNA probes detected by alkaline phosphatase and HRP histochemistry. *J. Neurosci. Methods* **50**, 145–152.

Baye, L. M., and Link, B. A. (2007). Interkinetic nuclear migration and the selection of neurogenic cell divisions during vertebrate retinogenesis. *J. Neurosci.* **27**, 10143–10152.

Beattie, C. E., Raible, D. W., Henion, P. D., and Eisen, J. S. (1999). Early pressure screens. *Methods Cell Biol.* **60**, 71–86.

Becker, T. S., Burgess, S. M., Amsterdam, A. H., Allende, M. L., and Hopkins, N. (1998). Not really finished is crucial for development of the zebrafish outer retina and encodes a transcription factor highly homologous to human nuclear respiratory factor-1 and avian initiation binding repressor. *Development* **125**, 4369–4378.

Bernardos, R. L., and Raymond, P. A. (2006). GFAP transgenic zebrafish. *Gene Expr. Patterns* **6**, 1007–1013.

Biehlmaier, O., Makhankov, Y., and Neuhauss, S. C. (2007). Impaired retinal differentiation and maintenance in zebrafish laminin mutants. *Invest. Ophthalmol. Vis. Sci.* **48**, 2887–2894.

Biehlmaier, O., Neuhauss, S. C., and Kohler, K. (2003). Synaptic plasticity and functionality at the cone terminal of the developing zebrafish retina. *J. Neurobiol.* **56**, 222–236.

Bodick, N., and Levinthal, C. (1980). Growing optic nerve fibers follow neighbors during embryogenesis. *Proc. Natl. Acad. Sci. U. S. A.* **77**, 4374–4378.

Branchek, T., and Bremiller, R. (1984). The development of photoreceptors in the zebrafish, *Brachydanio rerio*. I. Structure. *J. Comp. Neurol.* **224**, 107–115.

Brand, A. H., and Perrimon, N. (1993). Targeted gene expression as a means of altering cell fates and generating dominant phenotypes. *Development* **118**, 401–415.

Brennan, C., Monschau, B., Lindberg, R., Guthrie, B., Drescher, U., Bonhoeffer, F., and Holder, N. (1997). Two Eph receptor tyrosine kinase ligands control axon growth and may be involved in the creation of the retinotectal map in the zebrafish. *Development* **124**, 655–664.

Brockerhoff, S. E., Dowling, J. E., and Hurley, J. B. (1998). Zebrafish retinal mutants. *Vision Res* **38**, 1335–1339.

Brockerhoff, S. E., Hurley, J. B., Janssen-Bienhold, U., Neuhauss, S. C., Driever, W., and Dowling, J. E. (1995). A behavioral screen for isolating zebrafish mutants with visual system defects. *Proc. Natl. Acad. Sci. U. S. A.* **92**, 10545–10549.

Brockerhoff, S. E., Hurley, J. B., Niemi, G. A., and Dowling, J. E. (1997). A new form of inherited red-blindness identified in zebrafish. *J. Neurosci.* **17**, 4236–4242.

Brockerhoff, S. E., Rieke, F., Matthews, H. R., Taylor, M. R., Kennedy, B., Ankoudinova, I., Niemi, G. A., Tucker, C. L., Xiao, M., Cilluffo, M. C., Fain, G. L., and Hurley, J. B. (2003). Light stimulates a transducin-independent increase of cytoplasmic $Ca^{2+}$ and suppression of current in cones from the zebrafish mutant nof. *J. Neurosci.* **23**, 470–480.

Burckstummer, T., Bennett, K. L., Preradovic, A., Schutze, G., Hantschel, O., Superti-Furga, G., and Bauch, A. (2006). An efficient tandem affinity purification procedure for interaction proteomics in mammalian cells. *Nat. Methods* **3**, 1013–1019.

Burrill, J. D., and Easter, S. S. Jr. (1994). Development of the retinofugal projections in the embryonic and larval zebrafish (*Brachydanio rerio*). *J. Comp. Neurol.* **346**, 583–600.

Burrill, J., and Easter, S. (1995). The first retinal axons and their microenvironment in zebrafish cryptic pioneers and the pretract. *J. Neurosci.* **15**, 2935–2947.

Cajal, S. R. (1893). La retine des vertebres. *Cellule.* **9**, 17–257.

Cameron, D. A., and Carney, L. H. (2000). Cell mosaic patterns in the native and regenerated inner retina of zebrafish: implications for retinal assembly. *J. Comp. Neurol.* **416**, 356–367.

Cao, Y., Semanchik, N., Lee, S. H., Somlo, S., Barbano, P. E., Coifman, R., and Sun, Z. (2009). Chemical modifier screen identifies HDAC inhibitors as suppressors of PKD models. *Proc. Natl. Acad. Sci. U. S. A.* **106**, 21819–21824.

Cayouette, M., and Raff, M. (2003). The orientation of cell division influences cell-fate choice in the developing mammalian retina. *Development* **130**, 2329–2339.

Cayouette, M., Whitmore, A. V., Jeffery, G., and Raff, M. (2001). Asymmetric segregation of Numb in retinal development and the influence of the pigmented epithelium. *J. Neurosci.* **21**, 5643–5651.

Cedrone, C., Culasso, F., Cesareo, M., Zapelloni, A., Cedrone, P., and Cerulli, L. (1997). Prevalence of glaucoma in Ponza, Italy: a comparison with other studies. *Ophthalmic. Epidemiol.* **4**, 59–72.

Cerveny, K. L., Cavodeassi, F., Turner, K. J., de Jong-Curtain, T. A., Heath, J. K., and Wilson, S. W. (2010). The zebrafish flotte lotte mutant reveals that the local retinal environment promotes the differentiation of proliferating precursors emerging from their stem cell niche. *Development* **137**, 2107–2115.

Chinen, A., Hamaoka, T., Yamada, Y., and Kawamura, S. (2003). Gene duplication and spectral diversification of cone visual pigments of zebrafish. *Genetics* **163**, 663–675.

Choi, J., Dong, L., Ahn, J., Dao, D., Hammerschmidt, M., and Chen, J. N. (2007). FoxH1 negatively modulates flk1 gene expression and vascular formation in zebrafish. *Dev. Biol.* **304**, 735–744.

Chuang, J. C., Mathers, P. H., and Raymond, P. A. (1999). Expression of three Rx homeobox genes in embryonic and adult zebrafish. *Mech. Dev.* **84**, 195–198.

Clark, T. (1981). Visual responses in developing zebrafish (Brachydanio rerio). Ph. D. dissertation, University of Oregon, Eugene, OR.

Colbert, T., Till, B. J., Tompa, R., Reynolds, S., Steine, M. N., Yeung, A. T., McCallum, C. M., Comai, L., and Henikoff, S. (2001). High-throughput screening for induced point mutations. *Plant Physiol.* **126**, 480–484.

Collazo, A., Fraser, S. E., and Mabee, P. M. (1994). A dual embryonic origin for vertebrate mechanoreceptors. *Science* **264**, 426–430.

Collins, M. O., and Choudhary, J. S. (2008). Mapping multiprotein complexes by affinity purification and mass spectrometry. *Curr. Opin. Biotechnol.* **19**, 324–330.

Connaughton, V. P., Behar, T. N., Liu, W. L., and Massey, S. C. (1999). Immunocytochemical localization of excitatory and inhibitory neurotransmitters in the zebrafish retina. *Vis. Neurosci.* **16**, 483–490.

Cui, S., Otten, C., Rohr, S., Abdelilah-Seyfried, S., and Link, B. A. (2007). Analysis of aPKCλ and aPKCζ reveals multiple and redundant functions during vertebrate retinogenesis. *Mol. Cell. Neurosci.* **34**, 431–444.

Dahm, R., Schonthaler, H. B., Soehn, A. S., van Marle, J., and Vrensen, G. F. (2007). Development and adult morphology of the eye lens in the zebrafish. *Exp. Eye Res.* **85**, 74–89.

Dapson, R. W. (2007). Glyoxal fixation: how it works and why it only occasionally needs antigen retrieval. *Biotech. Histochem.* **82**, 161–166.

Das, T., Payer, B., Cayouette, M., and Harris, W. A. (2003). *In vivo* time-lapse imaging of cell divisions during neurogenesis in the developing zebrafish retina. *Neuron* **37**, 597–609.

Del Bene, F., Wehman, A. M., Link, B. A., and Baier, H. (2008). Regulation of neurogenesis by interkinetic nuclear migration through an apical-basal notch gradient. *Cell* **134**, 1055–1065.

Devoto, S. H., Melancon, E., Eisen, J. S., and Westerfield, M. (1996). Identification of separate slow and fast muscle precursor cells *in vivo*, prior to somite formation. *Development* **122**, 3371–3380.

Doerre, G., and Malicki, J. (2001). A mutation of early photoreceptor development, *mikre oko*, reveals cell–cell interactions involved in the survival and differentiation of zebrafish photoreceptors. *J. Neurosci.* **21**, 6745–6757.

Doerre, G., and Malicki, J. (2002). Genetic analysis of photoreceptor cell development in the zebrafish retina. *Mech. Dev.* **110**, 125–138.

Dowling, J. (1987). "The Retina". Harvard University Press, Cambridge, MA.

Doyon, Y., McCammon, J. M., Miller, J. C., Faraji, F., Ngo, C., Katibah, G. E., Amora, R., Hocking, T. D., Zhang, L., Rebar, E. J., Gregory, P. D., and Urnov, F. D., *et al*. (2008). Heritable targeted gene disruption in zebrafish using designed zinc-finger nucleases. *Nat. Biotechnol.* **26** 702–708.

Draper, B. W., Morcos, P. A., and Kimmel, C. B. (2001). Inhibition of zebrafish fgf8 pre-mRNA splicing with morpholino oligos: a quantifiable method for gene knockdown. *Genesis* **30**, 154–156.

Drescher, U., Bonhoeffer, F., and Muller, B. K. (1997). The Eph family in retinal axon guidance. *Curr. Opin. Neurobiol.* **7**, 75–80.

Driever, W., Solnica-Krezel, L., Schier, A. F., Neuhauss, S. C., Malicki, J., Stemple, D. L., Stainier, D. Y., Zwartkruis, F., Abdelilah, S., Rangini, Z., Belak, J., and Boggs, C. (1996). A genetic screen for mutations affecting embryogenesis in zebrafish. *Development* **123**, 37–46.

Dryja, T., and Li, T. (1995). Molecular genetics of retinitis pigmentosa. *Hum. Mol. Genet.* **4**, 1739–1743.

Duldulao, N. A., Lee, S., and Sun, Z. (2009). Cilia localization is essential for *in vivo* functions of the Joubert syndrome protein Arl13b/Scorpion. *Development* **136**, 4033–4042.

Easter, S. S., Jr., and Malicki, J. J. (2002). The zebrafish eye: developmental and genetic analysis. *Result Probl. Cell Differ*. **40**, 346–370.

Easter, S., and Nicola, G. (1996). The development of vision in the zebrafish (*Danio rerio*). *Dev. Biol.* **180**, 646–663.

Eisen, J. S., and Smith, J. C. (2008). Controlling morpholino experiments: don't stop making antisense. *Development* **135**, 1735–1743.

Ellingsen, S., Laplante, M. A., Konig, M., Kikuta, H., Furmanek, T., Hoivik, E. A., and Becker, T. S. (2005). Large-scale enhancer detection in the zebrafish genome. *Development* **132**, 3799–3811.

Emran, F., Rihel, J., Adolph, A. R., and Dowling, J. E. (2010). Zebrafish larvae lose vision at night. *Proc. Natl. Acad. Sci. U. S. A.* **107**, 6034–6039.

Emran, F., Rihel, J., Adolph, A. R., Wong, K. Y., Kraves, S., and Dowling, J. E. (2007). OFF ganglion cells cannot drive the optokinetic reflex in zebrafish. *Proc. Natl. Acad. Sci. U. S. A.* **104**, 19126–19131.

Fadool, J. M. (2003). Development of a rod photoreceptor mosaic revealed in transgenic zebrafish. *Dev. Biol.* **258**, 277–290.

Fadool, J. M., Brockerhoff, S. E., Hyatt, G. A., and Dowling, J. E. (1997). Mutations affecting eye morphology in the developing zebrafish (*Danio rerio*). *Dev. Genet.* **20**, 288–295.

Fadool, J. M., Hartl, D. L., and Dowling, J. E. (1998). Transposition of the mariner element from *Drosophila mauritiana* in zebrafish. *Proc. Natl. Acad. Sci. U. S. A.* **95**, 5182–5186.

Fashena, D., and Westerfield, M. (1999). Secondary motoneuron axons localize DM-GRASP on their fasciculated segments. *J. Comp. Neurol.* **406**, 415–424.

Foley, J. E., Maeder, M. L., Pearlberg, J., Joung, J. K., Peterson, R. T., and Yeh, J. R. (2009). Targeted mutagenesis in zebrafish using customized zinc-finger nucleases. *Nat. Protoc.* **4**, 1855–1867.

Fraser, S. (1992). Patterning of retinotectal connections in the vertebrate visual system. *Curr. Oppin. Neurobiol.* **2**, 83–87.

Fricke, C., Lee, J. S., Geiger-Rudolph, S., Bonhoeffer, F., and Chien, C. B. (2001). Astray, a zebrafish roundabout homolog required for retinal axon guidance. *Science* **292**, 507–510.

Gnuegge, L., Schmid, S., and Neuhauss, S. C. (2001). Analysis of the activity-deprived zebrafish mutant macho reveals an essential requirement of neuronal activity for the development of a fine-grained visuotopic map. *J. Neurosci.* **21**, 3542–3548.

Godinho, L., Mumm, J. S., Williams, P. R., Schroeter, E. H., Koerber, A., Park, S. W., Leach, S. D., and Wong, R. O. (2005). Targeting of amacrine cell neurites to appropriate synaptic laminae in the developing zebrafish retina. *Development* **132**, 5069–5079.

Goldsmith, P., Baier, H., and Harris, W. A. (2003). Two zebrafish mutants, ebony and ivory, uncover benefits of neighborhood on photoreceptor survival. *J. Neurobiol.* **57**, 235–245.

Golling, G., Amsterdam, A., Sun, Z., Antonelli, M., Maldonado, E., Chen, W., Burgess, S., Haldi, M., Artzt, K., Farrington, S., Lin, S. -Y., Nissen R. M., *et al*. (2002). Insertional mutagenesis in zebrafish rapidly identifies genes essential for early vertebrate development. *Nat. Genet.* **31** 135–140.

Gray, M. P., Smith, R. S., Soules, K. A., John, S. W., and Link, B. A. (2009). The aqueous humor outflow pathway of zebrafish. *Invest. Ophthalmol. Vis. Sci.* **50**, 1515–21.

Gross, J. M., and Perkins, B. D. (2008). Zebrafish mutants as models for congenital ocular disorders in humans. *Mol. Reprod. Dev.* **75**, 547–555.

Gross, J. M., Perkins, B. D., Amsterdam, A., Egana, A., Darland, T., Matsui, J. I., Sciascia, S., Hopkins, N., and Dowling, J. E. (2005). Identification of zebrafish insertional mutants with defects in visual system development and function. *Genetics* **170**, 245–261.

Guo, S., Wilson, S. W., Cooke, S., Chitnis, A. B., Driever, W., and Rosenthal, A. (1999). Mutations in the zebrafish unmask shared regulatory pathways controlling the development of catecholaminergic neurons. *Dev. Biol.* **208**, 473–487.

Haffter, P., Granato, M., Brand, M., Mullins, M. C., Hammerschmidt, M., Kane, D. A., Odenthal, J., van Eeden, F. J., Jiang, Y. J., Heisenberg, C. P., Kelsh, R. N., Furutani-Seiki, M., *et al*. (1996). The identification of genes with unique and essential functions in the development of the zebrafish, *Danio rerio*. *Development* **123**, 1–36.

Halloran, M. C., Sato-Maeda, M., Warren, J. T., Su, F., Lele, Z., Krone, P. H., Kuwada, J. Y., and Shoji, W. (2000). Laser-induced gene expression in specific cells of transgenic zebrafish. *Development* **127**, 1953–1960.

Halpern, M., Ho, R., Walker, C., and Kimmel, C. (1993). Induction of muscle pioneers and floor plate is distinguished by the zebrafish no tail mutation. *Cell* **75**, 99–111.

Hanker, J. S. (1979). Osmiophilic reagents in electronmicroscopic histocytochemistry. *Prog. Histochem. Cytochem.* **12**, 1–85.

Hartley, J. L., Temple, G. F., and Brasch, M. A. (2000). DNA cloning using *in vitro* site-specific recombination. *Genome Res.* **10**, 1788–1795.

Hartong, D. T., Berson, E. L., and Dryja, T. P. (2006). Retinitis pigmentosa. *Lancet* **368**, 1795–1809.

Hatta, K., Tsujii, H., and Omura, T. (2006). Cell tracking using a photoconvertible fluorescent protein. *Nat. Protoc.* **1**, 960–967.

Hauptmann, G., and Gerster, T. (1994). Two-color whole-mount *in situ* hybridization to vertebrate and *Drosophila* embryos. *Trends Genet.* **10**, 266.

Hinds, J., and Hinds, P. (1974). Early ganglion cell differentiation in the mouse retina: an electron microscopic analysis utilizing serial sections. *Dev. Biol.* **37**, 381–416.

Hisatomi, O., Satoh, T., Barthel, L. K., Stenkamp, D. L., Raymond, P. A., and Tokunaga, F. (1996). Molecular cloning and characterization of the putative ultraviolet- sensitive visual pigment of goldfish. *Vision Res.* **36**, 933–939.

Hitchcock, P. F., Macdonald, R. E., VanDeRyt, J. T., and Wilson, S. W. (1996). Antibodies against Pax6 immunostain amacrine and ganglion cells and neuronal progenitors, but not rod precursors, in the normal and regenerating retina of the goldfish. *J. Neurobiol.* **29**, 399–413.

Ho, R. K., and Kane, D. A. (1990). Cell-autonomous action of zebrafish spt-1 mutation in specific mesodermal precursors. *Nature* **348**, 728–730.

Holt, C., Bertsch, T., Ellis, H., and Harris, W. (1988). Cellular determination in the *Xenopus* retina is independent of lineage and birth date. *Neuron* **1**, 15–26.

Hong, C. C., Peterson, Q. P., Hong, J. Y., and Peterson, R. T. (2006). Artery/vein specification is governed by opposing phosphatidylinositol-3 kinase and MAP kinase/ERK signaling. *Curr. Biol.* **16**, 1366–1372.

Honig, M. G., and Hume, R. I. (1986). Fluorescent carbocyanine dyes allow living neurons of identified origin to be studied in long-term cultures. *J. Cell Biol.* **103**, 171–187.

Honig, M. G., and Hume, R. I. (1989). Dil and diO: versatile fluorescent dyes for neuronal labelling and pathway tracing. *Trends Neurosci.* **12**(333–335), 340–341.

Hu, M., and Easter, S. S. (1999). Retinal neurogenesis: the formation of the initial central patch of postmitotic cells. *Dev. Biol.* **207**, 309–321.

Hudak, L. M., Lunt, S., Chang, C. H., Winkler, E., Flammer, H., Lindsey, M., and Perkins, B. D. (2010). The intraflagellar transport protein ift80 is essential for photoreceptor survival in a zebrafish model of jeune asphyxiating thoracic dystrophy. *Invest. Ophthalmol. Vis. Sci.* **51**, 3792–3799.

Hyatt, G. A., Schmitt, E. A., Marsh-Armstrong, N., McCaffery, P., Drager, U. C., and Dowling, J. E. (1996). Retinoic acid establishes ventral retinal characteristics. *Development* **122**, 195–204.

Humphrey, C., and Pittman, F. (1974). A simple methylene blue-azure II-basic fuchsin stain for epoxy-embedded tissue sections. *Stain Technol.* **49**, 9–14.

Insinna, C., Pathak, N., Perkins, B., Drummond, I., and Besharse, J. C. (2008). The homodimeric kinesin, Kif17, is essential for vertebrate photoreceptor sensory outer segment development. *Dev. Biol.* **316**, 160–170.

Jacobson, M. (1991). "Developmental Neurobiology". Plenum Press, New York.

Jensen, A. M., Walker, C., and Westerfield, M. (2001). Mosaic eyes: a zebrafish gene required in pigmented epithelium for apical localization of retinal cell division and lamination. *Development* **128**, 95–105.

Jing, X., and Malicki, J. (2009). Zebrafish ale oko, an essential determinant of sensory neuron survival and the polarity of retinal radial glia, encodes the p50 subunit of dynactin. *Development* **136**, 2955–2964.

Jowett, T. (2001). Double *in situ* hybridization techniques in zebrafish. *Methods* **23**, 345–358.

Jowett, T., and Lettice, L. (1994). Whole-mount *in situ* hybridizations on zebrafish embryos using a mixture of digoxigenin- and fluorescein-labelled probes. *Trends Genet.* **10**, 73–74.

Kainz, P. M., Adolph, A. R., Wong, K. Y., and Dowling, J. E. (2003). Lazy eyes zebrafish mutation affects Müller glial cells, compromising photoreceptor function and causing partial blindness. *J. Comp. Neurol.* **463**, 265–280.

Karlsson, J., von Hofsten, J., and Olsson, P. E. (2001). Generating transparent zebrafish: a refined method to improve detection of gene expression during embryonic development. *Mar. Biotechnol. (NY)* **3**, 522–527.

Karlstrom, R. O., Trowe, T., Klostermann, S., Baier, H., Brand, M., Crawford, A. D., Grunewald, B., Haffter, P., Hoffmann, H., Meyer, S. U. *et al.* (1996). Zebrafish mutations affecting retinotectal axon pathfinding. *Development* **123**, 427–438.

Kaufman, C. K., White, R. M., and Zon, L. (2009). Chemical genetic screening in the zebrafish embryo. *Nat. Protoc.* **4**, 1422–1432.

Kawahara, A., Chien, C. B., and Dawid, I. B. (2002). The homeobox gene mbx is involved in eye and tectum development. *Dev. Biol.* **248**, 107–117.

Kawakami, K. (2004). Transgenesis and gene trap methods in zebrafish by using the Tol2 transposable element. *Methods Cell Biol.* **77**, 201–222.

Kawakami, K., Shima, A., and Kawakami, N. (2000). Identification of a functional transposase of the Tol2 element, an Ac-like element from the Japanese medaka fish, and its transposition in the zebrafish germ lineage. *Proc. Natl. Acad. Sci. U. S. A.* **97**, 11403–11408.

Kawakami, K., Takeda, H., Kawakami, N., Kobayashi, M., Matsuda, N., and Mishina, M. (2004). A transposon-mediated gene trap approach identifies developmentally regulated genes in zebrafish. *Dev. Cell* **7**, 133–144.

Kay, J. N., Finger-Baier, K. C., Roeser, T., Staub, W., and Baier, H. (2001). Retinal ganglion cell genesis requires lakritz, a zebrafish atonal homolog. *Neuron* **30**, 725–736.

Kay, J. N., Link, B. A., and Baier, H. (2005). Staggered cell-intrinsic timing of ath5 expression underlies the wave of ganglion cell neurogenesis in the zebrafish retina. *Development* **132**, 2573–2585.

Kay, J. N., Roeser, T., Mumm, J. S., Godinho, L., Mrejeru, A., Wong, R. O., and Baier, H. (2004). Transient requirement for ganglion cells during assembly of retinal synaptic layers. *Development* **131**, 1331–1342.

Kikuchi, Y., Segawa, H., Tokumoto, M., Tsubokawa, T., Hotta, Y., Uyemura, K., and Okamoto, H. (1997). Ocular and cerebellar defects in zebrafish induced by overexpression of the LIM domains of the islet-3 LIM/homeodomain protein. *Neuron* **18**, 369–382.

Kim, M. J., Kang, K. H., Kim, C. H., and Choi, S. Y. (2008). Real-time imaging of mitochondria in transgenic zebrafish expressing mitochondrially targeted GFP. *Biotechniques* **45**, 331–334.

Kimmel, C. B., Ballard, W. W., Kimmel, S. R., Ullmann, B., and Schilling, T. F. (1995). Stages of embryonic development of the zebrafish. *Dev Dyn* **203**, 253–310.

Kimmel, C. B., Sessions, S. K., and Kimmel, R. J. (1981). Morphogenesis and synaptogenesis of the zebrafish Mauthner neuron. *J. Comp. Neurol.* **198**, 101–120.

Kitambi, S. S., McCulloch, K. J., Peterson, R. T., and Malicki, J. J. (2009). Small molecule screen for compounds that affect vascular development in the zebrafish retina. *Mech. Dev.* **126**, 464–477.

Kitambi, S., Peterson, R., and Malicki, J. (2008). Small molecule screen for compounds that affect vascular development in the zebrafish retina. *Mech. Dev.* **126**, 464–477.

Kokel, D., Bryan, J., Laggner, C., White, R., Cheung, C. Y., Mateus, R., Healey, D., Kim, S., Werdich, A. A., Haggarty, S. J., Macrae, C. A., Shoichet, B., *et al.* (2010). Rapid behavior-based identification of neuroactive small molecules in the zebrafish. *Nat. Chem. Biol.* **6**, 231–237.

Kondrychyn, I., Garcia-Lecea, M., Emelyanov, A., Parinov, S., and Korzh, V. (2009). Genome-wide analysis of Tol2 transposon reintegration in zebrafish. *BMC Genomics* **10**, 418.

Kosodo, Y., Toida, K., Dubreuil, V., Alexandre, P., Schenk, J., Kiyokage, E., Attardo, A., Mora-Bermudez, F., Arii, T., Clarke, J. D., and Huttner, W. B. (2008). Cytokinesis of neuroepithelial cells can divide their basal process before anaphase. *EMBO J.* **27**, 3151–3163.

Koster, R. W., and Fraser, S. E. (2001). Tracing transgene expression in living zebrafish embryos. *Dev. Biol.* **233**, 329–346.

Krock, B. L., Bilotta, J., and Perkins, B. D. (2007). Noncell-autonomous photoreceptor degeneration in a zebrafish model of choroideremia. *Proc. Natl. Acad. Sci. U. S. A.* **104**, 4600–4605.

Krock, B. L., and Perkins, B. D. (2008). The intraflagellar transport protein IFT57 is required for cilia maintenance and regulates IFT-particle-kinesin-II dissociation in vertebrate photoreceptors. *J. Cell Sci.* **121**, 1907–1915.

Kwan, K. M., Fujimoto, E., Grabher, C., Mangum, B. D., Hardy, M. E., Campbell, D. S., Parant, J. M., Yost, H. J., Kanki, J. P., and Chien, C. B. (2007). The Tol2kit: a multisite gateway-based construction kit for Tol2 transposon transgenesis constructs. *Dev. Dyn.* **236**, 3088–3099.

Laessing, U., Giordano, S., Stecher, B., Lottspeich, F., and Stuermer, C. A. (1994). Molecular characterization of fish neurolin: a growth-associated cell surface protein and member of the immunoglobulin superfamily in the fish retinotectal system with similarities to chick protein DM-GRASP/SC-1/BEN. *Differentiation* **56**, 21–29.

Laessing, U., and Stuermer, C. A. (1996). Spatiotemporal pattern of retinal ganglion cell differentiation revealed by the expression of neurolin in embryonic zebrafish. *J. Neurobiol.* **29**, 65–74.

Larison, K., and Bremiller, R. (1990). Early onset of phenotype and cell patterning in the embryonic zebrafish retina. *Development* **109**, 567–576.

Lawson, N. D., and Weinstein, B. M. (2002). *In vivo* imaging of embryonic vascular development using transgenic zebrafish. *Dev. Biol.* **248**, 567–576.

Li, L., and Dowling, J. E. (1997). A dominant form of inherited retinal degeneration caused by a non-photoreceptor cell-specific mutation. *Proc. Natl. Acad. Sci. U. S. A.* **94**, 11645–11650.

Li, L., and Dowling, J. E. (2000). Disruption of the olfactoretinal centrifugal pathway may relate to the visual system defect in night blindness b mutant zebrafish. *J. Neurosci.* **20**, 1883–1892.

Li, Z., Hu, M., Ochocinska, M. J., Joseph, N. M., and Easter, S. S. Jr. (2000a). Modulation of cell proliferation in the embryonic retina of zebrafish (*Danio rerio*). *Dev. Dyn.* **219**, 391–401.

Li, Z., Joseph, N. M., and Easter, S. S. Jr. (2000b). The morphogenesis of the zebrafish eye, including a fate map of the optic vesicle. *Dev. Dyn.* **218**, 175–188.

Link, B. A., Fadool, J. M., Malicki, J., and Dowling, J. E. (2000). The zebrafish young mutation acts non-cell-autonomously to uncouple differentiation from specification for all retinal cells. *Development* **127**, 2177–2188.

Liu, I. S., Chen, J. D., Ploder, L., Vidgen, D., van der Kooy, D., Kalnins, V. I., and McInnes, R. R. (1994). Developmental expression of a novel murine homeobox gene (Chx10): evidence for roles in determination of the neuroretina and inner nuclear layer. *Neuron* **13**, 377–393.

Lowery, L. A., and Sive, H. (2004). Strategies of vertebrate neurulation and a re-evaluation of teleost neural tube formation. *Mech. Dev.* **121**, 1189–1197.

Macdonald, R., Barth, K. A., Xu, Q., Holder, N., Mikkola, I., and Wilson, S. W. (1995). Midline signalling is required for Pax gene regulation and patterning of the eyes. *Development* **121**, 3267–3278.

Macdonald, R., Scholes, J., Strahle, U., Brennan, C., Holder, N., Brand, M., and Wilson, S. W. (1997). The Pax protein Noi is required for commissural axon pathway formation in the rostral forebrain. *Development* **124**, 2397–2408.

Macdonald, R., and Wilson, S. (1997). Distribution of Pax6 protein during eye development suggests discrete roles in proliferative and differentiated visual cells. *Dev. Genes Evol.* **206**, 363–369.

Mack, A. F., and Fernald, R. D. (1995). New rods move before differentiating in adult teleost retina. *Dev. Biol.* **170**, 136–141.

Makhankov, Y. V., Rinner, O., and Neuhauss, S. C. (2004). An inexpensive device for non-invasive electroretinography in small aquatic vertebrates. *J. Neurosci. Methods* **135**, 205–210.

Malicki, J. (1999). Development of the retina. *Methods Cell Biol.* **59**, 273–299.

Malicki, J. (2000). Harnessing the power of forward genetics—Analysis of neuronal diversity and patterning in the zebrafish retina. *Trends Neurosci.* **23**, 531–541.

Malicki, J., and Driever, W. (1999). *Oko meduzy* mutations affect neuronal patterning in the zebrafish retina and reveal cell–cell interactions of the retinal neuroepithelial sheet. *Development* **126**, 1235–1246.

Malicki, J., Jo, H., and Pujic, Z. (2003). Zebrafish N-cadherin, encoded by the *glass onion* locus, plays an essential role in retinal patterning. *Dev. Biol.* **259**, 95–108.

Malicki, J., Jo, H., Wei, X., Hsiung, M., and Pujic, Z. (2002). Analysis of gene function in the zebrafish retina. *Methods* **28**, 427–438.

Malicki, J., Neuhauss, S. C., Schier, A. F., Solnica-Krezel, L., Stemple, D. L., Stainier, D. Y., Abdelilah, S., Zwartkruis, F., Rangini, Z., and Driever, W. (1996). Mutations affecting development of the zebrafish retina. *Development* **123**, 263–273.

Mangrum, W. I., Dowling, J. E., and Cohen, E. D. (2002). A morphological classification of ganglion cells in the zebrafish retina. *Vis. Neurosci.* **19**, 767–779.

Marcus, R. C., Delaney, C. L., and Easter, S. S. Jr. (1999). Neurogenesis in the visual system of embryonic and adult zebrafish (*Danio rerio*). *Vis. Neurosci.* **16**, 417–424.

Martinez-Morales, J. R., Del Bene, F., Nica, G., Hammerschmidt, M., Bovolenta, P., and Wittbrodt, J. (2005). Differentiation of the vertebrate retina is coordinated by an FGF signaling center. *Dev. Cell* **8**, 565–574.

Masai, I., Lele, Z., Yamaguchi, M., Komori, A., Nakata, A., Nishiwaki, Y., Wada, H., Tanaka, H., Nojima, Y., Hammerschmidt, M., Wilson, S. W., and Okamoto, H. (2003). N-cadherin mediates retinal lamination, maintenance of forebrain compartments and patterning of retinal neurites. *Development* **130**, 2479–2494.

Masai, I., Stemple, D. L., Okamoto, H., and Wilson, S. W. (2000). Midline signals regulate retinal neurogenesis in zebrafish. *Neuron* **27**, 251–263.

Masai, I., Yamaguchi, M., Tonou-Fujimori, N., Komori, A., and Okamoto, H. (2005). The hedgehog–PKA pathway regulates two distinct steps of the differentiation of retinal ganglion cells: the cell-cycle exit of retinoblasts and their neuronal maturation. *Development* **132**, 1539–1553.

McCallum, C. M., Comai, L., Greene, E. A., and Henikoff, S. (2000). Targeted screening for induced mutations. *Nat. Biotechnol.* **18**, 455–457.

Meng, X., Noyes, M. B., Zhu, L. J., Lawson, N. D., and Wolfe, S. A. (2008). Targeted gene inactivation in zebrafish using engineered zinc-finger nucleases. *Nat. Biotechnol.* **26**, 695–701.

Metcalfe, W. K. (1985). Sensory neuron growth cones comigrate with posterior lateral line primordial cells in zebrafish. *J. Comp. Neurol.* **238**, 218–224.

Metcalfe, W. K., Myers, P., Trevarrow, B., Bass, M., and Kimmel, C. (1990). Primary neurons that express the L2/HNK-1 carbohydrate during early development in the zebrafish. *Development* **110**, 491–504.

Moens, C. B., and Fritz, A. (1999). Techniques in neural development. *Methods Cell Biol.* **59**, 253–272.

Mohideen, M. A., Beckwith, L. G., Tsao-Wu, G. S., Moore, J. L., Wong, A. C., Chinoy, M. R., and Cheng, K. C. (2003). Histology-based screen for zebrafish mutants with abnormal cell differentiation. *Dev. Dyn.* **228**, 414–423.

Morris, A. C., Schroeter, E. H., Bilotta, J., Wong, R. O., and Fadool, J. M. (2005). Cone survival despite rod degeneration in XOPS-mCFP transgenic zebrafish. *Invest. Ophthalmol. Vis. Sci.* **46**, 4762–4771.

Muller, H. (1857). Anatomisch-physiologische untersuchungen uber die Retina bei Menschen und Wirbelthieren. *Z. Wiss. Zool.* **8**, 1–122.

Mullins, M. C., Hammerschmidt, M., Haffter, P., and Nusslein-Volhard, C. (1994). Large-scale mutagenesis in the zebrafish: in search of genes controlling development in a vertebrate. *Curr. Biol.* **4**, 189–202.

Mumm, J. S., Williams, P. R., Godinho, L., Koerber, A., Pittman, A. J., Roeser, T., Chien, C. B., Baier, H., and Wong, R. O. (2006). *In vivo* imaging reveals dendritic targeting of laminated afferents by zebrafish retinal ganglion cells. *Neuron* **52**, 609–621.

Muto, A., Orger, M. B., Wehman, A. M., Smear, M. C., Kay, J. N., Page-McCaw, P. S., Gahtan, E., Xiao, T., Nevin, L. M., Gosse, N. J., Staub, W., Finger-Baier, K., *et al.* (2005). Forward genetic analysis of visual behavior in zebrafish. *PLoS Genet.* **1**, e66.

Nagayoshi, S., Hayashi, E., Abe, G., Osato, N., Asakawa, K., Urasaki, A., Horikawa, K., Ikeo, K., Takeda, H., and Kawakami, K. (2008). Insertional mutagenesis by the Tol2 transposon-mediated enhancer trap approach generated mutations in two developmental genes: Tcf7 and synembryn-like. *Development* **135**, 159–169.

Nasevicius, A., and Ekker, S. C. (2000). Effective targeted gene "knockdown" in zebrafish. *Nat. Genet.* **26**, 216–220.

Nawrocki, W. (1985). Development of the neural retina in the zebrafish (*Brachydanio rerio*). Ph. D. dissertation, University of Oregon, Eugine, OR.

Neuhauss, S. C. (2003). Behavioral genetic approaches to visual system development and function in zebrafish. *J. Neurobiol.* **54**, 148–160.

Neuhauss, S. C., Biehlmaier, O., Seeliger, M. W., Das, T., Kohler, K., Harris, W. A., and Baier, H. (1999). Genetic disorders of vision revealed by a behavioral screen of 400 essential loci in zebrafish. *J. Neurosci.* **19**, 8603–8615.

Neumann, C. J., and Nuesslein-Volhard, C. (2000). Patterning of the zebrafish retina by a wave of sonic hedgehog activity. *Science* **289**, 2137–2139.

Nicolson, T., Rusch, A., Friedrich, R. W., Granato, M., Ruppersberg, J. P., and Nusslein-Volhard, C. (1998). Genetic analysis of vertebrate sensory hair cell mechanosensation: the zebrafish circler mutants. *Neuron* **20**, 271–283.

Norden, C., Young, S., Link, B. A., and Harris, W. A. (2009). Actomyosin is the main driver of interkinetic nuclear migration in the retina. *Cell* **138**, 1195–1208.

Nornes, H. O., Dressler, G. R., Knapik, E. W., Deutsch, U., and Gruss, P. (1990). Spatially and temporally restricted expression of Pax2 during murine neurogenesis. *Development* **109**, 797–809.

North, T. E., Goessling, W., Peeters, M., Li, P., Ceol, C., Lord, A. M., Weber, G. J., Harris, J., Cutting, C. C., Huang, P. *et al*. (2009). Hematopoietic stem cell development is dependent on blood flow. *Cell* **137**, 736–748.

North, T. E., Goessling, W., Walkley, C. R., Lengerke, C., Kopani, K. R., Lord, A. M., Weber, G. J., Bowman, T. V., Jang, I. H., Grosser, T., Fitzgerald, G. A., Daley, G. Q., *et al*. (2007). Prostaglandin E2 regulates vertebrate haematopoietic stem cell homeostasis. *Nature* **447**, 1007–1011.

Novak, A. E., and Ribera, A. B. (2003). Immunocytochemistry as a tool for zebrafish developmental neurobiology. *Methods Cell Sci.* **25**, 79–83.

Omori, Y., Zhao, C., Saras, A., Mukhopadhyay, S., Kim, W., Furukawa, T., Sengupta, P., Veraksa, A., and Malicki, J. (2008). Elipsa is an early determinant of ciliogenesis that links the IFT particle to membrane-associated small GTPase Rab8. *Nature Cell Biol.* **10**, 437–444.

Oxtoby, E., and Jowett, T. (1993). Cloning of the zebrafish krox-20 gene (krx-20) and its expression during hindbrain development. *Nucleic Acids Res.* **21**, 1087–1095.

Passini, M. A., Levine, E. M., Canger, A. K., Raymond, P. A., and Schechter, N. (1997). Vsx-1 and Vsx-2: differential expression of two paired-like homeobox genes during zebrafish and goldfish retinogenesis. *J. Comp. Neurol.* **388**, 495–505.

Pathak, N., Obara, T., Mangos, S., Liu, Y., and Drummond, I. A. (2007). The zebrafish fleer gene encodes an essential regulator of cilia tubulin polyglutamylation. *Mol. Biol. Cell* **18**, 4353–4364.

Pauls, S., Geldmacher-Voss, B., and Campos-Ortega, J. A. (2001). A zebrafish histone variant H2A.F/Z and a transgenic H2A.F/Z: GFP fusion protein for *in vivo* studies of embryonic development. *Dev. Genes Evol.* **211**, 603–610.

Perkins, B. D., Kainz, P. M., O'Malley, D. M., and Dowling, J. E. (2002). Transgenic expression of a GFP-rhodopsin COOH-terminal fusion protein in zebrafish rod photoreceptors. *Vis. Neurosci.* **19**, 257–264.

Peterson, R. E., Fadool, J. M., McClintock, J., and Linser, P. J. (2001). Müller cell differentiation in the zebrafish neural retina: evidence of distinct early and late stages in cell maturation. *J. Comp. Neurol.* **429**, 530–540.

Peterson, R. T., Link, B. A., Dowling, J. E., and Schreiber, S. L. (2000). Small molecule developmental screens reveal the logic and timing of vertebrate development. *Proc. Natl. Acad. Sci. U. S. A.* **97**, 12965–12969.

Peterson, R. T., Shaw, S. Y., Peterson, T. A., Milan, D. J., Zhong, T. P., Schreiber, S. L., MacRae, C. A., and Fishman, M. C. (2004). Chemical suppression of a genetic mutation in a zebrafish model of aortic coarctation. *Nat. Biotechnol.* **22**, 595–599.

Peterson, R. E., Tu, C., and Linser, P. J. (1997). Isolation and characterization of a carbonic anhydrase homologue from the zebrafish (*Danio rerio*). *J. Mol. Evol.* **44**, 432–439.

Plaster, N., Sonntag, C., Busse, C. E., and Hammerschmidt, M. (2006). p53 deficiency rescues apoptosis and differentiation of multiple cell types in zebrafish flathead mutants deficient for zygotic DNA polymerase delta1. *Cell Death Differ.* **13**, 223–235.

Poggi, L., Vitorino, M., Masai, I., and Harris, W. A. (2005). Influences on neural lineage and mode of division in the zebrafish retina *in vivo*. *J. Cell Biol.* **171**, 991–999.

Porteus, M. H., and Carroll, D. (2005). Gene targeting using zinc finger nucleases. *Nat. Biotechnol.* **23**, 967–973.

Prince, V. E., Joly, L., Ekker, M., and Ho, R. K. (1998). Zebrafish hox genes: genomic organization and modified colinear expression patterns in the trunk. *Development* **125**, 407–420.

Pujic, Z., and Malicki, J. (2001). Mutation of the zebrafish *glass onion* locus causes early cell-nonautonomous loss of neuroepithelial integrity followed by severe neuronal patterning defects in the retina. *Dev. Biol.* **234**, 454–469.

Pujic, Z., and Malicki, J. (2004). Retinal pattern and the genetic basis of its formation in zebrafish. *Semin. Cell Dev. Biol.* **15**, 105–114.

Pujic, Z., Omori, Y., Tsujikawa, M., Thisse, B., Thisse, C., and Malicki, J. (2006). Reverse genetic analysis of neurogenesis in the zebrafish retina. *Dev. Biol.* **293**, 330–347.

Raible, D. W., Wood, A., Hodsdon, W., Henion, P. D., Weston, J. A., and Eisen, J. S. (1992). Segregation and early dispersal of neural crest cells in the embryonic zebrafish. *Dev. Dyn.* **195**, 29–42.

Raymond, P., Barthel, L., and Curran, G. (1995). Developmental patterning of rod and cone photoreceptors in embryonic zebrafish. *J. Comp. Neurol.* **359**, 537–550.

Raymond, P., Barthel, L., Rounsifer, M., Sullivan, S., and Knight, J. (1993). Expression of rod and cone visual pigments in godfish and zebrafish: a rhodopsin-like gene is expressed in cones. *Neuron* **10**, 1161–1174.

Raz, E., van Luenen, H. G., Schaerringer, B., Plasterk, R. H., and Driever, W. (1998). Transposition of the nematode *Caenorhabditis elegans* Tc3 element in the zebrafish *Danio rerio*. *Curr. Biol.* **8**, 82–88.

Rembold, M., Loosli, F., Adams, R. J., and Wittbrodt, J. (2006). Individual cell migration serves as the driving force for optic vesicle evagination. *Science* **313**, 1130–1134.

Ren, J. Q., McCarthy, W. R., Zhang, H., Adolph, A. R., and Li, L. (2002). Behavioral visual responses of wild-type and hypopigmented zebrafish. *Vision Res.* **42**, 293–299.

Riley, B. B., Chiang, M., Farmer, L., and Heck, R. (1999). The deltaA gene of zebrafish mediates lateral inhibition of hair cells in the inner ear and is regulated by pax2.1. *Development* **126**, 5669–78.

Robinson, J., Schmitt, E., and Dowling, J. (1995). Temporal and spatial patterns of opsin gene expression in zebrafish (*Danio rerio*). *Vis. Neurosci.* **12**, 895–906.

Rodieck, R. W. (1973). "The Vertebrate Retina: Principles of Structure and Function". W. H. Freeman & Co., San Francisco, CA.

Roeser, T., and Baier, H. (2003). Visuomotor behaviors in larval zebrafish after GFP-guided laser ablation of the optic tectum. *J. Neurosci.* **23**, 3726–3734.

Sachidanandan, C., Yeh, J., Peteerson, Q., and Peteerson, R. (2008). Identification of a novel retinoid by small molecule screening with zebrafish embryos. *PLoS One* **3**, 1–9.

Sandell, J., Martin, S., and Heinrich, G. (1994). The development of GABA immunoreactivity in the retina of the zebrafish. *J. Comp. Neurol.* **345**, 596–601.

Sanes, J. R. (1993). Topographic maps and molecular gradients. *Curr. Opin. Neurobiol.* **3**, 67–74.

Sato, T., Takahoko, M., and Okamoto, H. (2006). HuC:Kaede, a useful tool to label neural morphologies in networks *in vivo*. *Genesis* **44**, 136–142.

Scheer, N., and Campos-Ortega, J. A. (1999). Use of the Gal4–UAS technique for targeted gene expression in the zebrafish. *Mech. Dev.* **80**, 153–158.

Scheer, N., Groth, A., Hans, S., and Campos-Ortega, J. A. (2001). An instructive function for Notch in promoting gliogenesis in the zebrafish retina. *Development* **128**, 1099–1107.

Scheer, N., Riedl, I., Warren, J. T., Kuwada, J. Y., and Campos-Ortega, J. A. (2002). A quantitative analysis of the kinetics of Gal4 activator and effector gene expression in the zebrafish. *Mech. Dev.* **112**, 9–14.

Schier, A. F., Neuhauss, S. C., Helde, K. A., Talbot, W. S., and Driever, W. (1997). The one-eyed pinhead gene functions in mesoderm and endoderm formation in zebrafish and interacts with no tail. *Development* **124**, 327–342.

Schmitt, E., and Dowling, J. (1994). Early eye morphogenesis in the zebrafish, *Brachydanio rerio*. *J. Comp. Neurol.* **344**, 532–542.

Schmitt, E. A., and Dowling, J. E. (1996). Comparison of topographical patterns of ganglion and photoreceptor cell differentiation in the retina of the zebrafish, *Danio rerio*. *J. Comp. Neurol.* **371**, 222–234.

Schmitt, E. A., and Dowling, J. E. (1999). Early retinal development in the zebrafish, *Danio rerio*: light and electron microscopic analyses. *J. Comp. Neurol.* **404**, 515–536

Schmitz, B., Papan, C., and Campos-Ortega, J. (1993). Neurulation in the anterior trunk of the zebrafish *Brachydanio rerio*. *Roux's Arch. Dev. Biol.* **202**, 250–259.

Schroeter, E. H., Wong, R. O., and Gregg, R. G. (2006). *In vivo* development of retinal ON-bipolar cell axonal terminals visualized in nyx: MYFP transgenic zebrafish. *Vis. Neurosci.* **23**, 833–843.

Scott, E. K., Mason, L., Arrenberg, A. B., Ziv, L., Gosse, N. J., Xiao, T., Chi, N. C., Asakawa, K., Kawakami, K., and Baier, H. (2007). Targeting neural circuitry in zebrafish using GAL4 enhancer trapping. *Nat. Methods* **4**, 323–326.

Seddon, J. (1994). Age-relatred macular degeneration: epidemiology. *In* "Principles and Practice of Ophthalmology" (B. Albert, and F. Jakobiec, eds.) pp. 1266–1274. Philadelphia

Seo, H. C., Drivenes, O., Ellingsen, S., and Fjose, A. (1998). Expression of two zebrafish homologues of the murine Six3 gene demarcates the initial eye primordia. *Mech. Dev.* **73**, 45–57.

Shaner, N. C., Patterson, G. H., and Davidson, M. W. (2007). Advances in fluorescent protein technology. *J. Cell. Sci.* **120**, 4247–4260.

Shields, C. R., Klooster, J., Claassen, Y., Ul-Hussain, M., Zoidl, G., Dermietzel, R., and Kamermans, M. (2007). Retinal horizontal cell-specific promoter activity and protein expression of zebrafish connexin 52.6 and connexin 55.5. *J. Comp. Neurol.* **501**, 765–779.

Sivasubbu, S., Balciunas, D., Davidson, A. E., Pickart, M. A., Hermanson, S. B., Wangensteen, K. J., Wolbrink, D. C., and Ekker, S. C. (2006). Gene-breaking transposon mutagenesis reveals an essential role for histone H2afza in zebrafish larval development. *Mech. Dev.* **123**, 513–529.

Solnica-Krezel, L., Schier, A., and Driever, W. (1994). Efficient recovery of ENU-induced mutations from the zebrafish germline. *Genetics* **136**, 1–20.

Soules, K. A., and Link, B. A. (2005). Morphogenesis of the anterior segment in the zebrafish eye. *BMC Dev. Biol.* **5**, 12.

Strahle, U., Blader, P., Adam, J., and Ingham, P. W. (1994). A simple and efficient procedure for non-isotopic *in situ* hybridization to sectioned material. *Trends Genet.* **10**, 75–76.

Streisinger, G., Singer, F., Walker, C., Knauber, D., and Dower, N. (1986). Segregation analyses and gene–centromere distances in zebrafish. *Genetics* **112**, 311–319.

Streisinger, G., Walker, C., Dower, N., Knauber, D., and Singer, F. (1981). Production of clones of homozygous diploid zebra fish (*Brachydanio rerio*). *Nature* **291**, 293–296.

Stuermer, C. A. (1988). Retinotopic organization of the developing retinotectal projections in the zebrafish embryo. *J. Neurosci*. **12**, 4513–4530.

Take-uchi, M., Clarke, J. D., and Wilson, S. W. (2003). Hedgehog signalling maintains the optic stalk–retinal interface through the regulation of Vax gene activity. *Development* **130**, 955–968.

Takechi, M., Hamaoka, T., and Kawamura, S. (2003). Fluorescence visualization of ultraviolet-sensitive cone photoreceptor development in living zebrafish. *FEBS Lett.* **553**, 90–94.

Takechi, M., and Kawamura, S. (2005). Temporal and spatial changes in the expression pattern of multiple red and green subtype opsin genes during zebrafish development. *J. Exp. Biol.* **208**, 1337–1345.

Taylor, M. R., Hurley, J. B., Van Epps, H. A., and Brockerhoff, S. E. (2004). A zebrafish model for pyruvate dehydrogenase deficiency: rescue of neurological dysfunction and embryonic lethality using a ketogenic diet. *Proc. Natl. Acad. Sci. U. S. A.* **101**, 4584–4589.

Thisse, B., Heyer, V., Lux, A., Alunni, V., Degrave, A., Seiliez, I., Kirchner, J., Parkhill, J. P., and Thisse, C. (2004). Spatial and temporal expression of the zebrafish genome by large-scale *in situ* hybridization screening. *Methods Cell Biol.* **77**, 505–519.

Tran, T. C., Sneed, B., Haider, J., Blavo, D., White, A., Aiyejorun, T., Baranowski, T. C., Rubinstein, A. L., Doan, T. N., Dingledine, R., and Sandberg, E. M (2007). Automated, quantitative screening assay for antiangiogenic compounds using transgenic zebrafish. *Cancer Res.* **67**, 11386–11392.

Trowe, T., Klostermann, S., Baier, H., Granato, M., Crawford, A. D., Grunewald, B., Hoffmann, H., Karlstrom, R. O., Meyer, S. U., Muller, B., Richter, S., Nüsslein-Volhard, C., *et al*. (1996). Mutations disrupting the ordering and topographic mapping of axons in the retinotectal projection of the zebrafish, *Danio rerio*. *Development* **123**, 439–450.

Tsujimura, T., Chinen, A., and Kawamura, S. (2007). Identification of a locus control region for quadruplicated green-sensitive opsin genes in zebrafish. *Proc. Natl. Acad. Sci. U. S. A.* **104**, 12813–12818.

Tsujikawa, M., and Malicki, J. (2004a). Genetics of photoreceptor development and function in zebrafish. *Int. J. Dev. Biol.* **48**, 925–934.

Tsujikawa, M., and Malicki, J. (2004b). Intraflagellar transport genes are essential for differentiation and survival of vertebrate sensory neurons. *Neuron* **42**, 703–716.

Turner, D., and Cepko, C. (1987). A common progenitor for neurons and glia persists in rat retina late in development. *Nature* **328**, 131–136.

Turner, D., Snyder, E., and Cepko, C. (1990). Lineage-independent determination of cell type in the embryonic mouse retina. *Neuron* **4**, 833–845.

Urasaki, A., Morvan, G., and Kawakami, K. (2006). Functional dissection of the Tol2 transposable element identified the minimal *cis*-sequence and a highly repetitive sequence in the subterminal region essential for transposition. *Genetics* **174**, 639–649.

van Eeden, F. J., Granato, M., Odenthal, J., and Haffter, P. (1999). Developmental mutant screens in the zebrafish. *Methods Cell Biol.* **60**, 21–41.

Varga, Z. M., Wegner, J., and Westerfield, M. (1999). Anterior movement of ventral diencephalic precursors separates the primordial eye field in the neural plate and requires cyclops. *Development* **126**, 5533–5546.

Vihtelic, T. S., Doro, C. J., and Hyde, D. R. (1999). Cloning and characterization of six zebrafish photoreceptor opsin cDNAs and immunolocalization of their corresponding proteins. *Vis. Neurosci.* **16**, 571–585.

Vihtelic, T. S., and Hyde, D. R. (2000). Light-induced rod and cone cell death and regeneration in the adult albino zebrafish (*Danio rerio*) retina. *J. Neurobiol.* **44**, 289–307.

Villefranc, J. A., Amigo, J., and Lawson, N. D. (2007). Gateway compatible vectors for analysis of gene function in the zebrafish. *Dev. Dyn.* **236**, 3077–3087.

Walker, C. (1999). Haploid screens and gamma-ray mutagenesis. *Methods Cell Biol.* **60**, 43–70.

Watanabe, T., and Raff, M. (1988). Retinal astrocytes are immigrants from the optic nerve. *Nature* **332**, 834–837.

Wei, X., and Malicki, J. (2002). Nagie oko, encoding a MAGUK-family protein, is essential for cellular patterning of the retina. *Nat. Genet.* **31**, 150–157.

Westerfield, M. (2000). "The Zebrafish Book. A Guide for the Laboratory Use of Zebrafish (*Danio rerio*)". University of Oregon Press, Eugene.

Wetts, R., and Fraser, S. (1988). Multipotent precursors can give rise to all major cell types of the frog retina. *Science* **239**, 1142–1145.

Wienholds, E., Schulte-Merker, S., Walderich, B., and Plasterk, R. H. (2002). Target-selected inactivation of the zebrafish rag1 gene. *Science* **297**, 99–102.

Wise, G., Dollery, C., and Henkind, P. (1971). "The Retinal Circulation". Harper & Row, New York.

Woo, K., and Fraser, S. E. (1995). Order and coherence in the fate map of the zebrafish nervous system. *Development* **121**, 2595–2609.

Wright, D. A., Thibodeau-Beganny, S., Sander, J. D., Winfrey, R. J., Hirsh, A. S., Eichtinger, M., Fu, F., Porteus, M. H., Dobbs, D., Voytas, D. F., and Joung, J. K. (2006). Standardized reagents and protocols for engineering zinc finger nucleases by modular assembly. *Nat. Protoc.* **1**, 1637–1652.

Xiao, T., Roeser, T., Staub, W., and Baier, H. (2005). A GFP-based genetic screen reveals mutations that disrupt the architecture of the zebrafish retinotectal projection. *Development* **132**, 2955–2967.

Yamaguchi, M., Fujimori-Tonou, N., Yoshimura, Y., Kishi, T., Okamoto, H., and Masai, I. (2008). Mutation of DNA primase causes extensive apoptosis of retinal neurons through the activation of DNA damage checkpoint and tumor suppressor p53. *Development* **135**, 1247–1257.

Yamaguchi, M., Imai, F., Tonou-Fujimori, N., and Masai, I. (2010). Mutations in N-cadherin and a Stardust homolog, Nagie oko, affect cell-cycle exit in zebrafish retina. *Mech. Dev.* **127**, 247–264.

Yamamoto, Y., and Jeffery, W. R. (2002). Probing teleost eye development by lens transplantation. *Methods* **28**, 420–426.

Yazulla, S., and Studholme, K. M. (2001). Neurochemical anatomy of the zebrafish retina as determined by immunocytochemistry. *J. Neurocytol.* **30**, 551–592.

Yeo, S. Y., Kim, M., Kim, H. S., Huh, T. L., and Chitnis, A. B. (2007). Fluorescent protein expression driven by her4 regulatory elements reveals the spatiotemporal pattern of Notch signaling in the nervous system of zebrafish embryos. *Dev. Biol.* **301**, 555–567.

Yu, C. J., Gao, Y., Willis, C. L., Li, P., Tiano, J. P., Nakamura, P. A., Hyde, D. R., and Li, L. (2007). Mitogen-associated protein kinase- and protein kinase A-dependent regulation of rhodopsin promoter expression in zebrafish rod photoreceptor cells. *J. Neurosci. Res.* **85**, 488–496.

Zhang, Y., McCulloch, K., and Malicki, J. (2009). Lens transplantation in zebrafish and its application in the analysis of eye mutants. *J Vis. Exp.*

Zhao, X. C., Yee, R. W., Norcom, E., Burgess, H., Avanesov, A. S., Barrish, J. P., and Malicki, J. (2006). The zebrafish cornea: structure and development. *Invest. Ophthalmol. Vis. Sci.* **47**, 4341–4348.

Zolessi, F. R., Poggi, L., Wilkinson, C. J., Chien, C. B., and Harris, W. A. (2006). Polarization and orientation of retinal ganglion cells *in vivo*. *Neural Dev.* **1**, 2.

Zon, L. I., and Peterson, R. T. (2005). *In vivo* drug discovery in the zebrafish. *Nat. Rev. Drug Discov.* **4**, 35–44.

# CHAPTER 7

# Photoreceptor Structure and Development: Analyses using GFP Transgenes

**Brian D. Perkins**[*] *and* **James M. Fadool**[†]

[*]Department of Biology, Texas A&M University, College Station, Texas

[†]Department of Biological Science, Florida State University, Tallahassee, Florida.

Abstract
I. Introduction
  A. Photoreceptor Anatomy and Biochemistry
  B. Photoreceptor Development
  C. Improvements in Transgenic Technology
II. Transport Mechanisms
III. Regulation of Photoreceptor Size
IV. Photoreceptor Synapse Structure
V. Regeneration
VI. Future Directions
VII. Conclusions
References

## Abstract

In recent years, studies of zebrafish rod and cone photoreceptors have yielded novel insights into the differentiation of distinct photoreceptor cell types and the mechanisms guiding photoreceptor regeneration following cell death, and they have provided models of human retinal degeneration. These studies were facilitated by the use of transgenic zebrafish expressing fluorescent reporter genes under the control of various cell-specific promoters. Improvements in transgenesis techniques (e.g., Tol2 transposition), the availability of numerous fluorescent reporter genes with different localization properties, and the ability to generate transgenes via recombineering (e.g., Gateway technology) have enabled researchers to quickly develop transgenic lines that improve our understanding of the causes of human blindness and ways to mitigate its effects.

Copyright © 2010 Elsevier Inc. All rights reserved.

978-0-12-384892-5
DOI: 10.1016/B978-0-12-384892-5.00007-4

# I. Introduction

More is known about photoreceptor cells than any other cell in the vertebrate retina. From early studies in psychophysics (Hecht *et al*., 1942) and on visual pigments (Wald, 1955), to the work on mechanisms of dark adaptation (Dowling, 1963), phototransduction (Yau, 1994), and inherited retinal disease (Dryja and Li, 1995), rod photoreceptors have been central to the understanding of retinal function and hereditary blindness disorders. Many of the mutations known to cause hereditary retinal degeneration affect rod-specific genes or otherwise interfere with rod function. For reasons still not fully understood, rod degeneration often leads to the secondary death of cone photoreceptors and the loss of color vision and eventually all vision. For decades, insights into the mechanisms of rod photoreceptor degeneration came from studies of naturally occurring mutations and gene knock-outs in nocturnal mammalian models such as rats and mice, whose retinas have ~95% rods. More recently, diseases primarily affecting cone photoreceptors, such as achromatopsia, have prompted investigations into the biochemical and physiological properties of cones. The zebrafish is a diurnal animal with a retina containing large numbers of diverse cone subtypes (Branchek, 1984; Branchek and Bremiller, 1984; Fadool, 2003; Raymond *et al*., 1993, 1995), which make zebrafish an ideal model to study the pathological mechanisms underlying both rod and cone degeneration, as well as to examine the capacity of the vertebrate retina to regenerate rods and cones.

## A. Photoreceptor Anatomy and Biochemistry

Both rod and cone photoreceptors are highly specialized cells with a unique morphology consisting of an elongated outer segment, connecting cilium, inner segment, cell body, and synaptic terminal (Fig. 1). The shape and morphology of the outer segments (OSs) usually distinguish the rods from the cones and provide the basis for their nomenclature. The OS consists of hundreds of tightly stacked membrane discs that contain the proteins necessary for phototransduction. Protein synthesis occurs in the inner segment, and molecules destined for the OS must be transported apically through the connecting cilium via a process known as intraflagellar transport (IFT) (see Insinna and Besharse, 2008 for a recent review). The inner segment also contains numerous mitochondria needed to provide the energy for the demands of protein synthesis, protein trafficking, and phototransduction. The synaptic terminals of rod photoreceptors, known as spherules, are typically smaller than the cone terminals, known as pedicles. Both spherules and pedicles are filled with synaptic vesicles, contain synaptic ribbons, and are presynaptic to the bipolar and horizontal cells.

Zebrafish possess one type of rod photoreceptor and four subtypes of cone photoreceptors. The zebrafish cone subtypes absorb light maximally in the red (570 nm), green (480 nm), blue (415 nm), and ultraviolet (362 nm) regions of the spectrum (Robinson *et al*., 1993). These cone types are also distinguishable morphologically; short and long single cones contain the ultraviolet (UV)- and blue-absorbing visual pigments, respectively, whereas the red- and green-sensitive visual pigments are found

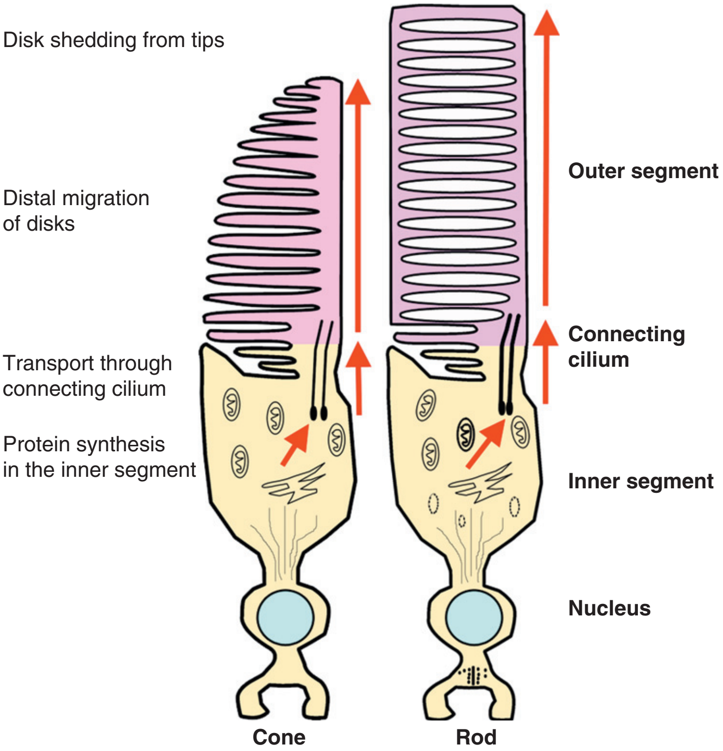
Disk shedding from tips
Distal migration of disks
Transport through connecting cilium
Protein synthesis in the inner segment
Outer segment
Connecting cilium
Inner segment
Nucleus
Cone
Rod

**Fig. 1** Anatomy cartoon diagrams of vertebrate cone (left) and rod (right) photoreceptors. Arrows indicate the direction of protein trafficking for most outer segment proteins. The outer segments are more darkly shaded and cellular processes relevant for outer segment development are outlined on the left.

in the principal and accessory members of the double cones (Robinson *et al*., 1993). The cone photoreceptors are arranged in a highly ordered crystalline mosaic, with rod inner segments projecting through the cone mosaic to surround the UV cones (Fadool, 2003). Additional details about the cone mosaic and cone physiology can be found in two recent review articles (Fadool and Dowling, 2008; Raymond and Barthel, 2004)

## B. Photoreceptor Development

In vertebrates, neurogenesis of the retina begins when proliferating neuroblasts exit the cell cycle and begin the process of differentiation. In most species, including zebrafish, cone differentiation occurs before rod differentiation. The expression of the zebrafish rod opsin gene begins at approximately 50 h post-fertilization (hpf) (Schmitt and Dowling, 1996) in a region of precocious neurogenesis in the ventral nasal retina referred to as the ventral patch. The red and blue cone opsin genes are also expressed at about 50 hpf while expression of the UV opsin gene is observed about 5 h later (Schmitt *et al*., 1999). Similarly, small clusters of rods and the red/green double cones are labeled with the monoclonal antibodies ROS-1 and Zpr-1, respectively, in whole mount at 50 hpf (Raymond *et al*., 1995). Given that the first cells in the outer nuclear layer (ONL) of the retina to become post-mitotic are seen between 43 and 48 hpf (Hu and Easter, 1999), it is likely that cell cycle exit precedes opsin expression by several hours. Cone differentiation occurs in a sweeping fashion from the ventronasal side of the choroid fissure to the dorsonasal retina and then to the dorsotemporal and ventrotemporal side of the choroid fissure (Raymond *et al*., 1995; Schmitt and Dowling, 1996). On the other hand, rod differentiation initiates in the ventral retina on the nasal side of the choroid fissure but soon crosses directly to the temporal side of the fissure. This ventral patch of rods grows symmetrically across the choroid fissure and increases in density while slowly expanding. Between 50 and 72 hpf, rods fill in the dorsal retina in a seemingly random fashion that does not resemble the wave of differentiation exhibited by all other retinal cell types (Raymond *et al*., 1995; Schmitt and Dowling, 1996). Despite similarities in timing of early rod and cone differentiation, zebrafish vision is predominantly cone driven for several days. Based upon behavioral studies and electroretinogram (ERG) recordings, rod function can first be demonstrated only between 14 and 21 days post-fertilization (dpf) (Bilotta *et al*., 2001; Saszik *et al*., 1999). Spectral sensitivity appears to be cone dominated through 15 dpf, and the rod contribution is not adult-like until close to 1 month of age (Bilotta *et al*., 2001; Saszik *et al*., 1999).

A number of intrinsic and extrinsic factors contribute to the specification, differentiation, and maturation of rods, but the story is far from complete. For example, the transcription factors neural retina leucine zipper (Nrl), cone–rod homeobox (*crx*) gene, *neuroD*, and *tbx2b* regulate distinct aspects of rod development (Alvarez-Delfin *et al*., 2009; Furukawa *et al*., 1997, 1999; Mears *et al*., 2001). Extrinsic factors known to promote rod specification and differentiation include sonic hedgehog (Shh) (Shkumatava *et al*., 2004; Stenkamp and Frey, 2003), taurine (Young and Cepko, 2004), fibroblast growth factor (Patel and McFarlane, 2000), and retinoic acid (Hyatt *et al*., 1996; Perkins *et al*., 2002). Given the potentially broad 12-h time window for cell cycle exit and differentiation of photoreceptors (~43–55 hpf), it is unclear if these extrinsic signals contribute equally to the specification and differentiation of rods and cones.

## C. Improvements in Transgenic Technology

The techniques to generate transgenic zebrafish have significantly improved in the last 5 years. In the past, linearized plasmid DNA containing the transgene was injected into the yolks of 1–4-cell-stage zebrafish embryos. In a small percentage of cases (typically 5–10%), the DNA randomly integrates into the genome of the germ cells. These “founder fish” produced transgenic progeny. As described in a previous review (Perkins *et al*., 2004), this approach was used to generate transgenic zebrafish lines that express GFP exclusively in rod photoreceptor cells (Fadool, 2003; Hamaoka *et al*., 2002; Kennedy *et al*., 2001; Perkins *et al*., 2002), one line that expresses GFP in all cone photoreceptors (Kennedy *et al*., 2007), and one line that selectively marks UV cones (Takechi *et al*., 2003). Today, transgenesis frequencies have been increased by creating plasmids that contain sequences recognized by a rare-cutting endonuclease, such as *I-SceI*, or by inserting the transgene into the Tol2 transposon (see Chapter 4). In both cases, the percentage of injected embryos transiently expressing the transgene is elevated severalfold, and the rate of germ line transmission has approached 70% (Balciunas *et al*., 2006). Construction of Tol2 vectors for transgenesis is now facilitated by the use of site-specific recombination cloning (Gateway®) technology, as part of the "Tol2kit" (Kwan *et al*., 2007). The Tol2kit consists of various plasmids containing Gateway recombination sequences. A functional Tol2 transposon may be rapidly assembled in a modular fashion by recombining a promoter-containing 5′ element, a 3′-tag, and a Tol2 transposon backbone. With these tools in hand, one can quickly construct Tol2 transposons and generate transgenic lines that express fluorescent markers behind cell-specific or inducible promoters and express proteins fused at the N- or C-terminus with fluorescent markers or protein purification tags, as well as other variations.

## II. Transport Mechanisms

Photoreceptor OSs rapidly turn over throughout the lives of photoreceptor cells; thus, efficient protein transport mechanisms provide photoreceptors with a sufficient supply of protein to replenish that lost during OS turnover. It is estimated that rhodopsin constitutes 90% of the total protein in the rod OS and therefore plays important roles in both the physiology and structural integrity of the photoreceptor (Nathans, 1992). As such, investigations into this process have primarily focused on the transport of rhodopsin.

The photoreceptor OS can be considered a specialized sensory cilium that concentrates opsin for light detection. All cilia consist of a microtubule-based axoneme surrounded by the ciliary membrane. Beginning at the basal body, the photoreceptor axoneme extends into a transition zone, known as the connecting cilium, and continues distally into the OS where it terminates near the tip as singlet microtubules (Insinna and Besharse, 2008). Disc membrane assembly occurs at the base of the OS, just beyond the distal end of the transition zone. A process known as intraflagellar transport, or IFT, transports opsin molecules through the connecting cilium where they then incorporate into newly assembled disc membranes (Insinna *et al*., 2008, 2009a; Marszalek *et al*., 2000; Pazour *et al*., 2002). IFT refers to the bidirectional movement of multisubunit IFT particles along the length of the ciliary axoneme. The IFT particle is composed of at least 18 distinct proteins and perhaps dozens of associated protein components and cargo molecules (Hao and Scholey, 2009). Although most OS proteins incorporate into disc membranes and are eventually shed from the distal tips of photoreceptors, IFT particles are believed to migrate along the length of the axoneme in both an anterograde and a retrograde manner. Evidence for this comes from transient transgenesis experiments where constructs containing IFT proteins fused to GFP were expressed using a zebrafish rhodopsin promoter (Insinna *et al*., 2009b; Kennedy *et al*., 2001; Luby-Phelps *et al*., 2008). Rod-specific overexpression of IFT20-GFP, IFT52-GFP, IFT57-GFP, and IFT88-GFP found localization of IFT proteins along the entire length of the axoneme, as well as the basal body and the connecting cilium.

Cilia formation and anterograde IFT movement require two kinesin motor proteins. The heterotrimeric kinesin-II motor, which is composed of the Kif3a and Kif3b kinesin subunits and a kinesin-associated protein (KAP) subunit, was first shown to be required for rod photoreceptors (Marszalek *et al*., 2000). Studies in *Caenorhabditis elegans*, however, revealed that a homodimeric kinesin-II motor, OSM-3, was also required for ciliogenesis in some sensory neurons. Insinna and colleagues (2008, 2009a) found that Kif17, the vertebrate homolog to OSM-3, was also essential for ciliogenesis and OS formation in zebrafish photoreceptors. The authors compared the roles of these different kinesin motors in photoreceptor function by creating new constructs that utilized the promoter for the zebrafish cone transducin alpha subunit (TαC) (Kennedy *et al*., 2007) to drive dominant-negative forms of either the *Xenopus* Kif3b (Lin-Jones *et al*., 2003) or the mouse Kif17 (Chu *et al*., 2006). In both cases, the motor domain of the kinesin protein was replaced by GFP. The 3.2 kilobase fragment of the TαC promoter drives expression in all cone subtypes, although the first observed expression of a GFP transgene does not occur until ~70 hpf, which is several hours after endogenous opsin expression (Kennedy *et al*., 2007). Overexpression of the dominant-negative Kif17 (DNKIF17) caused severe ablation of cone OSs, whereas the dominant-negative Kif3b (DNKIF3B) was less damaging to cones. In contrast, opsin mislocalization was observed in cells expressing DNKIF3B but not DNKIF17, suggesting that these two kinesins regulate trafficking of distinct cargoes (Insinna *et al*., 2009b).

## III. Regulation of Photoreceptor Size

The length of mature photoreceptor OSs remains almost constant through the daily balancing act of disc membrane renewal. Approximately 10% of the OS is shed from the apical tips and this material is replaced at the OS base on a daily basis. Almost nothing is known about the mechanisms that maintain OS at a constant size or the mechanisms that regulate the IFT process, thereby facilitating OS renewal. Recent work has suggested that the 4.1 protein, ezrin, radixin, moesin (FERM) protein Mosaic eyes may function to negatively regulate apical renewal of photoreceptors (Hsu *et al*., 2006). The zebrafish *mosaic eyes* (*moe*) gene is essential for proper retinal lamination (Jensen *et al*., 2001), thereby preventing analysis of photoreceptor morphology. The lamination defects could be rescued, however, through genetic mosaic analysis, which also revealed cell-autonomous functions for Moe. The rod-specific *(Tg)XOPS:GFP* transgene was placed on the *moe*$^{-/-}$ background to help visualize transplanted photoreceptors and to provide a means to measure cell volume. In the wild-type host retinas, GFP-expressing *moe*$^{-/-}$ rods adopted a normal morphology but the cell volume was nearly 50% greater than wild type at 6 dpf. Most of this increased volume appeared to be due to an increase in OS volume. The Moe protein directly interacted with a number of Crumbs proteins and this interaction suggests a potential regulatory mechanism for OS length. In *Drosophila*, overexpression of *crumbs* expands the apical domains of ectodermal epithelia (Wodarz *et al*., 1995) and lengthens the stalk region of photoreceptors (Pellikka *et al*., 2002). These results suggest a conserved mechanism whereby Crumbs proteins function positively in OS growth and Moe negatively regulates Crumbs function (Hsu *et al*., 2006).

## IV. Photoreceptor Synapse Structure

Genetic screens utilizing the optokinetic response (OKR) assay have successfully identified mutants that affect synaptic transmission between cone photoreceptors and bipolar cells of the inner retina (Brockerhoff *et al*., 1995; Muto *et al*., 2005; Van Epps *et al*., 2004). One such example is the *no optokinetic response c* (*nrc*) mutant, which disrupts the synaptojanin 1 protein. Synaptojanin 1 is a polyphosphoinositide phosphatase that regulates clathrin-mediated endocytosis at conventional synapses. In *nrc* mutant photoreceptor synapses, the ribbons formed normally but would “float” unanchored from the synaptic junction, fewer synaptic vesicles were present within the synapse, and the arciform density, which anchors the ribbon to the plasma membrane, was missing (Allwardt *et al*., 2001; Van Epps *et al*., 2004). Interestingly, changes in synaptic architecture could be observed using confocal microscopy of transgenic mutants (*Tg(TαC:GFP)nrc*). In wild-type cells expressing the *TαC:GFP* transgene, the cones form invaginating synapses that appear like a “donut” of fluorescence, with a dark center corresponding to the non-fluorescent bipolar cells. The mutant cone terminals were flattened and lacked the dark center, indicating that *nrc* mutant cones failed to form invaginating synapses with bipolar cells.

## V. Regeneration

Persistent neurogenesis and regeneration in the visual system of adult teleost fish have been valuable models of neural development. Zebrafish, like many teleosts, continue to grow throughout their life, and the increase in body mass is matched by an increase in the size of the eye and the area of the retina (Fernald, 1990; Johns, 1982; Johns and Fernald, 1981; Marcus *et al*., 1999; Otteson *et al*., 2001). In the adult, neurogenesis occurs from two distinct stem cell populations (Hecht *et al*., 1942): multipotent neural progenitors at the retinal margin, which can give rise to all retinal cell types except rods, and (Wald, 1955) slowly dividing stem cells within the ONL that serve as rod precursors. At the retinal margin, mitotic cells possess properties of stem cells, maintaining a balance between the self-renewal and the generation of multipotent neuroblasts that differentiate into all classes of neurons and glia. The spatial expression of proneural genes, cell-to-cell signaling molecules, and cellular differentiation markers recapitulates the temporal sequence observed during embryonic development. The identification of neurogenesis at the margin of the hatchling chick retina and the isolation of proliferative cells from the ciliary margin of rodents suggested an evolutionarily conserved system, although further experimental evidence is warranted (Ahmad, 2001; Cicero *et al*., 2009; Fischer and Reh, 2000; Haruta *et al*., 2001; Tropepe *et al*., 2000).

During post-embryonic growth in teleosts, new rods are generated in the central retina from a population of mitotic cells referred to as the rod progenitor lineage. As the animal grows, the retina is gradually stretched within the expanding optic cup, and cell density decreases for all cells except rod photoreceptors. Visual acuity is maintained by increasing the size of the retinal image proportional to that of the increase in eye size. Visual sensitivity, however, is maintained by the generation of new rods in the central retina from a population of mitotic cells referred to as rod progenitor cells (Johns, 1982; Johns and Fernald, 1981). The addition of new rods ensures a constant density across the ONL, thereby preserving scotopic sensitivity (Fernald, 1990; Johns, 1982). Rod progenitors were initially identified as proliferating cells that were distributed across the ONL and served as a source of newly generated rods (Johns, 1982; Johns and Fernald, 1981). These rod precursors proliferate at a low rate and subsequently differentiate into rod photoreceptors. Subsequent studies using multiple injections of tritiated thymidine or exposure to thymidine analogues revealed groups of mitotically active cells arranged in radial arrays spanning the inner nuclear layer (INL) and ONL. In histological sections, these “neurogenic clusters” appeared to migrate along Müller glia. The author proposed that the clusters of proliferating cells were rod progenitors that migrated to the outer retina and became the source of the rod precursors (Johns, 1982).

Perhaps more interesting is that in teleosts, including zebrafish, cell death resulting from mechanical damage, chemical toxicity, phototoxicity, or genetic lesions stimulates an increase in cellular proliferation in the INL and ONL, followed by regeneration of lost cell types, including damaged rod photoreceptors (Braisted *et al*., 1994; Fausett and Goldman, 2006; Vihtelic and Hyde, 2000; Wu *et al*., 2001), and recovery of vision (Mensinger and Powers, 1999). Until recently, the cellular and molecular processes underlying regeneration remained largely unknown; however, transgenic analysis of adult neurogenesis in zebrafish has contributed significantly to the understanding of the origin of the cells that maintain the regenerative potential and the genes that regulate regeneration of photoreceptor cells.

Several lines of evidence have identified a subpopulation of Müller glia as the origin of the “neurogenic clusters” that give rise to both the rod progenitor lineage and the multipotent stem cells observed in regenerating fish retinas (Bernardos *et al*., 2007; Fausett *et al*., 2008; Fimbel *et al*., 2007; Morris *et al*., 2008; Thummel *et al*., 2008; Yurco and Cameron, 2005). In both the intact juvenile retina and the following acute photoreceptor cell damage, double-labeling experiments demonstrated that these proliferating cells co-label for definitive markers of Müller cells, including glial fibrillary acid protein (GFAP), carbonic anhydrase, and glutamine synthetase. The most convincing evidence of the single origin for both of these processes was provided by Barnados *et al*. (Bernardos and Raymond, 2006; Bernardos *et al*., 2007) who used *Tg* *(gfap:GFP)$^{mi2002}$* transgenic zebrafish, in which regulatory elements of the zebrafish GFAP gene drove expression of cytoplasmic or nuclear-targeted GFP specifically in Müller glia. The authors used the persistence of GFP fluorescence as a lineage tracer to track the fates of cells derived from the Müller glia. Following bromodeoxyuridine (BrdU) labeling to identify mitotically active cells in the uninjured retina, the authors observed small numbers of BrdU+ cells in the INL and ONL, some of which were also GFP+. Following light damage, the number of mitotically active (i.e., BrdU+) GFP+ cells increased considerably and could be traced as clusters extending from the INL to the ONL where some co-labeled for the transcription factor Crx and other markers of differentiating photoreceptors. The authors concluded that the co-labeled cells were de-differentiated Müller glia and their progeny, which migrate from the INL into the ONL to form rod precursors and regenerated photoreceptors, respectively. It has also been demonstrated that constant intense light treatment of dark-adapted albino zebrafish selectively kills rod and cone photoreceptors in the central retina (Qin *et al*., 2009; Vihtelic and Hyde, 2000) and induces approximately 50% of the Müller glia to co-label for mitotic markers such as proliferating cell nuclear antigen (PCNA) (Thummel *et al*., 2008). Injection and electroporation of antisense morpholinos complementary to PCNA prior to retinal lesion led to a significant increase in the number of dying cells in the INL and reduced both the number of proliferating cells and the number of Müller glia in the region of the light damage (Thummel *et al*., 2008). These data suggest that following retinal lesion, asymmetric cell division of Müller glia generates a mitotic progenitor that gives rise to the neurogenic cluster while maintaining a constant population of Müller glia.

As regeneration progresses, the Müller-derived stem cells expressed numerous genes consistent with a photoreceptor developmental program. Following retinal damage, the Müller glial-derived mitotic cells initiate expression of retinal stem/progenitor cell markers, including *ascl1a, pax6, rx1, neurogenin1*, and *chx10* (Fausett and Goldman, 2006; Raymond *et al*., 2006; Thummel *et al*., 2010). As the retinal progenitors migrate from the INL to the ONL, Pax6 expression is lost and other transcription factors are expressed, most notably the basic helix-loop-helix gene *neurod*, and the cone–rod homeobox gene *crx*. Similarly, cell signaling molecules of the Notch–Delta pathway and its downstream effectors are also expressed (Raymond *et al*., 2006). These data suggest that progenitor cells produced in the INL in response to acute injury pass through a series of intervening, less-committed states prior to adopting a photoreceptor cell fate.

To uncover genes specifically expressed by the Müller glial-derived mitotic progenitors, the gene expression profiles were compared with those of GFP+ cells isolated from intact and light-lesioned *Tg(gfap:GFP)$^{mi2002}$* zebrafish retinas (Qin *et al*., 2009). Using fluorescence-activated cell sorting, the GFP+ cells were isolated from control retinas and retinas up to 36 h post light damage. Similar to other studies of changes in gene expression following acute damage, gene networks associated with increased proliferation, stress response, and neurogenesis were activated. The regeneration of the retina shares features common to other regenerating tissues including the heart and fin. Two genes required for fin and heart regeneration in zebrafish—*hspd1*, which encodes heat shock protein 60 and *mps1*, a protein kinase involved in mitotic checkpoint regulation—are upregulated in injury-activated Müller glia (Qin *et al*., 2009). Co-labeling confirmed that both genes were expressed in the mitotically activated Müller glia and their progeny. Quite fortuitously, mutant alleles exist in zebrafish for both of these genes. The mutant *no blastema* (*nbl*) is a temperature-sensitive null allele of *hspd1* that disrupts chaperone activity (Makino *et al*., 2005). *nightcap* (*ncp*) has a missense substitution in the conserved kinase domain of *mps1* and also exhibits a temperature-sensitive phenotype (Poss *et al*., 2002). By rearing fish at the non-permissive temperature, the authors demonstrated that both were required at different stages of cone photoreceptor regeneration following light damage.

Whereas current work in numerous species has focused on the Müller cells and the INL stem cells, understanding the regulation of rod progenitor cell activity may offer an alternative avenue to investigate the fundamental processes of photoreceptor replacement. Two previous limitations of such studies have been that rod precursors are relatively few in number and no definitive marker specific for the rod progenitors is available. The *XOPS-mCFP* transgenic line experiences selective degeneration of the rod photoreceptor cells due to the toxic effects of high-level expression of a rod-targeted fluorescent reporter gene (Morris and Fadool, 2005). This rod degeneration resulted in a loss of rod-mediated electrophysiological responses, but did not cause any secondary cone pathology. It was, however, accompanied by a significant increase in rod progenitor mitotic activity (Morris and Fadool, 2005). Similar to cone regeneration, the transcription factors NeuroD and Crx were upregulated in cells in the ONL. But, in contrast, expression of *nr2e3*—a rod determination gene found exclusively in post-mitotic differentiating rod photoreceptors—was also upregulated, whereas expression of *pax6* was not observed (Morris and Fadool, 2005). Immunolabeling of retinal cryosections with anti-BrdU showed no significant increase in INL BrdU+ cells or PCNA expression. The expression of genes with demonstrated roles in photoreceptor development, such as *neurod, crx*, and *nr2e3*, combined with the lack of *pax6* expression, suggests an early commitment of the mitotic rod precursors to the rod cell fate (Morris and Fadool, 2005). Supporting this conclusion, knock-down of both Pax6a and Pax6b resulted in increased numbers of rod precursors in the ONL without affecting rod regeneration (Thummel *et al*., 2010). Therefore, it appears that the rod progenitors in the ONL maintain the capacity to respond to rod photoreceptor degeneration without relying on increased activity of progenitor cells in the INL or the Müller glia. By contrast, cone-specific cell death resulting from mutation of the *pde6c* gene stimulates Müller glial proliferation in the absence of rod cell death (Morris *et al*., 2008) which we inferred that the retina responds to rod and cone cell death differently.

Others have demonstrated mitosis of Müller glia following a specific form of rod death. Regeneration following acute and specific loss of all mature rod photoreceptors was tested using the bacterial nitroreductase (NTR)/metronidazole cell ablation system (Montgomery *et al*., 2010). The authors describe two independent transgenic lines of zebrafish that express an NTR-EGFP fusion protein from the zebrafish rod opsin promoter. Similar lines have also been generated to induce the specific loss of bipolar cells in the retina (Montgomery *et al*., 2010). In the former studies, uniform expression of NTR-EGFP in all rod photoreceptors was observed in the *Tg(zop:nfsB-EGFP)*$^{nt19}$ line, whereas a subset of rods express NTR-EGFP in *Tg(zop:nfsB-EGFP)*$^{nt20}$ line. Treatment with metronidazole resulted in the death of all rods expressing the NTR-EGFP fusion protein. In contrast to what we observed in the *Tg(xops:mCFP)* transgenic line, metronidazole treatment of the *Tg(zop:nfsB-EGFP)*$^{nt19}$ fish increased Müller glial cell proliferation. However, the authors reported that only increased rod precursor cell proliferation was observed following treatment of the *Tg(zop:nfsB-EGFP)*$^{nt20}$ fish. Thus, acute loss of the majority of rod photoreceptors was sufficient to induce a Müller glial regeneration response, suggesting that the level of cell death is an important factor regulating increased proliferation of Muller glial versus rod progenitors.

These studies highlight the significant gains made possible by combining advances in many areas of zebrafish genetics such as the development of novel transgenic lines, application of cell sorting, gene profiling arrays, and cell ablation technologies. The ever-increasing utility of transgenic tools to investigate photoreceptor biology in zebrafish has mirrored many of the advances in other organ systems. The continuation of these studies should allow a more detailed characterization of the intrinsic properties of retinal stem cells, identification of the environmental signals that direct regeneration of the photoreceptor cells, and development of methods to manipulate cells to direct photoreceptor cell replacement.

## VI. Future Directions

Transgenic zebrafish are powerful tools to analyze photoreceptor morphology, cell biology, and regeneration. To date, studies have utilized transgenic technology to express intrinsic proteins behind very strong promoters (e.g., *Xenopus* opsin or cone transducin promoters). While deleterious effects of overexpressing some proteins have not yet been reported, it is likely that overexpression of some proteins cannot be tolerated by rods or cones. Future efforts to identify and characterize weakly and moderately expressing promoters will enhance the toolkit available to zebrafish researchers and reduce the chances of overexpression toxicity.

The role of extrinsic factors on photoreceptor development and differentiation has largely relied on loss of function strategies (e.g., mutagenesis and morpholino approaches) and overexpression following mRNA injection. In both cases, analysis on photoreceptors is often limited because many signaling molecules have essential roles much earlier in development and the embryos may not survive to later time points, or photoreceptor phenotypes may be reflect non-specific effects from general developmental abnormalities. Temporally regulated expression of transgenes is one potential method to bypass these limitations. The promoter of the heat shock protein, hsp70, allows transgene expression to be limited to those times when the animals are exposed to a brief heat shock. This temporal control of transgene expression can be used to drive expression of signaling molecules or dominant-negative forms of growth factor receptors during windows critical for photoreceptor development but well after critical developmental events, such as gastrulation or optic cup formation. These approaches will significantly enhance our understanding of how some molecules contribute to both photoreceptor differentiation and regeneration.

## VII. Conclusions

The study of photoreceptor cell structure and development has benefited from the use of transgenic zebrafish expressing cell-specific GFP reporter genes. At the moment there are several rod- and cone-specific GFP lines, and one cone subtype-specific line, namely that for UV opsin-expressing cones. Transgenic technology will greatly facilitate future studies of neuronal structure and function in zebrafish. Dozens of different transgenic zebrafish lines currently exist (Udvadia and Linney, 2003) and more specialized lines will no doubt appear in the future. The classic studies of Ramón y Cajal used Golgi staining to provide tremendous insights into the structure of retinal neurons in fixed tissue (Ramon and Cajal, 1911). With the increasing power of fluorescent imaging technology, questions about the development and function of neurons *in vivo* and in real time are being addressed. With the appropriate promoters, it should be possible to generate individual transgenic lines that express reporter genes within all subsets of the major classes of retinal cells. These lines could be used for rapid identification of specific cell types prior to electrophysiological recordings. Additionally, time-lapse imaging of individual cells or whole layers of cells could be used to study the timing and control of synaptogenesis *in vivo*, as seen from the report by Kay *et al*. (2004). Certainly the combination of these techniques with the wide assortment of zebrafish mutants will facilitate our understanding of neural development and function.

### References

Ahmad, I. (2001). *Invest. Ophthalmol. Vis. Sci.* **42**, 2743–2748.

Allwardt, B. A., Lall, A. B., Brockerhoff, S. E., and Dowling, J. E. (2001). *J. Neurosci.* **21**, 2330–2342.

Alvarez-Delfin, K., Morris, A. C., Snelson, C. D., Gamse, J. T., Gupta, T., Marlow, F. L., Mullins, M. C., Burgess, H. A., Granato, M., and Fadool, J. M. (2009). *Proc. Natl. Acad. Sci. U.S.A* **106**, 2023–2028.

Balciunas, D., Wangensteen, K. J., Wilber, A., Bell, J., Geurts, A., Sivasubbu, S., Wang, X., Hackett, P. B., Largaespada, D. A., McIvor, R. S., and Ekker, S. C. (2006). *PLoS Genet.* **2**, e169.

Bernardos, R. L., Barthel, L. K., Meyers, J. R., and Raymond, P. A. (2007). *J. Neurosci.* **27**, 7028–7040.

Bernardos, R. L., and Raymond, P. A. (2006). *Gene Expr. Patterns* **6**, 1007–1013.

Bilotta, J., Saszik, S., and Sutherland, S. E. (2001). *Dev. Dyn.* **222**, 564–570.

Braisted, J. E., Essman, T. F., and Raymond, P. A. (1994). *Development* **120**, 2409–2419.

Branchek, T. (1984). *J. Comp. Neurol.* **224**, 116–122.

Branchek, T., and Bremiller, R. (1984). *J. Comp. Neurol.* **224**, 107–115.

Brockerhoff, S. E., Hurley, J. B., Janssen-Bienhold, U., Neuhauss, S. C., Driever, W., and Dowling, J. E. (1995). *Proc. Natl. Acad. Sci. U.S.A* **92**, 10545–10549.

Chu, P. J., Rivera, J. F., and Arnold, D. B. (2006). *J. Biol. Chem.* **281**, 365–373.

Cicero, S. A., Johnson, D., Reyntjens, S., Frase, S., Connell, S., Chow, L. M., Baker, S. J., Sorrentino, B. P., and Dyer, M. A. (2009). *Proc. Natl. Acad. Sci. U.S.A* **106**, 6685–6690.

Dowling, J. E. (1963). *J. Gen. Physiol.* **46**, 1287–1301.

Dryja, T. P., and Li, T. (1995). *Hum. Mol. Genet.* **4**, 1739–1743.

Fadool, J. M. (2003). *Dev. Biol.* **258**, 277–290.

Fadool, J. M., and Dowling, J. E. (2008). *Prog. Retin. Eye Res.* **27**, 89–110.

Fausett, B. V., and Goldman, D. (2006). *J. Neurosci.* **26**, 6303–6313.

Fausett, B. V., Gumerson, J. D., and Goldman, D. (2008). *J. Neurosci.* **28**, 1109–1117.

Fernald, R. D. (1990). *J. Exp. Zool. Suppl.* **5**, 167–180.

Fimbel, S. M., Montgomery, J. E., Burket, C. T., and Hyde, D. R. (2007). *J. Neurosci.* **27**, 1712–1724.

Fischer, A. J., and Reh, T. A. (2000). *Dev. Biol.* **220**, 197–210.

Furukawa, T., Morrow, E. M., and Cepko, C. L. (1997). *Cell* **91**, 531–541.

Furukawa, T., Morrow, E. M., Li, T., Davis, F. C., and Cepko, C. L. (1999). *Nat. Genet.* **23**, 466–470.

Hamaoka, T., Takechi, M., Chinen, A., Nishiwaki, Y., and Kawamura, S. (2002). *Genesis* **34**, 215–220.

Hao, L., and Scholey, J. M. (2009). *J. Cell. Sci.* **122**, 889–892.

Haruta, M., Kosaka, M., Kanegae, Y., Saito, I., Inoue, T., Kageyama, R., Nishida, A., Honda, Y., and Takahashi, M. (2001). *Nat. Neurosci.* **4**, 1163–1164.

Hecht, S., Schlaer, S., and Pirenne, M. H. (1942). *J. Optic. Soc. Amer.* **38**, 196–208.

Hsu, Y. C., Willoughby, J. J., Christensen, A. K., and Jensen, A. M. (2006). *Development* **133**, 4849–4859.

Hu, M., and Easter, S. S. (1999). *Dev. Biol.* **207**, 309–321.

Hyatt, G. A., Schmitt, E. A., Fadool, J. M., and Dowling, J. E. (1996). *Proc. Natl. Acad. Sci. U.S.A* **93**, 13298–13303.

Insinna, C., and Besharse, J. C. (2008). *Dev. Dyn.* **237**, 1982–1992.

Insinna, C., Humby, M., Sedmak, T., Wolfrum, U., and Besharse, J. C. (2009a). *Dev. Dyn.* **238**, 2211–2222.

Insinna, C., Luby-Phelps, K., Link, B. A., and Besharse, J. C. (2009b). *Methods Cell Biol.* **93**, 219–234.

Insinna, C., Pathak, N., Perkins, B., Drummond, I., and Besharse, J. C. (2008). *Dev. Biol.* **316**, 160–170.

Jensen, A. M., Walker, C., and Westerfield, M. (2001). *Development* **128**, 95–105.

Johns, P. R. (1982). *J. Neurosci.* **2**, 178–198.

Johns, P. R., and Fernald, R. D. (1981). *Nature* **293**, 141–142.

Kay, J. N., Roeser, T., Mumm, J. S., Godinho, L., Mrejeru, A., Wong, R. O., and Baier, H. (2004). *Development* **131**, 1331–1342.

Kennedy, B. N., Alvarez, Y., Brockerhoff, S. E., Stearns, G. W., Sapetto-Rebow, B., Taylor, M. R., and Hurley, J. B. (2007). *Invest. Ophthalmol. Vis. Sci.* **48**, 522–529.

Kennedy, B. N., Vihtelic, T. S., Checkley, L., Vaughan, K. T., and Hyde, D. R. (2001). *J. Biol. Chem.* **276**, 14037–14043.

Kwan, K. M., Fujimoto, E., Grabher, C., Mangum, B. D., Hardy, M. E., Campbell, D. S., Parant, J. M., Yost, H. J., Kanki, J. P., and Chien, C. B. (2007). *Dev. Dyn.* **236**, 3088–3099.

Lin-Jones, J., Parker, E., Wu, M., Knox, B. E., and Burnside, B. (2003). *Invest. Ophthalmol. Vis. Sci.* **44**, 3614–3621.

Luby-Phelps, K., Fogerty, J., Baker, S. A., Pazour, G. J., and Besharse, J. C. (2008). *Vision Res.* **48**, 413–423.

Makino, S., Whitehead, G. G., Lien, C. L., Kim, S., Jhawar, P., Kono, A., Kawata, Y., and Keating, M. T. (2005). *Proc. Natl. Acad. Sci. U.S.A* **102**, 14599–14604.

Marcus, R. C., Delaney, C. L., and Easter, S. S., Jr. (1999). *Vis. Neurosci.* **16**, 417–424.

Marszalek, J. R., Liu, X., Roberts, E. A., Chui, D., Marth, J. D., Williams, D. S., and Goldstein, L. S. (2000). *Cell* **102**, 175–187.

Mears, A. J., Kondo, M., Swain, P. K., Takada, Y., Bush, R. A., Saunders, T. L., Sieving, P. A., and Swaroop, A. (2001). *Nat. Genet.* **29**, 447–452.

Mensinger, A. F., and Powers, M. K. (1999). *Vis. Neurosci.* **16**, 241–251.

Montgomery, J. E., Parsons, M. J., and Hyde, D. R. (2010). *J. Comp. Neurol.* **518**, 800–814.

Morris, A. C., and Fadool, J. M. (2005). *Physiol. Behav.* **86**, 306–313.

Morris, A. C., Scholz, T. L., Brockerhoff, S. E., and Fadool, J. M. (2008). *Dev. Neurobiol.* **68**, 605–619.

Muto, A., Orger, M. B., Wehman, A. M., Smear, M. C., Kay, J. N., Page-McCaw, P. S., Gahtan, E., Xiao, T., Nevin, L. M., Gosse, N. J., Staub, W., Finger-Baier, K., *et al.* (2005). *PLoS Genet.* **1**, e66.

Nathans, J. (1992). *Biochemistry* **31**, 4923–4931.

Otteson, D. C., D'Costa, A. R., and Hitchcock, P. F. (2001). *Dev. Biol.* **232**, 62–76.

Patel, A., and McFarlane, S. (2000). *Dev. Biol.* **222**, 170–180.

Pazour, G. J., Baker, S. A., Deane, J. A., Cole, D. G., Dickert, B. L., Rosenbaum, J. L., Witman, G. B., and Besharse, J. C. (2002). *J. Cell Biol.* **157**, 103–113.

Pellikka, M., Tanentzapf, G., Pinto, M., Smith, C., McGlade, C. J., Ready, D. F., and Tepass, U. (2002). *Nature* **416**, 143–149.

Perkins, B. D., Fadool, J. M., and Dowling, J. E. (2004). *Methods Cell Biol.* **76**, 315–331.

Perkins, B. D., Kainz, P. M., O'Malley, D. M., and Dowling, J. E. (2002). *Vis. Neurosci.* **19**, 257–264.

Poss, K. D., Nechiporuk, A., Hillam, A. M., Johnson, S. L., and Keating, M. T. (2002). *Development* **129**, 5141–5149.

Qin, Z., Barthel, L. K., and Raymond, P. A. (2009). *Proc. Natl. Acad. Sci. U.S.A* **106**, 9310–9315.

Ramon y Cajal, S. (1911). "Histologie du Systeme Nerveax de l'Homme et des Vertebres", Maloine, Paris.

Raymond, P. A., and Barthel, L. K. (2004). *Int. J. Dev. Biol.* **48**, 935–945.

Raymond, P. A., Barthel, L. K., Bernardos, R. L., and Perkowski, J. J. (2006). *BMC Dev. Biol.* **6**, 36.

Raymond, P. A., Barthel, L. K., and Curran, G. A. (1995). *J. Comp. Neurol.* **359**, 537–550.

Raymond, P. A., Barthel, L. K., Rounsifer, M. E., Sullivan, S. A., and Knight, J. K. (1993). *Neuron* **10**, 1161–1174.

Robinson, J., Schmitt, E. A., Harosi, F. I., Reece, R. J., and Dowling, J. E. (1993). *Proc. Natl. Acad. Sci. U.S. A* **90**, 6009–6012.

Saszik, S., Bilotta, J., and Givin, C. M. (1999). *Vis. Neurosci.* **16**, 881–888.

Schmitt, E. A., and Dowling, J. E. (1996). *J. Comp. Neurol.* **371**, 222–234.

Schmitt, E. A., Hyatt, G. A., and Dowling, J. E. (1999). *Vis. Neurosci.* **16**, 601–605.

Shkumatava, A., Fischer, S., Muller, F., Strahle, U., and Neumann, C. J. (2004). *Development*. **131**, 3849–3858

Stenkamp, D. L., and Frey, R. A. (2003). *Dev. Biol.* **258**, 349–363.

Takechi, M., Hamaoka, T., and Kawamura, S. (2003). *FEBS Lett.* **553**, 90–94.

Thummel, R., Enright, J. M., Kassen, S. C., Montgomery, J. E., Bailey, T. J., and Hyde, D. R. (2010). *Exp. Eye. Res.* **90**, 572–582.

Thummel, R., Kassen, S. C., Enright, J. M., Nelson, C. M., Montgomery, J. E., and Hyde, D. R. (2008). *Exp. Eye. Res.* **87**, 433–444.

Tropepe, V., Coles, B. L., Chiasson, B. J., Horsford, D. J., Elia, A. J., McInnes, R. R., and van der Kooy, D. (2000). *Science* **287**, 2032–2036.

Udvadia, A. J., and Linney, E. (2003). *Dev. Biol.* **256**, 1–17.

Van Epps, H. A., Hayashi, M., Lucast, L., Stearns, G. W., Hurley, J. B., De Camilli, P., and Brockerhoff, S. E. (2004). *J. Neurosci.* **24**, 8641–8650.

Vihtelic, T. S., and Hyde, D. R. (2000). *J. Neurobiol.* **44**, 289–307.

Wald, G. (1955). *Am. J. Ophthalmol.* **40**, 18–41.

Wodarz, A., Hinz, U., Engelbert, M., and Knust, E. (1995). *Cell* **82**, 67–76.

Wu, D. M., Schneiderman, T., Burgett, J., Gokhale, P., Barthel, L., and Raymond, P. A. (2001). *Invest Ophthalmol. Vis. Sci.* **42**, 2115–2124.

Yau, K. W. (1994). *Invest. Ophthalmol. Vis. Sci.* **35**, 9–32.

Young, T. L., and Cepko, C. L. (2004). *Neuron* **41**, 867–879.

Yurco, P., and Cameron, D. A. (2005). *Vision Res.* **45**, 991–1002.

## CHAPTER 8

# Physiological Recordings from Zebrafish Lateral-Line Hair Cells and Afferent Neurons

**Josef G. Trapani *and* Teresa Nicolson**
Howard Hughes Medical Institute, Oregon Hearing Research Center and Vollum Institute, Oregon Health and Science University, Portland, Oregon

Abstract
I. Introduction
II. Zebrafish Mounting and Immobilizing
    A. Anesthesia and Mounting of Larvae
    B. Immobilizing Larvae with α-Bungarotoxin
III. Microphonics
    A. Stimulation of Neuromast Hair Cells
    B. Microphonic Recordings from Neuromast Hair Cells
    C. Signal Collection and Analysis
    D. Confirming a Biologically Relevant Signal
IV. Action Currents
    A. Electrode and Recording Details
    B. Analysis of Action Currents
V. Summary
VI. Discussion
Acknowledgments
References

## Abstract

Sensory signal transduction, the process by which the features of external stimuli are encoded into action potentials, is a complex process that is not fully understood. In fish and amphibia, the lateral-line organ detects water movement and vibration and is critical for schooling behavior and the detection of predators and prey. The

METHODS IN CELL BIOLOGY, VOL. 100
Copyright © 2010 Elsevier Inc. All rights reserved.

978-0-12-384892-5
DOI: 10.1016/B978-0-12-384892-5.00008-6

lateral-line system in zebrafish serves as an ideal platform to examine encoding of stimuli by sensory hair cells. Here, we describe methods for recording hair-cell microphonics and activity of afferent neurons using intact zebrafish larvae. The recordings are performed by immobilizing and mounting larvae for optimal stimulation of lateral-line hair cells. Hair cells are stimulated with a pressure-controlled water jet and a recording electrode is positioned next to the site of mechanotransduction in order to record microphonics—extracellular voltage changes due to currents through hair-cell mechanotransduction channels. Another readout of the hair-cell activity is obtained by recording action currents from single afferent neurons in response to water-jet stimulation of innervated hair cells. When combined, these techniques make it possible to probe the function of the lateral-line sensory system in an intact zebrafish using controlled, repeatable, physiological stimuli.

## I. Introduction

The zebrafish has many features that make it a versatile model system for physiological studies. Larvae are optically transparent and genetically tractable, enabling one to express transgenic fluorescent proteins in target cells and subsequently visualize them in the intact organism. Furthermore, they are prolific egg layers, lines are simple to maintain, and large-scale mutagenesis screens are feasible. Finally, zebrafish larvae are well suited for electrophysiology, which provides a key method for answering fundamental questions in neurobiology (Ono *et al.*, 2001; Ribera and Nüsslein-Volhard, 1998; Smear *et al.*, 2007; Westerfield *et al.*, 1990). Researchers have used these advantages to advance fields ranging from development to cell biology and neuroscience (Feldman *et al.*, 1998; Patton and Zon, 2001; Söllner *et al.*, 2004b; Sumbre *et al.*, 2008; Whitfield *et al.*, 2002).

An important sensory feature of the larval zebrafish is its lateral-line system. Unlike mammals, in addition to auditory and vestibular organs, all fish and amphibia possess a lateral-line organ that is composed of sensory hair cells (Freeman, 1928; Ryder, 1884). Similar to auditory and vestibular sensory detection, the lateral line detects and encodes water motion through hair-cell mechanotransduction (Hoagland, 1933; Suckling and Suckling, 1950). Lateral-line hair cells are arranged together with support cells into rosette-like structures termed neuromast organs. These neuromasts are located along the surface of the animal (superficial neuromasts) and in fluid-filled subepidermal canals in adults (canal neuromasts). The accessibility of zebrafish neuromasts makes them an ideal platform for studying the molecular, cellular, and physiological features of sensory hair cells.

Here we describe in detail our method for recording activity from the lateral line of larval zebrafish. To date, we have recorded extracellular potentials from individual neuromasts and extracellular action currents from single afferent neurons. This preparation is highly suited for performing physiological studies because it utilizes intact animals and biologically relevant stimuli.

## II. Zebrafish Mounting and Immobilizing

The lateral-line system of larvae at 120 hours post fertilization (hpf) is composed of superficial neuromasts arranged around the head to form the anterior lateral line and along the trunk to form the posterior lateral line (Dambly-Chaudière *et al*., 2003). At this stage, all primary neuromasts are present along with a few immature secondary neuromasts still forming (Grant *et al*., 2005; Nuñez *et al*., 2009). Studies with primary neuromasts of the posterior lateral line are ideal because their planar polarity results in hair-cell activation with simple anterior–posterior deflections (López-Schier *et al*., 2004; Nicolson *et al*., 1998).

In order for routine, stereotyped access to neuromasts and afferent cell bodies of the posterior lateral line, larvae are mounted to a recording chamber with a circular opening (PC-R; Siskiyou, Inc. Grants Pass, OR, USA). This opening is covered by a square cover glass and coated with a 2 mm layer of silicone elastomer, Sylgard (#184; Dow Corning, Midland, MI, USA). Coating the chamber with Sylgard is ideal because of its elastic properties and relative optical clarity, which can be maintained with frequent recoating. The recording chamber fits within an adapter plate (PC-A; Siskiyou, Inc.), which allows the mounted larvae to be rotated 360°. Free rotation alleviates the need to mount the larva at a precise position relative to the recording chamber and pipette holders. Free rotation of the recording chamber also facilitates the proper alignment of all electrodes (Fig. 1A).

Prior to establishing a recording, an individual larva must be immobilized and mounted to the recording chamber. This is accomplished in two steps: first, the larva

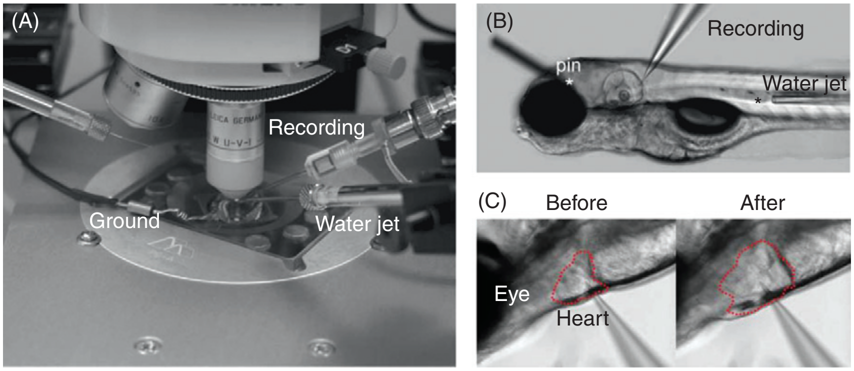

**Fig. 1** Setup for mounting and immobilizing zebrafish larva. (A) Photograph illustrating the position of the recording electrode and water-jet pipettes. A third pipette holder is shown on the left side of the image and can be used for dual recordings or as a stimulating electrode. Note the bath ground attaches to the recording chamber, which fits into the circular adapter plate allowing for 360° rotation of the preparation. (B) A 120 hpf larva is pinned to the Sylgard-lined chamber. In this image (10× objective), the recording electrode is positioned for action-current recordings from the posterior lateral-line ganglion. The water jet is positioned just posterior to a neuromast (black asterisk). Note the insertion point of the anterior pin (white asterisk). (C) Before and after α-bungarotoxin injection, which expanded the heart cavity (red dashed outline).

is anesthetized with tricaine and pinned to the Sylgard-lined chamber. Second, the larva is injected with a paralytic (α-bungarotoxin) into its heart and the anesthetic is removed before recording.

## A. Anesthesia and Mounting of Larvae

An individual larva is anesthetized in embryo media containing 0.02% tricaine methanesulfonate (MS-222; Sigma-Aldrich, St. Louis, MO, USA) for 30 s. Then, using a transfer pipette, the larva and a dropper full of solution are expelled onto the Sylgard-lined chamber. Next, with a dissecting microscope and two watchmaker's forceps (No. 5 Dumont), the larva is positioned on its right side in the center of the chamber and pinned with two tungsten pins. One pin is inserted just posterior to the eye and anterior to the ear (Fig. 1B). The other pin is inserted into the notochord near the end of the tail of the larva.

Pins are fabricated from tungsten rod (0.002 × 3 in., A-M Systems, Sequim, WA, USA). To aid in puncturing the skin, we first electrolytically sharpen one end of the rod using a 1 N NaOH solution and a 9 V battery. Then, a 90° bend is made 1 mm up from the tip end and the rod is cut to form a small, sharpened "L."

Using these techniques, the larva remains immobilized for the length of a given recording (2–30 min), although careful monitoring and readjustments of electrode position may be necessary for long-duration recordings. Conveniently, since larvae do not have gills at this stage, a perfusion setup is not necessary. During recordings, the heartbeat should remain regular, as hair cells are very sensitive to oxygen depletion.

## B. Immobilizing Larvae with α-Bungarotoxin

Electrophysiological recordings are precluded by the presence of the anesthetic tricaine, which blocks both neuronal activity and mechanotransduction channels. Therefore, to record lateral-line activity, larvae are immobilized with a paralytic so that the tricaine can be washed away. The paralytic, α-bungarotoxin, blocks the acetylcholine receptor at the zebrafish neuromuscular junction (Westerfield *et al.*, 1990). This toxin is a suitable paralytic for lateral-line recordings since immunohistochemistry with α-bungarotoxin antibodies confirmed labeling of muscle and did not label hair cells of the ear or neuromasts (unpublished observations).

The anesthetized larva is injected with α-bungarotoxin (125 μM) into the heart using a patch pipette with a tip diameter of 1–3 μm. The larva is positioned, and the heart injection is visualized, using the wide-field upright microscope used for our recordings. The α-bungarotoxin pipette is then mounted to the pipette holder that is used for water-jet stimulation; the output tubing of the pipette holder is temporarily switched to a pressure injector (Pressure System IIe, Toohey Company, Fairfield, NJ, USA). Once mounted, the α-bungarotoxin pipette is aligned perpendicular to the heart under a 10× microscope objective. Next, the pipette is advanced toward the heart, pressed against the skin, and then advanced further until the skin is penetrated. After the pipette is inside the heart cavity, a bolus of α-bungarotoxin is injected. Successful injection will result in an obvious expansion of the heart cavity (Fig. 1C). If necessary, inclusion of phenol red (10%) can increase visualization of the expelled α-bungarotoxin. Following injection, the pipette is retracted and the pinned larva is rinsed several times with standard extracellular solution [in mM: 130 NaCl, 2 KCl, 2 $CaCl_2$, 1 $MgCl_2$, and 10 4-(2-hydroxyethyl)-1-piperazineethanesulfonic acid (HEPES); 290 mOsm; pH 7.8]. The larva is left in 0.5–1 mL of solution for several minutes prior to recording to allow for effective tricaine removal.

## III. Microphonics

The term “microphonics” was first used (Adrian, 1931) to describe the cochlear AC potentials that Wever and Bray (1930) observed in recordings from cats. Microphonic potentials have since been found to represent the changes in extracellular potential that result from the inward flow of cations during gating of mechanotransduction channels located at the tips of hair-cell stereocilia (Beurg *et al*., 2009; Corey and Hudspeth, 1983; Jaramillo and Hudspeth, 1991). As a measure of the activity of mechanotransduction channels, microphonic recordings are useful for determining the amplitude and frequency of the transduction response in hair cells. The following methods can be used for recording and analyzing microphonics from individual neuromasts of the larval lateral line.

### A. Stimulation of Neuromast Hair Cells

At 120 hpf, larval neuromasts contain 9–14 hair cells. At the apical end of each hair cell is the stereociliary hair bundle. Each hair bundle is connected to a single kinocilium that extends roughly 20 μm into the aqueous medium. A gelatinous cupula covers and encompasses all of the kinocilia. Deflection of the cupula results in the concerted deflection of all kinocilia, which in turn deflects attached stereocilia (Netten and Kroese, 1987). Shearing of hair bundles ultimately opens mechanotransduction channels located at their tips (Beurg *et al*., 2009; Jaramillo and Hudspeth, 1991).

Stimulation of neuromast hair cells is performed with a pipette filled with extracellular solution that is driven by a pressure clamp (HSPC-1, ALA Scientific). This pipette, termed a water jet, should have a circular opening with a diameter of approximately 30 μm. To achieve this pipette shape, thick-walled (1.5 mm OD and 0.86 mm ID) borosilicate glass is fabricated from a single, hard pull (micropipette puller P-97; Sutter Instruments) that results in two pipettes with long, tapering ends. These two long ends are rubbed against each other until one end scores and cleanly breaks the other. Note that this process requires non-filament glass in order to have a clean tip break and laminar fluid flow.

The water-jet pipette is positioned approximately 100 μm from a given neuromast cupula. The height of the water jet should be slightly above the cupula and deflection by the water jet should be equal in forward and reverse directions.

## B. Microphonic Recordings from Neuromast Hair Cells

Electrodes for microphonic recordings are pulled to resemble standard patch electrodes using filament glass that is otherwise the same as the water-jet pipettes. Electrode outer tip diameters are of 1–3 µm and have resistances of approximately 3 MΩ when filled with extracellular solution. The recording electrode is mounted at a 45° angle from the water-jet pipette and positioned (using a 40× objective) at a height even with the stereocilia (Fig. 2A). Since mechanotransduction channels are located at the tips of stereocilia, the position of the recording electrode is critical for obtaining the largest possible microphonic signal. Proper position is important because lateral-line stereocilia are very short and difficult to visualize even with a 40× objective, where they appear as a dark spot at the apical surface of each hair cell (white-dashed circle in Fig. 2A).

On day 5, in addition to the primary posterior lateral-line neuromasts, secondary neuromasts are also forming (Grant *et al.*, 2005). Care should be taken to record exclusively from primary neuromasts, as secondary neuromasts activate with deflections of different polarities, which may give confounding results. Also, note that all solutions (water jet, electrode, and bath) should be identical to avoid junction potential errors.

## C. Signal Collection and Analysis

Microphonic potentials are recorded in current-clamp mode, sampled at 10 kHz, and filtered at 1 kHz. The voltage signal is then further amplified (10,000× final) and

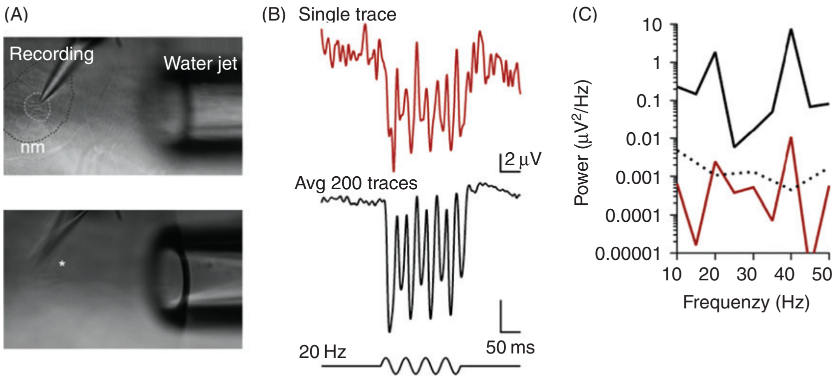

**Fig. 2** Microphonic recordings from posterior lateral-line neuromasts. (A) Images (40× objective) of the location of the recording electrode (top panel) and water-jet pipette (bottom panel) relative to a neuromast (nm; black dashed circle). The recording electrode is at the level of the hair-cell stereocilia, which are dark spots under DIC differential interference contrast (white dashed circle). The water-jet pipette is positioned approximately 100 µm from the neuromast. Note that the water-jet height is even with the top of the neuromast cupula (white asterisk). (B) An individual trace (red trace) from a microphonic recording, compared to an average of 200 consecutive traces (black trace), which illustrates the increase in signal-to-noise ratio with averaging. (C) Power spectrum from the individual trace (red line) and the average trace (black line) during the 200 ms sine wave stimulation. Note that the individual-trace power is barely distinguished from the power spectrum of the noise portion of the average trace (black dashed line).

filtered (50–100 Hz; eight-pole Bessel) by an additional amplifier (Model 440, Brownlee Precision). In order to drive the pressure clamp and record the microphonic potential simultaneously, a sinusoidal voltage command is delivered to the pressure clamp via an analog output from the recording amplifier. The pressure of the water jet can also be monitored by a feedback sensor on the pressure-clamp headstage and recorded simultaneously with acquisition software.

As microphonic signals are typically 10 μV, one should take care to effectively remove all electrical noise from the recording setup. Under ideal conditions, recording noise can be held to under 5 μV peak to peak, and microphonic signals can be seen without averaging traces (Fig. 2B). To overcome the variability of neuromast structure and the position of the recording electrode, one can quantify microphonic signals by determining the power of the total signal per unit frequency. The stimulus portion of the signal is analyzed with a power spectral density function (Fig. 2C). Power spectra will contain primary peaks at the stimulus frequency (1*f*) and at twice the frequency (2*f*); for a 20 Hz stimulus, this would result in peaks at 20 and 40 Hz, respectively (see Fig. 2C). These frequency components result from the presence of two groups of hair cells of different orientation that respond to stimuli of opposite polarity (Flock and Wersall, 1962; Ghysen and Dambly-Chaudière, 2007).

### D. Confirming a Biologically Relevant Signal

There are several qualifications and tests that help to determine whether a recorded microphonic signal is biologically relevant. If bidirectional stimuli (e.g., sine waves) are used, then the signal should contain the 2*f* frequency component. In addition, a biologically relevant signal should not be detected with stimulation perpendicular to the excitation axis of a neuromast. Furthermore, the microphonic signal should be blocked by mechanotransduction channel antagonists such as dihydrostreptomycin and amiloride (Farris *et al*., 2004). Microphonics should also be blocked by disruption of stereocilia tip links—components necessary for transduction. For example, chelating extracellular calcium with 1,2-bis(*o*-aminophenoxy)ethane-*N,N,N*’,*N*’-tetraacetic acid (BAPTA) or ethylene glycol tetraacetic acid (EGTA), both of which break tip links, abolishes microphonics (Assad *et al*., 1991). In addition, microphonics should be absent in larvae lacking mechanotransduction such as *cdh23* or *pcdh15* mutants (Nicolson *et al*., 1998; Seiler *et al*., 2005; Söllner *et al*., 2004a).

## IV. Action Currents

The neurotransmitter output of hair cells, which encodes the features of sensory stimuli, results from a unique process of graded transduction. Briefly, gating of mechanotransduction channels results in graded changes in hair-cell membrane potential, which drives graded synaptic vesicle fusion at specialized ribbon synapses. These graded signals are ultimately encoded as sequences of all-or-none action potentials (spikes) in afferent neurons.

When recorded in an extracellular loose-patch configuration, action potentials are measured as action currents. Typically, action-current recordings are less invasive and easier to establish than whole-cell recordings. Furthermore, lateral-line afferent neurons are ideal for this type of recording, as their dendrites are myelinated and spiking is absent without hair-cell neurotransmission (Obholzer *et al.*, 2008). These qualities imply that afferent spiking is evoked from spontaneous and stimulation-dependent release of neurotransmitter from hair cells. Thus, action-current recordings are sufficient for examining the temporal sequence of spikes, which provides a direct readout of the activity of innervated hair cells.

## A. Electrode and Recording Details

Extracellular recording electrodes are pulled in a similar fashion as microphonic electrodes except with longer shafts and outer tip diameters slightly smaller than 1 μm. Recording electrode resistances should range between 5 and 10 MΩ in extracellular solution. The recording electrode is positioned at an approximately 45° angle to the dorsal side of the pinned larva (Fig. 1B). The electrode should be positioned in the same optical plane as the middle of the posterior lateral line ganglion (PLLg). In a manner similar to α-bungarotoxin injection, the electrode is moved ventrally with increasing pressure against the fish skin until it advances through it. Often following the skin puncture, the pipette will move rapidly past the ganglion. If this occurs, then the electrode should be slowly retracted until it is within the membranous sack that encompasses the cell bodies. The electrode's position within the PLLg is confirmed by inflation of this sack with positive pipette pressure delivered via the electrode holder. Note that if necessary, the PLLg can be visualized using transgenic animals with fluorescently labeled lateral-line neurons (see both Nagiel *et al.*, 2008 and Obholzer *et al.*, 2008 for constructs).

To record from an individual lateral-line neuron, the electrode is moved against a desired cell and negative pipette pressure is applied (Fig. 3A).Recordings are made with the amplifier in voltage-clamp mode (command voltage = 0) with a 10 kHz sample rate and filtered at 1 kHz. For typical action-current recordings, the series resistance lies within a range of 30–80 MΩ. Confirmation of an established recording is seen first by the appearance of spontaneous spiking, after which the water jet is used to scan for the innervated neuromast, resulting in the conversion of spontaneous to phase-locked spiking.

Occasional application of positive pipette pressure is useful for both increasing the clarity of the ganglion and freeing any skin, cell, or tissue debris that may be obstructing the pipette tip. Also, on occasion, electrodes will rapidly form gigaohm seals, which predicts that whole-cell recordings of afferent neurons will be easily obtained.

## B. Analysis of Action Currents

In response to bidirectional stimulation of neuromast hair cells (e.g., sine waves), action-current recordings reveal phase-locked spiking to one direction of stimulation

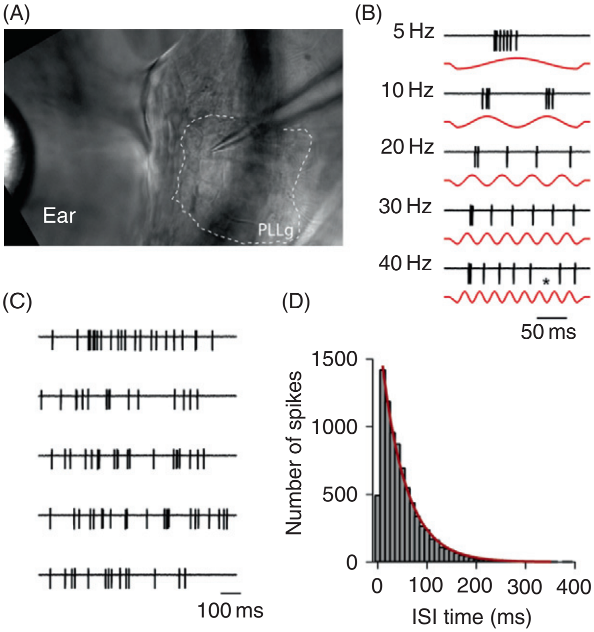

**Fig. 3** Action-current recordings from individual posterior lateral-line neurons. (A) Under DIC differential interference contrast optics with a 40× objective, the posterior lateral-line ganglion (PLLg; dashed-with line) is visible just posterior to the ear. The recording electrode is positioned in the anterior-dorsal portion of the PLLg, where the majority of cell bodies for the primary neuromasts are located. Note the otolith in the anterior side of the image. (B) Single traces of action currents in response to hair-cell stimulation at various frequencies. Note the spikes are phase-locked to just one direction of deflection. (C) Five consecutive 1 s traces of spontaneous spiking. The mean interspike interval (ISI) for 400 s of spiking was 50 ms. (D) Histogram representing the distribution of ISIs (10 ms bins) from 400 s of spiking by the cell shown in C. The histogram is best fit by a single-phase exponential decay equation (red line) with a tau of 50 ms.

(Obholzer *et al.*, 2008). This occurs because an individual afferent neuron innervates only one of the two populations of hair cells within a neuromast that all display the same hair-bundle polarity (Faucherre *et al.*, 2009; Nagiel *et al.*, 2008; Obholzer *et al.*, 2008). Spiking remains phase-locked with rates of stimulation approaching 100 Hz. At lower frequencies, spiking occurs with each deflection, while at higher frequencies, spikes do not occur with every deflection. In both cases, there is no loss of phase locking to the water-jet stimulus (Fig. 3B). Spike trains in response to continuous stimulation can be visualized with period histograms where individual spike times are binned and plotted relative to the unit period for a given stimulus frequency. The resulting series of unit spike times can be further transformed into unit vectors with corresponding, specific phase angles. Thus, the collection of spikes, now represented by a series of vectors, can be quantified for the degree of synchrony between the stimulus and response by calculating the vector strength ($r$) of the series (Goldberg and Brown, 1969). We recently utilized this method of analysis to quantify phase-locked activity in larvae with disrupted hair-cell endocytosis (Trapani *et al.*, 2009).

In the absence of sensory stimuli, spontaneous spiking is observed in afferent neurons of the auditory, vestibular, and lateral-line systems across species. This spontaneous spiking apparently results from neurotransmitter release from innervated hair cells (Annoni *et al*., 1984; Flock and Russell, 1976; Furukawa and Ishii, 1967; Siegel and Dallos, 1986; Starr and Sewell, 1991; Zimmerman, 1979). The most meaningful feature of spontaneous spiking is the time interval between two consecutive spikes, which is termed the interspike interval (ISI). The temporal pattern of the spontaneous activity can be analyzed using ISI histograms, where features of the histogram describe the nature of the activity. For example, if spikes are generated by a Poisson process, then the ISI histogram will be best fit by a single-phase exponential decay equation with the time constant (tau) corresponding to the recording's mean ISI time. Recording spontaneous action currents from a PLLg neuron results in a diverse range of ISI times (Fig. 3C). The ISI histogram of spontaneous spiking in Fig. 3D is best fit by a single exponential decay equation.

## V. Summary

In this chapter, we have described our methods for recording activity from the posterior lateral-line system of the larval zebrafish. While some of the details are specific for this particular preparation, a majority of the techniques are translatable to physiology in other areas of the fish. The mounting and immobilization of larvae, as well as the basic principles of the recording, will benefit any investigator looking to establish physiological recordings in live, intact larvae.

## VI. Discussion

The zebrafish is a genetically tractable vertebrate and a powerful platform for electrophysiological studies. The above preparation is extremely valuable in assessing sensory hair-cell function in various auditory/vestibular mutants. The ability to record both microphonics from hair cells and action currents from lateral-line neurons can help to pinpoint the nature of the defect in mutants and reveal the biological role of the protein of interest. Using these techniques provides important information about the impact of mutations affecting genes that are conserved in function from fish to humans. In addition, the preparation allows one to mechanically stimulate hair cells in an undissected animal with intact circuitry that receives sensory input for higher order processing. Such recordings are currently not possible with mammalian model systems.

Future experiments using the lateral-line system may include whole-cell patch clamp recordings from the afferent neuron and potentially from individual hair cells, which will further increase the capability of this preparation. Furthermore, the afferent neuron forms an unmyelinated basket beneath a given, innervated neuromast, and this presents the potential for postsynaptic recordings similar to those achieved in mice (Glowatzki and Fuchs, 2002). Experiments with a double patch-clamp amplifier, where one could simultaneously record activity at both the neuromast and the afferent neuron, would be extremely powerful for examining sensory signal encoding.

Over the past 10 years, the zebrafish community has developed a large number of mutant and transgenic zebrafish lines. Using either endogenous regulatory sequences or Gal4/UAS targeting allows for spatially and temporally restricted expression of proteins of interest and has created a large set of optogenetic tools: photoconvertible fluorescent proteins to visualize cells, light-gated ion channels to activate cells, genetically encoded voltage and calcium sensors to examine cellular activity, and genetically encoded proteins that poison synaptic transmission to deactivate cells. The combination of transgenic lines with hair cell and afferent-specific expression of these reporters together with the electrophysiology techniques described in this chapter presents the potential for experiments aimed at understanding the fundamental aspects of hair-cell processing and sensory signaling.

## Acknowledgments

Many thanks go to P. Brehm and H. Wen for initial instruction on mounting and paralyzing larvae, as well as technical advice. Thanks also to L. Trussell and K. Bender for comments and advice on recordings and data analysis.

## References

Adrian, E. D. (1931). The microphonic action of the cochlea: an interpretation of Wever and Bray's experiments. *J. Physiol.* **71**, 28–29.

Annoni, J. M., Cochran, S. L., and Precht, W. (1984). Pharmacology of the vestibular hair cell-afferent fiber synapse in the frog. *J. Neurosci.* **4**, 2106–2116.

Assad, J. A., Shepherd, G. M., and Corey, D. P. (1991). Tip-link integrity and mechanical transduction in vertebrate hair cells. *Neuron* **7**, 985–994.

Beurg, M., Fettiplace, R., Nam, J.-H., and Ricci, A. J. (2009). Localization of inner hair cell mechanotransducer channels using high-speed calcium imaging. *Nat. Neurosci.* **12**, 553–558.

Corey, D. P., and Hudspeth, A. J. (1983). Analysis of the microphonic potential of the bullfrog's sacculus. *J. Neurosci.* **3**, 942–961.

Dambly-Chaudière, C., Sapède, D., Soubiran, F., Decorde, K., Gompel, N., and Ghysen, A. (2003). The lateral line of zebrafish: a model system for the analysis of morphogenesis and neural development in vertebrates. *Biol. Cell* **95**, 579–587.

Farris, H. E., LeBlanc, C. L., Goswami, J., and Ricci, A. J. (2004). Probing the pore of the auditory hair cell mechanotransducer channel in turtle. *J. Physiol.* **558**, 769–792.

Faucherre, A., Pujol-Martí, J., Kawakami, K., and López-Schier, H. (2009). Afferent neurons of the zebrafish lateral line are strict selectors of hair-cell orientation. *PLoS One* **4**, e4477.

Feldman, B., Gates, M. A., Egan, E. S., Dougan, S. T., Rennebeck, G., Sirotkin, H. I., Schier, A. F., and Talbot, W. S. (1998). Zebrafish organizer development and germ-layer formation require nodal-related signals. *Nature* **395**, 181–185.

Flock, A. and Russell, I. (1976). Inhibition by efferent nerve fibres: action on hair cells and afferent synaptic transmission in the lateral line canal organ of the burbot *Lota lota*. *J. Physiol.* **257**, 45–62.

Flock, A., and Wersall, J. (1962). A study of the orientation of the sensory hairs of the receptor cells in the lateral line organ of fish, with special reference to the function of the receptors. *J. Cell Biol.* **15**, 19–27.

Freeman, W. (1928). The function of the lateral line organs. *Science* **68**, 205.

Furukawa, T., and Ishii, Y. (1967). Neurophysiological studies on hearing in goldfish. *J. Neurophysiol.* **30**, 1377–1403.

Ghysen, A., and Dambly-Chaudière, C. (2007). The lateral line microcosmos. *Genes Dev.* **21**, 2118–2130.

Glowatzki, E., and Fuchs, P. A. (2002). Transmitter release at the hair cell ribbon synapse. *Nat. Neurosci.* **5**, 147–154.

Goldberg, J. M. and Brown, P. B. (1969). Response of binaural neurons of dog superior olivary complex to dichotic tonal stimuli: some physiological mechanisms of sound localization. *J. Neurophysiol.* **32**, 613–36.

Grant, K. A., Raible, D. W., and Piotrowski, T. (2005). Regulation of latent sensory hair cell precursors by glia in the zebrafish lateral line. *Neuron* **45**, 69–80.

Hoagland, H. (1933). Electrical responses from the lateral-line nerves of catfish. I. *J. Gen Physiol.* **16**, 695–714.

Jaramillo, F., and Hudspeth, A. J. (1991). Localization of the hair cell's transduction channels at the hair bundle's top by iontophoretic application of a channel blocker. *Neuron* **7**, 409–420.

López-Schier, H., Starr, C. J., Kappler, J. A., Kollmar, R., and Hudspeth, A. J. (2004). Directional cell migration establishes the axes of planar polarity in the posterior lateral-line organ of the zebrafish. *Dev. Cell* **7**, 401–412.

Nagiel, A., Andor-Ardó, D., and Hudspeth, A. J. (2008). Specificity of afferent synapses onto plane-polarized hair cells in the posterior lateral line of the zebrafish. *J. Neurosci.* **28**, 8442–8453.

Nicolson, T., Rüsch, A., Friedrich, R. W., Granato, M., Ruppersberg, J. P., and Nüsslein-Volhard, C. (1998). Genetic analysis of vertebrate sensory hair cell mechanosensation: the zebrafish circler mutants. *Neuron* **20**, 271–283.

Nuñez, V. A., Sarrazin, A. F., Cubedo, N., Allende, M. L., Dambly-Chaudière, C., and Ghysen, A. (2009). Postembryonic development of the posterior lateral line in the zebrafish. *Evol. Dev.* **11**, 391–404.

Obholzer, N., Wolfson, S., Trapani, J. G., Mo, W., Nechiporuk, A., Busch-Nentwich, E., Seiler, C., Sidi, S., Söllner, C., Duncan, R. N., Boehland, A., and Nicolson, T. (2008). Vesicular glutamate transporter 3 is required for synaptic transmission in zebrafish hair cells. *J. Neurosci.* **28**, 2110–2118.

Ono, F., Higashijima, S., Shcherbatko, A., Fetcho, J. R., and Brehm, P. (2001). Paralytic zebrafish lacking acetylcholine receptors fail to localize rapsyn clusters to the synapse. *J Neurosci* **21**, 5439–5448.

Patton, E. E., and Zon, L. I. (2001). The art and design of genetic screens: zebrafish. *Nat. Rev. Genet.* **2**, 956–966.

Ribera, A. B., and Nüsslein-Volhard, C. (1998). Zebrafish touch-insensitive mutants reveal an essential role for the developmental regulation of sodium current. *J. Neurosci.* **18**, 9181–9191.

Ryder, J. A. (1884). The pedunculated lateral-line organs of *Gastrostomus*. *Science* **3**, 5.

Seiler, C., Finger-Baier, K. C., Rinner, O., Makhankov, Y. V., Schwarz, H., Neuhauss, S. C. F., and Nicolson, T. (2005). Duplicated genes with split functions: independent roles of protocadherin 15 orthologues in zebrafish hearing and vision. *Development* **132**, 615–623.

Siegel, J. H. and Dallos, P. (1986). Spike activity recorded from the organ of Corti. *Hear. Res.* **22**, 245–248.

Smear, M. C., Tao, H. W., Staub, W., Orger, M. B., Gosse, N. J., Liu, Y., Takahashi, K., Poo, M.-M., and Baier, H. (2007). Vesicular glutamate transport at a central synapse limits the acuity of visual perception in zebrafish. *Neuron* **53**, 65–77.

Starr, P. A., and Sewell, W. F. (1991). Neurotransmitter release from hair cells and its blockade by glutamate-receptor antagonists. *Hear. Res.* **52**, 23–41.

Suckling, E. E., and Suckling, J. A. (1950). The electrical response of the lateral line system of fish to tone and other stimuli. *J. Gen. Physiol.* **34**, 1–8.

Sumbre, G., Muto, A., Baier, H., and Poo, M.-M. (2008). Entrained rhythmic activities of neuronal ensembles as perceptual memory of time interval. *Nature* **456**, 102–106.

Söllner, C., Rauch, G.-J., Siemens, J., Geisler, R., Schuster, S. C., Müller, U., Nicolson, T., and Tübingen 2000 Screen Consortium (2004a). Mutations in cadherin 23 affect tip links in zebrafish sensory hair cells. *Nature* **428**, 955–959.

Söllner, C., Schwarz, H., Geisler, R., and Nicolson, T. (2004b). Mutated otopetrin 1 affects the genesis of otoliths and the localization of Starmaker in zebrafish. *Dev. Genes Evol.* **214**, 582–590.

Trapani, J. G., Obholzer, N., Mo, W., Brockerhoff, S. E., and Nicolson, T. (2009). Synaptojanin 1 is required for temporal fidelity of synaptic transmission in hair cells. *PLoS Genet.* **5**, e1000480.

Westerfield, M., Liu, D. W., Kimmel, C. B., and Walker, C. (1990). Pathfinding and synapse formation in a zebrafish mutant lacking functional acetylcholine receptors. *Neuron* **4**, 867–874.

Wever, E. G. and Bray, C. W. (1930). Action currents in the auditory nerve in response to acoustical stimulation. *Proc. Natl. Acad. Sci. U. S. A.* **16**, 344–350.

Whitfield, T. T., Riley, B. B., Chiang, M.-Y., and Phillips, B. (2002). Development of the zebrafish inner ear. *Dev. Dyn.* **223**, 427–458.

Zimmerman, D. M. (1979). Onset of neural function in the lateral line. *Nature* **282**, 82–84.

van Netten, S. M., and Kroese, A. B. (1987). Laser interferometric measurements on the dynamic behaviour of the cupula in the fish lateral line. *Hear. Res.* **29**, 55–61.

## CHAPTER 9

# Zebrafish Kidney Development

**Iain A. Drummond**[*] ***and*** **Alan J. Davidson**[†]

[*]Departments of Medicine and Genetics, Harvard Medical School and Nephrology Division, Massachusetts General Hospital, Charlestown, Massachusetts

[†]Center for Regenerative Medicine, Massachusetts General Hospital, Boston, Massachusetts

---

Abstract
I. Introduction
II. Structure of the Zebrafish Pronephros
III. Formation of the Pronephros
  A. Origin of the Nephrogenic Mesoderm
  B. Early Subdomains within the Nephrogenic Mesoderm
  C. Role of Retinoic Acid Signaling
  D. Role of Pax2a
  E. Role of the Endoderm
  F. Differentiation of the Tubular Epithelium
  G. Formation of the Glomerulus
  H. Formation of the Cloaca
IV. Methods to Study Pronephros Function
  A. Embryo Dissociation
  B. Isolation of Fluorescently Labeled Cells by Fluorescence Activated Cell Sorting (FACS)
  C. A Simple Assay for Glomerular Filtration
  D. Gentamicin Induced Kidney Tubule Injury in Embryos and Adults
  E. Adult Kidney Isolation
  F. Non-Lethal Surgical Access to the Adult Kidney
  G. Detecting and Imaging Zebrafish Cilia
  H. Histological Sectioning of Whole mount Stained Embryos
  I. Electron Microscopy Methods for Zebrafish
V. Conclusions
Acknowledgments
References

METHODS IN CELL BIOLOGY, VOL. 100
Copyright © 2010 Elsevier Inc. All rights reserved.

978-0-12-384892-5
DOI: 10.1016/B978-0-12-384892-5.00009-8

## Abstract

The zebrafish pronephric kidney provides a useful and relevant model of kidney development and function. It is composed of cell types common to all vertebrate kidneys and pronephric organogenesis is regulated by transcription factors that have highly conserved functions in mammalian kidney development. Pronephric nephrons are a good model of tubule segmentation and differentiation of epithelial cell types. The pronephric glomerulus provides a simple model to assay gene function in regulating cell structure and cell interactions that form the blood filtration apparatus. The relative simplicity of the pronephric kidney combined with the ease of genetic manipulation in zebrafish makes it well suited for mutation analysis and gene discovery, in vivo imaging, functional screens of candidate genes from other species, and cell isolation by FACS . In addition, the larval and adult zebrafish kidneys have emerged as systems to study kidney regeneration after injury. This chapter provides a review of pronephric structure and development as well as current methods to study the pronephros.

## I. Introduction

The kidney has two principal functions: to remove waste from the blood and to balance ion and metabolite concentrations in the blood within physiological ranges that support proper functioning of all other cells (Vize *et al*., 2002). Kidney function is achieved largely by first filtering the blood and then recovering useful ions and small molecules by directed epithelial transport. This work is performed by nephrons, the functional units of the kidney (Fig. 1). The nephron is comprised of a blood filter, called the glomerulus, attached to a tubular epithelium (Fig. 1C and D). The glomerulus contains specialized epithelial cells called podocytes that form a basket-like extension of cellular processes around a capillary tuft. The basement membrane between podocytes and capillary endothelial cells together with the specialized junctions between the podocyte cell processes (slit diaphragms) function as a blood filtration barrier, allowing passage of small molecules, ions, and blood fluid into the urinary space, while retaining high molecular weight proteins in the vascular system (Fig. 1; see also Fig. 12D). The blood filtrate travels down the lumen of the kidney tubule, encountering distinct proximal and distal tubule segments that modify the composition of the urine via specific solute transport activities. The urine is drained by the collecting ducts, which further modify its salt and water composition, until eventually being voided outside the body (Fig. 1; Vize *et al*., 2002).

In the course of vertebrate evolution, three distinct forms of kidneys of increasing complexity have been generated: the pronephros, mesonephros, and metanephros (Saxén, 1987). The pronephros is the first kidney to form during embryogenesis. In vertebrates with free-swimming larvae, including amphibians and teleost fish, the pronephros is the functional kidney of early larval life (Howland, 1921; Tytler, 1988; Tytler *et al*., 1996; Vize *et al*., 1997) and is required for proper osmoregulation (Howland, 1921). Later, in juvenile stages of fish and frog development, a mesonephros forms around and along the length of the pronephros and later serves as the final adult kidney. The metanephric kidney forms

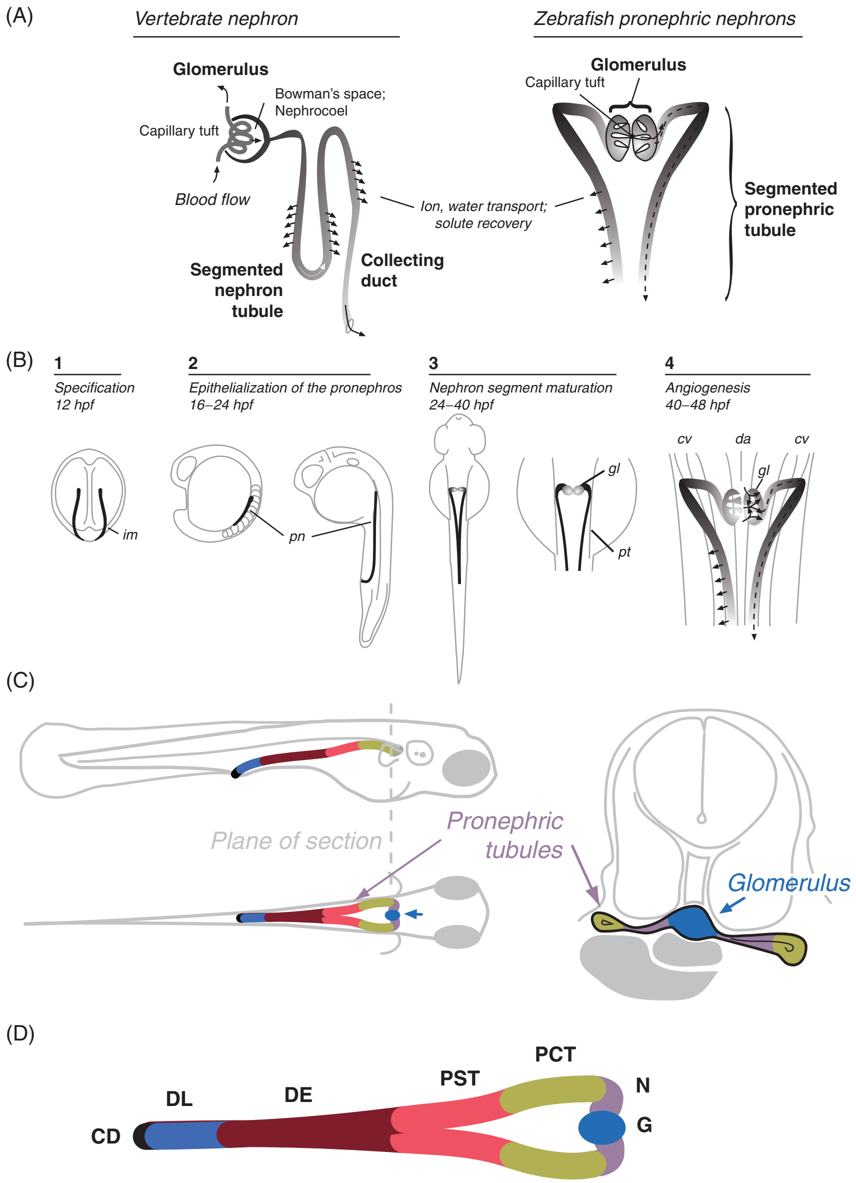
(A)
Vertebrate nephron
Glomerulus
Bowman's space; Nephrocoel
Capillary tuft
Blood flow
Segmented nephron tubule
Collecting duct
Ion, water transport; solute recovery
Zebrafish pronephric nephrons
Glomerulus
Capillary tuft
Segmented pronephric tubule
(B)
1
Specification
12 hpf
im
2
Epithelialization of the pronephros
16–24 hpf
pn
3
Nephron segment maturation
24–40 hpf
gl
pt
4
Angiogenesis
40–48 hpf
cv
da
cv
gl
(C)
Plane of section
Pronephric tubules
Glomerulus
(D)
CD
DL
DE
PST
PCT
N
G

**Fig. 1** The zebrafish pronephros. (A) Functional features of the vertebrate nephron and the zebrafish pronephric nephrons. See text for details. (B) Stages in zebrafish pronephric kidney development. (1) Specification of mesoderm to a nephric fate: expression patterns of pax2.1 and lim-1 define a posterior region of the intermediate mesoderm (im) and suggest that a nephrogenic field is established in early development. (2) Epithelialization of the pronephros (pn) follows somitogenesis and is complete by 24 hpf. (3) Patterning of the nephron gives rise to the pronephric glomerulus (gl) and pronephric tubules (pt). (4) Angiogenic sprouts from the dorsal aorta (da) invade the glomerulus and form the capillary loop. The cardinal vein (cv) is apposed to the tubules and receives recovered solutes. (C) Diagram of the mature zebrafish pronephric kidney in 3-day larva. A midline compound glomerulus connects to the segmented pronephric tubules that run laterally. The nephrons are joined at the cloaca where they communicate with the exterior. (D) Patterning of the pronephric nephron generates discrete segments: neck (N), proximal convoluted tubule (PCT), proximal straight tubule (PST), distal early (DE), late distal (DL), and collecting duct (CD).

exclusively in the amniotes (mammals, birds, and reptiles) and, in the case of mammals, is adapted for water retention and producing concentrated urine. Despite some differences in organ morphology between the various kidney forms, many common elements exist at the cellular and molecular level that can be exploited to further our general understanding of renal development and biology. In particular, the zebrafish pronephros has provided a useful model of nephrogenic mesoderm differentiation, kidney cell type differentiation, nephron patterning, kidney, vasculature interactions, glomerular function, and diseases affecting glomerular filtration and tubule lumen size, i.e., cystic kidney disease. While much remains to be done, the basic features of zebrafish pronephric development and patterning have emerged from studies using simple histology, cell lineage tracing, gene expression patterns, and analysis of zebrafish mutants affecting this process.

## II. Structure of the Zebrafish Pronephros

The zebrafish pronephros consists of only two nephrons with glomeruli fused at the embryo midline just ventral to the dorsal aorta (Fig. 1C) (Agarwal and John, 1988; Armstrong, 1932; Balfour, 1880; Drummond, 2000; Drummond *et al*., 1998; Goodrich, 1930; Hentschel and Elger, 1996; Marshall and Smith, 1930; Newstead and Ford, 1960; Tytler, 1988; Tytler *et al*., 1996). Historically, much of the tubular epithelium extending from the glomerulus to the cloaca has been referred to as pronephric duct. This nomenclature was based on the similar anatomical location of the pronephric or Wolffian ducts in amphibians, chickens, and mammals (Vize *et al*., 2002). However, based on new molecular data there is now a consensus that the tubular epithelium of the zebrafish pronephros is actually subdivided into two proximal tubule segments (proximal convoluted tubule (PCT) and proximal straight tubule (PST)) and two distal tubule segments (distal early (DE) and distal late (DL)) that are homologous in many ways to the segments of the mammalian nephron (Wingert and Davidson, 2008). What was previously considered “tubule” is now believed to represent a “neck” segment, such as that described in the adult kidneys of other teleosts (Kamunde and Kisia, 1994).

The PCT segment is structurally similar to the proximal tubules of the mammalian kidney, displaying a well-developed brush border and high columnar epithelial cells (Seldin and Giebisch, 1992). The proximal tubule in other vertebrates plays a major role in reabsorbing the bulk of the salts, sugars, and small proteins that pass through the glomerular filtration barrier (Vize *et al*., 2002). The zebrafish PCT expresses the endocytic receptors megalin and cubalin and takes up small fluorescent dextrans that pass through the glomerulus, consistent with a conserved absorptive function (Anzenberger *et al*., 2006). The PCT also expresses the chloride/bicarbonate anion exchanger AE2, the sodium/bicarbonate cotransporter NBC1, and the sodium/hydrogen exchanger NHE (Fig. 2A) (Nichane *et al*., 2006; Shmukler *et al*., 2005; Wingert *et al*., 2007), indicating a role in acid/base homeostasis which is also shared with proximal tubules in mammals.

The function of the PST segment is less clear. Markers of this segment include an aspartoacylase homolog (Fig. 2B), the zebrafish *starmaker* gene (Fig. 2C) (Sollner *et al*., 2003; Sprague *et al*., 2008), *slc13a1* (a sodium/sulfate symporter), and *trpm7*

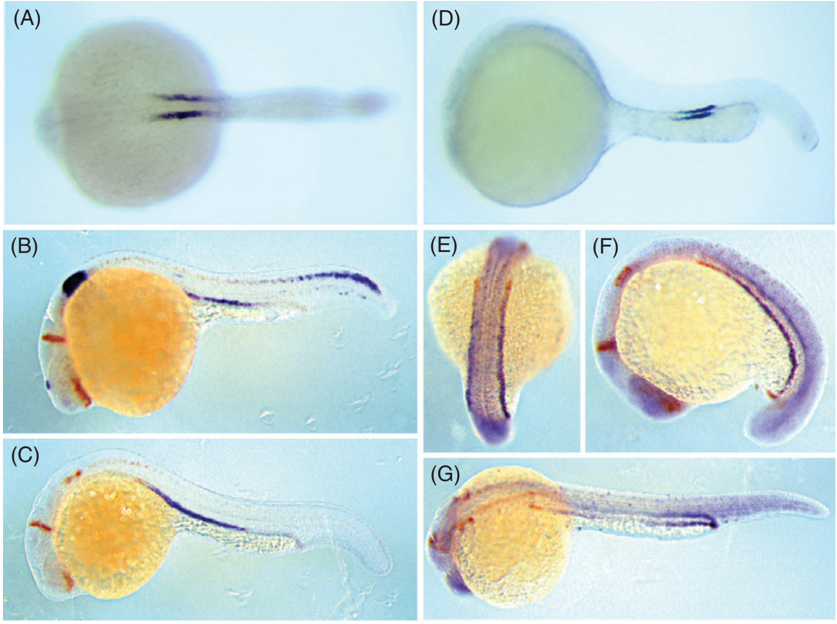

**Fig. 2** Ion transporter mRNA expression defines pronephric nephron segments. (A) The chloride–bicarbonate anion exchanger (AE2) is expressed in the proximal convoluted tubule. The proximal straight segment specifically expresses the zebrafish starmaker gene (B) and an *aspartoacylase* homolog (C). Early distal segments express the Na–K–Cl symporter *slc12a1* (D). Expression of a putative ABC transporter (ibd2207) is observed initially throughout most of the forming pronephric tubules at the 15-somite stage (E and F) but becomes restricted primarily to the late distal segment by 24 hpf (G). Embryos in parts B, C, E, F, and G are counterstained with *pax2a* probe in red for reference. (A and D, courtesy of Alan Davidson *et al.*; B, C, E, F, and G, courtesy of Neil Hukreide.)

(a monovalent cation channel). The nutria mutant lacks a functional trpm7 gene and exhibits kidney stone formation and skeletal defects (Elizondo *et al.*, 2005) suggesting a role for TrpM7 in calcium uptake from the tubular fluid. The observation that the PST specifically expresses a sulfate (slc13a3) and calcium (*trpm7*) transporter suggests that this segment may specialize in the uptake of particular ions.

The DE segment expresses *slc12a1* (aka the NKCC2 (Na–K–Cl) symporter) (Fig. 2D), which in mammals is exclusively expressed in the thick ascending limb (TAL) portion of the distal tubule (Igarashi *et al.*, 1995). This segment is also known as the "diluting segment" as it reduces the osmolarity of the urinary filtrate (Guggino *et al.*, 1988). Diluting segments in freshwater fish and terrestrial vertebrates play an important role in NaCl conservation (and in the case of birds and mammals, urine concentration; Dantzler, 2003). The activity of Slc12a1 is dependent upon the recycling of $K^+$ ions back to the tubular fluid via the apical Romk2 potassium channel and the transport of $Cl^-$ ions out of the cell via the Clckb chloride channel (Simon and Lifton, 1998). Consistent with the zebrafish DE segment functioning as a diluting segment, homologues of *Romk2* and *Clck* are also expressed by the DE (Wingert *et al.*, 2007).

The DL segment expresses *slc12a3*, encoding a NaCl cotransporter. In the mammalian nephron, this cotransporter is expressed in the distal convoluted tubule segment, which follows the TAL, and fine-tunes sodium and chloride absorption under hormonal regulation (Mastroianni *et al*., 1996; Simon *et al*., 1996). It is likely that the DL segment of the zebrafish pronephros has an analogous function, although this has yet to be confirmed. Some overlap exists between expression of what would be collecting duct markers in mammals (*c-ret, gata3*) and distal tubule markers (*slc12a3, clck*; Wingert *et al*., 2007) in the DL segment of the pronephros. Since freshwater vertebrates do not have concentrating kidneys, the lack of a significant segment expressing markers consistent with collecting duct identity is not unusual.

## III. Formation of the Pronephros

### A. Origin of the Nephrogenic Mesoderm

Cell labeling and lineage tracing in zebrafish gastrula stage embryos have demonstrated that cells destined to form the pronephros arise from the ventral mesoderm, in a region partially overlapping with cells fated to form blood (Fig. 3A) (Kimmel *et al*., 1990). These cells emerge shortly after the completion of epiboly as a band of tissue, the intermediate mesoderm (IM), at the posterior lateral edge of the paraxial mesoderm (Fig. 3B and C). In zebrafish, unlike other non-teleost vertebrates, the IM gives rise to both kidney and blood cells. The size and positioning of the IM are significantly influenced by dorsoventral and anterior–posterior axis patterning molecules, such as the ventralizing factors bone morphogenetic proteins (BMPs) and their inhibitors, and the Cdx family of homeobox genes (see Table I for a summary of zebrafish mutants with pronephric defects).

### B. Early Subdomains within the Nephrogenic Mesoderm

By the early stages of somitogenesis, the nephrogenic mesoderm component of the IM is clearly defined by the expression of renal markers such as the transcription factors *pax2a*, *pax8*, and *lhx1a*, which extend from the level of somite 3 to the cloaca (Carroll *et al*., 1999; Drummond, 2000; Heller and Brandli, 1999; Krauss *et al*., 1991; Majumdar

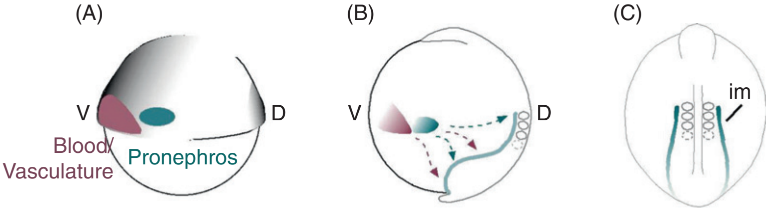

**Fig. 3** Origins of the intermediate mesoderm. (A) Approximate positions of cells in a shield stage embryo destined to contribute to the blood/vasculature and pronephric lineages in the ventral (V) germ ring. (D; dorsal shield). (B) Migration of cells during gastrulation to populate the intermediate mesoderm (im) (C).

**TABLE I**
**Zebrafish Mutants with Defects in Early Pronephros Formation**

| Mutant/gene | Gene product | Kidney phenotype | Reference |
|---|---|---|---|
| *swirl/bmp2b* | BMP ligand | Absent or reduced | Hild *et al.* (1999) |
| *snailhouse/bmp7a* | BMP ligand | Reduced | Kishimoto *et al.* (1997) |
| *somitabun/smad5* | BMP signal transducer | Reduced | Nguyen *et al.* (1998) |
| *lost-a-fin/alk8* | BMP receptor | Reduced | Mullins *et al.* (1996) |
| *chordino/chordin* | BMP antagonist | Expanded | Hammerschmidt *et al.* (1996b) |
| *kugelig/cdx4 and cdx1a* | Homeobox transcription factors | Posteriorly shifted | Davidson *et al.* (2003); Wingert *et al.* (2007) |
| *ntla and spadetail/tbx16* double mutants | Mesoderm inducing T-box transcription factors | Absent | Amacher *et al.* (2002) |

*et al.*, 2000; Mauch *et al.*, 2000; Pfeffer *et al.*, 1998; Puschel *et al.*, 1992). Based on the overlapping but distinct expression patterns of the transcription factor genes *wt1a, pax2a*, and *sim1a* in the IM, together with fate mapping analyses, it was initially shown that podocytes, neck (previously "tubule"), and proximal tubule cells (previously "duct") could be defined as sequential anterior to posterior subdomains of the IM (Fig. 4) (Serluca and Fishman, 2001). Further refinement of this observation suggests that podocytes and neck cells arise from the IM adjacent to somites 3–4 whereas the first proximal tubule segment descends from the IM level with somites 5–8 (Bollig *et al.*, 2009; Wingert *et al.*, 2007). It is likely that the other tubule segments are derived sequentially from more posterior subdomains of the IM, although this has yet to be confirmed by lineage labeling. The notion that IM at all axial levels contributes to the pronephros in zebrafish is in contrast to other non-teleost vertebrates where only the anterior portion of the IM adopts a renal fate and the duct elongates to the cloaca.

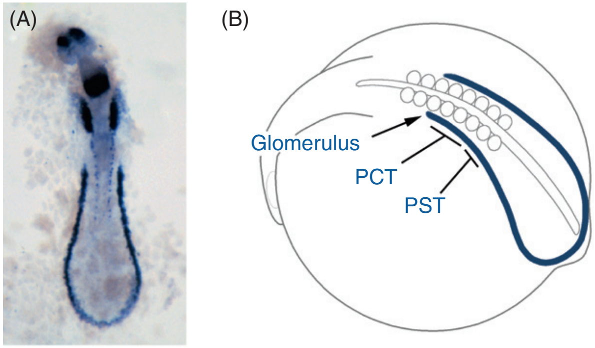

**Fig. 4** Derivation of the pronephros from the intermediate mesoderm. (A) The pax2.1 expression domain in early somitogenesis stage embryos defines a stripe of intermediate mesoderm fated to become the pronephric epithelia. (B) Fate map of the nephrogenic intermediate mesoderm derived from fluorescent dye uncaging lineage experiments. Proximal fates previously referred to as "tubule" are now more accurately defined as proximal convoluted tubule (PCT) and more distal fates previously referred to as "duct" are now more accurately termed proximal straight tubule (PST).

## C. Role of Retinoic Acid Signaling

Recently it was shown that retinoic acid (RA) signaling plays a major role in establishing the proximo-distal segmentation pattern of the pronephros (Wingert *et al*., 2007). Exposure of embryos to high RA doses induces the formation of expanded proximal tubule segments at the expense of the distal segments. Conversely, inhibition of RA synthesis with diethylaminobenzaldehyde (DEAB), a competitive inhibitor of the aldehyde dehydrogenase enzymes, favors distal nephron cell fates. DEAB could elicit these patterning effects when added at the end of gastrulation through to the beginning of somitogenesis, consistent with a requirement for RA during early IM patterning. In support of this, DEAB-treated embryos show a loss of proximally restricted genes such as *jagged-2a* and *delta-c* and a concomitant expansion in the distal marker *meccom* at the 8-somite stage (Wingert *et al*., 2007). RA may also function later in pronephric development as transgenic RA reporter embryos show significant activity in the pronephric tubules at the 18-somite stage (Perz-Edwards *et al*., 2001). The source of the RA is presumed to be the paraxial mesoderm, which expresses high levels of *aldh1a2* (aka *retinaldehyde dehydrogenase-2*).

In addition to tubule patterning defects, DEAB-treated embryos are also characterized by a loss of podocytes. Expression of *wt1a*, implicated in podocyte differentiation (Perner *et al*., 2007), is absent in DEAB-treated embryos from the subdomain of the IM fated to give rise to the glomerulus. Analysis of the *wt1a* promoter identified an RA-responsive element consistent with *wt1a* being a direct target of RA signaling (Bollig *et al*., 2009). Additional RA target genes that specify podocytes or maintain podocyte function (Vaughan *et al*., 2005) remain to be explored in zebrafish.

## D. Role of Pax2a

The paired domain transcription factor *pax2a* is now known to play a key role in establishing the boundary between podocytes and the neck segment. After initially being expressed throughout the nephrogenic mesoderm, *pax2a* becomes highly expressed in the neck segment (Krauss *et al*., 1991; Majumdar *et al*., 2000). Fish with mutations in *pax2a* (*no isthmus, noi*) show an expansion in the expression of the podocyte markers *wt1a* and *vegf* into the neck and possibly proximal tubule domain (Fig. 5). Although these proximal tubule cells maintain an epithelial character (no transdifferentiation to a podocyte morphology is observed), they fail to express normal markers of this segment (NaK ATPase and 3G8, a brush border marker) (Majumdar *et al*., 2000). The data suggest that *pax2a* plays an important role in defining the podocyte/neck/proximal tubule boundaries, possibly by repressing podocyte-specific genes in the neck and proximal tubule segments.

## E. Role of the Endoderm

Although pronephric development does not require proper development of the endoderm, overdevelopment of the endoderm can alter pronephric development (Mudumana *et al*., 2008). Knockdown of odd-skipped related1 gene (*osr1*), encoding

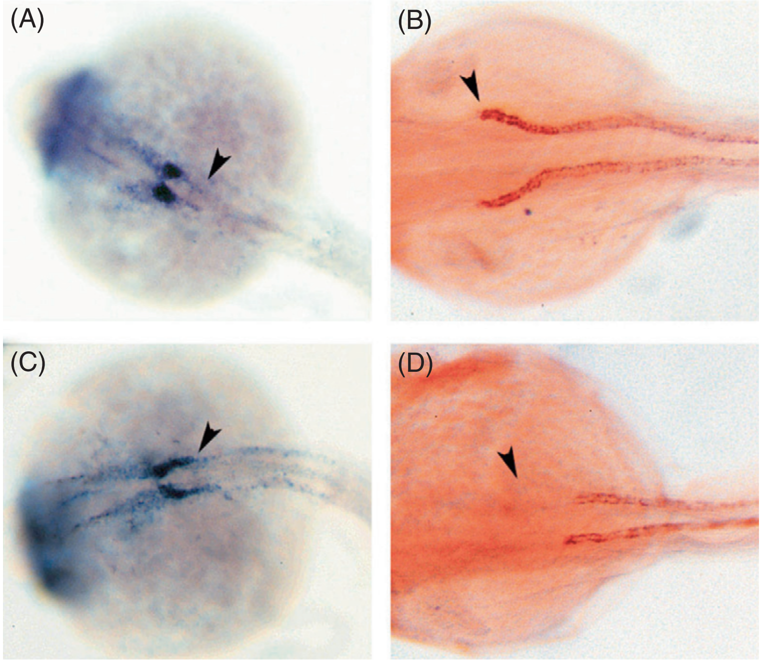

**Fig. 5** Formation of the glomerulus–tubule boundary is disrupted in *no isthmus* (*noi; pax2a*) mutants. Wholemount *in situ* hybridization with *wt1a* marks the presumptive podocytes in wildtype embryos (A). *wt1a* expression is caudally expanded into the anterior pronephric tubules in noi$^{tb21}$ mutant embryos (C) at 24 hpf (arrow in C). Wholemount antibody staining of wild-type (B) and noi$^{tb21}$ (D) embryos with mAb alpha6F which recognizes a Na$^+$/K$^+$ ATPase alpha1 subunit. alpha6F marks the pronephric epithelia in wild-type (arrows in B) and proximal tubule Na$^+$/K$^+$ ATPase expression is missing in noi$^{-/tb21}$ mutant embryos at 2.5 dpf (D).

a zinc finger transcription factor, causes expansion of endoderm that subsequently inhibits epithelialization of the proximal portion of the pronephros.

## F. Differentiation of the Tubular Epithelium

Tubule formation is mediated by a mesenchyme to epithelial transition, a process central to kidney formation in all vertebrates (Saxén, 1987). By the end of this transition, which is complete by 24 h post fertilization, the epithelial cells of the pronephros are polarized with apical and basolateral domains containing ion transport proteins (Fig. 6A) (Drummond *et al*., 1998). In addition, individual multiciliated cells, induced by notch signaling during mid-somitogenesis, are interspersed with transporting epithelial cells along the pronephros (Liu *et al*., 2007). Thus, tubule formation occurs simultaneously with patterning events that define functionally distinct epithelial cell types.

Establishment of cell–cell junctions is an essential step in separating apical and basolateral membrane domains and giving an epithelium its vectorial property. Cadherins are the major proteins of the adherens junction that maintain the integrity

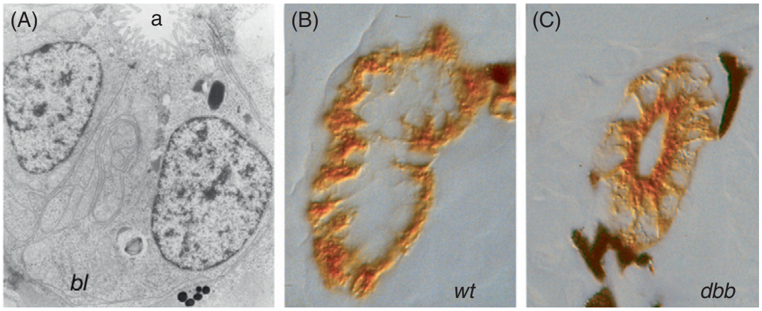

**Fig. 6** Epithelial cell polarity in the pronephric tubules. (A) Electron micrograph of 2.5-day pronephric tubule epithelial cells showing apical (A) brush border and basolateral cell surfaces and infoldings. Polarized distribution of the NaK ATPase in 2.5-day pronephric tubule epithelial cells visualized by the alpha6F monoclonal antibody is shown. The apical cell surface is devoid of staining while staining is strong on the basolateral cell surface and membrane infoldings (B). Double bubble mutant embryos (C) aberrantly express the NaK ATPase on the apical cytoplasm and cell membrane.

of epithelial sheets and separate apical and basolateral membrane domains. *cadherin17* is specifically expressed in the zebrafish nephrogenic mesoderm and persists in the pronephric epithelium (Horsfield *et al*., 2002). Knockdown of *cadherin17* causes a loss in renal epithelial cell-to-cell adhesion, failure of the ducts to fuse at the cloaca, and gaps between epithelial cells (Horsfield *et al*., 2002), thus demonstrating an essential role for *cadherin17* in tubule and duct morphogenesis.

Cell polarity and proper targeting of membrane transporters are essential for proper kidney ion transport and function. Several zebrafish mutants have been found to mistarget the NaK ATPase in the tubules from its normal basolateral membrane location to the apical membrane (Fig. 6) (Drummond *et al*., 1998). The activity of the NaK ATPase provides the motive force for many other coupled transport systems (Seldin and Giebisch, 1992); its mislocalization suggests that severe problems in osmoregulation exist in these mutants. In fact, these mutants later develop cysts in the pronephric tubule and the embryos eventually die of edema (Drummond *et al*., 1998).

## G. Formation of the Glomerulus

A major feature of the glomerular blood filter is the podocyte slit-diaphragm, a specialized adherens junction that forms between the finger-like projections of podocytes (podocyte foot processes) (Reiser *et al*., 2000). Failure of the slit-diaphragm to form results in leakage of high molecular weight proteins into the filtrate, a condition called proteinuria in human patients. Several disease genes with known function in the slit-diaphragm have been cloned. Nephrin is a transmembrane protein present in the slit diaphragm itself and is thought to contribute to the zipper-like extracellular structure between foot processes (Ruotsalainen *et al*., 1999). Podocin is a podocyte junction-associated protein (Roselli *et al*., 2002) that resembles stomatin proteins which play a role in regulating mechanosensitive ion channels (Tavernarakis and Driscoll, 1997).

Electron microscopy of the zebrafish pronephric glomerulus reveals that, like mammalian podocytes, zebrafish podocytes form slit diaphragms between their foot processes (Fig. 7D). Zebrafish homologs of *podocin* and *nephrin* are specifically expressed in podocytes as early as 24 hpf (Fig. 7E and F) and have been shown to be required for proper slit-diaphragm formation in pronephric podocytes (Kramer-Zucker *et al*., 2005b).

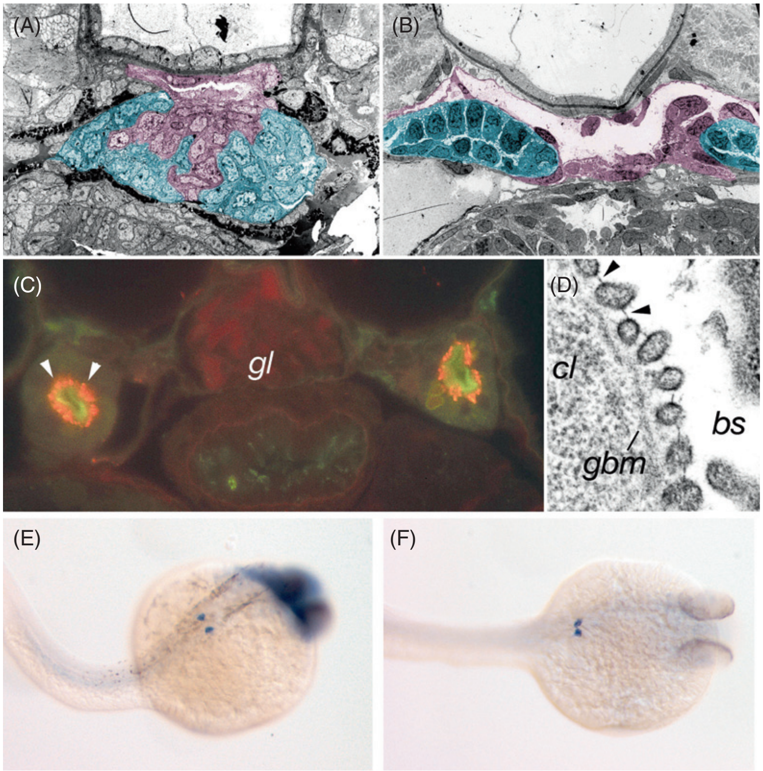

**Fig. 7** The glomerular capillary tuft and podocyte slit diaphragms. (A) An electron micrograph of the forming glomerulus at 2.5 dpf with invading endothelial cells from the dorsal aorta shaded in red and podocytes shaded in blue (image false-colored in Adobe Photoshop). (B) A similar stage glomerulus in the mutant island beat which lacks blood flow due to a mutation in an L-type cardiac-specific calcium channel. The endothelial cells and podocytes are present but the aorta has a dilated lumen surrounding the podocytes with no sign of glomerular remodeling and morphogenesis. (C) Rhodamine dextran filtration and uptake by pronephric epithelial cells. Lysine-fixable rhodamine dextran (10kDa) injected into the general circulation can be seen as red fluorescence in glomerular capillaries (gl), and filtered dye is seen in apical endosomes of pronephric tubule cells (arrowheads). Counterstain: FITC wheat germ agglutinin. (D) Electron micrograph of the glomerular basement membrane region in the glomerulus. Individual profiles of podocyte foot processes resting on the glomerular basement membrane (gbm) are connected by slit-diaphragms (arrowheads at top). cl, capillary lumen; bs, Bowman's space. Wholemount *in situ* hybridization shows expression of zebrafish podocin (E) and nephrin (F) specifically in the forming podocytes. (See Plate no. 9 in the Color Plate Section.)

Vascularization of the glomerulus occurs relatively late in development, after pronephric tubule development is complete (Armstrong, 1932; Drummond *et al*., 1998; Tytler, 1988). The bilateral glomerular primordia coalesce at 36–40 hpf ventral to the notochord, bringing the presumptive podocytes into contact with endothelial cells of the overlying dorsal aorta (Fig. 8) (Drummond, 2000; Drummond *et al*., 1998; Majumdar and Drummond, 1999). Podocytes express two known mediators of angiogenesis: *vascular endothelial growth factor* (*vegf*) and *angiopoietin2* (Carmeliet *et al*., 1996; Ferrara *et al*., 1996; Majumdar and Drummond, 1999, 2000; Pham *et al*., 2001; Shalaby *et al*., 1995). In a complementary manner, capillary-forming endothelial cells express *kdrl* (aka *flk1*), a VEGF receptor (Majumdar and Drummond, 1999). Between 40 and 48 hpf, kdrl-positive endothelial cells invade the glomerular epithelium and become surrounded by podocytes (Fig. 8) (Drummond *et al*., 1998). Vascular shear force is required to drive capillary formation as mutants lacking cardiac function, such as silent heart/cardiac troponin T and island beat/L-type cardiac calcium channel, fail to form a proper glomerular capillary tuft (Fig. 7A and B) (Rottbauer *et al*., 2001; Sehnert *et al*., 2002). Glomerular filtration begins around 48 hpf but is leaky at this time, allowing large molecular weight dextrans to pass into the tubules. Full maturation and size-selectivity occur at 4 days post-fertilization (dpf), concomitant with well-developed podocyte foot processes and endothelial cell fenestrations (Kramer-Zucker *et al*., 2005b).

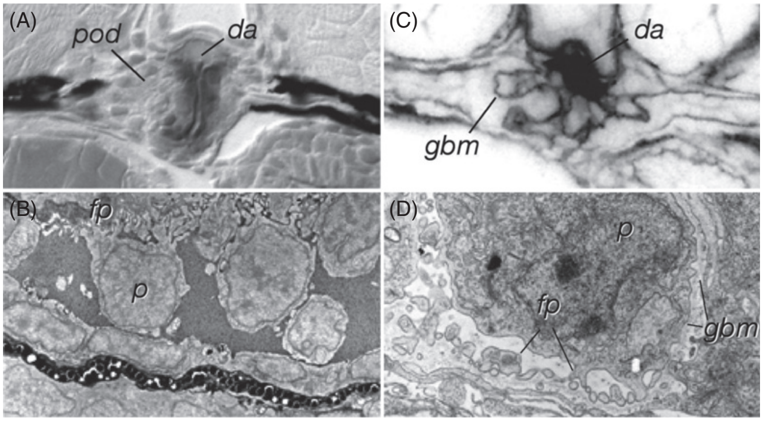

**Fig. 8** Interaction of pronephric podocytes with the vasculature. (A) Apposition of nephron primordia at the embryo midline in a 40 hpf zebrafish embryo. Aortic endothelial cells in the cleft separating the nephron primordia are visualized by endogenous alkaline phosphatase activity. Podocytes, pod; dorsal aorta, da. (B) Ultrastructure of the forming zebrafish glomerulus at 40 hpf. A longitudinal section shows podocytes (p) extending foot processes (fp) in a dorsal direction and in close contact with overlying capillary endothelial cells. (C) Rhodamine dextran (10,000 Dalton MW) injected embryos show dye in the dorsal aorta (da) and in the glomerular basement membrane (gbm) shown here graphically inverted from the original fluorescent image. (D) Podocyte foot process formation does not require signals from endothelial cells as evidenced by the appearance of foot processes (fp) in cloche mutant embryos which lack all vascular structures. Glomerular basement membrane, gbm; podocyte cell body, p.

### H. Formation of the Cloaca

Formation of the caudal pronephric opening or cloaca requires BMP signaling (Pyati *et al.*, 2006). The ligand involved here appears to be BMP4 since mutants lacking functional BMP4 exhibit failure to complete the fusion of the pronephric ducts with the epidermis and an absence of a pronephric opening (Stickney *et al.*, 2007), similar to the phenotype seen when a dominant negative BMP receptor is ectopically expressed late in development (Pyati *et al.*, 2006). These studies revealed that cloaca formation is likely to involve developmentally programmed cell death accompanied by cellular rearrangements within the terminus of the pronephric duct and the epidermis. Although zebrafish do not have a urinary bladder, the terminus of the pronephros may be homologous to the end of the common nephric duct in mammals which inserts into the bladder by a mechanism involving programmed cell death (Batourina *et al.*, 2005).

## IV. Methods to Study Pronephros Function

### A. Embryo Dissociation

Historically, the functional aspects of kidney epithelial ion transport have been studied using isolated single epithelial tubules in primary culture. This has not yet been achieved for zebrafish pronephric tubules. However, a useful first step in considering such an approach is larval tissue fractionation and tubule isolation (Fig. 9). Two to three day old zebrafish larvae show a remarkable resistance to collagenase digestion. However, a 1 h preincubation in dithiothreitol (DTT) or *N*-acetyl-cysteine, which degrade the protective mucous layer around the embryo, allows subsequent incubation in collagenase to be effective.

1. Anesthetize 2–3 day old larvae with 0.2% Tricaine.
2. Incubate larvae in 10 mM DTT or *N*-acetyl-cysteine in egg water for 1 h at room temperature.

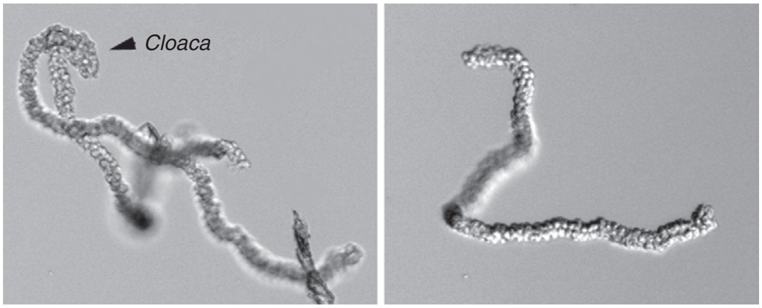

**Fig. 9** Isolated pronephric tubules. Two day old larvae were treated with 10 mM DTT followed by incubation in 5 mg/ml collagenase for 3 h at 28°C. Individual pronephric nephrons can be dissected away from trunk tissue, often with the cloaca intact (arrowhead), joining the bilateral tubules at the distal segment.

3. Wash the larvae 3–4 times with egg water to remove the DTT.
4. Incubate larvae at 28.5°C in 5 mg/ml collagenase in tissue culture medium or Hanks saline with calcium (Worthington) for 3–6 h.
5. Triturate the larvae gently 5 times with a "blue tip" 1000 µl pipet tip. The larvae should disaggregate into chunks of tissue.
6. Disperse the cell/tissue suspension into a 10 cm petri dish containing 10 ml of tissue culture medium or Hanks buffer.
7. Collect pronephric tubules by visual identification under a dissecting microscope.

## B. Isolation of Fluorescently Labeled Cells by Fluorescence Activated Cell Sorting (FACS)

The isolation of specific cells from transgenic embryos on the basis of fluorescent marker expression has numerous applications, including purification of cells for transplantation, preparation of cDNA libraries, and quantification of cell types in mutant or morpholino "knockdown" embryos.

1. Collect and dechorinate (if necessary) both transgenic embryos and non-transgenic controls and anesthetize with 0.2% Tricaine.
2. Transfer embryos to 1.5 ml microfuge tubes (no more than a 500 µl packed volume of embryos per tube) and wash 3 times with FACS buffer (0.9× phosphate buffered saline (PBS) + 5% fetal calf serum).
3. Homogenize the embryos with a microfuge pestle.
4. Spin down the cells for 3 min at 1500 g in a microcentrifuge.
5. Resuspend the cells in 500 ml FACS buffer.
6. Repeat the spinning and resuspending steps an additional 3 times.
7. Filter the cells by pipetting them through a 40 mm nylon cell strainer (Falcon 2340) into a 5 ml round-bottom tube (Falcon 2054) on ice.
8. Add propidium iodide (PI) to a final concentration of 1 µg/ml (to stain dead cells).
9. FACS the control non-transgenic cells on the basis of PI exclusion and reporter gene fluorescence (e.g., green fluorescence protein) in order to be able to set the gate for the transgenic sample. Repeat for the transgenic cells.
10. Collect positive cells in 500 ml of FACS buffer.

Note: A single sort usually gives only 70–80% purity. For ~95% purity it is recommended that the cells be double sorted. If RNA is to be collected from the cells then pellet the cells at 12,000 ***g*** in a microcentrifuge for 15 min and resuspend in a small volume of extraction buffer (e.g., Trizol).

## C. A Simple Assay for Glomerular Filtration

Filtration of blood by the glomerulus can be detected by injections of fluorescent compounds (10–70 kDa rhodamine dextran) into the general circulation and then monitoring the appearance of fluorescent endosomes in the apical cytoplasm of pronephric tubule cells (Fig. 7C) (Drummond *et al.*, 1998; Majumdar and Drummond, 2000). The ability to detect filtered dextrans in endocytic vesicles of the tubules has also been adapted to create an assay for disruption of the filtration barrier (i.e., proteinuria or nephrotic syndrome). Kramer-Zucker *et al*. demonstrated that large dextrans (500 kDa) do not significantly pass a normal glomerular filter while in embryos where orthologs of human nephrotic syndrome genes have been knocked down, passage of large dextrans could be observed as accumulation in tubule endocytic vesicles (Kramer-Zucker *et al*., 2005b). Filtered fluorescent dextrans can also be observed directly as they exit the pronephros at the cloaca in live larvae and used as a qualitative assay of the rate of pronephric fluid output (Kramer-Zucker *et al*., 2005a).

1. Embryos:

   1. Anesthetize 84 hpf embryos in 0.2% Tricaine and position them ventral side up in a 1% agarose injection mold. The age of the embryo is critical for this assay since younger embryos have leaky glomeruli (Kramer-Zucker, *et al*., 2005b).
   2. Using a microinjection device (e.g., Nanoject II from Drummond Scientific, Broomall, PA) fitted with a pulled glass capillary needle inject 5 nl of fluorescently labeled dextran (40 mg/ml in 150 mM NaCl; Invitrogen) into the cardiac venous sinus or alternatively into the cardinal vein in the posterior trunk (Fig. 10).
   3. Return embryo to egg water to recover.
   4. Uptake of the 40 kDa dextran by the PCT occurs within 24 hpf and can be imaged in live embryos. To detect the 500 kDa dextran it is necessary to fix and section the embryos (see Section IV-H) at the level of the PCT. If the glomerulus is leaky, fluorescent endosomes can be visualized in endocytic vesicles of PCT epithelial cells (similar to Fig. 7C).

2. Adults:

   1. Anesthetize an adult fish in 0.2% Tricaine.
   2. Lay the fish on its back on a wet tissue or paper towel.

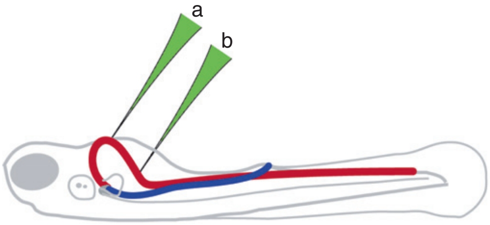

**Fig. 10** Assaying glomerular filtration by injection of labeled dextrans. The diagram shows a zebrafish larva positioned dorsal side down, exposing the sinus venosus/inflow tract of the heart circulation. Vasculature is depicted in red; the pronephros is in blue. (A) Sinus venosus injections are feasible in 2–3 dpf embryos. (B) By 3.5 dpf the inflow tract is shifted forward, making it necessary to inject dye in the descending cardinal vein. (See Plate no. 10 in the Color Plate Section.)

3. Using a 0.5 cc insulin syringe, inject 20 µl of 40 kDa fluorescein-labeled dextran (40 mg/ml; Invitrogen) into the intraperitoneal space by carefully inserting the needle into the abdomen at the ventral midline. Insert the needle at a shallow angle to avoid injecting the gut. Once through the skin, pull the needle slightly away from the fish to "tent" the skin and create a void space to inject into. The entire abdomen of the fish should swell as the dextran is injected.
4. Return fish to the tank to recover. Uptake of the dextran by the proximal tubule occurs within a few hours and persists for several days.

## D. Gentamicin Induced Kidney Tubule Injury in Embryos and Adults

Zebrafish and other teleosts have a remarkable capacity for kidney regeneration. Gentamicin is an antibiotic that in high enough doses induces necrosis of proximal tubule epithelial cells. Kidney damage in this model is repaired by the formation of new nephrons.

### 1. Embryos:

1. Dechorinate 50–55 hpf embryos and anesthetize in 0.2% Tricaine and positioned on their back in a 1% agarose injection mold.
2. Using a microinjection device (e.g. Nanoject II from Drummond Scientific, Broomall, PA) fitted with a pulled glass capillary needle inject 5 nl of gentamicin (5 mg/ml in 150 mM NaCl; Sigma) into the cardiac venous sinus or alternatively into the cardinal vein in the posterior trunk (Fig. 10).
3. Return embryo to egg water to recover. Marked pericardial and intracranial edema caused by a failure to osmoregulate will be apparent between 72 and 96 hpf. Histologically the PCT segment shows lysosomal phospholipidosis, flattening of the brush border, an accumulation of cellular debris in the lumen, and distention (Hentschel *et al*., 2005).

Note: If necessary, phenol red (0.25%) can be added to the gentamicin to positively identify successfully injected embryos.

### 2. Adults:

1. Anesthetize an adult fish in 0.2% Tricaine.
2. Lay the fish on its back on a wet tissue or paper towel.
3. Using a 0.5 cc insulin syringe, inject 20 µl of gentamicin (5 mg/ml) into the intraperitoneal space by carefully inserting the needle into the abdomen at the ventral midline. Insert the needle at a shallow angle to avoid injecting the gut. Once through the skin, pull the needle slightly away from the fish to "tent" the skin and create a void space to inject into. The entire abdomen of the fish should swell as the gentamicin is injected.
4. Return fish to the tank to recover. Necrosis of the proximal tubule occurs within 24 h.

Note: Expect 5–10% mortality. Do not feed the fish for 24 h to increase the survival rate.

## E. Adult Kidney Isolation

The adult (mesonephric or opisthonephric) kidney is located along the dorsal wall of the body cavity and can be divided into head, trunk (or saddle), and tail portions going from anterior to posterior (Fig. 11A). Two major collecting ducts run the length of the kidney and drain hundreds of nephrons. As in the pronephros, the mesonephric nephron is made up of a glomerulus, a neck segment, and two proximal and two distal tubule segments. The nephrons are branched predominantly at the DL segment, with occasional branching occurring at the DE segment.

1. Euthanize an adult fish by Tricaine overdose.
2. Using scissors, remove the head by cutting at the level of the gills (be careful to not cut beyond the posterior limit of the gill flap as the head kidney is located in this region).
3. Using scissors, make an excision along the ventral midline of the fish.
4. Carefully remove the gut and associated organs (liver, pancreas, etc.), gonads (testes or ovaries), and swim bladder using forceps. The kidney appears as a thin reddish organ with black melanocytes and is located along the dorsal side of the body wall.
5. Using forceps, score alongside each side of the kidney to sever the blood vessels entering the kidney and also to rupture a thin translucent membrane covering the kidney.
6. Starting at the head kidney, gently prize the tissue off the body wall. Although the kidney tissue has a gelatinous consistency it is possible to remove it intact. At the caudal end, use forceps to sever the relatively tough collecting ducts (these fuse at a urinary sinus near the cloaca).

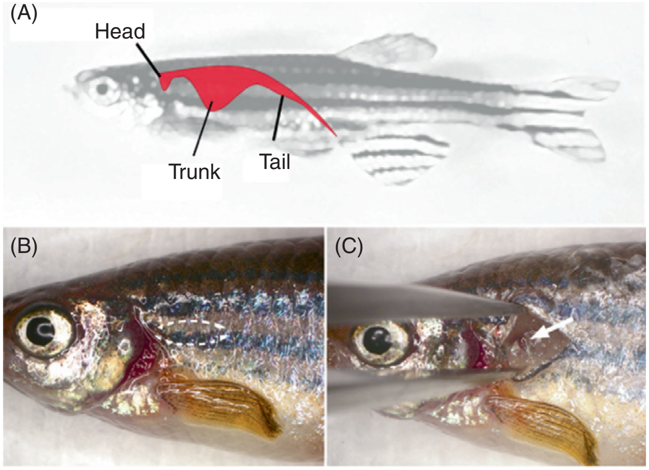

**Fig. 11** The adult (mesonephric or opisthonephric) kidney. (A) The adult kidney is located along the dorsal wall of the body cavity and can be divided into head, trunk (or saddle), and tail portions going from anterior to posterior. (B) The head kidney can be accessed surgically by making an incision in the upper part of the middle blue stripe near the gills (dotted region) and appears as a red mass (C; arrow).

## F. Non-Lethal Surgical Access to the Adult Kidney

Despite being located deep in the body cavity, the kidney can be non-lethally accessed. The head kidney, due to its lobular shape and anatomical position, can be exposed by a small lateral excision in the side of the fish.

1. Anesthetize an adult fish in 0.2% Tricaine.
2. Using forceps, remove the scales in the region just posterior to the gill flap.
3. Using a scalpel, make a 1–2mm cut level with the top of the middle blue stripe (see Fig. 11B). Initially make a shallow cut.
4. Use forceps to open the incision and cut progressively deeper until the dark red head kidney and underlying silver pigment (lining the anterior body cavity) are visible. Cells or dyes can be injected into the kidney using a fine gauge Hamilton syringe or glass needle.
5. Provided the excision is small, a suture is not needed to keep the wound closed and the fish can be returned to the tank to recover.

## G. Detecting and Imaging Zebrafish Cilia

Zebrafish are ideally suited for analysis of genes required for ciliogenesis and cilia function. Pronephric cilia have a "9 + 2" microtubule doublet organization and dynein arms characteristic of motile cilia and flagella and consistent with their proposed function in propelling fluid down the tubules (Kramer-Zucker *et al*., 2005a; Liu *et al*., 2007; Pathak *et al*., 2007). Cilia can be visualized using the anti-acetylated tubulin monoclonal antibody 6-11-B1 (Sigma T6793) as well as anti-gamma tubulin (GTU-88) and anti-polyglutamyl tubulin (B3).

| | | |
|---|---|---|
| Anti-acetylated tubulin (clone 6-11b-1) | Sigma | T6793 |
| Anti-polyglutamylated tubulin (clone B3) | Sigma | T9982 |
| Anti-gamma-tubulin (clone GTU-88) | Sigma | T6657 |

The protocol that follows is designed for use of these antibodies but can be adapted for other antibodies and other fixation methods.

### 1. Materials

PBS
DMSO
Tween 20
Normal goat serum (Sigma G9023)
Bovine serum albumin (BSA; Sigma A8022) or gelatin from cold water fish skin (Sigma G7765)
Methanol
Benzyl alcohol

Glycerol
*N*-propyl gallate
Formaldehyde
Hydrogen peroxide
SDS

## 2. Solutions

| | |
|---|---|
| PBST: | PBS + 0.5% tween20 |
| Blocking solution: | PBS with<br>1% DMSO<br>0.5% Tween20<br>1% BSA or 0.3% gelatin from cold water fish skin<br>10% normal goat serum |
| Incubation solution: | PBS with<br>1% DMSO<br>0.5% Tween20<br>2% normal goat serum |
| High-salt wash: | PBS with<br>1% DMSO<br>0.5% Tween20<br>2% normal goat serum<br>0.18% NaCl (final NaCl = 0.27%) |
| Dent's fixative: | 80% methanol<br>20% DMSO |
| Formaldehyde (BT) fix | 4% formaldehyde (from paraformaldehyde)<br>0.1 M phosphate buffer, pH 7.2<br>3% sucrose<br>0.12 mM $CaCl_2$ |
| Rehydration solutions:<br>75:25 MeOH/PBST<br>50:50 MeOH/PBST<br>25:75 MeO/PBST | |
| Antigen retrieval solution: | 1% SDS in PBS |
| Mounting medium: | 53% benzyl alcohol (by weight)<br>45% glycerol (by weight)<br>2% *N*-propyl gallate |

## 3. Methods

One of the main advantages of using zebrafish immunofluorescence is the transparency of their embryos. To achieve maximum embryo transparency, development of pigmentation can be blocked by raising embryos in 0.003% phenylthiourea (PTU) egg water. Alternatively embryos can be bleached with hydrogen peroxide after fixation (see below).

## 4. Fixation

1. Fix embryos in Dent's fixative for 3 h to overnight at room temperature. If necessary, remove pigment by bleaching fixed embryos overnight in 10% $H_2O_2$. After fixation embryos can be stored in 100% methanol at −20°C.
2. Rehydrate Dent's fixed embryos with graded changes of methanol/PBT:

   75:25 MeOH/PBT 15 min
   50:50 MeOH/PBT 15 min
   25:75 MeOH/PBT 15 min
   PBT

   Dent's fixative works well for antibodies that preferentially recognize denatured epitopes. If formaldehyde fixation is preferable, antigen retrieval can be performed by denaturing the embryos after formaldehyde fixation. For formaldehyde fixation fix 2 h to overnight at 4°C in BT fix and then wash twice in PBS. Permeabilize the embryos in cold acetone for 20 min at −20°C. Warm to room temperature and wash with PBS. For antigen retrieval (denaturation), incubate fixed embryos in 1% SDS/PBS for 15 min at room temperature followed by washing with PBS 4×5 min each.

## 5. Antibody Staining

3. Block non-specific binding by incubating fixed embryos for 2 h to overnight in Blocking solution. Incubations are done in eppendorf tubes at 4°C on a nutator rocking platform.
4. Incubate with primary antibody (6-11-B1 at 1:1000) in incubation solution overnight at 4°C. Monoclonal supernatants can be used at 1:50 to 1:25 dilution. Be aware that any primary antibody raised in rabbits should be affinity purified on antigen to avoid high background staining of larval fish skin. If necessary to economize on primary antibodies the incubation can be done in 50–100 µl without agitation.
5. After incubation with primary antibody, wash at least 4 × 30 min with incubation solution. Normal goat serum (2%) is included in all steps to reduce background. If background staining becomes a problem, the first wash after incubation with primary antibody can employ the "high-salt" wash. Subsequent washes are in the standard incubation solution.
6. Incubate with secondary antibody in incubation solution overnight. Alexa anti-mouse secondary antibodies (Invitrogen) work well at 1:1000 dilution. Following incubation, wash at least 4×30 min with incubation solution on a rocking platform. Although background staining with secondary antibodies is not common, a high-salt wash can be used to minimize non-specific staining.

### 6. Mounting the Sample for Confocal Microscopy

To minimize optical distortion caused by mismatch in refractive index of the sample, coverslips, and immersion oil, use a mounting medium that has the same refractive index (1.513) as the immersion oil. We make a mounting medium developed by Gustafsson *et al.* (1999) that is a mixture of glycerol and benzyl alcohol and contains an antifade compound (*N*-propyl gallate) that is essential for preventing signal bleaching, especially when using 488 nM fluorophores (fluroescein (FITC), Alexa 488) on large Z image stacks.

7. Embryos can be placed in mounting medium directly after washing. The difference in the density of the mounting medium and PBS is significant and causes turbulence but does not damage the sample. It is best to transfer embryos to mounting medium in a depression slide or directly on a microscope slide since the embryos become essentially invisible and can be hard to find in an eppendorf tube. Change to fresh mounting medium and transfer embryos to a standard microscope slide. Using small balls of modeling clay, support the edges of a coverslip to provide space for the embryo and coverslip the sample. Alternatively, make a coverslip bridge with additional coverslips as spacers. The orientation of the embryo can often be shifted by moving the coverslip. This sample configuration is suited for viewing with an upright microscope using a 63× oil immersion objective.

### 7. Alternate Protocols

**a. Visualization of Cilia with HRP/DAB** If visualization of cilia by light microscopy is desired, a horseradish peroxidase (HRP)-coupled secondary antibody can be used. To visualize HRP after washing out the secondary antibody:

1. Wash once in PBSBT (PBS/0.1% tween/0.2% BSA) for 5 min.
2. Incubate with 0.3 mg/ml Diamion Benzidine (DAB) and 0.5% $NiCl_2$ in PBSBT for 20 min.
3. Add $H_2O_2$ to 0.03% (1:1000 dilution of 30% stock) and monitor color development (check at 10 min).
4. Stop the reaction by rinsing in PBST and then PBS. Post fix in 2% formaldehyde/ 0.1% glutaraldehyde.

## H. Histological Sectioning of Whole mount Stained Embryos

Fluorescent signal from secondary antibodies is preserved in glycol methacrylate (JB4) embedded samples. This allows for histological sectioning of wholemount stained embryos and viewing 3–10 μm sections by standard wide-field epifluorescence. Longer wavelength excitation secondary antibodies, for instance Alexa 546 or rhodamine, should be used instead of FITC since fluorescein excitation wavelengths result in significant autofluorescence from the glycol methacrylate/JB4.

1. After the final wash following secondary antibody incubation, dehydrate embryos in sequential changes of 30, 50, 75, 85, and 95% ethanol.

2. Prepare catalyzed JB4 (Polysciences or Electron Microscopy Sciences) following the manufacturer's instructions. Dissolve 0.625 g powdered catalyst to 50 ml monomer solution A in a 50 ml tube. Wrap the tube in foil to protect it from light and store it at 4°C. The catalyzed JB4 making can be used for 1–2 weeks.
3. Remove final ethanol and add catalyzed JB4 solution to the dehydrated wholemount stained embryos. The embryos will float at the top of the solution and gradually sink as they become infiltrated. Leave at 4°C overnight.
4. Draw off the first solution of JB4 making sure to remove traces of ethanol that can inhibit hardening. Add the hardener (solution B) at 40 μl/ml to the embryos. Pour embryos in JB4 into a plastic mold, orient the embryos, and allow the JB4 to harden. Humidity and oxygen will inhibit hardening, so this step is best done in a sealed, desiccated chamber.
5. To embed embryos to cut them in cross section, first half fill a mold by pouring a bed of JB4 (0.7 ml) in the mold (15 mm × 15 mm) and let it harden. Then add stained embryos in final catalyzed JB4 plus hardener and orient them to be headed to the side of the mold. The "half blocks" of JB4 adhere well even if polymerized separately and this allows for rotating and mounting the final block to have embryos facing the knife for sectioning.
6. JB4 blocks require sectioning with glass knives. Use a Leica RM2255 or equivalent style microtome. JB-4 embedding kit and embedding molds can be purchased from Polysciences or Electron Microscopy Sciences (EMS).

## I. Electron Microscopy Methods for Zebrafish

Electron microscopy is a standard method required for assessing cellular structural defects. Electron microscopy on zebrafish is performed essentially the same as for other vertebrate tissues but with some alterations that accommodate the lower osmolarity of extracellular fluids in fish. Other modifications include use of tannic acid in the fixative to enhance contrast and use of partially reduced osmium that produces a less grainy final image.

### 1. Materials

(All available from Electron Microscopy Sciences)

Glutaraldehyde
Paraformaldehyde
Phosphate or cacodylate buffer
Sucrose
Tannic acid

### 2. Methods

1. Fix overnight at 4°C in

| | |
|---|---|
| 1.5% glutaraldehyde | 7.5 ml 10% stock |
| 1% paraformaldehyde | 3.125 ml 16% stock |

| | |
|---|---|
| 70 mM $NaPO_4$, pH 7.2 | 3.5 ml 1 M stock |
| 3% sucrose | 5 ml 30% stock |
| 0.1% tannic acid | 0.05 g |
| | Water to 50 ml |

EMS (Electron Microscopy Sciences) premade stocks can be used for the aldehydes; these come in sealed glass vials. Addition of tannic acid enhances the final contrast of the image, particularly of microtubules and other filamentous structures. Add the tannic acid just before fixation; it does not keep well. The buffer has a slightly lower osmolarity than a fixative for mammalian tissue.

2. Wash 3 × 5 min in 0.1 M cacodylate or phosphate buffer, pH 7.4.

   Avoid the use of mechanical rocking or mixing during the fixation and washes; the overall concern is to be as gentle as possible with the tissue to preserve structure.
3. Post fix in 1% $OsO_4$ plus potassium ferrocyanide for 1 h on ice:

   1 ml 4% $OsO_4$
   3 ml $H_2O$
   0.06 g potassium ferrocyanide

   This is partially reduced osmium; it produces less grainy images. If desired the potassium ferrocyanide may be omitted.
4. Wash 2 × 10 min in 0.1 M cacodylate or phosphate buffer, pH 7.4.
5. En bloc stain fixed embryos in 1% uranyl acetate in 0.1 M cacodylate pH 7.4 for 1 h at room temperature.
6. Wash 3 × 10 min in 0.1 M cacodylate or phosphate buffer, pH 7.4.
7. Dehydrate in 25, 50, 70, 80, 95, and 100% EtOH for 20–30 min each.
8. Dehydrate with 2 × 100% EtOH 20–30 min each.
9. Infiltrate with propylene oxide for 15–20 min (in a fume hood).
10. Mix the Epon 812 (or substitute epoxy embedding medium) according to the manufacturer's instructions.
11. Infiltrate with

| | |
|---|---|
| 25% | 30 min (25% Epon in propylene oxide) |
| 50% | 40 min |
| 75% | Overnight |
| 100% | 4 h |
| 100% | 1 h |

12. Embed embryos in fresh Epon in flat molds. Position embryo swimming toward the tip of the block for acquiring cross sections.
13. Harden at 60°C for 16 h.

The blocks are now ready for sectioning and staining. We use formvar-coated slot grids (Electron Microscopy Sciences; catalog # FF2010-Cu) to maximize visibility of the tissue in the sections.

## V. Conclusions

The zebrafish pronephric kidney represents one of the many vertebrate kidney forms that have evolved to solve the problem of blood fluid and electrolyte homeostasis in an osmotically challenging environment. Despite differences in organ morphology between the mammalian and teleost kidneys, many parallels exist at the cellular and molecular levels that can be exploited to further our understanding of kidney cell specification, epithelial tubule formation, and the tissue interactions that drive nephrogenesis. The same genes (for instance *pax*2) and cell types (for instance podocytes, endothelial cells, and tubular epithelial cells) are employed in the development and function of fish, frog, chicken, and mammalian kidneys. Genes mutated in human disease are also essential for the formation and function of the zebrafish pronephros. The zebrafish thus presents a useful and relevant model of vertebrate kidney development: its principal strengths lie in the ease with which it can be genetically manipulated and phenotyped so as to rapidly determine the function of genes and cell–cell interactions that underlie the development of all kidney forms.

### Acknowledgments

IAD was supported by NIH grants DK53093, DK071041, and DK070263 and by grants from the PKD foundation. AJD was supported by the NIH grant DK077186 and grants from the Harvard Stem Cell Institute, American Society of Nephrology, and the Cystinosis Research Foundation.

### References

Agarwal, S., and John, P. A. (1988). Studies on the development of the kidney of the guppy, Lebistes reticulatus. Part 1. The development of the pronephros. *J. Anim. Morphol. Physiol.* **35**, 17–24.

Amacher, S. L., Draper, B. W., Summers, B. R., Kimmel, C. B., (2002). The zebrafish T-box genes no tail and spadetail are required for development of trunk and tail mesoderm and medial floor plate. *Development*. **129**, 3311–3323.

Anzenberger, U., Bit-Avragim, N., Rohr, S., Rudolph, F., Dehmel, B., Willnow, T. E., and Abdelilah-Seyfried, S. (2006). Elucidation of megalin/LRP2-dependent endocytic transport processes in the larval zebrafish pronephros. *J. Cell Sci.* **119**, 2127–2137.

Armstrong, P. B. (1932). The embryonic origin of function in the pronephros through differentiation and parenchyma–vascular association. *Am. J. Anat.* **51**, 157–188.

Balfour, F. M. (1880). “A Treatise on Comparative Embryology”. Macmillan and Co., London.

Batourina, E., Tsai, S., Lambert, S., Sprenkle, P., Viana, R., Dutta, S., Hensle, T., Wang, F., Niederreither, K., McMahon, A. P., Carroll, T. J., and Mendelsohn, C. L. (2005). Apoptosis induced by vitamin A signaling is crucial for connecting the ureters to the bladder. *Nat. Genet.* **37**, 1082–1089.

Bollig, F., Perner, B., Besenbeck, B., Kothe, S., Ebert, C., Taudien, S., and Englert, C. (2009). A highly conserved retinoic acid responsive element controls wt1a expression in the zebrafish pronephros. *Development* **136**, 2883–2892.

Carmeliet, P., Ferreira, V., Breier, G., Pollefeyt, S., Kieckens, L., Gertsenstein, M., Fahrig, M., Vandenhoeck, A., Harpal, K., Eberhardt, C., Declercq, C., Pawling, J., *et al.* (1996). Abnormal blood vessel development and lethality in embryos lacking a single VEGF allele. *Nature* **380**, 435–439.

Carroll, T. J., Wallingford, J. B., and Vize, P. D. (1999). Dynamic patterns of gene expression in the developing pronephros of *Xenopus laevis*. *Dev. Genet.* **24**, 199–207.

Dantzler, W. H. (2003). Regulation of renal proximal and distal tubule transport: sodium, chloride and organic anions. *Comp. Biochem. Physiol. A Mol. Integr. Physiol.* **136**, 453–478.

Davidson, A. J., Ernst, P., Wang, Y., Dekens, M. P., Kingsley, P. D., Palis, J., Korsmeyer, S. J., Daley, G. Q., Zon, L. I., (2003). cdx4 mutants fail to specify blood progenitors and can be rescued by multiple hox genes. *Nature*. **425**, 300–306.

Drummond, I. A. (2000). The zebrafish pronephros: a genetic system for studies of kidney development. *Pediatr. Nephrol.* **14**, 428–435.

Drummond, I. A., Majumdar, A., Hentschel, H., Elger, M., Solnica-Krezel, L., Schier, A. F., Neuhauss, S. C., Stemple, D. L., Zwartkruis, F., Rangini, Z., Driever, W., and Fishman, M. C. (1998). Early development of the zebrafish pronephros and analysis of mutations affecting pronephric function. *Development* **125**, 4655–4667.

Elizondo, M. R., Arduini, B. L., Paulsen, J., MacDonald, E. L., Sabel, J. L., Henion, P. D., Cornell, R. A., and Parichy, D. M. (2005). Defective skeletogenesis with kidney stone formation in dwarf zebrafish mutant for trpm7. *Curr. Biol.* **15**, 667–671.

Ferrara, N., Carver-Moore, K., Chen, H., Dowd, M., Lu, L., O'Shea, K. S., Powell-Braxton, L., Hillan, K. J., and Moore, M. W. (1996). Heterozygous embryonic lethality induced by targeted inactivation of the VEGF gene. *Nature* **380**, 439–442.

Goodrich, E. S. (1930). "Studies on the Structure and Development of Vertebrates". Macmillan, London.

Guggino, W. B., Oberleithner, H., and Giebisch, G. (1988). The amphibian diluting segment. *Am. J. Physiol.* **254**, F615–F627.

Gustafsson, M. G., Agard, D. A., and Sedat, J. W. (1999). I5M: 3D widefield light microscopy with better than 100 nm axial resolution. *J. Microsc.* **195**, 10–16.

Hammerschmidt, M., Pelegri, F., Mullins, M. C., Kane, D. A., van Eeden, F. J., Granato, M., Brand, M., Furutani-Seiki, M., Haffter, P., Heisenberg, C. P., Jiang, Y. J., Kelsh, R. N., et al., (1996b). dino and mercedes, two genes regulating dorsal development in the zebrafish embryo. *Development*. **123**, 95–102.

Heller, N., and Brandli, A. W. (1999). Xenopus Pax-2/5/8 orthologues: novel insights into Pax gene evolution and identification of Pax-8 as the earliest marker for otic and pronephric cell lineages. *Dev. Genet.* **24**, 208–19.

Hentschel, H., and Elger, M. (1996). Functional morphology of the developing pronephric kidney of zebrafish. *J. Am. Soc. Nephrol.* **7**, 1598.

Hentschel, D. M., Park, K. M., Cilenti, L., Zervos, A. S., Drummond, I., and Bonventre, J. V. (2005). Acute renal failure in zebrafish: a novel system to study a complex disease. *Am. J. Physiol. Renal Physiol.* **288**, F923–F929.

Hild, M., Dick, A., Rauch, G. J., Meier, A., Bouwmeester, T., Haffter, P., Hammerschmidt, M., (1999). The smad5 mutation somitabun blocks Bmp2b signaling during early dorsoventral patterning of the zebrafish embryo. *Development*. **126**, 2149–2159.

Horsfield, J., Ramachandran, A., Reuter, K., LaVallie, E., Collins-Racie, L., Crosier, K., and Crosier, P. (2002). Cadherin-17 is required to maintain pronephric duct integrity during zebrafish development. *Mech. Dev.* **115**, 15–26.

Howland, R. B. (1921). Experiments on the effect of the removal of the pronephros of Ambystoma punctatum. *J. Exp. Zool.* **32**, 355–384.

Igarashi, P., Vanden Heuvel, G. B., Payne, J. A., and Forbush, B. III. (1995). Cloning, embryonic expression, and alternative splicing of a murine kidney-specific Na–K–Cl cotransporter. *Am. J. Physiol.* **269**, F405–F418.

Kamunde, C. N., and Kisia, S. M. (1994). Fine structure of the nephron in the euryhaline teleost, *Oreochromis niloticus*. *Acta Biol. Hung.* **45**, 111–121.

Kimmel, C. B., Warga, R. M., and Schilling, T. F. (1990). Origin and organization of the zebrafish fate map. *Development* **108**, 581–594.

Kishimoto, Y., Lee, K. H., Zon, L., Hammerschmidt, M., Schulte-Merker, S., (1997). The molecular nature of zebrafish swirl: BMP2 function is essential during early dorsoventral patterning. *Development*. **124**, 4457–4466.

Kramer-Zucker, A. G., Olale, F., Haycraft, C. J., Yoder, B. K., Schier, A. F., and Drummond, I. A. (2005a). Cilia-driven fluid flow in the zebrafish pronephros, brain and Kupffer's vesicle is required for normal organogenesis. *Development* **132**, 1907–1921.

Kramer-Zucker, A. G., Wiessner, S., Jensen, A. M., and Drummond, I. A. (2005b). Organization of the pronephric filtration apparatus in zebrafish requires Nephrin, Podocin and the FERM domain protein Mosaic eyes. *Dev. Biol.* **285**, 316–329.

Krauss, S., Johansen, T., Korzh, V., and Fjose, A. (1991). Expression of the zebrafish paired box gene pax[zf-b] during early neurogenesis. *Development* **113**, 1193–1206.

Liu, Y., Pathak, N., Kramer-Zucker, A., and Drummond, I. A. (2007). Notch signaling controls the differentiation of transporting epithelia and multiciliated cells in the zebrafish pronephros. *Development* **134**, 1111–1122.

Majumdar, A., and Drummond, I. A. (1999). Podocyte differentiation in the absence of endothelial cells as revealed in the zebrafish avascular mutant, cloche [In Process Citation]. *Dev. Genet.* **24**, 220–229.

Majumdar, A., and Drummond, I. A. (2000). The zebrafish floating head mutant demonstrates podocytes play an important role in directing glomerular differentiation. *Dev. Biol.* **222**, 147–157.

Majumdar, A., Lun, K., Brand, M., and Drummond, I. A. (2000). Zebrafish no isthmus reveals a role for pax2.1 in tubule differentiation and patterning events in the pronephric primordia. *Development* **127**, 2089–2098.

Marshall, E. K., and Smith, H. W. (1930). The glomerular development of the vertebrate kidney in relation to habitat. *Biol. Bull.* **59**, 135–153.

Mastroianni, N., De Fusco, M., Zollo, M., Arrigo, G., Zuffardi, O., Bettinelli, A., Ballabio, A., and Casari, G. (1996). Molecular cloning, expression pattern, and chromosomal localization of the human Na–Cl thiazide-sensitive cotransporter (SLC12A3). *Genomics* **35**, 486–493.

Mauch, T. J., Yang, G., Wright, M., Smith, D., and Schoenwolf, G. C. (2000). Signals from trunk paraxial mesoderm induce pronephros formation in chick intermediate mesoderm. *Dev. Biol.* **220**, 62–75.

Mudumana, S. P., Hentschel, D., Liu, Y., Vasilyev, A., and Drummond, I. A. (2008). odd skipped related1 reveals a novel role for endoderm in regulating kidney versus vascular cell fate. *Development* **135**, 3355–3367.

Mullins, M. C., Hammerschmidt, M., Kane, D. A., Odenthal, J., Brand, M., van Eeden, F. J., Furutani-Seiki, M., Granato, M., Haffter, P., Heisenberg, C. P., Jiang, Y. J., Kelsh, R. N., et al., (1996). Genes establishing dorsoventral pattern formation in the zebrafish embryo: the ventral specifying genes. *Development*. **123**, 81–93.

Newstead, J. D., and Ford, P. (1960). Studies on the development of the kidney of the Pacific Salmon, *Oncorhynchus forbuscha* (Walbaum). 1. The development of the pronephros. *Can. J. Zool.* **36**, 15–21.

Nguyen, V. H., Schmid, B., Trout, J., Connors, S. A., Ekker, M., Mullins, M. C. (1998). Ventral and lateral regions of the zebrafish gastrula, including the neural crest progenitors, are established by a bmp2b/swirl pathway of genes. *Dev. Biol*. **199**, 93–110.

Nichane, M., Van Campenhout, C., Pendeville, H., Voz, M. L., and Bellefroid, E. J. (2006). The $Na^+/PO^4$ cotransporter SLC20A1 gene labels distinct restricted subdomains of the developing pronephros in *Xenopus* and zebrafish embryos. *Gene Expr. Patterns* **6**, 667–672.

Pathak, N., Obara, T., Mangos, S., Liu, Y., and Drummond, I. A. (2007). The zebrafish fleer gene encodes an essential regulator of cilia tubulin polyglutamylation. *Mol. Biol. Cell* **18**, 4353–4364.

Perner, B., Englert, C., and Bollig, F. (2007). The Wilms tumor genes wt1a and wt1b control different steps during formation of the zebrafish pronephros. *Dev. Biol.* **309**, 87–96.

Perz-Edwards, A., Hardison, N. L., and Linney, E. (2001). Retinoic acid-mediated gene expression in transgenic reporter zebrafish. *Dev. Biol.* **229**, 89–101.

Pfeffer, P. L., Gerster, T., Lun, K., Brand, M., and Busslinger, M. (1998). Characterization of three novel members of the zebrafish Pax2/5/8 family: dependency of Pax5 and Pax8 expression on the Pax2.1 (noi) function. *Development* **125**, 3063–3074.

Pham, V. N., Roman, B. L., and Weinstein, B. M. (2001). Isolation and expression analysis of three zebrafish angiopoietin genes. *Dev. Dyn.* **221**, 470–474.

Puschel, A. W., Westerfield, M., and Dressler, G. R. (1992). Comparative analysis of Pax-2 protein distributions during neurulation in mice and zebrafish. *Mech. Dev.* **38**, 197–208.

Pyati, U. J., Cooper, M. S., Davidson, A. J., Nechiporuk, A., and Kimelman, D. (2006). Sustained Bmp signaling is essential for cloaca development in zebrafish. *Development* **133**, 2275–2284.

Reiser, J., Kriz, W., Kretzler, M., and Mundel, P. (2000). The glomerular slit diaphragm is a modified adherens junction. *J. Am. Soc. Nephrol.* **11**, 1–8.

Roselli, S., Gribouval, O., Boute, N., Sich, M., Benessy, F., Attie, T., Gubler, M. C., and Antignac, C. (2002). Podocin localizes in the kidney to the slit diaphragm area. *Am. J. Pathol.* **160**, 131–139.

Rottbauer, W., Baker, K., Wo, Z. G., Mohideen, M. A., Cantiello, H. F., and Fishman, M. C. (2001). Growth and function of the embryonic heart depend upon the cardiac-specific L-type calcium channel alpha1 subunit. *Dev. Cell* **1**, 265–275.

Ruotsalainen, V., Ljungberg, P., Wartiovaara, J., Lenkkeri, U., Kestila, M., Jalanko, H., Holmberg, C., and Tryggvason, K. (1999). Nephrin is specifically located at the slit diaphragm of glomerular podocytes. *Proc. Natl. Acad. Sci. U. S. A.* **96**, 7962–7967.

Saxén, L. (1987). “Organogenesis of the Kidney”. Cambridge University Press, New York.

Sehnert, A. J., Huq, A., Weinstein, B. M., Walker, C., Fishman, M., and Stainier, D. Y. (2002). Cardiac troponin T is essential in sarcomere assembly and cardiac contractility. *Nat. Genet.* **31**, 106–110.

Seldin, D. W., and Giebisch, G. H. (1992). “The Kidney: Physiology and Pathophysiology”. Raven Press, New York.

Serluca, F. C., and Fishman, M. C. (2001). Pre-pattern in the pronephric kidney field of zebrafish. *Development* **128**, 2233–2241.

Shalaby, F., Rossant, J., Yamaguchi, T. P., Gertsenstein, M., Wu, X. F., Breitman, M. L., and Schuh, A. C. (1995). Failure of blood-island formation and vasculogenesis in Flk-1-deficient mice. *Nature* **376**, 62–66.

Shmukler, B. E., Kurschat, C. E., Ackermann, G. E., Jiang, L., Zhou, Y., Barut, B., Stuart-Tilley, A. K., Zhao, J., Zon, L. I., Drummond, I. A., Vandorpe, D. H., Paw, B. H., *et al*. (2005). Zebrafish slc4a2/ae2 anion exchanger: cDNA cloning, mapping, functional characterization, and localization. *Am. J. Physiol. Renal Physiol.* **289**, F835–F849.

Simon, D. B., and Lifton, R. P. (1998). Ion transporter mutations in Gitelman’s and Bartter’s syndromes. *Curr. Opin. Nephrol. Hypertens.* **7**, 43–47.

Simon, D. B., Nelson-Williams, C., Bia, M. J., Ellison, D., Karet, F. E., Molina, A. M., Vaara, I., Iwata, F., Cushner, H. M., Koolen, M., Gainza, F. J., Gitleman, H. J., *et al*. (1996). Gitelman’s variant of Bartter’s syndrome, inherited hypokalaemic alkalosis, is caused by mutations in the thiazide-sensitive Na–Cl cotransporter. *Nat. Genet.* **12**, 24–30.

Sollner, C., Burghammer, M., Busch-Nentwich, E., Berger, J., Schwarz, H., Riekel, C., and Nicolson, T. (2003). Control of crystal size and lattice formation by starmaker in otolith biomineralization. *Science* **302**, 282–286.

Sprague, J., Bayraktaroglu, L., Bradford, Y., Conlin, T., Dunn, N., Fashena, D., Frazer, K., Haendel, M., Howe, D. G., Knight, J., Mani, P., Moxon, S. A., *et al*. (2008). The Zebrafish Information Network: the zebrafish model organism database provides expanded support for genotypes and phenotypes. *Nucleic Acids Res.* **36**, D768–D772.

Stickney, H. L., Imai, Y., Draper, B., Moens, C., and Talbot, W. S. (2007). Zebrafish bmp4 functions during late gastrulation to specify ventroposterior cell fates. *Dev. Biol.* **310**, 71–84.

Tavernarakis, N., and Driscoll, M. (1997). Molecular modeling of mechanotransduction in the nematode *Caenorhabditis* elegans. *Annu. Rev. Physiol.* **59**, 659–689.

Tytler, P. (1988). Morphology of the pronephros of the juvenile brown trout, *Salmo trutta*. *J. Morphol.* **195**, 189–204.

Tytler, P., Ireland, J., and Fitches, E. (1996). A study of the structure and function of the pronephros in the larvae of the turbot (*Scophthalmus maximus*) and the herring (*Clupea harengus*). *Mar. Fresh. Behav. Physiol.* **28**, 3–18.

Vaughan, M. R., Pippin, J. W., Griffin, S. V., Krofft, R., Fleet, M., Haseley, L., and Shankland, S. J. (2005). ATRA induces podocyte differentiation and alters nephrin and podocin expression *in vitro* and *in vivo*. *Kidney Int.* **68**, 133–144.

Vize, P. D., Seufert, D. W., Carroll, T. J., and Wallingford, J. B. (1997). Model systems for the study of kidney development: use of the pronephros in the analysis of organ induction and patterning. *Dev. Biol.* **188**, 189–204.

Vize, P. D., Woolf, A. S., and Bard, J. B. L. (2002). "The Kidney: From Normal Development to Congenital Diseases". Academic Press, Amsterdam and Boston.

Wingert, R. A., and Davidson, A. J. (2008). The zebrafish pronephros: a model to study nephron segmentation. *Kidney Int.* **73**, 1120–1127.

Wingert, R. A., Selleck, R., Yu, J., Song, H. D., Chen, Z., Song, A., Zhou, Y., Thisse, B., Thisse, C., McMahon, A. P., and Davidson, A. J. (2007). The cdx genes and retinoic acid control the positioning and segmentation of the zebrafish pronephros. *PLoS Genet.* **3**, 1922–1938.

# CHAPTER 10

# Molecular Regulation of Pancreas Development in Zebrafish

**Robin A. Kimmel** *and* **Dirk Meyer**
Institute of Molecular Biology, University of Innsbruck, A-6020 Innsbruck, Austria

Abstract
I. Introduction
II. Pancreas Development
  A. Morphogenesis
  B. Pancreas Specification
  C. Pancreas Cell Segregation into DB and VB
  D. Formation of the Dorsal Bud
  E. Beta-Cell Proliferation
III. Analysis of Beta-Cell Migration and Proliferation
  A. Time-Lapse Imaging of Beta-Cell Migration
  B. Pancreatic Beta-Cell Proliferation
IV. Future Directions
Acknowledgments
References

## Abstract

The pancreas is a vertebrate-specific organ of endodermal origin which is responsible for production of digestive enzymes and hormones involved in regulating glucose homeostasis, in particular insulin, deficiency of which results in diabetes. Basic research on the genetic and molecular pathways regulating pancreas formation and function has gained major importance for the development of regenerative medical approaches aimed at improving diabetes treatment. Among the different model organisms that are currently used to elucidate the basic pathways of pancreas development and regeneration, the zebrafish is distinguished by its unique opportunities to combine genetic and pharmacological approaches with sophisticated live-imaging methodology,

METHODS IN CELL BIOLOGY, VOL. 100
Copyright © 2010 Elsevier Inc. All rights reserved.

978-0-12-384892-5
DOI: 10.1016/B978-0-12-384892-5.00010-4

and by its ability to regenerate the pancreas within a short time. Here we review current perspectives and present methods for studying two important processes contributing to pancreas development and regeneration, namely cell migration via time-lapse micropscopy and cell proliferation via incorporation of nucleotide analog EdU, with a focus on the insulin-producing beta cells of the islet.

## I. Introduction

Pancreas from zebrafish and mammals show striking similarities in the molecular control of development, share cellular and subcellular architecture, and have a conserved physiological function. All of these criteria validate zebrafish as a relevant model for studying basic mechanisms of pancreas development and function. As in mammals, the zebrafish pancreas mostly consists of exocrine tissues, the acinar glands, that secrete inactive precursors of digestive enzymes (zymogens) into a branched intrapancreatic duct system. The intrapancreatic duct system transports these zymogens into the gut where they are activated by proteolytic cleavage. The endocrine hormones, including insulin, are produced in the pancreatic islets, which in mammals are termed islets of Langerhans. In fish and most mammals, these islets have a characteristic cellular architecture with a core of insulin-producing beta cells surrounded by a smaller number of up to four different cell types producing glucagon (alpha cells), somatostatin (delta cells), ghrelin (epsilon cells), and pancreatic polypeptide (PP cells). Islets are embedded in exocrine tissue and tightly connected to the vasculature through which they release endocrine hormones directly into the bloodstream.

Many adult tissues have the capacity to regenerate during a lifetime or after injury by proliferation of remaining cells, differentiation from multipotent precursor populations, or conversion from another mature cell type. From studies in rodents, there is evidence for all of these mechanisms contributing to homeostasis and response to injury in the pancreas, depending on the experimental manipulation and method of analysis. However, direct observation of transdifferentiation and migration to assemble into new islets is hampered by the inaccessibility of mouse embryos to direct observation during development. Studies in zebrafish have provided evidence for latent endocrine potential in cells of the pancreatic ductal system (Chung *et al*., 2010; Dong *et al*., 2007; Moro *et al*., 2009; Parsons *et al*., 2009) and emerging microscopic methods will enable close examination of regenerative processes.

## II. Pancreas Development

### A. Morphogenesis

In 2003, Field *et al.* (2003) showed that the zebrafish pancreas originates from two morphologically distinct endodermal structures that were initially termed posterior and anterior buds. In analogy to the dorsal and ventral pancreatic buds that build the pancreas

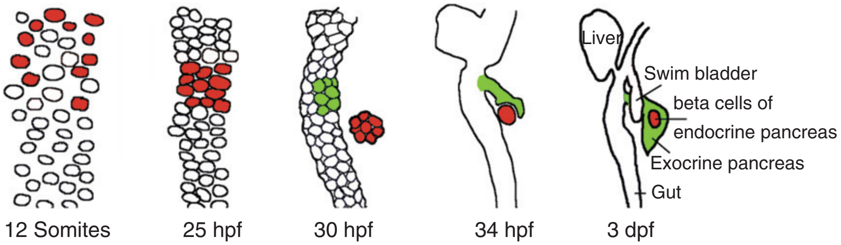

**Fig. 1** Zebrafish pancreas development. Dorsal bud endocrine precursors (dark gray) emerge within the endoderm during early somite stages. These cells cluster to form the islet at around 24 hpf, while the ventral bud (light gray) forms after 34 hpf, surrounds the islet, and expands to form the exocrine pancreas.

in amniotes, these terms later changed to dorsal bud (DB) and ventral bud (VB), even though the buds from zebrafish and amniotes have different cell morphological and differentiation properties. In particular, the earlier forming zebrafish DB is distinguished from its amniotic counterpart in that cells exclusively differentiate into endocrine cells. The DB becomes morphologically apparent at 24 hours post-fertilization (hpf) on the dorsal side of the gut where a first set of early forming endocrine cells assemble into the primary islet (Fig. 1). After 24 hpf the process of gut looping leads to displacement of the gut to the left side and of the DB islet to the right side of the embryo. The VB forms after 34 hpf from a population of gut cells positioned anterior to the islet. Between 34 and 48 hpf, VB cells migrate from the gut toward and later around the DB and thereby build a connection between the gut and the islet. Similar to the fate of both pancreatic buds in amniotes, the VB cells give rise to exocrine, duct, and late-forming endocrine cells (Field *et al*., 2003). Following cell-type specification, the exocrine (acinar) tissue expands posteriorly along the intestine and in parallel the intrapancreatic ductal system is established (Wan *et al*., 2006). After only 5 days, the zebrafish pancreas has a cellular composition and histology very similar to that of the adult mammalian pancreas (Pack *et al*., 1996; Parsons *et al*., 2009; Pauls *et al*., 2007; Yee *et al*., 2005). At this stage, the pancreas consists mainly of exocrine acinar tissue connected to the gut through a branching ductal system and a single islet with about 60 endocrine cells including about 35 insulin-producing beta cells. During postembryonic growth, the primary islet increases in size and additional smaller secondary islets form along the exocrine duct system (Parsons *et al*., 2009). In the adult animal, this expansion leads to the formation of several thousand beta cells distributed in a huge primary islet (diameter $> 240\,\mu m$) and several dozen secondary islets with diameters ranging from below $30\,\mu m$ to more than $100\,\mu m$ (Chen *et al*., 2007).

## B. Pancreas Specification

Over the past several years, enormous progress has been made in defining extrinsic and intrinsic factors that regulate pancreas formation starting with endodermal regionalization, through tissue specification, cell differentiation, and organ morphogenesis. At the onset of gastrulation, TGF-beta/Nodal signaling induces a subset of marginal cells to adopt an endodermal fate after which they initiate expression of endodermal markers such as *sox17, cas/sox32*, and *foxA2* (reviewed in Zorn and Wells, 2007). Endodermal cells internalize together with mesodermal cells, but remain in contact with the yolk surface where they adopt a flat morphology. Recently, it was shown that during early gastrulation, endoderm cells spread out by "random walk" which leads to the establishment of a non-continuous monolayer between the yolk and the mesoderm (Pezeron *et al*., 2008). After midgastrulation, endodermal cells change their behavior from random to directed migration which follows overall convergence-extension movement within the embryo. During these early stages, cells are exposed to various patterning signals that regionalize endodermal cells along the different body axes. Among them Hedgehog (Hh) signaling factors expressed in axial mesoderm and retinoic acid produced in presomitic mesoderm are both required during gastrulation to establish a region with competence for pancreatic differentiation. Hh-signaling mutants are characterized by a lack of DB with maintained but bilaterally duplicated VB and embryos deficient in retinoic acid (RA) synthesis or signaling are missing the entire pancreas (diIorio *et al*., 2002; Roy *et al*., 2001; Stafford and Prince, 2002).

The requirement for Hh signaling appears unique for zebrafish since in amniotes pancreas induction requires absence of Hh signaling. While the evolutionary causes for this difference remain to be investigated, experimental data suggest a role of early HH signals not for inducing DB fates but rather for preventing ventral signaling that blocks DB fates. In particular, in was shown that *smo/smoothened* mutant endoderm cells that are defective in intracellular transmission of Hh signaling are able to adopt DB fates when transplanted into an environment with wild-type endoderm (Chung and Stainier, 2008). Furthermore, cell autonomy studies with transgenic cells expressing a heat shock-inducible dominant-negative version of the bone morphogenetic protein (BMP) receptor Alk8 revealed that the inhibition of intracellular BMP signaling is sufficient to induce insulin expression in anterior endoderm, even in hh-deficient embryos (Chung *et al*., 2010). The data suggest that in fish, Hh signaling is required to block BMP signals on the dorsal side, thus restricting BMP signals to the ventral side and thereby preventing cell-autonomous block of pancreatic differentiation by BMP signaling.

Retinoic acid is required cell-autonomously during late gastrulation to refine the competence field for pancreas to a small region of anterior endoderm (Stafford and Prince, 2002; Stafford *et al*., 2006). A complex interplay between spatially and temporally regulated expression of RA-signaling agonists and antagonists regulates positioning of pancreatic precursors in the endoderm underlying the most anterior somites of the early-somite-stage embryo. Involved in this interplay are RA-producing enzyme (RALDH), RA-metabolizing enzymes (Cyp27a, b, c), different RA receptors, and Cdx transcription factors that inhibit RA functions on the transcriptional level (Kinkel and Prince, 2009; Kinkel *et al*., 2008).

## C. Pancreas Cell Segregation into DB and VB

As revealed by lineage tracing of individual endoderm cells from 12 hpf (6–8-somite stage) to 50 hpf, the precursors of both pancreatic buds, DB and VB, originate from the endodermal cells that underlie the first three somites of the early-somite-stage embryo (Ward *et al*., 2007). Cell-tracking studies further showed that only medial cells positioned directly adjacent to the notochord build the DB, while VB cells arise from the more lateral cells (Chung and Stainier, 2008; Ward *et al*., 2007). Notably, most of the medial cells contributed only to the DB while all lateral cells produced a larger progeny that contributed to the VB, intestine, and in the case of the most lateral cells also to liver. This implies that DB cells are specified before or during early somitogenesis while VB fates are determined later, after a few more rounds of proliferation. Furthermore, a nucleosome-targeted H2B-RFP fusion protein is retained and labels non-dividing cells in the DB at 52 hpf following injection of the coding mRNA at the one-cell stage, but is diluted and undetectable in VB cells, evidence supporting a difference in proliferative activity between these precursor populations (Hesselson *et al*., 2009).

Consistent with an early onset of endocrine differentiation in medial cells, they initiate expression of various transcription factors with conserved function in endocrine differentiation already during early somite stages (Argenton *et al*., 1999). Although not formally demonstrated, the notochord is implicated in promoting the separation of DB and VB fates and in inducing endocrine differentiation in flanking cells. Consistent with the latter, loss of the notochord in *flh* mutants causes a loss of DB as suggested by a lack or strong reduction of beta cells at 24 hpf (Biemar *et al*., 2001). Endocrine differentiation of DB cells is associated with the temporally and spatially restricted expression of various transcriptional regulators of endocrine fates. The recent reviews of Kinkel and Prince (2009) and Tiso *et al*. (2009) together with two recent reports on pancreatic *pax6* and *nkx6* functions (Binot *et al*., 2010; Verbruggen *et al*., 2010) provide an excellent overview of our current understanding of the functions of these genes and their interplay during early endocrine differentiation in zebrafish.

## D. Formation of the Dorsal Bud

Between 17 and 24 hpf, the endocrine cell progenitors rearrange from a linear assembly along the notochord into a single cluster, the DB, directly dorsal to the intestine and ventral to the notochord (Fig. 2). Time-lapse analysis of this process in embryos expressing GFP under the control of the *insulin* promoter (*Tg(ins:GFP)*) revealed that beta cells actively migrate to the level of the third somite where they aggregate to form the core of the islet (Huang *et al*., 2001; Kim *et al*., 2005). The migration path is consistent with the previously observed y-shaped expression of early endocrine markers, indicating that cells stay in close contact to the notochord during migration (Fig. 2).

The molecular mechanisms regulating migration and clustering of the DB cells are still unknown. Genetic screens, including two unpublished screens in our lab, have yielded only a few mutants with specific defects in islet morphogenesis (reviewed by Kinkel and Prince, 2009). These included mutants for *glypican4/knypek* and *tbx16/spadetail*, which both display a bilaterally split islet phenotype (Biemar *et al*., 2001)

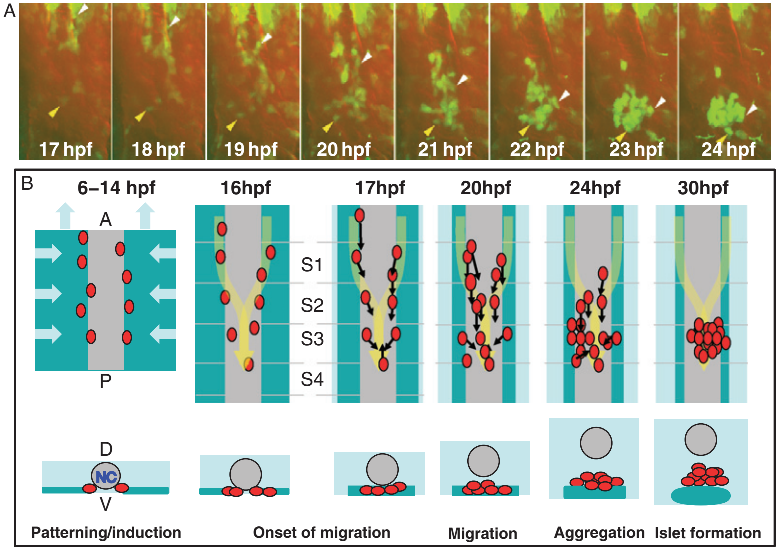

**Fig. 2** Beta-cell migration during islet formation. (A) Time-lapse series showing beta-cell migration using a *Tg(mnx1:GFP)* transgenic embryo. Arrowheads trace movement of individual cells. (B) Beta cells form in two domains located lateral to the notochord. Cells migrate posteriorly and converge between 17 and 24 hpf to the level of the third somite (S3) where they form a cluster ventral to the notochord (NC) and dorsal to the developing intestine. A, anterior; D, dorsal; P, posterior; V, ventral; S, somite. (See Plate no. 11 in the Color Plate Section.)

and affect cell polarity in the context of non-canonical Wnt signaling (*knypek*) and formation of mesoderm structures, respectively. Currently, only one pancreas-specific screen has been reported. Among other mutants, this screen yielded five novel mutants of currently unknown molecular nature in which endocrine cells are formed in normal numbers but aggregate in multiple scattered clusters (Kim *et al.*, 2006). While these scattered clusters are smaller in comparison to the wild-type DB, they still display the cellular architecture of the wild-type islet, indicating that posterior migration and clustering are regulated by separate pathways.

More recently, chemokine signaling by the Cxcr4a/Crxl12(Sdf1) receptor/ligand pair was shown to be required for correct pancreas morphogenesis (Mizoguchi *et al.*, 2008; Siekmann *et al.*, 2009). Similar to the phenotype of the type III mutants described by Kim *et al.* (2006), loss of chemokine function either by morpholino knock-down or in *cxcr4a* mutants causes scattered insulin expression and duplication or disrupted assembly of the later forming VB (Mizoguchi *et al.*, 2008). Currently, it is not clear if Cxcr4a has a direct role in migrating endocrine progenitor cells as expression of this receptor has not been reported for the time window of migration. However, *cxcr4* is expressed in the gastrula endoderm and Cxcr4a-Crxl12 signaling was shown to coordinate the movement between mesoderm and endoderm during gastrulation (Mizoguchi *et al.*, 2008; Nair and Schilling, 2008). As endoderm cells in *cxcr4a*-depleted embryos fail to align close to the notochord, observed pancreas phenotypes in *cxcr4a* mutants might result from the inability of endodermal cells to receive inductive signals from the notochord. Alternatively, Cxcr4a function in mesoderm adjacent to the islet could be required to establish the necessary environment for proper migration.

A similar mode of function has been suggested for non-canonical Wnt signaling. Interference with this pathway caused failure of anterior gut tube fusion with subsequent bilateral duplication of endocrine and exocrine pancreatic primordia (Matsui *et al*., 2005). In addition, morpholino knock-down of either the *frizzled2* receptor or its potential ligand *wnt5b* leads to scattered endocrine cells (Kim *et al*., 2005). As *frizzled2* is not expressed in the migrating cells but in neighboring cells, the data imply that *wnt5b/frizzled2* helps to establish the correct environment for directed migration.

## E. Beta-Cell Proliferation

Beta-cell number increases significantly during the transition from late embryonic to postnatal and juvenile stages in zebrafish as well as in mammals (Chen *et al*., 2007; Hanley *et al*., 2008; Moro *et al*., 2009; Parsons *et al*., 2009). Although recovery from beta-cell loss can occur during development, in patients with diabetes, the regenerative response is not sufficient to reestablish glucose homeostasis. In experimental models, re-expansion of the beta-cell population occurs following manipulations such as pancreatectomy or drug-induced beta-cell ablation (Curado *et al*., 2007; Levine and Itkin-Ansari, 2008; Moss *et al*., 2009; Pisharath *et al*., 2007). The existence of a proliferative compartment of beta cells or progenitors has been proposed to account for beta-cell expansion and regeneration, but has not been convincingly demonstrated. Studies in mouse have documented beta-cell self-renewal (Dor *et al*., 2004) and an absence of specialized progenitors (Teta *et al*., 2007), while other studies have found evidence for endogenous progenitor cells that can give rise to new beta cells (Inada *et al*., 2008; Xu *et al*., 2008). Beta cells in adult mice have extremely slow rates of replication (Teta *et al*., 2005), and no activation of beta-cell replication is seen in human diabetes patients (Butler *et al*., 2003, 2007), but an increase of duct-associated beta cells is associated with obesity (Butler *et al*., 2003).

The molecular control of beta-cell proliferation is not clearly defined, but, as in all cell types, involves a complex interplay of growth factors and external signals impacting on positive and negative regulators of the cell cycle. Specific D-type cyclin and cyclin-dependent kinases (Cdks), which interact to promote entry into the cell cycle, are expressed in the islet and their manipulation impacts beta-cell growth and proliferation (reviewed in Levine and Itkin-Ansari, 2008). For example, mice deficient in CDK4 or cyclin D2 showed impaired beta-cell proliferation and signs of insulin-dependent diabetes (Georgia and Bhushan, 2004; Rane *et al*., 1999; Tsutsui *et al*., 1999). A recent study demonstrated that chromatin modification regulates transcription of negative cell-cycle regulators from the *Ink4a/Arf* locus, causing changes in beta-cell proliferation during regeneration and aging (Dhawan *et al*., 2009).

**Table I**
**Studies of beta-cell proliferation in zebrafish**

| Treatment/detection | Stage | Finding | Reference |
|---|---|---|---|
| Pdx1-morpholino,[a] BrdU | 48–60 hpf | BrdU+ in pancreas, none in islet | Yee *et al.* (2001) |
| MTZ-ablation,[b] BrdU | 120 hpf | BrdU+/Ins+ in islet | Pisharath *et al.* (2007) |
| Time-lapse *Tg(Ins:GFP)* | 20–25 hpf | No beta-cell mitoses | Moro *et al.* (2009) |
| Time-lapse *Tg(Ins:GFP)* | 48–60 hpf | Beta-cell mitoses detected | Moro *et al.* (2009) |
| PCNA antibody | 48 hpf, 7 dpf | Rare PCNA+/Ins+ in islet | Moro *et al.* (2009) |
| Thymidine-kinase (TK)-ablation *Tg(Ins:TKGFP)* | 20 hpf–7 dpf | Reduced number of beta cells after treatment with ganciclovir (GCG) | Moro *et al.* (2009) |
| Adult islet homeostasis, BrdU | Adult (5, 9 months) | Rare proliferation of beta cells | Moro *et al.* (2009) |
| STZ-ablation,[c] MTZ-ablation, PCNA antibody | Adult | PCNA+ cells (peri-islet) increased, PCNA+/Ins+ unchanged | Moro *et al.* (2009) |
| Pancreatectomy, PCNA antibody | Adult | increased PCNA+/Ins+ cells | Moro *et al.* (2009) |
| EdU (injection) | 25–60 hpf, 60–120 hpf | EdU+ in pancreas, no EdU+ beta cells | Hesselson *et al.*, 2009 |

[a] Pdx1 morpholino treatment results in disruption of pancreas development at 2 dpf, with restoration by 5 dpf.
[b] MTZ treatment in zebrafish expressing nitroreductase (Ntr) from an insulin promoter causes beta cell apoptosis.
[c] STZ is a chemical toxin that specifically ablates beta cells.
dpf, days post-fertilization; hpf, hours post-fertilization; MTZ, metronidazole; PCNA, proliferating cell nuclear antigen; STZ, streptozotocin

Studies in zebrafish, examining normal development and regeneration, have variably found proliferative beta cells at low frequencies, with findings depending on stage and experimental protocol used (Table I). Recent studies quantitatively assessed beta-cell proliferation dynamics through embryonic development and into adulthood (Moro *et al.*, 2009), and following drug treatment and surgical manipulations widely used in mouse regeneration studies (Moss *et al.*, 2009), expanding the applicability of the zebrafish as a model organism for investigating beta-cell homeostasis and regeneration. In zebrafish, dividing cells can be detected in the three-dimensional context of a developing embryo and even within the living organism (Moro *et al.*, 2009) to help dissect both intrinsic and environmental regulators.

## III. Analysis of Beta-Cell Migration and Proliferation

### A. Time-Lapse Imaging of Beta-Cell Migration

Due to their small size and transparency, zebrafish embryos are a favored model for microscopic analyses of embryonic beta-cell formation and regeneration. Cells of interest tagged by expression of fluorescent proteins can be visualized in both fixed specimens and living embryos. The spectrum of fluorescent proteins (FPs) available for use in live imaging experiments have been steadily expanding to include not only a broad range of colors but also offering variants of other relevant properties such as brightness, photostability, phototoxicity, and maturation speed (for an extensive review, see Davidson and Campbell, 2009). The subcellular localization of the expressed FP(s) can reveal different aspects of biological processes and facilitate later analysis. Cytoplasmically expressed FPs render a cell's full morphological complexity but can cause difficulties in cell tracking and quantitative studies as particle detection algorithms may be unable to recognize individual cells within a closely spaced cluster. FPs fused to a nuclear localization signal (NLS) mark distinct entities which helps cell identification and tracking (Nowotschin *et al.*, 2009). However, the cell may be lost to tracking during cell division because after nuclear envelope breakdown the fluorescent signal becomes weak and diffusely distributed throughout the cell. This problem is avoided by using an FP–histone fusion, which becomes incorporated into the nucleosome and produces a robust signal throughout all stages of the cell cycle (Kanda *et al.*, 1998). FPs can also be localized to the plasma membrane or secretory apparatus through addition of sequences that direct lipid modification (Rhee *et al.*, 2006). This enables visualization of cell membrane dynamics during migration, including extension and retraction of membrane protrusions and intercellular bridge formation. The rapidly expanding research on pancreas development and regeneration has resulted in the generation of numerous transgenic fish lines that express FPs in beta cells or endocrine progenitors, or in associated cell types (Table II). Simultaneous demarcation of plasma membrane and cytoplasm or nucleus is possible through combinations of spectrally distinct FPs (Fig. 3); labeling of related cell populations by different fluorophores helps to orient the migration process within the embryo and provides a point of reference during cell tracking (Fig. 4).

### 1. Method: Analysis of DB Morphogenesis by Time-Lapse Laser-Scanning Microscopy

**a. Equipment** ***Microscope:*** Upright microscope (Zeiss LSM5 Exciter) with water dipping lens (40×).

***Software:*** Images collected using Zen 2008 software and analyzed with LSM Image Browser (Zeiss) or Imaris (Bitplane).

**b. Materials** ***Observation chamber***—Prepare an observation chamber by drilling a 1 cm diameter hole into the bottom of a 3.5 cm petri dish. Apply silicon glue around the edge of the circle on the bottom of the plate. Seal the opening by pressing a coverslip onto the glue.

***Egg water***—Dissolve 7.5 g Coral Pro Salt (Red Sea) in 25 l reverse osmosis $H_2O$.

***Low-melt agarose*** (Biozym, Vienna, Austria)—Prepare 1.2% low-melt agarose in egg water and place in a prewarmed 37°C waterbath.

***Tricaine*** (Sigma-Aldrich, Vienna, Austria)—Prepare 25× stock solution by dissolving 400 mg in ~97.9 ml $H_2O$, plus 2.1 ml Tris-HCl (pH 9.0). Adjust pH to 7.0. Store aliquots at –20°C.

**c. Imaging**

1. ***Temperature control:*** Imaging room should be maintained at a constant temperature. Adjust air conditioner/heater to give room temperature of approximately 28°C. Allow the room and equipment temperature to equilibrate before starting to image.

**Table II**
**Transgenic lines that label pancreatic cells**

| Gene | Name of transgenic line | Location | Cell type | References |
|---|---|---|---|---|
| ClaudinB | *Tg(-8.0cldnb:lynEGFP)zf106* | Membrane | Epithelia | Haas and Gilmour, (2006) |
| Elastase | *Tg(ela3l:EGFP)gz2* | Cytoplasm | Exocrine | Wan *et al*. (2006) |
| Endoderm | *Tg(XlEef1a1:GFP)s854* | Cytoplasm | Endoderm | Field *et al*. (2003) |
| Glucagon | *Tg(gcga:GFP)ia1* | Cytoplasm | Alpha cells | Zecchin *et al*. (2007) |
| Hb9/mnx1 | *Tg(mnx1:GFP)ml2* | Cytoplasm | Beta cells | Flanagan-Steet *et al*. (2005) |
| | *Tg(mnx1:mGFP)ml3* | Membrane | Beta cells | Flanagan-Steet *et al*. (2005) |
| | *Tg(mnx1:nucRFP)ml4* | Nuclear | Beta cells | Arkhipova and Meyer (personal communication) |
| Insulin | *Tg(-4.0ins:GFP)zf5* | Cytoplasm | Beta cells | Huang *et al*. (2001) |
| | *Tg(ins:CFP-NTR)s892* | Cytoplasm | Beta cells | Curado *et al*. (2007) |
| | *Tg(-1.0ins:eGFP)sc1* | Cytoplasm | Beta cells | Moro *et al*. (2009) |
| | *Tg(ins:dsRed)m1018* | Cytoplasm | Beta cells | Hesselson *et al*., 2009 |
| | *Tg(ins:eGFP)jh3/jh3* | Cytoplasm | Beta cells | Pisharath *et al*. (2007) |
| | *Tg(ins:Kaede)jh6/jh6* | Cytoplasm | Beta cells | Pisharath *et al*. (2007) |
| | *Tg(ins:mCherry)jh2* | Cytoplasm | Beta cells | Pisharath *et al*. (2007) |
| | *Tg(ins:nfsB-mCherry)jh4* | Cytoplasm | Beta cells | Pisharath *et al*. (2007) |
| | *Tg(ins:nfsB-mCherry)jh5/jh5* | Cytoplasm | Beta cells | Pisharath *et al*. (2007) |
| | *Tg(T2Kins:EGFP-mCherry)jh8* | Cytoplasm | Beta cells | Provost *et al*. (2007) |
| | *Tg(-1.2ins:TKGFP)* | Nuclear | Beta cells | Moro *et al*. (2009) |
| | *Tg(T2Kins:Hmgb1-eGFP)jh10* | Nuclear | Beta cells | Parsons *et al*. (2009) |
| | *Tg(ins:Gal4)m1080* | Nuclear | Beta cells | Zecchin *et al*. (2007) |
| NeuroD | *TgBAC(neurod:EGFP)nl1* | Cytoplasm | Endocrine | Obholzer *et al*. (2008) |
| Nkx2.2a | *Tg(-3.5nkx2.2a:GFP)ia3* | Cytoplasm | Duct | Pauls *et al*. (2007) |
| | *Tg(-8.5nkx2.2a:GFP)ia2* | Cytoplasm | Duct, endocrine | Pauls *et al*. (2007) |
| | *Tg(nkx2.2a:mEGFP)vu16* | Membrane | Endocrine | Ng *et al*. (2005) |
| Pax6b | *Tg(P0-pax6b:DsRed)ulg302* | Cytoplasm | Endocrine | Delporte *et al*. (2008) |
| | *Tg(P0-pax6b:GFP)ulg515* | Cytoplasm | Endocrine | Delporte *et al*. (2008) |
| Pdx1 | *Tg(-6.5pdx1:GFP)zf6* | Cytoplasm | Endocrine/beta cells | Huang *et al*. (2001) |
| Ptf1/P48 | *Tg(ptf1a:eGFP)jh1* | Cytoplasm | Exocrine | Godinho *et al*. (2005) |
| | *Tg(ptf1a:eGFP)jh7* | Cytoplasm | Exocrine | Park *et al*. (2008) |
| Somatostatin | *Tg(sst2:gfp)* | Cytoplasm | Delta cells | Li *et al*. (2009) |
| | *Tg(sst2:rfp)* | Cytoplasm | Delta cells | Li *et al*. (2009) |
| Sox17 | *Tg(-5.0sox17:EGFP)zf99* | Cytoplasm | Endoderm | Wilkins *et al*. (2008) |
| | *Tg(sox17:DsRed)s903* | Cytoplasm | Endoderm | Chung and Stainier (2008) |
| Tp1[a] | *Tg(Tp1bglob:eGFP)um14* | Cytoplasm | Notch-responsive cells | Parsons *et al*. (2009) |
| | *Tg(T2KTp1bglob:hmgb1-mCherry)ih11* | Nuclear | Notch-responsive cells | Parsons *et al*. (2009) |

[a] Tp1 is an artificial Notch-responsive element with 12 RBP-Jk binding sites
For further details, see also ZFIN (http://zfin.org).

2. ***Staging:*** Migration occurs between 16 hpf (14-somite stage) and 24 hpf.
   a. If the aquarium is coordinated with daylight, this is normally between 12 midnight and 8 AM
   b. To speed up development: If a 32°C incubator is used, time-lapse can be started at 10 PM

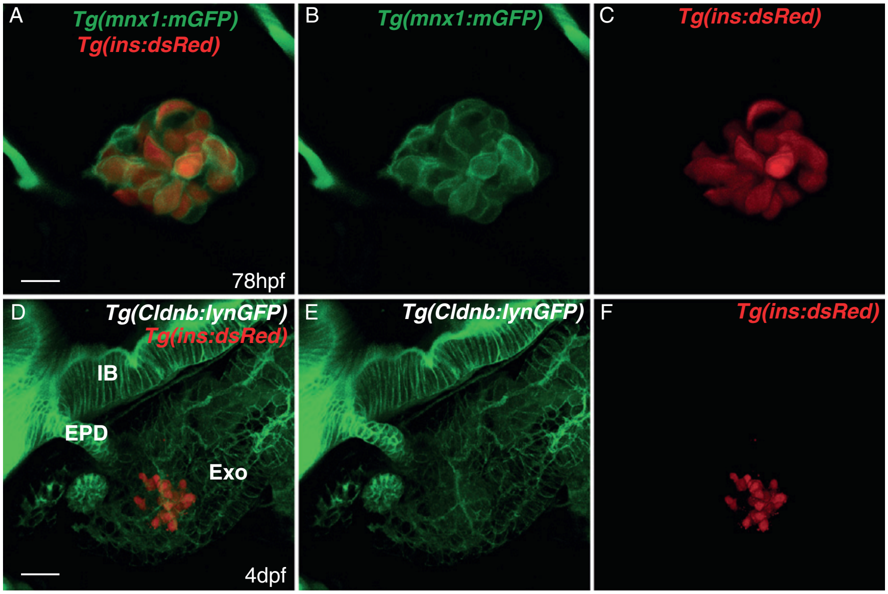

**Fig. 3** Visualizing beta cells using transgenic zebrafish lines. (A–C) z-stack projection obtained by imaging a living double transgenic *Tg(Hb9:mGFP; ins:dsRed)* embryo, lateral view at 78 hpf, showing both membrane-targeted GFP and cytoplasmic dsRed (A) or single fluorophores (B, C). (D–F) z-stack projection, ventral view of fixed embryo, double transgenic *Tg(Cldnb:lynEGFP; ins:dsRed)*. Membrane-targeted GFP expression from a *ClaudinB* promoter fragment (Haas and Gilmour, 2006) outlines epithelia of the developing gastrointestinal system, delineating the intestinal bulb (IB), extrapancreatic duct (EPD), and exocrine pancreas (Exo), while *Tg(ins:dsRed)* cells are seen in the islet. Scale bar in A = 10 μM and in D = 20 μM.

c. To slow down development:
  - Collect embryos after 11 AM.
  - Grow embryo overnight at 24°C.
  - Embryos reach 12–14-somite stage at 8 AM.

3. Manually remove chorion from embryo.
4. Fill opening in the observation dish with 0.2 ml low-melt agarose solution.
5. Immediately after, pick up an embryo in a minimal volume of egg water with a fire polished Pasteur pipette and let embryo sink to the outer surface.
6. Dip the tip of the pipette into the liquid agarose solution and the embryo will sink into the agarose.
7. For a dorsal view, orient the embryo under a stereomicroscope using a blunt probe such that the first somite is closest to the objective and let agarose harden.
8. Fill observation chamber with a maximal volume of 1X Tricaine-containing egg water.

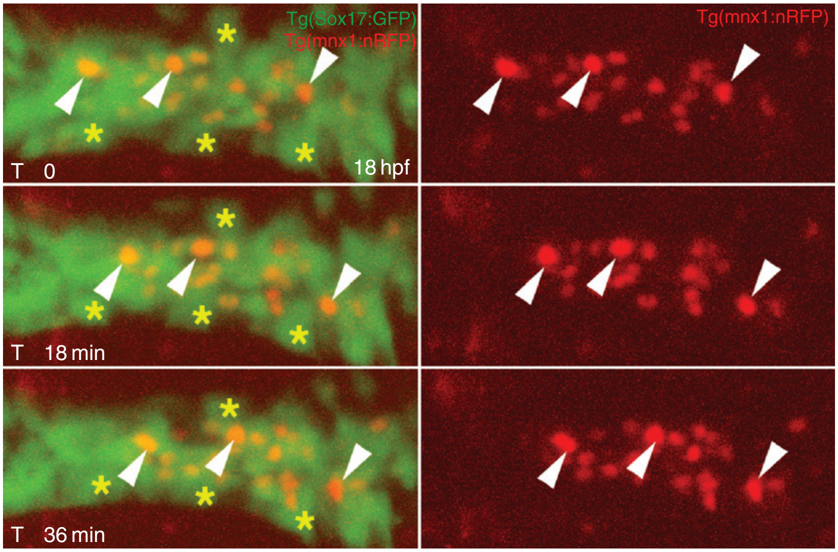

**Fig. 4** Time-lapse analysis of beta-cell migration. Three-dimensional projections from a time-lapse series imaging a double transgenic *Tg(sox17:GFP; mnx1:nucRFP)* embryo starting at 18 hpf. Images shown are spaced 18 min apart. Individual nucRFP-positive nuclei of beta cells (arrowheads) migrate relative to Sox17:GFP-labeled endoderm cells (asterisks).

9. Locate embryo and region of interest using bright-field and fluorescent illumination. Start imaging.
10. Due to the morphological changes during somitogenesis, the region of intertest may shift. Therefore, it is often necessary to frequently check on the scan, and if required to adjust microscope settings and stage.

**d. Imaging Parameters** Adjustable settings for time-lapse imaging include pinhole size, laser power, thickness of *z*-slice, number of slices, and time interval. Optimal settings must be determined empirically for each transgene and particular imaging experiment. Illumination is set depending on strength of signal to achieve an adequate signal-to-noise ratio while limiting photobleaching and phototoxicity. The necessary time interval depends on the speed of the process under observation. (For a discussion of optimizing parameters for image acquisition during time-lapse experiments, see Koster and Fraser, 2004.)

For an imaging experiment as shown in Figure 4, we typically collect 15–20 *z*-sections of 2–5 μM, with a total *z*-stack of 50–60 μM. The *z*-range is set to include several slices above and below the region of interest, which helps to ensure the full *z*-stack contains the area of interest even after some drift of the sample. For following individual cells during beta-cell migration, a time interval of 3–5 min is used.

## B. Pancreatic Beta-Cell Proliferation

Techniques to label and localize proliferative cells are well established in mice and have been adapted and utilized in zebrafish studies of pancreas development. Incorporation of the nucleotide analog BrdU into DNA establishes that a cell has passed through the cell cycle, which is detected following tissue fixation by antibody immunohistochemistry. The advantage of BrdU labeling is that the labeled cell and its progeny retain the label in their DNA, and incorporated BrdU remains detectable for up to six or seven cell divisions (Mandyam *et al*., 2007). Therefore, proliferative progenitors, once labeled, can be identified at later stages of differentiation and followed during migration.

However, there are several confounding factors that can complicate the interpretation of BrdU-labeling experiments. Bioavailability of BrdU, that is, the time window after administration in which incorporation into DNA can occur, has not been systematically studied in zebrafish embryos. In adult fish, it has been reported to be 4 h after injection (Reimer *et al*., 2008), while values ranging from 15 min up to 2 h have been estimated for labeling adult and perinatal mouse brain following systemic BrdU injection (Mandyam *et al*., 2007; Taupin, 2007). The duration of BrdU labeling after injection depends on route of delivery, permeability of tissue, as well as metabolism by the organism. Overestimating the labeling duration can lead to proliferation events going undetected.

Alternative markers for proliferative cells include antibodies for PCNA and Ki67. PCNA is a cofactor of DNA polymerase expressed during S-phase, but also during DNA repair, and has a long half-life. Therefore, PCNA may remain detectable long after cell-cycle exit, while Ki-67, a nuclear protein expressed throughout the cell cycle, has a very short half-life (Kee *et al*., 2002). Thus, Ki-67 is a more reliable marker of recent proliferation compared to PCNA, but as expression is soon lost, the newly generated cells can no longer be identified.

EdU is a recently introduced thymidine analog that, unlike BrdU, does not require DNA denaturation or antibody staining for its detection. The harsh denaturing treatment required to expose the BrdU epitope for antibody labeling damages the tissue and decreases reproducibility of the procedure, and may alter antibody epitopes which limit the ability to identify cell types based on co-expression of other markers. By contrast, EdU can be detected within intact double-stranded DNA with reagents that easily penetrate tissue (Salic and Mitchison, 2008), making this method highly suitable for labeling in whole mount. EdU can be visualized in combination with cells expressing transgenic reporters, or with proteins detected by antibody staining. Labeling of the developing pancreas by injection of EdU into zebrafish embryo yolk or pericardial space has been described (Anderson *et al*., 2009; Hesselson *et al*., 2009). With extended incubation in EdU, we have detected rare proliferation events in the slowly dividing beta-cell population (Fig. 5).

### 1. Method: Detection of Proliferation in Pancreas Using EdU

#### a. Materials

Click-It EdU Imaging Kit (product C10085, Invitrogen, Lofer, Austria)

EdU—Dissolve in 2 ml 1× PBS (final 10 mM). Store in aliquots at −20°C protected from light.

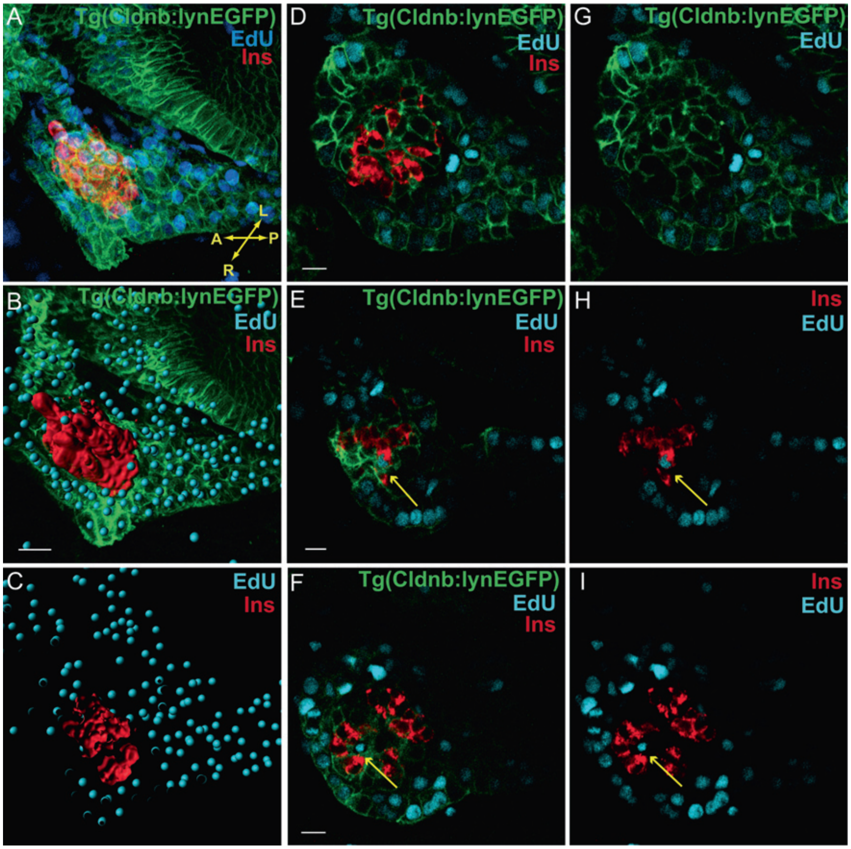
A
Tg(Cldnb:lynEGFP)
EdU
Ins
L
A
P
R
D
Tg(Cldnb:lynEGFP)
EdU
Ins
G
Tg(Cldnb:lynEGFP)
EdU
B
Tg(Cldnb:lynEGFP)
EdU
Ins
E
Tg(Cldnb:lynEGFP)
EdU
Ins
H
Ins
EdU
C
EdU
Ins
F
Tg(Cldnb:lynEGFP)
EdU
Ins
I
Ins
EdU

**Fig. 5** Identification of proliferating cells in developing pancreas. (A) Confocal projection of *Tg(Cldnb:lynEGFP)* larva at 72 hpf following 48 h of EdU labeling. Most exocrine cells are EdU+. (B) Same data set as in A, with a surface rendering of the insulin domain and EdU+ nuclei represented by a spot-detection algorithm. (C) Cutting plane through the insulin surface shown in B to demonstrate the absence of EdU+ nuclei within the insulin domain. (D–I) Single plane views of embryos treated as in A, showing an example of no proliferating cells in the islet (D, G), an EdU+/insulin+ cell (E, H; arrow), and an EdU+/insulin- islet cell (F, I; arrow). Scale bar in B = 15 μM and in D–F = 10 μM. A, anterior; P, posterior; L, left; R, right. (See Plate no. 12 in the Color Plate Section.)

AlexaFluor Azide—Dissolve in 70 μl DMSO. Store in aliquots at −20°C protected from light.

Reaction Buffer D (10×) stock solution—Store at 4°C.

Additive F—Add 2 ml ddH$_2$O. Mix well and store in aliquots at −20°C

CuSO4—Store at 4°C

Other Reagents

BSA

DMSO
MeOH
4% PFA (prepared fresh)
PBS
Proteinase K—10 mg/ml stock solution, aliquot and store at –20°C
Triton X-100
Tween-20
Normal Goat Serum
PBST—PBS + 0.1% Tween-20
PTU—For 10× stock solution, dissolve 304 mg powder in 1 l $ddH_2O$
Blocking solution—1% DMSO/1% Triton X-100/2% NGS/1% BSA in PBS

1. Collect embryos. From 22 hpf onward, include 1X PTU in egg water to inhibit pigmentation. Incubate to desired stage. (This protocol has been tested on embryos 48 hpf and older.)
2. Transfer embryos to EdU solution (final concentration 0.5 mM in 0.4% DMSO/1X PTU/egg water). Incubate at 28°C.
3. After desired incubation period, wash embryos in egg water, transfer to fresh egg water (with PTU), or continue to fixation.
4. Fix in 4% PFA (made fresh) at room temperature for 3 h, or 4°C overnight on rocker.
5. Wash 3× in PBST for 5 min each.
6. Wash in 100% MeOH for 5 min. Change to fresh MeOH. Incubate at –20°C for 2 h (longer storage at –20°C is possible).
7. Rehydrate through MeOH/PBST series: 75% MeOH/PBST, 50% MeOH/PBST, 25% MeOH/PBST. Incubate for 5 min each.
8. Wash 3× in PBST.
9. Manually deyolk embryos.
10. Treat with Proteinase K diluted to 10 μg/ml in PBST at room temperature for 45 min.
11. Refix for 15 min in 4%PFA/PBST at room temperature. Wash 3× in PBST.
12. Incubate embryos in 1% DMSO/0.5% Triton in PBS × 20 min at RT.
13. Wash with PBST. Remove as much PBST as possible.
14. Add *staining solution*: (for 500 μl/100 μl per tube of embryos)

| | |
|---|---|
| **44 μl** | 1× Click-iT Reaction Buffer |
| **10 μl** | $CuSO_4$ |
| **2.5 μl** | Fluorescent dye azide |
| **50 μl** | Reaction Buffer Additive |
| **394 μl** | $ddH_2O$ |

15. Incubate for 2 h at room temperature in the dark.
16. Rinse 3× with PBST.
17. Proceed to antibody staining, starting with a minimum of 1 h incubation in blocking solution. We typically incubate with primary antibody diluted in blocking solution overnight at 4°C, followed by washes in 1% BSA/0.3% Triton

in PBS, overnight incubation with secondary antibody at 4°C followed by washes in PBST. (Keep embryos protected from light throughout.)

18. Imaging. For an experiment as shown in Figure 5, we use Alexa-Azide 647 (Invitrogen), and the following antibodies: rabbit anti-GFP (Torrey Pines Biolabs, East Orange, NJ, USA), guinea-pig anti-insulin (Dako, Vienna, Austria), anti-rabbit Alexa 488 (Invitrogen), anti-guinea pig Alexa-555 (Invitrogen).

## IV. Future Directions

Cell proliferation and migration are developmental events critical for assembly of the mature pancreatic islet. Recent advances in labeling methods and microscopy, combined with the visualization benefits of zebrafish, enable high-resolution detection of these processes during normal development and following genetic manipulations. Fluorescent probes fused to proteins subject to ubiquitin-mediated degradation at particular parts of the cell cycle provide a real-time read-out of the cell-cycle phase in living cells (Sakaue-Sawano *et al.*, 2008). By using transgenic lines expressing these proteins, it becomes possible to visualize cell-cycle dynamics in real-time within living organisms, in conjunction with other biological processes such as migration. A better understanding of how beta-cell proliferation and migration are coordinately regulated will provide important insights for diabetes therapies for which not only production of sufficient numbers of replacement beta cells is required, but also the assembly of an appropriate three-dimensional structure is a necessary prerequisite for fully functional regulation of glucose homeostasis.

## Acknowledgments

The authors would like to thank Mayra Eduardoff and Valeriya Arkhipova for help with protocols, technical assistance, and useful discussions; Pia Aanstad for insightful comments; Jochen Holzschuh and lab members for sharing protocols; and Darren Gilmour for the *Tg(cldnb:lynGFP)* line. This work is supported in part by FWF grants to D.M. and R.A.K.

## References

Anderson, R. M., Bosch, J. A., Goll, M. G., Hesselson, D., Dong, P. D., Shin, D., Chi, N. C., Shin, C. H., Schlegel, A., Halpern, M., *et al.* (2009). Loss of Dnmt1 catalytic activity reveals multiple roles for DNA methylation during pancreas development and regeneration. *Dev. Biol.* **334**, 213–223.

Argenton, F., Zecchin, E., and Bortolussi, M. (1999). Early appearance of pancreatic hormone-expressing cells in the zebrafish embryo. *Mech. Dev.* **87**, 217–221.

Biemar, F., Argenton, F., Schmidtke, R., Epperlein, S., Peers, B., and Driever, W. (2001). Pancreas development in zebrafish: Early dispersed appearance of endocrine hormone expressing cells and their convergence to form the definitive islet. *Dev. Biol.* **230**, 189–203.

Binot, A. C., Manfroid, I., Flasse, L., Winandy, M., Motte, P., Martial, J. A., Peers, B., and Voz, M. L. (2010). Nkx6.1 and nkx6.2 regulate alpha- and beta-cell formation in zebrafish by acting on pancreatic endocrine progenitor cells. *Dev. Biol.* **340**, 397–407.

Butler, A. E., Galasso, R., Meier, J. J., Basu, R., Rizza, R. A., and Butler, P. C. (2007). Modestly increased beta cell apoptosis but no increased beta cell replication in recent-onset type 1 diabetic patients who died of diabetic ketoacidosis. *Diabetologia* **50**, 2323–2331.

Butler, A. E., Janson, J., Bonner-Weir, S., Ritzel, R., Rizza, R. A., and Butler, P. C. (2003). Beta-cell deficit and increased beta-cell apoptosis in humans with type 2 diabetes. *Diabetes* **52**, 102–110.

Chen, S., Li, C., Yuan, G., and Xie, F. (2007). Anatomical and histological observation on the pancreas in adult zebrafish. *Pancreas* **34**, 120–125.

Chung, W. S., Andersson, O., Row, R., Kimelman, D., and Stainier, D. Y. (2010). Suppression of Alk8-mediated Bmp signaling cell-autonomously induces pancreatic beta-cells in zebrafish. *Proc. Natl. Acad. Sci. U.S.A* **107**, 1142–1147.

Chung, W. S., and Stainier, D. Y. (2008). Intra-endodermal interactions are required for pancreatic beta cell induction. *Dev. Cell* **14**, 582–593.

Curado, S., Anderson, R. M., Jungblut, B., Mumm, J., Schroeter, E., and Stainier, D. Y. (2007). Conditional targeted cell ablation in zebrafish: A new tool for regeneration studies. *Dev. Dyn.* **236**, 1025–1035.

Davidson, M. W., and Campbell, R. E. (2009). Engineered fluorescent proteins: Innovations and applications. *Nat. Methods* **6**, 713–717.

Delporte, F. M., Pasque, V., Devos, N., Manfroid, I., Voz, M. L., Motte, P., Biemar, F., Martial, J. A., and Peers, B. (2008). Expression of zebrafish pax6b in pancreas is regulated by two enhancers containing highly conserved cis-elements bound by PDX1, PBX and PREP factors. *BMC Dev. Biol.* **8**, 53.

Dhawan, S., Tschen, S. I., and Bhushan, A. (2009). Bmi-1 regulates the Ink4a/Arf locus to control pancreatic beta-cell proliferation. *Genes Dev.* **23**, 906–911.

diIorio, P. J., Moss, J. B., Sbrogna, J. L., Karlstrom, R. O., and Moss, L. G. (2002). Sonic hedgehog is required early in pancreatic islet develo. *Dev. Biol.* **244**, 75–84.

Dong, P. D., Munson, C. A., Norton, W., Crosnier, C., Pan, X., Gong, Z., Neumann, C. J., and Stainier, D. Y. (2007). Fgf10 regulates hepatopancreatic ductal system patterning and differentiation. *Nat. Genet.* **39**, 397–402.

Dor, Y., Brown, J., Martinez, O. I., and Melton, D. A. (2004). Adult pancreatic beta-cells are formed by self-duplication rather than stem-cell differentiation. *Nature* **429**, 41–46.

Field, H. A., Dong, P. D., Beis, D., and Stainier, D. Y. (2003). Formation of the digestive system in zebrafish. II. Pancreas morphogenesis. *Dev. Biol.* **261**, 197–208.

Flanagan-Steet, H., Fox, M. A., Meyer, D., and Sanes, J. R. (2005). Neuromuscular synapses can form in vivo by incorporation of initially aneural postsynaptic specializations. *Development* **132**, 4471–4481.

Georgia, S., and Bhushan, A. (2004). Beta cell replication is the primary mechanism for maintaining postnatal beta cell mass. *J. Clin. Invest.* **114**, 963–968.

Godinho, L., Mumm, J. S., Williams, P. R., Schroeter, E. H., Koerber, A., Park, S. W., Leach, S. D., and Wong, R. O. (2005). Targeting of amacrine cell neurites to appropriate synaptic laminae in the developing zebrafish retina. *Development* **132**, 5069–5079.

Haas, P., and Gilmour, D. (2006). Chemokine signaling mediates self-organizing tissue migration in the zebrafish lateral line. *Dev. Cell* **10**, 673–680.

Hanley, N. A., Hanley, K. P., Miettinen, P. J., and Otonkoski, T. (2008). Weighing up beta-cell mass in mice and humans: Self-renewal, progenitors or stem cells? *Mol. Cell. Endocrinol.* **288**, 79–85.

Hesselson, D., Anderson, R. M., Beinat, M., and Stainier, D. Y. (2009). Distinct populations of quiescent and proliferative pancreatic beta-cells identified by HOTcre mediated labeling. *Proc. Natl. Acad. Sci. U.S.A* **106**, 14896–14901.

Huang, H., Vogel, S. S., Liu, N., Melton, D. A., and Lin, S. (2001). Analysis of pancreatic development in living transgenic zebrafish embryos. *Mol. Cell. Endocrinol.* **177**, 117–124.

Inada, A., Nienaber, C., Katsuta, H., Fujitani, Y., Levine, J., Morita, R., Sharma, A., and Bonner-Weir, S. (2008). Carbonic anhydrase II-positive pancreatic cells are progenitors for both endocrine and exocrine pancreas after birth. *Proc. Natl. Acad. Sci. U.S.A* **105**, 19915–19919.

Kanda, T., Sullivan, K. F., and Wahl, G. M. (1998). Histone-GFP fusion protein enables sensitive analysis of chromosome dynamics in living mammalian cells. *Curr. Biol.* **8**, 377–385.

Kee, N., Sivalingam, S., Boonstra, R., and Wojtowicz, J. M. (2002). The utility of Ki-67 and BrdU as proliferative markers of adult neurogenesis. *J. Neurosci. Meth.* **115**, 97–105.

Kim, H. J., Schleiffarth, J. R., Jessurun, J., Sumanas, S., Petryk, A., Lin, S., and Ekker, S. C. (2005). Wnt5 signaling in vertebrate pancreas development. *BMC Biol.* **3**, 23.

Kim, H. J., Sumanas, S., Palencia-Desai, S., Dong, Y., Chen, J. N., and Lin, S. (2006). Genetic analysis of early endocrine pancreas formation in zebrafish. *Mol. Endocrinol.* **20**, 194–203.

Kinkel, M. D., Eames, S. C., Alonzo, M. R., and Prince, V. E. (2008). Cdx4 is required in the endoderm to localize the pancreas and limit beta-cell number. *Development* **135**, 919–929.

Kinkel, M. D., and Prince, V. E. (2009). On the diabetic menu: Zebrafish as a model for pancreas development and function. *Bioessays* **31**, 139–152.

Koster, R. W., and Fraser, S. E. (2004). Time-lapse microscopy of brain development. *Methods Cell Biol.* **76**, 207–235.

Levine, F., and Itkin-Ansari, P. (2008). Beta-cell regeneration: Neogenesis, replication or both? *J. Mol. Med.* **86**, 247–258.

Li, Z., Wen, C., Peng, J., Korzh, V., and Gong, Z. (2009). Generation of living color transgenic zebrafish to trace somatostatin-expressing cells and endocrine pancreas organization. *Differentiation* **77**, 128–134.

Mandyam, C. D., Harburg, G. C., and Eisch, A. J. (2007). Determination of key aspects of precursor cell proliferation, cell cycle length and kinetics in the adult mouse subgranular zone. *Neuroscience* **146**, 108–122.

Matsui, T., Raya, A., Kawakami, Y., Callol-Massot, C., Capdevila, J., Rodriguez-Esteban, C., and Izpisua Belmonte, J. C. (2005). Noncanonical Wnt signaling regulates midline convergence of organ primordia during zebrafish development. *Genes Dev.* **19**, 164–175.

Mizoguchi, T., Verkade, H., Heath, J. K., Kuroiwa, A., and Kikuchi, Y. (2008). Sdf1/Cxcr4 signaling controls the dorsal migration of endodermal cells during zebrafish gastrulation. *Development* **135**, 2521–2529.

Moro, E., Gnugge, L., Braghetta, P., Bortolussi, M., and Argenton, F. (2009). Analysis of beta cell proliferation dynamics in zebrafish. *Dev. Biol.* **332**, 299–308.

Moss, J. B., Koustubhan, P., Greenman, M., Parsons, M. J., Walter, I., and Moss, L. G. (2009). Regeneration of the pancreas in adult zebrafish. *Diabetes* **58**, 1844–1851.

Nair, S., and Schilling, T. F. (2008). Chemokine signaling controls endodermal migration during zebrafish gastrulation. *Science* **322**, 89–92.

Ng, A. N., de Jong-Curtain, T. A., Mawdsley, D. J., White, S. J., Shin, J., Appel, B., Dong, P. D., Stainier, D. Y., and Heath, J. K. (2005). Formation of the digestive system in zebrafish: III. Intestinal epithelium morphogenesis. *Dev. Biol.* **286**, 114–135.

Nowotschin, S., Eakin, G. S., and Hadjantonakis, A. K. (2009). Live-imaging fluorescent proteins in mouse embryos: Multi-dimensional, multi-spectral perspectives. *Trends Biotechnol.* **27**, 266–276.

Obholzer, N., Wolfson, S., Trapani, J. G., Mo, W., Nechiporuk, A., Busch-Nentwich, E., Seiler, C., Sidi, S., Sollner, C., Duncan, R. N., *et al.* (2008). Vesicular glutamate transporter 3 is required for synaptic transmission in zebrafish hair cells. *J. Neurosci.* **28**, 2110–2118.

Pack, M., Solnica-Krezel, L., Malicki, J., Neuhauss, S. C., Schier, A. F., Stemple, D. L., Driever, W., and Fishman, M. C. (1996). Mutations affecting development of zebrafish digestive organs. *Development* **123**, 321–328.

Park, S. W., Davison, J. M., Rhee, J., Hruban, R. H., Maitra, A., and Leach, S. D. (2008). Oncogenic KRAS induces progenitor cell expansion and malignant transformation in zebrafish exocrine pancreas. *Gastroenterology* **134**, 2080–2090.

Parsons, M. J., Pisharath, H., Yusuff, S., Moore, J. C., Siekmann, A. F., Lawson, N., and Leach, S. D. (2009). Notch-responsive cells initiate the secondary transition in larval zebrafish pancreas. *Mech. Dev.* **126**, 898–912.

Pauls, S., Zecchin, E., Tiso, N., Bortolussi, M., and Argenton, F. (2007). Function and regulation of zebrafish nkx2.2a during development of pancreatic islet and ducts. *Dev. Biol.* **304**, 875–890.

Pezeron, G., Mourrain, P., Courty, S., Ghislain, J., Becker, T. S., Rosa, F. M., and David, N. B. (2008). Live analysis of endodermal layer formation identifies random walk as a novel gastrulation movement. *Curr. Biol.* **18**, 276–281.

Pisharath, H., Rhee, J. M., Swanson, M. A., Leach, S. D., and Parsons, M. J. (2007). Targeted ablation of beta cells in the embryonic zebrafish pancreas using E. coli nitroreductase. *Mech. Dev.* **124**, 218–229.

Provost, E., Rhee, J., and Leach, S. D. (2007). Viral 2A peptides allow expression of multiple proteins from a single ORF in transgenic zebrafish embryos. *Genesis* **45**, 625–629.

Rane, S. G., Dubus, P., Mettus, R. V., Galbreath, E. J., Boden, G., Reddy, E. P., and Barbacid, M. (1999). Loss of Cdk4 expression causes insulin-deficient diabetes and Cdk4 activation results in beta-islet cell hyperplasia. *Nat. Genet.* **22**, 44–52.

Reimer, M. M., Sorensen, I., Kuscha, V., Frank, R. E., Liu, C., Becker, C. G., and Becker, T. (2008). Motor neuron regeneration in adult zebrafish. *J. Neurosci.* **28**, 8510–8516.

Rhee, J. M., Pirity, M. K., Lackan, C. S., Long, J. Z., Kondoh, G., Takeda, J., and Hadjantonakis, A. K. (2006). In vivo imaging and differential localization of lipid-modified GFP-variant fusions in embryonic stem cells and mice. *Genesis* **44**, 202–218.

Roy, S., Qiao, T., Wolff, C., and Ingham, P. W. (2001). Hedgehog signaling pathway is essential for pancreas specification in the zebrafish embryo. *Curr. Biol.* **11**, 1358–1363.

Sakaue-Sawano, A., Kurokawa, H., Morimura, T., Hanyu, A., Hama, H., Osawa, H., Kashiwagi, S., Fukami, K., Miyata, T., Miyoshi, H., *et al.* (2008). Visualizing spatiotemporal dynamics of multicellular cell-cycle progression. *Cell* **132**, 487–498.

Salic, A., and Mitchison, T. J. (2008). A chemical method for fast and sensitive detection of DNA synthesis in vivo. *Proc. Natl. Acad. Sci. U.S.A* **105**, 2415–2420.

Siekmann, A. F., Standley, C., Fogarty, K. E., Wolfe, S. A., and Lawson, N. D. (2009). Chemokine signaling guides regional patterning of the first embryonic artery. *Genes Dev.* **23**, 2272–2277.

Stafford, D., and Prince, V. E. (2002). Retinoic acid signaling is required for a critical early step in zebrafish pancreatic development. *Curr. Biol.* **12**, 1215–1220.

Stafford, D., White, R. J., Kinkel, M. D., Linville, A., Schilling, T. F., and Prince, V. E. (2006). Retinoids signal directly to zebrafish endoderm to specify insulin-expressing beta-cells. *Development* **133**, 949–956.

Taupin, P. (2007). BrdU immunohistochemistry for studying adult neurogenesis: Paradigms, pitfalls, limitations, and validation. *Brain Res. Rev.* **53**, 198–214.

Teta, M., Long, S. Y., Wartschow, L. M., Rankin, M. M., and Kushner, J. A. (2005). Very slow turnover of beta-cells in aged adult mice. *Diabetes* **54**, 2557–2567.

Teta, M., Rankin, M. M., Long, S. Y., Stein, G. M., and Kushner, J. A. (2007). Growth and regeneration of adult beta cells does not involve specialized progenitors. *Dev. Cell* **12**, 817–826.

Tiso, N., Moro, E., and Argenton, F. (2009). Zebrafish pancreas development. *Mol. Cell. Endocrinol.* **312**, 24–30.

Tsutsui, T., Hesabi, B., Moons, D. S., Pandolfi, P. P., Hansel, K. S., Koff, A., and Kiyokawa, H. (1999). Targeted disruption of CDK4 delays cell cycle entry with enhanced p27(Kip1) activity. *Mol. Cell. Biol.* **19**, 7011–7019.

Verbruggen, V., Ek, O., Georlette, D., Delporte, F., Von Berg, V., Detry, N., Biemar, F., Coutinho, P., Martial, J. A., Voz, M. L., *et al.* (2010). The Pax6b homeodomain is dispensable for pancreatic endocrine cell differentiation in zebrafish. *J. Biol. Chem.* **285**, 13863–13873.

Wan, H., Korzh, S., Li, Z., Mudumana, S. P., Korzh, V., Jiang, Y. J., Lin, S., and Gong, Z. (2006). Analyses of pancreas development by generation of gfp transgenic zebrafish using an exocrine pancreas-specific elastaseA gene promoter. *Exp. Cell Res.* **312**, 1526–1539.

Ward, A. B., Warga, R. M., and Prince, V. E. (2007). Origin of the zebrafish endocrine and exocrine pancreas. *Dev. Dyn.* **236**, 1558–1569.

Wilkins, S. J., Yoong, S., Verkade, H., Mizoguchi, T., Plowman, S. J., Hancock, J. F., Kikuchi, Y., Heath, J. K., and Perkins, A. C. (2008). Mtx2 directs zebrafish morphogenetic movements during epiboly by regulating microfilament formation. *Dev. Biol.* **314**, 12–22.

Xu, X., D'Hoker, J., Stange, G., Bonne, S., De Leu, N., Xiao, X., Van de Casteele, M., Mellitzer, G., Ling, Z., Pipeleers, D., *et al.* (2008). Beta cells can be generated from endogenous progenitors in injured adult mouse pancreas. *Cell* **132**, 197–207.

Yee, N. S., Lorent, K., and Pack, M. (2005). Exocrine pancreas development in zebrafish. *Dev. Biol.* **284**, 84–101.

Yee, N. S., Yusuff, S., and Pack, M. (2001). Zebrafish pdx1 morphant displays defects in pancreas development and digestive organ chirality, and potentially identifies a multipotent pancreas progenitor cell. *Genesis* **30**, 137–140.

Zecchin, E., Filippi, A., Biemar, F., Tiso, N., Pauls, S., Ellertsdottir, E., Gnugge, L., Bortolussi, M., Driever, W., and Argenton, F. (2007). Distinct delta and jagged genes control sequential segregation of pancreatic cell types from precursor pools in zebrafish. *Dev. Biol.* **301**, 192–204.

Zorn, A. M., and Wells, J. M. (2007). Molecular basis of vertebrate endoderm development. *Int. Rev. Cytol.* **259**, 49–111.

# CHAPTER 11

# Monitoring Sleep and Arousal in Zebrafish

**Jason Rihel**[*], **David A. Prober**[†], *and* **Alexander F. Schier**[*,‡,§,¶]

[*]Department of Molecular and Cellular Biology, Harvard University, Cambridge, Massachusetts

[†]Division of Biology, California Institute of Technology, Pasadena, California

[‡]Division of Sleep Medicine, Harvard University, Cambridge, Massachusetts

[§]Center for Brain Science, Harvard University, Cambridge, Massachusetts

[¶]Harvard Stem Cell Institute, Harvard University, Cambridge, Massachusetts

---

I. Introduction
II. Behavior, Genetics, and Pharmacology of Zebrafish Sleep
    A. Behavior
    B. Genetics and Pharmacology
III. Methods for Monitoring Sleep/Wake Behavior in Zebrafish
    A. Methodological Considerations—from *Drosophila* to *Danio*
    B. Experimental Design and Setup
    C. Monitoring and Analysis of Sleep/Wake Behaviors
IV. Conclusion
References

## Abstract

Zebrafish has emerged in the past 5 years as a model for the study of sleep and wake behaviors. Experimental evidence has shown that periods of behavioral quiescence in zebrafish larvae and adults are sleep-like states, as these rest bouts are regulated by the circadian cycle, are associated with decreases in arousal, and are increased following rest deprivation. Furthermore, zebrafish share with mammals a hypocretin/orexin system that promotes wakefulness, and drugs that alter mammalian sleep have similar effects on zebrafish rest. In this chapter, we review the zebrafish sleep literature and describe a long-term, high-throughput monitoring system for observing sleep and wake behaviors in larval zebrafish.

Copyright © 2010 Elsevier Inc. All rights reserved.

978-0-12-384892-5
DOI: 10.1016/B978-0-12-384892-5.00011-6

## I. Introduction

Sleep is essential, time consuming, and conserved across the animal kingdom, yet it remains one of the major mysteries of biology. What is the function of sleep, and how is it regulated by genes and neurons? Since the discovery of characteristic electroencephalographic (EEG) signatures for states of sleep and waking in the late 1930s (Davis *et al.*, 1937), mammalian model systems have dominated sleep research. However, behavioral observations over the past decade have demonstrated that non-mammalian systems, including *Drosophila* (Hendricks *et al.*, 2000; Shaw *et al.*, 2000), *Caenorhabditis elegans* (Raizen *et al.*, 2008; Van Buskirk and Sternberg, 2007), and zebrafish (Prober *et al.*, 2006; Yokogawa *et al.*, 2007; Zhdanova *et al.*, 2001), have sleep-like states. These "simple" model systems allow researchers to bring large-scale genetics and *in vivo* imaging to bear on fundamental questions of sleep biology. Zebrafish is an attractive model because it combines the facile genetics of invertebrates with brains that are morphologically and molecularly analogous to mammals. In this chapter, we review the progress of sleep studies in zebrafish and discuss the high-throughput methods (Fig. 1) we have developed to study larval zebrafish sleep/wake behaviors.

## II. Behavior, Genetics, and Pharmacology of Zebrafish Sleep

### A. Behavior

Sleep is a period of reversible, inattentive behavioral quiescence that can be distinguished from quiet wakefulness using several behavioral criteria (Borbely and

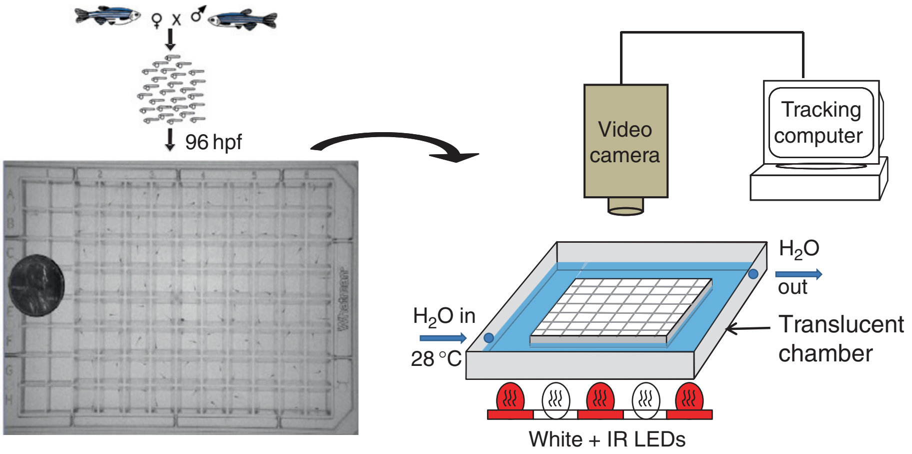

**Fig. 1** High-throughput tracking of zebrafish locomotor behavior. Zebrafish larvae older than 96 hpf are placed into a 96-well plate filled with blue water. The plate is then placed into a translucent chamber that is illuminated from the bottom continuously by infrared (IR) light emitting diodes (LEDs) and from 9:00 AM to 11:00 PM with white LEDs. Water heated to 28°C is pumped continuously through (water goes in and out of the chamber) the plate chamber to maintain temperature and humidity. The plate is observed by a video camera connected to a computer with video tracking software. The chamber, lights, and camera are housed inside a box (not shown) to prevent extraneous light from interfering with the experiment. Modified from Fig. 4 in Prober *et al.*, 2006.

Tobler, 1996; Campbell and Tobler, 1984; Cirelli, 2009). Sleep-like rest periods are typically associated with a species-specific posture and location, and are regulated in a circadian (about 24 h) manner (Borbely and Tobler, 1996). Importantly, sleep is associated with an increased arousal threshold in response to stimuli, although strong stimuli can still wake the animal (thereby distinguishing sleep from coma or stupor). Finally, sleep is thought to be under homeostatic control, such that depriving an animal of sleep results in a subsequent increase in the duration or intensity of sleep, known as sleep rebound (Borbely and Tobler, 1996). Using automated tracking systems to observe individual animals for several days (see Section III), a variety of non-mammalian model systems, including fruit flies (Hendricks *et al*., 2000; Shaw *et al*., 2000), *C. elegans* (Raizen *et al*., 2008; Van Buskirk and Sternberg, 2007), and both larval (Prober *et al*., 2006; Zhdanova *et al*., 2001) and adult zebrafish (Yokogawa *et al*., 2007), have been shown to exhibit sleep-like states that meet these behavioral criteria.

### 1. Criterion 1—Quiescent Behavior Regulated by an Endogenous Circadian Rhythm

Zebrafish larvae first exhibit active spontaneous locomotor activity around 96 h post fertilization (hpf), shortly after inflation of the swim bladder (Hurd and Cahill, 2002; Prober *et al*., 2006). When maintained on a 14 h:10 h light:dark cycle, these swim bouts occur maximally during the lights-on phase and are tightly synchronized with the light stimulus (Fig. 2A). If raised on a light:dark cycle and then transferred to constant dark conditions, the spontaneous locomotor activity of >96 hpf larvae and adults continues to cycle with a circadian rhythm of ~25–25.5 h, with the phase set by the prior entraining light:dark cycle (Hurd and Cahill, 2002; Hurd *et al*., 1998). These observations demonstrate that zebrafish have an endogenously controlled circadian rhythm behavior that can be entrained by light. Consistent with the behavioral observations, rhythmic components of the molecular machinery that controls circadian rhythms in *Drosophila* and mammals also exhibit rhythmic expression with a light-entrainable circadian period in zebrafish. Such genes include the zebrafish orthologs of *Period1* (Dekens and Whitmore, 2008), *Period3* (Kaneko and Cahill, 2005; Pando *et al*., 2001), *Clock* (Whitmore *et al*., 1998), *Cryptochrome* (Kobayashi *et al*., 2000), and the clock-binding partner *Bmal* (Cermakian *et al*., 2000).

### 2. Criterion 2—Increased Arousal Threshold/Decreased Responsiveness during Quiescence

Throughout the 24 h light:dark cycle, zebrafish larvae exhibit bouts of quiescence that can last for several minutes or longer (Fig. 2B and C) and that occur maximally at night. During these quiescent periods, both zebrafish larvae and adults have an accompanying increase in arousal threshold, as measured by a decreased responsiveness of larvae to taps at night versus the day (Zhdanova *et al*., 2001), an increase in response time to large changes in light intensity (Prober *et al*., 2006), or a decreased responsiveness to electrical stimuli in adults (Yokogawa *et al*., 2007). By correlating the length of a quiescent bout with the concomitant change in arousal state, sleep is defined as a quiescent bout lasting at least 1 min in larvae and at least 6 s in adults. This definition of a sleep-like state has served well in the analysis of molecules that regulate sleep and has been effective in uncovering conserved pathways (see Section II-B). The definition can now be refined by testing changes in arousal across multiple sensory modalities,

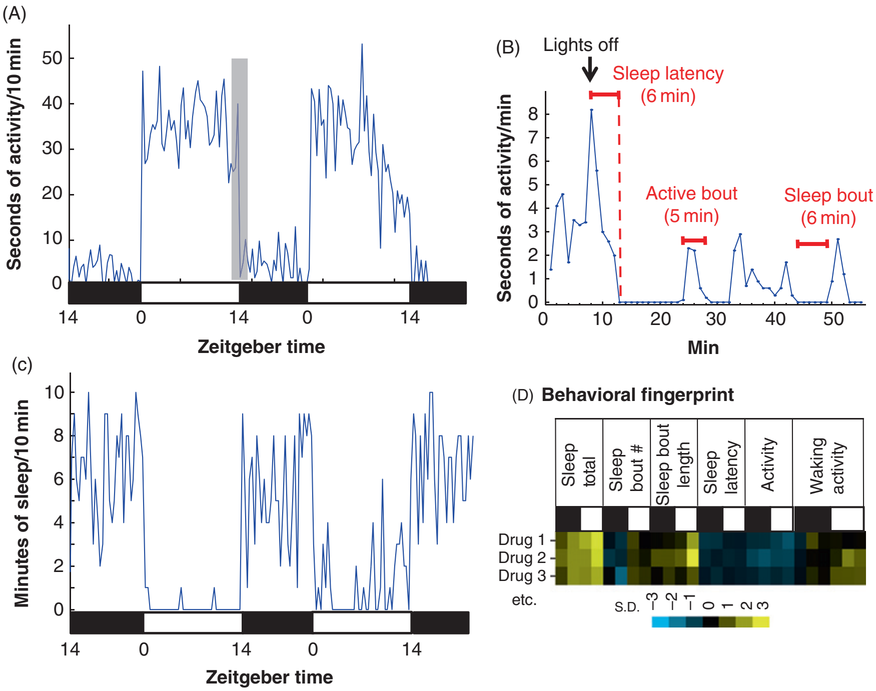

**Fig. 2** Zebrafish sleep/wake data. (A) The average activity of a single wild type larva is plotted per 10 min for two light:dark cycles starting at ~110 hpf. Activity occurs maximally during each day period. The gray area is expanded in (B). Zeitgeber time 0 = lights on; 14 = lights off. (B) The average activity of the same fish in (A) (gray area), expanded and replotted per 1 min. Examples of sleep latency, sleep bout, sleep bout length, active bout, and active bout length are indicated. (C) The behavior of the same fish shown in (A) and (B), plotted as minutes of sleep per 10 min. Sleep occurs maximally during each night period. (D) By normalizing each behavioral parameter to wild type controls, the data can be transformed into a behavioral fingerprint. Each square of the fingerprint represents the average relative value in standard deviations (black, higher than controls; white, lower than controls) for a single behavioral measurement. The black and white bars across the top represent night and day measurements, respectively. In this example, fingerprints are shown for three different drugs that increase sleep bout lengths, leading to increased total sleep.

experimental conditions, and behavioral situations, including a detailed analysis of changes in arousal states during different times of the day and night. For example, a recent report notes that larval respiration rate is reduced and arousal threshold elevated in nighttime rest compared to daytime rest (Zhdanova, 2006), indicating that these two quiescent states may not be equivalent. We also observe changes in average sleep bout length and in waking activity (see section III.C for details) during the day and night that may reflect underlying differences between these states (Table I).

### 3. Criterion 3—Sleep Rebound Following Sleep Deprivation (Homeostatic Regulation of Sleep)

Two studies have demonstrated an increase in total sleep amount in larval and adult zebrafish following nighttime sleep deprivation. Zhdanova and colleagues used a

**TABLE I**
**Typical Sleep/Wake Measures Obtained from Wild Type Larvae (TLAB × TLAB Cross) in a 14 h:10 h Light:Dark Cycle**

| | Mean | (± SD) | Median |
|---|---|---|---|
| TOTAL SLEEP (minutes) | | | |
| Day 6 | 189 | 138 | 135 |
| Day 7 | 110 | 127 | 60 |
| Night 6 | 252 | 125 | 240 |
| Night 7 | 219 | 118 | 202 |
| # SLEEP BOUTS | | | |
| Day 6 | 29 | 21 | 24 |
| Day 7 | 37 | 34 | 26 |
| Night 6 | 58 | 23 | 57 |
| Night 7 | 64 | 20 | 63 |
| SLEEP LENGTH (minutes) | | | |
| Day 6 | 7.7 | 5.4 | 6.6 |
| Day 7 | 2.8 | 1.9 | 2.3 |
| Night 6 | 4.5 | 2.8 | 3.9 |
| Night 7 | 3.5 | 2.4 | 3.1 |
| SLEEP LATENCY (minutes) | | | |
| Day 6 | 24.8 | 70.6 | 4 |
| Day 7 | 59.2 | 147.0 | 7 |
| Night 6 | 21.2 | 28.0 | 13 |
| Night 7 | 19.6 | 27.0 | 14 |
| AVERAGE ACTIVITY (seconds/minute) | | | |
| Day 6 | 4.04 | 1.88 | 3.90 |
| Day 7 | 4.18 | 1.95 | 4.00 |
| Night 6 | 0.85 | 0.46 | 0.78 |
| Night 7 | 0.85 | 0.42 | 0.79 |
| WAKING ACTIVITY (seconds/minute) | | | |
| Day 6 | 5.01 | 1.67 | 4.80 |
| Day 7 | 4.58 | 1.88 | 4.30 |
| Night 6 | 1.29 | 0.50 | 1.21 |
| Night 7 | 1.21 | 0.41 | 1.19 |

$n = 321$; 14 h Day, 10 h Night
Each parameter (±SD) was calculated from the behavioral data of 321 wild type larvae. Day 6 starts at 120 hpf, and night 6 starts at 134 hpf. Day 7 starts at 144 hpf, and night 7 starts at 158 hpf. Sleep latency at night is calculated as the time from lights out to the first sleep bout; sleep latency during the day is calculated as the time from lights on to the first sleep bout.

mechanical shaker to deprive larvae of rest during the day and the night and found that night time deprivation decreased subsequent larval locomotor activity more than day time deprivation (Zhdanova *et al*., 2001). Furthermore, following nighttime sleep deprivation, the larvae had an increased arousal threshold response to a tap stimulus. Together, these data suggest that nighttime deprivation causes a sleep rebound in both the amount and the depth of sleep. However, the decrease in general locomotion may indicate that the mechanical deprivation had caused some harm or stress. A long-term behavioral assessment demonstrating a return to baseline activity levels would help clarify this point. Furthermore, it is unclear whether the arousal threshold changes occurred specifically during times of sleep-like states (see Section II-A, criterion 2). Large changes in arousal states during waking activity may also be an indicator of poor health. In another study, adult zebrafish were deprived of rest for 6 h with either electric shocks or light (Yokogawa *et al.*, 2007). Shock-induced deprivation at night resulted only in a modest rebound in total sleep relative to yoked controls; changes in arousal threshold following deprivation were not examined. Curiously, light-induced deprivation resulted in no observed sleep rebound, which may reflect a strong masking effect of light or the effect of light on the circadian rhythm in zebrafish.

Although these results are encouraging, much more work needs to be done to firmly establish that rest is under homeostatic control in zebrafish. In particular, it remains to be demonstrated that either the depth or duration of sleep rebound increases with increasing amounts of sleep deprivation. Also underexplored are the behavioral consequences of short- and long-term sleep deprivation, including the time course of the return to normal sleep patterns and altered performance in behavioral tasks (see Zhdanova, 2006). Finally, rebound sleep following short-term exposure to arousing drugs or genetic manipulations that dramatically reduce total sleep (see Section II-B) should also be investigated, as these treatments may represent less invasive and more reproducible methods for sleep deprivation.

## B. Genetics and Pharmacology

Genetic and pharmacological experiments in zebrafish indicate that mechanisms that regulate mammalian sleep are conserved in zebrafish. Of these, the most studied is the hypocretin/orexin (Hcrt) system, which has been shown to increase wakefulness in mammals (Sakurai, 2007). Hcrt peptide is produced by a population of hypothalamic neurons that project throughout the brain, particularly to other known wake-promoting centers (Peyron *et al.*, 1998). Deficiency in Hcrt signaling can be caused by loss-of-function mutations in the peptide (Chemelli *et al.*, 1999) or its receptors (Lin *et al.*, 1999; Willie *et al.*, 2003) or by a selective loss of Hcrt-producing neurons (Hara *et al.*, 2001; Peyron *et al.*, 2000; Thannickal *et al.*, 2000). In mammals, loss of Hcrt signaling leads to narcolepsy, a disease characterized by excessive daytime sleepiness, unstable sleep/wake states, and sudden loss of muscle tone during waking. Larval and adult zebrafish express their single *hcrt* ortholog in a small number of hypothalamic neurons that project to putative wake-promoting centers of the brain and down the spinal cord, regions that also express the single *hcrt* receptor (Appelbaum *et al.*, 2009; Faraco *et al.*, 2006; Kaslin *et al.*, 2004; Prober *et al.*, 2006). As expected for a wake-promoting peptide, overexpression of *hcrt* in larval zebrafish leads to increased wakefulness at the expense of rest (Prober *et al.*, 2006). Furthermore, *in vivo* observation of Hcrt neural activity using the bioluminescent reporter GFP-Aequorin reveals that they are maximally active during episodes of spontaneous locomotor activity and inactive during rest (Naumann *et al.*, 2010), consistent with results obtained in mammals (Lee *et al.*, 2005; Mileykovskiy *et al.*, 2005). Finally, adult zebrafish with mutations in the Hcrt receptor exhibit sleep fragmentation (Yokogawa *et al.*, 2007), another hallmark of narcolepsy (Mochizuki *et al*., 2004; Overeem *et al*., 2001). Taken together, these data confirm that at least some aspects of Hcrt's regulatory role in sleep/wake behavior are preserved in zebrafish.

There are some discrepancies between the Hcrt data obtained in larvae and adults that should be noted. Paradoxically, Hcrt receptor mutant adults were reported to have a small decrease in sleep at night and to be slightly hyperactive at night, although the latter effect was only significant compared to unrelated non-mutagenized wild type animals (Yokogawa *et al*., 2007). These effects were not seen in Hcrt receptor mutant larvae under constant dim light conditions (Appelbaum *et al*., 2009). In addition, some behavioral effects (e.g., hypoactivity and increased sleep in constant dark) appear only in Hcrt receptor heterozygotes (Yokogawa *et al*., 2007). The reasons for these discrepancies are unclear but might include background mutations or the small number of adults that were analyzed. In addition, injection of a very high dose (280–2800 pmol/g body weight) of Hcrt peptide into adult zebrafish brains led to a slight decrease in activity (Yokogawa *et al*., 2007). This observation contrasts with the long-term and strong increase in wakefulness following Hcrt overexpression in zebrafish larvae (Prober *et al*., 2006) and the arousing effects of moderate levels (2.8–28 pmol/g body weight) of Hcrt peptide injected into adult goldfish (Nakamachi *et al*., 2006). Additional genetic studies and more extensive behavioral analyses will be needed to resolve these discrepancies. Currently, the preponderance of evidence indicates that Hcrt has arousing effects in teleosts, and that loss of Hcrt receptor in adults leads to fragmented sleep/wake states, as in mammals.

Other evidence for the conservation of sleep-regulatory mechanisms in zebrafish comes from pharmacological studies. Tests of known sedative and hypnotic compounds, including the hormone melatonin (Zhdanova *et al*., 2001), the GABA receptor agonists baclofen, phenobarbital, and diazepam (Renier *et al*., 2007; Zhdanova *et al*., 2001), and the alpha-2 adrenergic receptor agonist clonidine (Ruuskanen *et al*., 2005), demonstrated that these compounds dose-dependently decrease locomotor activity and increase rest in zebrafish larvae 2–3 h following drug treatment. We have confirmed and extended these results through an unbiased screen of the long-term (3 days) effects of nearly 4000 small molecules on larval zebrafish sleep/wake behaviors. We found that many modulators of neurotransmitter systems, including the noradrenaline, serotonin, dopamine, GABA, glutamate, histamine, adenosine, and melatonin systems, induce similar sleep/wake phenotypes in zebrafish as observed in mammals (Rihel *et al*., 2010).

Overall, the behavioral, genetic, and pharmacological evidence indicates that a sleep-like state exists in both larval and adult zebrafish and that this state is regulated by mechanisms that are conserved among vertebrates. Now that the conceptual groundwork for studying sleep in zebrafish has been established, future screens and experiments can begin to dissect novel mechanisms of sleep/wake regulation in earnest. Indeed, the pharmacological screen has already identified several pathways, including the ether-a-go-go related gene (ERG) potassium channel, verapamil-sensitive L-type calcium channels, and the immunomodulatory nuclear factor of activated T cells (NFAT) and nuclear factor kappa B (NF-$\kappa$B) pathways, as targets for future zebrafish sleep/wake studies (Rihel *et al*., 2010).

## III. Methods for Monitoring Sleep/Wake Behavior in Zebrafish

### A. Methodological Considerations—from *Drosophila* to *Danio*

Two major methods have been used to track locomotor behavior of animals, either by counting the number of times an animal breaks an infrared beam or by direct analysis of movements captured by video. Pioneering work on circadian rhythms (Konopka and Benzer, 1971) and sleep (Hendricks *et al.*, 2000; Shaw *et al.*, 2000) in *Drosophila* predominantly used the infrared beam break method, which measures when the fly crosses an infrared beam in the center of a tube. Some work on zebrafish (Hurd *et al.*, 1998) and goldfish (Azpeleta *et al.*, 2010; Iigo and Tabata, 1996; Vera *et al.*, 2007) also used this method to assess locomotion. Although useful for low time-resolution analysis of circadian rhythms, the beam break method suffers from blind spots, where an animal may move without crossing the beam. Indeed, a direct comparison of results from infrared beam breaks to direct video recording suggests that the beam break method can overestimate total sleep in flies by 10–90% (Zimmerman *et al.*, 2008). More fine-scale measures of sleep structure, including sleep latency, sleep bout number, and sleep bout length (see Section III-C for descriptions of these measures), can be even more dramatically overestimated (Zimmerman *et al.*, 2008). In addition, to obtain an accurate assessment of these important sleep parameters, individual animals must be tracked unambiguously throughout the experiment. Because sleep bouts occur non-simultaneously among individuals, methods that average activity across a population of animals lack details of sleep architecture. While methods that allow for the simultaneous and unambiguous tracking of animals within the same arena are under development (Branson *et al.*, 2009; Grover *et al.*, 2009; Kato *et al.*, 2004; Straw *et al.*, 2010), most available methods require animals to be individually housed.

There are a growing number of methods for automated detection of zebrafish locomotion using video-based analysis. These include commercially available zebrafish tracking systems from Noldus Information Technology (http://www.noldus.com) and Viewpoint Life Sciences, Inc. (http://www.vplsi.com) as well as custom algorithms designed for the analysis of short-term responses to stimuli captured by a high-speed camera (e.g., Burgess and Granato, 2007; Fontaine *et al.*, 2008). To simultaneously observe hundreds of animals over several days with minimal user input, we use a relatively simple frame-by-frame background subtraction method within an analysis suite from Viewpoint Life Sciences. We find that counting pixel changes per frame at a low frame rate (15 frames per second) gives a reliable readout of the timing and duration of each larva's locomotor activity and rest for days or weeks of continuous behavioral recording.

### B. Experimental Design and Setup

Because sleep behavior can be strongly influenced by prior environmental conditions and experiences (Ganguly-Fitzgerald *et al.*, 2006 and personal observation), the conditions for raising larvae prior to behavioral testing must be rigorously maintained. Following fertilization, embryos and larvae are raised from a single cell on a 14 h:10 h light:dark (LD) cycle at 28°C in petri dishes with conventional embryo water at a density of no more than 50 larvae per 100 mm dish. If the effect of a mutation or a transgene (e.g., heat shock driving Hcrt overexpression; Prober *et al.*, 2006) on behavior is being tested, all comparisons are ideally done within the same clutch or batch, raised in the same petri dish, and not pre-sorted by genotype. Each day, the dishes are cleared of any sick larvae, water levels are readjusted as necessary, and the chorions are removed post hatching.

Between 96 and 110 hpf, single larvae are placed into each well of a flat-bottom, square-well 96-well plate (650 µl well volume, Whatman) filled with embryo blue water. For the best optical properties, each well is filled so that the meniscus is flat and nearly flush with the top of the well. To test the long-term behavioral effects of small molecules, drugs may be added directly to the wells at this time by pipetting compound dissolved in DMSO. Usually the desired final concentration of drug in each well is between 100 nM and 1 mM, and the final DMSO concentration should not exceed 1% (above this level, DMSO can have behavioral consequences).

The 96-well plate is then placed into the zebrafish tracking setup (custom modified from Viewpoint Life Sciences; see Fig. 1). Inside a box, the plate chamber is illuminated continuously with an infrared LED panel and from 9:00 AM to 11:00 PM with white LEDs. The plate is monitored by a video camera (Dinion one-third inch Monochrome Bosch camera) fitted with a fixed-angle megapixel lens (50 mm focal length; Computar) and a filter that transmits infrared light. To slightly humidify the box and maintain a constant temperature, distilled water heated to 28°C is continuously pumped through the plate chamber. Embryo water is added daily to each well to maintain high water levels. Although the larvae need not be fed until the 7th day of development, paramecia can also be added to each well daily (they will not be detected by the software). By adding paramecia to the wells, we have monitored larvae in the same 96-well plate continuously from day 4 to day 14 of development without a noticeable decline in health (JR, unpublished data). Older animals can be monitored in plates with larger well sizes (e.g., 6-, 12-, and 24-well plates).

## C. Monitoring and Analysis of Sleep/Wake Behaviors

To collect the movement data from each larva in the 96-well plate, we use Viewpoint Life Sciences Videotrack software running in the quantization mode. In this software package, a detection threshold is set to distinguish the dark fish from the white background (in our setup, the threshold is 40, although this value depends on the infrared lighting used). For each camera frame, any pixels darker than this threshold that change are detected as a movement and stored in a raw data file as pixels changed per frame for each larva. These data are further processed by setting a threshold value for the number of pixels that must change to constitute larval movement instead of random pixel noise (the “freeze” threshold; for our experimental setups, a cutoff of 4 pixels). The data are then converted into total seconds spent moving per minute for each larva by summing the total time of pixel changes that exceed the threshold. A sample 56 h activity trace from a single fish is plotted in Fig. 2A.

From the activity data of each larva, we use custom-designed Matlab code to extract multiple additional parameters that measure the amount and structure of sleep for each day and night (Fig. 2B and Table I).

### 1. Total Sleep

We define sleep in larval zebrafish as a continuous period of inactivity that lasts at least 1 min, because 1 min of inactivity at night is associated with increased response latencies to changes in light intensity (Prober *et al*., 2006). We measure the total sleep for each day and night period and plot the average sleep per 10 min to generate a sleep time course (Fig. 2C). Based on recent wild type data from our lab ($n = 321$ animals, TLAB × TLAB cross), zebrafish larvae sleep at night on average 235 min each 10 h night (23.5 min/h), but individual larvae can vary considerably from this value (Table I).

### 2. Sleep Bout Number and Sleep Bout Length

A sleep bout is defined as a continuous period of inactivity lasting 1 min or longer (see Fig. 2B). Because each larva has numerous sleep bouts that are interrupted by brief awakenings, plotting the sleep bout length distribution for each larva can also be useful. At night, larvae have on average 61 sleep bouts, with each bout lasting an average of 4 min (Table I).

### 3. Sleep Latency

Sleep latency is defined as the amount of time from the start of each day and night period until the first sleep bout (see Fig. 2B). Following lights out, wild type (TLAB × TLAB cross) larvae have sleep latencies at night averaging about 20 min (Table I).

### 4. Average Activity per Waking Minute

Changes in a larva's locomotor behavior could be due to perturbations in muscle control and coordination, altered stress or arousal state, or other general health deficits. For example, an unhealthy larva with increased sleep may also move considerably less during active swimming. By measuring the average activity only during bouts of waking activity, we can assess whether the overall health and swimming ability of the fish have been compromised. Average activity per waking minute is calculated for each day and night period by summing the total activity and dividing by the number of active minutes (total active minutes = total time - total sleep time). This measure can also be used to determine whether an experimental perturbation causes a larva to be hyperactive when awake. In our experimental apparatus, wild type larvae have an average waking activity of 4.8 s per minute during the day and 1.3 s per minute at night (Table I).

These measures of sleep structure are biologically important, providing information about the initiation, maintenance, and timing of sleep. Given that these parameters can be selectively perturbed by pharmacological agents (Rihel *et al*., 2010), they are likely controlled by at least partially independent regulatory mechanisms. These parameters can be presented as a multi-dimensional "behavioral fingerprint" to facilitate comparisons among multiple genotypes, experimental manipulations, or small molecules. Each measurement is normalized to matched controls and then combined to create a vector that accounts for all of the parameters (see Fig. 2D; Rihel *et al*., 2010). Clustering algorithms and principal component analyses can be used to organize large datasets by phenotype and to uncover small molecules or genotypes that have similar effects across multiple zebrafish sleep/wake behavioral parameters.

## IV. Conclusion

Only a decade old, the study of sleep in non-mammalian systems is still in its infancy. While early zebrafish sleep studies have focused on establishing the existence of behavioral sleep regulated by conserved mechanisms, the challenge ahead is to use the zebrafish sleep model to uncover heretofore unsuspected aspects of the neuronal and genetic control of sleep/wake regulation. Recent studies that potentially link Hcrt signaling to pineal gland regulation (Appelbaum *et al*., 2009) and that uncover novel small molecule regulators of sleep/wake states (Rihel *et al*., 2010) may represent two such discoveries.

A major advantage of the zebrafish system is the ability to efficiently perform genetic and pharmacological screens in a cost-, space-, and labor-effective manner. With this in mind, we have described an automated high-throughput method for observing long-term sleep/wake behavior in larval zebrafish. This methodology is highly flexible and can easily be adapted to other behaviors, for example to observe larval responses to temperature, vibration, noxious chemicals, and changes in light intensity (Emran *et al*., 2007, 2008, 2010; Prober *et al*., 2008). In principle, the behavioral space of future screens could be expanded by testing these and other behavioral modalities in conjunction with long-term sleep/wake behavioral monitoring, incorporating all the data into a single multi-dimensional behavioral fingerprint. Such screens could not only uncover novel mutants that affect specific behaviors but also identify correlated sets of behaviors that are regulated by similar underlying mechanisms. With new techniques to directly observe neural activity in behaving zebrafish, including neuroluminescence, whole-brain calcium imaging, and optogenetic techniques to manipulate the activity of neurons with light, future studies will also begin to directly elucidate the activities and functions of neural circuits that underlie sleep/wake behaviors.

## References

Appelbaum, L., Wang, G. X., Maro, G. S., Mori, R., Tovin, A., Marin, W., Yokogawa, T., Kawakami, K., Smith, S. J., Gothilf, Y., Mignot, E., and Mourrain, P. (2009). Sleep–wake regulation and hypocretin–melatonin interaction in zebrafish. *Proc. Natl. Acad. Sci. U. S. A.* **106**, 21942–21947.

Azpeleta, C., Martinez-Alvarez, R. M., Delgado, M. J., Isorna, E., and De Pedro, N. (2010). Melatonin reduces locomotor activity and circulating cortisol in goldfish. *Horm. Behav.* **57**, 323–329.

Borbely, A. A., and Tobler, I. (1996). Sleep regulation: Relation to photoperiod, sleep duration, waking activity, and torpor. *Prog. Brain Res.* **111**, 343–348.

Branson, K., Robie, A. A., Bender, J., Perona, P., and Dickinson, M. H. (2009). High-throughput ethomics in large groups of *Drosophila*. *Nat. Methods* **6**, 451–457.

Burgess, H. A., and Granato, M. (2007). Modulation of locomotor activity in larval zebrafish during light adaptation. *J. Exp. Biol.* **210**, 2526–2539.

Campbell, S. S., and Tobler, I. (1984). Animal sleep: A review of sleep duration across phylogeny. *Neurosci. Biobehav. Rev.* **8**, 269–300.

Cermakian, N., Whitmore, D., Foulkes, N. S., and Sassone-Corsi, P. (2000). Asynchronous oscillations of two zebrafish CLOCK partners reveal differential clock control and function. *Proc. Natl. Acad. Sci. U. S. A.* **97**, 4339–4344.

Chemelli, R. M., Willie, J. T., Sinton, C. M., Elmquist, J. K., Scammell, T., Lee, C., Richardson, J. A., Williams, S. C., Xiong, Y., Kisanuki, Y., et al. (1999). Narcolepsy in orexin knockout mice: Molecular genetics of sleep regulation. *Cell* **98**, 437–451.

Cirelli, C. (2009). The genetic and molecular regulation of sleep: From fruit flies to humans. *Nat. Rev. Neurosci.* **10**, 549–560.

Davis, H., Davis, P. A., Loomis, A. L., Harvey, E. N., and Hobart, G. (1937). Changes in human brain potentials during the onset of sleep. *Science* **86**, 448–450.

Dekens, M. P., and Whitmore, D. (2008). Autonomous onset of the circadian clock in the zebrafish embryo. *EMBO J.* **27**, 2757–2765.

Emran, F., Rihel, J., Adolph, A. R., and Dowling, J. E. (2010). Zebrafish larvae lose vision at night. *Proc. Natl. Acad. Sci. U. S. A.* **107**, 6034–6039.

Emran, F., Rihel, J., Adolph, A. R., Wong, K. Y., Kraves, S., and Dowling, J. E. (2007). OFF ganglion cells cannot drive the optokinetic reflex in zebrafish. *Proc. Natl. Acad. Sci. U. S. A.* **104**, 19126–19131.

Emran, F., Rihel, J., and Dowling, J. E. (2008). A behavioral assay to measure responsiveness of zebrafish to changes in light intensities. *J. Vis. Exp* **20**, http://www.jove.com/index/details.stp?id=923, doi: 10.3791/923.

Faraco, J. H., Appelbaum, L., Marin, W., Gaus, S. E., Mourrain, P., and Mignot, E. (2006). Regulation of hypocretin (orexin) expression in embryonic zebrafish. *J. Biol. Chem.* **281**, 29753–29761.

Fontaine, E., Lentink, D., Kranenbarg, S., Muller, U. K., van Leeuwen, J. L., Barr, A. H., and Burdick, J. W. (2008). Automated visual tracking for studying the ontogeny of zebrafish swimming. *J. Exp. Biol.* **211**, 1305–1316.

Ganguly-Fitzgerald, I., Donlea, J., and Shaw, P. J. (2006). Waking experience affects sleep need in *Drosophila*. *Science* **313**, 1775–1781.

Grover, D., Yang, J., Ford, D., Tavare, S., and Tower, J. (2009). Simultaneous tracking of movement and gene expression in multiple *Drosophila melanogaster* flies using GFP and DsRED fluorescent reporter transgenes. *BMC Res. Notes* **2**, 58.

Hara, J., Beuckmann, C. T., Nambu, T., Willie, J. T., Chemelli, R. M., Sinton, C. M., Sugiyama, F., Yagami, K., Goto, K., Yanagisawa, M., and Sakurai, T. (2001). Genetic ablation of orexin neurons in mice results in narcolepsy, hypophagia, and obesity. *Neuron* **30**, 345–354.

Hendricks, J. C., Finn, S. M., Panckeri, K. A., Chavkin, J., Williams, J. A., Sehgal, A., and Pack, A. I. (2000). Rest in *Drosophila* is a sleep-like state. *Neuron* **25**, 129–138.

Hurd, M. W., and Cahill, G. M. (2002). Entraining signals initiate behavioral circadian rhythmicity in larval zebrafish. *J. Biol. Rhythms* **17**, 307–314.

Hurd, M. W., Debruyne, J., Straume, M., and Cahill, G. M. (1998). Circadian rhythms of locomotor activity in zebrafish. *Physiol. Behav.* **65**, 465–472.

Iigo, M., and Tabata, M. (1996). Circadian rhythms of locomotor activity in the goldfish *Carassius auratus*. *Physiol. Behav.* **60**, 775–781.

Kaneko, M., and Cahill, G. M. (2005). Light-dependent development of circadian gene expression in transgenic zebrafish. *PLoS Biol.* **3**, e34.

Kaslin, J., Nystedt, J. M., Ostergard, M., Peitsaro, N., and Panula, P. (2004). The orexin/hypocretin system in zebrafish is connected to the aminergic and cholinergic systems. *J. Neurosci.* **24**, 2678–2689.

Kato, S., Nakagawa, T., Ohkawa, M., Muramoto, K., Oyama, O., Watanabe, A., Nakashima, H., Nemoto, T., and Sugitani, K. (2004). A computer image processing system for quantification of zebrafish behavior. *J. Neurosci. Methods* **134**, 1–7.

Kobayashi, Y., Ishikawa, T., Hirayama, J., Daiyasu, H., Kanai, S., Toh, H., Fukuda, I., Tsujimura, T., Terada, N., Kamei, Y., Yuba, S., Iwai, S., et al. (2000). Molecular analysis of zebrafish photolyase/cryptochrome family: Two types of cryptochromes present in zebrafish. *Genes Cells* **5**, 725–738.

Konopka, R. J., and Benzer, S. (1971). Clock mutants of *Drosophila melanogaster*. *Proc. Natl. Acad. Sci. U. S. A.* **68**, 2112–2116.

Lee, M. G., Hassani, O. K., and Jones, B. E. (2005). Discharge of identified orexin/hypocretin neurons across the sleep–waking cycle. *J. Neurosci.* **25**, 6716–6720.

Lin, L., Faraco, J., Li, R., Kadotani, H., Rogers, W., Lin, X., Qiu, X., de Jong, P. J., Nishino, S., and Mignot, E. (1999). The sleep disorder canine narcolepsy is caused by a mutation in the hypocretin (orexin) receptor 2 gene. *Cell* **98**, 365–376.

Mileykovskiy, B. Y., Kiyashchenko, L. I., and Siegel, J. M. (2005). Behavioral correlates of activity in identified hypocretin/orexin neurons. *Neuron* **46**, 787–798.

Mochizuki, T., Crocker, A., McCormack, S., Yanagisawa, M., Sakurai, T., and Scammell, T. E. (2004). Behavioral state instability in orexin knock-out mice. *J. Neurosci.* **24**, 6291–6300.

Nakamachi, T., Matsuda, K., Maruyama, K., Miura, T., Uchiyama, M., Funahashi, H., Sakurai, T., and Shioda, S. (2006). Regulation by orexin of feeding behaviour and locomotor activity in the goldfish. *J. Neuroendocrinol.* **18**, 290–297.

Naumann, E. A., Kampff, A. R., Prober, D. A., Schier, A. F., and Engert, F. (2010). Monitoring neural activity with bioluminescence during natural behavior. *Nat. Neurosci.* **13**, 513–520.

Overeem, S., Mignot, E., van Dijk, J. G., and Lammers, G. J. (2001). Narcolepsy: Clinical features, new pathophysiologic insights, and future perspectives. *J. Clin. Neurophysiol.* **18**, 78–105.

Pando, M. P., Pinchak, A. B., Cermakian, N., and Sassone-Corsi, P. (2001). A cell-based system that recapitulates the dynamic light-dependent regulation of the vertebrate clock. *Proc. Natl. Acad. Sci. U. S. A.* **98**, 10178–10183.

Peyron, C., Faraco, J., Rogers, W., Ripley, B., Overeem, S., Charnay, Y., Nevsimalova, S., Aldrich, M., Reynolds, D., Albin, R., Li, R., Hungs, M., et al. (2000). A mutation in a case of early onset narcolepsy and a generalized absence of hypocretin peptides in human narcoleptic brains. *Nat. Med.* **6**, 991–997.

Peyron, C., Tighe, D. K., van den Pol, A. N., de Lecea, L., Heller, H. C., Sutcliffe, J. G., and Kilduff, T. S. (1998). Neurons containing hypocretin (orexin) project to multiple neuronal systems. *J. Neurosci.* **18**, 9996–10015.

Prober, D. A., Rihel, J., Onah, A. A., Sung, R. J., and Schier, A. F. (2006). Hypocretin/orexin overexpression induces an insomnia-like phenotype in zebrafish. *J. Neurosci.* **26**, 13400–13410.

Prober, D. A., Zimmerman, S., Myers, B. R., McDermott, B. M. Jr., Kim, S. H., Caron, S., Rihel, J., Solnica-Krezel, L., Julius, D., Hudspeth, A. J., and Schier. A. F. (2008). Zebrafish TRPA1 channels are required for chemosensation but not for thermosensation or mechanosensory hair cell function. *J. Neurosci.* **28**, 10102–10110.

Raizen, D. M., Zimmerman, J. E., Maycock, M. H., Ta, U. D., You, Y. J., Sundaram, M. V., and Pack, A. I. (2008). Lethargus is a *Caenorhabditis elegans* sleep-like state. *Nature* **451**, 569–572.

Renier, C., Faraco, J. H., Bourgin, P., Motley, T., Bonaventure, P., Rosa, F., and Mignot, E. (2007). Genomic and functional conservation of sedative-hypnotic targets in the zebrafish. *Pharmacogenet. Genomics* **17**, 237–253.

Rihel, J., Prober, D. A., Arvanites, A., Lam, K., Zimmerman, S., Jang, S., Haggarty, S. J., Kokel, D., Rubin, L. L., Peterson, R. T., and Schier., A. F. (2010). Zebrafish behavioral profiling links drugs to biological targets and rest/wake regulation. *Science* **327**, 348–351.

Ruuskanen, J. O., Peitsaro, N., Kaslin, J. V., Panula, P., and Scheinin, M. (2005). Expression and function of alpha-adrenoceptors in zebrafish: Drug effects, mRNA and receptor distributions. *J. Neurochem.* **94**, 1559–1569.

Sakurai, T. (2007). The neural circuit of orexin (hypocretin): Maintaining sleep and wakefulness. *Nat. Rev. Neurosci.* **8**, 171–181.

Shaw, P. J., Cirelli, C., Greenspan, R. J., and Tononi, G. (2000). Correlates of sleep and waking in *Drosophila melanogaster*. *Science* **287**, 1834–1837.

Straw, A. D., Branson, K., Neumann, T. R., and Dickinson, M. H. (2010). Multi-camera real-time three-dimensional tracking of multiple flying animals. *J. R. Soc. Interface*, doi:10.1098/rsif.2010.0230.

Thannickal, T. C., Moore, R. Y., Nienhuis, R., Ramanathan, L., Gulyani, S., Aldrich, M., Cornford, M., and Siegel, J. M. (2000). Reduced number of hypocretin neurons in human narcolepsy. *Neuron* **27**, 469–474.

Van Buskirk, C., and Sternberg, P. W. (2007). Epidermal growth factor signaling induces behavioral quiescence in *Caenorhabditis elegans*. *Nat. Neurosci.* **10**, 1300–1307.

Vera, L. M., De Pedro, N., Gomez-Milan, E., Delgado, M. J., Sanchez-Muros, M. J., Madrid, J. A., and Sanchez-Vazquez, F. J. (2007). Feeding entrainment of locomotor activity rhythms, digestive enzymes and neuroendocrine factors in goldfish. *Physiol. Behav.* **90**, 518–524.

Whitmore, D., Foulkes, N. S., Strahle, U., and Sassone-Corsi, P. (1998). Zebrafish Clock rhythmic expression reveals independent peripheral circadian oscillators. *Nat. Neurosci.* **1**, 701–707.

Willie, J. T., Chemelli, R. M., Sinton, C. M., Tokita, S., Williams, S. C., Kisanuki, Y. Y., Marcus, J. N., Lee, C., Elmquist, J. K., Kohlmeier, K. A., Leonard, C. S., Richardson, J. A., et al. (2003). Distinct narcolepsy syndromes in Orexin receptor-2 and Orexin null mice: Molecular genetic dissection of non-REM and REM sleep regulatory processes. *Neuron* **38**, 715–730.

Yokogawa, T., Marin, W., Faraco, J., Pezeron, G., Appelbaum, L., Zhang, J., Rosa, F., Mourrain, P., and Mignot, E. (2007). Characterization of sleep in zebrafish and insomnia in hypocretin receptor mutants. *PLoS Biol.* **5**, e277.

Zhdanova, I. V. (2006). Sleep in zebrafish. *Zebrafish* **3**, 215–226.

Zhdanova, I. V., Wang, S. Y., Leclair, O. U., and Danilova, N. P. (2001). Melatonin promotes sleep-like state in zebrafish. *Brain Res.* **903**, 263–268.

Zimmerman, J. E., Raizen, D. M., Maycock, M. H., Maislin, G., and Pack, A. I. (2008). A video method to study *Drosophila* sleep. *Sleep* **31**, 1587–1598.

## CHAPTER 12

# Use of Flatbed Transparency Scanners in Zebrafish Research: Versatile and Economical Adjuncts to Traditional Imaging Tools for the *Danio rerio* Laboratory

**Charles A. Lessman**[*], **Michael R. Taylor**[†], **Wilda Orisme**[†], ***and* Ethan A. Carver**[‡]

[*]Department of Biological Sciences, The University of Memphis, Memphis, Tennessee

[†]Department of Chemical Biology and Therapeutics, St. Jude Children's Research Hospital, Memphis, Tennessee

[‡]Department of Biological and Environmental Sciences, The University of Tennessee-Chattanooga, Chattanooga, Tennessee

---

Abstract
- I. Introduction
- II. Scanner Basics
  - A. Resolution and Bit Depth
  - B. Temperature and Fluidics
  - C. Image Acquisition with Scanners
  - D. Macroscheduler: A Mouse–Keyboard Macro for Automation of Scans
  - E. ImageJ: Image Analysis Program for Animation, Manipulation, and Analysis of Image Stacks
- III. Motility Analysis
  - A. Computer-aided Screening: Survey of Development after Microinjection or Other Treatment
  - B. Motility of Wild-type Zebrafish Embryos and Larvae
  - C. Computer-aided Larval Motility Screen (CALMS)
  - D. Determining Embryo Movement over Time (*x*–*y* Coordinates)
  - E. Drug Screens: Effect on Motility

Copyright © 2010 Elsevier Inc. All rights reserved.

978-0-12-384892-5
DOI: 10.1016/B978-0-12-384892-5.00012-8

- F. Vision Mutants: Mutant Phenotype versus Wild Type
- G. Colorimetric Potential of Scanners: pH Indicators

IV. Oocyte and Egg Assays
- A. Computer-aided Meiotic Maturation Assay: Quantification of Oocyte Maturation
- B. Osmoregulation during Oocyte Maturation
- C. Egg Activation Assay (EggsAct)

V. Using Scanners to Count and Measure
- A. Oocyte, Egg, and Embryo Counting by Scanners
- B. Scanner Imaging of Juveniles and Adults

VI. Other Potential Applications of Scanners

VII. Summary: Inexpensive Adjunct to Microscopy

Acknowledgments

References

## Abstract

Flatbed transparency scanners are typically relegated to routine office tasks, yet they do offer a variety of potentially useful imaging tools for the zebrafish laboratory. These include motility screens, oocyte maturation and egg activation assays as well as counting and measuring tasks. When coupled with Macroscheduler (http://www.mjtnet.com) and ImageJ (http://rsbweb.nih.gov/ij), the scanner becomes a stable platform for imaging large arrays of zebrafish oocytes, embryos, larvae, and adults. Such large arrays are a prerequisite to the development of high-throughput screens for small molecules as potential therapeutic drugs in the treatment of many diseases including cancer and epilepsy. Thus the scanner may have a role in adapting zebrafish to future drug and mutagenesis screening. In this chapter, some of the uses of scanners are outlined to bring attention to the potentials of this simple-to-use, flexible, inexpensive device for the zebrafish research community.

## I. Introduction

One of the remarkable features of the zebrafish embryo is its transparent optical properties, which provides exceptional opportunities for imaging scientists. An underutilized and perhaps overlooked imaging tool for the zebrafish community is the common office scanner used routinely to image documents, photos, and films. In this chapter, some of the imaging possibilities will be reviewed in order to bring attention to the range of uses such a commonly available device can have for the zebrafish researcher. The goal here is to demonstrate that the transparency scanner can provide additional imaging capabilities to the laboratory that complement the stereoscope, fluorescent, and confocal microscopes used routinely in zebrafish work. A particularly important feature of these scanners is their large imaging surface upon which may be scanned one or more multiwell plates or Petri dishes or large arrays of immobilized adults. While digital cameras fitted with macro lenses may also be used for this type of imaging, the scanner, by contrast, provides a stable platform complete with both transmitted and reflective lighting and constant 1× magnification with a focal plane that will not change over time.

We have used scanners to automate screens of zebrafish motility mutants (Lessman, 2002, 2004) to complement the earlier procedures involving manual observation methods of screening (Granato *et al*., 1996). In addition, we have adapted scanners for analysis of zebrafish oocyte maturation (Lessman *et al*., 2007). In this chapter we expand on these methods and introduce new methods to image zebrafish with flatbed transparency scanners.

## II. Scanner Basics

Flatbed transparency scanners consist of a glass sheet that makes up the imaging surface below which is driven a linear charge-coupled device (CCD) by a binary stepper motor with associated belt drive. In the reflected mode, light comes from a bulb below the glass to reflect the image onto the CCD as it passes under the object. In the transmitted mode, a light source (transparency adapter) produces light from above the object and passes through to the CCD moving below. For most zebrafish work, especially embryos and oocytes, the transmitted mode provides the most informative imaging. However, for adults and in some cases larvae, the reflective mode is more appropriate. Depending on the scanner, the bed can be the size of a standard sheet of paper or larger in reflected mode while the transmitted mode generally provides a smaller, yet useful scanned area such as one or more 96- or 384-well plates. Scanners are particularly well suited for following large arrays of oocytes, embryos, or larvae over time (i.e., minutes to days); however, they are not very useful for capturing rapid events (seconds or less). Scans take a few seconds to a few minutes depending upon the resolution, bit depth, speed of data pipeline to the computer as well as the CPU speed. An 8-bit, 1200-dpi scan of a 96-well plate should be possible in about 20 s with most scanners and computer systems available today.

We have successfully used a variety of scanners over the last 10 years including a high-resolution (for its day) Relisys scanner, HP scanjets, Umax Astra 6700, and most recently the Epson photo V500. The scanner software bundled with the scanner was compatible with Macroscheduler to allow for automated scanning. Most of the software included scanner-specific drivers, although even MS Windows has some limited capability to drive scanners. We have used ArtScan (Relisys), HP Director (HP scanjet), SilverFast SE (Umax), and Epson Scan (Epson photo V500) scanner software.

### A. Resolution and Bit Depth

Scanner resolution along the *x*-axis depends on the number of individual elements in the linear CCD, whereas in the *y*-axis it is the stepper motor and drive system that determines resolution. Optical resolution is the limit imposed by the hardware and in most modern scanners is 1200 × 1200 dpi or better. It should be noted that scanners may be advertised with significantly higher resolution but this is usually interpolated resolution or empty magnification that replaces a single pixel with multiple smaller, but identical pixels. Bit depth refers to the binary array of intensity bins producing an image. An 8-bit grayscale image has 255 shades of gray, from white to black. A 1-bit image is either black or white with no shades of gray; this is the type of image used by image analysis programs for measuring areas or other quantitative data in an image. A red, blue, green (RGB) image is a 24-bit image with 8 bits for each color, i.e., 255 shades of intensity for each of the three primary colors. Higher bit depth such as 12- or 16-bit grayscale or 48-bit color is advertised in the scanner literature, but, like interpolation, does not add significantly to the image quality in terms of suitability for image analysis and quantification. Higher resolution and bit depth quickly produces very large image files that may overwhelm even rather substantial modern workstations. So in this case, bigger is not necessarily better.

## B. Temperature and Fluidics

Scanners produce some heat when powered up, which is useful in zebrafish work because the optimal temperature is 28°C for these animals, especially the embryos. Use of a simple thermistor probe on the operating scanner bed gives a convenient temperature reading that will average about 2°C above ambient. In air-conditioned laboratories, a black plastic sheet or an opaque box fitted over the scanner bed may be used to further elevate the bed temperature and eliminate stray ambient light. We have used small thermostatically controlled ceramic space heaters or small incandescent desk lamps to provide additional heat when needed. Another issue is fluid media temperature. Cold media, for example fish salines stored in refrigerators until use for oocyte work, should be 28°C prior to addition to plates or dishes. Otherwise gas bubbles will form that obscure imaging and, in the case of oocytes and embryos, the attached bubbles can actually cause the cells to float around in the wells, which produces disconcerting, spurious movement between scans. For most imaging tasks, an uncovered plate provides the best images; however, long-term scanning (i.e., overnight) requires covered plates or the addition of media via peristaltic pump. Condensation in the case of covered wells can obscure images if temperature differentials are great. Media reservoirs, in the latter case, should also be warmed to 28°C before pumping onto plates. Obviously, a siphon or overflow port should be provided to vent the excess liquid (Fig. 1).

The edges of the glass scanner bed should be sealed to the scanner chassis with a thin film of clear silicone glue; this will prevent spills from entering the underlying compartment containing the electronic components. Various vessels may be used to hold oocytes, embryos, larvae, and adults during scanning. Nunc rectangular (cat # 176600) plates fitted with plastic screen (plastic canvas or needlepoint screen #10 mesh with 10 square perforations per inch, available at most hobby stores) provide a suitable substrate for perfusing media over oocytes or chorionated embryos in the same

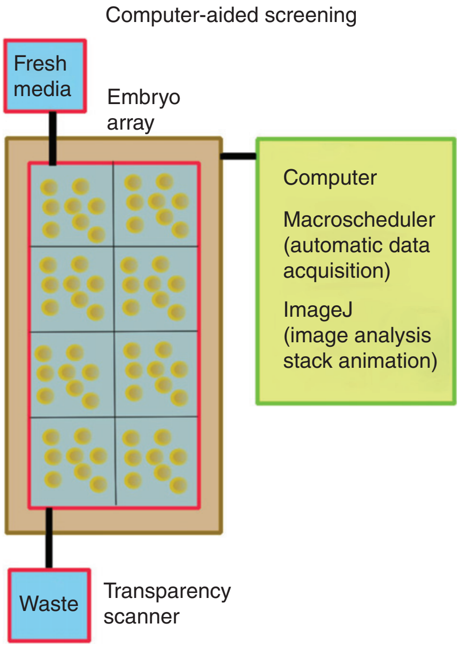
Computer-aided screening
Fresh media
Embryo array
Computer
Macroscheduler (automatic data acquisition)
ImageJ (image analysis stack animation)
Waste
Transparency scanner

**Fig. 1** Diagram of a flatbed transparency scanner and computer system for zebrafish imaging. Embryos are arrayed in a multiwell plate on the scanner bed (transparency adapter has been removed); shown is the optional media input and outflow via peristaltic pumps. The scanner is controlled by a macroprogram (Macroscheduler: http://www.mjtnet.com) to automatically acquire images at user-defined intervals. ImageJ (http://rsbweb.nih.gov/ij) is subsequently used to import the image sequence into a stack for animation and image analysis.

liquid compartment, yet maintaining relative positions on the plate. Gluing the ~1-mm mesh screen to the plate bottom provides shallow wells to keep embryos separated and in place (Lessman, 2004). Such plates can carry 100 oocytes or embryos per square inch, so that a Nunc plate with an area of 15 square inches could hold 1500 embryos in individual wells from which particular embryos could be retrieved after scanning. Multiwell plates with round-bottom or U-shaped wells help center the oocyte or embryo in the well and reduce wall effects; however, most common multiwell plates can be used for scanning (Fig. 2). Bubbles are a particularly troublesome problem when using 384-well plates; however, brief centrifugation of the media-filled plate prior to oocyte or embryo loading will remove most of the bubbles.

## C. Image Acquisition with Scanners

For most scanner software, avoid using the full-auto scanning features. Instead select manual mode to set up the scanner for research scanning. There are three main settings to choose prior to image acquisition. (1) The initial decision is to choose

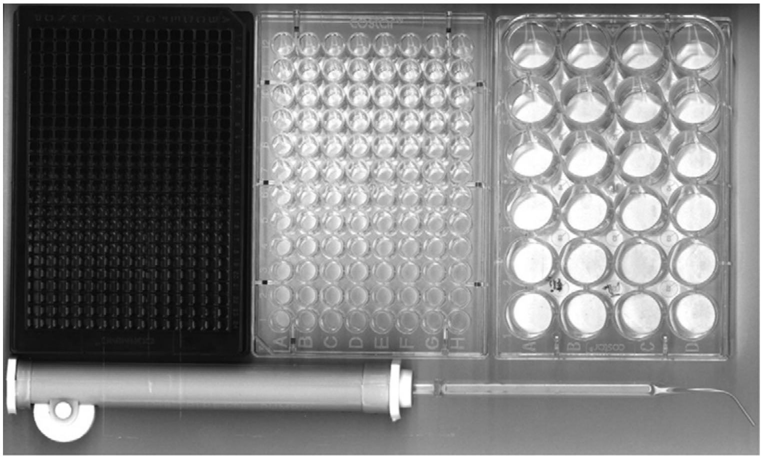

**Fig. 2** Multiwell plates and pipette pump for use in imaging arrays of zebrafish oocytes, embryos, and larvae with transparency scanners. A black-walled 384-well plate with clear flat bottom (left) is useful for high-density embryo imaging; 96-well round-bottom plate (middle) works especially well with oocytes, embryos, and larvae; the 24-well plate (right) may be used to image multiple oocytes per well and allows greater free movement for single larva. The pipette pump (bottom) has a Pasteur pipette with tip bent in flame for reaching into individual wells. This figure was produced by imaging with an Umax Astra 6700 reflective mode scanner at 1200 dpi and 8-bit grayscale.

reflective or transmitted mode for the scan; this decision will be dictated by the zebrafish stage being imaged. The opaque adults and older juveniles are best imaged with reflective lighting, while oocytes, embryos, and larvae are visualized in more detail by transmitted light. Most scanners that have transparency adapters will have this option; if not, the machine is likely a reflected mode-only scanner and may require the purchase of an optional transparency adapter. Many of the newer scanners have transparency adapters built into the lids; these will work provided the lid can accommodate the thickness of the Petri plate or multiwall plate holding the fish. (2) The second option to select is the resolution (i.e., 1200 dpi or higher). There is little to be gained by setting the resolution higher than the optical resolution of the scanner. Also, file size and scan time increase with higher resolution settings. (3) Third is a choice of 8-bit grayscale or 24-bit color; use color only if there is a need, as color scans will be three times larger and take longer to scan. The other options available, such as sharpening or automatic brightness–contrast adjustment, are not recommended; these can always be applied later. If incorporated in the scan, these options are applied after the image is already in memory but before it has been saved to disk, thus adding to scan time. Run a prescan to bring the scanned image onto the computer screen. Using the rectangular marquee tool, select the area of the image you want to scan. Select the area carefully since this saves time in initial scanning and reduces the need to crop unwanted areas later. Finally, click on the scan button; a dialog box will appear to request a filename or a default sequentially numbered filename will be used.

## D. Macroscheduler: A Mouse–Keyboard Macro for Automation of Scans

For sequential time-lapse scan series, a macro program such as Macroscheduler (http://www.mjtnet.com) is needed for unattended scanner operation. After installing the program, Macroscheduler will reside in memory; click on the gear icon found in the resident program toolbar to bring a dialog box on screen. Select record, give the macro a filename, and then begin recording by clicking on scan (the initial scan must be done manually to set up the conditions and area to be scanned as well as the directory and default filename series). A dialog box will appear with the default sequential filename automatically assigned; click on OK or save and the scanner will scan the area and save the file. After the scanner is finished, stop recording the macro by pressing ctrl-alt-s. Double click on the newly created macro that should appear on a list of available macros and select run when from the menu. Select the day of week, time to begin scanning, and scan interval. If multiple days are selected, the scanner will run throughout that time frame. Minimize the macroscheduler window and monitor the computer to ensure that the automated scanning will proceed. The gear icon will flash when the macro is running. Before the macro has been initiated, it is recommended to disconnect the computer from the Internet and shut off antivirus or other programs that might produce unwanted popups or other dialog-status boxes that can interfere with the macro. Since the macro will carry out mouse moves and keystrokes, moving the scanner windows after the initial macroprogramming or using the computer while the macro is running will prematurely stop the scan series.

## E. ImageJ: Image Analysis Program for Animation, Manipulation, and Analysis of Image Stacks

ImageJ is freely available from the NIH Web site (http://rsb.info.nih.gov/ij) bundled with Java (Abramoff *et al*., 2004). Most PC users will need the 32-bit version for Windows machines; additional versions are available for Macs and Unix machines as is a 64-bit version for Windows 7. ImageJ is being constantly updated and we have used versions 1.40 through 1.43 for most of the work presented here. Image stacks are sequential images in memory that ImageJ can animate, manipulate, and analyze; the stack will be the sum of all the image data, so if a single image is 5 MB then an image stack of 100 images will be 0.5 GB. In order to address enough RAM to put a large stack in memory, the memory option will need to be specified under the edit menu. Up to 75% of RAM may be specified, with the upper limit for the 32-bit version being around 1.6 GB. Nevertheless, we have found 1.3 GB to be a useful maximum, and, depending upon the particular computer, instability often occurs above this limit. However, with both 64-bit Windows and 64-bit Java, ImageJ may address over 1.7 GB according to the website. A number of plugins and macros are available for ImageJ and are listed at the Web site. Some that are needed for this chapter include bij plugin (http://webscreen.ophth.uiowa.edu/bij) for registering stacks (aligns the stack on an inanimate region of interest (ROI)), and stack combiner (puts two stacks together in parallel) and stack concatenator (puts two stacks together in series). The stepper motors in scanners are binary driven and some uncertainty is inherent in the exact positioning of the scan head; thus on animation the image stack may chatter one or more pixels reflecting the hardware limitations. The bji plugin, specifically the **register ROI** plugin, will remove this chatter by aligning the image stack on an inanimate portion of the image such as a portion of the plate between wells. Newer versions of ImageJ come bundled with many useful plugins and macros; plugins are usually initiated from the plugins menu when an image or stack is open and some selection made. Macros are usually compiled by the user in the plugin menu prior to their first use when ImageJ is opened. The documentation for ImageJ is found on the Web site, and an active user-group is available for help with specific issues pertaining to ImageJ.

## III. Motility Analysis

### A. Computer-aided Screening: Survey of Development after Microinjection or Other Treatment

This procedure has been described previously (Lessman, 2002, 2004) and allows detection of motility mutants during the first 72 h of zebrafish development. Here we will describe using computer-aided screening (CAS) to screen embryo development after injection. Following injection of early embryos with various substances (e.g., morpholinos, transgene constructs, antibodies, or drugs), arraying them in 96-well, round-bottom plates and scanning in transparency mode at intervals from 10 to 60 min will provide the researcher with a developmental record of their experiment. Since the yolk cell undergoes cytolysis and turns opaque at death (Fig. 3), yolky zebrafish embryos are well suited for toxicity assays.

### B. Motility of Wild-type Zebrafish Embryos and Larvae

Use of transparency scanners for continual or intermittent imaging of zebrafish embryos and larvae permits time-lapse visualization of development and of the movement of the developing fish over time. Image stacks compressed by *z*-projection of minimum density (i.e., dark pixels) in ImageJ produce single images depicting a summary of movement at different embryonic stages (Fig. 4). The *z*-projections are useful when a single image is needed to portray the extent of movement over time. The stack of images is particularly useful since it may be animated and the researcher can see the motility directly, and the center of mass (density) function of ImageJ may be used to generate quantitative data on the movement of individuals over time.

### C. Computer-aided Larval Motility Screen (CALMS)

The protocol for detecting motility mutants during the larval stage (i.e., after 72 h of development) has been detailed earlier (Lessman, 2004). Using computer-aided larval motility screen (CALMS), movement of individual larva is followed over time, and the center of mass (image density) is computed. The standard deviation of the *x*- and *y*-coordinates gives an indication of degree of movement within the well. These

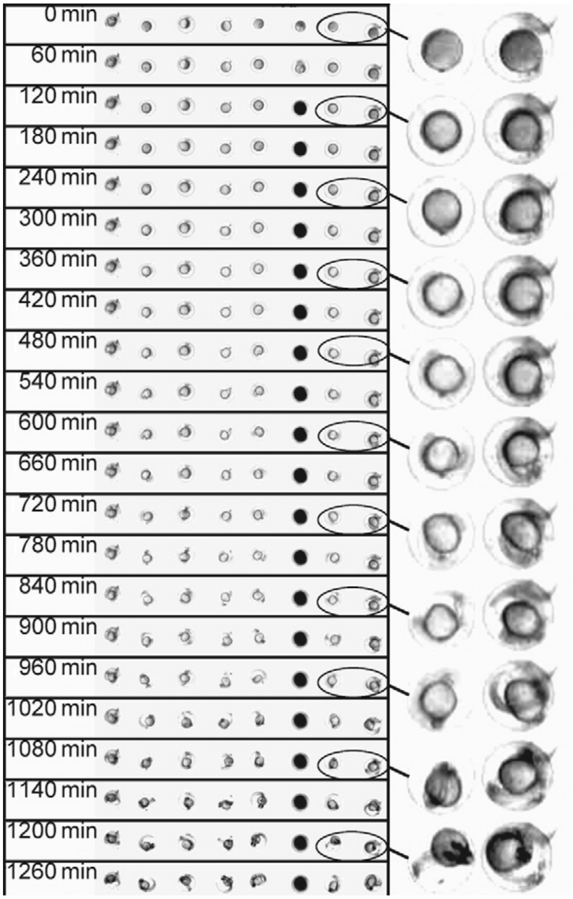
0 min
60 min
120 min
180 min
240 min
300 min
360 min
420 min
480 min
540 min
600 min
660 min
720 min
780 min
840 min
900 min
960 min
1020 min
1080 min
1140 min
1200 min
1260 min

**Fig. 3** Use of CAS to follow microinjected embryos through development. In this example, eight early cleavage stage embryos were injected into the yolk cell with 1 nl of distilled water and allowed to recover before distributing into individual wells of a 96-well round-bottom plate. Hourly scanning (1200 dpi, 8-bit grayscale) was started at the late blastula or early gastrula stage. This montage was created from the image stack by selecting **stack** from the **image** menu of ImageJ using the **montage** option. Cytolysis occurred to the third embryo from the right. Major developmental events such as gastrulation, neurulation, somitogenesis, pigment cell migration, and motility are readily apparent in the other embryos. Insets on the right are enlargements of the circled embryos.

are plotted, and clustering of points is indicative of similar phenotypes in mutagenesis screens or, for pharmacological studies, similar drug-treatment effects.

## D. Determining Embryo Movement over Time (*x*–*y* Coordinates)

Once an image stack is loaded in ImageJ, the position of each embryo can be determined using the center of mass function in the particle analyzer menu (Protocol 1).

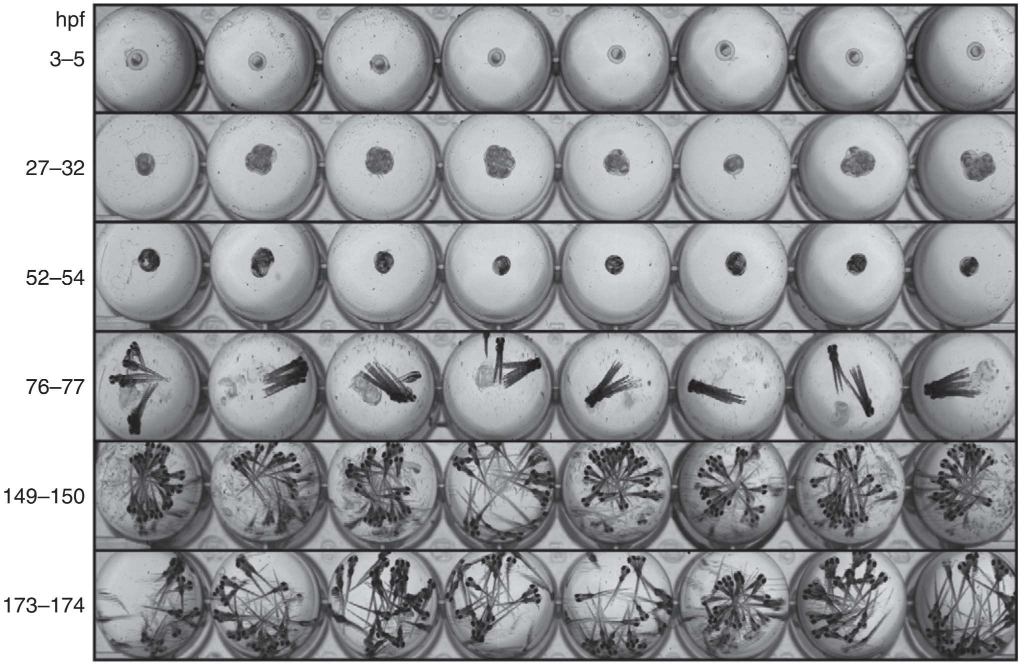

**Fig. 4** *z*-Projection of scanner images of eight wild-type zebrafish embryos at different hours post fertilization (hpf). The apparent multiple exposures are due to the single embryo or larva moving between scans. Scans at 1200-dpi, 8-bit grayscale were made every 10 min during the times indicated on the left, and a minimum density *z*-projection (darkest pixels) was made to summarize the stage-specific movements (Protocol 1, step 16).

The program calculates the coordinates of the greatest optical density for each ROI and all images in the stack. In order to specify what wells are to be analyzed, a thresholded 1-bit binary image of the wells should be made and the resulting mask sent to the ROI manager. This set of ROIs can be saved and reused with other similar plates. A simple way to do this is to fill an empty plate with a dark dye such as neutral red, trypan blue, or methylene blue and scan it, carefully selecting the area of the plate from edge to edge and top to bottom. This is important since it will be used as a template for all other similar plates subsequently scanned; therefore, the procedure is reiterated here and in the outline protocol below. Open the image in ImageJ and **adjust threshold** under the **image** menu such that the dyed wells are highlighted. After pressing OK the image will become a 1-bit black and white binary image. Open the **analyze particles** option under the analyze menu and check the **add to manager** box. After pressing OK the ROI manager window should appear with the ROIs for the plate. **Show all** will highlight the ROIs in numbered circles on the original image. **Save** the ROIs as **96well ROI.zip** or other identifying filename for subsequent use. If extraneous portions of the plate appear highlighted the remedy is to go back to analyze particles and specify 0.8–1.0

circularity to specify the circular wells. The area size range of the wells can also be specified to further eliminate unwanted ROIs.

**Protocol 1.** Determination of relative movement in time-lapse scans of zebrafish embryos and larvae.

1. Load image stack in ImageJ by selecting **import** from **file** menu; if necessary, register the stack (bij plugin; http://webscreen.ophth.uiowa.edu/bij) by specifying an ROI around a portion of the plate or dish (inanimate object) using the rectangle tool. Use **register ROI** to align all images in the stack from **plugin** menu under **bji plugins**.
2. Create a mask of the wells to be analyzed as follows: Threshold an image of the type of plate being used (e.g., 96-well) under **image** menu **adjust** > **threshold** as described above in Section D. Adjust sliders until the wells are highlighted—it may be necessary to fill wells with a dark dye such as methylene blue or trypan blue. Once wells are selected, press **apply** and the image should revert to a binary black and white image. In **analyze** menu, press **set measurements** and check box for area. Under the **analyze** menu, select **analyze particles** and select **outlines** in show dialog box; press **OK** to get results table and drawing showing numbered outlines of particles measured. Note the area size of the wells; extraneous portions will also be measured but they will be eliminated in the next step.
3. Again go to **analyze particles** in **analyze** menu and insert a range of area values that approximate the well areas from the results table. Delete the results table and the drawing showing outlines from the preliminary run. Also under **circularity** set the range to be 0.8–1.0 (high circularity) and check box for **add to manager**, then press OK. The ROI manager window should open along with a new results table and drawing showing the measured outlines of particles, or in this case the wells.
4. In the ROI manager select **save** to put the ROIs of wells into an ROI.zip file.
5. Open **ROI manager** (**analyze** menu under **tools**).
6. In **analyze** menu select **set measurements**; select **center of mass**.
7. In **ROI manager**, open ROI.zip file from thresholded 1-bit plate image.
8. Use **show all** in ROI manager to determine whether the ROIs match the image stack.
9. Use **multi-measure** in ROI manager to obtain measurements specified in set measurements.
10. Data will be arrayed in the results window; click **select all** under **edit** menu and **copy** to spreadsheet for further manipulation.
11. In **MS Excel**, use standard deviation (**stdev**) function to determine the variation in $x$- and $y$-coordinates for each embryo.
12. Copy and paste special (check values and transpose options) to give a column of data on new sheet.
13. Create a macro to reformat the single column into $x, y$ data pairs as follows (under **tools** in excel 2003 or **developer** menu in 2007 version). Use shortcut **ctrl-z**, be sure **relative cell reference** option is checked and cut the $y$ value (second number in the column) and paste into the empty column next to the $x$ value; go to the second $y$ value in the first column and press **ctrl-z**. Stop recording the macro.

14. Go to the third *y* value in the original column and press **ctrl-z**, the macro should loop and move all the remaining *y* values next to their respective *x* values. The spaces will be ignored when plotted.
15. Create a scatterplot indicating the *x* and *y* columns in the plot window.
16. Create a summary *z*-projection of image stack; under **image** menu select **stacks** and **z-projection.** A window will appear with options for the type of projection desired; generally we project the darkest pixels of each slice in the stack. For bright objects (e.g., birefringence) the maximum density projection results in the most satisfactory image.

## E. Drug Screens: Effect on Motility

Scanners may be used to analyze the effects of drugs and small molecules on the motility of larval zebrafish. Variations in responses to a pharmacological agent may be visualized and quantified. Subsequent mating and generational breeding could lead to lines of fish with different responses to specific drugs and the genes that contribute to the overall response. Researchers could use this technology to screen for genes that are involved in complex behavioral traits.

Here we test pentylene tetrazole (ptz) for its effect on day 3 larval motility (Figs. 5 and 6). This convulsant agent has been shown to elicit seizures and promote increased motility in zebrafish (Baraban *et al*., 2005, 2007). Furthermore, zebrafish provide a

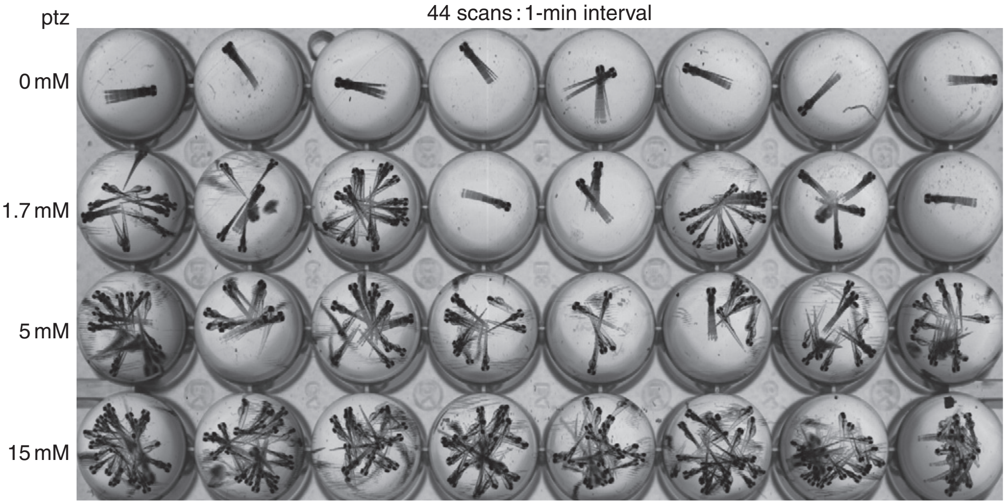

**Fig. 5** CALMS *z*-projection of 3-day larvae treated with different doses of the convulsant agent pentylene tetrazole (ptz). Scans acquired every minute for 44 min at 1200-dpi, 8-bit grayscale. A single larva is placed in each well. The resulting image stack may be animated (Supplement Movie 1; http://www.elsevierdirect.com/companions/9780123848925) or in this case a *z*-axis projection using the minimum density function (i.e., darkest pixels) was made (Protocol 1, step 16).

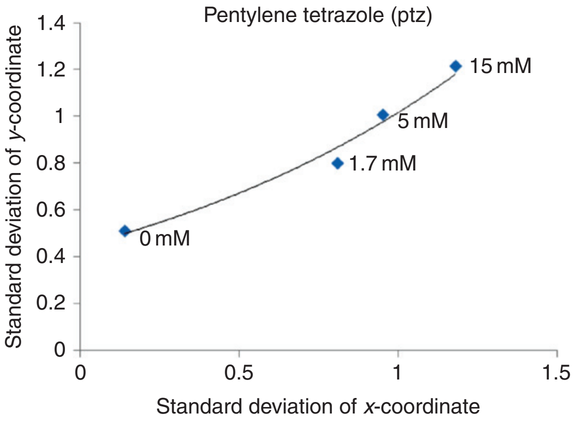

**Fig. 6** Mean of standard deviation of *x*- and *y*-coordinates of center of mass (density) with different doses of pentylene tetrazole. *N* equals eight larvae per dose. Scanned every minute for 44 min at 1200-dpi, 8-bit grayscale (Protocol 1).

tractable vertebrate system to screen for antiepileptic drugs and genes involved in seizure disorders (Baraban *et al*., 2005, 2007; Berghmans *et al*., 2007).

The dose–response curve (Fig. 6) indicates that ptz induces a dose-dependent increase in motility (hypermotility) in day 3 larvae (Protocol 1).

## F. Vision Mutants: Mutant Phenotype versus Wild Type

Motility defects in mutant zebrafish larvae may be found in screens using CALMS (Lessman, 2004). Here we apply CALMS as an additional screen for vision-defective mutants, since we hypothesize that visually impaired or blind larvae may have altered motility (Protocol 1). To test this hypothesis, the vision mutant *laj*$^{s304}$ (Muto *et al*., 2005) was screened at day 7 for the optokinetic response (OKR) (Brockerhoff *et al*., 1995) and then subsequently assayed using CALMS (Fig. 7). The difference between the motilities of mutant and wild-type embryos was statistically significant, but there was some overlap between the mutant and wild-type sibs. This result suggests that additional cues, such as lateral line input, compensate or provide primary directives for movement within the confines of a well. This also agrees with the normal (i.e., 1.0) score this mutant obtained in a spontaneous swimming assay (Muto *et al*., 2005).

## G. Colorimetric Potential of Scanners: pH Indicators

In theory, color scanners should be able to detect color changes while monitoring movement or development simultaneously. To test this, phenol red pH indicator dye was used in the bathing media of the larvae in 96-well plates. Preliminary trials with concentrations between 0.001% and 0.25% indicated that a level of 0.01% phenol red

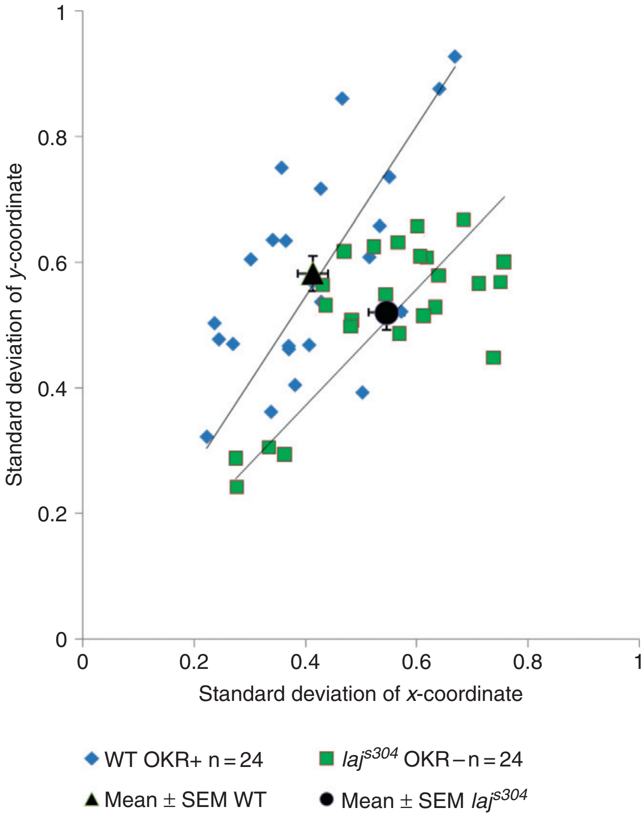

**Fig. 7** Motility differences in *laj*$^{s304}$ mutant (Muto *et al*., 2005) and wild-type (wt) sibs using CALMS. A single spawn from a *laj*$^{s304}$ heterozygote cross was screened using the optokinetic response (OKR) assay (Brockerhoff *et al*., 1995) and the mutants (24) and wt sibs (24) were arrayed into a 96-well round-bottom plate and scanned every minute for 33 min at 1200 dpi and 8-bit grayscale. The *x*–*y* coordinates were computed from the stack by ImageJ and the standard deviations were computed in MS Excel and the result plotted. The data are shown as standard deviation of *x*- and *y*-coordinates with the mean, SEM, and trendlines shown (Protocol 1).

provided sufficient detectable color without affecting the viability of embryos. Since 24-bit images are not compatible for thresholding and image density measurements, the stack was split into separate RGB channels (in ImageJ: **image** menu, select **color** then **split channels**). The green channel showed the greatest intensity change as expected for a red-to-yellow color change with acid production by larvae. The green channel stack was used to determine *x*–*y* coordinate changes (Protocol 1) and green intensity change for each corresponding well (Fig. 8). Plumes of yellow, denoting acid associated with larvae especially near the gills, could be seen upon stack animation (Fig. 9; Supplement Movie 2).

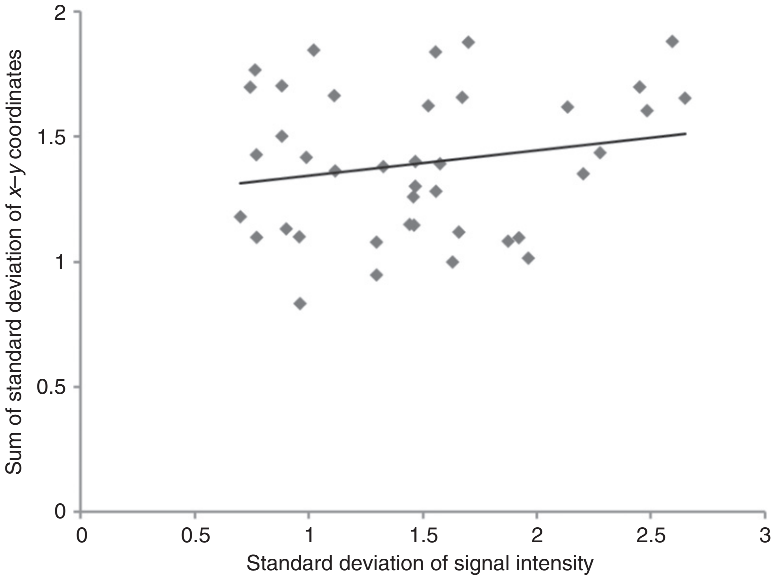

**Fig. 8** General relationship between degree of larval movement (*y*-axis) (Protocol 1) and change in pH as a function of green intensity (*x*-axis). Some correlation between the extent of movement and pH indicator color change is apparent, but additional factors, such as basal metabolism, likely account for much of the variation.

## IV. Oocyte and Egg Assays

### A. Computer-aided Meiotic Maturation Assay: Quantification of Oocyte Maturation

This technique was described previously (Lessman *et al.*, 2007). The basis for this assay is the clearing of oocytes as they undergo meiotic maturation (Lessman *et al.*, 2007; Selman *et al.*, 1993, 1994). Fully grown oocytes (~0.5–0.7 mm) are harvested from the ovary of a killed gravid female and placed into multiwell plates in groups (i.e., 24-well plate) or singly (i.e., 96-well round-bottom plate) with an appropriate media such as Cortland's fish saline containing (g/l) NaCl 7.25, $CaCl_2$ 0.23, $MgSO_4$ 0.23, KCl 0.38, HEPES acid 1.9, HEPES salt 3.1, penicillin 30 mg/l, and streptomycin 50 mg/l, pH 7.8 (Wolf and Quimby, 1969) or Leibovitz L-15 cell culture medium. The normal inducer of maturation is 17α-20β-dihydroxyprogesterone (DHP) which elicits oocyte clearing in a dose-dependent manner (Fig. 10). Previously, oocyte maturation was scored as a quantal endpoint assay—that is, cleared oocytes were counted along with those that remained opaque at the end of a predetermined incubation period (Selman *et al.*, 1993, 1994). Computer-aided meiotic maturation assay (CAMMA) follows each oocyte over time. Thus, the investigator can determine the clearing of individual oocytes and quantify the temporal changes (Fig. 11); this provides more useful information about treatment effects. CAMMA for multiple

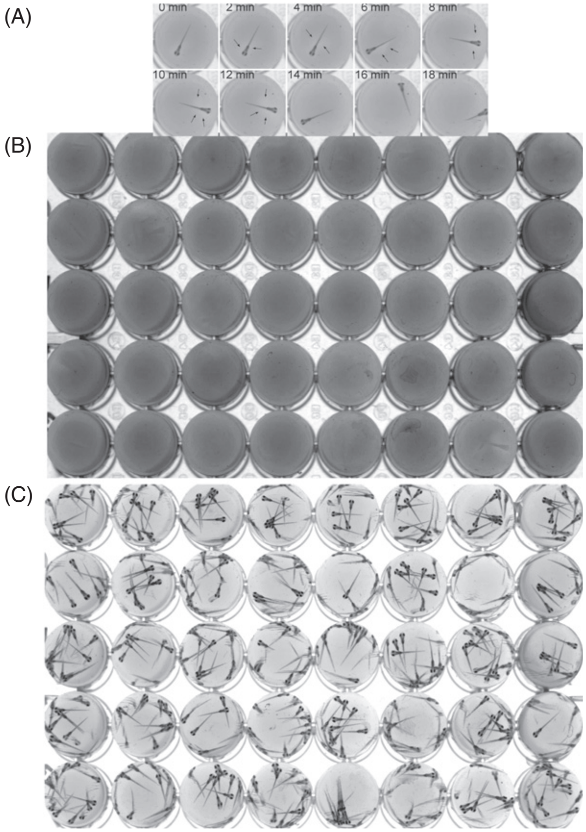

**Fig. 9** Use of colorimetric capability of scanners to relate movement and pH change. Wild-type AB 7-day larvae were loaded individually into the wells of a 96-well round-bottom plate containing 0.01% phenol red, 0.015 M NaCl, 0.1 mM KCl, 0.1 mM $CaCl_2$, 0.1 mM $MgSO_4$, and 1 mM Tris (pH 7.2), and the plate was scanned at 2-min intervals (1200 dpi, 24-bit color). (A) Eight-bit green channel showing a single well with larva surrounded by plumes of lighter (yellow in color image) area (arrows) (Supplement Movie 2; http://www.elsevierdirect.com/companions/9780123848925). (B) Eight-bit *z*-projection of green channel maximum intensity (brightest pixels) showing areas of change, especially around larva. (C) Eight-bit *z*-projection of minimum intensity showing larval position changes over 24 min of observation period.

oocytes per well is given in Protocol 2. CAMMA for single oocytes in 96-well round-bottom plates is similar to the protocol for CAS or CALMS except that average density is the main measurement desired rather than center of mass density (Fig. 12).

**Protocol 2.** Semi-automated CAMMA for 24-well plate or other cultureware containing more than one cell per well.

1. **Import** images in **image** menu into stack and animate (backslash or **image** menu **stacks** then **animation options**) to visualize results.
2. Register stack if necessary (register ROI plugin).

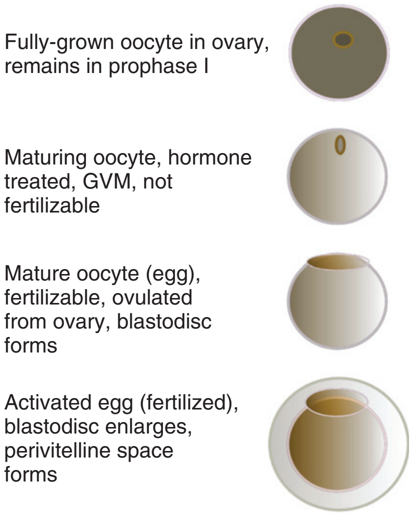
Fully-grown oocyte in ovary, remains in prophase I
Maturing oocyte, hormone treated, GVM, not fertilizable
Mature oocyte (egg), fertilizable, ovulated from ovary, blastodisc forms
Activated egg (fertilized), blastodisc enlarges, perivitelline space forms

**Fig. 10** Diagram of changes during zebrafish oocyte maturation and egg activation. During oocyte maturation, the prophase I oocyte (dark oocyte nucleus or germinal vesicle, GV) is converted to a metaphase II egg (GV breaks down after migrating to the animal pole) and the ooplasm clears. During egg activation the blastodisc at the animal pole enlarges and the elevation of the chorion produces the perivitelline space.

3. Use oval selection tool and produce round selection by pressing **shift and left mouse button** to encompass all oocytes in a well.
4. Under **image** menu, select **duplicate**, check box for entire stack.
5. Repeat for each well providing a filename for the well (e.g., well A1).
6. To make an ROI set for each well, activate the stack and in **image** menu **duplicate** the first image (do not check the box for entire stack).

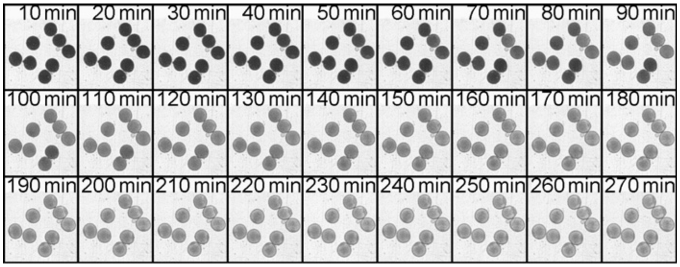
10 min
20 min
30 min
40 min
50 min
60 min
70 min
80 min
90 min
100 min
110 min
120 min
130 min
140 min
150 min
160 min
170 min
180 min
190 min
200 min
210 min
220 min
230 min
240 min
250 min
260 min
270 min

**Fig. 11** Maturation of fully grown, prophase I zebrafish ovarian oocytes treated with 10 ng/ml 17α-20β-dihydroxyprogesterone. Oocytes from a single well of a 24-well plate (28°C) were scanned every 10 min at 1200 dpi and 8-bit grayscale in transparency mode (Supplement Movie 3; http://www.elsevierdirect.com/companions/9780123848925). Oocytes clear and develop a blastodisc at the animal pole. This figure shows a group of eight oocytes from the well that were subjected to signal intensity analysis (Protocol 2); the results are plotted in Fig. 12.

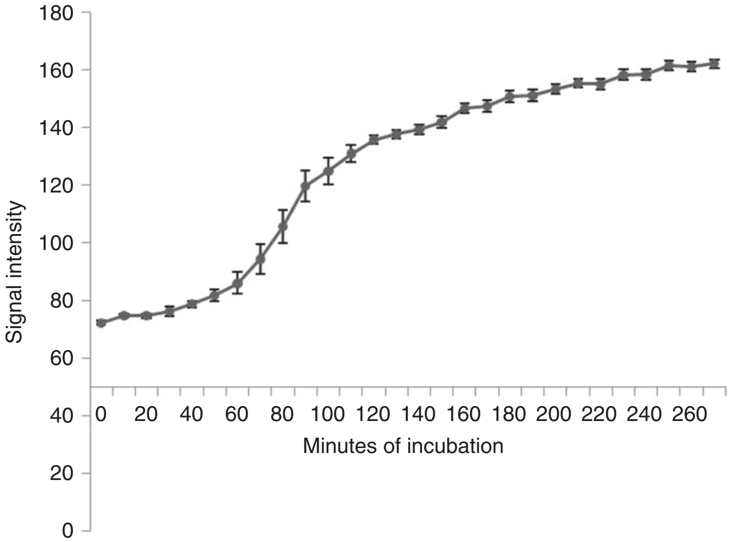

**Fig. 12** CAMMA analysis of the maturation (clearing) of the eight oocytes depicted in Fig. 11. Signal intensity data are given as mean±SEM in 8-bit grayscale (i.e., 0 equals black, 255 equals white).

7. Under **edit** menu, select **clear outside.**
8. Use **adjust threshold** under **image** menu; move sliders to highlight oocytes and **apply**.
9. Under **process** menu, select **binary** and **fill holes** to uniformly highlight oocytes.
10. Oocytes that are touching need to be separated using the **watershed** function in the **binary** selection of the **process** menu.
11. Produce ROI set by using **particle analyzer** under **analyze** menu and selecting **direct to manager**; the ROI set may be saved.
12. **Set measurements** of average density, area, and options such as feret's diameter under **analyze** menu.
13. In **ROI manager**, select **more** then **multiple measure**. Selecting **show all** will indicate the numbered areas to be measured.
14. Results will appear in a new window. The data are then transferred to a spreadsheet for analysis.

The temporal change in the signal intensity of individual oocytes may also be followed by CAMMA as shown in Fig. 13.

## B. Osmoregulation during Oocyte Maturation

As oocytes mature and are ovulated, they leave the ionic environment of the ovary and are deposited in freshwater during oviposition. Immature oocytes, taken directly from the ovary by dissection, cytolyse when placed in freshwater (Lessman,

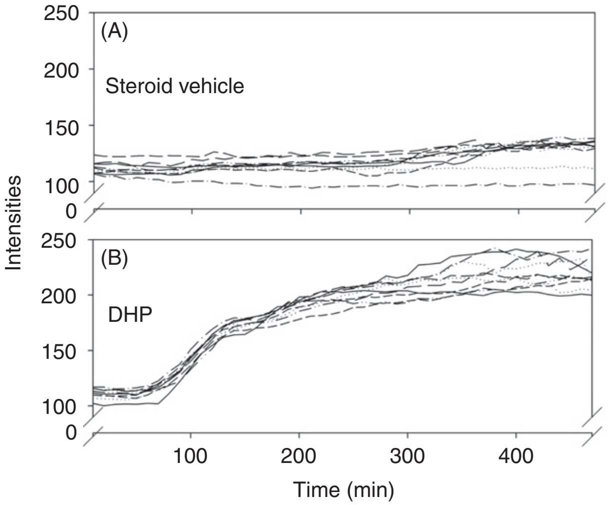

**Fig. 13** Signal intensity plots of individual zebrafish oocytes ($n = 10$) versus time of incubation with either vehicle control (A) or 10 ng/ml 17α-20β-dihydroxyprogesterone (DHP) (B). Each line represents a single oocyte analyzed by CAMMA.

unpublished). The osmoregulation assay determines the time course of acquisition by maturing oocytes of the capacity to osmoregulate in freshwater. In this example, fully grown oocytes were incubated with 10 ng/ml DHP in 100% Cortland's and, at 1-h intervals, eight oocytes were placed individually into the wells of successive rows (96-well round-bottom plate) containing 200 µl of 5% Cortland's saline. Scans were made every 10 min at 1200 dpi, 8-bit. A montage of the resulting images is shown in Fig. 14 and a count of cytolysed eggs is given in Fig. 15.

## C. Egg Activation Assay (EggsAct)

Zebrafish eggs obtained from anesthetized gravid females or from progestogen-matured oocytes may be assayed for their ability to undergo a cortical response and formation of the perivitelline space (Fig. 16) by following Protocol 3 (Fig. 17). This can be combined with *in vitro* fertilization if sperm suspensions are added to the freshwater used to initiate activation.

**Protocol 3**. Egg activation assay (EggsAct).

1. Place individual eggs into wells containing 50 µl 100% Cortland's in a 96-well round-bottom plate.
2. Position the plate on the scanner bed.
3. Replace media in wells with 200 µl 5% Cortland's using a multichannel pipette.
4. Begin a scan series at 1200 dpi, 8-bit, every 1–5 min for at least 30 min total.
5. Stack the resulting scans in ImageJ.

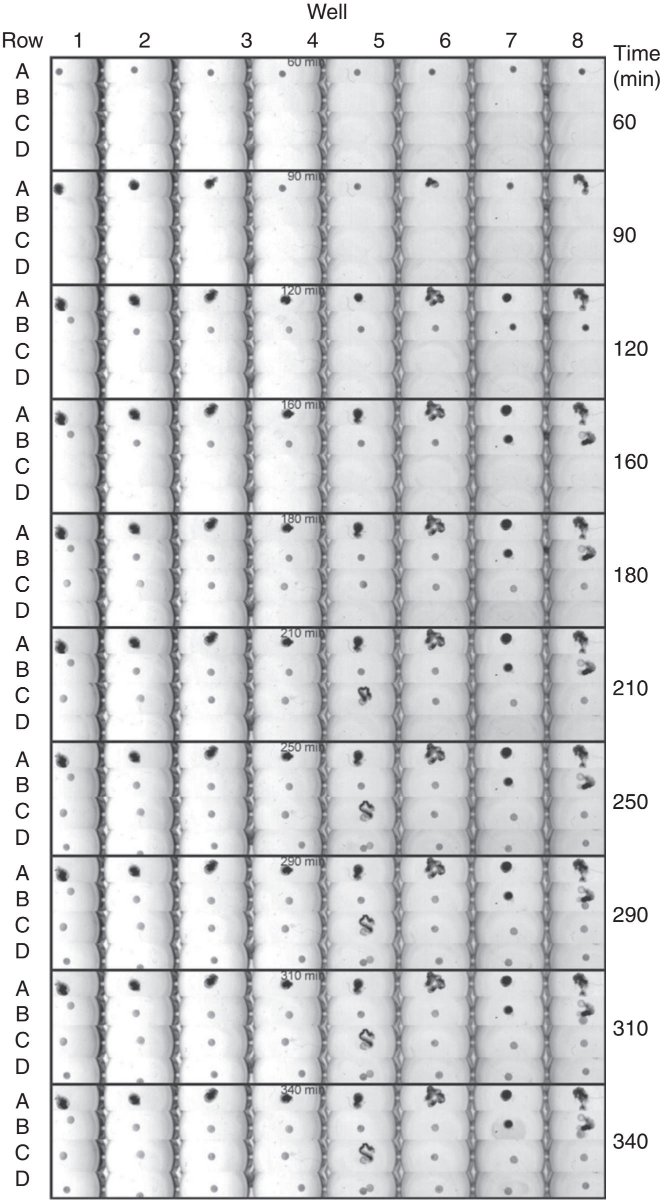
Well
Row
1
2
3
4
5
6
7
8
Time (min)
A
B
C
D
60 min
90 min
120 min
160 min
180 min
210 min
250 min
290 min
310 min
340 min
60
90
120
160
180
210
250
290
310
340

**Fig. 14** Development of osmoregulation in maturing zebrafish oocytes. Fully grown ovarian oocytes were treated with 10 ng/ml 17α-20β-dihydroxyprogesterone in 100% Cortland's solution at time 0, and at hourly intervals, eight oocytes were transferred individually into the wells of successive rows of a 96-well plate. Each well contained 5% Cortland's solution (Wolf and Quimby, 1969). Oocytes that have not developed osmoregulatory capacity undergo cytolysis and turn opaque (i.e., all at 60 min); increasing numbers of oocytes remain viable after 120-min incubation with DHP, coincident with oocyte maturation (Supplement Movie 4; http://www.elsevierdirect.com/companions/9780123848925).

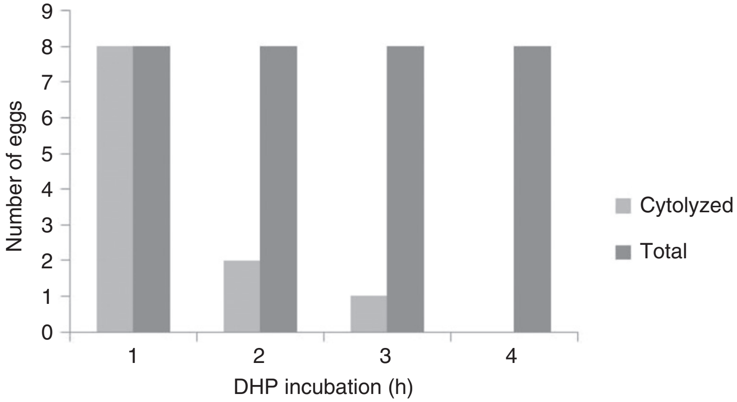

**Fig. 15** Cytolysis of zebrafish oocytes subjected to osmoregulatory shock as a function of maturation. The number of cytolysed eggs is plotted as a function of time of incubation with 17α-20β-dihydroxyprogesterone (DHP) prior to osmotic shock. Data taken from last image of Fig. 14 (340 min).

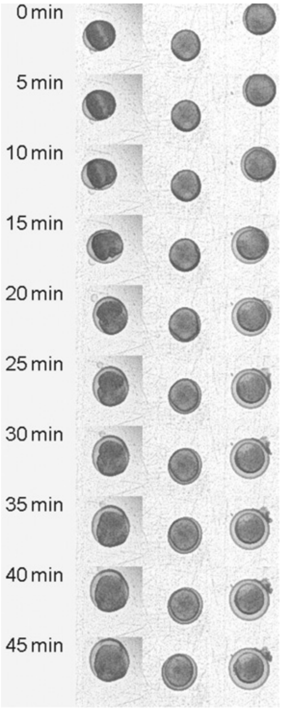

**Fig.16** Montage of 17α-20β-dihydroxyprogesterone-matured zebrafish oocytes (eggs) undergoing activation in low ionic strength media (5% Cortland's balanced fish saline). Note the formation of the perivitelline space and elevation of the chorion (Supplement Movie 5; http://www.elsevierdirect.com/companions/9780123848925).

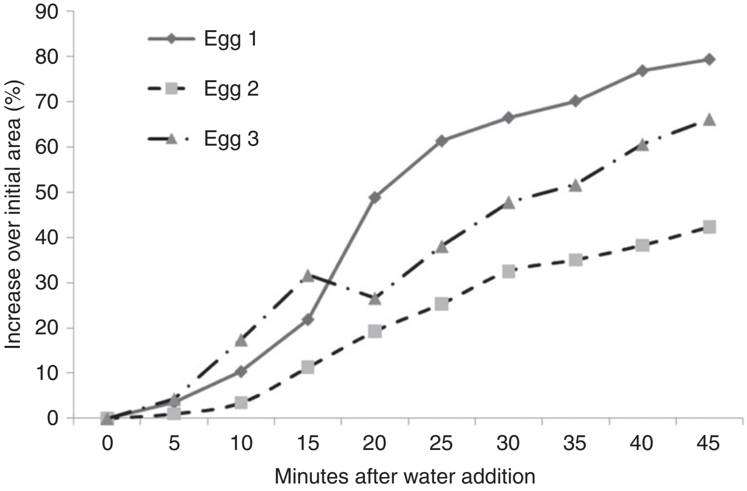

**Fig. 17** Results of the egg activation assay (EggsAct) for the three eggs imaged in Fig. 16 (Protocol 3).

6. For each egg to be analyzed, select and duplicate the well containing the egg.
7. Make a **montage** under the **stacks** selection of **image** menu using 1 as **scale factor**.
8. **Adjust** the **threshold** and apply to make 1-bit binary image; if necessary use **fill holes** option from **process** menu.
9. **Set measurements** in **analyze** menu to include area; use the **analyze particles** selection under **analyze** menu to return areas of eggs in montage.
10. Copy the results into MS Excel and calculate the percent area change by dividing the area at $t = 0$ into the area obtained at each time point multiplied by 100.
11. Repeat steps 6–10 for each egg and plot results (Fig. 17).

## V. Using Scanners to Count and Measure

### A. Oocyte, Egg, and Embryo Counting by Scanners

Scanned images of dishes containing oocytes, eggs, or embryos can be easily counted using Protocol 4 (Fig. 18). It is important to remove, as much as possible, extraneous material such as scales, fish waste, uneaten food, and debris that may produce errors in embryo counts. In the case of oocytes, complete dissociation of the ovarian fragments produces the most accurate counts.

**Protocol 4.** Semi-automated zebrafish embryo counting with ImageJ.

1. Open ImageJ program. In **file** menu, **open** the image to be analyzed. Use the **magnify tool** to increase or decrease magnification so that you can see the embryos.

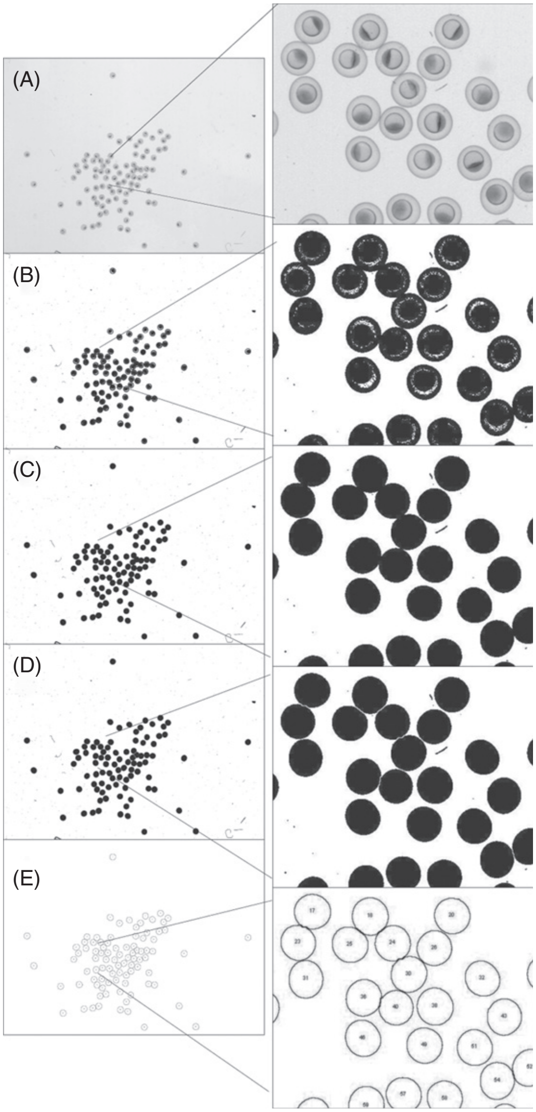

**Fig. 18** Counting zebrafish embryos. Scanned image (A) of blastula-stage embryos was thresholded to produce a 1-bit binary image (B). Under process menu, selection of the fill holes function of the binary option transforms embryos to filled circles (C). Next the watershed function of the binary option is used to separate touching embryos (D). Finally the analyze particles' function under the analyze menu is used to count embryos (E). A total of 90 embryos are present and accurately counted (Protocol 4).

2. **Adjust threshold** (under **image** menu select **adjust**), set sliders so that only embryos are highlighted, then select **apply**. It may be impossible to exclude all debris, but try to minimize selecting debris while maximizing embryo selection.
3. Crop image using rectangle tool to remove extra areas if possible (under **image** menu: **crop**).
4. Under **process** menu select **binary** then **fill holes.**
5. Under **process** menu select **binary** then **watershed** to separate those embryos that are still touching.
6. Run a preliminary analysis: under **analyze** menu select **analyze particles** (under **show**, select **outlines** and check **show results** box); known embryos should give areas of about 2000 pixels (at 1200-dpi scan) on the **results** window and **circularity** should be set for 0.6–1.0. This will give particles both larger and smaller than embryos, but look at the numbered outlines and pick some that are known embryos and check their area on the results list. Delete the preliminary results and the window showing particle outlines.
7. Under **analyze** menu select **analyze particles** and set minimum and maximum size to include all embryos (try 1600–2600 to start). Compare the original image with the drawing to see if all embryos have in fact been counted.
8. In **results** window, **select all** under **edit** menu and paste to excel spreadsheet.

## B. Scanner Imaging of Juveniles and Adults

### 1. Morphometrics and Archival Images

Protocol 5 provides a rapid method to obtain archival images of anesthetized larvae, juveniles, and adults (Fig. 19). Different images collected at a single resolution (i.e., 1200 dpi) may be compared directly, and morphometrics may be obtained from the images as outlined in this protocol.

**Protocol 5.** Imaging adult zebrafish using the reflected mode at 1200 dpi and using ImageJ to measure standard length (snout to caudal peduncle).

1. Obtain an image of anesthetized adults (0.04% tricaine methane sulfonate).
2. **Open** the image in ImageJ and under **analyze** menu, select **calibrate**.
3. In window type in 1200 for pixel number and 25.4 in actual distance.
4. Use mm as units.
5. Using the line tool, draw a line from the snout to caudal peduncle and under the **analyze** menu, select **measurement**.
6. A results window will appear with the measurement in mm.
7. Repeat for other fish in image or make other morphometric determinations.

### 2. Tumors or Abnormal Morphologies

Scanners may also provide a convenient imaging tool for routine measurements of tumors or other abnormalities (Fig. 20). An example used here is the nerve sheath and abdominal tumor prone tp53$^{-/-}$ line (Berghmans *et al*., 2005). Anesthetized adults may be

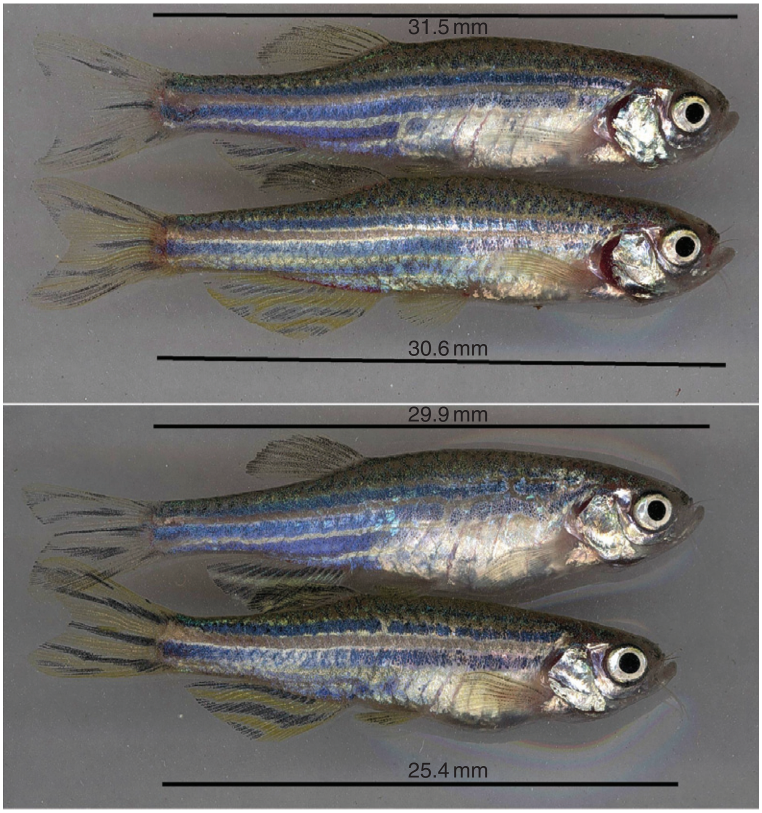

**Fig. 19** Morphometric measurements and archival imaging of zebrafish. Reflected mode scanning of adult zebrafish (1200 dpi, 24-bit color). Two spawning pairs of adults were anesthetized in 0.04% tricaine methane sulfonate (females on top). The lines above or below each fish represent the standard length from snout to caudal peduncle determined with ImageJ from the scanned image (Protocol 5).

scanned in reflective mode at weekly intervals, for example, to follow tumor development and to allow measurement of tumor extent or size change. A scanner in the fish room could be devoted to this task. Efforts in the zebrafish research community are under way to develop high-throughput zebrafish bioassays for human cancers (Snaar-Jagalska and ZF-Cancer Consortium, 2009) as well as tumor assays after cancer cell transplantation (Taylor and Zon, 2009). Scanners may prove useful in these future endeavors.

## VI. Other Potential Applications of Scanners

Theoretically, scanners should be able to detect fluorescent molecules in zebrafish. Light-emitting diodes (LEDs) of the appropriate wavelength could be used along with

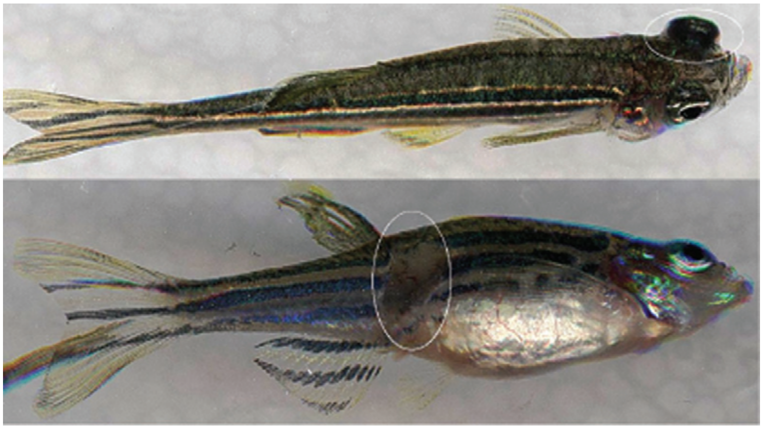

**Fig. 20** Documentation of disease and abnormal morphology in adult zebrafish. Adult tp53$^{-/-}$ zebrafish with spontaneous eye tumor (top) and abdominal tumor (bottom) were scanned at 1200-dpi, 24-bit color in reflected mode. Some of the affected areas are circled.

an appropriate barrier filter placed between the plate bearing the fish and the CCD to allow detection. Diode lasers may also be suitable for illuminating samples via fiber optics or prisms on the scanner bed. Developing a suitable scanner system for detection of fluorescent molecules in zebrafish embryos, larvae, and adults in large arrays is a worthwhile future endeavor. The ability to quickly identify embryos expressing fluorescent molecules from large arrays would be useful in high-throughput assays, for example, in the nile red obesity assay (Jones *et al*., 2008).

Myofibrils in zebrafish larval muscle illuminated by plane-polarized light produce anisotropy or birefringence (Granato *et al*., 1996). Transparency scanners can easily produce birefringence by placing multiwell plates between crossed polarizing film on the scanner bed. Two sheets of the polarizing film, when turned 90° from each other, prevent light from passing through unless the light is refracted by something between the polarizers.

Sheets of colored filter (e.g., Wratten filters) may also be used to illuminate embryos or larvae with different wavelengths by placing the sheet between the light source and the animals. This could be useful in behavioral studies. With the appropriate combination of filters above and below the fish, various fluorescent or colored molecules may be visualized.

Scanners may also be used for imaging developing embryos of other fish species, especially if the embryos have some degree of transparency. We have successfully imaged channel catfish embryos (*Ictalurus punctatus*) with transparency scanners. These embryos are relatively large (~3 mm) and semi-transparent, and require about 7 days at 25°C to develop. In order to scan during the entire course of development, peristaltic pumps were used to produce fresh laminar flow of media over the embryos. Other important food species such as rainbow trout or salmon could also be imaged;

however, these cold water species would require scanning in a cold room or low-temperature incubator. We have tested scanners in environments as low as 2°C and found them to be functional and reliable over the course of days.

## VII. Summary: Inexpensive Adjunct to Microscopy

The flatbed transparency scanner is inexpensive, simple to use, and provides a stable imaging platform for large arrays of zebrafish oocytes, embryos, larvae, and adults. Coupled with Macroscheduler and ImageJ, the scanner can produce quantitative data for numerous research endeavors. We have outlined a few of the possible uses of this commonly available device and look forward to new uses that can arise from the vibrant, creative zebrafish research community.

## Acknowledgments

This chapter was written while CAL was on sabbatical from the University of Memphis and hosted by St. Jude Children's Research Hospital and the University of Tennessee-Chattanooga. We thank the members of the Taylor and Carver laboratories for their suggestions and assistance. We thank the personnel of the Stoneville, MS USDA Catfish Facility, for providing channel catfish embryos. This work was supported in part by a Hartwell grant to MRT and an NIH grant to EAC.

## References

Abramoff, M. D., Magelhaes, P. J., and Ram, S. J. (2004). Image processing with ImageJ. *Biophotonics Int.* **11**, 36–42.

Baraban, S. C., Dinday, M. T., Castro, P. A., Chege, S., Guyenet, S., and Taylor, M. R. (2007). A large-scale mutagenesis screen to identify seizure-resistant zebrafish. *Epilepsia* **48**, 1151–1157.

Baraban, S. C., Taylor, M. R., Castro, P. A., and Baier, H. (2005). Pentylenetetrazole induced changes in zebrafish behavior, neural activity and c-fos expression. *Neuroscience* **131**, 759–768.

Berghmans, S., Hunt, J., Roach, A., and Goldsmith, P. (2007). Zebrafish offer the potential for a primary screen to identify a wide variety of potential anticonvulsants. *Epilepsy Res.* **75**, 18–28.

Berghmans, S., Murphey, R. D., Wienholds, E., Neuberg, D., Kutok, J. L., Fletcher, C. D. M., Morris, J. P., Liu, T. X., Schulte-Merker, S., Kanki, J. P., Plasterk, R., Zon, L. I., *et al*. (2005). tp53 mutant zebrafish develop malignant peripheral nerve sheath tumors. *Proc. Natl. Acad. Sci. U. S. A.* **102**, 407–412.

Brockerhoff, S. E., Hurley, J. B., Janssen-Bienhold, U., Neuhauss, S. C. F., Driever, W., and Dowling, J. E. (1995). A behavioral screen for isolating zebrafish mutants with visual system defects. *Proc. Natl. Acad. Sci. U. S. A.* **92**, 10545–10549.

Granato, M., van Eeden, F. J., Schach, U., Trowe, T., Brand, M., Furutani-Seiki, M., Haffter, P., Hammerschmidt, M., Heisenberg, C. P., Jiang, Y. P., Kane, D. A., Kelsh, R. N., *et al*. (1996). Genes controlling and mediating locomotion behavior of the zebrafish embryo and larva. *Development* **123**, 399–413.

Jones, K. S., Alimov, A. P., Rilo, H. L., Jandacek, R. J., Woollett, L. A., and Penberthy, W. T. (2008). A high throughput live transparent animal bioassay to identify non-toxic small molecules or genes that regulate vertebrate fat metabolism for obesity drug development. *Nutr. Metab.* **5**, 23–33.

Lessman, C. A. (2002). Use of computer-aided-screening (CAS) for detection of motility mutants in zebrafish embryos. *Real-Time Imaging* **8**, 189–201.

Lessman, C. A. (2004). Computer-aided screening for zebrafish embryonic motility mutants. *Methods Cell Biol.* **76**, 285–313.

Lessman, C. A., Nathani, R., Uddin, R., Walker, J., and Liu, J. (2007). Computer-aided meiotic maturation assay (CAMMA) of zebrafish (*Danio rerio*) oocytes *in vitro*. *Mol. Reprod. Dev.* . **74**, 97–107.

Muto, A., Orger, M. B., Wehman, A. M., Smear, M. C., Kay, J. N., Page-McCaw, P. S., Gahtan, E., Xiao, T., Nevin, L. M., Gosse, N. J., Staub, W., Finger-Baier, K., *et al*. (2005). Forward genetic analysis of visual behavior in zebrafish. *PLoS Genet.* **1**, 575–588.

Rasband, W. S. (1997–2009). ImageJ. U. S. National Institutes of Health, Bethesda, Maryland, USA, http://rsb.info.nih.gov/ij/.

Selman, K., Petrino, T. R., and Wallace, R. A. (1994). Experimental conditions for oocyte maturation in the zebrafish, *Brachydanio rerio*. *J. Exp. Zool.* **269**, 538–550.

Selman, K., Wallace, R. A., Sarka, A., and Qi, X. (1993). Stages of oocyte development in the zebrafish, *Brachydanio rerio*. *J. Morphol.* **218**, 203–224.

Snaar-Jagalska, E. B. and ZF-CANCER Consortium (2009). ZF-CANCER: developing high-throughput bioassays for human cancers in zebrafish. *Zebrafish* **6**, 441–443.

Taylor, A. M., and Zon, L. I. (2009). Zebrafish tumor assays: the state of transplantation. *Zebrafish* **6**, 339–346.

Wolf, K., and Quimby, M. C. (1969). Fish cell and tissue culture. *In* “Fish Physiology” (Hoar, W. S., and Randall, D. J., eds.) **Vol. 3**, pp. 293–312, Academic Press, New York.

# SUBJECT INDEX

Note: The letters '*f*' and '*t*' following the locators refer to figures and tables respectively.

**A**

Achromatopsia, 155, 206
Action currents
  analysis of, 226–228
    hair-cell endocytosis, 227
    interspike interval (ISI), 228
    neuromast hair cells (sine waves), 226–227
    spiking, 227
  electrode and recording details, 226
    from individual posterior lateral-line neurons, 226*f*
    posterior lateral line ganglion (PLLg), 226
    voltage-clamp mode recordings, 226
Adult kidney isolation, 249
Albinism, 60
Alkaline phosphatase (AP) staining for 3 dpf embryos, 28, 38–39
  materials, 38–39
    fixation buffer, 38
    rinse buffer, 38
    staining buffer, 39
    staining solution, 39
  protocol, 39
Anaplastic lymphoma kinase *(ALK)* gene, 145
Angiopoietin2, 244
Anterior neural plate (ANP), 76*f*, 77, 167
Antibodies, 166–172
  antibody staining, 166, 171
  anti-GABA staining, 171
  antigen retrieval, 171
  confocal microscopy, 170
  conventional epifluorescence microscopy, 171
  GABA staining protocol, 172
  glyoxal-based fixatives, 170
  labeling with, 9
    Alcam-a (zn-5/zn-8, monoclonal antibodies), 9
    anti-acetylated tubulin (Sigma), 9
    anti-DsRed (mCherry, Clontech), 9
    anti-GFP (Invitrogen), 9
    anti-tagRFP (Invitrogen) antibodies, 9
    standard whole-mount antibody staining techniques, 9
    zn-5/8 staining, 9
Anti-gamma aminobutyric acid (GABA) staining, 170
Anti-gamma tubulin (GTU-88), 171, 250
Antigen retrieval, pretreatments, 104–105
  citrate retrieval, 104
  hydrochloric acid pretreatment, 104
Anti-polyglutamyl tubulin (B3), 278
Artificial cerebrospinal fluid (ACSF), 107
Auerbach plexus (myenteric plexus), 130
Autonomic nervous system (ANS), 128–130

**B**

BAPTISM (birthdating analysis by photoconverted fluorescent protein tracing in vivo combined with subpopulation markers), 96
Behavior/genetics/pharmacology
  criterion 1—quiescent behavior regulation, 283
    endogenous circadian rhythm, 283
    genes in zebrafish orthologs, 283
    light:dark cycle, 283
  criterion 2—quiescence, 283–284
    decreased responsiveness, 283
    increased arousal threshold, 283
    sleep-like state, definition, 283
    sleep/wake measures from wild type larvae, 285*t*
    zebrafish sleep/wake data, 284*f*
  criterion 3—sleep deprivation, 284–286
    homeostatic regulation of sleep, 284–286
    light deprivation, 286
    nighttime sleep deprivation, 284–285
    rebound sleep, 286
    shock deprivation at night, 286
  hypocretin/orexin (Hcrt) system, 286
  larval/adult zebrafish, sleep-like state in, 287
  neurotransmitter systems, 287
  non-mammalian model systems, 283
  pharmacological screen, pathways, 287
  sleep-like rest periods, 283
Berlin blue dye, 31, 36
Beta cell migration and proliferation, 268–276
  studies of, 268*t*
  time-lapse imaging of, 268–273
  visualization, 271*f*

Blastomere transplantation, 93, 100, 177–178
Blood vessels in zebrafish, imaging, 27–52
  imaging vascular gene expression, 29–30
  non-vital blood vessel imaging
    AP staining for 3 dpf embryos, 38–39
    micro-dye/-resin injection, 31–38
  vital imaging of blood vessels
    microangiography, 41–45
    in transgenic zebrafish, 45–51
Bone morphogenetic proteins (BMP) signaling, 130, 238, 264
  PHOX2B, 132
  proneural gene, Mash-1, 132
BRAD1 (BRCA1-associated domain 1 located at 2q35), 145
Breeding schemes, 187–188
  early pressure technique, 188
  in F1/F3 generation embryos, 187
  mutagenized animals (G0), 187
  screening strategies, 187–188
Bromodeoxyuridine (BrdU), 95
  injections, 179
  intraperitoneal injections of adult fish, 105–106
  labeling, 179
  tracing and marker analysis
    quiescent radial glial cells (state I progenitors), 80
    radial glial cells (state II progenitors), 80

## C

Cadherins
  cadherin17, 242
  N-cadherin, 15*t*, 98*t*, 132
  VE-cadherin, 29
Caged fluorescent dyes, 87
CAMP and MAPK signaling, 133
Carbocyanine dyes
  DiI, DiO, DiA, or DiD (Invitrogen), 9
Cell ablation methods, 102
  diphtheria toxin, use of, 102
  ganciclovir, 103
  KillerRed, 103
  laser-mediated cell ablation, 102
  prodrug (metronidazole), conversion of, 103
  thymidine kinase–ganciclovir, 103
Cell-autonomy of gene function, 17–19
  early transplants at blastula stage, 17
  entire eye primordia, transplanting, 17
  transplants at later stage, 17–19
Cell culture derivation, 59–60
  blastomere cells, 59
  medaka karyotype, 60
  nucleolar cycle, 60
  pure haploid ES cells, 60, 61*f*
  uniparental haploidy
    Albinism, 60
    haploid metaphases, 60
    haploid syndrome, 60
Cell cycle events, 95–96
  BAPTISM, 96
  Fucci, 96
  S-phase, BrdU incorporation, 96
Central nervous system (CNS), 74–75, 80, 89, 94, 96, 100, 130, 139–140, 142, 143*f*, 154–155
Charge-coupled device (CCD), 297, 320
Chemokine signaling, 266
Chlorodeoxyuridine (CldU), 96
Chromaffin cells, 129
  neural crest (NC), 129
  sympathoadrenal (SA) cell, 129
Cilia, zebrafish, 250
  alternate protocols, 253
  confocal microscopy, 253
  fixation, 252
  materials, 250–251
  methods, 251–252
  solutions, 251
Cloaca formation, 245
Cloning
  animal, 63
  Gateway
    destination vectors, 185
    entry vectors, 185
    Tol2-based zebrafish destination vector, 184
  positional and candidate, 191
    of *nagie oko locus,* 191
    standard steps, 191
Computer-aided larval motility screen (CALMS), 302–303, 306*f*, 307, 308*f*, 310
Computer-aided meiotic maturation assay (CAMMA)
  quantal endpoint assay, 309
  quantification of oocyte maturation, 309–312
  semi-automated CAMMA, 310–312
Computer-aided screening (CAS)
  survey of development after microinjection or other treatment, 302
  use of, 303*f*
Cone–rod homeobox *(crx)* gene, 208, 213–214
Confocal microscopy, 5*f*, 6, 6*f*–7*f*, 13, 19*f*, 95, 170–171, 211, 253, 296
Cyclin-dependent kinases (Cdks), 267
Cystic kidney disease, 236

## D

DAB (3,3’-diaminobenzidine) staining
  antibody staining, 166
  photoconversion, 166
  retrograde labeling, 166
*Danio rerio,* 134
  *See also* Flatbed transparency scanners in zebrafish research, use of
dHAND, 131*f*, 133, 136*t*, 137*f*
Diethylaminobenzaldehyde (DEAB), 240
Digital scanned laser light sheet fluorescence microscopy (DSLM), 95
Diluting segment, 237
Dopamine-β-hydroxylase (dbh), 131*f*, 133, 139
Dorsal bud (DB), 263
  endocrine differentiation, 265
  formation, 265–267
*Drosophila* to *Danio,* methodological considerations, 288
  direct analysis of movements by video, 288
  fine-scale measures of sleep structure
    sleep bout length, 288
    sleep bout number, 288
    sleep latency, 288
  infrared beam break method, 288
  video-based analysis
    Noldus Information Technology, 288
    Viewpoint Life Sciences, 288
Drug screens, effect on motility, 306–307
  CALMS z-projection of 3-day larvae, 306*f*
  dose–response curve, 307
  mean of standard deviation of x- and y-coordinates, 307*f*
  pentylene tetrazole (ptz), testing of, 306
Duct markers, 238
Dye injection method
  of embryos and early larvae, 36–38
  of juvenile and adult zebrafish, 38
  materials, 36
  and mounting of developing zebrafish, 37*f*

## E

Egg activation assay (EggsAct), 313–316
  17α-20β-dihydroxyprogesterone-matured zebrafish oocytes, 315*f*
  results of, 316*f*
eHAND, 133
Electroencephalographic (EEG) signatures, 282
Electron microscopy, 254–255
  materials, 254
  methods, 254–255
Electroretinography (ERG), 180
  d-wave, 180
  large positive b-wave, 180
  small negative a-wave, 180
Embryo dissociation, 245–246
Embryogenesis, 62, 95, 134–135, 154, 161–162, 166, 176, 187, 234
Embryo movement over time (x–y coordinates), 303–306
  particle analyzer menu, 303–304
  in time-lapse scans, determination of, 305–306
Embryonic stem (ES) cells, 55–68
Enhanced green fluorescent protein (EGFP), 5*f*, 7, 18*f*–19*f*, 20, 39, 40–41, 40*t*, 45–46, 50, 90*t*–91*t*, 101*t*, 102*t*, 175, 214–215, 270*t*, 271*f*, 274*f*
Enhancer trap (ET) screens, 21, 92*t*, 185
Enteric nervous systems (ENS), 128–129, 137, 143
Epson photo V500, 297
  Epson Scan scanner software, 297
Ethynyldeoxyuridine (EdU), 96, 262, 268*t*, 273, 274*f*, 275

## F

Fate-mapping studies
  late gastrulation, 155
  neurulation, 155
    neural keel, 155
    optic lobes, 155
Fibroblast growth factors (FGFs), 130
  Fgf signaling, 79, 92*t*, 130
Fight-or-flight response, 129
Flatbed transparency scanners in zebrafish research, 295–321, 299*f*
  motility analysis
    CALMS, 302–303
    CAS, 302
    drug screen effects on, 306–307
    embryo movement over time (x–y coordinates), 303–306
    pH indicators, 306–307
    vision mutants, mutant phenotype *vs.* wild type, 306
    of wild-type zebrafish embryos and larvae, 302
  oocyte and egg assays
    CAMMA, 309–312
    egg activation assay (EggsAct), 313–316
    osmoregulation during oocyte maturation, 312–313
  potential applications of scanners, 319–321
  scanner basics
    image acquisition with scanners, 299–300

Flatbed transparency scanners in zebrafish research *(cont.)*
    imageJ, 301–302
    mouse–keyboard macro for automation of scans, 301
    resolution and bit depth, 297–298
    temperature and fluidics, 298–299
  using scanners to count and measure
    oocyte/egg/embryo counting by scanners, 316–318
    scanner imaging of juveniles and adults, 318–319
Fluorescence activated cell sorting (FACS), 179, 213, 246
Fluorescent proteins (FPs), 7, 173–176, 268–269
  advantages, 176
  Dronpa green fluorescence, 176
  green fluorescent protein (GFP), 174
  photoconvertible FPs, 175
  recombination cloning approaches, 176
  red fluorescent protein (RFP), 174
  uses of
    monitoring of fate/differentiation/cell physiology, 175
    visualization of gene activity, 174
    visualization of subcellular localization of proteins, 174–175
Forward genetics, 185–191
  breeding schemes, 187–188
  mutagenesis approaches, 186–187
  mutant strains, 191
  phenotype detection methods, 188–191
  positional and candidate cloning, 191
Fucci (fluorescent ubiquitination-based cell cycle indicator), 99

## G

Gal4-specific Upstream Activating Sequence (UAS) promoter (UAS:GFP), 90
Gateway cloning
  destination vectors, 185
  entry vectors, 185
  Tol2-based zebrafish destination vector, 184
Gene expression, manipulating, 101–103
  gain-of-function approaches, 97
  loss-of-function studies, 97
  mutagenesis screens, 97
  spatial control of genetic manipulations, 100–101
    blastomere transplantation, 100
    cell-type-specific manipulations, 101, 101*t*
    Cre-loxP system, 101
    Gal4-UAS bipartite system, 100
    genetic perturbations, 100
  temporally controlled genetic manipulations, 101–103
    chemical compound, administration of, 101
    Cre-LoxP system, 101
    drug tamoxifen, administration of, 101
    heat shock promoter (hsp70), 101
    steroid Mifepristone, administration of, 101
    Tet system in mammals, 101
    time controlled cell-type-specific manipulation, 102*t*
  TILLING libraries, 97
Gene function, 65–67
  germline chimera formation, 65
  in haploid ES cells, 66
  in theory, 66–67
    genomic PCR, 67
    p53, 66–67
    RT-PCR, 67
Gene function in zebrafish retina
  forward genetics, 185–191
    breeding schemes, 187–188
    mutagenesis approaches, 186–187
    mutant strains, 191
    phenotype detection methods, 188–191
    positional and candidate cloning, 191
  reverse genetic approaches, 182–185
    approaches to gene overexpression, 184–185
    loss-of-function analysis, 182–183
Gene overexpression, 184–185
  GAL4–UAS overexpression system, 185
  GAL4–VP16 fusion protein, 184
  Gateway cloning, 184
  recombination cloning-based strategies, 184
  RNA or DNA injections, 184
  terminal inverted repeats (TIRs), 184
  T2KXIG, 184
  Tol2 transposon-based vectors, 184
Gentamicin induced kidney tubule injury, 248
  adults, 248
  embryos, 248
Ghrelin, 262
Glial cells generation, 74–75
  astrocytic function in brain, 80
  of oligodendrocytes, 80
  radial glial cells, molecular markers, 80
Glial fibrillary acid protein (GFAP), 78*t*, 82*t*, 90*t*, 89–90, 88*f*, 169*t*, 212–213
Gliogenesis, 74
Glomerular filtration, 244
  assay for, 246–247

- adults, 247–248
- embryos, 247
- blood filter, 242
- capillary tuft, 243*f*
- formation of glomerulus, 242–244
- glomerulus–tubule boundary, 241*f*

Glucagon, 262, 270

Green fluorescent protein (GFP), 8*t*, 9, 16, 19*f*, 40*t*, 45, 63, 65*f*, 88*f*, 90*t*–92*t*, 94–95, 101–102, 101*t*, 167*t*–169*t*, 173*f*, 174–176, 182, 190, 205–216, 265, 266*f*, 268*t*, 270*t*, 271*f*, 272*f*, 276, 286

## H

Hank's buffered salt solution (HBSS), 106

Haploid embryos, production of, 59, 59*f*
- androgenesis, 59
- gynogenesis, 59
  - albino medaka strains (i1 and i3), 59
- haploid syndrome, 59

Haploid ES cell
- characterization of, 62
- culture, 57–58
- lines, generation of stable, 61–62
  - clonal growth, 61
  - flow cytometry analyses, 62
  - medaka gynogenetic ES cells, 61

Haploid genetic screens, 67
- chemical mutagenesis, 67
- gene targeting, 67
- gene transfer technology, 67
- mutagenesis screening, 67

Haploid syndrome, 59–60

Heat-shocks to induce misexpression, 16–17
- focal heat shock method, 17
  - using optical fiber, 17
  - using sharpened soldering iron, 17
- global heat shocks, 17
- hsp70l promoter, 16–17

Hedgehog (Hh) signaling, 264

Helix-loop-helix gene *neurod,* 213

Holly, 65

Horseradish peroxidase (HRP) staining, 173*f*, 178

HP scanjets, 297
- HP Director, 297

$H^3$-thymidine labeling, 179

## I

ImageJ, 301–302
- bij plugin, 301
  - register ROI plugin, 302
- 32-bit version for Windows machines, 301
- dark pixels, 302
- image stacks, 301
- stack combiner, 301
- stepper motors, 301–302

Imaging blood vessels in transgenic zebrafish, 45–51
- confocal microangiography, 45
- germline transgenic zebrafish
  - *fli1a:EGFP* transgenic lines, 45–46
  - murine Tie2-GFP, 45
  - tissue-specific expression of fluorescent proteins, 45
- long-term mounting for time-lapse imaging
  - materials, 46–47
  - method, 47–49
  - mounting animals in imaging chambers, 49–50
- multiphoton time-lapse imaging, 50–51

Immunohistochemistry
- fixation of adult brain, 103
- on vibratome sections, 103

Immunostaining, 62, 81, 104

Induced pluripotent stem (iPS) cells, 56

*In situ* hybridization
- fixation of adult brain, 103
- on gelatine–albumin sections, 104
- on whole mount adult brains, 104

Insulin, 105, 248, 262–267, 270*t*, 274*f*, 276

Interkinetic nuclear migration (INM), 75, 96

Intermediate mesoderm (IM), 238
- pronephros, derivation of, 239*f*
- sequential anterior, 239

Intraflagellar transport (IFT), 181, 206, 209–210

Intrapancreatic duct system, 262

*In vivo* imaging, 93–95
- confocal microscopy, 95
- DSLM, 95
- fate tracking, 94
- light microscopy, 95
- melanin formation
  - iridophores (roy orbison embryos), 93
  - melanophores (nacre embryos), 93
- multicolor imaging, 94
- multiphoton microscopy, 95
- pigmentation mutants, 94
- spinning disk confocals, 95
- two-photon excitation, 94
- UV light irradiation, 94
- *in vivo* time-lapse imaging, 94

*In vivo* single cell electroporation, 10

Iododeoxyuridine (IdU), 96, 179

Islets of Langerhans, 262

J

June, Joubert, and Hermansky–Pudlak syndromes, 155
Juvenile/adult stages, neurogenesis at, 80
  BrdU tracing and marker analysis
    quiescent radial glial cells (state I progenitors), 80
    radial glial cells (state II progenitors), 79
  generation of neurons, 80
  neural progenitors in adult brain, 88*f*
  proneural genes, 80
  radial glial/early differentiation markers, 80
  zones of proliferation, 80

K

Kidney
  epithelial ion transport, 245
  functions, 234
  mesonephros, 234
  metanephros, 234
  nephrons, 234
  pronephros, 234

L

Labeling methods, protocols for, 11–13
  precise labeling with intra-retinal injection of lipophilic dyes
    protocol, 11–12
    solutions needed, 11
  single cell *in vivo* electroporation
    protocol, 12–13
    solutions needed, 12
Lens transplantation, 177
Light-emitting diodes (LEDs), 319
Light-sensing photoreceptors, 155
Lipofections/electroporations of adult brain *in vivo,* 96*f*, 106
Lipophilic dyes, labeling with, 9–10
  advantages, 10
  DiI (red) and DiO (green)
    dye-coated microneedle, 10
    vibrating-needle injection apparatus, 9
    “whole eye fills” technique, 9
  lipophilic carbocyanine dyes
    DiI, DiO, DiA, or DiD (Invitrogen), 9
Lipophilic tracers, 228–229
  carbocyanine dyes (DiI and DiO), 228
Live cells labeling methods, 81–88
  blastomere transplantation, 93
  caged fluorescent dyes, 87
  electroporation and lipofections, 93
  lineage analysis, 81
  mosaic labeling, 88
  photolysis, 87
  stable transgenic lines, 89–90
    expression of KalTA4, 90
    Gal4-specific UAS promoter (UAS:GFP), 90
    green fluorescent protein (GFP), 89
  transient expression of RNA and DNA, 88–89
    targeting neural plate by injection, 89*f*
  ubiquitous labeling, 88
  *in vivo* imaging, *See In vivo* imaging
Long-term, high-throughput sleep/wake monitoring, 291–292
  DMSO concentration, 289
  infrared LED panel, 289
  single cell on 14/10 h light/dark (LD) cycle, 288–289
Long-term mounting for time-lapse imaging
  materials, 46–47
  method, 47–49
    mounting animals in imaging chambers, 49–50
    preparation of imaging chambers, 47–49
  mounting zebrafish embryos and larvae for, 48*f*–49*f*
Loss-of-function analysis, 182–183
  antisense-based interference, 182
  morpholino-modified oligonucleotides
    disadvantages, 183
    Gene Tools LLC (designing morpholinos), 183
    RTPCR (splice-site morpholinos), 183
  mutagenesis approaches in zebrafish
    DNA sequences, 183
    ZFNs, 183
  TILLING, 183

M

Macroscheduler, 301
Mammalian achaete-scute homolog (Mash-1), 131*f*, 132–133, 137
MAPK pathway, 145
*Meccom,* 240
Medaka haploid embryonic stem cells, 55–68
  applications of
    analysis of gene function, 65–67
    haploid genetic screens, 67
    semicloning, 63–65
  haploid ES cell culture, 57–58
    in *Drosophila,* 57
    first mouse ES cells, 58
    in frog, 57
    in human, 57

  haploidy in evolution, 57
    asexual reproduction, 57
    honeybee (invertebrates), 57
    meiosis, 57
    plantlets, 57
    yeast (single-celled eukaryotic organisms), 57
  methods
    cell culture derivation, 59–60
    characterization of haploid ES cells, 62
    culture condition, 60
    generation of stable haploid ES cell lines, 61–62
    production of haploid embryos, 59
    stable growth and genetic stability, 62–63
  rationale, 58
Meissners plexus (submucosal plexus), 130
Mesonephros, 234
Metanephric kidney, 234
Metanephros, 234
Microangiography, 41–45
  of developing zebrafish embryos and larvae, 43*f*
  experimental procedure, 43–45
  materials, 41–42
    PEG-coated non-targeted QDs, 42
    Quantum dots (QD), 42
  preparation of apparatus, 42–43
    glass microinjection needles, 42
    for holding embryos, 42–43
    holding pipettes, 42
    for microinjection, 42
Micro-dye and micro-resin injection, 31–38
  classical dye or resin injection methods, 31
  corrosive resin casting method, 31
  dye injection method
    materials, 36
    protocol, 36–38
  Florence Sabin (vascular embryologists), 31
  resin injection method
    materials, 31
    protocol, 31
Microphonics
  biologically relevant signal, 225
    bidirectional stimuli (sine waves), 225
    dihydrostreptomycin and amiloride, 225
  recordings from neuromast hair cells, 224
    mechanotransduction channels, 224
    posterior lateral-line neuromasts, 224*f*
    secondary neuromasts, 224
    standard patch electrodes, 224
  signal collection and analysis, 224–225
  stimulation of neuromast hair cells, 223
    stereociliary hair bundle, 223
    water jet pipette, 223
Microsurgery tool (Fine Science Tools 10055-12), 106
Midgastrulation, 264
Molecular markers, 81
  antibodies and antisense RNA probes, 81
    distinct cellular states, 82*t*–87*t*
    neuronal identity markers, 84*t*–87*t*
  immunostaining and *in situ* hybridization, 81
  phosphohistone H3, 81
  proliferating cell nuclear antigen (PCNA), 81
  use of, 166–176
    antibodies, 166–172
    cell class-specific markers, 166
    endogenous transcripts and proteins, 166
    fluorescent proteins (FPs), 173–176
    lipophilic tracers, 172–173
    mRNA Probes, 172
    to study zebrafish retina, 167*t*–169*t*
    transverse sections through center of zebrafish eye, 170*f*–171*f*
Monitoring sleep and arousal in zebrafish, 281–291
  behavior
    criterion 1—quiescent behavior regulation, 283
    criterion 2—quiescence, 283–284
    criterion 3—sleep deprivation, 284–286
  *Drosophila* to *Danio,* methodological considerations, 288
  genetics and pharmacology, 286–287
  high-throughput tracking of zebrafish locomotor behavior, 282*f*
  long-term, high-throughput sleep/wake monitoring, 289–290
  of sleep/wake behaviors
    average activity per waking minute, 290–291
    sleep bout number/length, 290
    sleep latency, 290
    total sleep, 290
Morphogenesis, 28, 52, 75, 76*f*, 88, 135, 158–159, 161, 176, 191, 243*f*, 262–263, 265–266, 269
Morphogenetic events, early, 155–157, 156*f*
  choroid fissure forms, 157
  fate-mapping studies, 155
  invagination, 157
  lens rudiment, 156*f*, 157
  optic cup, sheets of cells in
    cuboidal pigmented epithelium (pe), 157
    pseudostratified columnar neuroepithelium (rne), 157
  optic stalk, 157
  retinal pigmented epithelium (RPE), 157
Morpholino knockdown embryos, 266–267

Morpholino oligonucleotides (MOs) injections, 13, 16
  hsp70l heat shock promoter, 16
  morpholino oligonucleotides (MOs), 16
  protein translation, 16
  splicing of pre-mRNAs, 16
  transcription factor *atoh7,* 16
Mosaic analysis
  genetic approaches in *Drosophila,* 177
  in mosaic animals, 179
  quality of transplantation needle, 178
    features, 178
    preparation (beveler and microforge), 178
  tracer purity, 178
  UV illumination, 177
  *The Zebrafish Book,* 178
  in zebrafish retina, 179
Mounting and immobilizing, zebrafish, 221*f*
  anesthesia and mounting of larvae, 222
  coating chamber with Sylgard, 221
  immobilizing larvae with α-Bungarotoxin, 222–223
    α-bungarotoxin (125 μM) injection, 222
    electrophysiological recordings, 222
    2-hydroxyethyl-1-piperazineethanesulfonic acid (HEPES), 223
    inclusion of phenol red, 222–223
  larva anesthetized with tricaine, 221
  lateral-line system of larvae, 221
  paralytic (α-bungarotoxin), 222
  recording chamber with circular opening (PC-R), 221
  studies with primary neuromasts, 221
mRNA Probes, 172
  alkaline phosphatase (AP), 172
  *in situ* hybridization, 172
  *in situ* reagents, 172
Multiphoton time-lapse imaging, 50–51
  4-D imaging, 50
  multiphoton transgenic blood vessel imaging, 51
  PTU, 50
  three dimensionality, 50
  tricaine (MS-222), use of, 50
Multiple endocrine neoplasia syndromes type IIA and type IIB (MEN IIA/B), 129
Mutagenesis approaches, 186–187
  *N*-ethyl-*N*-nitrosourea (ENU), use of, 186
  insertional mutagenesis strategies, 186
  retroviral mutagenesis, 186
  transposon-based mutagenesis
    enhancer or gene trap vectors, 186
    hAT (Tol2) families, 186
    Tc-1/mariner (Sleeping beauty), 186

**N**

Nephrin, 242, 243*f*
Nephrogenic mesoderm
  origin of, 238
  subdomains, early, 238–239
Nephrons, 234, 235*f*, 236, 245*f*, 248–249
Neural crest (NC) cells
  chromaffin cells, 129
  development and migration, 135–136
    fate decisions, 135–136
    migration and cell fate specification, 135
  formation and fate specification of, 130
  neuregulin-1 pathway, 132
  premigratory stage, 130
  progenitors, 130
    bone morphogenetic proteins (BMPs), 130
    fibroblast growth factors (FGFs), 130
    retinoic acid (RA), 130
    *Snai11/2/Tfap2α/Foxd3,* genes, 130
    Wnt signaling, 130
  restricting NC cell migration, 132
  ventrolateral migration, 132
Neural plate
  fate map/neurogenesis/early proneural clusters, 76*f*
  molecular determinants/patterning of, 77
    anterior neural plate (ANP), 77
    BMP signaling, 77
    neural crest and Rohon-Beard neurons, 77
    neural progenitors, 77
    SoxB transcription factors, 77
  and tube formation, 75
    brain regions and markers, 75
    fate mapping study, 75
    interkinetic nuclear migration (INM), 75
    Par3, localization of, 75
    6–10 somite stages, 75
    structural proteins, localization of, 75
    two-dimensional neural plate (gastrulation), 75
    ZO1 and N cadherin, localization of, 75
Neural retina leucine zipper (Nrl), 208
Neuroblastoma (NB)
  aberrant MYCN expression, 145
  allelic losses, 145
  anaplastic lymphoma kinase *(ALK)* gene, 145
  cytogenetic analyses, 145
  embryonic tumor of PSNS, 144
  *PHOX2B* gene, 145
  signaling pathways
    MAPK pathway, 145
    PI3K/Akt pathway, 145
    STAT3 pathway, 145

  - single nucleotide polymorphisms, 145
    - BRAD1 (BRCA1-associated domain 1 located at 2q35), 145
    - putative gene FLJ22536 at 6p22, 145
  - studies in zebrafish, 145–146
    - morpholinos and shRNA techniques, 146
    - murine transgenic mice, 145–146
    - new zebrafish model of NB, 146
    - TILLING, 146
    - *in vivo* animal model of NB, 145
    - Zinc-Finger Nuclease strategies, 146
  - tumor suppressor genes (KIF1B and miR34a), 145
- Neurogenesis, 73–107, 157–159
  - cell cycle, changes in, 158
    - lakritz gene, 158
  - cell fate determination, 159
  - classes of neurons, 159
    - ganglion cell differentiation, 159
  - in development and adult brain
    - formation of neural plate/tube, 75
    - generation of glial cells, 79–80
    - molecular determinants/patterning of neural plate, 77
    - neurogenesis at juvenile/adult stages, 80
    - proneural domains/lateral inhibition/neurogenic cascade, 77–84
    - signaling centers and downstream neuronal specification, 79
    - zones of delayed differentiation, 78
  - methods in developing and adult brain
    - expression of genes, manipulation, 97–99
    - to follow cell cycle events, 95–96
    - methods to label live cells, 81–88
    - molecular markers, 981
    - for targeted cell ablations, 103
    - *in vivo* imaging, 93–95
  - mitotic divisions, 158
  - photoreceptor morphogenesis, 159
    - photoreceptor mosaic, 160
    - types of photoreceptor cells, 159–160
  - postmitotic neurons, 159
  - protocols to study adult neurogenesis
    - fixation of adult brain, 103
    - immunohistochemistry on vibratome sections, 103
    - intraperitoneal injections of BrdU, 105–106
    - lipofections/electroporations of adult brain *in vivo,* 105
    - pretreatments, antigen retrieval, 104
    - *in situ* hybridization, 104
    - slice culture, 107
    - sterile filter, 107
  - retinal neuroepithelium, 157*f*, 158
  - two-photon imaging studies, 158
  - in zebrafish retina, 173*f*
- Neurotransmitters, 129
- Non-neuronal tissues, 161
  - choroidal and retinal vasculatures, 161
  - other non-neuronal ocular tissues, 161
  - transgenic lines, 161
- Non-vital blood vessel imaging
  - alkaline phosphatase staining for 3 dpf embryos, 38–39
  - micro-dye and micro-resin injection, 31–38
- Noradrenergic neurons, differentiation of, 139–141
  - expression of Hu proteins, 139
  - expression of noradrenalin and genes
    - dopamine-β-hydroxylase (dbh), 139
    - tyrosine hydroxylase (th), 138–140
  - phenylethanolamine-*N*-methyltransferase (PNMT), 140
    - mRNA *in situ* hybridization assays, 140
  - sympathoadrenal derivatives in embryonic and juvenile zebrafish, 141*f*
  - tyrosine hydroxylase gene *(th2),* 139
- Normal goat serum (NGS), 104–105, 250–252, 275
- Nuclear localization signal (NLS), 269
- Nucleolar silver staining, 60

## O

- Oocyte and egg assays
  - CAMMA, 309–310, 312, 312*f*, 313*f*
    - changes during oocyte maturation and egg activation, 311*f*
    - prophase I zebrafish ovarian oocytes, 311*f*
  - egg activation assay (EggsAct), 313–316
  - individual zebrafish oocytes *vs.* time of incubation, 313*f*
  - osmoregulation during oocyte maturation, 312–313, 314*f*
    - cytolysis of zebrafish oocytes, 315*f*
- Oocyte/egg/embryo counting by scanners, 316–318
  - counting zebrafish embryos, 317*f*
  - semi-automated zebrafish embryo counting with ImageJ, 316–318
- Optokinetic response (OKR), 164*t*, 180, 190, 211, 307, 308*f*
- Organ morphogenesis, 263
- *Oryzias latipes* (fish medaka), 57
- Osmoregulation during oocyte maturation, 312–313
  - fully grown oocytes, 313
  - immature oocytes, 312–313
  - oviposition, 312

## P

Pancreas development, 263*f*
  beta-cell proliferation, 267–268, 268*t*, 273–276
  cell segregation into DB and VB, 264–265
  dorsal bud, formation, 265–267
  morphogenesis, 262–263
  specification, 261–262
Paraformaldehyde (PFA), 11, 38–39, 103, 107, 170, 251, 254, 275
Pedicles, 206
Peripheral autonomic nervous system, 128–129
Peripheral sympathetic nervous system (PSNS) development, 127–146
  molecular pathways of, 130–134
    bHLH transcription factor HAND2 (dHAND), 133
    bilateral migration of SA cells, 130
    dose-dependent BMP signaling, 132, 134
    HAND1 (eHAND), 133
    homeobox proteins PHOX2A, 133
    NC cells, *See* Neural crest (NC) cells
    neuronal and noradrenergic differentiation of SA progenitors, 130
    neurotrophic factors (NGF and NT-3), 133
    PHOX2A and PHOX2B, 133
    PSNS neurons, 130
    zebrafish *(Danio rerio),* 134
    zinc-finger proteins GATA-2/3, 133
  mutations affecting, 142–144
    isolation of PSNS mutants in zebrafish, 143*f*
    lockjaw or mount blanc mutant (tfap2a), 143
    NC fate specification, 143
    nosedive mutant, 143
    retinoic acid (RA) signaling pathways, 144
    SCG formation, 142
    sympathetic mutant 1 (sym1), 142–143
    *th* mRNA whole-mount in situ hybridization, 142
    zebrafish colorless (cls) mutant, 142–143
    zebrafish hands off mutant, 144
  peripheral autonomic nervous system, 128–129
  PSNS development in zebrafish, 134–144, 137*f*
    differentiation of noradrenergic neurons, 139–141
    gene expression in migrating SA progenitors, 136–138
    modeling of sympathetic ganglia, 141–142
    murine gene knockout models, 135
    neural crest development and migration, 135–136
    neuronal differentiation and coalescence, 138
    new gene identification for, 135
    phenotype-based genetic screens, 134
Phenotype detection methods, 188–191
  behavioral tests, 190
  DiI and DiO labeling, 189
  genetic screen, 189
  large-scale mutagenesis screens, 188
  metabolic pathways or DNA replication machinery, 188
  mutant phenotype recognition strategy, 188
  optokinetic response, 190
  optomotor response, lack of, 189
  transgenic GFP lines, 190
  visual inspection screens, 189
Phenylethanolamine-*N*-methyltransferase (PNMT), 136*t*, 139, 142
1-Phenyl-2-thiourea (PTU), 12, 20–21, 43, 46–47, 49–50, 94, 162, 252, 275
Pheochromocytomas, 129
pH indicators, colorimetric potential of scanners, 307–309
  24-bit images, 308
  color scanners, 307
  green channel stack, 308
  phenol red pH indicator dye, 307
  relationship between degree of larval movement, 309*f*
  use of colorimetric capability of scanners, 310*f*
Phosphate-buffered saline (PBS), 11–12, 104–105, 107, 170, 246, 250–253, 273
Photoreceptor cells
  cones
    double cones, 160
    green and red opsin genes, 160
    long and short single cones, 160
  rods, 159
Photoreceptor structure and development: analyses using GFP transgenes, 205–216
  anatomy and biochemistry, 206–207
    cone photoreceptors, 206
    cone subtypes, 206
    intraflagellar transport (IFT), 206
    outer segments (OSs), 206
    spherules and pedicles, 206
    vertebrate cone (left) and rod (right) photoreceptors, 206, 207*f*
  development, 207–208
    cone differentiation, 207–208
    electroretinogram (ERG) recordings, 208
    intrinsic and extrinsic factors, 208
    rod differentiation, 208
  regeneration, 211–215

    - bromodeoxyuridine (BrdU) labeling, 213
    - cell death, 212
    - co-labeling, 214
    - damaged rod photoreceptors, 212
    - markers of Müller cells, 212
    - neurogenic clusters, 212
    - Notch–Delta pathway, 213
    - ONL and INL, 213–214
    - post-embryonic growth in teleosts, 212
    - proliferating cell nuclear antigen (PCNA), 213
    - recovery of vision, 212
    - XOPS-mCFP transgenic line, 214
  - size, regulation of, 210–211
    - crumbs in *Drosophila,* overexpression of, 211
    - FERM protein Mosaic eyes, 210
    - rod-specific *(Tg)XOPS:GFP* transgene, 210
    - zebrafish mosaic eyes (moe) gene, 210
  - synapse structure, 211
    - confocal microscopy of transgenic mutants *(Tg(TαC:GFP)nrc),* 211
    - no optokinetic response c (nrc) mutant, 211
    - optokinetic response (OKR) assay, 211
    - synaptojanin 1, 211
  - transgenic technology, improvements in, 208–209
    - “founder fish”, 208
    - I-SceI, rare-cutting endonuclease, 209
    - site-specific recombination cloning (Gateway®) technology, 209
  - transport mechanisms, 209–210
    - connecting cilium, 209
    - heterotrimeric kinesin-II motor, 210
    - intraflagellar transport (IFT), 209–210
    - Kif3b (DNKIF3B), 210
    - photoreceptor OSs, 209
    - studies in *Caenorhabditis elegans,* 210
    - studies in *Xenopus* Kif3b or mouse Kif17, 210
- PI3K/Akt pathway, 145
- Podocin, 242–243
- Podocytes, 234, 239–244, 256
- Proliferating cell nuclear antigen (PCNA), 81, 96, 213–214, 268, 273
- Proliferation in pancreas using EdU, 273–276
- Pronephric cilia, 250
- Pronephric duct, 236, 245
- Pronephric podocytes, 243, 244*f*
- Pronephros, 234, 235*f*, 247
  - division
    - distal early (DE), 236
    - distal late (DL), 236
    - proximal convoluted tubule (PCT), 236
    - proximal straight tubule (PST), 236
  - structure of, 236–237
- Pronephros formation
  - cloaca formation, 245
  - endoderm, role of, 240
  - glomerulus formation, 242–244
  - nephrogenic mesoderm
    - origin of, 238
    - subdomains, early, 238–239
  - *pax2a,* role of, 240
  - retinoic acid signaling, role of, 240
  - tubular epithelium, differentiation, 241–242
  - zebrafish mutants with defects, 239*t*
- Pronephros function, methods to study
  - adult kidney isolation, 249
  - electron microscopy methods for zebrafish
    - materials, 254
    - methods, 254–255
  - embryo dissociation, 245–246
  - fluorescently labeled cells by FACS, 246
  - gentamicin induced kidney tubule injury, 248
    - adults, 248
    - embryos, 248
  - glomerular filtration, assay for, 246–247
    - adults, 247–248
    - embryos, 247
  - histological sectioning of wholemount stained embryos, 253–254
  - non-lethal surgical access to adult kidney, 250
  - zebrafish cilia, 250
    - alternate protocols, 253
    - antibody staining, 252
    - confocal microscopy, mounting sample for, 253
    - fixation, 252
    - materials, 250–251
    - methods, 251–252
    - solutions, 251
- Proneural domains/lateral inhibition/neurogenic cascade, 77–84
  - antibodies and antisense probes, 82*t*
    - distinct cellular states, 82*t*–87*t*
    - neuronal identity markers, 84*t*–85*t*
  - Cdkn1c and histone deacetylase, 78
  - 2 days post-fertilization (dpf), 77
  - family of Hairy/Enhancer of Split genes, 78
  - 18 h post-fertilization (hpf), 77
  - Notch ligands and receptors, 78
  - proneural/neurogenic genes, 78
  - “salt and pepper” pattern, 78
- Proteinuria or nephrotic syndrome, 242, 247
- Proximal convoluted tubule (PCT), 235–237, 239, 247–248
- Proximal straight tubule (PST), 236–237, 267

## R

- RA-producing enzyme (RALDH), 264
- Recordings from lateral-line hair cells/afferent neurons, physiological, 219–229
  - action currents
    - analysis of action currents, 226–228
    - electrode and recording details, 226
  - microphonics
    - biologically relevant signal, 225
    - recordings from neuromast hair cells, 224
    - signal collection and analysis, 224–225
    - stimulation of neuromast hair cells, 223, 226
  - zebrafish mounting and immobilizing, 221–223
    - anesthesia and mounting of larvae, 222
    - immobilizing larvae with α–Bungarotoxin, 222–223
- Regeneration, 211–215
  - expression of *nr2e3,* 214
  - fin and heart regeneration
    - *hspd1*, 213–214
    - *mps1*, 214
  - GFP fluorescence, 213
  - identification of neurogenesis, 212
  - inner nuclear layer (INL), 212
  - metronidazole treatment, 215
  - Müller glial-derived mitotic cells, 213
  - neurogenic clusters, 212
  - *no blastema (nbl),* 214
  - NTR-EGFP fusion protein, 214
  - *pax6* expression, 213–214
  - post-embryonic growth in teleosts, 212
  - proliferating cell nuclear antigen (PCNA), 213
  - rod progenitor cells, 212, 214
  - subpopulation of Müller glia, 212
  - uncovering genes, 213
  - visual sensitivity, 212
  - XOPS-mCFP transgenic line, 214
- Region of interest (ROI), 96, 272, 301–302, 304–305, 310–312
- Relisys scanner
  - ArtScan (Relisys), 297
- Resin injection method, 31*f*, 31–32, 38, 40
  - experimental procedure, 34–36
    - digestion of tissue, 36
    - fixation with 2% glutaraldehyde, 35
    - mixing resin, 35
    - saline buffer, 34–35
    - scanning electron microscopy, 36
  - materials, 31
  - preparation of apparatus, 31–33
    - glass needles, 32–33, 32*f*
    - for injecting fixative, 33, 33*f*
    - for injecting physiological saline buffer, 33, 33*f*
    - for injecting resin, 33
    - paraffin bed, 31–32, 32*f*
    - resin for injection, preparation of, 33–34, 34*f*
- Retina in zebrafish model, 153–192
  - analysis of gene function
    - forward genetics, 185–191
    - reverse genetic approaches, 182–185
  - analysis of wild-type and mutant visual system
    - behavioral studies, 180
    - biochemical approaches, 181
    - cell and tissue interactions, 177–179
    - cell movements and lineage relationships, 176
    - cell proliferation, 179
    - chemical screens, 181–182
    - electrophysiological analysis of retinal function, 180–181
    - histological analysis, 162–166
    - molecular markers, use of, 166–176
  - development of
    - early morphogenetic events, 155–157
    - neurogenesis, 158–160
    - non-neuronal tissues, 161
    - retinotectal projections, 160–161, 172, 177
  - histology of, 157*f*
- Retinal axon guidance in zebrafish, analyzing, 3–22
  - perturbing retinotectal system
    - injecting DNA or MOs, 16
    - protocols for transplants, 19–21
    - retinotectal mutants, 13–16
    - transplanting to test cell-autonomy of function, 17–19
    - using heat-shocks to induce misexpression, 16–17
    - zebrafish retinotectal projection, 5*f*, 18*f*–19*f*
  - visualizing retinal axons
    - labeling with antibodies, 9
    - labeling with lipophilic dyes, 9–10
    - methods for, 6*f*–7*f*
    - protocols for labeling methods, 11–13
    - time-lapse imaging, 11
    - transgenic lines, 7–9
    - transiently expressing DNA constructs, 10
    - *in vivo* single cell electroporation, 10
- Retinal ganglion cells (RGCs), 4–10, 12–13, 17, 19–21, 84, 86, 161, 189
- Retinoic acid (RA), 130, 264
  - signaling, 144, 240, 264
- Retinotectal mutants, 13–16, 14*t*–15*t*
  - ace/fgf8, 16
  - *astray/robo2* genes, 16

  *gdf6a and collagenIVa5,* 16
  *pou4f3: mGFP* transgenic line, 16
  projection, 5*f*–7*f*, 18*f*–19*f*
  regulators of axon guidance or brain patterning
    adhesion molecule *N-cadherin,* 13
    receptor *robo2 or patched1,* 13
    transcription factor *lhx2,* 13
Retinotectal projections, 160–161
  ganglion cell axons, 160–161
  optic nerve head, 160
  optic tectum, 160–161
  optic tract, 161
Retinotectal system, perturbation
  cell-autonomy, 17–19
  heat-shocks to induce misexpression, 16–17
  injecting DNA or MOs, 16
  protocols for transplants, 19–21
  retinotectal mutants, 13–16, 14*t*–15*t*
  zebrafish retinotectal projection, 5*f*–7*f*
Reverse genetic approaches, 182–185
  approaches to gene overexpression, 184–185
  loss-of-function analysis, 182–183
Reverse transcription polymerase chain reaction (RTPCR), 183

## S

SA progenitors, gene expression in migrating, 136–138
  cyclops mutant, 137
  expression of bmp, 137*f*, 138
  expression of conserved PSNS genes, 136*t*
  gene knockdown techniques, 138
  noradrenergic differentiation, 138
  no tail mutants, 137
  *phox2a/phox2b/gata-2/3/hand2* genes, 137
  soulless, 138
  zash1a gene (homolog of Mash-1), 137
Scanners
  to count and measure
    oocyte/egg/embryo counting by scanners, 316–318
    scanner imaging of juveniles and adults, 318–319
  image acquisition with, 299–300
    8-bit grayscale or 24-bit color, 300
    rectangular marquee tool, 300
    reflective or transmitted mode, 300
    resolution, selection of, 300
  imageJ, 301–302
  imaging of juveniles and adults, 318–319
    documentation of disease and abnormal morphology, 320*f*
    morphometrics and archival images, 319*f*, 320*f*
    tumors or abnormal morphologies, 318–319
  Macroscheduler, 301
  multiwell plates/pipette pump in imaging arrays, 300*f*
  pH indicators, 307–309
  potential applications of, 319–321
    catfish embryos *(Ictalurus punctatus),* 320
    diode lasers, 320
    light-emitting diodes (LEDs), 319–320
    myofibrils in zebrafish larval muscle, 320
    sheets of colored filter (Wratten filters), 320
    transparency scanners, 320
  resolution and bit depth, 297–298
    8-bit grayscale image, 298
    optical resolution, 298
    12- or 16-bit grayscale or 48-bit color (higher bit depth), 298
    red, blue, green (RGB) image (24-bit image), 298
  temperature and fluidics, 298–299
    cold media, 298
    long-term scanning, 298
    multiwell plates, 299, 300f
    Nunc rectangular plates, 298
    simple thermistor probe, 298
Semicloning, 63–65
  animal cloning, 63
  first semicloned medaka (Holly), 65
  and germline transmission, 64*f*–65*f*
  human ES cell derivation, 63
  i1 and i3 males, test-crosses to, 65
  intracytoplasmic sperm injection, 63
  NT1, 63
  nuclear reprogramming, 63
Signaling centers and downstream neuronal specification, 79
  FGF signaling activity, 79
  manipulation of whole embryo, 97*t*–98*t*
  mutants affecting neuronal specification, 99*t*
  transgenic lines to visualize distinct states and fates, 90*t*–91*t*
  Uas effector lines, 92*t*
  V3 and KA″/KA′ interneurons, 79–80
  Wnt signaling activity, 79
Sleep, zebrafish
  behavior, 282–286
  genetics and pharmacology, 286–287
Sleep bout, 284–285, 288, 290
Sleep latency, 284–285, 288, 290
Sleep rebound, 283–286

Sleep/wake behaviors
  average activity per waking minute, 290–291
  sleep bout number/length, 290
  sleep latency, 290
  total sleep, 290
Slice culture, 74, 81, 107
*Smo/smoothened* mutant endoderm cells, 264
Somatostatin, 82, 168*t*, 262, 270
Somitogenesis, 235, 238–239, 241, 265, 272, 303
Sonic hedgehog (Shh), 15, 79, 132, 174, 208
Spherules, 206
Stable growth and genetic stability
  diploidization and haploidization, 62–63
  ES cell lines, 62–63
  HX cell lines, 62–63
Standard whole-mount antibody staining, 9
*Starmaker* gene, 236, 237f
STAT3 pathway, 145
Sterile filter
  brain embedding, cutting, and culture, 107
  fixation, 107
Sympathetic ganglia
  modeling of, 141–142
    neurotrophic factors (NGF and NT-3), 141
    pan-neuronal marker, 16A11, expression of, 141
    Rohon-Beard sensory neurons, 141
    *TrkA* expression, 141
  neuronal differentiation and coalescence into, 138
    expression of BMPs, 138
    pan-neuronal antibody 16A11, 138
    superior cervical ganglion (SCG) complex, 138
Sympathetic nervous system
  adenosine triphosphate, 129
  long adrenergic postganglia, 129
  preganglionic neurons, 129
  smooth muscle cells (cardiac muscle cells), 129

## T

Teleost retinae, 154
Terminal inverted repeats (TIRs), 184
TGF-beta/Nodal signaling, 263
Thick ascending limb (TAL), 237
TILLING (Targeting induced local lesions in genomes), 97, 99*t*, 146, 163, 183
Time-lapse imaging, 11, 268–272, 300*f*
  confocal or two-photon microscopy, 11
Tissue specification, 263
Tol2kit, 209
Transgenesis, 209
Transgenic lines, 7–9
  advantages, 7
  enhanced green FP (EGFP), 7
  fluorescent proteins (FPs), 7
  Gal4-VP16, 7
  GAP-43, N-terminal palmitoylation sequence, 7
  *isl2b* and *atoh7* genes, 7
  labeling RGCs, 8*t*
  and pancreatic cells, 270*t*
  *pou4f3* genes, 7
Transplants, protocols for, 19–21
  blastula transplants, 19–20
  late topographic transplants
    protocol, 20–21
    solutions needed, 20
Transport mechanisms, 209–210
Tubule formation, 241
Tyrosine hydroxylase (th), 81, 84*t*, 131, 133, 139, 145, 168*t*, 171*f*, 189

## U

Umax Astra 6700, 297, 300
  SilverFast SE (Umax), 297

## V

Vascular endothelial growth factor (vegf), 244
Vascular gene expression, imaging, 29–30
  Disabled-2 (Dab2), cytosolic adaptor, 30
  ephb4, venous marker, 30
  immunohistochemistry, 29
  marker genes used in zebrafish vasculature research, 29*t*
  Prox-1 and Lyve-1, lymphatic endothelial markers, 30
  *in situ* hybridization, 29
    *fli1a* and *scl* genes, 29
    *kdrl* and *flt4* genes, 29–30
    other genes *(efnb2/grl/Dll4/Tbx20/notch5),* 30
    *tie2* and *cdh5* genes, 29
Ventral bud (VB), 263–266
Vision mutants, mutant phenotype *vs.* wild type, 307
  motility differences in laj$^{s304}$ mutant and wild-type (wt) sibs, 308f
  optokinetic response (OKR), 307
Visualizing retinal axons
  labeling with antibodies, 9
  labeling with lipophilic dyes, 9–10
  protocols for labeling methods, 11–13
  time-lapse imaging, 11
  transgenic lines, 7–9
  transiently expressing DNA constructs, 10
  *in vivo* single cell electroporation, 10

- Vital dyes, 135
- Vital imaging of blood vessels
  - confocal microangiography, 39–41, 45
  - confocal or multiphoton microscope, 44
  - high-resolution imaging, 40
  - imaging blood vessels in transgenic zebrafish, 45–51
  - microangiography, 41–45
  - multiphoton time-lapse imaging, 41, 50–51
  - transgenic lines expressing nuclear-targeted EGFP
    - artery/venous sprouts *Tg(flt1:YFP; kdrl: mCherryRed),* 41
    - *Tg(fli1a:EGFP–cdc42wt)*$^{y48}$, 41
    - *Tg(fli1a:EGFP; gata1:DsRed),* 41
    - *Tg(fli1a:EGFP; kdrl:ras-cherry),* 41
    - *Tg(fli1a:nEGFP)*$^{y7}$, 41
    - *Tg(gata1:DsRed)*$^{sd2}$, 41
  - zebrafish *fli1a:EGFP/kdrl:EGFP,* 40
  - zebrafish transgenic lines for time-lapse vascular imaging, 40*t*

## W

- Wild-type and mutant visual system, analysis of
  - behavioral studies, 180
    - escape response, 180
    - optokinetic response, 180
    - optomotor response, 180
    - phototaxis, 180
    - startle response, 180
  - biochemical approaches, 181
    - co-immunoprecipitation, 181
    - tandem affinity purification (TAP) tag, 181
  - cell and tissue interactions, 177–179
    - advantages and disadvantages, 179
    - conventional or confocal miscroscopy, 178
    - enzymatic detection reactions, 178
    - fluorophore-conjugated tracer, 178
    - HRP-conjugated streptavidin version, 178
    - mCFP Q01 line, 179
    - mosaic analysis, 177–179
    - transplantation techniques, 177
  - cell movements and lineage relationships, 176
    - Caged flourescein, 176
    - iontophoresis, 176
    - *Xenopus laevis,* iontophoretic cell labeling in, 176
    - zebrafish retina, lineage analysis in, 176
  - cell proliferation, 179
    - bromodeoxyuridine (BrdU) injections, 179
    - fluorescence activated cell sorting (FACS), 179
    - H$^3$-thymidine labeling, 179
  - chemical screens, 181–182
    - chemical compound libraries, 182
    - flk-GFP transgenic line, 182
    - phenotype detection approaches, 182
    - small-molecule screening, 182
  - electrophysiological analysis of retinal function, 180–181
    - electroretinography (ERG), 180–181
    - ganglion cell function, 181
    - OFF response, 180
    - retinal responses, 180
  - histological analysis, 162–166
    - DAB-labeled, 166
    - electron microscopy, 162, 166
    - epoxy resins, 162
    - light microscopy, 162
  - molecular markers, use of, 166–176
    - antibodies, 166–172
    - cell class-specific markers, 166
    - endogenous transcripts and proteins, 166
    - fluorescent proteins, 173–176
    - lipophilic tracers, 172–173
    - mRNA Probes, 172
  - studies of zebrafish retina and their sources/examples of use, 163*t*–165*t*
- Wild-type zebrafish embryos and larvae, motility of, 302
  - z-Projection of scanner images, 304*f*
- Wnt signaling, 79, 130, 265, 267
- Wolffian ducts, 236

## Z

- *The Zebrafish Book,* 178
- Zebrafish Model Organism Database (ZFIN), 8, 191
- Zinc finger nucleases (ZFNs), 97, 183
- Zn-5/8 staining, 9
- Zymogens, 262

# VOLUMES IN SERIES

**Founding Series Editor**
**DAVID M. PRESCOTT**

**Volume 1 (1964)**
**Methods in Cell Physiology**
*Edited by David M. Prescott*

**Volume 2 (1966)**
**Methods in Cell Physiology**
*Edited by David M. Prescott*

**Volume 3 (1968)**
**Methods in Cell Physiology**
*Edited by David M. Prescott*

**Volume 4 (1970)**
**Methods in Cell Physiology**
*Edited by David M. Prescott*

**Volume 5 (1972)**
**Methods in Cell Physiology**
*Edited by David M. Prescott*

**Volume 6 (1973)**
**Methods in Cell Physiology**
*Edited by David M. Prescott*

**Volume 7 (1973)**
**Methods in Cell Biology**
*Edited by David M. Prescott*

**Volume 8 (1974)**
**Methods in Cell Biology**
*Edited by David M. Prescott*

**Volume 9 (1975)**
**Methods in Cell Biology**
*Edited by David M. Prescott*

**Volume 10 (1975)**
**Methods in Cell Biology**
*Edited by David M. Prescott*

**Volume 11 (1975)**
**Yeast Cells**
*Edited by David M. Prescott*

**Volume 12 (1975)**
**Yeast Cells**
*Edited by David M. Prescott*

**Volume 13 (1976)**
**Methods in Cell Biology**
*Edited by David M. Prescott*

**Volume 14 (1976)**
**Methods in Cell Biology**
*Edited by David M. Prescott*

**Volume 15 (1977)**
**Methods in Cell Biology**
*Edited by David M. Prescott*

**Volume 16 (1977)**
**Chromatin and Chromosomal Protein Research I**
*Edited by Gary Stein, Janet Stein, and Lewis J. Kleinsmith*

**Volume 17 (1978)**
**Chromatin and Chromosomal Protein Research II**
*Edited by Gary Stein, Janet Stein, and Lewis J. Kleinsmith*

**Volume 18 (1978)**
**Chromatin and Chromosomal Protein Research III**
*Edited by Gary Stein, Janet Stein, and Lewis J. Kleinsmith*

**Volume 19 (1978)**
**Chromatin and Chromosomal Protein Research IV**
*Edited by Gary Stein, Janet Stein, and Lewis J. Kleinsmith*

**Volume 20 (1978)**
**Methods in Cell Biology**
*Edited by David M. Prescott*

## Advisory Board Chairman
## KEITH R. PORTER

**Volume 21A (1980)**
**Normal Human Tissue and Cell Culture, Part A: Respiratory, Cardiovascular, and Integumentary Systems**
*Edited by Curtis C. Harris, Benjamin F. Trump, and Gary D. Stoner*

**Volume 21B (1980)**
**Normal Human Tissue and Cell Culture, Part B: Endocrine, Urogenital, and Gastrointestinal Systems**
*Edited by Curtis C. Harris, Benjamin F. Trump, and Gray D. Stoner*

**Volume 22 (1981)**
**Three-Dimensional Ultrastructure in Biology**
*Edited by James N. Turner*

**Volume 23 (1981)**
**Basic Mechanisms of Cellular Secretion**
*Edited by Arthur R. Hand and Constance Oliver*

**Volume 24 (1982)**
**The Cytoskeleton, Part A: Cytoskeletal Proteins, Isolation and Characterization**
*Edited by Leslie Wilson*

**Volume 25 (1982)**
**The Cytoskeleton, Part B: Biological Systems and *In Vitro* Models**
*Edited by Leslie Wilson*

**Volume 26 (1982)**
**Prenatal Diagnosis: Cell Biological Approaches**
*Edited by Samuel A. Latt and Gretchen J. Darlington*

## Series Editor

## LESLIE WILSON

**Volume 27 (1986)**
**Echinoderm Gametes and Embryos**
*Edited by Thomas E. Schroeder*

**Volume 28 (1987)**
***Dictyostelium discoideum:* Molecular Approaches to Cell Biology**
*Edited by James A. Spudich*

**Volume 29 (1989)**
**Fluorescence Microscopy of Living Cells in Culture, Part A: Fluorescent Analogs, Labeling Cells, and Basic Microscopy**
*Edited by Yu-Li Wang and D. Lansing Taylor*

**Volume 30 (1989)**
**Fluorescence Microscopy of Living Cells in Culture, Part B: Quantitative Fluorescence Microscopy—Imaging and Spectroscopy**
*Edited by D. Lansing Taylor and Yu-Li Wang*

**Volume 31 (1989)**
**Vesicular Transport, Part A**
*Edited by Alan M. Tartakoff*

**Volume 32 (1989)**
**Vesicular Transport, Part B**
*Edited by Alan M. Tartakoff*

**Volume 33 (1990)**
**Flow Cytometry**
*Edited by Zbigniew Darzynkiewicz and Harry A. Crissman*

**Volume 34 (1991)**
**Vectorial Transport of Proteins into and across Membranes**
*Edited by Alan M. Tartakoff*

**Selected from Volumes 31, 32, and 34 (1991)**
**Laboratory Methods for Vesicular and Vectorial Transport**
*Edited by Alan M. Tartakoff*

**Volume 35 (1991)**
**Functional Organization of the Nucleus: A Laboratory Guide**
*Edited by Barbara A. Hamkalo and Sarah C. R. Elgin*

**Volume 36 (1991)**
***Xenopus laevis:* Practical Uses in Cell and Molecular Biology**
*Edited by Brian K. Kay and H. Benjamin Peng*

## Series Editors
## LESLIE WILSON AND PAUL MATSUDAIRA

**Volume 37 (1993)**
**Antibodies in Cell Biology**
*Edited by David J. Asai*

**Volume 38 (1993)**
**Cell Biological Applications of Confocal Microscopy**
*Edited by Brian Matsumoto*

**Volume 39 (1993)**
**Motility Assays for Motor Proteins**
*Edited by Jonathan M. Scholey*

**Volume 40 (1994)**
**A Practical Guide to the Study of Calcium in Living Cells**
*Edited by Richard Nuccitelli*

**Volume 41 (1994)**
**Flow Cytometry, Second Edition, Part A**
*Edited by Zbigniew Darzynkiewicz, J. Paul Robinson, and Harry A. Crissman*

**Volume 42 (1994)**
**Flow Cytometry, Second Edition, Part B**
*Edited by Zbigniew Darzynkiewicz, J. Paul Robinson, and Harry A. Crissman*

**Volume 43 (1994)**
**Protein Expression in Animal Cells**
*Edited by Michael G. Roth*

**Volume 44 (1994)**
***Drosophila melanogaster:* Practical Uses in Cell and Molecular Biology**
*Edited by Lawrence S. B. Goldstein and Eric A. Fyrberg*

**Volume 45 (1994)**
**Microbes as Tools for Cell Biology**
*Edited by David G. Russell*

**Volume 46 (1995)**
**Cell Death**
*Edited by Lawrence M. Schwartz and Barbara A. Osborne*

**Volume 47 (1995)**
**Cilia and Flagella**
*Edited by William Dentler and George Witman*

**Volume 48 (1995)**
***Caenorhabditis elegans:* Modern Biological Analysis of an Organism**
*Edited by Henry F. Epstein and Diane C. Shakes*

**Volume 49 (1995)**
**Methods in Plant Cell Biology, Part A**
*Edited by David W. Galbraith, Hans J. Bohnert, and Don P. Bourque*

**Volume 50 (1995)**
**Methods in Plant Cell Biology, Part B**
*Edited by David W. Galbraith, Don P. Bourque, and Hans J. Bohnert*

**Volume 51 (1996)**
**Methods in Avian Embryology**
*Edited by Marianne Bronner-Fraser*

**Volume 52 (1997)**
**Methods in Muscle Biology**
*Edited by Charles P. Emerson, Jr. and H. Lee Sweeney*

**Volume 53 (1997)**
**Nuclear Structure and Function**
*Edited by Miguel Berrios*

**Volume 54 (1997)**
**Cumulative Index**

**Volume 55 (1997)**
**Laser Tweezers in Cell Biology**
*Edited by Michael P. Sheetz*

**Volume 56 (1998)**
**Video Microscopy**
*Edited by Greenfield Sluder and David E. Wolf*

**Volume 57 (1998)**
**Animal Cell Culture Methods**
*Edited by Jennie P. Mather and David Barnes*

**Volume 58 (1998)**
**Green Fluorescent Protein**
*Edited by Kevin F. Sullivan and Steve A. Kay*

**Volume 59 (1998)**
**The Zebrafish: Biology**
*Edited by H. William Detrich III, Monte Westerfield, and Leonard I. Zon*

**Volume 60 (1998)**
**The Zebrafish: Genetics and Genomics**
*Edited by H. William Detrich III, Monte Westerfield, and Leonard I. Zon*

**Volume 61 (1998)**
**Mitosis and Meiosis**
*Edited by Conly L. Rieder*

**Volume 62 (1999)**
***Tetrahymena thermophila***
*Edited by David J. Asai and James D. Forney*

**Volume 63 (2000)**
**Cytometry, Third Edition, Part A**
*Edited by Zbigniew Darzynkiewicz, J. Paul Robinson, and Harry Crissman*

**Volume 64 (2000)**
**Cytometry, Third Edition, Part B**
*Edited by Zbigniew Darzynkiewicz, J. Paul Robinson, and Harry Crissman*

**Volume 65 (2001)**
**Mitochondria**
*Edited by Liza A. Pon and Eric A. Schon*

**Volume 66 (2001)**
**Apoptosis**
*Edited by Lawrence M. Schwartz and Jonathan D. Ashwell*

**Volume 67 (2001)**
**Centrosomes and Spindle Pole Bodies**
*Edited by Robert E. Palazzo and Trisha N. Davis*

**Volume 68 (2002)**
**Atomic Force Microscopy in Cell Biology**
*Edited by Bhanu P. Jena and J. K. Heinrich Hörber*

**Volume 69 (2002)**
**Methods in Cell-Matrix Adhesion**
*Edited by Josephine C. Adams*

**Volume 70 (2002)**
**Cell Biological Applications of Confocal Microscopy**
*Edited by Brian Matsumoto*

**Volume 71 (2003)**
**Neurons: Methods and Applications for Cell Biologist**
*Edited by Peter J. Hollenbeck and James R. Bamburg*

**Volume 72 (2003)**
**Digital Microscopy: A Second Edition of Video Microscopy**
*Edited by Greenfield Sluder and David E. Wolf*

**Volume 73 (2003)**
**Cumulative Index**

**Volume 74 (2004)**
**Development of Sea Urchins, Ascidians, and Other Invertebrate Deuterostomes: Experimental Approaches**
*Edited by Charles A. Ettensohn, Gary M. Wessel, and Gregory A. Wray*

**Volume 75 (2004)**
**Cytometry, 4th Edition: New Developments**
*Edited by Zbigniew Darzynkiewicz, Mario Roederer, and Hans Tanke*

**Volume 76 (2004)**
**The Zebrafish: Cellular and Developmental Biology**
*Edited by H. William Detrich, III, Monte Westerfield, and Leonard I. Zon*

**Volume 77 (2004)**
**The Zebrafish: Genetics, Genomics, and Informatics**
*Edited by William H. Detrich, III, Monte Westerfield, and Leonard I. Zon*

**Volume 78 (2004)**
**Intermediate Filament Cytoskeleton**
*Edited by M. Bishr Omary and Pierre A. Coulombe*

**Volume 79 (2007)**
**Cellular Electron Microscopy**
*Edited by J. Richard McIntosh*

**Volume 80 (2007)**
**Mitochondria, 2nd Edition**
*Edited by Liza A. Pon and Eric A. Schon*

**Volume 81 (2007)**
**Digital Microscopy, 3rd Edition**
*Edited by Greenfield Sluder and David E. Wolf*

**Volume 82 (2007)**
**Laser Manipulation of Cells and Tissues**
*Edited by Michael W. Berns and Karl Otto Greulich*

**Volume 83 (2007)**
**Cell Mechanics**
*Edited by Yu-Li Wang and Dennis E. Discher*

**Volume 84 (2007)**
**Biophysical Tools for Biologists, Volume One: *In Vitro* Techniques**
*Edited by John J. Correia and H. William Detrich, III*

**Volume 85 (2008)**
**Fluorescent Proteins**
*Edited by Kevin F. Sullivan*

**Volume 86 (2008)**
**Stem Cell Culture**
*Edited by Dr. Jennie P. Mather*

**Volume 87 (2008)**
**Avian Embryology, 2nd Edition**
*Edited by Dr. Marianne Bronner-Fraser*

**Volume 88 (2008)**
**Introduction to Electron Microscopy for Biologists**
*Edited by Prof. Terence D. Allen*

**Volume 89 (2008)**
**Biophysical Tools for Biologists, Volume Two: *In Vivo* Techniques**
*Edited by Dr. John J. Correia and Dr. H. William Detrich, III*

**Volume 90 (2008)**
**Methods in Nano Cell Biology**
*Edited by Bhanu P. Jena*

**Volume 91 (2009)**
**Cilia: Structure and Motility**
*Edited by Stephen M. King and Gregory J. Pazour*

**Volume 92 (2009)**
**Cilia: Motors and Regulation**
*Edited by Stephen M. King and Gregory J. Pazour*

**Volume 93 (2009)**
**Cilia: Model Organisms and Intraflagellar Transport**
*Edited by Stephen M. King and Gregory J. Pazour*

**Volume 94 (2009)**
**Primary Cilia**
*Edited by Roger D. Sloboda*

**Volume 95 (2010)**
**Microtubules, in vitro**
*Edited by Leslie Wilson and John J. Correia*

**Volume 96 (2010)**
**Electron Microscopy of Model Systems**
*Edited by Thomas Müeller-Reichert*

**Volume 97 (2010)**
**Microtubules: In Vivo**
*Edited by Lynne Cassimeris and Phong Tran*

**Volume 98 (2010)**
**Nuclear Mechanics & Genome Regulation**
*Edited by G. V. Shivashankar*

**Volume 99 (2010)**
**Calcium in Living Cells**
*Edited by Michael Whitaker*